Linear Parameter-Varying Control of Systems of High Complexity

Christian Hoffmann

LINEAR PARAMETER-VARYING CONTROL OF SYSTEMS OF HIGH COMPLEXITY

Vom Promotionsausschuss der
Technischen Universität Hamburg-Harburg

zur Erlangung des akademischen Grades

Doktor-Ingenieur (Dr.-Ing.)

genehmigte Dissertation

von
CHRISTIAN HOFFMANN

aus
Bremerhaven, Bremen, Deutschland

2016

Umschlagsfotografie: Julian Theis

Vorsitzende des Promotionsverfahrens: Prof. Dr. Sibylle Schupp

1. Gutachter: Prof. Dr. Herbert Werner
2. Gutachter: Dr. James Whidborne
weitere Gutachter: Prof. Dr.-Ing. Robert Seifried
Prof. Dr.-Ing. Uwe Weltin

Tag der mündlichen Prüfung: 04. Dezember 2015

1. Auflage 2016

Dedicated to my Family
and Loved ones.

ZUSAMMENFASSUNG

IN der vorliegenden Arbeit werden Regelstrecken als *Lineare parameterveränderliche* (LPV)-Systeme betrachtet, die einen hohen Aufwand in der Modellierung sowie der Synthese und Implementierung entsprechender LPV-Regler aufweisen können, weil sie entweder stark nichtlinear gekoppelte Systeme mit vielen Parametern darstellen, oder aus einer großen Anzahl verteilter, interagierender LPV-Subsysteme bestehen. Für komplexe LPV Systeme der ersten Klasse werden systematische Werkzeuge zur exakten mathematischen Modellierung mit verringerter Komplexität bereitgestellt und deren gewinnbringende Verwendung im Rahmen von erweiterten LPV-Reglersynthesemethoden behandelt. Der grundsätzliche Ansatz beruht dabei auf einer Überführung nichtlinearer Differentialgleichungen in eine Deskriptor-LPV-Zustandsraumdarstellung, einer automatisierten Parametrierung und möglichen Approximation mit Hilfe einer Hauptachsentransformation. Einflüsse auf den Rechenaufwand während der Synthese und Implementierung werden identifiziert und durch mathematisch equivalente Umformulierungen reduziert. Die Methoden werden an den nichtlinearen Modellen eines industriellen Roboters und eines *Control Moment Gyroscopes* (CMG) validiert. Dabei gelingt es, LPV-Regler für die exakten und für die approximierten Modelle zu synthetisieren und mit niedrigem Implementierungsaufwand experimentell zu validieren.

Des Weiteren wird zunächst ein allgemeines Framework für die Formulierung verteilter LPV Systeme eingeführt. Ein Aufstellen der Synthesebedingungen für ein solches verteiltes System erlaubt die Reduktion der Synthesekomplexität durch strukturelle Randbedingungen auf Entscheidungsvariablen. So lassen sich Bedingungen formulieren, die in ihrer Ordnung der Komplexität der eines einzelnen Subsystems multipliziert mit der Anzahl unterschiedlicher Subsystemdynamiken entsprechen. Die Diagonalisierbarkeit der Interaktionsmatrizen wird durch Transformationen gewährleistet, die zu virtuellen symmetrischen oder normalen Interaktionsmatrizen führen. Da solche Matrizen durch unitäre Transformationen diagonalisiert werden können, wird die direkte Komplexitätsreduktion der Synthesebedingungen durch eine Kongruenztransformation bestimmter Matrixungleichungen und somit die Berücksichtigung zeitvariabler, gerichteter Topologien ermöglicht. Die vorgestellten Methoden werden sowohl an einem numerischen Beispiel als auch anhand der Formationsregelung nichtlinearer Quadrotor-Helikopter in der Simulation validiert.

SUMMARY

THE present work considers plant representations in the framework of *linear parameter-varying* (LPV) systems that may involve a high degree of complexity. This class contains nonlinear systems that lead to high costs in modeling, synthesis and implementation of associated LPV controllers on the one hand as well as systems consisting of a large number of LPV subsystems interconnected through a possibly time-varying topology on the other hand. For complex LPV systems of the first kind, the contribution of this thesis consists in the development of systematic tools for mathematically exact modeling with reduced complexity and the subsequent efficient exploitation by extended LPV synthesis methods. The fundamental approach follows a translation of nonlinear differential equations into a descriptor state space LPV representation, parameterization and possible approximation by means of a principle component analysis. The synthesis conditions and implementation are analyzed in terms of their respective computational effort and reduced by mathematically equivalent modification. The methods are validated on nonlinear models of an industrial robot and a *Control Moment Gyroscope* (CMG). LPV controllers are synthesized for both the exact as well as the approximated models and experimentally implemented with low computational costs.

Furthermore, a general framework for the representation of distributed LPV systems is introduced. A straightforward formulation of synthesis conditions for the entire system allows reducing the synthesis complexity via the introduction of structural constraints on decision variables. In this vein, synthesis conditions are formulated whose complexity ranges in the order of a single subsystem times the number of different subsystem dynamics. The diagonalizability of interaction matrices is achieved by a transformation that leads to virtual symmetric or normal interaction matrices. Such matrices can be diagonalized by unitary transformations, which allows the direct congruence transformation of synthesis conditions for the consideration of time-varying, directed topologies. The presented methods are evaluated against state-of-the-art techniques and validated in a numerical example as well as in a simulated leader-follower-based formation of a group of heterogeneous nonlinear quadrotor helicopters interconnected through arbitrary directed topologies.

KURZZUSAMMENFASSUNG

Der Entwurf von Reglern für komplexe nichtlineare Regelstrecken im Framework *Linear Parameterveränderlicher* (LPV) Systeme führt zu hohem Modellierungs-, Synthese- und Implementierungsaufwand. Zugleich können Regelstrecken durch eine verteilte Struktur ähnlicher interagierender LPV-Subsysteme eine hohe Komplexität erlangen. Die vorliegende Arbeit behandelt Methoden zur Modellierung komplexer LPV-Systeme, sowohl im Sinne nichtlinearer, als auch verteilter Regelstrecken, und beinhaltet verbesserte Entwurfswerkzeuge, die zu niedrigerem Synthese- und Implementierungsaufwand führen.

ABSTRACT

The controller design for complex nonlinear systems using the framework of *linear parameter-varying* (LPV) systems often leads to high costs in modeling, synthesis and implementation. Interconnected LPV subsystems also yield complex systems. This thesis presents methods for the modeling of complex LPV systems, in the sense of nonlinear as well as interconnected subsystems and introduces improved controller synthesis tools that lead to reduced synthesis and implementation costs.

ACKNOWLEDGMENTS

THE present thesis is the result of about four years of work at the Institute of Control Systems, Hamburg University of Technology. It has been heavily supported by colleagues, friends and much more experienced researchers. Without all of their inspiration, guidance and friendly advice, this thesis would not have turned out the way it did or would probably not even have come into existence. First and foremost, I am grateful to my supervisor, Prof. Dr. Herbert Werner, for many reasons. Among them, I am humbly acknowledging the amount of trust put in me. Letting students off the leash can spur creativity and a sense of identification with the work. On the other hand, I do not want to deny the occasional nudges, scientific rigor in seminars and attention to mathematical details that did not let me stray too far from the red thread. In my opinion Prof. Dr. Werner has supervised me with an ever present sense of integrity and respect for theoretical science.

My former fellow Ph.D. student colleagues Dr.-Ing. Georg Pangalos, Dr.-Ing. Annika Eichler and Dr.-Ing. Qin Liu made my stay at the Institute of Control Systems all the more pleasurable, such that soon colleagues turned into friends. I am especially grateful to Annika Eichler for the many opportunities to collaborate—I am still sorry for thinking much slower at times. A warm and special thanks also goes to Dr.-Ing. Hossam Seddik Abbas, Dr.-Ing. Ahsan Ali and Dr.-Ing. Mahdi Hashemi. Not only did they provide a heartwarmingly open culture of asking questions until the matter was understood, but they also provided a most welcome warm start to my research by openly sharing unsolved issues of their work on which we then collaborated. In times, such as this, I am fortunate enough to have observed in them faithful and open-minded believers in Islam—an experience that, I believe, built strong mutual respect. I am confident that in this regard they are not exceptions. It is uplifting nonetheless that having worked and laughed with them provided living proof that islamophobics are wrong.

Nowadays, it appears a custom that many researchers spend the last lines acknowledging the time his or her beloved significant others have sacrificed while the author was in the final stages of writing up. In fact, in my case things are a little different—or at least, I choose not to see it that way. For one thing, friends and family have kept me busy with the other beautiful things in life, which provided distraction and thus the necessary endurance and a sense of fun in the matters related to my science. Although hours have undoubtedly been long during part of my studies, I feel that I have been most enthusiastic about my work, whenever it was in balance with my private life. This is why I'd like to express my deep gratitude to my brother Sascha and my mother and father, Iris and Thomas, for insisting in not sacrificing anything, but rather not letting work drown out precious personal moments. The happiest part then began, when I was in the final stages of writing

up, which was also when I fell in love with Lydia. Let's just say that I believe that under the influence of love and peace of mind, creativity can flourish and in that regard and many others, I am very grateful that Lydia is a part of my life.

All that being said, this doctoral thesis is just that—a doctoral thesis. However small, it may be a stepping stone for future researchers and practitioners and if that holds true, I will be grateful to those having the patience to read through it and to those dropping me a line or two to point out mistakes or simply to tell me that it was of some use.

Speaking of mistakes, I would like to conclude by thanking the people that provided aid in correcting numerous errors (not only typographical ones) in the thesis: Anne Pape, Clara Schmale, David Coverly, Dagmar Pohl, Hauke Gravenkamp, Hossam Seddik Abbas, Jonas Krone, Klemens Jagieniak, Lydia Herzog, Marc Bahde, Robinson Peric, Sascha Hoffmann and Tobias Mörke. Thank you very much for your time and efforts!

Christian Hoffmann, April 24th, 2016

CONTENTS

1

INTRODUCTION

NOWADAYS, modern control systems are implemented digitally and can often be updated and improved at little cost. Systems can be designed with a highly integrated control system in mind that is in fact essential for operation. In classical control, systems are often engineered in such a manner that a suitable control strategy for the entire operating envelope can be devised by means of simple analysis and synthesis tools[1]. This would typically involve the design of separate, cascaded subsystem controllers in a hierarchical order.

That means that higher level controllers rely on the closed-loop performance provided by lower level controllers. While such a systematic, sometimes iterative approach is attractive and can lead to robust designs, in engineering ≪interactions are essential≫ [9] and can be exploited to improve performance. Taking interactions into account introduces complexity into the system modeling, design and controller synthesis phase, as elaborated in the following quote of Aström and Kumar.

≪There is a general tendency that engineering systems are becoming more complex. Complexity is created by many mechanisms: size, interaction and complexity of the subsystems are three factors that contribute.≫

Aström and Kumar [9], p. 28

---

[1] As in the original meaning of the greek words: ἀνάλυσιζ — analysis: ≪decomposition≫; σύνθεσιζ — sýnthesis: ≪combination≫.

In this thesis, the «mechanisms» considered that induce complexity of a system are the following two: Intricate nonlinear behaviour of lumped systems, the interconnection of a potentially very large number of subsystems, or a combination of the two, result in systems of a high degree of complexity that require special techniques for control.

The linear parameter-varying (LPV) framework has been proven to be a suitable tool for dealing with measurable changes in the plant dynamics and nonlinear couplings via «gain-scheduling» controller design in a systematic fashion [134]. The attractiveness of the framework not only resides in its systematic synthesis tools, but also in the closed-loop stability and performance guarantees that come along with them. However, in many cases the available tools fail to appropriately scale with the complexity of the LPV systems considered and are intractable to apply.

Figure 1.1b illustrates the benefits of taking into account intricate nonlinear couplings in controller designs over neglecting them via linearized models. The considered plant is a control moment gyroscope[2], which exhibits strong nonlinear couplings between the controlled angles q_3 and q_4, cf. Fig. 1.1a. As apparent, cross-

(a) A control moment gyroscope.

(b) Simulation results of reference tracking.
(——) Nonlinear LPV controller designed by the methods of this thesis.
(——) $\mathcal{H}_\infty$-LTI controller.
(·····) Reference trajectory.
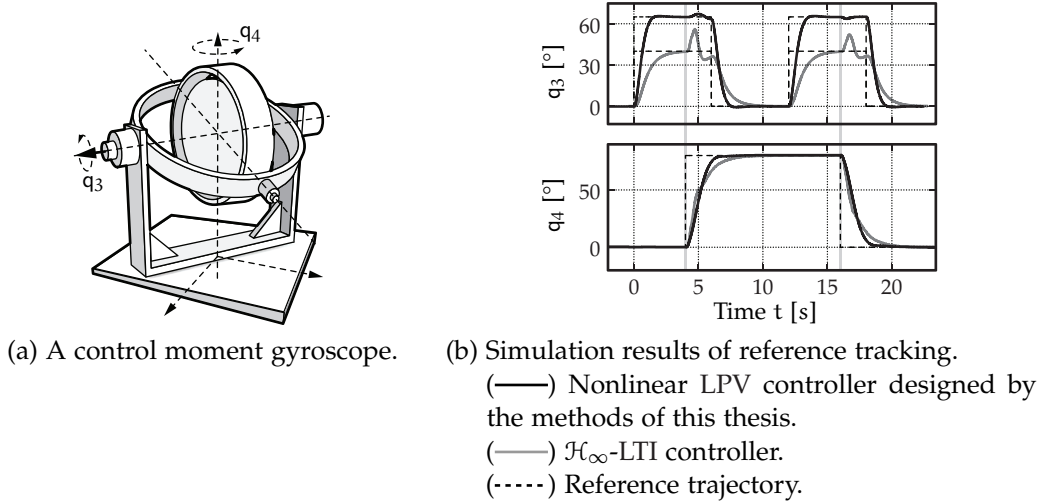
Figure 1.1: Illustrative example of benefits of linear parameter-varying vs. linear time-invariant control on the basis of a control moment gyroscope.

coupling effects are significantly decreased while the rise times are at least maintained. Furthermore, the reference of the linear control loop had to be reduced to avoid instability.

Furthermore, when dealing with identical or similar systems interconnected through a possibly time-varying topology, a suitable synthesis algorithm would have to take into account dynamic interactions and potential loss of interconnec-

---

2 The control moment gyroscope will be introduced in detail in Chap. 4, Sect. 4.7.

tion in the same instance. As it turns out, essential methods borrowed from LPV controller synthesis can be employed to cater to this need.

In the course of this thesis, practical methods will be developed that lead to gain-scheduled controllers for plants with complicated nonlinear couplings which can be implemented with low computational cost. This can be attained by improved synthesis methods taking into account the accurate plant dynamics, or by novel, systematic approximation and modeling methods. If such subsystems modeled in the LPV framework are connected to form an interconnected LPV system on a larger scale, methods are developed whose computational effort during synthesis does not scale with the number of subsystems.

The remainder of this chapter provides a brief historical background of LPV systems in Sect. 1.1, motivation and objectives in Sect. 1.2, a detailed list of the main contributions as well as an outline of this thesis in Sect. 1.3 and 1.4, respectively.

1.1 Historical Background

THE systematic design of controllers that are able to guarantee stability and a high level of performance for nonlinear and time-varying (TV) plants has been an active field of research since at least from the beginning of the 1970s [E83]. Research has shifted from focusing primarily on optimality to also taking into account robustness against parameter variations [120]. If these parameters can be measured online, gain-scheduling can be performed, which classically involves the interpolation or switching between linear time-invariant (LTI) controllers designed independently on a set of operating points [85]. This controller design approach is well-known to only provide rigorous stability and performance guarantees for sufficiently slow parameter variations [136]. However, it is still widely used in practice—often successfully.

The seminal work of Shamma [133, 135] first introduced the paradigm of LPV models for the systematic analysis and design of gain-scheduled controllers. LPV models are introduced as linear state space models whose matrices depend on time-varying parameters. The dynamics of an LPV system are therefore linear but time-varying [138]. Special classes of nonlinear systems which can be naturally covered by the LPV framework [138] are, e. g., hybrid dynamical systems [121] and jump linear systems/switched linear systems [22]. The suitability of the LPV framework for the control of general nonlinear systems arises from the fact that nonlinear state space models can be brought into the so-called quasi-linear parameter-varying (Q-LPV) form [83–85], in which parameters can be functions of the states, inputs or outputs, instead of only exogenous signals. In light of this, LPV models are often derived from systems described by nonlinear differential equations that are obtained from physical relations, e. g., by balancing generalized flows or potentials. Such equations may yield transcendental, rational or polynomial terms in the states, inputs and outputs, which are covered by parameter variations. Such endogenous parameter definitions have become popular to tackle a variety of nonlinear control

problems. See Sect. 3.2 for a survey. This approach is relatively straightforward for systems, whose component parameters, like inertias, stiffnesses, inertances, resistances, etc., are state-dependent. Hard nonlinearities such as stiction, hysteresis or saturation are more difficult to handle, as are systems with nonlinearly coupled modes. The success of controller synthesis for the latter depends on the non-unique choice of LPV parameters, see, e. g., [E47, E69].

For the above systems, LPV controller synthesis is attractive as a straightforward extension of LTI control methodologies, such as sensitivity shaping and modeling tools. Early synthesis methods were limited to slow parameter variations [137] but over the years methods have been derived that allow arbitrarily fast parameter variations, [3, 5, 6, 124, 125, 129, 130, 161, 164]. Incorporating knowledge on bounds on the parameters' rate of variation can be used to reduce conservatism and has been explored, e. g., in [3, 163].

Even though the LPV methodology has been introduced over 25 years ago [133, 135] and is nowadays theoretically well-founded, the LPV methodology still appears to be not be widely used in industrial applications. It is also stated that LPV methods are difficult to apply to plants of industrial complexity due to considerable computational burdens [E21] potential numerical issues during synthesis [E83] and the lack of systematic LPV modeling tools [E60]. As mentioned above, this thesis aims to contribute to resolving some of these issues.

1.2 Motivation and Objectives

Despite extensive studies in LPV control, few methods can be applied systematically—or only with severe drawbacks—to design controllers for complex LPV plants. Consequently, this thesis essentially deals with the analysis and control of systems with a high degree of complexity using and extending available LPV methodologies. Since in this thesis *complexity* may arise from both intricate nonlinear ordinary differential equations of lumped LPV systems as well as from the interconnection of a potentially very large number of LPV subsystems, the thesis is structured in two parts for which the main motivational aspects are listed as follows.

1.2.1 *Part I—LPV Control of Complex Lumped Systems*

As the data from a preliminary survey suggests [59][3] only few experimentally validated controller designs are reported for plants with seven or more scheduling parameters. In this survey, an attempt at a decision tree for LPV controller synthesis is made for complex LPV systems, which is shown in Fig. 1.2. This tree focuses on the major available standard output-feedback (OF) LPV controller synthesis techniques, whose association with the respective LPV modeling frameworks is depicted in Fig. 1.3. The decision tree is to be traversed by evaluating questions

---

3 Presented in extended form in Sect. 3.2

about the associated numbers of parameters and block sizes indicated by n_ρ, n_δ, n_θ and n_Δ as well as the convexity of the range of admissible parameter values $\boldsymbol{\rho}$. Here, it is assumed that an LPV model with general parameter-dependence on the parameter vector ρ is available and suitable rational or affine representations in terms of the parameter vectors δ and θ, respectively, can be found. While it may well be claimed that this assumption holds in general, the methods used to arrive at rational, affine or even at the general LPV representation are highly non-trivial to begin with. The matter of conservatism is further deeply entwined with the chosen parameterization due to so-called overbounding in the parameter space and relaxations used during synthesis. The question of whether a particular approach delivers the required performance is posed at the very end, as it is hard to predict. Following the approach to prefer simpler solutions, the only given answer is to switch to parameter-dependent Lyapunov functions (PDLFs) in case of excessive conservatism. Thus it may be argued that the decision tree in fact lacks *feedback*: A mechanism and a systematic approach in case the available tools reach dead ends in terms of excessive conservatism or excessive implementation complexity.
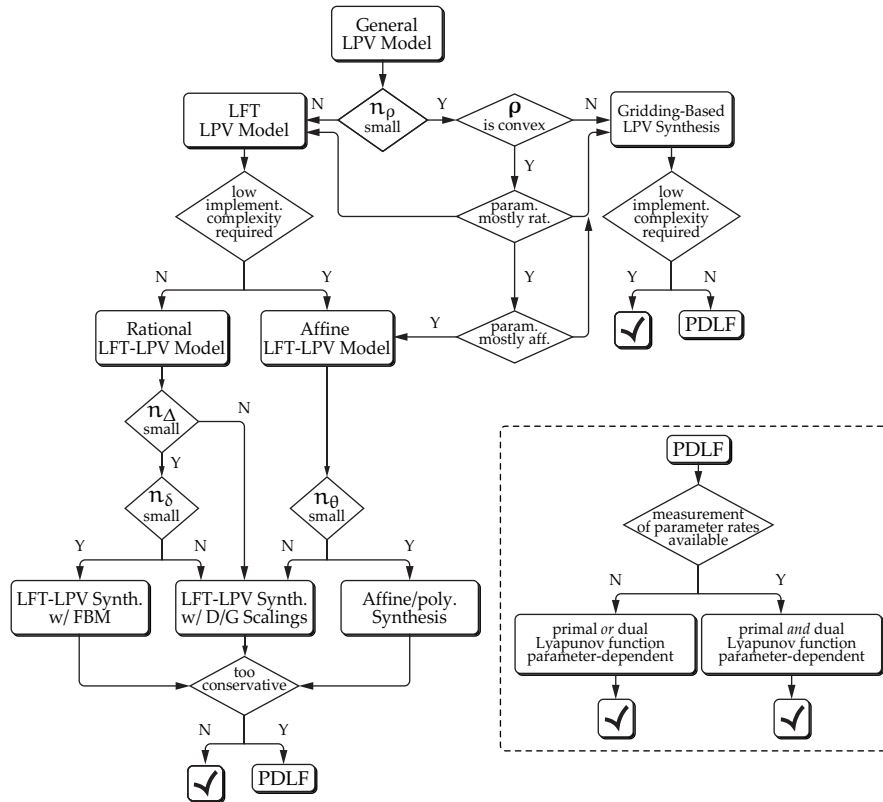
Figure 1.2: A first attempt at a decision tree for LPV controller synthesis for complex LPV systems.
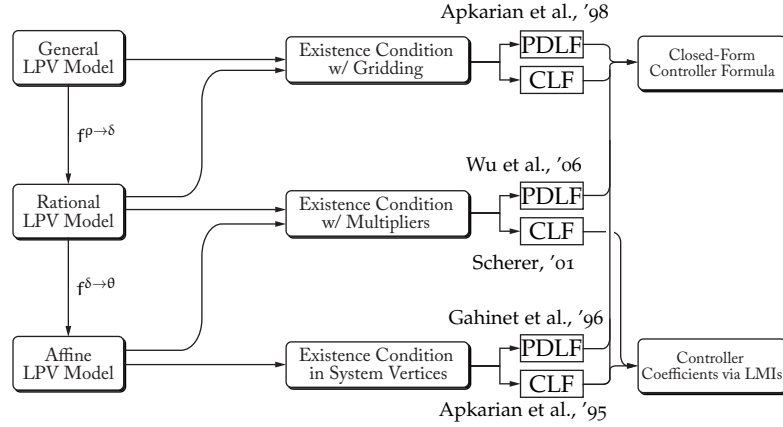
Figure 1.3: Standard OF LPV controller synthesis techniques associated with the respective LPV modeling frameworks.

LPV MODELING AND MODEL COMPLEXITY ASSESSMENT

The decision tree of Fig. 1.3 is the result of an empirical analysis of the model complexities and associated synthesis techniques in [59] and is further supported by preliminary research that led to the results presented in this thesis. In order to be applicable by control designers, a suite of tools is required that can—at least to a certain degree—provide an *a priori* assessment of model, synthesis and implementation complexities. Such tools quickly lead to an attempt to unify the modeling approach, in order to maintain comparable quantifiers for complexity. Even though the mere number of scheduling parameters may bear limited meaning as a measure of complexity, it is still desirable to be able to derive parameterizations with a minimum number of parameters.

Systematic LPV modeling tools have been proposed in [E60, 146], which allow to arrive at LPV models from nonlinear differential equations. While in [E60] a more rigorous mathematical language is employed than in [146], the work in [E60] focuses on affine LPV model representations only, which were believed to yield low-complexity controllers. This is not entirely untrue, but a rigorous enumeration of complexity figures for a quantitative comparison has not yet been performed.

Therefore, one of the goals of this thesis is to introduce novel systematic methods for arriving at general and rational LPV model factorizations and embed these in an extendable framework that essentially allows to characterize all possible factorizations. As a consequence, an algorithm is provided that can be tuned towards low-complexity LPV models or in favor of maintaining coupling terms.

LPV MODEL APPROXIMATION

The method of parameter set mapping (PSM) as introduced in [79] has been proven to be capable of providing good approximations of relatively complex models [E37]. However, as formulated initially, it relies on simulation-based or experimental data of trajectories that traverse the entire operating envelope of interest. This necessi-

tates the availability of a controller that can provide closed-loop stability and an appropriate amount of performance in this range. Accordingly, the LPV controller design is limited to the purpose of improving performance instead of enlarging the available range of operation, which can be amended by methods that are not based on data. In addition, the application of PSM to rational, so-called linear fractional transformation (LFT)-based LPV models usually has the undesirable effect of actually increasing the model complexity in terms of the parameter block dimensions, denoted n_Δ in Fig. 1.2. Consequently, a further goal of this thesis is to provide novel methods for the approximation of rational LPV models.

SYNTHESIS METHODS OF LOW COMPLEXITY
The design of the decision tree shown in Fig. 1.2 mainly stems from the fact that complexity in LPV controller synthesis grows exponentially with the number of scheduling parameters. This holds true for conditions based on a so-called gridding for general parameter-dependency, full-block multipliers (FBMs) for LFT-LPV representations as well as conditions for polytopic LPV models. In these cases this ultimately limits the number of parameters that can be considered to only a few.

The thesis thus further focuses on model representations and improving synthesis conditions, such that the increase in synthesis complexity with the increase in model complexity is less severe. It is aimed at illustrating the benefits on a plant, for which it was previously impossible to consider exact LPV plant representations in modeling and synthesis. As a result of the research efforts presented in this thesis, the decision tree will be revised in the conclusions of Sect. 11.2.

1.2.2 *Part II—Control of Interconnected LPV Systems*

In interconnected systems theory it is often desired to reach a global, common goal by means of local interaction and information processing. The underlying rationale is to aim for *resilient* systems in a sense that is often stated to transcend the control theoretic term «robustness». At the dawn of the age of cyber physical systems (CPSs)—a term coined «to describe the increasingly tight coupling of control, computing, communication and networking» [9]—the requirement on a system to be «resilient» includes the ability to recover and withstand the influence of hostile and malicious actors [119]. In view of the research field of «glocal control»[4], hybrid systems are the next evolutionary step from robust systems [118], meaning that, e.g., even social components play an important role not to be dismissed during the design of such a distributed system. However, it appears as though more issues on the lower levels of control still need to be resolved, to which this thesis aims to contribute.

Despite a wealth of research, it is still robustness against failing communication links, failing subsystems, heterogeneity in the subsystem dynamics, or any combination of these that needs to be adressed further. For instance, distributed control

---

[4] Global control by local interactions.

systems should ideally be scalable, s. t. the introduction of additional agents or subsystems does not require the complete redesign of the control structure. In essence, it is desired to combine the universal applicability of the methods presented in [80] with the scalability of the methods proposed by [98]. Figure 1.4 visualizes the essential approach on the example of a multi-agent system (MAS): A synthesis framework is sought that can handle heterogeneous, nonlinear subsystems with physical or virtual time-varying and directed interconnections, while offering synthesis complexity in the order of a single subsystem. Each type of subsystem is associated with a respective type of controller, while the entirety of controllers inherit the interaction topology of the interconnected plant. Even though, this problem is easy to grasp, it becomes arguably more interesting in the face of physical interconnections between the agents.
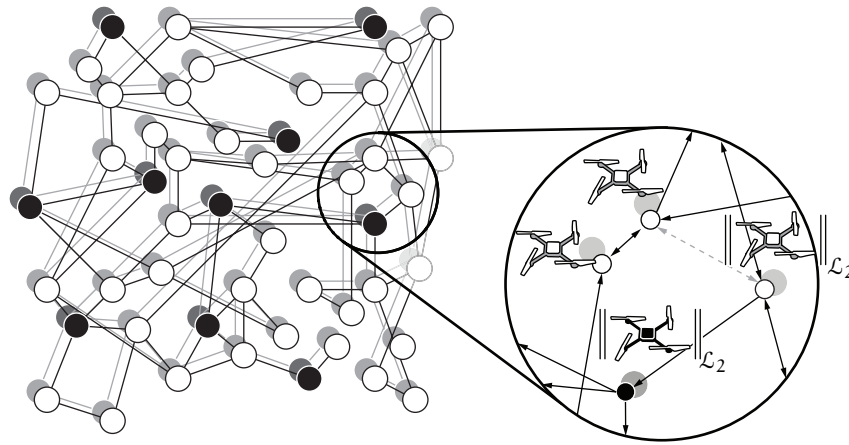
Figure 1.4: An exemplary heterogeneous MAS with nonlinear dynamics and a visualization for synthesis conditions with complexity in the order of a single subsystem. Circles of different shades indicate heterogeneity in the subsystems. Connecting lines indicate interaction, and the fact that each circle has a superimposed companion illustrates that each subsystem has its own local controller.

A General Framework for Interconnected Systems Modeling
A particular goal of this thesis resides in proposing a framework for the modeling of interconnected systems that encompasses the universal applicability of the one defined in [80], i. e., freedom in defining virtual (communication) and physical couplins, while allowing for the exploitation of graph theory [109] to limit/reduce the complexity of synthesis and analysis conditions to yield scalable distributed controller synthesis methods.

Arbitrary, Directed and Switching Interconnection Topologies
Owing to the limitations incurred by particular decomposition methods, e. g., [97], synthesis conditions that provide optimization over a performance index and still allow for arbitrary, directed and switching interconnections with low conservatism

are not readily available. The thesis therefore also contains improved methods for this purpose and relates them to existing ones.

Nonlinear and Heterogeneous Subsystem Dynamics

The efficiency of many tools for interconnected systems is achieved by considering identical subsystems, e. g., [24]. However, real-world systems usually involve some degree of heterogeneity, which may arise from changed dynamics or locally varying operating points. A goal of this thesis is therefore to address this issue and extend synthesis methods accordingly.

Scalable and Convex Synthesis Conditions

Methods for cooperative controller synthesis that allow the addition of new agents at any time, e. g., [115], rely on non-convex optimization, since they are posed as robust control problems. A further goal of this thesis is to investigate to which extent the methods proposed in this thesis can be applied to turn distributed controller synthesis into convex optimization problems and therefore simplify the synthesis process.

1.3 Main Contributions

The main contributions of this thesis are listed below—structured in two parts according to the considered mechanisms that incur increased complexity.

1.3.1 *Part I—LPV Control of Complex Lumped Systems*

Within this thesis, contributions to the LPV control of complex lumped systems are devoted to the development of a systematic modeling framework by extending the automated derivation of LPV factorizations from intricate nonlinear ordinary differential equations (ODEs) and by proposing descriptor representation-based compact LFT-LPV parameterizations. The highlights are summarized in the following items:

- A tool for the detailed analysis for the *a priori* assessment of synthesis and implementation complexity for each of the respective major LPV modeling frameworks is summarized in Sect. 3.1 in Tabs. 3.1–3.4 on pp. 83–84 and pp. 89–90, respectively.

- A versatile and tunable heuristic approach to the LPV factorization of nonlinear vectors occurring in state space representations is presented in Sect. 4.3 on pp. 105. It employs a mathematical nomenclature to allow for further, potentially more rigorous optimization criteria to be applied to it.

- An explicit compact LFT parameterization of descriptor LPV models is developed in Sect. 4.4 on pp. 117, which allows for automatic LPV parameterization and approximation by employing Lma. 4.2 on p. 126 and associated corollar-

ies presented in Sect. 4.5 on pp. 123. The procedure is summarized in Alg. 4.1 on p. 137.

- In Chap. 5, a reduction of synthesis and implementation complexity for both output-feedback and state-feedback LPV controller synthesis by improved linear matrix inequality (LMI) conditions is achieved via Cor. 5.1 on p. 160 and Prop. 5.1 on p. 172, respectively.

The methods are applied in detail to the LPV modeling (Sects. 4.6 and 4.7) and control (Chap. 6) of a three-degree of freedom (3-DOF) robotic manipulator and a four-degree of freedom (4-DOF) control moment gyroscope (CMG). Preliminary results w. r. t. the robotic manipulator have been experimentally validated in [E48], whereas novel experimental validations of the extended methods are presented for the CMG in this thesis. Using the above methods, for the first time controllers that guarantee closed-loop stability and performance are synthesized directly based on the exact model of the CMG, while reductions in synthesis time reach up to 90 %.

1.3.2 *Part II—Control of Interconnected LPV Systems*

The core methods developed within this thesis associated with the synthesis of distributed controllers are summarized in the following highlights:

- A compact modeling framework is developed in Chap. 8 on pp. 249 that allows for a wide range of interconnected systems with both physical and virtual interconnections.

- Propositions 9.1, 9.2 and 9.3 on pp. 253–259 are developed as solutions to Prob. 9.1 on p. 251, which consists in finding an equivalent representation of any interconnection matrix that involves a normal matrix.

- Based on these, in Chap. 9, the analysis result for heterogeneous groups of interconnected LPV subsystems in Thm. 9.2 on p. 263 can be reduced in complexity by applying Lma. 9.1 on p. 266. The lemma formalizes the congruence transformation on the associated LMIs, in order to obtain decoupled conditions in Thm. 9.3 on p. 269.

- Scalable existence conditions for distributed LPV controllers are presented in Thm. 9.6 on p. 272 that can be solved efficiently as standard gain-scheduling problems. This as the approach poised for applying recently developed advanced techniques in LPV gain-scheduling using dynamic multipliers to it.

- Application examples presented in Chap. 10 indicate both the relatively low conservatism that may be introduced via the proposed methods and the benefits over existing methods. Section 10.2.1 establishes the performance norm-optimal formation control problem subject to directed and time-varying interconnection topologies as well as LPV agents as a convex (gain-scheduling) synthesis problem, instead of as a non-convex robust control problem.

In summary, methods are developed that allow for the synthesis of distributed controllers for

- interconnected heterogeneously scheduled LPV subsystems,

- subsystems with heterogeneous dynamics,

- interconnections that are both virtual and physical,

- directed and switching interconnection topologies.

Furthermore, the developed synthesis tools have the following properties:

- Synthesis complexity in the order of a single subsystem,

- Synthesis conditions posed as a convex optimization problem in terms of LMIs,

- Guaranteed stability and upper bounds on the achievable control performance.

The synthesis techniques presented herein consequently combine the universal applicability of the approach presented in [80] with the scalability of the methods proposed by [98].

1.4 THESIS OUTLINE

THE thesis is structured as follows, cf. Fig. 1.5: After the introduction in Chap. 1, Chap. 2 continues with the presentation of the fundamental concepts in LPV theory that are relevant for both of the subsequent parts. From here the reader may continue with either Part I or Part II. Part I is dedicated to the development of methods for synthesizing LPV controllers for complex lumped systems, while Part II focuses on the distributed controller synthesis for interconnected LPV systems. Both parts start with an investigation of the current state of the art in Chap. 3 and 7, respectively, to further illustrate the focus and direction of the research presented in this thesis. The advances in both areas are to a large extent enabled by the development of improved modeling tools and new perspectives proposed in Chap. 4 and 8. The new, extended or modified representations are then exploited in the subsequent Chap. 5 and 9, where advances in the synthesis tools are presented. Before the consolidation of the results in conclusions and an outlook in Part III, application examples for both lumped systems and interconnected systems are discussed in Chap. 6 and 10.

```
┌─────────────────┐
│    Chap. 1      │
│  Introduction   │
└─────────────────┘
         │
         ▼
┌─────────────────────┐
│      Chap. 2        │
│   LPV Systems —     │
│  Representations and│
│ Controller Synthesis│
└─────────────────────┘
```

Chap. 3
Applied LPV
Control —
A Survey

Chap. 4
Compact LFT-LPV
Modeling

Chap. 5
LPV Controller
Synthesis for
Complex Systems

Chap. 6
Application
Examples

Part I
LPV Control of
Complex Lumped
Systems

Chap. 7
State of the Art

Chap. 8
A Compact
Modeling
Framework

Chap. 9
Synthesis of
Distributed LPV
Controllers

Chap. 10
Application
Examples

Part II
Control of
Interconnected
LPV Systems

Chap. 11
Summary and
Conclusions

Chap. 12
Outlook

Part III
Summary,
Conclusions and
Outlook

Figure 1.5: Outline of the thesis.

2

LPV SYSTEMS — REPRESENTATIONS AND CONTROLLER
SYNTHESIS

*≪There is nothing so practical
as a good theory.≫*

Kurt Lewin, Marrow, 1969

THIS chapter introduces the basic theory of LPV model realizations and as-
sociated synthesis techniques. Sect. 2.1 defines and reviews terminology and
methods w. r. t. general, LFT-based and affine/polytopic LPV representations.
Sect. 2.2 reviews the fundamentals of LPV system stability and performance analy-
sis by convex optimization. Sect. 2.3 illustrates the extension to well-known con-
troller synthesis methods associated with the respective types of LPV representa-
tions.

A special in-depth treatment is provided for the construction of LPV controllers
in conjunction with multiplier-based LFT-LPV controller synthesis using constant
Lyapunov functions under special consideration of structural multiplier constraints.
This material lays the groundwork for the subsequent development of synthesis
methods in

Part I, allowing for the efficient synthesis of LPV controllers that result in low
computational load during online implementation,

Part II, allowing for the efficient synthesis of distributed LPV controllers that in-
herit the interconnection topology from the interconnected system.

2.1 State Space Representations of Linear Parameter-Varying Systems

I N the following LPV model representations are reviewed in the order of increased restrictions on the type of parameter dependency. General LPV systems are introduced in Sect. 2.1.1, followed by LFT-LPV systems that allow for rational parameter dependency in Sect. 2.1.2. Affine representations are introduced in Sect. 2.1.3 and a discussion on the parameter reduction technique denoted «parameter set mapping» follows in Sect. 2.1.4.

2.1.1 General Representations

An LPV system is defined as the combination of a mathematical system representation, e. g., in state space form, and a set of admissible parameter trajectories.

Definition 2.1 (Parameter Variation Set [160])
Given a compact set $\rho \subseteq \mathbb{R}^{n_\rho}$, the parameter variation set $\mathcal{F}_\rho$ denotes a set of piecewise continuous functions mapping $\mathbb{R}^+$ into ρ with a finite number of discontinuities in any interval.

Remark 2.1 *This thesis' notation widely follows [160], s. t. $\rho(t) \in \mathcal{F}_\rho$ denotes time-varying trajectories, whereas $\rho \in \rho$ denotes a vector in a compact subset of $\mathbb{R}^{n_\rho}$.*

Definition 2.2 (General LPV System [133])
A dynamic system that can be written in the form

$$\mathcal{T}_\rho : \begin{cases} \begin{bmatrix} \dot{\mathfrak{x}} \\ z \end{bmatrix} = \begin{bmatrix} \mathcal{A}\big(\rho(t)\big) & \mathcal{B}_{\mathrm{p}}\big(\rho(t)\big) \\ \mathcal{C}_{\mathrm{p}}\big(\rho(t)\big) & \mathcal{D}_{\mathrm{pp}}\big(\rho(t)\big) \end{bmatrix} \begin{bmatrix} \mathfrak{x} \\ w \end{bmatrix} \\ \rho(t) \in \mathcal{F}_\rho, \end{cases} \tag{2.1}$$

is called a «general LPV system», where $\mathfrak{x} \in \mathbb{R}^{n_{\mathfrak{x}}}$, $w \in \mathbb{R}^{n_w}$, $z \in \mathbb{R}^{n_z}$, are the state, input and output signal vectors of the system, respectively, and the system's state space model matrix $T_\rho\big(\rho(t)\big) \in \mathcal{C}^0(\mathbb{R}^{n_\rho}, \mathbb{R}^{(n_x+n_z)\times(n_x+n_w)})$, with

$$T_\rho\big(\rho(t)\big) = \begin{bmatrix} \mathcal{A}\big(\rho(t)\big) & \mathcal{B}_{\mathrm{p}}\big(\rho(t)\big) \\ \mathcal{C}_{\mathrm{p}}\big(\rho(t)\big) & \mathcal{D}_{\mathrm{pp}}\big(\rho(t)\big) \end{bmatrix}, \tag{2.2}$$

is a continuous matrix-valued function of the parameter vector

$$T_\rho\big(\rho(t)\big) \in \mathcal{C}^0(\mathbb{R}^{n_\rho}, \mathbb{R}^{(n_x+n_z)\times(n_x+n_w)}).$$

Furthermore, continuous, measurable quantities $\rho(t)$ that range in some set of continuous admissible trajectories $\mathcal{F}_\rho$ are denoted as «scheduling signals».

The parameter vector

$$\rho(t) = \left[\rho_1(t), \rho_2(t), \ldots, \rho_{n_\rho}(t) \right]^\top \in \boldsymbol{\rho} \subseteq \mathbb{R}^{n_\rho}, \tag{2.3}$$

may be associated with bounded rates of change if the admissible trajectories are piecewise continuously differentiable. Denote the rate of change of the parameter vector

$$\dot{\rho}(t) = \sigma(t) = \left[\sigma_1(t), \sigma_2(t), \ldots, \sigma_{n_\rho}(t) \right]^\top \in \boldsymbol{\sigma} \subseteq \mathbb{R}^{n_\rho}, \tag{2.4}$$

where $\boldsymbol{\sigma}$ denotes a compact subset of the vector space $\mathbb{R}^{n_\rho}$.

Definition 2.3 (Rate-Bounded Parameter Trajectory Set [160])
The set $\mathcal{F}_\rho^\sigma$ denotes a set of admissible rate-bounded trajectories

$$\mathcal{F}_\rho^\sigma = \left\{ \rho(t) \in \mathcal{C}^1(\mathbb{R}^+, \mathbb{R}^{n_\rho}) \mid (\rho(t), \sigma(t)) \in (\boldsymbol{\rho} \times \boldsymbol{\sigma}), \ \forall t \geqslant 0 \right\}. \tag{2.5}$$

Let the input-output operator associated with $\mathcal{T}_\rho$ be denoted T_ρ. It is obtained via

$$T_\rho\big(\rho(t)\big) = \frac{1}{s} I_{n_{\mathfrak{r}}} \star T_\rho\big(\rho(t)\big) = \left[\begin{array}{c|c} \mathcal{A}\big(\rho(t)\big) & \mathcal{B}_p\big(\rho(t)\big) \\ \hline \mathcal{C}_p\big(\rho(t)\big) & \mathcal{D}_{pp}\big(\rho(t)\big) \end{array} \right] \tag{2.6}$$

The following definition is introduced to consider LPV systems with bounds on the parameters' rate of change.

Definition 2.4 (LPV System with Rate-Bounded Trajectories [160])
An LPV system $\mathcal{T}_\rho$ as defined in (2.1) associated with bounds on the parameters' rate of change is denoted

$$\mathcal{T}_\rho^\sigma \triangleq \left\{ T_\rho\big(\rho(t)\big) \mid \rho(t) \in \mathcal{F}_\rho^\sigma \right\}. \tag{2.7}$$

Remark 2.2 *Note at this point that the system $\mathcal{T}_\rho^\sigma$ may explicitly depend on $\sigma(t)$, e.g., when it represents the closed loop of an LPV system and controller, where the controller has been synthesized by methods that result in explicit dependence of the controller's system matrix on $\sigma(t)$ [3, 160].*

LPV systems can be used to represent nonlinear systems through the notion of quasi-LPV systems

Definition 2.5 (Quasi-LPV System [160])
An LPV system $\mathcal{T}_\rho$ or $\mathcal{T}_\rho^\sigma$ as from Defs. 2.2 or 2.4 is denoted a «quasi-LPV» system, if the parameters are functions of the system's endogeneous signals, such as states, inputs or outputs.

$$\rho(t) = \rho\big(t, \mathfrak{r}(t), w(t), z(t)\big). \tag{2.8}$$

Consequently, an LPV system whose parameters only depend on exogenous signals is referred to as a pure LPV system.

With

$$\underline{\rho}_i \stackrel{\triangle}{=} \min_{t \geqslant 0} \rho_i(t), \quad \overline{\rho}_i \stackrel{\triangle}{=} \max_{t \geqslant 0} \rho_i(t),$$

$$\underline{\sigma}_i \stackrel{\triangle}{=} \min_{t \geqslant 0} \sigma_i(t), \quad \overline{\sigma}_i \stackrel{\triangle}{=} \max_{t \geqslant 0} \sigma_i(t), \quad \forall i \in \{1, \dots, n_\rho\},$$

it is possible to find more explicit characterizations of the compact sets, such as hyperboxes

$$\mathrm{hyp}\,(\boldsymbol{\rho}) = \left\{ \rho(t) \;\middle|\; \underline{\rho}_i \leqslant \rho_i(t) \leqslant \overline{\rho}_i, \; \forall i \in \{1, \dots, n_\rho\} \right\} \supseteq \boldsymbol{\rho} \text{ and} \tag{2.9}$$

$$\mathrm{hyp}\,(\boldsymbol{\sigma}) = \left\{ \sigma(t) \;\middle|\; \underline{\sigma}_i \leqslant \sigma_i(t) \leqslant \overline{\sigma}_i, \; \forall i \in \{1, \dots, n_\rho\} \right\} \supseteq \boldsymbol{\sigma}. \tag{2.10}$$

Furthermore, the convex hulls conv $(\boldsymbol{\rho})$ and conv $(\boldsymbol{\sigma})$ denote the smallest convex sets containing all admissible parameter vectors. Consequently,

$$(\boldsymbol{\rho} \times \boldsymbol{\sigma}) \subseteq (\mathrm{conv}\,(\boldsymbol{\rho}) \times \mathrm{conv}\,(\boldsymbol{\sigma})) \subseteq (\mathrm{hyp}\,(\boldsymbol{\rho}) \times \mathrm{hyp}\,(\boldsymbol{\sigma})).$$

(a) General LPV plant $\mathcal{T}_\rho$.

(b) General LPV plant as an interconnection of the parameter-dependent system state space model matrix T_ρ and integrators.
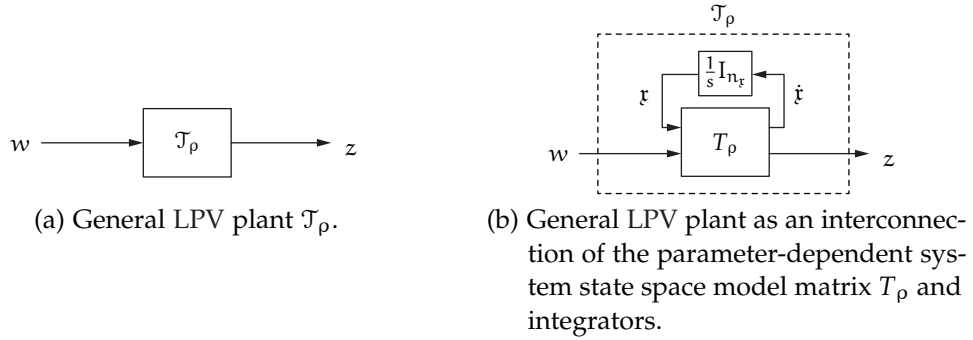
Figure 2.1: General LPV plant.

As evident from Fig. 2.1a, the symbol $\mathcal{T}_\rho$ is used in diagrams to denote the LPV system associated with the admissible set of trajectories. An LPV representation such as (2.1) is denoted *general*, since no further requirement on the parameter-dependency is imposed. The parameters are assumed to be directly measureable online and may appear in the system's state space model matrix as arguments of any arbitrary nonlinear function. More restrictive assumptions on the kind of parameter-dependency, e. g., rational dependency, facilitate the convexification of analysis and synthesis conditions by rendering tools such as the full-block $\mathcal{S}$-Procedure applicable [125]. As will be seen later, this usually comes at the expense of one or multiple of the following items:

- Increased conservatism due to overbounding [79],

- Increased synthesis complexity due to additional decision variables in LMI-based conditions [E48, 60],

- Increased modeling effort and ambiguity/non-uniqueness in LPV representations [58, 78].

While these may appear as discouraging downsides, so-called LFT-based LPV representations are able to offer significant advantages in synthesis and implementation complexity, especially when the number of parameters is large. A quantification of the incurred increase in complexity is presented in Sect. 3.1.

2.1.2 *Linear Fractional Representations*

For the purpose of rewriting an LPV system (2.1) with general dependence on the parameters $\rho(t)$ in the form of an linear fractional representation (LFR), transcendental functions are required to be covered up by newly introduced parameters. This new set of parameters will be denoted LFT *parameters* and is collected in a vector $\delta(t)$ ranging in an admissible compact set denoted $\boldsymbol{\delta} \subseteq \mathbb{R}^{n_\delta}$.

$$\delta(t) = \left[\delta_1(t), \delta_2(t), \ldots, \delta_{n_\delta}(t)\right]^\top \in \boldsymbol{\delta} \subseteq \mathbb{R}^{n_\delta}. \tag{2.11}$$

Associated bounded rates of change are denoted

$$\dot{\delta}(t) = \eta(t) = \left[\eta_1(t), \eta_2(t), \ldots, \eta_{n_\delta}(t)\right]^\top \in \boldsymbol{\eta} \subseteq \mathbb{R}^{n_\delta}, \tag{2.12}$$

where $\boldsymbol{\eta}$ denotes a set of admissible rates.

Remark 2.3 *Transcendental functions «transcend» algebra in the sense that they cannot be expressed in terms of a finite sequence of the algebraic operations of addition, multiplication and root extraction [147].*

To obtain an LFT-LPV representation from a general LPV representation, introduce the nonlinear, continuous and continuously differentiable injective mapping

$$f^{\rho \to \delta} \in \mathcal{C}^1(\boldsymbol{\rho}, \mathbb{R}^{n_\delta}), \quad \rho(t) \mapsto f^{\rho \to \delta}\big(\rho(t)\big) \triangleq \delta(t). \tag{2.13}$$

Remark 2.4 *Note that here the mapping $f^{\rho \to \delta} \in \mathcal{C}^1(\boldsymbol{\rho}, \mathbb{R}^{n_\delta})$ is only required to be continuous and continuously differentiable on the domain $\boldsymbol{\rho}$.*

The rates of the LFT parameters can be obtained via

$$\eta(t) = \dot{\delta}(t) = \frac{d\delta(\rho)}{d\rho}\dot{\rho}(t) = \frac{d}{d\rho}f^{\rho \to \delta}\big(\rho(t)\big)\sigma(t). \tag{2.14}$$

After the definition of the mapping $f^{\rho \to \delta}$, an LFR of the LPV plant is given by the following.

Definition 2.6 (LFT-LPV System Representation [5])
The model (2.1) rewritten in the form

$$
\mathcal{T}_\delta : \begin{cases} \begin{bmatrix} \dot{\mathfrak{x}} \\ p_\Delta \\ z \end{bmatrix} = \begin{bmatrix} \mathcal{A} & \mathcal{B}_\Delta & \mathcal{B}_p \\ \mathcal{C}_\Delta & \mathcal{D}_{\Delta\Delta} & \mathcal{D}_{\Delta p} \\ \mathcal{C}_p & \mathcal{D}_{p\Delta} & \mathcal{D}_{pp} \end{bmatrix} \begin{bmatrix} \mathfrak{x} \\ q_\Delta \\ w \end{bmatrix} , \\ q_\Delta = \Delta\big(\delta(t)\big) p_\Delta, \quad \delta(t) \in \mathcal{F}_\delta \end{cases} \tag{2.15}
$$

is called an «LFT-LPV system», where $q_\Delta \in \mathbb{R}^{n_{q_\Delta}}$, $p_\Delta \in \mathbb{R}^{n_{p_\Delta}}$ denote the parameter channel of the system. The parameter $\delta(t)$ is restricted to a set of admissible trajectories $\mathcal{F}_\delta$ and the parameter block $\Delta\big(\delta(t)\big)$ is a continuous matrix-valued function of the LFT parameter vector $\delta(t)$

$$
\Delta\big(\delta(t)\big) \in \mathcal{C}^0(\mathbb{R}^{n_\delta}, \mathbb{R}^{n_{q_\Delta} \times n_{p_\Delta}}).
$$

Note that due to the LFT approach, time-varying parameters and constant model matrices are separated. By defining the system's state space model matrix as

$$
T_\delta \triangleq \begin{bmatrix} \mathcal{A} & \mathcal{B}_\Delta & \mathcal{B}_p \\ \mathcal{C}_\Delta & \mathcal{D}_{\Delta\Delta} & \mathcal{D}_{\Delta p} \\ \mathcal{C}_p & \mathcal{D}_{p\Delta} & \mathcal{D}_{pp} \end{bmatrix} \tag{2.16}
$$

the input-output operator T_δ is obtained via

$$
\mathsf{T}_\delta = \frac{1}{s} I_{n_{\mathfrak{x}}} \star T_\delta = \left[\begin{array}{c|cc} \mathcal{A} & \mathcal{B}_\Delta & \mathcal{B}_p \\ \hline \mathcal{C}_\Delta & \mathcal{D}_{\Delta\Delta} & \mathcal{D}_{\Delta p} \\ \mathcal{C}_p & \mathcal{D}_{p\Delta} & \mathcal{D}_{pp} \end{array} \right] . \tag{2.17}
$$

Figures 2.2a and 2.2b illustrate the separation of constant/dynamic LTI and

(a) LFT-LPV plant as an interconnection of the LTI plant T_δ and the parameter block $\Delta(t)$.

(b) LFT-LPV plant as an interconnection of the constant system state space model matrix T_δ, integrators and the parameter block $\Delta(t)$.
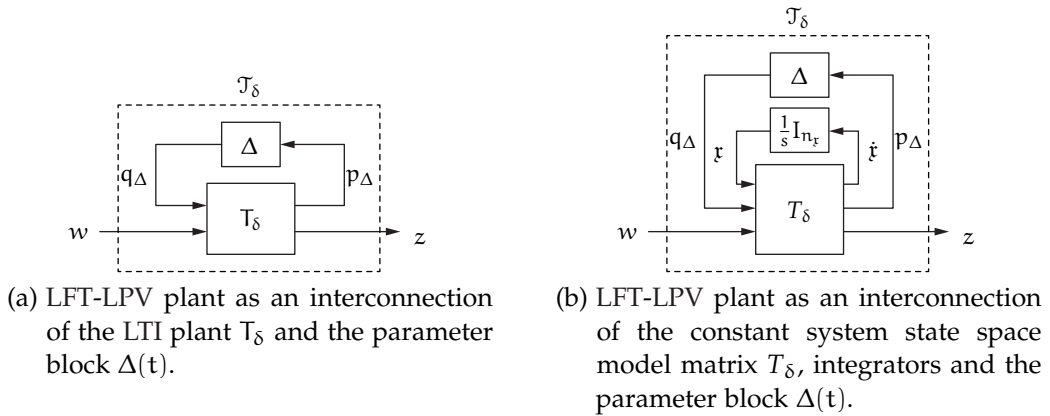
Figure 2.2: LFT-LPV plant.

parameter-dependent parameter block. The parameter-dependent input-output operator

$$\Delta\big(\delta(t)\big) \star T_\delta = \left[\begin{array}{c|c} \mathcal{A}\big(\delta(t)\big) & \mathcal{B}_p\big(\delta(t)\big) \\ \hline \mathcal{C}_p\big(\delta(t)\big) & \mathcal{D}_{pp}\big(\delta(t)\big) \end{array}\right] \tag{2.18}$$

$$= \left[\begin{array}{c|c} \mathcal{A} & \mathcal{B}_p \\ \hline \mathcal{C}_p & \mathcal{D}_{pp} \end{array}\right] + \left[\begin{array}{c} \mathcal{B}_\Delta \\ \hline \mathcal{D}_{p\Delta} \end{array}\right] \Delta\big(\delta(t)\big)\Big(I - D_{\Delta\Delta}\Delta\big(\delta(t)\big)\Big)^{-1} \left[\begin{array}{c|c} \mathcal{C}_\Delta & \mathcal{D}_{\Delta p} \end{array}\right]$$

in turn recovers the LPV representation $\mathcal{T}_\delta$, when it is associated with the set of admissible trajectories $\mathcal{F}_\delta$. The general LPV representation $\mathcal{T}_\rho$ is obtained if the LFT parameters are substituted by using the mapping $\delta(t) = f^{\rho\to\delta}\big(\rho(t)\big)$ and considering the set of admissible trajectories $\mathcal{F}_\rho$. In fact, the set of admissible trajectories $\mathcal{F}_\delta$ is derived from $\mathcal{F}_\rho$, in the sense that

$$\mathcal{F}_\delta = \Big\{\delta\big(\rho(t)\big) = f^{\rho\to\delta}\big(\rho(t)\big)\,\Big|\, \rho(t) \in \mathcal{F}_\rho\Big\}. \tag{2.19}$$

As before, the LFT-LPV system $\mathcal{T}_\delta$ as defined in (2.15) associated with bounds on the parameters' rate of change is denoted

$$\mathcal{T}_\delta^\eta \triangleq \big\{\Delta(t) \star T_\delta \mid \delta(t) \in \mathcal{F}_\delta^\eta\big\}, \tag{2.20}$$

where the set $\mathcal{F}_\delta^\eta$ is the set of admissible rate-bounded trajectories

$$\mathcal{F}_\delta^\eta = \Big\{\delta(t) \in \mathcal{C}^1(\mathbb{R}^+, \mathbb{R}^{n_\delta}) \,\Big|\, (\delta(t), \eta(t)) \in (\delta \times \eta),\ \forall t \geqslant 0\Big\}. \tag{2.21}$$

The parameter block may typically assume block-diagonal form

$$\Delta(t) = \operatorname*{diag}_{i=1}^{n_\delta}\big(\delta_i(t)I_{r_{\delta,i}}\big),$$

for which then $n_{q_\Delta} = n_{p_\Delta} = \sum_{i=1}^{n_\delta} r_{\delta,i}$. However, the techniques presented in [124, 125] allow fully populated parameter blocks, which will play a central role in this thesis. Furthermore, such representations can yield non-square parameter blocks. Throughout the thesis, it is required that the LFR is well-posed, i.e., $(I - D_{\Delta\Delta}\Delta(t))$ is invertible for all admissible parameter values.

As before, with $\underline{\delta}_i = \min_{t\geqslant 0}\delta_i(t)$, $\bar{\delta}_i = \max_{t\geqslant 0}\delta_i(t)$, $\underline{\eta}_i = \min_{t\geqslant 0}\eta_i(t)$ and $\bar{\eta}_i = \max_{t\geqslant 0}\eta_i(t)$, $\forall i \in \{1,\dots,n_\delta\}$, it is possible to find hyperboxes

$$\operatorname{hyp}(\delta) = \big\{\delta(t) \mid \underline{\delta}_i \leqslant \delta_i(t) \leqslant \bar{\delta}_i,\ \forall i \in \{1,\dots,n_\delta\}\big\} \supseteq \delta \text{ and} \tag{2.22}$$

$$\operatorname{hyp}(\eta) = \Big\{\eta(t) \,\Big|\, \underline{\eta}_i \leqslant \eta_i(t) \leqslant \bar{\eta}_i,\ \forall i \in \{1,\dots,n_\delta\}\Big\} \supseteq \eta. \tag{2.23}$$

The convex hulls $\operatorname{conv}(\delta)$ and $\operatorname{conv}(\eta)$ again denote the smallest convex sets containing all admissible trajectories of the LFT parameters, s. t.

$$(\delta \times \eta) \subseteq (\operatorname{conv}(\delta) \times \operatorname{conv}(\eta)) \subseteq (\operatorname{hyp}(\delta) \times \operatorname{hyp}(\eta)).$$

It is apparent that the compact sets δ and η are obtained by (2.13) and (2.14). Continuity on ρ and continuous differentiability of (2.13), together with the compactness of both ρ and σ guarantee the compactness of δ and η.

Definition 2.7 (Mixed General/LFT-LPV System Representation [161])
The model (2.1) rewritten in the form

$$
\mathcal{T}^{\sigma,\eta}_{\rho,\delta} : \begin{cases} \begin{bmatrix} \dot{\mathfrak{r}} \\ p_\Delta \\ z \end{bmatrix} = \begin{bmatrix} \mathcal{A}\big(\rho(t)\big) & \mathcal{B}_\Delta\big(\rho(t)\big) & \mathcal{B}_p\big(\rho(t)\big) \\ \mathcal{C}_\Delta\big(\rho(t)\big) & \mathcal{D}_{\Delta\Delta}\big(\rho(t)\big) & \mathcal{D}_{\Delta p}\big(\rho(t)\big) \\ \mathcal{C}_p\big(\rho(t)\big) & \mathcal{D}_{p\Delta}\big(\rho(t)\big) & \mathcal{D}_{pp}\big(\rho(t)\big) \end{bmatrix} \begin{bmatrix} \mathfrak{r} \\ q_\Delta \\ w \end{bmatrix}, \\[4ex] q_\Delta = \Delta\big(\delta(t)\big)p_\Delta, \quad \delta(t) \in \mathcal{F}^\eta_\delta, \quad \rho(t) \in \mathcal{F}^\sigma_\rho \end{cases}
\tag{2.24}
$$

is called a «Mixed General/LFT-LPV system», where $q_\Delta \in \mathbb{R}^{n_{q_\Delta}}$, $p_\Delta \in \mathbb{R}^{n_{p_\Delta}}$ denote the LFT parameter channel of the system defining rational dependence on the parameter $\delta(t)$ via the continuous matrix-valued function

$$
\Delta\big(\delta(t)\big) \in \mathcal{C}^0(\mathbb{R}^{n_\delta}, \mathbb{R}^{n_{q_\Delta} \times n_{p_\Delta}}).
$$

The parameter $\delta(t)$ is restricted to the rate-bounded set of admissible trajectories $\mathcal{F}^\eta_\delta$ and is assumed to be disjoint from the parameter $\rho(t)$, which in turn is restricted to rate-bounded set of admissible trajectories $\mathcal{F}^\sigma_\rho$.

Definitions of state space system matrix and input-output operator follow from analogy.

2.1.3 *Affine/Polytopic Representations*

A special case of LFT-LPV representations are systems, which are affinely dependent on the parameters. For the purpose of rewriting an LFT-LPV system (2.15) in the form of an LFR with affine parameter-dependence, again new parameters need to be introduced to cover rational functions. This new set of parameters will be denoted *affine parameters* and is collected in a vector $\theta(t)$ ranging in an admissible set denoted $\theta \subseteq \mathbb{R}^{n_\theta}$.

$$
\theta(t) = \Big[\theta_1(t), \theta_2(t), \dots, \theta_{n_\theta}(t)\Big]^\top \in \theta \subseteq \mathbb{R}^{n_\theta}.
\tag{2.25}
$$

Associated bounded rates of change are denoted

$$
\dot{\theta}(t) = \nu(t) = \Big[\nu_1(t), \nu_2(t), \dots, \nu_{n_\theta}(t)\Big]^\top \in \boldsymbol{\nu} \subseteq \mathbb{R}^{n_\theta},
\tag{2.26}
$$

where $\boldsymbol{\nu}$ denotes a set of admissible rates.

To obtain an affine LPV representation from an LFT-LPV representation, introduce the nonlinear, continuous and continuously differentiable injective mapping from δ to $\mathbb{R}^{n_\theta}$

$$
f^{\delta\to\theta} \in \mathcal{C}^1(\delta, \mathbb{R}^{n_\theta}), \quad \delta(t) \mapsto f^{\delta\to\theta}\big(\delta(t)\big) \overset{\triangle}{=} \theta(t).
\tag{2.27}
$$

Consider the derivation of affine parameters as a concatenation of the mappings $f^{\rho\to\delta}$ and $f^{\delta\to\theta}$, s. t.

$$f^{\rho\to\theta} = \left(f^{\delta\to\theta} \circ f^{\rho\to\delta}\right) \in \mathcal{C}^2(\boldsymbol{\rho}, \mathbb{R}^{n_\theta}),$$

$$\rho(t) \mapsto f^{\rho\to\theta}\big(\rho(t)\big) = f^{\delta\to\theta}\left(f^{\rho\to\delta}\big(\rho(t)\big)\right) \stackrel{\triangle}{=} \theta(t). \tag{2.28}$$

The rates of the affine parameters can be obtained via

$$\nu(t) = \dot{\theta}(t) = \frac{d\theta(\delta)}{d\delta}\dot{\delta}(t) = \frac{d\theta(\delta)}{d\delta}\frac{d\delta(\rho)}{d\rho}\eta(t). \tag{2.29}$$

Again, the mapping $f^{\delta\to\theta}$ is not unique but always injective.

Denote an LFT-LPV plant with affine parameter-dependency by

$$\mathcal{T}_\theta : \begin{cases} \begin{bmatrix} \dot{\mathfrak{x}} \\ p_\Theta \\ z \end{bmatrix} = \begin{bmatrix} \mathcal{A} & \mathcal{B}_\Theta & \mathcal{B}_p \\ \hline \mathcal{C}_\Theta & 0 & \mathcal{D}_{\Theta p} \\ \mathcal{C}_p & \mathcal{D}_{p\Theta} & \mathcal{D}_{pp} \end{bmatrix} \begin{bmatrix} \mathfrak{x} \\ q_\Theta \\ w \end{bmatrix}, \\ q_\Theta = \Theta\big(\theta(t)\big)p_\Theta, \quad \theta(t) \in \mathcal{F}_\theta \end{cases} \tag{2.30}$$

where $q_\Theta \in \mathbb{R}^{n_{q_\Theta}}$, $p_\Theta \in \mathbb{R}^{n_{p_\Theta}}$ denote the modified parameter channels of the system and $\mathcal{F}_\theta$ represents the set of admissible trajectories. Note that the affine nature of the plant is evident from $D_{\Theta\Theta} = 0$.

As before, $\Theta(t)$ is a continuous matrix-valued function of the affine parameter vector $\theta(t)$, $\Theta\big(\theta(t)\big) \in \mathcal{C}^0(\theta, \mathbb{R}^{n_{q_\Theta} \times n_{p_\Theta}})$, and may typically assume diagonal form

$$\Theta\big(\theta(t)\big) = \operatorname*{diag}_{i=1}^{n_\theta}\big(\theta_i(t)I_{r_{\theta,i}}\big), \tag{2.31}$$

for which then $n_\Theta = \sum_{i=1}^{n_\theta} r_{\theta,i}$. Again, full parameter blocks can be considered, but in the light of a reduced implementation complexity, the diagonal structure is advantageous, [57]. Define symbols T_θ and T_θ associated with the system's state space model matrix and input-output operator as before, respectively. The parameter-dependent input-output operator

$$\Theta(t) \star \mathsf{T}_\theta = \begin{bmatrix} \mathcal{A}\big(\theta(t)\big) & \mathcal{B}_p\big(\theta(t)\big) \\ \hline \mathcal{C}_p\big(\theta(t)\big) & \mathcal{D}_{pp}\big(\theta(t)\big) \end{bmatrix} \tag{2.32}$$

eventually recovers the LPV representation $\mathcal{T}_\theta$, when it is associated with the set of admissible trajectories $\mathcal{F}_\theta$. The general LPV representation $\mathcal{T}_\rho$ is obtained if the parameters are substituted by using the mapping $\theta(t) = f^{\rho\to\theta}\big(\rho(t)\big)$ and considering the set of admissible trajectories $\mathcal{F}_\delta$. The affine LPV system $\mathcal{T}_\theta$ as defined in (2.30) associated with bounds on the affine parameters' rate of change is denoted

$$\mathcal{T}_\theta^\gamma \stackrel{\triangle}{=} \big\{\Theta\big(\theta(t)\big) \star \mathsf{T}_\theta \mid \theta(t) \in \mathcal{F}_\theta^\gamma\big\}, \tag{2.33}$$

where the set $\mathcal{F}_\theta^\gamma$ is the set of admissible rate-bounded trajectories

$$\mathcal{F}_\theta^\gamma = \left\{ \theta(t) \in \mathcal{C}^1(\mathbb{R}^+, \mathbb{R}^{n_\theta}) \;\middle|\; (\theta(t), \nu(t)) \in (\boldsymbol{\theta} \times \boldsymbol{\nu}), \; \forall t \geqslant 0 \right\}. \tag{2.34}$$

With the extreme values $\underline{\theta}_i = \min_{t \geqslant 0} \theta_i(t)$, $\overline{\theta}_i = \max_{t \geqslant 0} \theta_i(t)$, $\underline{\nu}_i = \min_{t \geqslant 0} \nu_i(t)$ and $\overline{\nu}_i = \max_{t \geqslant 0} \nu_i(t)$, $\forall i \in \{1, \ldots, n_\theta\}$, it is possible to find hyperboxes

$$\text{hyp}(\boldsymbol{\theta}) = \left\{ \theta(t) \;\middle|\; \underline{\theta}_i \leqslant \theta_i(t) \leqslant \overline{\theta}_i, \; \forall i \in \{1, \ldots, n_\theta\} \right\} \supseteq \boldsymbol{\theta} \text{ and} \tag{2.35}$$

$$\text{hyp}(\boldsymbol{\nu}) = \left\{ \nu(t) \mid \underline{\nu}_i \leqslant \nu_i(t) \leqslant \overline{\nu}_i, \; \forall i \in \{1, \ldots, n_\theta\} \right\} \supseteq \boldsymbol{\nu}. \tag{2.36}$$

The convex hulls $\text{conv}(\boldsymbol{\theta})$ and $\text{conv}(\boldsymbol{\nu})$ again denote the smallest convex sets containing all admissible trajectories of the LFT parameters, s.t.

$$(\boldsymbol{\theta} \times \boldsymbol{\nu}) \subseteq (\text{conv}(\boldsymbol{\theta}) \times \text{conv}(\boldsymbol{\nu})) \subseteq (\text{hyp}(\boldsymbol{\theta}) \times \text{hyp}(\boldsymbol{\nu})).$$

Analogously to (2.32), the parameter-dependent state space model matrix $T_\rho(\rho(t)) = \Theta(t) \star T_\theta$ can be computed. An alternative exists in representing this state space model matrix as an affine function of the parameters $\theta_i(t)$

$$\begin{bmatrix} \mathcal{A}(\theta(t)) & \mathcal{B}_\mathrm{P}(\theta(t)) \\ \hline \mathcal{C}_\mathrm{P}(\theta(t)) & \mathcal{D}_\mathrm{PP}(\theta(t)) \end{bmatrix} = \begin{bmatrix} \mathcal{A}_0 & \mathcal{B}_{\mathrm{P},0} \\ \hline \mathcal{C}_{\mathrm{P},0} & \mathcal{D}_{\mathrm{PP},0} \end{bmatrix} + \sum_{i=1}^{n_\theta} \theta_i(t) \begin{bmatrix} \mathcal{A}_i & \mathcal{B}_{\mathrm{P},i} \\ \hline \mathcal{C}_{\mathrm{P},i} & \mathcal{D}_{\mathrm{PP},i} \end{bmatrix}.$$

From this affine decomposition, a matrix polytope can be constructed from a finite number n_v of «vertex matrices». Each admissible state space model matrix can be constructed from a weighted sum of these vertex matrices by deriving the barycentric coordinates α_l, $\forall l \in \{1, \ldots, n_v\}$ from the corresponding polytope in the parameter vectors $\theta(t)$. For this purpose, let $\theta_{v,l}$, $\forall l \in \{1, \ldots, n_v\}$, denote the vertices spanning the polytope in the parameter range, i.e., the convex hull $\text{conv}(\boldsymbol{\theta})$, s.t.

$$\text{conv}(\boldsymbol{\theta}) = \text{conv}(\theta_{v,l}, \; l \in \{1, \ldots, n_v\})$$

$$\triangleq \left\{ \sum_{l=1}^{n_v} \alpha_l \theta_{v,l} \;\middle|\; \alpha_l \geqslant 0, \; \sum_{l=1}^{n_v} \alpha_l = 1 \right\}. \tag{2.37}$$

Denote the corresponding matrix polytope by

$$\text{conv}(S_l, \; l \in \{1, \ldots, n_v\}) \triangleq \left\{ \sum_{l=1}^{n_v} \alpha_l S_l \;\middle|\; \alpha_l \geqslant 0, \; \sum_{l=1}^{n_v} \alpha_l = 1 \right\}. \tag{2.38}$$

$$\text{where } S_l = \begin{bmatrix} \mathcal{A}(\theta(t)) & \mathcal{B}_\mathrm{P}(\theta(t)) \\ \hline \mathcal{C}_\mathrm{P}(\theta(t)) & \mathcal{D}_\mathrm{PP}(\theta(t)) \end{bmatrix} \Bigg|_{\theta(t)=\theta_{v,l}} \tag{2.39}$$

Note that the parameter signal vectors $\rho_{v,l}$ that map into the parameter vertices $\theta_{v,l}$ via

$$\theta_{v,l} = f^{\rho \to \theta}(\rho_{v,l}), \quad l \in \{1, \ldots, n_v\},$$

do not necessarily belong to the admissible range ρ, since the vertices are required to form a convex region in terms of θ, whereas neither ρ nor θ are required to denote convex sets. This results in so-called «overbounding» [79].

A formula for determining the barycentric coordinates $\alpha_l, \forall l \in \{1, \ldots, n_v\}$ for a parameter vector $\theta(t)$ ranging in a simple polytope is given in [158], detailed in App. A.6 on p. 324.

2.1.4 *Parameter Set Mapping*

LPV controller synthesis may prove intractable in face of a large number of parameters or excessive overbounding. A systematic, but heuristic technique to approximate any given set of parameters by a set containing fewer parameters has been proposed [79] and is generally denoted PSM. Since the method is based on a principle component analysis (PCA), it also provides the option to change the coordinate base of the parameters without approximation. The technique has so far been applied to affine LPV models, e.g., [E36, E37, E44, E45, 57, E46, E60, 76, 110], and will be developed here in this venue.

The objective of PSM is to find a linear (approximating) mapping

$$f^{\theta \to \phi} \in \mathcal{C}^1(\theta, \mathbb{R}^{n_\phi}), \quad \theta(t) \mapsto f^{\theta \to \phi}(\theta(t)) \triangleq \phi(t). \tag{2.40}$$

that maps the plant's parameter vector $\theta(t) \in \mathbb{R}^{n_\theta}$ into a (reduced) parameter vector $\phi(t) \in \mathbb{R}^{n_\phi}$, $n_\phi \leqslant n_\theta$. In [E60, 79], normalization of the parameters θ is assumed, s.t. $|\theta_i| \leqslant 1$, $i \in \{1, \ldots, n_\theta\}$ and the parameters have zero mean w.r.t. the data on which PCA is performed.

More specifically, the linear map can be written as

$$\phi(t) = U_N U \theta(t), \quad U \in \mathbb{R}^{n_\phi \times n_\theta}, \quad UU^\top = I. \tag{2.41}$$

$$\text{where with } U = [u_{ij}], \ U_N = \operatorname*{diag}_{i=1}^{n_\phi} \left(\Big(\sum_{j=1}^{n_\theta} |u_{ij}| \Big)^{-1} \right)$$

is used for normalizing the new parameter set, s.t. $|\phi_i| \leqslant 1$, $i \in \{1, \ldots, n_\phi\}$. Since the mapping is static, one may easily obtain compact sets for the new parameter set and it's rate of variation

$$\phi(t) = \left[\phi_1(t), \phi_2(t), \ldots, \phi_{n_\phi}(t) \right]^\top \in \boldsymbol{\phi} \subseteq \mathbb{R}^{n_\phi}, \tag{2.42}$$

$$\dot{\phi}(t) = \psi(t) = \left[\psi_1(t), \psi_2(t), \ldots, \psi_{n_\phi}(t) \right]^\top \in \boldsymbol{\psi} \subseteq \mathbb{R}^{n_\phi}. \tag{2.43}$$

If the matrix U has been obtained, the original parameters $\theta(t)$ can be substituted for via

$$\hat{\theta}(t) = U^\top U_N^{-1} \phi(t), \tag{2.44}$$

which allows to rewrite (approximate) the LPV system (2.30) with the input-output operator

$$
\begin{aligned}
T_\phi\big(\phi(t)\big) &= \left[\begin{array}{c|c} \mathcal{A}\big(\phi(t)\big) & \mathcal{B}_p\big(\phi(t)\big) \\ \hline \mathcal{C}_p\big(\phi(t)\big) & \mathcal{D}_{pp}\big(\phi(t)\big) \end{array}\right] \\
&= \left[\begin{array}{c|c} \mathcal{A}_0 & \mathcal{B}_{p,0} \\ \hline \mathcal{C}_{p,0} & \mathcal{D}_{pp,0} \end{array}\right] + \sum_{j=1}^{n_\phi} \phi_j(t) \left[\begin{array}{c|c} \hat{\mathcal{A}}_j & \hat{\mathcal{B}}_{p,j} \\ \hline \hat{\mathcal{C}}_{p,j} & \hat{\mathcal{D}}_{pp,j} \end{array}\right].
\end{aligned}
$$

2.1.4.1 *Obtaining the Mapping by Principle Component Analysis*

In order to obtain the projection U, a data matrix Ξ is constructed, containing horizontally concatenated sampled parameter vectors θ. In [79], it is proposed to obtain the parameter vector samples by recording experimental trajectories, which limits the applicability to stable plants or unstable plants stabilized by some preliminary controller. In the second case, such a controller needs to be able to operate the plant in all relevant operating conditions, a requirement that may in some cases only be fulfilled by a suitable nonlinear controller to begin with.

An alternative is presented in [57], which relies on sampled parameter vectors obtained from a gridding of the set of admissible trajectories $\mathcal{F}_\rho$ of measurable signals that comprise the general LPV parameters. A more pragmatic, but possible conservative way exists in gridding the compact set of admissible parameter vectors ρ instead.

The data matrix is therefore constructed from the finite set of parameter vector samples $\rho^{(1)}, \ldots, \rho^{(n_d)}$ covering the operating range:

$$
\Xi = \begin{bmatrix} \theta\big(\rho^{(1)}\big) & \ldots & \theta\big(\rho^{(n_d)}\big) \end{bmatrix}. \tag{2.45}
$$

If ρ ranges in a hyperbox, the number of samples from gridding each parameter ρ_i, $i \in \{1, \ldots, n_\rho\}$, over n_g evenly spaced grid points is $n_d = n_g^{n_\rho}$. A singular value decomposition of the data matrix

$$
\Xi = \begin{bmatrix} U_\phi & U_\theta \end{bmatrix} \begin{bmatrix} \Sigma_\phi & 0 & 0 \\ 0 & \Sigma_\theta & 0 \end{bmatrix} \begin{bmatrix} V_\phi^\top \\ V_\theta^\top \\ V_0^\top \end{bmatrix}, \tag{2.46}
$$

yields $U = \begin{bmatrix} U_\phi & U_\theta \end{bmatrix}^\top$, if no approximation is desired and $U = U_\phi^\top$, if an approximation is sought that represents the given data well enough based on the significant singular values in Σ_ϕ. In such a case the corresponding data matrix in terms of samples of the new parameters ϕ is $\Xi_\phi = \Sigma_\phi V_\phi^\top$.

2.1.4.2 *The Effect on the Order of Linear Fractional Representations*

Denote the corresponding (approximated) LPV plant in LFR form by

$$
\mathcal{T}_{\phi}^{\psi} : \begin{cases} \begin{bmatrix} \dot{x} \\ \hline p_{\Phi} \\ z \end{bmatrix} = \begin{bmatrix} \mathcal{A} & \mathcal{B}_{\Phi} & \mathcal{B}_{p} \\ \hline \mathcal{C}_{\Phi} & 0 & \mathcal{D}_{\Phi p} \\ \mathcal{C}_{p} & \mathcal{D}_{p\Phi} & \mathcal{D}_{pp} \end{bmatrix} \begin{bmatrix} x \\ \hline q_{\Phi} \\ w \end{bmatrix}, \\ q_{\Phi} = \Phi(t) p_{\Phi}. \quad \phi(t) \in \mathcal{F}_{\phi}^{\psi} \end{cases}
\tag{2.47}
$$

While the affine representation of the input-output operator is reduced in complexity, since the summation goes from 1 to $n_{\phi} \leqslant n_{\theta}$, the size of the LFT parameter block $\Phi(\phi(t)) \in \mathcal{C}^{0}(\mathbb{R}^{n_{\phi}}, \mathbb{R}^{n_{\Phi} \times n_{\Phi}})$, in diagonal form

$$
\Phi(t) = \underset{i=1}{\overset{n_{\phi}}{\operatorname{diag}}} \left(\phi_{i}(t) I_{r_{\phi,i}} \right),
$$

—hence the order of the LFR—is increased, s. t. $n_{\Phi} \geqslant n_{\Theta}$. To see this, first note that for affine parameter-dependence the minimum order of an LFR results from the rank of the matrix coefficients [166]. The increase in order due to PSM ensues from the fact that for each $\hat{\theta}_{i}(t)$ that is substituted from (2.48) by

$$
\hat{\theta}_{i}(t) = \sum_{j=1}^{n_{\phi}} u_{ji} u_{N,j}^{-1} \phi_{j}(t),
\tag{2.48}
$$

a linear combination of matrices each of rank $I_{r_{\theta,i}}$ is turned into

$$
\begin{aligned}
\sum_{i=1}^{n_{\theta}} \theta_{i}(t) \begin{bmatrix} \mathcal{A}_{i} & \mathcal{B}_{p,i} \\ \hline \mathcal{C}_{p,i} & \mathcal{D}_{pp,i} \end{bmatrix} &= \sum_{i=1}^{n_{\theta}} \sum_{j=1}^{n_{\phi}} u_{ji} u_{N,j}^{-1} \phi_{j}(t) \begin{bmatrix} \mathcal{A}_{i} & \mathcal{B}_{p,i} \\ \hline \mathcal{C}_{p,i} & \mathcal{D}_{pp,i} \end{bmatrix} \\
&= \sum_{j=1}^{n_{\phi}} \phi_{j}(t) \sum_{i=1}^{n_{\theta}} u_{ji} u_{N,j}^{-1} \begin{bmatrix} \mathcal{A}_{i} & \mathcal{B}_{p,i} \\ \hline \mathcal{C}_{p,i} & \mathcal{D}_{pp,i} \end{bmatrix} \\
&= \sum_{j=1}^{n_{\phi}} \phi_{j}(t) \begin{bmatrix} \hat{\mathcal{A}}_{j} & \hat{\mathcal{B}}_{p,j} \\ \hline \hat{\mathcal{C}}_{p,j} & \hat{\mathcal{D}}_{pp,j} \end{bmatrix},
\end{aligned}
\tag{2.49}
$$

where now the rank of the new matrices in (2.49) is given by

$$
\min_{i \in \{1,\ldots,n_{\theta}\}} r_{\theta,i} \leqslant \operatorname{rank}\left(\begin{bmatrix} \hat{\mathcal{A}}_{j} & \hat{\mathcal{B}}_{p,j} \\ \hline \hat{\mathcal{C}}_{p,j} & \hat{\mathcal{D}}_{pp,j} \end{bmatrix} \right) = r_{\phi,j} \leqslant n_{\theta},
$$

because in general $u_{ji} \neq 0$. This simple insight illustrates that LFT-LPV synthesis based on LPV plants approximated via PSM can in fact become more complex.

A simple trick to prevent such an increase in the size of the parameter block follows from the observation that many entries u_{ij} are in fact very close to zero. By letting for some small $\varepsilon \ll 1$

$$
u_{ij} = \begin{cases} u_{ij} & , \; |u_{ij}| > \varepsilon \\ 0 & , \; |u_{ij}| < \varepsilon \end{cases}, \quad (i,j) \in (\{1,\ldots,n_{\phi}\} \times \{1,\ldots,n_{\theta}\}),
$$

the numerical rank of the matrices in (2.49) is usually significantly reduced, s.t. $n_\Phi \leqslant n_\Theta$. The additional approximation error incurred by this procedure can be easily checked and is usually small [E45].

2.2 Analysis of Linear Parameter-Varying Systems

In this section, the necessary tools for stability and performance analysis of LPV systems are reviewed. Sects. 2.2.1 and 2.2.2 develop the notions of Lyapunov stability as well as the induced $\mathcal{L}_2$-norm as stability and performance frameworks, respectively. Sect. 2.2.3 is devoted to the full-block $\mathcal{S}$-Procedure (FBSP) as a tool to render parameter-dependent matrix inequalities solvable by a finite number of LMIs. Eventually, Sect. 2.2.4 presents analysis results for the stability and performance of LPV systems that can be verified by semi-definite programs (SDPs).

2.2.1 *Stability Analysis of LPV Systems*

For LPV systems the locations of the poles of the LTI systems obtained by freezing the parameter values do not provide a conclusive statement about the stability of the LPV system [4]. Lyapunov arguments are therefore employed to obtain sufficient conditions for the stability of LPV systems. Since LPV representations can be used to define nonlinear and/or time-varying system behaviour, speaking of «stability» as a system property require justifying assumptions. First, consider a general parameter-dependent, autonomous, nonlinear and time-varying system

$$\begin{cases} \dot{\mathfrak{x}}(t) & = f\big(t, \mathfrak{x}(t), \rho(t)\big), \\ y(t) & = h\big(t, \mathfrak{x}(t), \rho(t)\big), \\ \text{with} \quad 0 = f\big(t, \bar{\mathfrak{x}}, \rho(t)\big), \ \bar{y} = h\big(t, \bar{\mathfrak{x}}, \rho(t)\big), \ \forall t \in \mathbb{R}^+. \end{cases} \tag{2.50}$$

with the nonlinear functions $f\big(t, \mathfrak{x}(t), \rho(t)\big) \in \mathcal{C}^0\big(\mathbb{R}^+ \times \mathbb{R}^{n_{\mathfrak{x}}} \times \boldsymbol{\rho}, \ \mathbb{R}^{n_{\mathfrak{x}}}\big)$ as well as $h\big(t, \mathfrak{x}(t), \rho(t)\big) \in \mathcal{C}^0\big(\mathbb{R}^+ \times \mathbb{R}^{n_{\mathfrak{x}}} \times \boldsymbol{\rho}, \ \mathbb{R}^{n_y}\big)$.

Remark 2.5 *Explicit dependence on time in (2.50) could as well be absorbed in the parameter $\rho(t)$. Further, even in equilibrium $\rho(t)$ may be time-varying, if it does not affect the state equilibrium.*

Definition 2.8 (Stability [156])
An equilibrium $\bar{\mathfrak{x}}$ of system (2.50) is stable if for every $\varepsilon_i > 0$ there exists an $\varepsilon_o(\varepsilon_i) > 0$, s. t.,

$$\|\mathfrak{x}(0) - \bar{\mathfrak{x}}\| < \varepsilon_i \quad \Longrightarrow \quad \|\mathfrak{x}(t) - \bar{\mathfrak{x}}\| < \varepsilon_o, \quad \forall t \in \mathbb{R}^+.$$

Definition 2.9 (Attractiveness [156])
An equilibrium $\bar{\mathfrak{x}}$ of system (2.50) is attractive if there exists an $\varepsilon_i > 0$, s. t.,

$$\|\mathfrak{x}(0) - \bar{\mathfrak{x}}\| < \varepsilon_i \quad \Longrightarrow \quad \lim_{t \to \infty} \mathfrak{x}(t) = \bar{\mathfrak{x}}.$$

Definition 2.10 (Asymptotic Stability [156])
An equilibrium $\bar{\mathfrak{x}}$ of system (2.50) is asymptotically stable if it is both stable and attractive.

Figures 2.3a and 2.3b illustrate these stability concepts. Note that an intuitive description of trajectories of asymptotically stable equilibria can be given by curves that

- converge to the equilibrium, and

- stay within a certain distance of the equilibrium before.

(a) Definition of stability.　　(b) Definition of attractiveness.
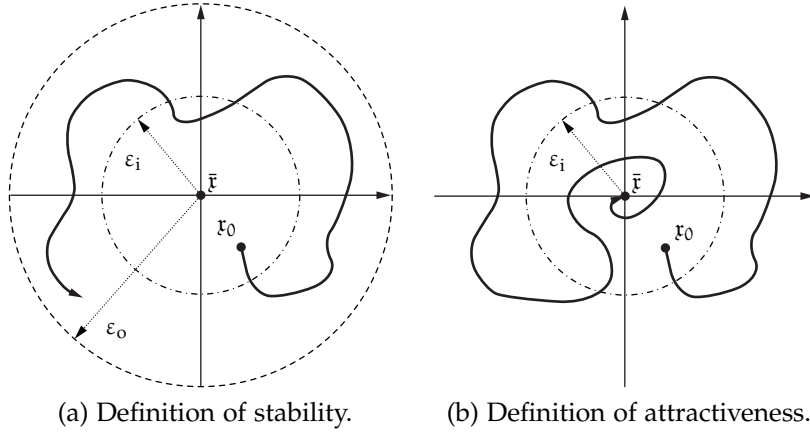
Figure 2.3: Definitions of stability and attractiveness [156].

Definition 2.11 (Derivative of a Function Along a Trajectory [156])
Let $V\big(t, \mathfrak{x}(t), \rho(t)\big) \in \mathcal{C}^1\big(\left(\mathbb{R}^+ \times \mathbb{R}^{n_{\mathfrak{x}}} \times \boldsymbol{\rho}\right), \mathbb{R}\big)$. *Then*

$$\partial \mathcal{V}\big(t, \mathfrak{x}(t), \rho(t), \dot{\rho}(t)\big) \stackrel{\triangle}{=} \frac{\partial V(\cdot)}{\partial t} + \frac{\partial V(\cdot)}{\partial \mathfrak{x}(t)} f\big(t, \mathfrak{x}(t), \rho(t)\big) + \frac{\partial V(\cdot)}{\partial \rho(t)} \dot{\rho}(t)$$

is called the «derivative of V along the trajectories of (2.50)». As a short-hand notation $\dot{\mathcal{V}}\big(t, \mathfrak{x}(t), \rho(t)\big) = \partial \mathcal{V}\big(t, \mathfrak{x}(t), \rho(t), \dot{\rho}(t)\big)$ *is often used.*

Let the equilibrium state $\bar{\mathfrak{x}}$, w. l. o. g., be the origin, $\bar{\mathfrak{x}} = 0$. The following is a preliminary result for the convenient characterization of stability of LPV systems by matrix inequalities.

Theorem 2.1 (Lyapunov Stability [156])
Consider system (2.50). The equilibrium $\bar{\mathfrak{x}}$ *is stable, if there exists a function* $V\big(t, \mathfrak{x}(t), \rho(t)\big) \in \mathcal{C}^1\big(\left(\mathbb{R}^+ \times \mathbb{R}^{n_{\mathfrak{x}}} \times \boldsymbol{\rho}\right), \mathbb{R}\big)$ *and a constant* r, *s. t.,* $\forall t \in \mathbb{R}^+$

$$V\big(t, \mathfrak{x}(t), \rho(t)\big) > 0, \quad \forall \mathfrak{x} \neq 0$$

and

$$\dot{V}\big(t, \mathfrak{x}(t), \rho(t)\big) \leqslant 0, \quad \forall \mathfrak{x} \in \mathcal{B}_r \stackrel{\triangle}{=} \{\mathfrak{x} \in \mathbb{R}^{n_{\mathfrak{x}}} \mid \|\mathfrak{x}\| < r\}.$$

The equilibrium is asymptotically stable, if

$$\dot{V}\big(t, \mathfrak{x}(t), \rho(t)\big) < 0, \quad \forall \mathfrak{x} \in \mathcal{B}_r \backslash \{0\} \triangleq \{\mathfrak{x} \in \mathbb{R}^{n_{\mathfrak{x}}} \mid \|\mathfrak{x}\| < r, \ \mathfrak{x} \neq 0\}.$$

$\square$

Theorem 2.1 provides only a sufficient condition in general, but can be shown to be also necessary for LTI systems [156]. Furthermore, it is a local result, in the sense that a positive constant r is required, s. t. the conditions of Thm. 2.1 are satisfied in a ball with radius r. For LTI systems global (asymptotic) stability coincides with local (asymptotic) stability of the origin and one can take the limit $\lim_{r \to \infty} \mathcal{B}_r = \mathbb{R}^{n_{\mathfrak{x}}}$.

When considering the LPV system $\mathcal{T}_\rho$ as defined in (2.1), with $w(t) = 0$, in the case that $\mathcal{A}\big(\rho(t)\big)$ is non-singular for all times, $\bar{\mathfrak{x}} = 0$ is the only possible equilibrium. By making this assumption in the following, stability will be referred to as a property of an LPV system, even though for nonlinear systems, stability is in general not a system property, rather than the property of a trajectory or point in state space.

Parameter-dependent quadratic Lyapunov functions are employed to arrive at the well-known result for parameter-dependent asymptotic stability of the LPV system $\mathcal{T}_\rho^\sigma$ *over* $\rho \times \sigma$.

Definition 2.12 (Parameter-Dependent Quadratic Lyapunov Function)
A function $V : (\mathbb{R}^{n_{\mathfrak{x}}} \times \rho) \mapsto \mathbb{R}$

$$V\big(\mathfrak{x}(t), \rho(t)\big) = \mathfrak{x}(t)^\top \mathcal{X}\big(\rho(t)\big)\mathfrak{x}(t), \quad \forall \rho \in \rho$$

with the «Lyapunov matrix» $\mathcal{X}\big(\rho(t)\big) \in \mathcal{C}^1(\rho, \mathcal{S}^{n_{\mathfrak{x}}})$, $\mathcal{X}\big(\rho(t)\big) \succ 0$ *is called a «parameter-dependent quadratic Lyapunov function».*

First introduce the definition of the derivative of $\mathcal{X}\big(\rho(t)\big)$ along the trajectories of (2.1) by defining the function $\partial \mathcal{X} : (\rho \times \sigma) \mapsto \mathcal{S}^{n_{\mathfrak{x}}}$

$$\partial \mathcal{X}\big(\rho(t), \sigma(t)\big) \triangleq \frac{\partial \mathcal{X}\big(\rho(t)\big)}{\partial \rho(t)}\sigma(t) = \sum_{i=1}^{n_\rho} \frac{\partial \mathcal{X}\big(\rho(t)\big)}{\partial \rho_i(t)}\sigma_i(t)$$

Remark 2.6 *It can be shown that the conditions of Thm. 2.2 in fact guarantee exponential stability [E19], i.e., with a small value $\varepsilon > 0$ and $\alpha I \preccurlyeq \mathcal{X} \preccurlyeq \beta I$ one can show that $\|\mathfrak{x}\|^2 \leqslant \frac{\beta}{\alpha}e^{-\frac{\varepsilon}{\beta}t}\|\mathfrak{x}_0\|^2$, where $\mathfrak{x}_0 = \mathfrak{x}(0)$.*

Theorem 2.2 (Parameter-Dependent Stability of LPV Systems [160])
The system $\mathcal{T}_\rho^\sigma$ as defined in (2.1), with $w(t) = 0$, $\forall t \geqslant 0$, is asymptotically stable over $\rho \times \sigma$ if there exists $\mathcal{X}(\rho) \in \mathcal{C}^1(\rho, \mathcal{S}^{n_{\mathfrak{x}}})$, $\mathcal{X}(\rho) \succ 0$, s. t.

$$\begin{bmatrix} \bullet \\ \bullet \end{bmatrix}^\top \begin{bmatrix} \partial \mathcal{X}(\rho, \sigma) & \mathcal{X}(\rho) \\ \mathcal{X}(\rho) & 0 \end{bmatrix} \begin{bmatrix} I \\ \mathcal{A}(\rho) \end{bmatrix} \prec 0, \quad \forall (\rho, \sigma) \in (\rho \times \sigma) \tag{2.51}$$

$\square$

Proof: Consider the parameter-dependent quadratic Lyapunov function $V : (\mathbb{R}^{n_{\mathfrak{x}}} \times \boldsymbol{\rho}) \mapsto \mathbb{R}$

$$V(\mathfrak{x}, \rho) = \mathfrak{x}^\top \mathcal{X}(\rho)\mathfrak{x} \geqslant 0, \quad \forall \rho \in \boldsymbol{\rho}$$

Considering this along solutions of the system $\mathcal{T}_\rho$, one may write

$$\dot{V}(\mathfrak{x}(t), \rho(t)) = \begin{bmatrix} \bullet \\ \bullet \end{bmatrix}^\top \begin{bmatrix} \dot{\mathcal{X}}(\rho(t)) & \mathcal{X}(\rho(t)) \\ \mathcal{X}(\rho(t)) & 0 \end{bmatrix} \begin{bmatrix} \mathfrak{x}(t) \\ \dot{\mathfrak{x}}(t) \end{bmatrix} < 0 \qquad (2.52)$$

Observe that along solution trajectories $\dot{\mathcal{X}}(\rho(t)) = \partial\mathcal{X}(\rho(t), \sigma(t))$, as well as $\dot{\mathfrak{x}}(t) = \mathcal{A}(\rho(t))\mathfrak{x}(t)$, s. t., by Def. 2.11 this yields

$$\dot{V}(\mathfrak{x}(t), \rho(t)) = \mathfrak{x}(t)^\top \begin{bmatrix} \bullet \\ \bullet \end{bmatrix}^\top \begin{bmatrix} \partial\mathcal{X}(\rho(t), \sigma(t)) & \mathcal{X}(\rho(t)) \\ \mathcal{X}(\rho(t)) & 0 \end{bmatrix} \begin{bmatrix} I \\ \mathcal{A}(\rho(t)) \end{bmatrix} \mathfrak{x}(t) < 0,$$

$$= \mathfrak{x}^\top \left(\mathcal{X}(\rho)\mathcal{A}(\rho)^\top + \mathcal{A}(\rho)\mathcal{X}(\rho) + \partial\mathcal{X}(\rho, \sigma) \right) \mathfrak{x}.$$

From here, observe that $\dot{V}(\mathfrak{x}(t), \rho(t)) < 0$, $\forall \mathfrak{x}(t) \in \mathbb{R}^{n_{\mathfrak{x}}}$, $\mathfrak{x}(t) \neq 0$, if (2.51) holds. $\blacksquare$

Another notion of stability often encountered in the context of LPV systems is the notion of «quadratic stability» [17].

Theorem 2.3 (Quadratic Stability of LPV Systems [17, 160])
The system $\mathcal{T}_\rho$ as defined in (2.1), with $w(t) = 0$, $\forall t \geqslant 0$, is asymptotically stable over $\boldsymbol{\rho}$ if there exists $\mathcal{X} \in \mathbb{S}^{n_{\mathfrak{x}}}$, $\mathcal{X} \succ 0$, s. t.

$$\begin{bmatrix} \bullet \\ \bullet \end{bmatrix}^\top \begin{bmatrix} 0 & \mathcal{X} \\ \mathcal{X} & 0 \end{bmatrix} \begin{bmatrix} I \\ \mathcal{A}(\rho) \end{bmatrix} \prec 0, \quad \forall \rho \in \boldsymbol{\rho} \qquad (2.53)$$

$\square$

The test for quadratic stability in Thm. 2.3 is not only recovered by considering a constant quadratic Lyapunov function $V(\mathfrak{x}) = \mathfrak{x}^\top \mathcal{X}\mathfrak{x}$ in the first place, but also follows quite naturally, if the parameters $\rho(t)$ are allowed to vary arbitrarily fast, i. e., $\boldsymbol{\sigma} = \mathbb{R}^{n_\rho}$. In this case $\partial\mathcal{X}(\rho, \sigma)$ can become unbounded and (2.51) can only be satisfied, if $\mathcal{X}(\rho(t)) \stackrel{\triangle}{=} \mathcal{X}$ is chosen independent of ρ, i. e., $\mathcal{X} \in \mathbb{S}^{n_{\mathfrak{x}}}$. Then $\partial\mathcal{X}(\rho, \sigma) = 0$, since $\partial\mathcal{X}(\rho(t))/\partial\rho(t) = 0$. If the parameters $\rho(t)$ are assumed constant, however, the Lyapunov matrix can still be parameter-dependent and $\partial\mathcal{X}(\rho, \sigma)$ in (2.51) simply vanishes due to $\boldsymbol{\sigma} = \{0\}$.

Remark 2.7 *The term «quadratic stability» somewhat arbitrarily draws from the fact that it is derived based on a quadratic and constant Lyapunov function $V(\mathfrak{x}) = \mathfrak{x}^\top \mathcal{X}\mathfrak{x}$. In some literature, e. g., [17], this is in fact used as its definition, which allows to coin (2.53) a* necessary and sufficient *condition for quadratic stability.*

The above arguments can be drawn upon for each individual parameter $\rho_i(t)$, $i \in \{1, \ldots, n_\rho\}$, s.t. single parameters can be allowed to vary arbitrarily fast or be constant, while the rate of change of others is constrained by known bounds [E19].

For Q-LPV systems, i.e., when the parameters are functions of endogeneous signals $\mathfrak{x}(t)$, $w(t)$ or $z(t)$, the Lyapunov stability conditions are again local conditions in the sense that statements about stability only hold true within bounds on the state $\mathfrak{x}(t)$ that imply $(\rho(\cdot), \sigma(\cdot)) \in (\boldsymbol{\rho} \times \boldsymbol{\sigma})$.

Remark 2.8 *A mixture between constant, switching or smoothly time-varying parameters occurs naturally in the context of the control of interconnected LPV systems. Such scenarios are considered in Part II of the thesis.*

2.2.2 The Induced $\mathcal{L}_2$-Norm as a Performance Measure

The following definitions are introduced to facilitate the introduction of the induced $\mathcal{L}_2$-system norm as a performance measure in LPV system analysis and controller synthesis.

Definition 2.13 (Vector Norm)
For a vector $z = \begin{bmatrix} z_1, z_2, \ldots, z_n \end{bmatrix} \in \mathbb{R}^n$, $z_i \in \mathbb{R}$, $\forall i \in \{1, \ldots, n\}$, the p-norm, $p \in \mathbb{N}$ is defined as

$$\|z\|_p \triangleq \left(\sum_{i=1}^{n} |z_i|^p \right)^{\frac{1}{p}}.$$

The Euclidean *norm is obtained for $p = 2$ and denoted as*

$$\|z\| = \sqrt{z^\top z}.$$

Remark 2.9 *The superscript attached to the $\mathcal{L}_2$-signal spaces, denoting the dimension of the vector valued signals, is often omitted if clear from the context.*

In this thesis, the primary performance specification considered will be in terms of the induced $\mathcal{L}_2$-gain, as system norm induced by the $\mathcal{L}_2$-signal norm.

Definition 2.14 ($\mathcal{L}_2$-Signal Norm [160])
For a signal $z(t) : \mathbb{R}^+ \mapsto \mathbb{R}^n$, the $\mathcal{L}_2$-norm is defined as

$$\|z(t)\|_2 \triangleq \sqrt{\int_0^\infty z^\top(\tau) z(\tau) d\tau}.$$

Definition 2.15 ($\mathcal{L}_2$-Signal Space [160])
A signal $z(t) : \mathbb{R}^+ \mapsto \mathbb{R}^n$ is said to be in the space $\mathcal{L}_2^n$, i.e., $z(t) \in \mathcal{L}_2^n$, if $\|z(t)\|_2$ is finite. The space $\mathcal{L}_2^n$ is therefore defined as

$$\mathcal{L}_2^n \triangleq \left\{ z(t) : \mathbb{R}^+ \mapsto \mathbb{R}^n \mid \|z(t)\|_2 < \infty \right\}.$$

Definition 2.16 (Induced $\mathcal{L}_2$-System Norm [112, 125, 160])
For a parameter-dependent stable system $\mathcal{T}_\rho^\sigma : \mathcal{L}_2 \mapsto \mathcal{L}_2$ as defined in (2.1) with zero initial condition $\mathfrak{x}(0) = 0$ and with input $w(t)$ and output $z(t)$, the induced $\mathcal{L}_2$-norm is defined as

$$\left\| \mathcal{T}_\rho^\sigma \right\|_{\mathcal{L}_2} \triangleq \sup_{\rho(t) \in \mathcal{F}_\rho^\sigma} \sup_{w(t) \neq 0,\ w(t) \in \mathcal{L}_2} \frac{\|z(t)\|_2}{\|w(t)\|_2}.$$

A condition for an upper bound on the induced $\mathcal{L}_2$-system norm $\|\mathcal{T}_\rho\|_{\mathcal{L}_2} < \gamma$ is a special case of a more general constraint on the input and output signals in the form of an integral quadratic constraint (IQC) [3, 104, 112].

$$\lim_{T \to \infty} \int_0^T \begin{bmatrix} w(t) \\ z(t) \end{bmatrix}^\top \begin{bmatrix} Q_p & S_p \\ S_p^\top & R_p \end{bmatrix} \begin{bmatrix} w(t) \\ z(t) \end{bmatrix} dt \leqslant 0 \tag{2.54}$$

For the special choice

$$\Gamma = \begin{bmatrix} Q_p & S_p \\ S_p^\top & R_p \end{bmatrix} = \begin{bmatrix} -\gamma I & 0 \\ 0 & \gamma^{-1} I \end{bmatrix} \tag{2.55}$$

one arrives at the relation $\|z(t)\|_2^2 \leqslant \gamma^2 \|w(t)\|_2^2$.

Remark 2.10 *The induced $\mathcal{L}_2$-system norm reduces to the $\mathcal{H}_\infty$-system norm, if the system $\mathcal{T}_\rho = \mathcal{T}$ denotes an LTI system. The $\mathcal{H}_\infty$-norm can then be defined by $\|\mathcal{T}\|_\infty \triangleq \sup_{\omega \in \mathbb{R}} \overline{\sigma}(\mathcal{T}(j\omega))$.*

2.2.3 *The Full-Block $\mathcal{S}$-Procedure*

Both parameter-dependent stability and performance criteria can be combined into a single condition. For this purpose, the full-block $\mathcal{S}$-Procedure is first introduced as a tool to combine various conditions. It is then specialized for later application on matrix inequalities with outer blocks that depend rationally on parameters.

In the theorem stated below and interpretations following a behavioral approach, the family of subspaces $\mathcal{W}(\rho) \subseteq \mathbb{R}^n$ is the system with signals ζ, from which $V(\rho) \in \mathcal{C}^0(\boldsymbol{\rho}, \mathbb{S}^{q \times n})$ selects interconnection variables that are constrained to reside in $\mathcal{S}(\rho)$. Continuous parameterizations are given in terms of $\rho \in \boldsymbol{\rho}$. The resulting «perturbed» system is denoted $\mathcal{B}(\rho)$. Further $U \in \mathbb{R}^{p \times n}$ and $Q(\rho) \in \mathcal{C}^0(\boldsymbol{\rho}, \mathbb{S}^p)$ are used to form an implicit negativity condition that is supposed to hold *on* $\mathcal{B}(\rho)$, i.e., for all perturbations of $\mathcal{W}(\rho)$ [123].

Theorem 2.4 (Full-Block $\mathcal{S}$-Procedure [125])
Let the family of subspaces $\mathcal{W}(\rho) \subseteq \mathbb{R}^n$ depend continuously on $\rho \in \boldsymbol{\rho}$, where $\boldsymbol{\rho}$ is a compact set. Let further $U \in \mathbb{R}^{p \times n}$, $V(\rho) \in \mathcal{C}^0(\boldsymbol{\rho}, \mathbb{S}^{q \times n})$ and $Q(\rho) \in \mathcal{C}^0(\boldsymbol{\rho}, \mathbb{S}^p)$. Define

$$\mathcal{B}(\rho) \triangleq \{\zeta \in \mathcal{W}(\rho) \mid V(\rho)\zeta \in \mathcal{S}(\rho)\}.$$

(i) *The condition*

$$U^\top Q(\rho) U \prec 0 \quad on \quad \mathcal{B}(\rho), \quad \forall \rho \in \boldsymbol{\rho} \tag{2.56}$$

holds iff there exists a multiplier M *with*

$$M \succcurlyeq 0 \quad on \quad \mathcal{S}(\rho), \quad \forall \rho \in \boldsymbol{\rho} \tag{2.57}$$

which satisfies

$$U^\top Q(\rho) U + V(\rho)^\top M V(\rho) \prec 0 \quad on \quad \mathcal{W}(\rho), \quad \forall \rho \in \boldsymbol{\rho}. \tag{2.58}$$

(ii) *Suppose there exists a subspace* $\mathcal{W}_0(\rho)$ *with*

$$U^\top Q(\rho) U \succcurlyeq 0 \quad on \quad \mathcal{W}_0(\rho) \subset \mathcal{W}(\rho) \tag{2.59}$$

and $\dim(V\mathcal{W}_0)(\rho) + \dim(\mathcal{S}(\rho)) \geqslant q$. *Then Conds. (2.57) and (2.58) imply*

$$V\mathcal{W}_0(\rho) \oplus \mathcal{S}(\rho) = \mathbb{R}^q \quad \forall \rho \in \boldsymbol{\rho} \tag{2.60}$$

$\square$

Proof: The theorem and its proof are presented in full detail in [125] for the case that $Q \in \mathbb{S}^p$, $V \in \mathbb{R}^{q \times n}$ are constant and $\mathcal{W}(\rho)$ and consequently $\mathcal{W}_0(\rho)$ denote fixed subspaces, rather than families of subspaces parameterized by ρ. However, the statements hold in full analogy and only item (i) is proved again:

(i) First show that Conds. (2.57) and (2.58) imply Cond. (2.56). For this purpose choose any $\zeta \in \mathcal{B}(\rho)$ with $\zeta \neq 0$. Since $\zeta \in \mathcal{W}(\rho)$ conclude from (2.58)

$$\zeta^\top U^\top Q(\rho) U \zeta < -\zeta^\top V(\rho)^\top M V(\rho) \zeta \quad \forall \rho \in \boldsymbol{\rho}.$$

Due to $V(\rho)\zeta \in \mathcal{S}(\rho)$, one has

$$M \succcurlyeq 0 \quad on \quad \mathcal{S}(\rho) \iff \zeta^\top V(\rho)^\top M V(\rho) \zeta \geqslant 0, \quad \forall \rho \in \boldsymbol{\rho},$$

from which it follows that

$$\zeta^\top U^\top Q(\rho) U \zeta < 0 \quad \forall \rho \in \boldsymbol{\rho}.$$

$\blacksquare$

It may seem counter-intuitive that the full-block $\mathcal{S}$-Procedure is presented here with possibly parameter-dependent $Q(\rho) \in \mathcal{C}^0(\boldsymbol{\rho}, \mathbb{S}^p)$, $V(\rho) \in \mathcal{C}^0(\boldsymbol{\rho}, \mathbb{R}^{q \times n})$ and the family of subspaces $\mathcal{W}(\rho) \subseteq \mathbb{R}^n$, as it is widely used with the main purpose of turning a parameter-dependent inequality (2.56) into a parameter-independent inequality and an inequality with more easily tractable parameter-dependency on the multiplier. As will be seen later, the additional parameter-dependency is introduced to facilitate a formal and unified view on the full-block $\mathcal{S}$-Procedure as a

tool to combine multiple constraints on a system's signals. This is illustrated by the derivation of the well-known Bounded Real Lemma.

Furthermore, it might be desired to carry over only some of the parameters in ρ to the «multiplier condition» (2.57), while others remain in the «nominal condition» (2.58). For this purpose, partition $\rho = \begin{bmatrix} \rho_1^\top, & \rho_2^\top \end{bmatrix}^\top$ with $\rho_1 \in \boldsymbol{\rho}_1$, $\rho_2 \in \boldsymbol{\rho}_2$ and consider, e.g., $Q(\rho_1)$, $\mathcal{W}(\rho_1)$, $V(\rho_1)$ and $\mathcal{S}(\rho_2)$, in order to require Cond. (2.57) to hold $\forall \rho_1 \in \boldsymbol{\rho}_1$ and Cond. (2.58) $\forall \rho_2 \in \boldsymbol{\rho}_2$. Different schemes, e.g., gridding the parameter range or the introduction of further multipliers, can then be employed individually to test the conditions.

An alternative representation of the space $\mathcal{B}(\rho)$ is found in the theorem's proof in [125] as well as in [124, 163]:

$$\mathcal{B}(\rho) \triangleq \left\{ \zeta \in \mathcal{W}(\rho) \mid V(\rho)\zeta \in \ker\!\big(\mathcal{S}^\perp(\rho)\big) \right\},$$

where «ker» denotes the Kernel and $\mathcal{S}^\perp(\rho) = I - \Pi_\mathcal{S}(\rho)$ denotes the complementary space of $\mathcal{S}(\rho)$, since $\Pi_\mathcal{S}(\rho)$ in turn denotes the orthogonal projector onto $\mathcal{S}(\rho)$. The basic difference in the representation thus resides in whether an implicit description of a constraint is available that relates signals to remain in an *image* or *kernel space*. This is precisely the difference in approaches Scherer on the one hand and Iwasaki et al. on the other hand took in their work [66, 125].

The full-block $\mathcal{S}$-Procedure can be specialized and compactly presented for linear fractional parameter dependency. In the following lemma, the separation of parameters into some that are supposed to remain in the nominal condition and others that only carry over to the multiplier condition is made explicit. This result has been employed in, e.g., [161, 163].

Lemma 2.1 (Full-Block $\mathcal{S}$-Procedure for LFRs [163])
Given parameters ρ and δ, each confined to a compact set, i.e., $\rho \in \boldsymbol{\rho}$ and $\delta \in \boldsymbol{\delta}$. The quadratic matrix inequality

$$B(\rho,\delta)^\top Q(\rho) B(\rho,\delta) \prec 0, \quad \forall\, (\rho,\delta) \in (\boldsymbol{\rho} \times \boldsymbol{\delta}) \tag{2.61}$$

with $Q(\rho) \in \mathcal{C}^0(\boldsymbol{\rho}, \mathbb{S}^p)$ and

$$B(\rho,\delta) = \Delta(\delta) \star \begin{bmatrix} W_{11}(\rho) & W_{12}(\rho) \\ W_{21}(\rho) & W_{22}(\rho) \end{bmatrix}, \quad \Delta(\delta) : \mathbb{R}^{n_\delta} \mapsto \mathbb{R} \tag{2.62}$$

holds iffthere exists a multiplier M, s.t.

$$\begin{bmatrix} \bullet \\ \bullet \end{bmatrix}^\top \begin{bmatrix} M & 0 \\ 0 & Q(\rho) \end{bmatrix} \begin{bmatrix} W_{11}(\rho) & W_{12}(\rho) \\ I & 0 \\ W_{21}(\rho) & W_{22}(\rho) \end{bmatrix} \prec 0, \quad \forall \rho \in \boldsymbol{\rho} \tag{2.63}$$

$$\begin{bmatrix} \bullet \\ \bullet \end{bmatrix}^\top M \begin{bmatrix} I \\ \Delta(\delta) \end{bmatrix} \succcurlyeq 0, \quad \forall \delta \in \boldsymbol{\delta}. \tag{2.64}$$

□

Proof: In analogy to Thm. 2.4 define

$$U = \begin{bmatrix} 0 & 0 & I \end{bmatrix}, \quad \zeta \triangleq \begin{bmatrix} p \\ q \\ w \end{bmatrix}, \quad V = \begin{bmatrix} I & 0 & 0 \\ 0 & I & 0 \end{bmatrix},$$

$$\mathcal{W}(\rho) \triangleq \operatorname{im}\left(\begin{bmatrix} W_{11}(\rho) & W_{12}(\rho) \\ I & 0 \\ W_{21}(\rho) & W_{22}(\rho) \end{bmatrix} \right), \quad S(\delta) \triangleq \operatorname{im}\left(\begin{bmatrix} I \\ \Delta(\delta) \end{bmatrix} \right),$$

s.t. the image

$$\operatorname{im}\left(\mathcal{B}(\rho, \delta) \right) = W_{22}(\rho) + W_{21}(\rho)\Delta(\delta)\left(I - W_{11}(\rho)\Delta(\delta) \right)^{-1} W_{12}(\rho),$$

$\delta \in \boldsymbol{\delta}$ can simply be represented by

$$\operatorname{im}\left(\mathcal{B}(\rho, \delta) \right) = B(\rho, \delta) : \begin{cases} \begin{bmatrix} p \\ z \end{bmatrix} = \begin{bmatrix} W_{11}(\rho) & W_{12}(\rho) \\ W_{21}(\rho) & W_{22}(\rho) \end{bmatrix} \begin{bmatrix} q \\ w \end{bmatrix}, \rho \in \boldsymbol{\rho} \\ q = \Delta(\delta)p, \quad \delta \in \boldsymbol{\delta} \end{cases}$$

as illustrated in Fig. 2.4. Straightforward substitution into (2.58) results in Conds. (2.63) and (2.64). ∎
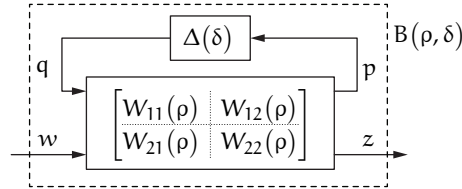
Figure 2.4: LFR of $B(\rho, \delta)$.

As a predecessor, the normal S-Procedure (SP) [17] fulfills virtually the same purpose as the FBSP with the drawback that conservatism is incurred, since only a single scalar multiplier is introduced per additional quadratic constraint.

Theorem 2.5 (S-Procedure [17])
Let $Q_0, Q_1, \ldots, Q_p$ be quadratic functions in the variable $\zeta \in \mathbb{R}^n$,

$$Q_i(\zeta) \triangleq \zeta^\top W_i \zeta + 2w_i^\top \zeta + v_i, \quad i \in \{0, \ldots, p\},$$

where $W_i \in S^n$. Then

$$Q_0(\zeta) \leqslant 0 \quad for \quad \zeta \in \mathcal{B} \triangleq \{\zeta \in \mathbb{R}^n \mid Q_i(\zeta) \leqslant 0, \, i \in \{0, \ldots, p\}\}, \tag{2.65}$$

holds if there exist $m_i \geqslant 0$, $i \in \{0, \dots, p\}$, *s. t.*

$$Q_0(\zeta) - \sum_{i=1}^{p} m_i Q_i(\zeta) \leqslant 0 \quad for \quad \zeta \in \mathbb{R}^n. \tag{2.66}$$

If $p = 1$, *Cond.* (2.66) *implies* (2.65), *provided that there exists some* ζ_0 *that satisfies the strict inequality* $Q_1(\zeta_0) < 0$. □

Proof: The proof can be found in [4]. ∎

The FBSP will prove to be a central tool in this thesis. Its usefulness in convexifying parameter-dependent linear matrix inequalitiess (PDLMIs) with complex parameter-dependency will be used to render complex synthesis and analysis problems tractable. The generality of the FBSP approach over the normal SP further allows to trade complexity in solving SDPs versus conservatism, by the imposition of structural constraints on the multipliers.

2.2.4 *Stability and Performance Analysis*

2.2.4.1 *The Parameter-Dependent Bounded Real Lemma*

The parameter-dependent Bounded Real Lemma (PDBRL) presents the main tool for LPV system analysis and controller synthesis. It is the origin of extending well-known LTI system analysis and synthesis methods to the parameter-dependent case. In the following, a formal derivation via the FBSP and dualization will be reviewed, followed by a discussion on the major obstacles in solving the LPV system analysis problem by convex optimization. This establishes the primary tools necessary to advance to the synthesis of LPV controllers.

Theorem 2.6 (PDBRL [E19, 160])
The system $\mathcal{T}_\rho^\sigma$ *as defined in* (2.7), *is asymptotically stable over* $\rho \times \sigma$ *and has an induced* $\mathcal{L}_2$-*norm bounded from above by* γ *if there exist a positive definite, symmetric matrix* $\mathcal{X}(\rho) \in \mathcal{C}^1(\rho, \mathbb{S}^{n_f})$, $\mathcal{X}(\rho) \succ 0$ *and* $\gamma > 0$ *that satisfy*

$$\begin{bmatrix} \bullet \\ \bullet \end{bmatrix}^\top \begin{bmatrix} \partial \mathcal{X}(\rho, \sigma) & \mathcal{X}(\rho) & \\ \mathcal{X}(\rho) & 0 & \\ \hline & & \Gamma \end{bmatrix} \begin{bmatrix} I & 0 \\ \mathcal{A}(\rho) & \mathcal{B}_p(\rho) \\ \hline 0 & I \\ \mathcal{C}_p(\rho) & \mathcal{D}_{pp}(\rho) \end{bmatrix} \prec 0, \ \forall\, (\rho, \sigma) \in (\rho \times \sigma) \tag{2.67}$$

□

Proof: It is the aim to combine the Conds. (2.52) , (2.54), i.e., more specifically using (2.55). Classically, performance constraints are considered in the context of robust stability analysis and small gain arguments [166]. For this purpose consider Fig. 2.5 as the uncertainty interconnection, where $\gamma \in \delta \overset{\triangle}{=} \mathbb{R}^+$, s. t. $\|\Delta_p\|_2 \leqslant \gamma^{-1}$ and $w(t) = \Delta_p z(t)$. Using the bound on the uncertainty, observe that

$$w(t)^\top w(t) = z(t)^\top \Delta_p^\top \Delta_p z(t) \leqslant \gamma^{-2} z(t)^\top z(t).$$

Such an inequality lends itself for direct use with the $\mathcal{S}$-Procedure, but here it is desired to investigate how the full-block $\mathcal{S}$-Procedure can be applied.
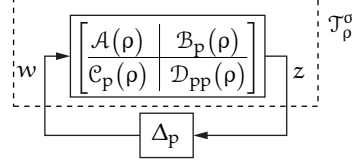
Figure 2.5: Uncertainty representation for performance.

Therefore, take

$$
U = \begin{bmatrix} I & 0 & 0 & 0 \\ 0 & I & 0 & 0 \end{bmatrix}, \quad \zeta \triangleq \begin{bmatrix} \mathfrak{x} \\ \dot{\mathfrak{x}} \\ w \\ z \end{bmatrix}, \quad V = \begin{bmatrix} 0 & 0 & I & 0 \\ 0 & 0 & 0 & I \end{bmatrix},
$$

$$
\mathcal{W}(\rho) \triangleq \mathrm{im}\left(\begin{bmatrix} I & 0 \\ \mathcal{A}(\rho) & \mathcal{B}_{\mathrm{P}}(\rho) \\ 0 & I \\ \mathcal{C}_{\mathrm{P}}(\rho) & \mathcal{D}_{\mathrm{PP}}(\rho) \end{bmatrix} \right), \quad \mathcal{S}(\delta) \triangleq \mathcal{S}(\gamma) = \mathrm{im}\left(\begin{bmatrix} \Delta_{\mathrm{P}} \\ I \end{bmatrix} \right),
$$

$$
Q(\rho) \triangleq \begin{bmatrix} \partial \mathcal{X}(\rho, \sigma) & \mathcal{X}(\rho) \\ \mathcal{X}(\rho) & 0 \end{bmatrix},
$$

s. t. by the full-block $\mathcal{S}$-Procedure for Conds. (2.52) and (2.55) to hold it is required that

$$
\begin{bmatrix} \bullet \\ \bullet \end{bmatrix}^\top M \begin{bmatrix} \Delta_{\mathrm{P}} \\ I \end{bmatrix} \succcurlyeq 0 \quad \forall \gamma \in \delta \tag{2.68}
$$

which satisfies

$$
\begin{bmatrix} \bullet \\ \bullet \end{bmatrix}^\top Q(\rho) \begin{bmatrix} I & 0 \\ \mathcal{A}(\rho) & \mathcal{B}_{\mathrm{P}}(\rho) \end{bmatrix} + \begin{bmatrix} \bullet \\ \bullet \end{bmatrix}^\top M \begin{bmatrix} 0 & I \\ \mathcal{C}_{\mathrm{P}}(\rho) & \mathcal{D}_{\mathrm{PP}}(\rho) \end{bmatrix} \prec 0 \quad \forall \rho \in \boldsymbol{\rho}. \tag{2.69}
$$

Observe now that a particular (parameter-dependent) choice for M that always guarantees (2.68) is $M = \Gamma = \mathrm{diag}\left(-\gamma I, \gamma^{-1} I \right)$, which also satisfies condition (2.55). ■

Remark 2.11 *How to prove the* PDBRL *based on inductive* trajectory arguments *is shown in, e. g., [E19, E83]. A constructive proof for the parameter-independent case is given in [112] based on* Finsler's Lemma *and the* $\mathcal{S}$-Procedure.

A dual version of the Bounded Real Lemma can be obtained by applying Lma. A.6, respectively, Lma. A.7—both on page 321— on Cond. (2.67). This concept of duality is essential to the derivation of convex controller synthesis methods,

in which the controller parameters are first eliminated from both primal and dual LMI formulations. Dualization of matrix inequalities quadratic in nature, as those shown above, appears a purely «mechanical» exercise. This is the motivation for representing LMIs in this way, rather than in expanded form, which is—in turn—more suitable for applying the Schur complement. The following theorem presents the dualized Bounded Real Lemma.

Theorem 2.7 (Dual PDBRL [E19])

The system $\mathcal{T}_\rho^\sigma$ as defined in (2.7), is asymptotically stable over $\boldsymbol{\rho} \times \boldsymbol{\sigma}$ and has an induced $\mathcal{L}_2$-norm bounded from above by γ if there exist a positive definite, symmetric matrix $\mathcal{Y}(\rho) \in \mathcal{C}^1(\boldsymbol{\rho}, S^{n_x})$, $\mathcal{Y}(\rho) \succ 0$ and $\gamma > 0$ that satisfy

$$\begin{bmatrix} \bullet \\ \bullet \end{bmatrix}^\top \left[\begin{array}{cc:c} 0 & \mathcal{Y}(\rho) & \\ \mathcal{Y}(\rho) & \partial\mathcal{Y}(\rho,\sigma) & \\ \hdashline & & \Gamma^{-1} \end{array}\right] \left[\begin{array}{cc} -\mathcal{A}^\top(\rho) & -\mathcal{C}_p^\top(\rho) \\ \hdashline I & 0 \\ \hdashline -\mathcal{B}_p^\top(\rho) & -\mathcal{D}_{pp}^\top(\rho) \\ 0 & I \end{array}\right] \succ 0,$$

$$\forall (\rho, \sigma) \in (\boldsymbol{\rho} \times \boldsymbol{\sigma}) \qquad (2.70)$$

□

Proof: The proof follows from direct application of Lma. A.7 on page 321 and by defining $\mathcal{Y}(\rho) \triangleq \mathcal{X}^{-1}(\rho)$. A useful technicality to observe—due to Eq. (A.1) given on p. 315 in the appendix—exists in

$$\begin{bmatrix} \partial\mathcal{X}(\rho,\sigma) & \mathcal{X}(\rho) \\ \mathcal{X}(\rho) & 0 \end{bmatrix} \begin{bmatrix} 0 & \mathcal{Y}(\rho) \\ \mathcal{Y}(\rho) & \partial\mathcal{Y}(\rho,\sigma) \end{bmatrix} = \begin{bmatrix} I & 0 \\ 0 & I \end{bmatrix}. \qquad (2.71)$$

■

2.2.4.2 *Solving the Analysis Condition*

Obtaining a solution to the PDBRL and therefore proving both asymptotic stability and an upper bound on the induced $\mathcal{L}_2$-gain of system $\mathcal{T}_\rho^\sigma$ essentially requires to minimize the performance index γ subject to finding a matrix-valued positive definite function $\mathcal{X}(\rho) \succ 0$. Thus, when considering «LPV system analysis», it is formally referred to the following problem definition.

Problem 2.1 (LPV System Analysis)

To certify asymptotic stability and an upper bound γ on the performance channel $w \to z$ of the LPV system $\mathcal{T}_\rho^\sigma$ solve

$$\min_{\mathcal{X}(\rho) \succ 0} \gamma \quad subject\ to \quad (2.67). \qquad (2.72)$$

□

In order to efficiently solve Prob. 2.1, remedies for the following obstacles have to be found.

LYAPUNOV MATRIX ANSATZ

The Lyapunov matrix may have an arbitrary dependence on the parameter ρ. Since the analysis condition is only sufficient, no statement about the system's stability can be made, if a particular Ansatz does not lead to a feasible solution to the matrix inequality.

CONVEXIFICATION

Condition (2.67) has to be evaluated on infinitely many points in the parameter range. A heuristic approach exists in evaluating a sufficiently dense grid over ρ. Since $\partial \mathcal{X}(\rho, \sigma)$ is affine in σ, it suffices to check only extremal values of the parameters' rate of change.

SIGMONIAL INEQUALITY

Condition (2.67) is a «sigmonial» matrix inequality in γ. A simple Schur complement would be required to render it affine. However, the choice $\Gamma = \text{diag}(-\gamma^2 I, I)$ fulfills the performance IQC, as well. The sigmonial choice will prove useful in the projection-based controller synthesis approach explained in Sect. 2.3.

As will be seen later, the Ansatz for the Lyapunov matrix has a great impact on the complexity of the semi-definite programming problem to be solved. Some systematic approaches have been presented in [E19, 65]. However, to the best of the author's knowledge, their suitability is based on simple heuristics, such as mimicking the plant's parameter-dependency.

In order to be able to convexly solve Cond. (2.67), methods based on the different LPV modeling paradigms

(a) general LPV representations,

(b) LFT-LPV representations,

(c) affine/polytopic representations,

as well as a mixture of the above have been devised.

While general LPV representations usually prescribe the application of gridding, affine LPV representations can yield matrix inequalities that can be solved in the vertices of the parameter ranges. The associated techniques are explained in more detail in Sect. 2.3, where the synthesis approaches are considered. A detailed approach for a convexification of the analysis condition (2.67) based on the FBSP is presented next, which can be applied if LFRs of both system matrices and a quadratic Lyapunov matrix Ansatz are considered. The more general result obtained analogously to [163] using a PDLF is presented first.

Theorem 2.8 (PDBRL w/ Multipliers, PDLF [E46, 163])

The system $\mathfrak{T}_\delta^\eta$ as defined in (2.20), is asymptotically stable over $\delta \times \eta$ and has an induced $\mathcal{L}_2$-norm from $w \to z$ bounded from above by γ if for a quadratic function

$$\mathfrak{X}(\delta) = \mathfrak{Q}(\delta)^\top \mathfrak{X} \mathfrak{Q}(\delta) \in \mathcal{C}^1(\delta, \mathbb{S}^{n_{\mathfrak{x}}}), \quad \mathfrak{X}(\delta) \succ 0 \; \forall \delta \in \delta,$$

$$\text{with} \quad \mathfrak{Q}(\delta) = \Delta_\mathfrak{Q}(\delta) \star \begin{bmatrix} \mathfrak{Q}_{11} & \mathfrak{Q}_{12} \\ \hline \mathfrak{Q}_{21} & \mathfrak{Q}_{22} \end{bmatrix} \in \mathcal{C}^1(\delta, \mathbb{R}^{n_{\mathfrak{x}} \times n_{\mathfrak{x}}})$$

there exist $\mathfrak{X} = \mathfrak{X}^\top \in \mathbb{S}^{n_{\mathfrak{x}}}$, $\mathfrak{M} = \mathfrak{M}^\top$, $\mathfrak{N} = \mathfrak{N}^\top$ and $\gamma > 0$ that satisfy

$$\begin{bmatrix} \bullet \\ \bullet \end{bmatrix}^\top \begin{bmatrix} \mathfrak{M} & & \\ & 0 & \mathfrak{X} \\ & \mathfrak{X} & 0 \\ & & \Gamma \end{bmatrix} \begin{bmatrix} \mathcal{B}_{11} & \mathcal{B}_{12} \\ I & 0 \\ \mathcal{B}_{21} & \mathcal{B}_{22} \end{bmatrix} \prec 0, \tag{2.73}$$

$$\begin{bmatrix} \bullet \\ \bullet \end{bmatrix}^\top \begin{bmatrix} \mathfrak{N} & \\ & \mathfrak{X} \end{bmatrix} \begin{bmatrix} \mathfrak{Q}_{11} & \mathfrak{Q}_{12} \\ I & 0 \\ \mathfrak{Q}_{21} & \mathfrak{Q}_{22} \end{bmatrix} \succ 0, \tag{2.74}$$

$$\begin{bmatrix} \bullet \\ \bullet \end{bmatrix}^\top \mathfrak{M} \begin{bmatrix} I \\ \hline \Delta_\mathcal{B}(\delta) \end{bmatrix} \succ 0, \; \forall \delta \in \delta \tag{2.75}$$

$$\begin{bmatrix} \bullet \\ \bullet \end{bmatrix}^\top \mathfrak{N} \begin{bmatrix} I \\ \hline \Delta_\mathfrak{Q}(\delta) \end{bmatrix} \prec 0, \; \forall \delta \in \delta \tag{2.76}$$

where

$$\mathcal{B}(\delta) = \mathcal{U}(\delta)\mathcal{G}(\delta) = \Delta_\mathcal{B}(\delta) \star \begin{bmatrix} \mathcal{B}_{11} & \mathcal{B}_{12} \\ \mathcal{B}_{21} & \mathcal{B}_{22} \end{bmatrix}, \tag{2.77}$$

$$\Delta_\mathcal{B} = \begin{bmatrix} \Delta_\mathcal{U}(\delta, \eta) & \\ & \Delta(\delta) \end{bmatrix},$$

$$\mathcal{U}(\delta, \eta) = \begin{bmatrix} \mathfrak{Q}(\delta) & 0 & \\ \partial\mathfrak{Q}(\delta, \eta) & \mathfrak{Q}(\delta) & \\ \hline & & I \; 0 \\ & & 0 \; I \end{bmatrix} = \Delta_\mathcal{U}(\delta, \eta) \star \begin{bmatrix} \mathcal{U}_{11} & \mathcal{U}_{12} \\ \mathcal{U}_{21} & \mathcal{U}_{22} \end{bmatrix}, \tag{2.78}$$

$$\mathcal{G}(\delta) = \begin{bmatrix} I & 0 \\ \mathcal{A}(\delta) & \mathcal{B}_p(\delta) \\ \hline 0 & I \\ \mathcal{C}_p(\delta) & \mathcal{D}_{pp}(\delta) \end{bmatrix} = \Delta(\delta) \star \begin{bmatrix} \mathcal{G}_{11} & \mathcal{G}_{12} \\ \mathcal{G}_{21} & \mathcal{G}_{22} \end{bmatrix}, \tag{2.79}$$

$$\begin{bmatrix} \mathcal{B}_{11} & \mathcal{B}_{12} \\ \mathcal{B}_{21} & \mathcal{B}_{22} \end{bmatrix} = \begin{bmatrix} \mathcal{U}_{11} & \mathcal{U}_{12}\mathcal{G}_{21} & \mathcal{U}_{12}\mathcal{G}_{22} \\ 0 & \mathcal{G}_{11} & \mathcal{G}_{12} \\ \mathcal{U}_{21} & \mathcal{U}_{22}\mathcal{G}_{21} & \mathcal{U}_{22}\mathcal{G}_{22} \end{bmatrix}. \tag{2.80}$$

$\square$

Proof: The proof is immediate from the quadratic construction of the Lyapunov matrix and application of Lma. 2.1 on p. 36. The derivation of (2.78) and (2.79), respectively, are given in App. B.1 on p. 325. ∎

In some applications, transcendental functions may incur excessive amounts of overbounding, when covered in a rational parameterization. In such cases, it may be desirable to pull out only those parameters that fit well into the LFT framework, while others remain in the LFT system matrices as general parameters, according to Def. 2.7. The following result ensues from applying the FBSP w. r. t. the LFT channel of such a mixed general/LFT-LPV representation, while keeping the parameter-dependency of the Lyapunov function restricted to the general LPV parameters $\rho(t)$.

Theorem 2.9 (PDBRL w/ Multipliers, Mixed PDLF/PiDLF [161])

The system $\mathfrak{T}_\delta$ as defined in (2.15), is asymptotically stable over $\boldsymbol{\rho} \times \boldsymbol{\sigma} \times \boldsymbol{\delta}$ and has an induced $\mathcal{L}_2$-norm bounded from above by γ if there exist $\mathfrak{X}(\rho) \in \mathcal{C}^1(\rho, \mathbb{S}^{n_F})$, $\mathfrak{X}(\rho) \succ 0$, $\mathcal{M} = \mathcal{M}^\top$ and $\gamma > 0$ that satisfy

$$\begin{bmatrix} \bullet \\ \bullet \end{bmatrix}^\top \begin{bmatrix} \mathcal{M} & & \\ & \partial\mathfrak{X}(\rho,\sigma) & \mathfrak{X}(\rho) \\ & \mathfrak{X}(\rho) & 0 \\ & & & \Gamma \end{bmatrix} \begin{bmatrix} \mathcal{G}_{11}(\rho) & \mathcal{G}_{12}(\rho) \\ I & 0 \\ \mathcal{G}_{21}(\rho) & \mathcal{G}_{22}(\rho) \end{bmatrix} \prec 0, \quad \begin{array}{c} \forall (\rho,\sigma) \\ \in (\boldsymbol{\rho} \times \boldsymbol{\sigma}) \end{array} \tag{2.81}$$

$$\begin{bmatrix} \bullet \\ \bullet \end{bmatrix}^\top \mathcal{M} \begin{bmatrix} I \\ \Delta(\delta) \end{bmatrix} \succ 0, \quad \forall \delta \in \boldsymbol{\delta}. \tag{2.82}$$

with

$$\mathcal{G}(\rho,\delta) = \begin{bmatrix} I & 0 \\ \mathcal{A}(\rho,\delta) & \mathcal{B}_P(\rho,\delta) \\ 0 & I \\ \mathcal{C}_P(\rho,\delta) & \mathcal{D}_{PP}(\rho,\delta) \end{bmatrix} = \Delta(\delta) \star \begin{bmatrix} \mathcal{G}_{11}(\rho) & \mathcal{G}_{12}(\rho) \\ \mathcal{G}_{21}(\rho) & \mathcal{G}_{22}(\rho) \end{bmatrix},$$

$$\begin{bmatrix} \mathcal{G}_{11}(\rho) & \mathcal{G}_{12}(\rho) \\ \mathcal{G}_{21}(\rho) & \mathcal{G}_{22}(\rho) \end{bmatrix} = \begin{bmatrix} \mathcal{D}_{\Delta\Delta}(\rho) & \mathcal{C}_\Delta(\rho) & \mathcal{D}_{\Delta P}(\rho) \\ 0 & I & 0 \\ \mathcal{B}_\Delta(\rho) & \mathcal{A}(\rho) & \mathcal{B}_P(\rho) \\ 0 & 0 & I \\ \mathcal{D}_{P\Delta}(\rho) & \mathcal{C}_P(\rho) & \mathcal{D}_{PP}(\rho) \end{bmatrix}. \tag{2.83}$$

$\square$

Proof: The proof follows from applying the FBSP on Cond. 2.67 from Thm. 2.6 with respect to an LFT interconnection of a subset of parameters, in which the plant is rational. ∎

For completeness, the dual version is also presented.

Theorem 2.10 (Dual PDBRL w/ Multipliers, Mixed PDLF/PiDLF [161])

The system $\mathcal{T}_\delta$ as defined in (2.15), is asymptotically stable over $\rho \times \sigma \times \delta$ and has an induced $\mathcal{L}_2$-norm bounded from above by γ if there exist $\mathcal{Y}(\rho) \in \mathcal{C}^1(\rho, S^{n_r})$, $\mathcal{Y}(\rho) \succ 0$, $\mathcal{N} = \mathcal{N}^\top$ and $\gamma > 0$ that satisfy

$$\begin{bmatrix} \bullet \\ \bullet \end{bmatrix}^\top \begin{bmatrix} \mathcal{N} & & \\ & 0 & \mathcal{Y}(\rho) \\ & \mathcal{Y}(\rho) & \partial\mathcal{Y}(\rho,\sigma) \\ & & & \Gamma^{-1} \end{bmatrix} \begin{bmatrix} I & 0 \\ \mathcal{H}_{11}(\rho) & \mathcal{H}_{12}(\rho) \\ \mathcal{H}_{21}(\rho) & \mathcal{H}_{22}(\rho) \end{bmatrix} \succ 0, \quad \begin{array}{c} \forall (\rho,\sigma) \\ \in (\rho \times \sigma) \end{array} \tag{2.84}$$

$$\begin{bmatrix} \bullet \\ \bullet \end{bmatrix}^\top \mathcal{N} \begin{bmatrix} -\Delta^\top(\delta) \\ I \end{bmatrix} \prec 0, \quad \forall \delta \in \delta. \tag{2.85}$$

with

$$\mathcal{H}(\rho,\delta) = \begin{bmatrix} -\mathcal{A}^\top(\rho,\delta) & -\mathcal{C}_p^\top(\rho,\delta) \\ I & 0 \\ -\mathcal{B}_p^\top(\rho,\delta) & -\mathcal{D}_{pp}^\top(\rho,\delta) \\ 0 & I \end{bmatrix} = -\Delta^\top(\delta) \star \begin{bmatrix} \mathcal{H}_{11}(\rho) & \mathcal{H}_{12}(\rho) \\ \mathcal{H}_{21}(\rho) & \mathcal{H}_{22}(\rho) \end{bmatrix},$$

$$\begin{bmatrix} \mathcal{H}_{11}(\rho) & \mathcal{H}_{12}(\rho) \\ \mathcal{H}_{21}(\rho) & \mathcal{H}_{22}(\rho) \end{bmatrix} = \begin{bmatrix} -\mathcal{D}_{\Delta\Delta}^\top(\rho) & -\mathcal{B}_\Delta^\top(\rho) & -\mathcal{D}_{p\Delta}^\top(\rho) \\ -\mathcal{C}_\Delta^\top(\rho) & -\mathcal{A}^\top(\rho) & -\mathcal{C}_p^\top(\rho) \\ 0 & I & 0 \\ -\mathcal{D}_{\Delta p}^\top(\rho) & -\mathcal{B}_p^\top(\rho) & -\mathcal{D}_{pp}^\top(\rho) \\ 0 & 0 & I \end{bmatrix} \tag{2.86}$$

$\square$

Proof: The proof follows from applying Lma. A.7 on page 321 to Conds. (2.81) and (2.82). Observe that $\mathcal{N} = \mathcal{M}^{-1}$ and $\mathcal{Y}(\rho) = \mathcal{X}^{-1}(\rho)$. $\blacksquare$

When the plant is purely parameterized within the LFT framework and a parameter-independent Lyapunov function (PiDLF) is chosen in the conditions of the previous theorems, a simplified special case is obtained as follows.

Theorem 2.11 (PDBRL w/ Multipliers, PiDLF [125])

The system $\mathcal{T}_\delta$ as defined in (2.15), is asymptotically stable over δ and has an induced $\mathcal{L}_2$-norm bounded from above by γ if there exist $\mathcal{X} = \mathcal{X}^\top \in S^{n_r}$, $\mathcal{X} \succ 0$, $\mathcal{M} = \mathcal{M}^\top$ and $\gamma > 0$ that satisfy

$$\begin{bmatrix} \bullet \\ \bullet \end{bmatrix}^\top \begin{bmatrix} \mathcal{M} & & \\ & 0 & \mathcal{X} \\ & \mathcal{X} & 0 \\ & & & \Gamma \end{bmatrix} \begin{bmatrix} \mathcal{G}_{11} & \mathcal{G}_{12} \\ I & 0 \\ \mathcal{G}_{21} & \mathcal{G}_{22} \end{bmatrix} \prec 0, \tag{2.87}$$

$$\begin{bmatrix} \bullet \\ \bullet \end{bmatrix}^\top \mathcal{M} \begin{bmatrix} I \\ \Delta(\delta) \end{bmatrix} \succ 0, \quad \forall \delta \in \delta. \tag{2.88}$$

with $\mathcal{G}_{ij}$, $i,j \in \{1,2\}$ from (2.83), where the vector of general LPV parameters $\rho(t)$ is empty.

$\square$

Proof: The proof follows from taking $\mathcal{Q}_{\mathcal{X}}(\delta) = I_{n_r}$ in Thm. 2.8. ∎

Again, for completeness, the dual version is presented.

Theorem 2.12 (Dual PDBRL w/ Multipliers, PiDLF [125])
The system $\mathcal{T}_\delta$ as defined in (2.15), is asymptotically stable over δ and has an induced $\mathcal{L}_2$-norm bounded from above by γ if there exist $\mathcal{Y} = \mathcal{Y}^\top \in \mathbb{S}^{n_r}$, $\mathcal{Y} \succ 0$, $\mathcal{N} = \mathcal{N}^\top$ and $\gamma > 0$ that satisfy

$$\begin{bmatrix} \bullet \\ \vdots \\ \bullet \end{bmatrix}^\top \begin{bmatrix} \mathcal{N} & & \\ & 0\ \mathcal{Y} & \\ & \mathcal{Y}\ 0 & \\ & & \Gamma^{-1} \end{bmatrix} \begin{bmatrix} I & 0 \\ \mathcal{H}_{11} & \mathcal{H}_{12} \\ \mathcal{H}_{21} & \mathcal{H}_{22} \end{bmatrix} \succ 0, \tag{2.89}$$

$$\begin{bmatrix} \bullet \\ \bullet \end{bmatrix}^\top \mathcal{N} \begin{bmatrix} -\Delta^\top(\delta) \\ I \end{bmatrix} \prec 0, \quad \forall \delta \in \boldsymbol{\delta}. \tag{2.90}$$

with $\mathcal{H}_{ij}$, $i,j \in \{1,2\}$ from (2.86), where the vector of general LPV parameters $\rho(t)$ is empty.
□

Proof: The proof follows from applying Lma. A.7 on page 321 to Conds. (2.87) and (2.88). Thus, observe that $\mathcal{N} = \mathcal{M}^{-1}$ and $\mathcal{Y} = \mathcal{X}^{-1}$. ∎

2.2.5 *Multiplier Constraints*

As mentioned earlier, the benefit of applying the FBSP mainly resides in separating parameter-independent from parameter-dependent conditions, the latter of which being only quadratic in the parameter blocks.

For illustration, we consider multiplier conditions of the form (2.88) and partition the multiplier into a 2×2 block matrix conformable with the dimensions of Δ. For the subsequent discussion, however, potentially complex-valued parameter blocks are considered. Thus, the multiplier conditions are of the form

$$\begin{bmatrix} \bullet \\ \bullet \end{bmatrix}^* \begin{bmatrix} \mathcal{M}_{11} & \mathcal{M}_{12} \\ \mathcal{M}_{12}^\top & \mathcal{M}_{22} \end{bmatrix} \begin{bmatrix} I \\ \Delta(\delta) \end{bmatrix} \succ 0, \quad \forall \delta \in \boldsymbol{\delta}, \tag{2.91}$$

$$\begin{bmatrix} \bullet \\ \bullet \end{bmatrix}^* \begin{bmatrix} \mathcal{N}_{11} & \mathcal{N}_{12} \\ \mathcal{N}_{12}^\top & \mathcal{N}_{22} \end{bmatrix} \begin{bmatrix} -\Delta^*(\delta) \\ I \end{bmatrix} \prec 0, \quad \forall \delta \in \boldsymbol{\delta}. \tag{2.92}$$

The concepts presented here extend naturally to the dual multiplier condition or parameter blocks composed from multiple subblocks. Since the set $\boldsymbol{\delta}$ is not necessarily convex, the evaluation of the multiplier condition is usually performed on the hyperbox or convex hull containing $\boldsymbol{\delta}$. In addition, the imposition of inertia or structural constraints potentially facilitates an efficient evaluation at the cost of increased conservatism. Note that due to the fact that $0 \in \{\Delta(\delta) \mid \delta \in \boldsymbol{\delta}\}$, one has $\mathcal{M}_{11} \succ 0$, $\mathcal{N}_{22} \prec 0$.

Full-Block Multipliers

Full-block multipliers avoid any structural constraints on the multipliers. Concavity constraints (or convexity constraints in the dual multiplier condition (2.92)) introducing low conservatism can be formulated if the following set is considered [E19, 125],

$$\Delta_{LR} \triangleq \left\{ \sum_{j=1}^{N_\Delta} L_j \Delta_j(\delta) R_j^\top \;\middle|\; \Delta_j(\delta) \in \Delta_j \right\}, \tag{2.93}$$

where Δ_j are compact sets that define size and structure of the blocks $\Delta_j(\delta)$ and L_j, R_j have full column rank. The following result is due to simple convexity arguments.

Lemma 2.2 (Evaluation of Multiplier Conditions [125])
Let $\Delta(\delta) \in \Delta_{LR}$. Then

$$\begin{bmatrix} \bullet \\ \bullet \end{bmatrix}^* \begin{bmatrix} \mathcal{M}_{11} & \mathcal{M}_{12} \\ \mathcal{M}_{12}^\top & \mathcal{M}_{22} \end{bmatrix} \begin{bmatrix} I \\ \Delta(\delta) \end{bmatrix} \succ 0, \quad \forall \Delta(\delta) \in \Delta_{LR}. \tag{2.94}$$

implies the satisfaction of the condition for $\Delta(\delta) \in \mathrm{conv}\,(\Delta_{LR})$ and in particular Cond. (2.91), if

$$L_j^\top \mathcal{M}_{22} L_j \prec 0, \quad \forall j \in \{1, \ldots, N_\Delta\}. \tag{2.95}$$

$\square$

The decomposition using matrices L_j and R_j of full column rank is non-unique and may affect the conservatism introduced via the concavity constraints. In practice, evaluating (2.94) is performed on on the vertices of $\mathrm{conv}\,(\Delta)$.

The set Δ_{LR} is rather general and more explicit descriptions are common in the literature, e. g., [5, 124]. Consider the following example.

Example 2.1 (Block-Diagonal Parameter Block Decomposition)
Consider a parameter block in block-diagonal form

$$\Delta(\delta) = \operatorname*{diag}_{j=1}^{N_\Delta}\big(\Delta_j(\delta)\big) \in \mathcal{C}^0(\mathbb{R}^{n_\delta}, \mathbb{R}^{n_{q_\Delta} \times n_{p_\Delta}}), \tag{2.96}$$

for which $\Delta_j \in \mathcal{C}^0(\mathbb{R}^{n_\delta}, \mathbb{R}^{n_{q_\Delta,j} \times n_{p_\Delta,j}})$ and thus $n_{q_\Delta} = \sum_{j=1}^{N_\Delta} n_{q_\Delta,j}$ and $n_{p_\Delta} = \sum_{j=1}^{N_\Delta} n_{p_\Delta,j}$. This block can be written as

$$\Delta(\delta) = \sum_{j=1}^{N_\Delta} L_j \Delta_j L_j^\top,$$

where

$$L_j = \operatorname*{col}_{i=1}^{N_\Delta}\left(\delta_{ji} I_{n_{q_{\Delta,j}}}\right), \qquad \delta_{ji} = \begin{cases} 1 & , j = 1 \\ 0 & , \textit{otherwise.} \end{cases}$$

Note that the blocks $\Delta_j(\delta)$ may or may not have a structure with repeated parameters δ on the diagonal as in Ex. 2.2. □

If the parameter block takes the form of a diagonal matrix with repeated parameters, the decomposition simplifies. Consider the following example.

Example 2.2 (Diagonal Parameter Block Decomposition)
Consider a parameter block of the typical form

$$\Delta(\delta) = \operatorname*{diag}_{i=1}^{n_\delta}\left(\delta_i I_{r_{\delta,i}}\right) \in \mathcal{C}^0(\mathbb{R}^{n_\delta}, \mathbb{R}^{n_\Delta \times n_\Delta}), \tag{2.97}$$

for which $n_\Delta = \sum_{i=1}^{n_\delta} r_{\delta,i}$. This block can be written as

$$\Delta(\delta) = \sum_{i=1}^{n_\delta} \delta_i L_i L_i^\top,$$

where

$$L_j = \operatorname*{col}_{i=1}^{n_\delta}\left(\delta_{ji} I_{r_{\delta,j}}\right), \qquad \delta_{ji} = \begin{cases} 1 & , j = 1 \\ 0 & , \textit{otherwise.} \end{cases}$$

In this case $N_\Delta = n_\delta$. □

While Exs. 2.1 and 2.2 provide illustration on how to construct decompositions of a parameter block that result in different concavity constraints, an often used limiting case exists in choosing $L_j = I_{n_{q_\Delta}}$ and $N_\Delta = 1$, which simply results in

$$\mathcal{M}_{22} \prec 0.$$

Such a simple inertia hypothesis clearly allows to evaluate Cond. (2.91) on $\operatorname{conv}(\delta)$ or $\operatorname{hyp}(\delta)$ independently of the actual structure of Δ and with the only requirement that $\Delta(\delta)$ is affinely dependent on the parameters δ_i, $i \in \{1, \ldots, n_\delta\}$. In this case evaluating the multiplier condition on $\operatorname{hyp}(\delta)$ amounts to 2^{n_δ} LMI constraints. This inertia hypothesis appears to be essential for a practically valid construction of a controller's parameter block, as will become evident later [125, 143].

In the following, the term «full-block multiplier» will refer to imposing only the inertia constraints $\mathcal{M}_{11} \succ 0$ and $\mathcal{M}_{22} \prec 0$ on the multiplier, if not stated otherwise.

D/G-scaling Constraints

D/G-scaling (D/G-S) constraints impose structural requirements on the multiplier, characterized by the following set.

$$\mathcal{M}_{D/G}(\Delta) \triangleq \left\{ \mathcal{M} = \begin{bmatrix} \mathcal{M}_{11} & \mathcal{M}_{12} \\ \mathcal{M}_{12}^\top & \mathcal{M}_{22} \end{bmatrix} \in \mathbb{S}^{(n_{p_\Delta} + n_{q_\Delta})}, \left| \begin{array}{l} \mathcal{M}_{12}\Delta = \Delta\mathcal{M}_{12}, \quad \mathcal{M}_{11}\Delta = \Delta\mathcal{M}_{11}, \\ \mathcal{M}_{12} = -\mathcal{M}_{12}^\top, \quad \mathcal{M}_{11} = -\mathcal{M}_{22}, \end{array} \forall \Delta \in \mathbf{\Delta} \right. \right\} \tag{2.98}$$

Remark 2.12 *The name «D/G-scalings» is owed to the application of these constraints in* μ*-theory, e.g., in [39, 53, 130].*

It is easy to verify that in the case of normalized bounds on real-valued parameters $|\delta_i| \leqslant 1$, $\forall i \in \{1, \ldots, n_\delta\}$, multipliers belonging to the set $\mathcal{M}_{D/G}(\Delta)$ trivially satisfy matrix inequalities of the form (2.91), where inertia hypotheses are implied by $0 \in \mathbf{\Delta}$.

A scaled version of D/G-S due to [130], takes into account bounds on δ_i, $i \in \{1, \ldots, n_\delta\}$ ranging in a hyperbox hyp (δ). For this purpose, assume bounds on the parameter values $\delta_i \in [\underline{\delta}_i, \overline{\delta}_i] \subset \mathbb{R}$, with

$$\underline{\delta}_i = \min_{t \geqslant 0} \delta_i(t), \quad \overline{\delta}_i = \max_{t \geqslant 0} \delta_i(t), \quad \forall i \in \{1, \ldots, n_\delta\},$$

The following two sets characterize the corresponding multipliers.

$$\hat{\mathcal{M}}_{D/G}(\Delta) \triangleq \left\{ \mathcal{M} = \begin{bmatrix} S_{11} & S_{12} \\ S_{12} & S_{22} \end{bmatrix} \begin{bmatrix} \mathcal{M}_{11} & 0 \\ 0 & \mathcal{M}_{11} \end{bmatrix} + \begin{bmatrix} 0 & \mathcal{M}_{12} \\ \mathcal{M}_{12}^\top & 0 \end{bmatrix} \right. \tag{2.99}$$

$$\begin{bmatrix} \mathcal{M}_{11} & \mathcal{M}_{12} \\ \mathcal{M}_{12}^\top & \mathcal{M}_{22} \end{bmatrix} \in \mathcal{M}_{D/G}(\Delta),$$

$$S^{(i)} = \begin{bmatrix} S_{11}^{(i)} & S_{12}^{(i)} \\ S_{12}^{(i)} & S_{22}^{(i)} \end{bmatrix} = \begin{bmatrix} -2\underline{\delta}_i\overline{\delta}_i I_{r_{\delta,i}} & (\underline{\delta}_i + \overline{\delta}_i)I_{r_{\delta,i}} \\ (\underline{\delta}_i + \overline{\delta}_i)I_{r_{\delta,i}} & -2I_{r_{\delta,i}} \end{bmatrix},$$

$$S_{kl} = \operatorname*{diag}_{i=1}^{n_\delta} \left(S_{kl}^{(i)} \right), \quad \begin{array}{l} \forall (k,l) \in \{1,2\} \times \{1,2\}, \\ \forall i \in \{1, \ldots, n_\delta\} \end{array} \right\}$$

$$\hat{\mathcal{N}}_{D/G}(\Delta) \triangleq \left\{ \mathcal{N} = \begin{bmatrix} \tilde{S}_{11} & \tilde{S}_{12} \\ \tilde{S}_{12} & \tilde{S}_{22} \end{bmatrix} \begin{bmatrix} \mathcal{N}_{11} & 0 \\ 0 & \mathcal{N}_{11} \end{bmatrix} + \begin{bmatrix} 0 & \mathcal{N}_{12} \\ \mathcal{N}_{12}^\top & 0 \end{bmatrix} \right| \qquad (2.100)$$

$$\begin{bmatrix} \mathcal{N}_{11} & \mathcal{N}_{12} \\ \mathcal{N}_{12}^\top & \mathcal{N}_{22} \end{bmatrix} \in \mathcal{M}_{D/G}(\Delta),$$

$$S^{(i)^{-1}} = \begin{bmatrix} \tilde{S}_{11}^{(i)} & \tilde{S}_{12}^{(i)} \\ \tilde{S}_{12}^{(i)} & \tilde{S}_{22}^{(i)} \end{bmatrix} = \frac{1}{(\underline{\delta}_i - \overline{\delta}_i)^2} \begin{bmatrix} 2I_{r_{\delta,i}} & (\underline{\delta}_i + \overline{\delta}_i)I_{r_{\delta,i}} \\ (\underline{\delta}_i + \overline{\delta}_i)I_{r_{\delta,i}} & 2\underline{\delta}_i\overline{\delta}_i I_{r_{\delta,i}} \end{bmatrix},$$

$$\tilde{S}_{kl} = \operatorname*{diag}_{i=1}^{n_\delta}\left(\tilde{S}_{kl}^{(i)}\right), \quad \begin{array}{l} \forall\,(k,l) \in \{1,2\} \times \{1,2\}, \\ \forall i \in \{1,\dots,n_\delta\} \end{array} \Bigg\}$$

Remark 2.13 *Since diagonal* LFT *parameter blocks can always be normalized, it may appear superfluous to introduce scaled multiplier conditions. However, in the context of distributed controller synthesis detailed in Part II of this thesis, such an approach is beneficial.*

Figures 2.6a and 2.6b illustrate the concavity and convexity constraints for the primal and dual multiplier conditions, respectively.

(a) Concavity of primal multiplier constraint for parameter δ_i, where the multiplier constraint reduces to $\mathcal{M}(\delta) = -2\underline{\delta}_i\overline{\delta}_i + 2(\underline{\delta}_i+\overline{\delta}_i)\delta_i-2\delta_i^2 > 0$.

(b) Convexity of dual multiplier constraint for parameter δ_i, where the multiplier constraint reduces to $\mathcal{N}(\delta) = 2\underline{\delta}_i\overline{\delta}_i-2(\underline{\delta}_i+\overline{\delta}_i)\delta_i+2\delta_i^2 < 0$.
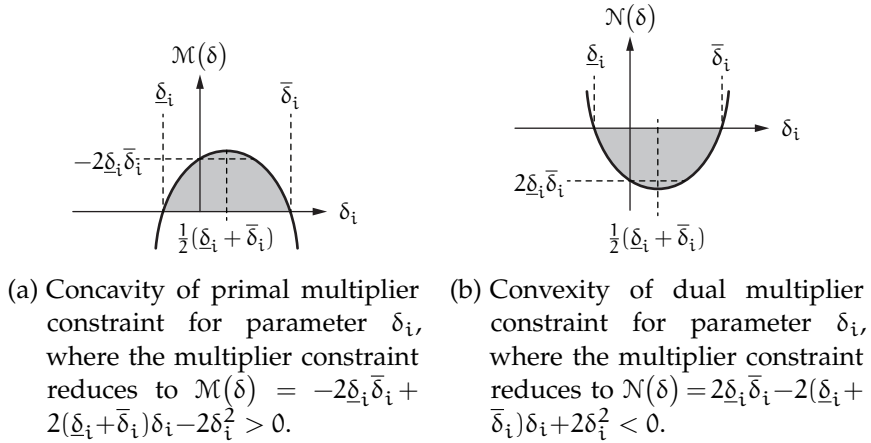
Figure 2.6: Concavity and convexity of primal and dual multiplier constraints for parameter δ_i.

Lemma 2.3 (D/G-scaling [130])
Under the assumption of a diagonal parameter block of the form

$$\Delta(\delta) = \operatorname*{diag}_{i=1}^{n_\delta}(\delta_i I_{r_{\delta,i}}) \in \mathcal{C}^0(\mathbb{R}^{n_\delta}, \mathbb{R}^{n_\Delta \times n_\Delta}),$$

and bounds on the parameter values $\delta_i \in \left[\underline{\delta}_i, \overline{\delta}_i\right] \subset \mathbb{R}$, with

$$\underline{\delta}_i = \min_{t \geqslant 0} \delta_i(t), \quad \overline{\delta}_i = \max_{t \geqslant 0} \delta_i(t), \quad \forall i \in \{1,\dots,n_\delta\},$$

the choice of multiplier structure $\mathcal{M} \in \hat{\mathbf{M}}_{D/G}(\Delta)$ decouples Cond. (2.91) into the n_δ trivially fulfilled conditions

$$\begin{bmatrix} \bullet \\ \hdashline \bullet \end{bmatrix}^\top \mathcal{M}^{(i)} \begin{bmatrix} I \\ \hdashline \delta_i I_{r_{\delta,i}} \end{bmatrix} \succ 0, \qquad \begin{array}{l} \forall \delta_i \in \left[\underline{\delta}_i, \overline{\delta}_i\right], \\ \forall i \in \{1, \dots, n_\delta\}. \end{array} \tag{2.101}$$

$$\mathcal{M}^{(i)} = \begin{bmatrix} S_{11}^{(i)} & S_{12}^{(i)} \\ S_{12}^{(i)} & S_{22}^{(i)} \end{bmatrix} \begin{bmatrix} \mathcal{M}_{11}^{(i)} & 0 \\ 0 & \mathcal{M}_{11}^{(i)} \end{bmatrix} + \begin{bmatrix} 0 & \mathcal{M}_{12}^{(i)} \\ \mathcal{M}_{12}^{(i)\top} & 0 \end{bmatrix}, \tag{2.102}$$

with

$$\mathcal{M}_{11} = \operatorname*{diag}_{i=1}^{n_\delta} \left(\mathcal{M}_{11}^{(i)} \right) \succ 0, \qquad \mathcal{M}_{11}^{(i)} \in \mathbf{S}^{r_{\delta,i} \times r_{\delta,i}},$$

$$\mathcal{M}_{12} = \operatorname*{diag}_{i=1}^{n_\delta} \left(\mathcal{M}_{12}^{(i)} \right) = -\mathcal{M}_{12}^\top, \quad \mathcal{M}_{12}^{(i)} \in \mathbb{R}^{r_{\delta,i} \times r_{\delta,i}}.$$

For the structural choice on the dual multiplier $\mathcal{N} \in \hat{\mathbf{N}}_{D/G}(\Delta)$, the dual multiplier condition is decoupled to the n_δ trivially fulfilled conditions

$$\begin{bmatrix} \bullet \\ \hdashline \bullet \end{bmatrix}^\top \mathcal{N}^{(i)} \begin{bmatrix} -\delta_i I_{r_{\delta,i}} \\ \hdashline I \end{bmatrix} \prec 0, \qquad \begin{array}{l} \forall \delta_i \in \left[\underline{\delta}_i, \overline{\delta}_i\right], \\ \forall i \in \{1, \dots, n_\delta\}, \end{array} \tag{2.103}$$

$$\mathcal{N}^{(i)} = \begin{bmatrix} \tilde{S}_{11}^{(i)} & \tilde{S}_{12}^{(i)} \\ \tilde{S}_{12}^{(i)} & \tilde{S}_{22}^{(i)} \end{bmatrix} \begin{bmatrix} \mathcal{N}_{11}^{(i)} & 0 \\ 0 & \mathcal{N}_{11}^{(i)} \end{bmatrix} + \begin{bmatrix} 0 & \mathcal{N}_{12}^{(i)} \\ \mathcal{N}_{12}^{(i)\top} & 0 \end{bmatrix}, \tag{2.104}$$

with

$$\mathcal{N}_{11} = \operatorname*{diag}_{i=1}^{n_\delta} \left(\mathcal{N}_{11}^{(i)} \right) \succ 0, \qquad \mathcal{N}_{11}^{(i)} \in \mathbf{S}^{r_{\delta,i} \times r_{\delta,i}},$$

$$\mathcal{N}_{12} = \operatorname*{diag}_{i=1}^{n_\delta} \left(\mathcal{N}_{12}^{(i)} \right) = -\mathcal{N}_{12}^\top, \quad \mathcal{N}_{12}^{(i)} \in \mathbb{R}^{r_{\delta,i} \times r_{\delta,i}}.$$

$\square$

Proof: Only the fulfillment of the primal multiplier is proven and since the decoupling resulting from the structural constraints is obvious, it suffices to consider a parameter block with only a single parameter δ resulting in a multiplier condition

$$\begin{bmatrix} \bullet \\ \hdashline \bullet \end{bmatrix}^\top \begin{bmatrix} -2\underline{\delta}\overline{\delta}\mathcal{M}_{11} & (\underline{\delta} + \overline{\delta})\mathcal{M}_{11} + \mathcal{M}_{12} \\ (\underline{\delta} + \overline{\delta})\mathcal{M}_{11} - \mathcal{M}_{12} & -2\mathcal{M}_{11} \end{bmatrix} \begin{bmatrix} I \\ \delta I \end{bmatrix} \succ 0, \ \forall \delta \in \left[\underline{\delta}, \overline{\delta}\right].$$

Since $\mathcal{M}_{11} \succ 0$, an expansion yields the condition

$$-2\underline{\delta}\overline{\delta} + 2(\underline{\delta} + \overline{\delta})\delta - 2\delta^2 \succ 0, \quad \forall \delta \in \left[\underline{\delta}, \overline{\delta}\right],$$

which has both roots at $\underline{\delta}$ and $\overline{\delta}$, constant curvature and is positive in between. $\blacksquare$

Example 2.3 (Commutativity w/ Block-Diagonal Parameter Blocks)
Consider again a parameter block in block-diagonal form (2.96). Note that any parameter block of this form commutes with matrices composed as

$$\mathcal{M}_{kl} = \operatorname*{diag}_{i=1}^{N_\Delta}\left(\mathcal{M}_{kl}^{(i)} I_{n_{\Delta_i}}\right), \quad \mathcal{M}_{kl}^{(i)} \in \mathbb{R},$$

rendering the multiplier actually diagonal. Furthermore, the skew-symmetry requirement on $\mathcal{M}_{12}$ enforces $\mathcal{M}_{12} = 0$. □

The commutativity requirement on the blocks $\mathcal{M}_{kl}$ and Δ imposes a sparsity pattern $\mathcal{M}_{kl}$ that depends on the shape of Δ. Also consider the following example. Commutativity with respect to diagonal parameter blocks forces fewer multiplier variables to be zero.

Example 2.4 (Commutativity w/ Diagonal Parameter Blocks)
Consider again a parameter block of the typical form (2.97). Note that any parameter block of this form commutes with matrices composed as

$$\mathcal{M}_{kl} = \operatorname*{diag}_{i=1}^{n_\delta}\left(\mathcal{M}_{kl}^{(i)}\right), \quad \mathcal{M}_{kl}^{(i)} \in \mathbb{S}^{r_{\delta,i} \times r_{\delta,i}}.$$

□

For diagonal parameter blocks, such constraints will prove beneficial in LFT-LPV synthesis based on PIDLFs, since they allow the controller's parameter block $\Delta^K(\delta)$ to be simply chosen as a copy of the plant's parameter block, i.e., $\Delta^K(\delta) = \Delta^P(\delta)$. Block-diagonal parameter blocks will most likely lead to an excessive amount of conservatism due to the commutativity requirements.

Note also that commutativity constraints emerge naturally from the channel-wise application of the FBSP (Thm. 2.4) or SP (Thm. 2.5) [123], i.e., taking into account each parameter δ_i, $i \in \{1, \ldots, n_\delta\}$ with its repetition one at a time.

D-scaling Constraints
D-scaling (D-S) constraints impose stronger structural requirements on the multiplier, by requiring the off-diagonal blocks to be zero. While being more conservative for real-valued diagonal parameter blocks of the typical form (2.97), e.g., shown on p. 47, they allow for complex-valued parameter blocks

$$\Delta(\delta) = \operatorname*{diag}_{i=1}^{n_\delta}(\delta_i I_{r_{\delta,i}}) \in \mathcal{C}^0(\mathbb{C}^{n_\delta}, \mathbb{C}^{n_\Delta \times n_\Delta}). \tag{2.105}$$

D-S constraints are characterized by the following set.

$$\mathbf{M}_D(\Delta) \triangleq \left\{ \mathcal{M} = \begin{bmatrix} \mathcal{M}_{11} & 0 \\ 0 & \mathcal{M}_{22} \end{bmatrix} \in \mathbb{S}^{(n_{p_\Delta}+n_{q_\Delta})}, \right.$$
$$\left. \mathcal{M}_{11}\Delta = \Delta\mathcal{M}_{11}, \; \mathcal{M}_{11} = -\mathcal{M}_{22}, \forall \Delta \in \mathbf{\Delta} \right\} \tag{2.106}$$

Again, it is easy to verify that in the case of normalized bounds on complex-valued parameters $|\delta_i| \leqslant 1, \forall i \in \{1, \ldots, n_\delta\}$, multipliers belonging to the set $\mathbf{M}_D(\Delta)$ trivially satisfy matrix inequalities of the form (2.91), where inertia hypotheses are implied by $0 \in \mathbf{\Delta}$.

It is possible to formally define shifted D-Ss, as well. A scaled version of D/G-S due to [130], takes into account bounds on δ_i, $i \in \{1, \ldots, n_\delta\}$ ranging in a hyperbox $\mathrm{hyp}(\delta)$. The following two sets characterize the corresponding multipliers.

$$\hat{\mathbf{M}}_D(\Delta) \triangleq \left\{ \mathcal{M} = \begin{bmatrix} S_{11} & S_{12} \\ S_{12} & S_{22} \end{bmatrix} \begin{bmatrix} \mathcal{M}_{11} & 0 \\ 0 & \mathcal{M}_{11} \end{bmatrix} \; \middle| \; \begin{bmatrix} \mathcal{M}_{11} & 0 \\ 0 & \mathcal{M}_{22} \end{bmatrix} \in \mathbf{M}_D(\Delta), \right.$$
$$S^{(i)} = \begin{bmatrix} S_{11}^{(i)} & S_{12}^{(i)} \\ S_{12}^{(i)} & S_{22}^{(i)} \end{bmatrix} = \begin{bmatrix} (\delta_{i,r}^2 - \delta_{i,c}^2)I_{r_{\delta,i}} & \delta_{i,c}I_{r_{\delta,i}} \\ \delta_{i,c}I_{r_{\delta,i}} & -I_{r_{\delta,i}} \end{bmatrix}$$
$$\left. S_{kl} = \operatorname*{diag}_{i=1}^{n_\delta}\left(S_{kl}^{(i)}\right), \quad \begin{array}{l} \forall (k,l) \in \{1,2\} \times \{1,2\}, \\ \forall i \in \{1, \ldots, n_\delta\} \end{array} \right\} \tag{2.107}$$

$$\hat{\mathbf{N}}_D(\Delta) \triangleq \left\{ \mathcal{N} = \begin{bmatrix} \tilde{S}_{11} & \tilde{S}_{12} \\ \tilde{S}_{12} & \tilde{S}_{22} \end{bmatrix} \begin{bmatrix} \mathcal{N}_{11} & 0 \\ 0 & \mathcal{N}_{11} \end{bmatrix} \; \middle| \; \begin{bmatrix} \mathcal{N}_{11} & \mathcal{N}_{12} \\ \mathcal{N}_{12}^\top & \mathcal{N}_{22} \end{bmatrix} \in \mathbf{M}_D(\Delta), \right.$$
$$S^{(i)-1} = \begin{bmatrix} \tilde{S}_{11}^{(i)} & \tilde{S}_{12}^{(i)} \\ \tilde{S}_{12}^{(i)} & \tilde{S}_{22}^{(i)} \end{bmatrix} = \frac{1}{\delta_{i,r}^2} \begin{bmatrix} I_{r_{\delta,i}} & \delta_{i,c}I_{r_{\delta,i}} \\ \delta_{i,c}I_{r_{\delta,i}} & -(\delta_{i,r}^2 - \delta_{i,c}^2)I_{r_{\delta,i}} \end{bmatrix}$$
$$\left. \tilde{S}_{kl} = \operatorname*{diag}_{i=1}^{n_\delta}\left(\tilde{S}_{kl}^{(i)}\right), \quad \begin{array}{l} \forall (k,l) \in \{1,2\} \times \{1,2\}, \\ \forall i \in \{1, \ldots, n_\delta\} \end{array} \right\} \tag{2.108}$$

The geometric interpretation of the parameterization of the scalings becomes ap-
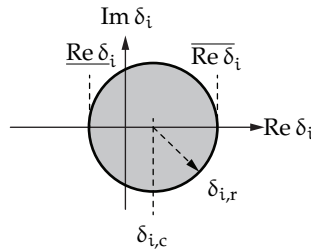
Figure 2.7: Ball region constraints for parameter δ_i.

parent by noticing that they confine each δ_i to balls with radius $\delta_{i,r}$ and center $\delta_{i,c}$. The corollary below follows from Lma. 2.3.

Corollary 2.1 (D-Scaling [130])
Under the assumption of a diagonal parameter block of the form

$$\Delta(\delta) = \operatorname*{diag}_{i=1}^{n_\delta}(\delta_i I_{r_{\delta,i}}) \in \mathcal{C}^0(\mathbb{C}^{n_\delta}, \mathbb{C}^{n_\Delta \times n_\Delta}),$$

and bounds on the parameter values $|\delta_i - \delta_{i,c}| \leqslant \delta_{i,r}$, with $\delta_{i,c}, \delta_{i,r} \in \mathbb{C}$, the choice of multiplier structure $\mathcal{M} \in \hat{\mathcal{M}}_D(\Delta)$ decouples Cond. (2.91) into n_δ trivially fulfilled conditions.

For the structural choice on the dual multiplier $\mathcal{N} \in \hat{\mathcal{N}}_D(\Delta)$, the dual multiplier condition is decoupled into n_δ trivially fulfilled conditions. □

Proof: The proof follows directly from Lma. 2.3. ■

D/G*-scaling Constraints
Analogously to D/G-S constraints that require the parameters to be purely real, D/G*-scaling (D/G*-S) constraints can be defined that require a zero real part for complex parameters. For this purpose, consider parameter blocks of the form

$$\Delta(\delta) = \operatorname*{diag}_{i=1}^{n_\delta}(\delta_i I_{r_{\delta,i}}) \in \mathcal{C}^0(j\mathbb{R}^{n_\delta}, j\mathbb{R}^{n_\Delta \times n_\Delta}). \tag{2.109}$$

D/G*-S constraints are characterized by the following set.

$$\mathcal{M}_{D/G^*}(\Delta) \triangleq \left\{ \mathcal{M} = \begin{bmatrix} \mathcal{M}_{11} & \mathcal{M}_{12} \\ \mathcal{M}_{12} & \mathcal{M}_{22} \end{bmatrix} \in \mathbb{S}^{(n_{p_\Delta} + n_{q_\Delta})}, \; \middle| \begin{array}{l} \mathcal{M}_{12}\Delta = \Delta\mathcal{M}_{12}, \quad \mathcal{M}_{11}\Delta = \Delta\mathcal{M}_{11}, \\ \mathcal{M}_{12} = \mathcal{M}_{12}^\top, \qquad \mathcal{M}_{11} = -\mathcal{M}_{22}, \end{array} \; \forall \Delta \in \boldsymbol{\Delta} \right\} \tag{2.110}$$

As before, it is easy to verify that in the case of normalized bounds on the parameters $|\delta_i| \leqslant 1$, $\forall i \in \{1, \ldots, n_\delta\}$, multipliers belonging to the set $\mathcal{M}_{D/G^*}(\Delta)$ trivially satisfy matrix inequalities of the form (2.91), where inertia hypotheses are implied by $0 \in \boldsymbol{\Delta}$. The difference to D/G-S resides in the off-diagonal blocks required to be symmetric instead of skew-symmetric. Due to the conjugate transpose of the scalar purely imaginary parameters, terms associated with the off-diagonal blocks cancel.

A scaled version of D/G*-S, takes into account bounds on $\delta_i \in j\mathbb{R}$, $i \in \{1, \ldots, n_\delta\}$ ranging in a hyperbox $\operatorname{hyp}(\delta)$. For this purpose, assume bounds on the parameter values $\delta_i \in j\left[\underline{\delta}_i, \overline{\delta}_i\right] \subset j\mathbb{R}$, with

$$\underline{\delta}_i = \min_{t \geqslant 0} \operatorname{Im} \delta_i(t), \quad \overline{\delta}_i = \max_{t \geqslant 0} \operatorname{Im} \delta_i(t), \quad \forall i \in \{1, \ldots, n_\delta\},$$

The following two sets characterize the corresponding multipliers.

$$
\hat{\mathcal{M}}_{D/G^*}(\Delta) \triangleq \left\{ \mathcal{M} = \begin{bmatrix} S_{11} & S_{12} \\ S_{12} & S_{22} \end{bmatrix} \begin{bmatrix} \mathcal{M}_{11} & 0 \\ 0 & \mathcal{M}_{11} \end{bmatrix} + \begin{bmatrix} 0 & \mathcal{M}_{12} \\ \mathcal{M}_{12} & 0 \end{bmatrix} \right| \tag{2.111}
$$

$$
\begin{bmatrix} \mathcal{M}_{11} & \mathcal{M}_{12} \\ \mathcal{M}_{12} & \mathcal{M}_{22} \end{bmatrix} \in \mathcal{M}_{D/G^*}(\Delta),
$$

$$
S^{(i)} = \begin{bmatrix} S_{11}^{(i)} & S_{12}^{(i)} \\ S_{12}^{(i)} & S_{22}^{(i)} \end{bmatrix} = \begin{bmatrix} -2\underline{\delta}_i\overline{\delta}_i I_{r_{\delta,i}} & (\underline{\delta}_i + \overline{\delta}_i)I_{r_{\delta,i}} \\ (\underline{\delta}_i + \overline{\delta}_i)I_{r_{\delta,i}} & -2I_{r_{\delta,i}} \end{bmatrix},
$$

$$
\left. S_{kl} = \operatorname*{diag}_{i=1}^{n_\delta}\left(S_{kl}^{(i)}\right), \quad \begin{array}{l} \forall\,(k,l) \in \{1,2\} \times \{1,2\}, \\ \forall i \in \{1,\dots,n_\delta\} \end{array} \right\}
$$

$$
\hat{\mathcal{N}}_{D/G^*}(\Delta) \triangleq \left\{ \mathcal{N} = \begin{bmatrix} \tilde{S}_{11} & \tilde{S}_{12} \\ \tilde{S}_{12} & \tilde{S}_{22} \end{bmatrix} \begin{bmatrix} \mathcal{N}_{11} & 0 \\ 0 & \mathcal{N}_{11} \end{bmatrix} + \begin{bmatrix} 0 & \mathcal{N}_{12} \\ \mathcal{N}_{12} & 0 \end{bmatrix} \right| \tag{2.112}
$$

$$
\begin{bmatrix} \mathcal{N}_{11} & \mathcal{N}_{12} \\ \mathcal{N}_{12} & \mathcal{N}_{22} \end{bmatrix} \in \mathcal{M}_{D/G^*}(\Delta),
$$

$$
S^{(i)-1} = \begin{bmatrix} \tilde{S}_{11}^{(i)} & \tilde{S}_{12}^{(i)} \\ \tilde{S}_{12}^{(i)} & \tilde{S}_{22}^{(i)} \end{bmatrix} = \frac{1}{(\underline{\delta}_i - \overline{\delta}_i)^2} \begin{bmatrix} 2I_{r_{\delta,i}} & (\underline{\delta}_i + \overline{\delta}_i)I_{r_{\delta,i}} \\ (\underline{\delta}_i + \overline{\delta}_i)I_{r_{\delta,i}} & 2\underline{\delta}_i\overline{\delta}_i I_{r_{\delta,i}} \end{bmatrix},
$$

$$
\left. \tilde{S}_{kl} = \operatorname*{diag}_{i=1}^{n_\delta}\left(\tilde{S}_{kl}^{(i)}\right), \quad \begin{array}{l} \forall\,(k,l) \in \{1,2\} \times \{1,2\}, \\ \forall i \in \{1,\dots,n_\delta\} \end{array} \right\}
$$

Corollary 2.2 (D/G*-Scaling)
Under the assumption of a diagonal parameter block of the form

$$
\Delta(\delta) = \operatorname*{diag}_{i=1}^{n_\delta}\left(\delta_i I_{r_{\delta,i}}\right) \in \mathcal{C}^0(j\mathbb{R}^{n_\delta}, j\mathbb{R}^{n_\Delta \times n_\Delta}),
$$

and bounds on the parameter values $\delta_i \in j\left[\underline{\delta}_i, \overline{\delta}_i\right] \subset j\mathbb{R}$, with

$$
\underline{\delta}_i = \min_{t \geqslant 0} \operatorname{Im} \delta_i(t), \quad \overline{\delta}_i = \max_{t \geqslant 0} \operatorname{Im} \delta_i(t), \quad \forall i \in \{1,\dots,n_\delta\},
$$

the choice of multiplier structure $\mathcal{M} \in \hat{\mathcal{M}}_{D/G^*}(\Delta)$ decouples Cond. (2.91) into n_δ trivially fulfilled conditions.

For the structural choice on the dual multiplier $\mathcal{N} \in \hat{\mathcal{N}}_{D/G^*}(\Delta)$, the dual multiplier condition is decoupled into n_δ trivially fulfilled conditions. □

Proof: The proof follows directly from Lma. 2.3. ∎

2.3 GAIN-SCHEDULED LINEAR PARAMETER-VARYING CONTROLLER SYNTHESIS

IN this section, the previous analysis results are extended to synthesis through the derivation of existence conditions resulting from the elimination of the controller parameters. Closed-loop representations are introduced in Sect. 2.3.2 and the controller elimination approach is detailed in Sect. 2.3.2. Sects. 2.3.3–2.3.5 treat the special cases of gridding-, polytopic- or multiplier-based solution of the associated LMIs and the implications w. r. t. controller construction.

2.3.1 Closed-Loop Representations

Consider an open-loop LPV system in general LPV representation of the form

$$
\mathcal{P}_\rho^\sigma : \begin{cases} \begin{bmatrix} \dot{x} \\ z \\ y \end{bmatrix} = \left[\begin{array}{c:cc} A\big(\rho(t)\big) & B_p\big(\rho(t)\big) & B_u\big(\rho(t)\big) \\ C_p\big(\rho(t)\big) & D_{pp}\big(\rho(t)\big) & D_{pu}\big(\rho(t)\big) \\ C_y\big(\rho(t)\big) & D_{yp}\big(\rho(t)\big) & D_{yu}\big(\rho(t)\big) \end{array} \right] \begin{bmatrix} x \\ w \\ u \end{bmatrix} \\ \qquad \rho(t) \in \mathcal{F}_\rho^\sigma, \end{cases}
\tag{2.113}
$$

where $x \in \mathbb{R}^{n_x}$, $u \in \mathbb{R}^{n_u}$, $y \in \mathbb{R}^{n_y}$, $w \in \mathbb{R}^{n_w}$, $z \in \mathbb{R}^{n_z}$, are the open-loop state, control input, measured output and performance signal vectors of the system, respectively. The definitions of the symbols as from Sects. 2.1.1–2.1.3 for the system's state space model matrix $P_\rho\big(\rho(t)\big)$ and input-output operator $P_\rho\big(\rho(t)\big)$ extend naturally to this representation. The system is illustrated in Fig. 2.8a.

Consider as well an LFR of the open-loop LPV system, illustrated in Fig. 2.8b,

$$
\mathcal{P}_\delta^\eta : \begin{cases} \begin{bmatrix} \dot{x} \\ p_\Delta^p \\ z \\ y \end{bmatrix} = \left[\begin{array}{c:ccc} A & B_\Delta & B_p & B_u \\ C_\Delta & D_{\Delta\Delta} & D_{\Delta p} & D_{\Delta u} \\ C_p & D_{p\Delta} & D_{pp} & D_{pu} \\ C_y & D_{y\Delta} & D_{yp} & D_{yu} \end{array} \right] \begin{bmatrix} x \\ q_\Delta^p \\ w \\ u \end{bmatrix} \\ \qquad q_\Delta = \Delta^P(t)p_\Delta, \quad \delta(t) \in \mathcal{F}_\delta^\eta, \end{cases}
\tag{2.114}
$$

where $q_\Delta \in \mathbb{R}^{n_{q_\Delta}^P}$, $p_\Delta \in \mathbb{R}^{n_{p_\Delta}^P}$.

(a) Generalized plant in general LPV representation $\mathcal{P}_\rho^\sigma$.

(b) Generalized LPV plant in linear fractional representation $\mathcal{P}_\delta^\eta$.
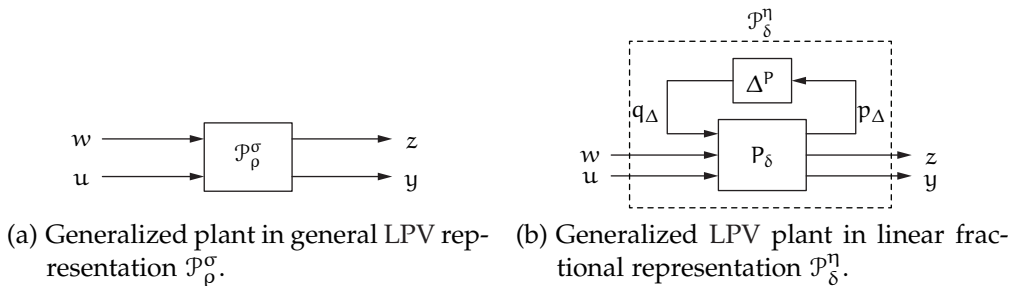
Figure 2.8: Generalized plant.

Consider an output-feedback LPV controller of the form

$$\mathcal{K}_\rho^\sigma : \begin{cases} \begin{bmatrix} \dot{x}^K \\ u \end{bmatrix} = \left[\begin{array}{c:c} A^K(\rho(t), \sigma(t)) & B_y^K(\rho(t)) \\ \hdashline C_u^K(\rho(t)) & D_{uy}^K(\rho(t)) \end{array} \right] \begin{bmatrix} x^K \\ y \end{bmatrix} \\ \rho(t) \in \mathcal{F}_\rho^\sigma, \end{cases}$$ (2.115)

where $x^K \in \mathbb{R}^{n_x^K}$, is the controller's state. An LFR of the controller can take the form

$$\mathcal{K}_\delta^\eta : \begin{cases} \begin{bmatrix} \dot{x}^K \\ u \\ p_\Delta^K \end{bmatrix} = \left[\begin{array}{c:cc} A^K & B_y^K & B_\Delta^K \\ \hdashline C_u^K & D_{uy}^K & D_{u\Delta}^K \\ C_\Delta^K & D_{\Delta y}^K & D_{\Delta\Delta}^K \end{array} \right] \begin{bmatrix} x^K \\ y \\ q_\Delta^K \end{bmatrix} \\ q_\Delta^K = \Delta^K(t) p_\Delta^K, \quad \delta(t) \in \mathcal{F}_\delta^\eta, \end{cases}$$ (2.116)

where $q_\Delta^K \in \mathbb{R}^{n_{q_\Delta}^K}$, $p_\Delta^K \in \mathbb{R}^{n_{p_\Delta}^K}$. As apparent from Eq. (2.115), the controller is generally allowed to depend also on the parameters' rate of change σ. Thus an LFR of the controller incorporates a parameter block $\Delta^K(\delta(t), \eta(t))$ that is a continuous matrix-valued function of the LFT parameter vector $\delta(t)$ *and* the associated rates $\eta(t)$.

$$\Delta^K(\delta(t), \eta(t)) \in \mathcal{C}^0(\boldsymbol{\delta} \times \boldsymbol{\eta}, \ \mathbb{R}^{n_{q_\Delta}^K \times n_{p_\Delta}^K}).$$

The interconnections

$$\mathcal{T}_\rho^\sigma = \mathcal{P}_\rho^\sigma \star \mathcal{K}_\rho^\sigma, \qquad \mathcal{T}_\delta^\eta = \mathcal{P}_\delta^\eta \star \mathcal{K}_\delta^\eta$$ (2.117)

denote the closed loop as illustrated in Figs. 2.9a–2.9b for general and LFT-LPV representations.

An explicit formula for the parameter-dependent closed-loop state space matrix linear in the controller matrix $K_\rho(\rho)$ can be obtained for plants with $D_{yu}(\rho) = 0$.

$$T_\rho(\rho) = T_{0,\rho}(\rho) + W_\rho(\rho) K_\rho(\rho) V_\rho(\rho) = \left[\begin{array}{c:c} \mathcal{A}(\rho) & \mathcal{B}_p(\rho) \\ \hdashline \mathcal{C}_p(\rho) & \mathcal{D}_{pp}(\rho) \end{array} \right]$$ (2.118)

$$= \left[\begin{array}{cc:c} A(\rho) & 0 & B_p(\rho) \\ 0 & 0 & 0 \\ \hdashline C_p(\rho) & 0 & D_{pp}(\rho) \end{array} \right] + \left[\begin{array}{c:c} 0 & B_u(\rho) \\ I & 0 \\ \hdashline 0 & D_{pu}(\rho) \end{array} \right] \times$$

$$\left[\begin{array}{c:c} A^K(\rho, \sigma) & B_y^K(\rho) \\ \hdashline C_u^K(\rho) & D_{uy}^K(\rho) \end{array} \right] \left[\begin{array}{cc:c} 0 & I & 0 \\ \hdashline C_y(\rho) & 0 & D_{yp}(\rho) \end{array} \right]$$ (2.119)

For LFRs, obtaining the closed-loop state space matrix linear in the controller matrix K_δ can be obtained by less restrictive assumptions on the plant. Specifically, for plants for which $D_{yu} = 0$, one has

$$T_\delta = T_{0,\delta} + W_\delta K_\delta V_\delta = \begin{bmatrix} \mathcal{A} & \mathcal{B}_\Delta & \mathcal{B}_p \\ \hline \mathcal{C}_\Delta & \mathcal{D}_{\Delta\Delta} & \mathcal{D}_{\Delta p} \\ \mathcal{C}_p & \mathcal{D}_{p\Delta} & \mathcal{D}_{pp} \end{bmatrix} \quad (2.120)$$

$$= \begin{bmatrix} A & 0 & B_\Delta & 0 & B_p \\ 0 & 0 & 0 & 0 & 0 \\ \hline C_\Delta & 0 & D_{\Delta\Delta} & 0 & D_{\Delta p} \\ 0 & 0 & 0 & 0 & 0 \\ \hline C_p & 0 & D_{p\Delta} & 0 & D_{pp} \end{bmatrix} + \begin{bmatrix} 0 & B_u & 0 \\ I & 0 & 0 \\ \hline 0 & D_{\Delta u} & 0 \\ 0 & 0 & I \\ \hline 0 & D_{pu} & 0 \end{bmatrix} \times$$

$$\begin{bmatrix} A^K & B^K_y & B^K_\Delta \\ \hline C^K_u & D^K_{uy} & D^K_{u\Delta} \\ C^K_\Delta & D^K_{\Delta y} & D^K_{\Delta\Delta} \end{bmatrix} \begin{bmatrix} 0 & I & 0 & 0 & 0 \\ C_y & 0 & D_{y\Delta} & 0 & D_{yp} \\ 0 & 0 & 0 & I & 0 \end{bmatrix} \quad (2.121)$$

The closed-loop parameter block is therefore

$$\Delta\big(\delta(t),\eta(t)\big) = \begin{bmatrix} \Delta^P(\bullet) & \\ & \Delta^K(\bullet) \end{bmatrix} \in \mathcal{C}^0(\delta \times \eta,\ \mathbb{R}^{n_{q_\Delta} \times n_{p_\Delta}}),$$

where $n_{p_\Delta} = n^P_{p_\Delta} + n^K_{p_\Delta}$ and $n_{q_\Delta} = n^P_{q_\Delta} + n^K_{q_\Delta}$.

(a) Closed-Loop interconnection of generalized LPV plant and LPV controller in general LPV representation $\mathcal{T}^\sigma_\rho$.

(b) Closed-Loop interconnection of generalized LPV plant and LPV controller in LFR $\mathcal{T}^\eta_\delta$.
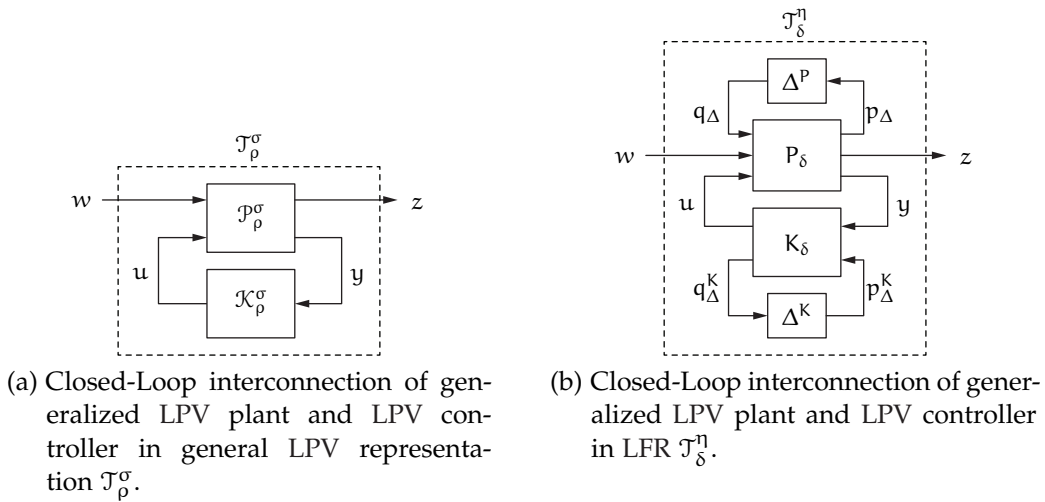
Figure 2.9: Closed-Loop interconnection of generalized LPV plant and LPV controller.

2.3.2 Controller Elimination and Explicit Solutions

A particular approach to LPV output-feedback or state-feedback controller synthesis is based on first eliminating the controller variables and obtaining conditions on the existence of stabilizing controllers that guarantee some degree of performance for the entire range of parameters. After such existence conditions have been solved, the controller parameters can be obtained by algebraic manipulations or by solving additional LMI problems.

For the purpose of the presentation of these techniques, consider the following assumptions on the plant [163].

(A2.1) **Parameter-Dependent Stabilizability:**
The pair $\big(A(\rho), B_u(\rho)\big)$ is parameter-dependent stabilizable for all $\rho(t) \in \mathcal{F}_\rho^\sigma$.

(A2.2) **Parameter-Dependent Detectability:**
The pair $\big(A(\rho), C_y(\rho)\big)$ is parameter-dependent detectable for all $\rho(t) \in \mathcal{F}_\rho^\sigma$.

(A2.3) **Full Output Gain Rank:**
The matrix $\big[C_y(\rho) \; D_{yp}(\rho)\big]$ has full row rank for all $\rho(t) \in \mathcal{F}_\rho^\sigma$.

(A2.4) **Full Input Gain Rank:**
The matrix $\big[B_u^\top(\rho) \; D_{pu}^\top(\rho)\big]$ has full row rank for all $\rho(t) \in \mathcal{F}_\rho^\sigma$.

(A2.5) **Strictly Proper System:**
There is no direct feedthrough in the control channel, i. e.,
$D_{yu}(\rho) = 0$.

(A2.6) **Absence of Performance Feedthrough:**
There is no direct feedthrough in the performance channel, i. e., $D_{pp}(\rho) = 0$.

Ass. (A2.1)–(A2.4), guarantee the existence of a stabilizing output-feedback LPV controller. Ass. (A2.5)–(A2.6) simplify the controller formula presented later on. The following theorem provides conditions on the existence of a stabilizing gain-scheduled output-feedback controller that guarantees a certain performance of the closed-loop system.

Theorem 2.13 (Controller Existence Conditions [3, 163])
Under Ass. (A2.1)–(A2.4), there exists a controller $\mathcal{K}_\rho^\sigma$ that renders the closed-loop system $\mathcal{T}_\rho^\sigma$ as defined in (2.7) asymptotically stable over $\boldsymbol{\rho} \times \boldsymbol{\sigma}$ with an induced $\mathcal{L}_2$-norm from $w \to z$ bounded from above by $\gamma > 0$, if there exist $R(\rho) \in \mathcal{C}^1(\boldsymbol{\rho}, \mathbb{S}^{n_x})$, $S(\rho) \in \mathcal{C}^1(\boldsymbol{\rho}, \mathbb{S}^{n_x})$ with $R(\rho) \succ 0$, $S(\rho) \succ 0$ that satisfy $\forall \, (\rho, \sigma) \in (\boldsymbol{\rho} \times \boldsymbol{\sigma})$

$$\mathcal{L}_R(\rho,\sigma) = N_R^\top(\rho) \begin{bmatrix} \bullet \\ \bullet \end{bmatrix}^\top \begin{bmatrix} \partial R(\rho,\sigma) & R(\rho) & \\ R(\rho) & 0 & \\ \hline & & \Gamma \end{bmatrix} \begin{bmatrix} I & 0 \\ A(\rho) & B_P(\rho) \\ \hline 0 & I \\ C_P(\rho) & D_{PP}(\rho) \end{bmatrix} N_R(\rho) \prec 0, \qquad (2.122)$$

$$\mathcal{L}_S(\rho, \sigma) = N_S^\top(\rho) \begin{bmatrix} \bullet \\ \bullet \end{bmatrix}^\top \begin{bmatrix} \begin{array}{cc} 0 & S(\rho) \\ S(\rho) & \partial S(\rho, \sigma) \end{array} & \\ & \Gamma^{-1} \end{bmatrix} \begin{bmatrix} -A^\top(\rho) & -C_p^\top(\rho) \\ I & 0 \\ \hline -B_p^\top(\rho) & -D_{pp}^\top(\rho) \\ 0 & I \end{bmatrix} N_S(\rho) \succ 0, \quad (2.123)$$

as well as $\forall \rho \in \boldsymbol{\rho}$

$$\mathcal{L}_{RS}(\rho) = \begin{bmatrix} R(\rho) & I \\ I & S(\rho) \end{bmatrix} \succ 0, \quad (2.124)$$

where

$$N_R(\rho) = \ker\left(\begin{bmatrix} C_y(\rho) & D_{yp}(\rho) \end{bmatrix}\right), \quad (2.125)$$

$$N_S(\rho) = \ker\left(\begin{bmatrix} B_u^\top(\rho) & D_{pu}^\top(\rho) \end{bmatrix}\right). \quad (2.126)$$

$\square$

Proof: The proof follows from the application of Lma. A.8 on page 321, using both Cond. (2.67) and its dual (2.70). Partition $\mathcal{X}(\rho)$ from Cond. (2.67) and $\mathcal{Y}(\rho)$ from Cond. (2.70) with dimensions compatible with the block matrix $\mathcal{A}(\rho)$ from (2.118) as

$$\mathcal{X}(\rho) = \begin{bmatrix} R(\rho) & R_1(\rho) \\ R_1^\top(\rho) & R_2(\rho) \end{bmatrix}, \quad \mathcal{Y}(\rho) = \mathcal{X}^{-1}(\rho) = \begin{bmatrix} S(\rho) & S_1(\rho) \\ S_1^\top(\rho) & S_2(\rho) \end{bmatrix}$$

and observe that only both upper left blocks of the Lyapunov matrices remain after eliminating the controller. Condition (2.124) results from the coupling condition on the primal and dual Lyapunov matrices $\mathcal{X}(\rho)\mathcal{Y}(\rho) = I$. To see this, employ the congruence transformation

$$T_S = \begin{bmatrix} S(\rho) & I \\ S_1^\top(\rho) & 0 \end{bmatrix}, \quad T_R = \begin{bmatrix} I & R(\rho) \\ 0 & R_1^\top(\rho) \end{bmatrix},$$

s.t.

$$T_S^\top \mathcal{X}(\rho) T_S = T_R^\top \mathcal{Y}(\rho) T_R = \begin{bmatrix} S(\rho) & I \\ I & R(\rho) \end{bmatrix} \succ 0.$$

$\blacksquare$

Under the Ass. (A2.5) and (A2.6), the following formulae can be used to contruct the output-feedback controller $\mathcal{K}_\rho^\sigma$ [161, 163] once a solution to the conditions of Thm. 2.13 has been obtained, s.t. both $R(\rho)$ and $S(\rho)$ are known.

(i) Let $M(\rho)N^\top(\rho) = I - S(\rho)R(\rho)$ and define

$$F(\rho) = -\left(D_{pu}^\top(\rho)D_{pu}(\rho)\right)^{-1}\left(\gamma B_u^\top(\rho)S^{-1}(\rho) + D_{pu}^\top(\rho)C_p(\rho)\right), \quad (2.127)$$

$$L(\rho) = -\left(\gamma R^{-1}(\rho)C_y^\top(\rho) + B_p(\rho)D_{yp}^\top(\rho)\right)\left(D_{yp}(\rho)D_{yp}^\top(\rho)\right)^{-1}, \quad (2.128)$$

(ii) Using these definitions, the state space matrix $K_\rho^\sigma(\rho, \sigma)$ is constructed from

$$A^K(\rho, \sigma) = -N^{-1}(\rho)\Big(-R(\rho)\partial S(\rho) - N(\rho)\partial M^\top(\rho)$$

$$+ A^\top(\rho) + R(\rho)\Big(A(\rho) + B_u(\rho)F(\rho) + L(\rho)C_y(\rho)\Big)S(\rho)$$

$$+ \gamma^{-1}R(\rho)\Big(B_p(\rho) + L(\rho)D_{yp}(\rho)\Big)B_p^\top(\rho)$$

$$+ \gamma^{-1}C_p(\rho)\Big(C_p^\top(\rho) + D_{pu}(\rho)F(\rho)\Big)S(\rho)\Big)M^{-\top}(\rho), \quad (2.129)$$

$$B_y^K(\rho) = N^{-1}(\rho)R(\rho)L(\rho), \quad (2.130)$$

$$C_u^K(\rho) = F(\rho)S(\rho)M^{-\top}(\rho), \quad (2.131)$$

$$D_{uy}^K(\rho) = 0. \quad (2.132)$$

In the state-feedback case, Ass. (A2.2) is not required due to the full information on the system's state. Consequently, Ass. (A2.3) is trivially fulfilled, as are Ass. (A2.5) and (A2.6). Thus, further assumptions on the plant are

(A2.7) $C_y(\rho(t)) = I$ and $D_{yp}(\rho(t)) = 0$.

In [160], more strict assumptions on the plant matrices are made, s.t. the generalized plant has the form

$$P_\rho(\rho(t)) = \begin{bmatrix} A(\rho(t)) & B_p(\rho(t)) & B_u \\ \begin{bmatrix} C_{p,1} \\ C_{p,2} \end{bmatrix} & 0 & \begin{bmatrix} 0 \\ I \end{bmatrix} \\ I & 0 & 0 \end{bmatrix}. \quad (2.133)$$

While this simplifies the solution and is in general not difficult to fulfill, a more general solution with a state-feedback gain formula as from Eq. (2.127) can be obtained as follows.

The following theorem provides conditions on the existence of a stabilizing gain-scheduled state-feedback controller that guarantees a certain performance of the closed-loop system.

Theorem 2.14 (State-Feedback Controller Synthesis [160])
Under Ass. (A2.1) and (A2.4)–(A2.7), there exists a state-feedback controller gain $F(\rho)$ that renders the closed-loop system $\mathcal{T}_\rho^\sigma$ as defined in (2.7) asymptotically stable over $\rho \times \sigma$ with an induced $\mathcal{L}_2$-norm from $w \to z$ bounded from above by $\gamma > 0$, if there exists $S(\rho) \in \mathcal{C}^1(\rho, \mathbb{S}^{n_x})$ with $S(\rho) \succ 0$ that satisfies

$$N_S^\top(\rho)\begin{bmatrix} \bullet \\ \bullet \\ \bullet \end{bmatrix}^\top \begin{bmatrix} \begin{array}{cc} 0 & S(\rho) \\ S(\rho) & \partial S(\rho, \sigma) \end{array} & \\ & \Gamma^{-1} \end{bmatrix} \begin{bmatrix} -A^\top(\rho) & -C_p^\top(\rho) \\ I & 0 \\ -B_p^\top(\rho) & 0 \\ 0 & I \end{bmatrix} N_S(\rho) \succ 0, \quad \begin{array}{c} \forall (\rho, \sigma) \\ \in (\boldsymbol{\rho} \times \boldsymbol{\sigma}) \end{array}$$

$$(2.134)$$

where

$$N_S = \ker\left(\begin{bmatrix} B_u^\top(\rho) & D_{pu}^\top(\rho) \end{bmatrix}\right).$$

The parameter-dependent state-feedback gain is then given by Eq. (2.127). □

    Proof: The proof can be found in App. B.2 on p. 327. ∎

    The problem of synthesizing an estimator gain $L(\rho)$ is the dual problem to synthesizing a state-feedback gain $F(\rho)$ and is performed using the primal matrix inequality Cond. (2.122) and the observer gain formula (2.128). The required associated dual assumption on the plant matrices is then

    (**A2.8**) $B_u\big(\rho(t)\big) = 0$ and $D_{pu}\big(\rho(t)\big) = I.$

2.3.3 *Gridding-Based Synthesis*

In gridding-based LPV synthesis approaches [3, 160] the inequalities (2.122)–(2.124) are solved on a set of points covering the parameter signal range and their associated rates of variation $\rho \times \sigma$. An evenly spaced grid can be chosen, but also additional points can be added by the designer, where a higher density is required. Note that the terms $\partial R(\rho, \sigma)$ and $\partial S(\rho, \sigma)$ and accordingly the matrix inequalities (2.122)–(2.123) are affine in the parameters' rate of change σ using a PDLF Ansatz, s. t. only the extremes need to be checked.

    The technique is applicable to LPV plants with general parameter-dependency, requiring neither polytopic nor LFT representations. Since the gridding is not restricted to convex regions, model elements such as look-up tables (LUTs) can be readily incorporated in the design. Accordingly, the Lyapunov variable can be parameterized by general parameter-dependency. Since this approach does not provide any rigorous guarantees for closed-loop stability and performance, the analysis inequality (2.67) is usually checked on a much denser grid *a posteriori*. It, however, suffices to perform eigenvalue tests, instead of solving semi-definite programs again, [73].

    If this analysis step fails, the grid density is increased (at least locally) and the synthesis step is repeated. An iteration between analysis and synthesis is conducted until local guarantees are established on a sufficiently dense grid.

    The implementation of the controller is computationally inexpensive, but may require large amounts of memory, in order to store the local controllers. The implementation scheme may consider an interpolation or a switching between local controllers. In general, this approach is limited to few scheduling signals because of the exponential increase in grid points, hence memory requirements or interpolation complexity. Closed-form controller formulae can be applied instead, shifting the complexity to online computing. Especially in the light of microprocessors limited in precision and/or computing power, the gridded LUT-based implementation is attractive, but applies to the other synthesis methods as well. I. e., also controller matrices K_δ or K_δ derived from polytopic and LFT-based controller representations can be gridded in terms of the scheduling signals ρ and implemented in LUTs.

If observer-based state-feedback synthesis is performed, parameter-dependent state-feedback matrices of both observer and controller can be computed online each essentially by a single matrix inversion without the need to store multiple controllers in memory [E83–E85]. Via a loop-shaping approach frequency-dependent characteristics as in the output-feedback case can be achieved, while observer and state-feedback gains can be synthesized sequentially via projection or a linearizing change of variables each at the cost of approximately the analysis problem (2.67) instead of the two projected LMIs. This can—in some sense—alleviate the relatively high complexity of the gridding approach.

2.3.4 *Polytopic Synthesis*

If the system $\mathcal{P}_\rho^\sigma$ as defined in (2.113) admits an affine/polytopic LPV representation $\mathcal{P}_\theta^\gamma$ with

$$
P_\theta\big(\theta(t)\big) = \left[\begin{array}{c|cc} A\big(\theta(t)\big) & B_p\big(\theta(t)\big) & B_u \\ \hline C_p\big(\theta(t)\big) & D_{pp} & D_{pu} \\ C_y & D_{yp} & 0 \end{array}\right]
$$

and the parameter-dependence of the Lyapunov variables $R(\theta)$ and $S(\theta)$ is dropped at the expense of conservatism, the existence conditions (2.122)–(2.124) can be solved in the vertices $\theta_{v,l}$, $l \in \{1, \dots, n_v\}$ of the convex hull $\mathrm{conv}\,(\theta)$ that includes the parameter set θ [6]. If the conditions are solved on the hyperbox $\mathrm{hyp}\,(\theta)$, one has $n_v = 2^{n_\theta}$.

If $R(\theta)$ and $S(\theta)$ are chosen to depend affinely on the parameters θ, a multi-convexity approach [42] can be used to introduce additional constraints

$$
\frac{\partial^2}{\partial \theta_i^2} \mathcal{L}_R\big(\theta, \nu\big) \succcurlyeq 0, \quad \frac{\partial^2}{\partial \theta_i^2} \mathcal{L}_S\big(\theta, \nu\big) \preccurlyeq 0, \quad i \in \{1, \dots, n_\theta\}. \tag{2.135}
$$

These conditions allow to still solve the inequalities on a finite set of vertices [42]. If the performance channel, or more specifically matrices $B_p\big(\theta(t)\big)$ and $C_p\big(\theta(t)\big)$ are parameter-independent, the multi-convexity constraints can be reduced to

$$
\frac{\partial^2}{\partial \theta_i^2} \Big(\partial R(\theta, \nu) + R(\theta) A(\theta) + A^\top(\theta) R(\theta) \Big) \succcurlyeq 0, \quad i \in \{1, \dots, n_\theta\},
$$

$$
-\frac{\partial^2}{\partial \theta_i^2} \Big(\partial S(\theta, \nu) + S(\theta) A^\top(\theta) + A(\theta) S(\theta) \Big) \preccurlyeq 0, \quad i \in \{1, \dots, n_\theta\}.
$$

Matrix inequalities (2.122)–(2.123) will be affine in ν and assuming that $n_\nu \leqslant n_\theta$ of the parameters have a non-zero rate of change and/or are considered in the parameter-dependent Lyapunov function (PDLF), the number of vertices increases to $n_v = 2^{n_\theta + n_\nu}$.

The controller is computed online as a weighted sum of the vertex controllers, which may be obtained explicitly. So-called overbounding may occur, i. e., guarantees are provided for portions of the scheduling signal range, that are not physically

admissible. In many applications, the parameter polytope can be optimized to either cover the parameter set more closely and/or use less vertices than incurred by naively considering a hyperbox.

2.3.5 *Multiplier-Based Synthesis*

By means of the FBSP and a quadratic Ansatz for PDLFs, the controller existence conditions of Thm. 2.13 can be formulated as a convex optimization problem as follows.

Theorem 2.15 (Controller Existence Conditions, PDLF [163])
Under Ass. (A2.1)–(A2.6), there exists a controller $\mathcal{K}_\delta^\eta$ given by Eqs. (2.127)–(2.132) that renders the closed-loop system $\mathcal{T}_\delta^\eta$ as defined in (2.20) asymptotically stable over $\delta \times \eta$ with an induced $\mathcal{L}_2$-norm from $w \to z$ bounded from above by $\gamma > 0$, if there exist $M \in S^{(n_{P_\Delta}^R + n_{q_\Delta}^R)}$, $N \in S^{(n_{P_\Delta}^S + n_{q_\Delta}^S)}$, $P \in S^{(n_{P_\Delta}^{RS} + n_{q_\Delta}^{RS})}$ and for quadratic functions

$$R(\delta) = Q_R(\delta)^\top R Q_R(\delta) \in \mathcal{C}^1(\delta, S^{n_x}), \quad R(\delta) \succ 0 \; \forall \delta \in \delta,$$
$$S(\delta) = Q_S(\delta)^\top S Q_S(\delta) \in \mathcal{C}^1(\delta, S^{n_x}), \quad S(\delta) \succ 0 \; \forall \delta \in \delta,$$

with

$$Q_R(\delta) = \Delta_R(\delta) \star \begin{bmatrix} Q_{R,11} & Q_{R,12} \\ Q_{R,21} & Q_{R,22} \end{bmatrix} \in \mathcal{C}^1(\delta, \mathbb{R}^{n_R \times n_x})$$

$$Q_S(\delta) = \Delta_S(\delta) \star \begin{bmatrix} Q_{S,11} & Q_{S,12} \\ Q_{S,21} & Q_{S,22} \end{bmatrix} \in \mathcal{C}^1(\delta, \mathbb{R}^{n_S \times n_x})$$

there exist $R \in S^{n_R}$, $S \in S^{n_S}$ and $\gamma > 0$ that satisfy

$$\mathcal{L}_{R,M} = \begin{bmatrix} \bullet \\ \bullet \\ \bullet \end{bmatrix}^\top \begin{bmatrix} M & & \\ & \begin{matrix} 0 & R \\ R & 0 \end{matrix} & \\ & & \Gamma \end{bmatrix} \begin{bmatrix} B_{R,11} & B_{R,12} \\ I & 0 \\ B_{R,21} & B_{R,22} \end{bmatrix} \prec 0, \tag{2.136}$$

$$\mathcal{L}_{S,N} = \begin{bmatrix} \bullet \\ \bullet \\ \bullet \end{bmatrix}^\top \begin{bmatrix} N & & \\ & \begin{matrix} 0 & S \\ S & 0 \end{matrix} & \\ & & \Gamma^{-1} \end{bmatrix} \begin{bmatrix} I & 0 \\ B_{S,11} & B_{S,12} \\ B_{S,21} & B_{S,22} \end{bmatrix} \succ 0, \tag{2.137}$$

$$\mathcal{L}_{RS,P} = \begin{bmatrix} \bullet \\ \bullet \\ \bullet \end{bmatrix}^\top \begin{bmatrix} P & & \\ & \begin{matrix} R & 0 \\ 0 & S \end{matrix} & \\ & & \begin{matrix} 0 & I \\ I & 0 \end{matrix} \end{bmatrix} \begin{bmatrix} B_{RS,11} & B_{RS,12} \\ I & 0 \\ B_{RS,21} & B_{RS,22} \end{bmatrix} \succcurlyeq 0, \tag{2.138}$$

and

$$\mathcal{L}_M(\delta, \eta) = \begin{bmatrix} \bullet \\ \bullet \end{bmatrix}^\top M \begin{bmatrix} I \\ \hline \Delta_{B_R}(\delta, \eta) \end{bmatrix} \succ 0, \ \forall (\delta, \eta) \in (\boldsymbol{\delta} \times \boldsymbol{\eta}) \tag{2.139}$$

$$\mathcal{L}_N(\delta, \eta) = \begin{bmatrix} \bullet \\ \bullet \end{bmatrix}^\top N \begin{bmatrix} \Delta_{B_S}(\delta, \eta) \\ \hline I \end{bmatrix} \prec 0, \ \forall (\delta, \eta) \in (\boldsymbol{\delta} \times \boldsymbol{\eta}) \tag{2.140}$$

$$\mathcal{L}_P(\delta) = \begin{bmatrix} \bullet \\ \bullet \end{bmatrix}^\top P \begin{bmatrix} I \\ \hline \Delta_{B_{RS}}(\delta) \end{bmatrix} \prec 0, \ \forall \delta \in \boldsymbol{\delta} \tag{2.141}$$

where the definitions of the outer factors is given in full detail in Sect. B.3 in the appendix.
□

Proof: The proof follows from application of the FBSP on the conditions of Thm. 2.13 [163]. ■

The somewhat complicated formulae for the matrix inequalities in Thm. 2.15 allow to prove the existence of a gain-scheduled controller via the parameter-independent matrix inequalities (2.136)–(2.138) and the multiplier conditions (2.139) and (5.13) that are now only quadratic in the parameters. Before detailing how to solve these parameter-dependent matrix inequalities efficiently, simplified conditions for the case, when only some of the parameters are treated via an LFR and multiplier techniques are presented, while the Lyapunov variables are dependent on general parameters. The following result follows from first applying the FBSP on the PDBRL with respect to parameters pulled out in an LFT interconnection and the subsequent application of the Parameter Elimination Lemma A.8.

Theorem 2.16 (Controller Existence Conditions, PDLF [161])
Under Ass. (A2.1)–(A2.4), there exists a controller $\mathcal{K}_\rho^\sigma$ that renders the closed-loop system $\mathcal{T}_\rho^\sigma$ as defined in (2.7) in mixed general/LFT-LPV form as given in (2.24) asymptotically stable over $\boldsymbol{\rho} \times \boldsymbol{\sigma}$ with an induced $\mathcal{L}_2$-norm from $w \to z$ bounded from above by $\gamma > 0$, if there exist $R(\rho) \in \mathcal{C}^1(\boldsymbol{\rho}, \mathbb{S}^{n_x}), S(\rho) \in \mathcal{C}^1(\boldsymbol{\rho}, \mathbb{S}^{n_x})$ with $R(\rho) \succ 0, S(\rho) \succ 0$ and $M \in \mathbb{S}^{(n_{q_\Delta}^P + n_{p_\Delta}^P)}, N \in \mathbb{S}^{(n_{q_\Delta}^P + n_{p_\Delta}^P)}$ that satisfy

$$\mathcal{L}_{R,M}(\rho, \sigma) = N_{R,M}^\top(\rho) \begin{bmatrix} \bullet \\ \bullet \end{bmatrix}^\top \begin{bmatrix} M & & & \\ & \partial R(\rho, \sigma) & R(\rho) & \\ & R(\rho) & 0 & \\ & & & \Gamma \end{bmatrix}$$

$$\times \begin{bmatrix} G_{R,11}(\rho) & G_{R,12}(\rho) \\ I & 0 \\ \hline G_{R,21}(\rho) & G_{R,22}(\rho) \end{bmatrix} N_{R,M}(\rho) \prec 0, \ \begin{matrix} \forall (\rho, \sigma) \\ \in (\boldsymbol{\rho} \times \boldsymbol{\sigma}) \end{matrix} \tag{2.142}$$

$$
\mathcal{L}_{S,N}(\rho,\sigma) = N_{S,N}^{\top}(\rho)
\begin{bmatrix} \bullet \\ \bullet \end{bmatrix}^{\top}
\left[\begin{array}{c:cc:c}
N & & & \\ \hdashline
& 0 & S(\rho) & \\
& S(\rho) & \partial S(\rho,\sigma) & \\ \hdashline
& & & \Gamma^{-1}
\end{array}\right]
\tag{2.143}
$$

$$
\times
\left[\begin{array}{cc}
I & 0 \\ \hdashline
G_{S,11}(\rho) & G_{S,12}(\rho) \\ \hdashline
G_{S,21}(\rho) & G_{S,22}(\rho)
\end{array}\right]
N_{S,N}(\rho) \succ 0,
\begin{array}{c}
\forall\,(\rho,\sigma) \\
\in (\boldsymbol{\rho}\times\boldsymbol{\sigma})
\end{array}
$$

$$
\mathcal{L}_{RS}(\rho) =
\begin{bmatrix}
R(\rho) & I \\
I & S(\rho)
\end{bmatrix} \succ 0, \quad \forall \rho \in \boldsymbol{\rho},
\tag{2.144}
$$

$$
\mathcal{L}_{M}(\delta) =
\begin{bmatrix} \bullet \\ \bullet \end{bmatrix}^{\top}
M
\left[\begin{array}{c}
I \\ \hdashline
\Delta^{P}(\delta)
\end{array}\right] \succ 0, \quad \forall \delta \in \boldsymbol{\delta}
\tag{2.145}
$$

$$
\mathcal{L}_{N}(\delta) =
\begin{bmatrix} \bullet \\ \bullet \end{bmatrix}^{\top}
N
\left[\begin{array}{c}
-\Delta^{P\top}(\delta) \\ \hdashline
I
\end{array}\right] \prec 0, \quad \forall \delta \in \boldsymbol{\delta}
\tag{2.146}
$$

where

$$
N_{R,M}(\rho) = \ker\left(\begin{bmatrix} D_{y\Delta}(\rho) & C_{y}(\rho) & D_{yp}(\rho) \end{bmatrix}\right),
\tag{2.147}
$$

$$
N_{S,N}(\rho) = \ker\left(\begin{bmatrix} D_{\Delta u}^{\top}(\rho) & B_{u}^{\top}(\rho) & D_{pu}^{\top}(\rho) \end{bmatrix}\right).
\tag{2.148}
$$

and

$$
\begin{bmatrix}
G_{R,11}(\rho) & G_{R,12}(\rho) \\ \hdashline
G_{R,21}(\rho) & G_{R,22}(\rho)
\end{bmatrix} =
\left[\begin{array}{c:cc}
D_{\Delta\Delta}(\rho) & C_{\Delta}(\rho) & D_{\Delta p}(\rho) \\ \hdashline
0 & I & 0 \\
B_{\Delta}(\rho) & A(\rho) & B_{p}(\rho) \\ \hdashline
0 & 0 & I \\
D_{p\Delta}(\rho) & C_{p}(\rho) & D_{pp}(\rho)
\end{array}\right]
\tag{2.149}
$$

$$
\begin{bmatrix}
G_{S,11}(\rho) & G_{S,12}(\rho) \\ \hdashline
G_{S,21}(\rho) & G_{S,22}(\rho)
\end{bmatrix} =
\left[\begin{array}{c:cc}
-D_{\Delta\Delta}^{\top}(\rho) & -B_{\Delta}^{\top}(\rho) & -D_{p\Delta}^{\top}(\rho) \\
-C_{\Delta}^{\top}(\rho) & -A^{\top}(\rho) & -C_{p}^{\top}(\rho) \\ \hdashline
0 & I & 0 \\ \hdashline
-D_{\Delta p}^{\top}(\rho) & -B_{p}^{\top}(\rho) & -D_{pp}^{\top}(\rho) \\
0 & 0 & I
\end{array}\right]
\tag{2.150}
$$

$\square$

Proof: The proof follows from application of the Parameter Elimination Lemma A.8 on page 321 on the conditions of Thm. 2.9 and its dual [161]. ∎

The result of Thm. 2.16 is easily specialized to the fully PıDLF case [125] and is presented for completeness. Instead of Ass. (A2.5) a milder assumption can be used on the LFT-LPV plant representation:

(**A2.9**) There is no direct feedthrough in the control channel, i. e.,
$D_{yu} = 0$.

Theorem 2.17 (Controller Existence Conditions, PiDLF [124, 125])

Under Ass. (A2.9), there exists a controller $\mathcal{K}_\delta$ that renders the closed-loop system $\mathcal{T}_\delta$ as defined in (2.15) asymptotically stable over δ with an induced $\mathcal{L}_2$-norm from $w \to z$ bounded from above by $\gamma > 0$, if there exist $R, S \in \mathbb{S}^{n_x}$ with $R \succ 0$, $S \succ 0$ and $M \in \mathbb{S}^{(n_{q_\Delta}^P + n_{p_\Delta}^P)}$, $N \in \mathbb{S}^{(n_{q_\Delta}^P + n_{p_\Delta}^P)}$ that satisfy

$$\mathcal{L}_{R,M} = N_R^\top \begin{bmatrix} \bullet \\ \vdots \\ \bullet \end{bmatrix}^\top \begin{bmatrix} M & & \\ & \begin{matrix} 0 & R \\ R & 0 \end{matrix} & \\ & & \Gamma \end{bmatrix} \begin{bmatrix} G_{R,11} & G_{R,12} \\ I & 0 \\ G_{R,21} & G_{R,22} \end{bmatrix} N_R \prec 0, \tag{2.151}$$

$$\mathcal{L}_{S,N} = N_S^\top \begin{bmatrix} \bullet \\ \vdots \\ \bullet \end{bmatrix}^\top \begin{bmatrix} N & & \\ & \begin{matrix} 0 & S \\ S & 0 \end{matrix} & \\ & & \Gamma^{-1} \end{bmatrix} \begin{bmatrix} I & 0 \\ G_{S,11} & G_{S,12} \\ G_{S,21} & G_{S,22} \end{bmatrix} N_R \succ 0, \tag{2.152}$$

$$\mathcal{L}_{R,S} = \begin{bmatrix} R & 0 \\ 0 & S \end{bmatrix} \succcurlyeq 0, \tag{2.153}$$

and

$$\mathcal{L}_M(\delta) = \begin{bmatrix} \bullet \\ \vdots \\ \bullet \end{bmatrix}^\top M \begin{bmatrix} I \\ \Delta^P \end{bmatrix} \succ 0, \quad \forall \delta \in \boldsymbol{\delta} \tag{2.154}$$

$$\mathcal{L}_N(\delta) = \begin{bmatrix} \bullet \\ \vdots \\ \bullet \end{bmatrix}^\top N \begin{bmatrix} -\Delta^{P\top} \\ I \end{bmatrix} \prec 0, \quad \forall \delta \in \boldsymbol{\delta} \tag{2.155}$$

where

$$N_R = \ker\left(\begin{bmatrix} D_{y\Delta} & C_y & D_{yp} \end{bmatrix}\right), \quad N_S = \ker\left(\begin{bmatrix} D_{\Delta u}^\top & B_u^\top & D_{pu}^\top \end{bmatrix}\right).$$

and $G_{R,ij}$, $G_{S,ij}$, $i, j \in \{1, 2\}$ from (B.6) and (B.8). □

Proof: The proof follows from application of the Parameter Elimination Lemma A.8 on page 321 on the conditions of Thm. 2.11 and its dual Thm. 2.12 [125]. ∎

The resemblance of the conditions of Thm. 2.17 with the conditions of Thm. 2.15 for the special case that PiDLFs are used is striking. However, note that due to the fact that the Parameter Elimination Lemma A.8 and FBSP are applied in reversed order as compared to Thm. 2.15, the elimination of the controller is performed via parameter-independent kernel matrices. Consequently, an even larger reduction in the size of the multiplier conditions is achieved than when considering PiDLFs in Thm. 2.15. A further advantage resides in the fact that from the multipliers M and N as well as from the Lyapunov variables R and S, the closed-loop multiplier $\mathcal{M}$ and Lyapunov matrix $\mathcal{X}$ can be reconstructed by algebraic manipulations. Under the constraint that FBM are chosen, these algebraic reconstructions allow to find a

parameter block $\Delta^K(\delta)$ that renders the multiplier condition in Thm. 2.11 fulfilled, while the controller matrices can be obtained by solving matrix inequality (2.87). After a Schur complement this boils down to an LMI in the controller variables.

2.3.5.1 *Controller Construction in the* PDLF *Case*

Since Thm. 2.15 simply results from the application of the FBSP to the projected PDBRL of Thm. 2.13, the closed-form formulae (2.127)–(2.132) apply directly.

2.3.5.2 *Controller Construction in the mixed* PDLF/PiDLF *Case*

The controller construction in the mixed gridding/multiplier-based synthesis framework presented in Thm. 2.16 [161] consequently requires a mixture of the techniques for the algebraic reconstruction of the closed-loop multiplier $\mathcal{M}$ and the construction of the controller's parameter block $\Delta^K(\Delta^P)$ with the algebraic computation of controller variables. The result of a special case from [161] is highlighted here, which provides the additional important result that an LFT-LPV controller can always be chosen to depend affinely on its parameter block, if the generalized plant has affine dependence on the parameter block, as well. The explicit result can be found in App. B.4 on p. 330.

The details of the algebraic reconstruction of the closed-loop multiplier $\mathcal{M}$ do not differ from the fully PiDLF case and are presented in the subsequent section.

2.3.5.3 *Controller Construction in the* PiDLF *Case*

Formulae (2.127)–(2.132) simplify considerably for PiDLFs and can be completely devoid of matrix inverses if the matrices $D_{pu}(\rho)$ and $D_{yp}(\rho)$ related to the performance channel are parameter-independent. A symbolic preprocessing might therefore yield controller formulae that are inexpensive to evaluate in each instant.

However, it may be often desirable to impose further optimization criteria on controller variables, such as minimizing the spectral radius of the matrix A^K in an LFR. Obtaining an explicit LFR of the controller by solving matrix inequality (2.87) for the controller variables therefore provides means for systematic implementation and further optimization within the limits of the existence guarantees. In order to do so, the closed-loop Lyapunov matrix $\mathcal{X}$ and multiplier $\mathcal{M}$ need to be reconstructed.

Reconstruction of the Closed-Loop Lyapunov Matrix
From the relation of the Lyapunov variables R and S to the closed-loop Lyapunov matrix $\mathcal{X}$ and its inverse $\mathcal{Y}$

$$\mathcal{X} = \begin{bmatrix} R & \bullet \\ \bullet & \bullet \end{bmatrix}, \quad \mathcal{X}^{-1} = \mathcal{Y} = \begin{bmatrix} S & \bullet \\ \bullet & \bullet \end{bmatrix},$$

the closed-loop Lyapunov matrix is reconstructed as

$$\mathcal{X} = \begin{bmatrix} R & Z \\ Z^\top & (Z^\top(R-S^{-1})Z)^{-1} \end{bmatrix} \succ 0, \tag{2.156}$$

where the columns of Z form an orthogonal basis of $\mathrm{im}(R-S^{-1})$ [125]. In fact, any non-singular matrix Z would be valid, but experience suggests better numerical behaviour with an orthogonal matrix. Since from (2.153) and by a Schur Complement argument $(R-S^{-1}) \succ 0$, one can observe that from Lma. A.1 on page 315, the $(1,1)$-block of $\mathcal{X}^{-1}$ is indeed

$$\left(R - ZZ^\top(R-S^{-1})ZZ^\top\right)^{-1} = S.$$

RECONSTRUCTION OF THE CLOSED-LOOP MULTIPLIER
Quite analogously to the reconstruction of the closed-loop Lyapunov matrix, the closed-loop multiplier has to be obtained. However, instead of a simple positive-definiteness requirement, the closed-loop multiplier has to fulfill a closed-loop quadratic matrix inequality, which contains a further unknown—the controller's parameter block that implements the actual scheduling policy. In the following, it is detailed how this policy is influenced by closed-loop multiplier reconstruction, which in turn is influenced by structural constraints imposed during the solution of the existence conditions.

Lemma 2.4 (Reconstruction of the Closed-Loop Multiplier)
Let the elements of M and N satisfy the existence conditions (2.151), (2.152) and (2.154), as well as the inertia hypotheses associated with FBM

$$M_{11} \succ 0, \quad M_{22} \prec 0, \quad N_{11} \prec 0, \quad N_{22} \succ 0,$$

Then, a reconstruction of the closed-loop multiplier

$$\mathcal{M} = \begin{bmatrix} \mathcal{M}_{11} & \mathcal{M}_{12} \\ \mathcal{M}_{12}^\top & \mathcal{M}_{22} \end{bmatrix} = \mathcal{N}^{-1} = \begin{bmatrix} \mathcal{N}_{11} & \mathcal{N}_{12} \\ \mathcal{N}_{12}^\top & \mathcal{N}_{22} \end{bmatrix}^{-1} \tag{2.157}$$

that satisfies

$$\begin{bmatrix} \bullet \\ \hdashline \bullet \end{bmatrix}^* \mathcal{M} \left[\begin{array}{c} I \\ \hline I \\ \hdashline \Delta^P(\delta) \\ \hline \Delta^K(\delta) \end{array} \right] \succ 0, \ \forall \delta \in \boldsymbol{\delta}, \tag{2.158}$$

for a suitable choice of $\Delta^K(\delta)$ is given by

$$\mathcal{M} = \Psi \begin{bmatrix} I \\ & T^\top \end{bmatrix} \begin{bmatrix} M & I \\ I & (M-N^{-1})^{-1} \end{bmatrix} \begin{bmatrix} I \\ & T \end{bmatrix} \Psi, \tag{2.159}$$

where T *is a suitable non-singular matrix and*

$$\Psi = \begin{bmatrix} I_{n_\Delta} & 0 & 0 & 0 \\ 0 & 0 & I_{n_\Delta} & 0 \\ 0 & I_{n_\Delta} & 0 & 0 \\ 0 & 0 & 0 & I_{n_\Delta} \end{bmatrix}.$$

□

Proof: Observe that

$$\Psi \mathcal{M} \Psi = \begin{bmatrix} M & \bullet \\ \bullet & \bullet \end{bmatrix}, \quad \Psi \mathcal{N} \Psi = \begin{bmatrix} N & \bullet \\ \bullet & \bullet \end{bmatrix},$$

s. t. any extension

$$\Psi \mathcal{N} \Psi = (\Psi \mathcal{M} \Psi)^{-1} = \left(\begin{bmatrix} I \\ & T^\top \end{bmatrix} \begin{bmatrix} M & I \\ I & (M - N^{-1})^{-1} \end{bmatrix} \begin{bmatrix} I \\ & T \end{bmatrix} \right)^{-1}$$

using a non-singular matrix T fulfills the duality constraints. The proof of the existence of a suitable parameter block of the controller $\Delta^K(\delta)$ associated with a suitable matrix T is provided by the following lemmas. ■

Lemma 2.5 (Parameter Block Construction, FBM [E21, 124])
Under the hypotheses of Lma. 2.4, the selection of $\mathsf{T} = \begin{bmatrix} \mathsf{T}_1 & \mathsf{T}_2 \end{bmatrix}$, *s. t.* T_1 *and* T_2 *satisfy*

$$\mathsf{T}_1^\top \left(\left(M - N^{-1} \right)^{-1} - \begin{bmatrix} 0 & 0 \\ 0 & M_{22}^{-1} \end{bmatrix} \right) \mathsf{T}_1 \prec 0, \tag{2.160}$$

$$\mathsf{T}_2^\top \left(\left(M - N^{-1} \right)^{-1} - \begin{bmatrix} M_{11}^{-1} & 0 \\ 0 & 0 \end{bmatrix} \right) \mathsf{T}_2 \succ 0, \tag{2.161}$$

permits the choice for the controller's parameter block

$$\Delta^K(\delta) = -\mathcal{W}_{22} + \begin{bmatrix} \mathcal{W}_{21} & \mathcal{V}_{12}^\top \end{bmatrix} \begin{bmatrix} \mathcal{U}_{11} & \mathcal{W}_{11}^\top + \Delta^{P\top} \\ \mathcal{W}_{11} + \Delta^P & \mathcal{V}_{11} \end{bmatrix}^{-1} \begin{bmatrix} \mathcal{U}_{12} \\ \mathcal{W}_{12} \end{bmatrix}, \tag{2.162}$$

where

$$\mathcal{M}_{11} - \mathcal{M}_{12} \mathcal{M}_{22}^{-1} \mathcal{M}_{12}^\top \triangleq \mathcal{U} = \begin{bmatrix} \mathcal{U}_{11} & \mathcal{U}_{12} \\ \mathcal{U}_{12}^\top & \mathcal{U}_{22} \end{bmatrix} \succ 0,$$

$$-\mathcal{M}_{22}^{-1} \triangleq \mathcal{V} = \begin{bmatrix} \mathcal{V}_{11} & \mathcal{V}_{12} \\ \mathcal{V}_{12}^\top & \mathcal{V}_{22} \end{bmatrix} \succ 0,$$

$$\mathcal{M}_{22}^{-1} \mathcal{M}_{12}^\top \triangleq \mathcal{W} = \begin{bmatrix} \mathcal{W}_{11} & \mathcal{W}_{12} \\ \mathcal{W}_{21} & \mathcal{W}_{22} \end{bmatrix}.$$

$\square$

Proof: The proof is given in App. B.5 on p. 332, providing some additional insight over the one shown in [124]. ∎

The inertia hypotheses guarantee the existence of an explicit formula for the parameter block $\Delta^K(\delta)$ as opposed to the more general controller scheduling policy presented in [125]. This is therefore regarded the practically valid approach [142, 143]. In constrast, in the face of relaxed inertia hypotheses resulting from conditions proposed in Lma. 2.2, the controller's scheduling function is formulated as an orthogonal projector onto some potentially varying eigenspace, which may be difficult to compute online. This indicates that the particular choice of the controller's parameter block (2.162) is by no means unique. An even more general representation, albeit involving more complex computations, is presented in [143].

The controller's parameter block presented in Lma. 2.5 (an LFR) requires computing an inverse online, which consumes additional processing power. Hence, simpler choices of parameter blocks may be desired. The following lemma provides conditions that make the choice $\Delta^K(\delta) = \Delta^P(\delta)$ admissible.

Lemma 2.6 (Parameter Block Copy [74])
Under the hypotheses of Lma. 2.4 and the additional conditions

$$\begin{bmatrix} M_{11} & I \\ I & N_{11} \end{bmatrix} \succ 0, \quad \begin{bmatrix} M_{22} & I \\ I & N_{22} \end{bmatrix} \prec 0, \tag{2.163}$$

$$\begin{bmatrix} \bullet \\ \bullet \end{bmatrix}^\top \left(M - N^{-1} \right) \begin{bmatrix} I \\ \Delta^P(\delta) \end{bmatrix} \succ 0, \ \forall \delta \in \boldsymbol{\delta}, \tag{2.164}$$

the selection $T = M - N^{-1}$ *permits the choice for the controller's parameter block*

$$\Delta^K(\delta) = \Delta^P(\delta) \tag{2.165}$$

$\square$

Proof: The proof is given in App. B.6 on p. 334. ∎

It is evident from the proof that the crucial condition to satisfy is indeed (2.164), which is non-trivial since it involves the inverse of N. However, it can be shown that D/G-S constraints together with the coupling conditions (2.163) guarantee the satisfaction of (2.164) [74] as shown in the next corollary.

Corollary 2.3 (D/G-S Constraints [74, 130])
If the multipliers M and N satisfying Conds. (2.151), (2.152), (2.154) and (2.155) are coupled as in Cond. (2.163) and, in addition, satisfy the structural constraints

$$M \in \mathcal{M}_{D/G}(\Delta), \quad N \in \mathcal{N}_{D/G}(\Delta),$$

Condition (2.164) holds and the choice $\Delta^K(\delta) = \Delta^P(\delta)$ *is admissible, if* $\|\Delta^P\| < 1$. $\square$

Proof: Observe that the coupling conditions (2.163) imply the inertia hypotheses

$$M_{11} \succ 0, \quad M_{22} \prec 0, \quad N_{11} \prec 0, \quad N_{22} \succ 0,$$

as well as $M_{11} - \tilde{N}_{11} \succ 0$. It is easy to show that the structural constraints imposed on N imply that N^{-1} inherits these structural constraints as well [E21]. Expand Cond. (2.164) to obtain

$$M_{11} - \tilde{N}_{11} + \Delta^{P*}\Delta^P \left(M_{22} - \tilde{N}_{22} \right) \succ 0. \tag{2.166}$$

From the D/G-S constraints, one indeed has

$$M_{22} - \tilde{N}_{22} = -\left(M_{11} - \tilde{N}_{11} \right),$$

which renders (2.166) satisfied for all Δ^P with $\|\Delta^P\| < 1$. ∎

Corollary 2.4 (Shifted D/G-S Constraints)
Assume a diagonal parameter block of the form

$$\Delta^P(\delta) = \operatorname*{diag}_{i=1}^{n_\delta}\left(\delta_i I_{r_{\delta,i}} \right) \in \mathcal{C}^0(\mathbb{R}^{n_\delta}, \mathbb{R}^{n_\Delta \times n_\Delta}), \tag{2.167}$$

and bounds on the parameter values $\delta_i \in \left[\underline{\delta}_i, \overline{\delta}_i \right]$, with

$$\underline{\delta}_i = \min_{t \geqslant 0} \delta_i(t), \quad \overline{\delta}_i = \max_{t \geqslant 0} \delta_i(t), \quad \forall i \in \{1, \dots, n_\delta\}.$$

Then the multipliers M and N satisfy Conds. (2.152), (2.154) and (2.164) admitting the choice $\Delta^K(\delta) = \Delta^P(\delta)$, if they are coupled as in Cond. (2.163) and, in addition, are chosen as

$$M \in \hat{\mathcal{M}}_{D/G}(\Delta), \quad N \in \hat{\mathcal{N}}_{D/G}(\Delta),$$

□

Proof: First note that
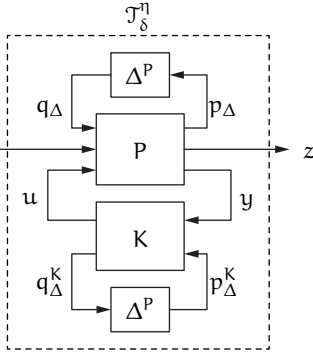
$$N^{-1} = \begin{bmatrix} \operatorname*{diag}_{i=1}^{n_\delta}\left(S_{11}^{(i)} \tilde{N}_{11}^{(i)} \right) & \operatorname*{diag}_{i=1}^{n_\delta}\left(S_{12}^{(i)} \tilde{N}_{11}^{(i)} + \tilde{N}_{12}^{(i)} \right) \\ \operatorname*{diag}_{i=1}^{n_\delta}\left(S_{12}^{(i)} \tilde{N}_{11}^{(i)} - \tilde{N}_{12}^{(i)} \right) & \operatorname*{diag}_{i=1}^{n_\delta}\left(S_{22}^{(i)} \tilde{N}_{11}^{(i)} \right) \end{bmatrix}.$$

Consequently, the same line of argumentation as in Cor. 2.3 applies with the addition of scalings and a constant term as in the proof of Lma. 2.3. ∎

Summary: Full-Block Multipliers vs. D/G-scalings
In LFT-LPV controller synthesis with PiDLFs as per [125], FBMs and D/G-S constraints are alternatives, between which the control engineer may choose according to the requirements on the control system design. For complex LPV systems, FBMs may be prohibitively complex in terms of synthesis and implementation complexity, even though they may strongly decrease the incurred conservatism. Tab. 2.1 compares advantages and disadvantages with respect to the two choices.

Table 2.1: Comparison of LFT-LPV-based FBM and D/G-S-based synthesis with PiDLFs based on the methods published in [125].

D/G-S		FBMs	
✓	Controller parameter block can be copied from plant.	✗	Controller parameter block is an LFT in terms of the plant's parameter block.
✓	Low synthesis complexity as multiplier vertex conditions are trivially fulfilled.	✗	Multiplier conditions need to be evaluated in vertices of matrix polytopes, the number of which increases exponentially with the number of parameters.
✗	Conservative in general.	✓	Reduced conservatism.
✗	Rendered overly conservative for full parameter blocks due to commutativity requirements. Only really suitable for diagonal parameter blocks.	✓	Can handle full and non-square parameter blocks.

Part I

LINEAR PARAMETER-VARYING CONTROL OF
COMPLEX LUMPED SYSTEMS

The application of the linear parameter-varying (LPV) modeling and
controller synthesis methodology to complex lumped plants, i. e., non-
distributed systems that result in intricate mathematical representations,
is a challenging task. The first part of this thesis introduces methods
that facilitate the derivation of low complexity LPV representations in
a compact modeling framework and their subsequent exploitation in
tractable synthesis algorithms.

3

LINEAR PARAMETER-VARYING CONTROL — A SURVEY OF COMPLEXITY AND APPLICATIONS

*≪Examine the contents,
not the bottle.≫*

The Talmud

Tʜɪs chapter aims at investigating ≪complexity≫ induced by the LPV controller synthesis methods reviewed in Chap. 2. For this purpose, in Sect. 3.1 quantities are proposed from which the intricacy of a particular controller synthesis algorithm and the subsequent online controller implementation can be assessed. The result is a tool set consisting of formulae compiled in comprehensive tables that allow the *a priori* assessment of

(i) implementation complexity in terms of the required number of arithmetic operations in each sampling instant and the number of scalar variables to be stored,

(ii) synthesis complexity in terms of the number of decision variables and the total size of the linear matrix inequality (LMI) to be solved.

The quantities can be evaluated once an LPV model of the desired type is available and the associated synthesis method is decided upon.

In Sect. 3.2, the chapter continues to survey literature reporting experimental or high-fidelity simulation-based validations of LPV control schemes and investigates the complexity of the respective problems. The survey is an empirical and quantitative statement that reflects open questions in the design of LPV controllers for complex plants.

3.1 Complexity in Linear Parameter-Varying Control

THE choice of the modeling framework and associated synthesis techniques affect both the complexities encountered during implementation and synthesis. In this section the involved complexity is analyzed, in order to generate numerical indicators for benefits and drawbacks of the individual approaches *a priori*. In the following, results from a thorough investigation of LPV controller synthesis and implementation complexity, conducted in [58], are presented.

For the sake of simplicity, signal and parameter values are assumed to range inside a hyperbox, which in most cases will mark an upper bound on the complexity. Furthermore, the discussion is restricted for the most part to the synthesis and implementation of state space output-feedback LPV controllers (2.115) of full order ($n_x^K = n_x$).

Four types of complexities are considered: The number of arithmetic operations to compute a value A, which at some point is referenced to be computed by a certain formula $A = f(x)$, is denoted $a[A]$. The multiplications, additions, divisons, etc., involved are assumed clear from the context by the explicit formula $f(x)$.

Similarly, the number of scalar values required to store the variables, from which A can be computed, is denoted by $m[A]$ and acts as a measure for memory requirements. Furthermore, the size of an LMI $\mathcal{L} \prec 0$, or $\mathcal{L} \succ 0$, is written as $s[\mathcal{L}]$ and is provided only in terms of one dimension, since LMIs are symmetric and square. The associated number of decision variables is given by $d[\mathcal{L}]$. If, e.g., $\mathcal{L}$ solely contains the matrix variables X, Y, one may also write $d[\mathcal{L}] = d[X] + d[Y]$.

The notational shortcut

$$m_{abcd} \stackrel{\triangle}{=} n_a + n_b + n_c + n_d$$

is used, with

$$a, b, c, d \in \{x, u, y, w, z, \Delta, \{\}, \ldots\},$$

s.t., e.g., $m_{xu} = n_x + n_u$ or $m_{xw\Delta^P u} = n_x + n_w + n_\Delta^P + n_u$.

Both the computational costs and memory requirements of elementary matrix operations are listed in Tabs. A.1 and A.2. These provide the basis of the following complexity assessment and will be frequently used without further reference.

Preliminary results of this section have been previously published in [58]. Several mistakes are corrected and non-square parameter blocks are considered.

3.1.1 *Implementation Complexity*

3.1.1.1 *General Complexity*

Updating the states and calculating the outputs is assumed to consume the same amount of arithmetic operations for each output-feedback-based method, which amounts to

$$a\left[[\dot{x}^{K\top}, u^\top]^\top\right] \leqslant (n_x + n_u)\,(2(n_x + n_y) - 1) \tag{3.1}$$

arithmetic operations once the state space matrices of the controller at a particular time instant are available. In contrast, a state-feedback controller requires

$$a[u] \leqslant n_u(2n_x - 1). \tag{3.2}$$

once the state-feedback gain matrix $F(\rho)$, as from (2.127) has been computed.

If the projection approach considered in Thm. 2.13 is applied, formulae (2.127)–(2.132) have to be used for the implementation of parameter-dependent Lyapunov function (PDLF)-based controllers, independent of the LPV framework (polytopic, linear fractional transformation (LFT)-based, gridding) considered. The reason for this resides in the fact that the construction of the closed-loop Lyapunov matrix $\mathcal{X}(\rho)$—even if carried out symbolically—results in a rational parameter-dependence and a convex search for the controller variables is only possible by again solving a gridded LMI problem based on Thm. (2.6).

The case where the controller depends on rates of change is considered practically undesirable and therefore the analysis is restricted to Eqs. (2.127)–(2.132) when the Lyapunov variable S is chosen parameter-independent, whereas $R(\rho)$ may be chosen parameter-dependent. A straightforward factorization is then $M(\rho) = I - S(\rho)R(\rho)$ and $N^\top(\rho) = I$. The opposite choice results in similar complexity. Computing the resulting formulae then amounts to

$$\begin{aligned}
a\left[K_\rho(\rho)\right] \leqslant &\, a\left[P_\rho(\rho)\right] + a\left[F(\rho)\right] + a\left[L(\rho)\right] + a\left[M(\rho)\right] \\
&+ a\left[A^K(\rho)\right] + a\left[B_y^K(\rho)\right] + a\left[C_u^K(\rho)\right].
\end{aligned}$$

For implementation, the generalized plant model matrices in (2.113) are required and it is assumed that their evaluation can be performed efficiently enough, such that the cost in arithmetic operations is negligible. The actual memory and evaluation costs then depend on the parameterization of $R(\rho)$. For the remainder, the intuitive heuristic choice for the Lyapunov function basis is chosen that aims at reflecting the parameter-dependency of the plant. Therefore $a\left[R(\rho)\right]$ will depend on the framework, the plant is modeled in. Once $R(\rho)$ is constructed online, however, its inversion requires

$$a\left[M^{-\top}(\rho)\right] \approx a\left[R^{-1}(\rho)\right] \leqslant \tfrac{2}{3}n_x^3$$

operations. Note that this complexity is absorbed in $a\big[F(\rho)\big]$. Furthermore, one has $a\big[M(\rho)\big] \leqslant n_x + 2n_x^3$. In the following enumeration of complexities care has been taken to maintain an economic sequence of operations, s. t., e. g., the inversion of $M(\rho)$ is considered in $a\big[A^K(\rho)\big]$, but not in $a\big[C_u^K(\rho)\big]$, as an efficient implementation will store the result of the inversion for multiple uses.

$$a\big[F(\rho)\big] \leqslant 2n_u^2 n_z + \tfrac{2}{3}(n_u^3 + n_x^3) + n_u(2n_x - 1)n_x$$
$$+ 2n_u n_x + n_u(2n_z - 1)n_x + n_u(2n_u - 1)n_x$$
$$a\big[L(\rho)\big] \leqslant 2n_x^2 n_y + n_x(2n_w - 1)n_y + n_x n_y + 2n_y^2 n_w + \tfrac{2}{3}n_y^3$$
$$a\Big[A^K(\rho)\Big] \leqslant 7n_x^2 + n_x n_w + n_x n_z + n_x(2n_y - 1)(n_x + n_w)$$
$$+ (n_x + n_z)(2n_u - 1)n_x + n_x(2n_x - 1)(5n_x + n_z)$$
$$+ n_x^2(2n_w - 1) + \tfrac{2}{3}n_x^3$$
$$a\Big[B_y^K(\rho)\Big] \leqslant n_x(2n_x - 1)n_u$$
$$a\Big[C_u^K(\rho)\Big] \leqslant n_x(2n_x - 1)(n_y + n_x)$$

In addition to evaluating the Lyapunov variable online, which costs $a\big[R(\rho)\big]$, this results in a total number of arithmetic operations to evaluate the controller's state space matrices from (2.127)–(2.132)

$$a\big[K_\rho(\rho)\big] \leqslant \tfrac{46}{3}n_x^3 + (6m_{uy} + 2m_{wz} - 2)n_x^2$$
$$+ (n_w + m_{uz}(2n_u - 1) + 2n_u n_z - m_{uyw} + 4n_y n_w + 1)n_x$$
$$+ 2n_z n_u^2 + 2n_w n_y^2 + \tfrac{2}{3}n_u^3 + \tfrac{2}{3}n_y^3. \tag{3.3}$$

In many cases the performance channel related matrices will be parameter-independent. If in addition, $C_y(\rho)$ is also parameter-independent, $L(\rho) \in \mathbb{R}^{n_x \times n_y}$ can be computed offline and the number of required computational steps is reduced. The same applies to the alternative practical case, where $R(\rho)$ instead of $S(\rho)$ is chosen constant and performance channel and input matrices are parameter-independent.

The memory requirements to store the plant matrices of general dependency on the scheduling signals are approximated by $(D_{pp} = 0, D_{yu} = 0)$

$$m\big[P_\rho(\rho)\big] \approx (n_x + n_z + n_y)(n_x + n_w + n_u) - n_z n_w - n_y n_u.$$

Furthermore, $m[S] = m\big[S^{-1}\big] = n_x(n_x + 1)/2$. For the remainder, the memory requirement $m[\gamma]$ will be neglected. Thus the total required scalar variables to be stored amount to

$$m\big[K_\rho(\rho)\big] \approx m\big[P_\rho(\rho)\big] + 2m[S] + m\big[R(\rho)\big]$$
$$\approx n_x(n_x + 1) + (n_x + n_z + n_y)(n_x + n_w + n_u)$$
$$- n_z n_w - n_y n_u + m\big[R(\rho)\big]$$

A particularly efficient implementation can be performed for state-feedback LPV controllers. It is possible to evaluate the state-feedback gain $F(\rho) = -\left(\gamma B_u^\top(\rho) R(\rho)^{-1} + C_p(\rho)\right)$ by

$$a[F(\rho)] \leqslant a[R(\rho)] + \tfrac{2}{3} n_x^3 + n_u(2n_x - 1)n_x + n_u n_x.$$

Here, only two plant matrices and a single inversion need to be calculated, which makes up the main computational load [E85].

3.1.1.2 *Polytopic LPV Controllers*

Parameter-Independent Lyapunov Functions
Polytopic LPV controllers synthesized based on parameter-independent Lyapunov functions (PiDLFs) can be implemented by the interpolation of the state space matrices of the linear time-invariant (LTI) vertex controllers. Therefore, one has:

$$K_\theta(\theta) = \begin{bmatrix} A^K(\rho) & B_y^K(\rho) \\ C_u^K(\rho) & D_{uy}^K(\rho) \end{bmatrix} = \sum_{l=1}^{n_v} \alpha_l K_\theta(\theta_{v,l}). \tag{3.4}$$

The associated number of arithmetic operations is

$$a[K_\theta(\theta)] \leqslant (2^{n_\theta+1} - 1)(n_x + n_u)(n_x + n_y), \tag{3.5}$$

which results from scaling each of the $n_v = 2^{n_\theta}$ vertex controllers by the respective α_l and then calculating the controller as a weighted sum by $2^{n_\theta} - 1$ matrix additions. In addition, the algorithm given in [158] to compute the barycentric coordinates α from the affine parameters θ requires approximately

$$a[\alpha] \leqslant n_v a[\alpha_l] = n_v \left(O(n_\theta^3) + n_\theta^2 + n_\theta - 1 \right).$$

When the parameters range in a hyperbox, the computation of the involved determinants is always one, which yields

$$a[\alpha] \leqslant 2^{n_\theta} \left(n_\theta^2 + n_\theta - 1 \right).$$

In contrast, the Matlab implementation of the command polydec requires

$$a[\alpha] \leqslant \sum_{i=1}^{n_\theta} (a[t_i] + a[c_i])$$

$$= 3n_\theta + 2\frac{1 - 2^{n_\theta+1}}{1 - 2} = 2^{n_\theta+2} + 3n_\theta - 2,$$

with $a[t_i] = 3$, $a[c_i] = 2^{i+1}$ and using the geometric series $\sum_{i=0}^{n} a^i = \frac{1-a^{n+1}}{1-a}$. Note that this is only valid for parameters ranging in a hyperbox, but also that it is always less costly than the algorithm proposed by [158].

Storing the controller matrices in the $n_v = 2^{n_\theta}$ vertices requires

$$m\big[K_\theta(\theta)\big] \approx 2^{n_\theta}(n_x + n_u)(n_x + n_y). \tag{3.6}$$

If either an offline preprocessing can be applied, which converts the convex coordinates back into the affine LPV parameter coordinates, or the synthesis for an affine LPV plant is carried out using multiplier-based LFT methods with additional constraints, [E21, E45, 57, E46], the exponential growth can be reduced to linear growth and barycentric coordinates need no longer be computed online:

$$a\big[K_\theta(\theta)\big] \leqslant 2n_\theta(n_x + n_u)(n_x + n_y),$$
$$m\big[K_\theta(\theta)\big] \approx (n_\theta + 1)(n_x + n_u)(n_x + n_y).$$

In the subsequent summary, it will be assumed that the implementation of affine controllers is carried out in this more efficient way.

Parameter-Dependent Lyapunov Functions
Using PDLFs in conjunction with the multi-convexity approach results in a controller which is no longer affine in the parameters θ, but rational. Therefore, the explicit formulae (2.127)–(2.132) have to be used, the complexity of which has already been discussed. Assuming the Lyapunov matrix has been parameterized as

$$R(\rho) = R + \sum_{i=r}^{s} \theta_i(\rho)R_i, \quad n_\theta^R = s - r. \tag{3.7}$$

its online construction requires

$$a\big[R(\rho)\big] \leqslant 2n_\theta^R n_x^2, \quad m\big[R(\rho)\big] \approx \tfrac{1}{2}\left(n_\delta^R + 1\right)n_x(n_x + 1)$$

operations and stored scalars, respectively.

3.1.1.3 *LFT-Based LPV Controllers*

Parameter-Independent Lyapunov Functions
The computation of LFT-based controllers is of polynomial order:

$$a\big[K_\delta(\delta)\big] \leqslant n_{q_\Delta}^K \left(2n_{p_\Delta}^K - 1\right)(n_x + n_y) + 2n_{q_\Delta}^K(n_x + n_y)(n_x + n_u)$$
$$\dots + a\big[\Psi^K(\delta)\big] + a\big[\Delta^K(\delta)\big], \tag{3.8}$$

where $\Psi^K(\delta) = \Delta^K(\delta)(I - D_{\Delta\Delta}^K\Delta^K(\delta))^{-1}$, $\Delta^K(\delta) \in \mathbb{R}^{n_{q_\Delta}^K \times n_{p_\Delta}^K}$. For the computation of $\Psi^K(\delta)$, note that due to the «push-through rule», it follows that

$$\Psi^K(\delta) = \Delta^K(\delta)(I - D_{\Delta\Delta}^K\Delta^K(\delta))^{-1} = (I - \Delta^K(\delta)D_{\Delta\Delta}^K)^{-1}\Delta^K(\delta),$$

which allows to choose the size of the matrix of which an inverse is to be computed between $n_{p_\Delta}^K \times n_{p_\Delta}^K$ and $n_{q_\Delta}^K \times n_{q_\Delta}^K$. For non-square parameter blocks, this can significantly reduce the computational burden. Accordingly, one has

$$
a\left[\Psi^K(\delta)\right] \leqslant \begin{cases} n_{p_\Delta}^{K2}\left(2n_{q_\Delta}^K - 1\right) + n_{p_\Delta}^K\left(\tfrac{2}{3}n_{p_\Delta}^{K2} + 1\right) \\ \qquad + n_{q_\Delta}^K n_{p_\Delta}^K\left(2n_{p_\Delta}^K - 1\right) \qquad , n_{q_\Delta}^K \geqslant n_{p_\Delta}^K \\ n_{q_\Delta}^{K2}\left(2n_{p_\Delta}^K - 1\right) + n_{q_\Delta}^K\left(\tfrac{2}{3}n_{q_\Delta}^{K2} + 1\right) \\ \qquad + n_{q_\Delta}^K n_{p_\Delta}^K\left(2n_{q_\Delta}^K - 1\right) \qquad , n_{q_\Delta}^K < n_{p_\Delta}^K \end{cases} \tag{3.9}
$$

Note that for PiDLF-based synthesis of LFT-LPV controllers using a full-block S-Procedure (FBSP) approach, the LFT channel sizes of the controller are usually inherited from the plant, thus $n_{q_\Delta}^K = n_{q_\Delta}^P$ and $n_{p_\Delta}^K = n_{p_\Delta}^P$.

Memory requirements amount to

$$
m\left[K_\delta(\delta)\right] \leqslant (n_x + n_{q_\Delta}^K + n_u)(n_x + n_{p_\Delta}^K + n_y) + m\left[\Delta^K(\delta)\right]. \tag{3.10}
$$

The terms $a\left[\Delta^K(\delta)\right]$ and $m\left[\Delta^K(\delta)\right]$ arise due to the scheduling block $\Delta^K(\delta)$ being constructed as an LFT based on $\Delta^P(\delta)$ as detailed in Lma. 2.5 on p. 69 [124]. The computation of the controller's parameter block therefore requires

$$
a\left[\Delta^K(\delta)\right] \leqslant 3n_{q_\Delta}^P n_{p_\Delta}^P + \tfrac{2}{3}(n_{q_\Delta}^P + n_{p_\Delta}^P)^3
$$
$$
+ (2n_{q_\Delta}^P + n_{p_\Delta}^P)\left(2(n_{q_\Delta}^P + n_{p_\Delta}^P) - 1\right)n_{p_\Delta}^P. \tag{3.11}
$$

Due to the symmetry, the inversion can possibly be performed more efficiently, which has been neglected here. Taking into account the symmetry of the matrices $\mathcal{U}_{11}$ and $\mathcal{V}_{11}$ from Eq. (2.162) in Lma. 2.5, however, the memory requirements amount to

$$
m\left[\Delta^K(\delta)\right] = 7(n_{q_\Delta}^P + n_{p_\Delta}^P)\left((n_{q_\Delta}^P + n_{p_\Delta}^P) + 1\right). \tag{3.12}
$$

As detailed in Lma. 2.3 on p. 49, at the price of increased conservatism the choice $\Delta^K = \Delta^P$ can be made admissible [E21] by additional constraints on multipliers. Neglecting the cost of evaluating Δ^P, both memory requirements and arithmetic operations are then negligible.

Parameter-Dependent Lyapunov Functions

In the case of PDLFs and LFT-based synthesis methods, the Lyapunov variable can be parameterized in a multitude of ways and an affine parameterization is most likely not the best choice. Therefore, consider an ansatz which—in a sense—mimics the rational parameter-dependence of the plant [66]:

$$
R(\rho) = Q_R^\top(\delta) R Q_R(\delta)
$$
$$
= \begin{bmatrix} \bullet \\ \bullet \end{bmatrix}^\top \begin{bmatrix} R_0 & R_\Delta \\ R_\Delta^\top & 0 \end{bmatrix} \begin{bmatrix} I \\ \Delta^P(\delta)\left(I - D_{\Delta\Delta}\Delta^P(\delta)\right)^{-1} C_\Delta \end{bmatrix}, \tag{3.13}
$$

with $R \in S^{(n_x + n_{q_\Delta}^P)}$. For controller implementation, evaluating (2.127)–(2.132) is required and the complexity again follows from (3.3) with

$$a\left[R(\rho)\right] \leqslant n_{q_\Delta}^P \left(2n_{p_\Delta}^P - 1\right) n_x + \left(2n_{q_\Delta}^P + 1\right) n_x^2 + a\left[\Psi^P(\delta)\right],$$
$$\text{with } a\left[\Psi^P(\delta)\right] \leqslant n_{p_\Delta}^{P2} \left(2n_{q_\Delta}^P - 1\right) + n_{p_\Delta}^P \left(\tfrac{2}{3}n_{p_\Delta}^{P2} + 1\right).$$

Storing the Lyapunov variables requires

$$m\left[R(\rho)\right] = \tfrac{1}{2}n_x(n_x + 1) + \left(n_{q_\Delta}^P + n_{p_\Delta}^P\right)^2. \tag{3.14}$$

However, the evaluation of $K_\delta(\delta)$ can possibly be performed more efficiently via first evaluating (2.127)–(2.132) offline symbolically [E69]. It may then be put into LFT form by tools available in the Control System Toolbox of Matlab or the linear fractional representation (LFR)-toolbox available from the German Aerospace Center (DLR) [52]. In this case, it is difficult to predict the size of the parameter block $\Delta^K(\delta)$, which will no longer match the size of the block $\Delta^P(\delta)$. Then again both (3.8) and (3.10) apply, but with $n_{q_\Delta}^K \neq n_{q_\Delta}^P$ and $n_{p_\Delta}^K \neq n_{p_\Delta}^P$.

3.1.1.4 *Gridding-Based LPV Controllers*

PARAMETER-INDEPENDENT LYAPUNOV FUNCTIONS
Gridding-based LPV controllers can be implemented online by the formulae (2.127)–(2.132). For PIDLFs the computation simplifies drastically, as, e. g., the factorization problem and many multiplications can be performed offline. However, as shown in [59], very few experimental results using the gridding technique with PIDLFs have been reported.

Apart from using the explicit formulae, it is also possible to store precomputed controllers on some parameter grid, which does not necessarily need to match the one used to solve the synthesis LMIs. If an evenly spaced grid of n_g points per parameter dimension is assumed, the required memory amounts to

$$m\left[K_\rho(\rho)\right] = n_g^{n_\rho}(n_x + n_u)(n_x + n_y). \tag{3.15}$$

It is clear that an interpolation for intermediate grid points requires a number of arithmetic operations in the same order as in the polytopic case:

$$a\left[K_\rho(\rho)\right] \leqslant (2^{n_\rho + 1} - 1)(n_x + n_u)(n_x + n_y).$$

This approach, which resembles the complexity of classical gain-scheduling techniques, can therefore quickly become intractable and control engineers might opt for switching between controller parameters or the above mentioned closed-form formulae instead.

Table 3.1: Implementation complexity of LPV controllers in terms of arithmetic operations vs. synthesis technique.

Technique		Arithmetic operations	
PDLF		Total	In parts
Grid.	$\times$	$a[K_\rho(\rho)] - a[M^{-\top}] - a[R^{-1}]$	$a[M^{-\top}] \approx a[R^{-1}] \leqslant {}^2\!/_3 n_x^3$
	$\checkmark$	$a[K_\rho(\rho)] + a[R(\rho)]$	$a[R(\rho)] = 2n_\theta^R n_x^2$
LFT	FBM	$a[K_\delta(\delta)] + a[\Psi] + a[\Delta^K(\delta)]$	$a[\Psi] = n_{p_\Delta}^{P2}\left(2n_{q_\Delta}^P - 1\right) + n_{p_\Delta}^P\left({}^2\!/_3 n_{p_\Delta}^{P2} + 1\right)$
	D/G-S	$a[K_\delta(\delta)] + a[\Psi]$	$a[\Delta^K(\delta)] = 3n_{q_\Delta}^P n_{p_\Delta}^P + {}^2\!/_3 m_{q_\Delta^P p_\Delta^P}^3$
	$\times$		$\qquad + (2n_{q_\Delta}^P + n_{p_\Delta}^P)(2m_{q_\Delta^P p_\Delta^P} - 1)n_{p_\Delta}^P$
	D/G-S	$a[K_\theta(\theta)]$	$a[K_\delta(\delta)] = n_{q_\Delta}^P m_{xy}\left((2n_{p_\Delta}^P - 1) + 2m_{xu}\right)$
	w/ Θ		$a[K_\theta(\theta)] = n_{q_\Theta}^P m_{xu}(2m_{xy} + 1)$
	$\checkmark$	$a[K_\rho(\rho)] + a[R(\delta)]$	$a[R(\delta)] = n_{q_\Delta}^P\left(2n_{p_\Delta}^P - 1\right)n_x + \left(2n_{q_\Delta}^P + 1\right)n_x^2$
			$\qquad + a[\Psi]$
Poly.	$\times$	Polytopic: $a[K_\theta(\theta)] + a[\alpha]$	$a[\alpha] = 2^{n_\theta + 2} + 3n_\theta - 2$
			$a[K_\theta(\theta)] = (2^{n_\theta + 1} - 1)m_{xu}m_{xy}$
		Affine: $a[K_\theta(\theta)]$	$a[K_\theta(\theta)] = 2n_\theta m_{xu}m_{xy}$
	$\checkmark$	$a[K_\rho(\rho)] + a[R(\theta)]$	$a[R(\theta)] = 2n_\theta^R n_x^2$

$$a[K_\rho(\rho)] = {}^{46}\!/_3 n_x^3 + (6m_{uy} + 2m_{wz} - 2)n_x^2 + (n_w + m_{uz}(2n_u - 1) + 2n_u n_z$$
$$- m_{uyw} + 4n_y n_w + 1)n_x + 2n_z n_u^2 + 2n_w n_y^2 + {}^2\!/_3 n_u^3 + {}^2\!/_3 n_y^3$$

PARAMETER-DEPENDENT LYAPUNOV FUNCTIONS
When a PDLF with affine parameter dependence is used, the LMIs need only be evaluated at the extrema of the parameter's rate of variation, since these still enter the LMIs in an affine way. This amounts to doubling the grid points, but requires an interpolation at least in terms of the variation in the rate of change.

3.1.1.5 *Implementation Complexity — Summary*

Tabs. 3.1 and 3.2 summarize LPV controller implementation complexity for the different synthesis methods by giving an overview of the required number of arithmetic operations to calculate the controller's state space system matrix *K* in its respective LPV representations and the associated requirements on the memory, respectively.

Table 3.2: Implementation complexity of LPV controllers in terms of memory requirements vs. synthesis technique.

Technique			Memory requirements	
	PDLF		Total	In parts
Grid.	$\times$		$m\left[P_\rho(\rho)\right] + 4m[R] + m\left[M^{-\top}\right]$	$m[R] = {}^1\!/_2 n_x(n_x+1)$ $m\left[M^{-\top}\right] = n_x^2$
	$\checkmark$		$m\left[P_\rho(\rho)\right] + m\left[R(\rho)\right] + 2m[S]$	$m\left[R(\rho)\right] = {}^1\!/_2 n_x(n_x+1)(n_\theta^R+1)$ $m[S] = {}^1\!/_2 n_x(n_x+1)$
LFT	$\times$	FBM	$m\left[K_\delta(\delta)\right] + m\left[\Delta^K(\delta)\right]$	$m\left[\Delta^K(\delta)\right] = 7 m_{q_\Delta^P p_\Delta^P}\left(m_{q_\Delta^P p_\Delta^P}+1\right)$
		D/G-S	$m\left[K_\delta(\delta)\right]$	$m\left[K_\delta(\delta)\right] = m_{x q_\Delta^P u} m_{x p_\Delta^P y}$
		D/G-S w/ Θ	$m\left[K_\theta(\theta)\right]$	$m\left[K_\theta(\theta)\right] = m_{x q_\Theta^P u} m_{x p_\Theta^P y} - m_{q_\Theta^P p_\Theta^P}^2$
	$\checkmark$		$m\left[P_\rho(\rho)\right] + m\left[R(\delta)\right] + 2m[S]$	$m\left[R(\delta)\right] = {}^1\!/_2 n_x(n_x+1) + m_{q_\Delta^P p_\Delta^P}^2$ $m[S] = {}^1\!/_2 n_x(n_x+1)$
Poly.	$\times$		Polytopic: $m\left[K_\theta(\theta)\right]$	$m\left[K_\theta(\theta)\right] = 2^{n_\theta} m_{xu} m_{xy}$
			Affine: $m\left[K_\theta(\theta)\right]$	$m\left[K_\theta(\theta)\right] = (n_\theta+1) m_{xu} m_{xy}$
	$\checkmark$		$m\left[P_\rho(\rho)\right] + m\left[R(\theta)\right] + 2m[S]$	$m\left[R(\theta)\right] = {}^1\!/_2 n_x(n_x+1)(n_\theta^R+1)$ $m[S] = {}^1\!/_2 n_x(n_x+1)$

$m\left[P_\rho(\rho)\right] = m_{xzy} m_{xwu} - n_z n_w - n_y n_u$

3.1.2 *Synthesis Complexity*

In the following both the total size of the LMI resulting from the diagonal concatenation of multiple LMI conditions and the number of decision variables are assessed.

3.1.2.1 *Polytopic LPV Synthesis*

Synthesis complexity is first assessed for PIDLFs.

PARAMETER-INDEPENDENT LYAPUNOV FUNCTIONS
The size of the LMIs $\mathcal{L}_R(\rho)$ (2.122) and $\mathcal{L}_S(\rho)$ (2.123) is determined by (dependency on σ is dropped due to PIDLFs)

$$s\big[\mathcal{L}_R(\rho)\big] = (n_x + n_w - n_y) + n_z \quad \text{and}$$
$$s\big[\mathcal{L}_S(\rho)\big] = (n_x + n_z - n_u) + n_w.$$

Note that in order to solve the LMIs a Schur complement with respect to $\frac{1}{\gamma}$ has to be taken each, which accounts for the additional terms n_z and n_w. The dimensions of the basis forming the null spaces $N_R(\rho)$ and $N_S(\rho)$ are due to the assumptions on the full row rank, which means that it is derived by the number of columns minus the number of rows, respectively.

Furthermore, if evaluated in a hyperbox the number of LMIs grows with $O(2^{n_\theta})$. Together with the Lyapunov variable coupling condition of size $2n_x$, the total size of the LMI amounts to

$$2^{n_\theta} \left(2(n_x + n_w + n_z) - (n_y + n_u)\right) + 2n_x.$$

The associated number of decision variables of the existence conditions are limited to the Lyapunov variables R and S and amount to $n_x(n_x + 1)$. When solving for the controller in the vertices, one may again obtain $m\big[K_\theta(\theta)\big]$ from (3.6), although closed-form formulae (2.127)–(2.132) can also be used, as performed in the Matlab implementation hinfgs.

PARAMETER-DEPENDENT LYAPUNOV FUNCTIONS
The parameterization of the Lyapunov functions has a strong impact on the synthesis complexity. Assume again that while $S(\theta) = S$ is chosen constant, $R(\theta)$ is parameterized as (3.7). The number of decision variables therefore increases to $n_x(n_x + 1)(1 + {}^1\!/_2 n_\theta^R)$. Furthermore, the LMI (2.122) has to be evaluated on $2^{n_\theta + n_\theta^R}$ vertices when considering the extremal values of $(\theta, \nu) \in \theta \times \nu$. The multi-convexity approach further introduces n_θ^R additional LMI constraints of size $\text{rank}(N_R) + n_z$. The second multi-convexity constraint is not required if only $R(\theta)$ is parameter-dependent. Furthermore, as above, it is assumed that B_p is parameter-independent, s. t. only LMIs of size n_x are introduced.

Additionally, the coupling (2.124) needs to be verified on the $2^{n_\theta^R}$ vertices. In conclusion the total size of the LMI is

$$\left(2^{n_\theta + n_\theta^R}\right)(n_x + n_w + n_z - n_u)$$
$$+ 2^{n_\theta}(n_x + n_w + n_z - n_y) + n_\theta^R n_x + 2^{n_\theta^R + 1} n_x.$$

3.1.2.2 *LFT-Based LPV Synthesis*

A core advantage in the synthesis of LPV controllers based on the LFT paradigm and the FBSP consists in a decoupling of parameter-dependent from parameter-independent LMIs. In addition, the multiplier conditions are quadratic in the parameters and therefore easily convexified by inertia hypotheses (multi-convexity) even in the case of rational parameter-dependence of the plant.

PARAMETER-INDEPENDENT LYAPUNOV FUNCTIONS
After application of the Schur complement, the nominal LMIs $\mathcal{L}_{R,M}$ (2.151) and $\mathcal{L}_{S,N}$ (2.152) are of the size

$$s[\mathcal{L}_{R,M}] = (n_x + n_w + n_{p_\Delta}^P + n_{q_\Delta}^P - n_y) + n_z \quad \text{and}$$
$$s[\mathcal{L}_{S,N}] = (n_x + n_z + n_{p_\Delta}^P + n_{q_\Delta}^P - n_u) + n_w,$$

which is again derived from the dimensions of the null spaces as explained above. The Lyapunov variable coupling condition $\mathcal{L}_{R,S}$ (2.153) is again of size $2n_x$ and the multiplier conditions $\mathcal{L}_M(\delta)$ (2.154) and $\mathcal{L}_N(\delta)$ (2.155) are both of size $n_{p_\Delta}^P + n_{q_\Delta}^P$.

With the multi-convexity constraints associated with full-block multiplier (FBM) as detailed in Lma. 2.4 on page 68, the multiplier conditions $\mathcal{L}_M(\delta)$ (2.154) and $\mathcal{L}_N(\delta)$ (2.155) have to be evaluated at vertices of the convex hull conv (δ) of the parameter range. Assuming a hyperbox, one has 2^{n_δ} LMI constraints on each multiplier and a total size of the concatenated LMIs of

$$2(2n_x + n_w + n_z + n_{p_\Delta}^P + n_{q_\Delta}^P) - (n_y + n_u) + 2^{n_\delta + 1}(n_{p_\Delta}^P + n_{q_\Delta}^P).$$

As before, the Lyapunov variables require $n_x(n_x + 1)$ decision variables and the major increase is due to the size of the multipliers, which can be structurally constrained. The FBMs M and N each require $(n_{p_\Delta}^P + n_{q_\Delta}^P)(2(n_{p_\Delta}^P + n_{q_\Delta}^P) + 1)$ decision variables. The use of D/G-scalings (D/G-Ss) and the associated commutativity requirement on all blocks of M and N with $\Delta^P(\delta)$ essentially reduces the number of decision variables to the case, in which several multiplier conditions involving only a single parameter are solved simultaneously. Then, the individual multiplier block sizes are inferred from the parameter's repetitions, leading to a total of

$$\sum_{i=1}^{n_\delta} r_{\delta,i}(r_{\delta,i} + 1) + r_{\delta,i}(r_{\delta,i} - 1) = 2 \sum_{i=1}^{n_\phi} r_{\delta,i}^2$$

decision variables for M and N. Consequently parameter blocks have to be square, s. t. one may define $n_\Delta^P \triangleq n_{p_\Delta}^P = n_{q_\Delta}^P$. Without *a priori* knowledge of the number of repetitions, the limiting cases can be considered: Take $n_\delta \to n_\Delta^P$, which leads to $r_{\delta,i} = 1$, $i \in \{1, \ldots, n_\delta\}$ and therefore the number of decision variables collapses to $2n_\delta$. If $n_\delta \to 1$, D/G-Ss are lossless [105], since a FBM is implied. This yields $2n_\Delta^{P\,2}$ decision variables for both multipliers. Note that D/G-Ss render the multiplier conditions trivially fulfilled, s. t. the total size of the LMI reduces to

$$2(2n_x + n_w + n_z + n_\Delta^P) - (n_y + n_u). \tag{3.16}$$

When solving for the controller variables, the number of decision variables adheres to $m[K_\delta(\delta)]$ from (3.10). Again, closed-form formulae (2.127)–(2.132) can also be used.

PARAMETER-DEPENDENT LYAPUNOV FUNCTIONS
Consider again the approach to mimic the plant's parameter-dependence in the Lyapunov variable, more specifically the choice shown in Eq. (3.13), which introduces $m[R(\rho)] = {}^1/_2 n_x(n_x + 1) + (n_{p_\Delta}^P + n_{q_\Delta}^P)^2$ decision variables, as obvious from (3.14).

When non-constant null spaces $N_R(\delta)$ and $N_S(\delta)$ are considered, the sizes of the resulting parameter blocks associated with the outer factors in (2.73) and (2.74) result from

$$\Delta_{B_R} = \mathrm{diag}\Big(\partial\Delta^P, \Delta^P, \Delta^P, \Delta^P, \Delta^P\Big) \in \mathbb{R}^{(n_{q_\Delta^R} \times n_{p_\Delta^R})},$$
$$\Delta_{B_S} = \mathrm{diag}\Big(-\Delta^{P\top}, -\Delta^{P\top}\Big) \in \mathbb{R}^{(n_{q_\Delta^S} \times n_{p_\Delta^S})},$$
$$\Delta_{B_{RS}} = \mathrm{diag}\Big(\Delta^P, \Delta^P\Big) \in \mathbb{R}^{(n_{q_\Delta^{RS}} \times n_{p_\Delta^{RS}})},$$

and are upper bounded by

$$n_{p_\Delta^R} = 5n_{p_\Delta}^P, \quad n_{q_\Delta^R} = 5n_{q_\Delta}^P,$$
$$n_{p_\Delta^S} = 2n_{q_\Delta}^P, \quad n_{q_\Delta^S} = 2n_{p_\Delta}^P,$$
$$n_{p_\Delta^{RS}} = 2n_{p_\Delta}^P, \quad n_{q_\Delta^{RS}} = 2n_{q_\Delta}^P.$$

At the cost of an increased number of states n_x, in this approach it will usually be beneficial to pre- and postfilter, reducing the problem to the sizes

$$n_{p_\Delta^R} = 4n_{p_\Delta}^P, \quad n_{q_\Delta^R} = 4n_{q_\Delta}^P,$$
$$n_{p_\Delta^S} = n_{q_\Delta}^P, \quad n_{q_\Delta^S} = n_{p_\Delta}^P.$$

For this case, LMIs (2.136)–(2.138) jointly have the size

$$2(n_x + n_w + n_z) - (n_y + n_u) + n_{q_\Delta^R} + n_{q_\Delta^S} + (n_{q_\Delta^{RS}} + 2n_x)$$
$$= 2(n_x + n_w + n_z) - (n_y + n_u) + 5n_{q_\Delta}^P + n_{p_\Delta}^P + 2n_x.$$

In order to evaluate the multiplier conditions (2.139) via FBMs, also the rates of change have to be taken into account for conditions on M, which requires the formulation of 2^{2n_δ} LMI constraints. In total the multiplier conditions form an LMI of size

$$2^{n_\delta}(2^{n_\delta}n_{p_\Delta^R} + n_{p_\Delta^S} + n_{p_\Delta^{RS}}) = 2^{n_\delta}(2^{n_\delta}4n_{q_\Delta}^P + n_{p_\Delta}^P + n_{q_\Delta}^P)$$

containing

$$(n_{q_\Delta}^P + n_{p_\Delta}^P)(3(n_{q_\Delta}^P + n_{p_\Delta}^P) + 1)$$

decision variables. Again, using D/G-S, the multiplier conditions are trivially fulfilled and the number of multiplier related decision variables reduces to

$$3\sum_{i=1}^{n_\delta} r_{\delta,i}^2 + \sum_{i=1}^{n_\delta}(3r_{\delta,i})^2 = 12\sum_{i=1}^{n_\delta} r_{\delta,i}^2,$$

when treating rates of change independently and regarding the repeated Δ^P-block structure as a single block with three times the repetitions for each parameter δ_i.

3.1.2.3 *Gridding-Based LPV Synthesis*

PARAMETER-INDEPENDENT LYAPUNOV FUNCTIONS
For n_g equidistant grid points between the minimum and maximum value of a scheduling signal, the number of LMI constraints grow with $O(n_g^{n_\rho})$. The size of the LMIs derived from (2.122) and (2.123) is identical to the polytopic case by a Schur complement, which leads to a total size of the LMI of

$$n_g^{n_\rho}(2(n_x + n_w + n_z) - (n_y + n_u)) + 2n_x. \tag{3.17}$$

As before, the only decision variables of the existence conditions are the Lyapunov variables R and S and amount to $n_x(n_x + 1)$. When solving for the controller in the grid points, one needs to solve for $n_g^{n_\rho} \cdot m[K_\rho(\rho)]$ variables as obtained from (3.15). More typically the closed-form formulae (2.127)–(2.132) are used, which further reduce in online complexity for constant Lyapunov functions.

PARAMETER-DEPENDENT LYAPUNOV FUNCTIONS
As in the previous approaches, the parameterization of the Lyapunov functions has a strong impact on the synthesis complexity. Assume again that while $S(\rho) = S$ is chosen constant, $R(\rho)$ is chosen parameter-dependent. Following the heuristic to mimic the plant's parameter-dependence, it appears a natural choice to consider the parameterization (3.7), which leads to $n_x(n_x + 1)(1 + {}^1/_2 n_\delta^R)$ decision variables. However, the Lyapunov matrix can also be chosen to depend on the scheduling signals ρ directly. In any case, the rates of change η or σ do not have to be gridded, since they enter the matrix inequality in an affine manner. Therefore, LMI (2.122)

Table 3.3: Synthesis complexity of LPV controllers: No. of dec. vars vs. synth. tech.

Technique		Number of decision variables	
PDLF		Total	In parts
Grid.	$\times$	$d[R] + d[S]$	$d[R] = d[S] = {}^1\!/_2 n_x(n_x + 1)$
	$\checkmark$	$d[R(\rho)] + d[S]$	$d[R(\rho)] = {}^1\!/_2 n_x(n_x + 1)(n_\theta^R + 1)$
LFT	$\times$ FBM	$d[R] + d[S] + d[M] + d[N]$	$d[R] = d[S] = {}^1\!/_2 n_x(n_x + 1)$ $d[M] = d[N] = {}^1\!/_2 m_{p_\Delta^P q_\Delta^P}(m_{p_\Delta^P q_\Delta^P} + 1)$
	$\times$ D/G-S	$d[R] + d[S] + d[M] + d[N]$	$d[R] = d[S] = {}^1\!/_2 n_x(n_x + 1)$ $d[M] = d[N] = \sum_{i=1}^{n_\delta} r_{\delta,i}^2$ $2n_\delta \leqslant d[M] \leqslant 2n_\Delta^{P\,2}$
	$\checkmark$ FBM	$d[R(\delta)] + d[S]$ $+ d[M] + d[N] + d[P]$	$d[R(\delta)] = {}^1\!/_2 n_x(n_x + 1) + {}^1\!/_4 m_{p_\Delta^P q_\Delta^P}^2$ $d[S] = {}^1\!/_2 n_x(n_x + 1)$ $d[M] = 2 m_{p_\Delta^P q_\Delta^P}(4 m_{p_\Delta^P q_\Delta^P} + 1)$ $d[N] = d[P] = {}^1\!/_2 m_{p_\Delta^P q_\Delta^P}(m_{p_\Delta^P q_\Delta^P} + 1)$
	$\checkmark$ D/G-S	$d[R(\delta)] + d[S]$ $+ d[M] + d[N] + d[P]$	$d[R(\delta)] = {}^1\!/_2 n_x(n_x + 1) + n_\Delta^{P\,2}$ $d[S] = {}^1\!/_2 n_x(n_x + 1)$ $d[M] = 10 \sum_{i=1}^{n_\delta} r_{\delta,i}^2$ $d[N] = d[P] = \sum_{i=1}^{n_\delta} r_{\delta,i}^2$
Poly	$\times$	$d[R] + d[S]$	$d[R] = d[S] = {}^1\!/_2 n_x(n_x + 1)$
	$\checkmark$	$d[R(\theta)] + d[S]$	$d[R(\theta)] = {}^1\!/_2 n_x(n_x + 1)(n_\theta^R + 1)$

has to be evaluated on $2^{n_\delta^R} n_g^{n_\rho}$ grid points, whereas LMI (2.123) is still only considered in $n_g^{n_\rho}$ grid points. For affine parameterizations of the Lyapunov variable, the coupling (2.124) needs to be verified on $2^{n_\delta^R}$ vertices, whereas—perhaps more typically—it is gridded over the $n_g^{n_\rho}$ grid points. In conclusion the total size of the LMI is

$$2^{n_\delta^R} n_g^{n_\rho} \left(2(n_x + n_w + n_z) - (n_y + n_u)\right) + 2^{n_\delta^R + 1} n_x. \tag{3.18}$$

3.1.2.4 *Synthesis Complexity — Summary*

Tabs. 3.3 and 3.4 summarize LPV controller synthesis complexity.

Table 3.4: Synthesis complexity of LPV controllers: LMI size vs. synth. tech.

Technique		Size of LMI (existence conditions)	
PDLF		Total	In parts
Grid.	×	$n_g^{n_\rho}\left(s[\mathcal{L}_R(\rho)] + s[\mathcal{L}_S(\rho)]\right) + s[\mathcal{L}_{RS}(\rho)]$	$s[\mathcal{L}_R(\rho)] = m_{xzw} - n_y$ $s[\mathcal{L}_S(\rho)] = m_{xzw} - n_u$ $s[\mathcal{L}_{RS}(\rho)] = 2n_x$
	✓	$n_g^{n_\rho}\left(2^{n_\theta^R} s[\mathcal{L}_R(\rho,\sigma)] + s[\mathcal{L}_S(\rho)] + s[\mathcal{L}_{RS}(\rho)]\right)$	$s[\mathcal{L}_R(\rho,\sigma)] = m_{xzw} - n_y$ $s[\mathcal{L}_S(\rho)] = m_{xzw} - n_u$ $s[\mathcal{L}_{RS}(\rho)] = 2n_x$
LFT	FBM ×	$s[\mathcal{L}_{R,M}] + s[\mathcal{L}_{S,N}] + s[\mathcal{L}_{RS}] + 2^{n_\delta}\left(s[\mathcal{L}_M(\delta)] + s[\mathcal{L}_N(\delta)]\right)$	$s[\mathcal{L}_{R,M}] = m_{xq_\Delta^P zw} - n_y$ $s[\mathcal{L}_{S,N}] = m_{xp_\Delta^P zw} - n_u$ $s[\mathcal{L}_{RS}] = 2n_x$ $s[\mathcal{L}_M(\delta)] = n_{q_\Delta^P},\, s[\mathcal{L}_N(\delta)] = n_{p_\Delta^P}$
	D/G-S ×	$s[\mathcal{L}_{R,M}] + s[\mathcal{L}_{S,N}] + s[\mathcal{L}_{RS}]$	$s[\mathcal{L}_{R,M}] = m_{x\Delta^P zw} - n_y$ $s[\mathcal{L}_{S,N}] = m_{x\Delta^P zw} - n_u$ $s[\mathcal{L}_{RS}] = 2n_x$
	FBM ✓	$s[\mathcal{L}_{R,M}] + s[\mathcal{L}_{S,N}] + s[\mathcal{L}_{RS,P}] + 2^{2n_\delta} s[\mathcal{L}_M(\delta,\eta)] + 2^{n_\delta}\left(s[\mathcal{L}_N(\delta)] + s[\mathcal{L}_P(\delta)]\right)$	$s[\mathcal{L}_{R,M}] = m_{xzw} + 4n_{q_\Delta^P} - n_y$ $s[\mathcal{L}_{S,N}] = m_{xzw} + n_{p_\Delta^P} - n_u$ $s[\mathcal{L}_M(\delta,\eta)] = 4n_{q_\Delta^P},\, s[\mathcal{L}_P(\delta)] = n_{q_\Delta^P}$ $s[\mathcal{L}_{RS,P}] = 2n_x + n_{q_\Delta^P},\, s[\mathcal{L}_N(\delta)] = n_{p_\Delta^P}$
	D/G-S ✓	$s[\mathcal{L}_{R,M}] + s[\mathcal{L}_{S,N}] + s[\mathcal{L}_{RS,P}]$	$s[\mathcal{L}_{R,M}] = m_{xzw} + 4n_\Delta^P - n_y,$ $s[\mathcal{L}_{S,N}] = m_{xzw} + n_\Delta^P - n_u,$ $s[\mathcal{L}_{RS,P}] = 2n_x + n_\Delta^P$
Poly	×	$2^{n_\theta}\left(s[\mathcal{L}_R(\theta)] + s[\mathcal{L}_S(\theta)]\right) + s[\mathcal{L}_{RS}]$	$s[\mathcal{L}_R(\theta)] = m_{xzw} - n_y$ $s[\mathcal{L}_S(\theta)] = m_{xzw} - n_u,\, s[\mathcal{L}_{RS}] = 2n_x$
	✓	$2^{n_\theta + n_\theta^R} s[\mathcal{L}_R(\theta,\nu)] + 2^{n_\theta} s[\mathcal{L}_S(\theta)] + 2^{n_\theta^R} s[\mathcal{L}_{RS}(\theta)] + n_\theta^R s\left[\frac{\partial^2}{\partial\theta_i^2}\mathcal{L}_R(\theta,\nu)\right]$	$s\left[\frac{\partial^2}{\partial\theta_i^2}\mathcal{L}_R(\theta,\nu)\right] = n_x$

3.2 Fields of Application and Associated Methods

The following survey of LPV control applications associated with the respective fundamental modeling and controller design methods—polytopic, multiplier-based and gridding-based—is extended from [59]. It has been updated to include the most recent publications and serves the purpose to assess the range of applications, the associated model complexity and synthesis method used to solve the control problem.

As previously reported in [59], experimental LPV control applications reported in the literature are ranging over a wide array of different subjects from robotic manipulators to micro-systems and various academic examples. In aerospace applications, even though many simulation results are available, relatively little experimental work is reported. This is likely due to the high effort and risks involved, e. g., in undertaking actual flight tests, and the possibly classified status of the respective military flight test reports. However, in this field and also other fields dealing with highly complex systems, the usual controller validation procedure involves so-called high-fidelity (HiFi) simulations—sometimes also denoted «industry-grade simulations»—as an intermediate step in-between «desktop analysis» and experimental validation. In aerospace applications, HiFi simulations are often performed in the form of pilot-in-the-loop (PIL) experiments with highly accurate flight simulators, see, e. g., [H7]. Due to the high requirements on their accuracy, HiFi simulation-based validations are included in this section's survey. References pointing to HiFi simulation-validated results are distinguished by the letter «H» preceding the reference number, whereas experimental work is indicated by an «E». «Low-fidelity» simulation results are not explicitly identified.

In the following, a chronological overview over the range of applications using the different synthesis techniques is given. Figure 3.1 shows a time-line, listing and classifying results by year and synthesis technique.

One of the more recent lines of research involved the control of the F-16 Variable stability In-flight Simulator Test Aircraft (VISTA), a highly maneuverable aircraft with relaxed airframe induced stability [H1, H3]. Civil research focuses more on safety issues and has spawned fault-tolerant controller and fault detection and isolation (FDI) filter designs in the LPV framework. The Advanced Fault Diagnosis for Sustainable Flight Guidance and Control (ADDSAFE)[1] project incorporates HiFi simulations of Boieng aircraft to validate these schemes [H4, H16, H28, H29, H31].

Wind energy systems, for instance, can be validated using the Fatigue, Aerodynamics, Structures, and Turbulence (FAST) software [68], a freely available HiFi

---

[1] http://addsafe.deimos-space.com/
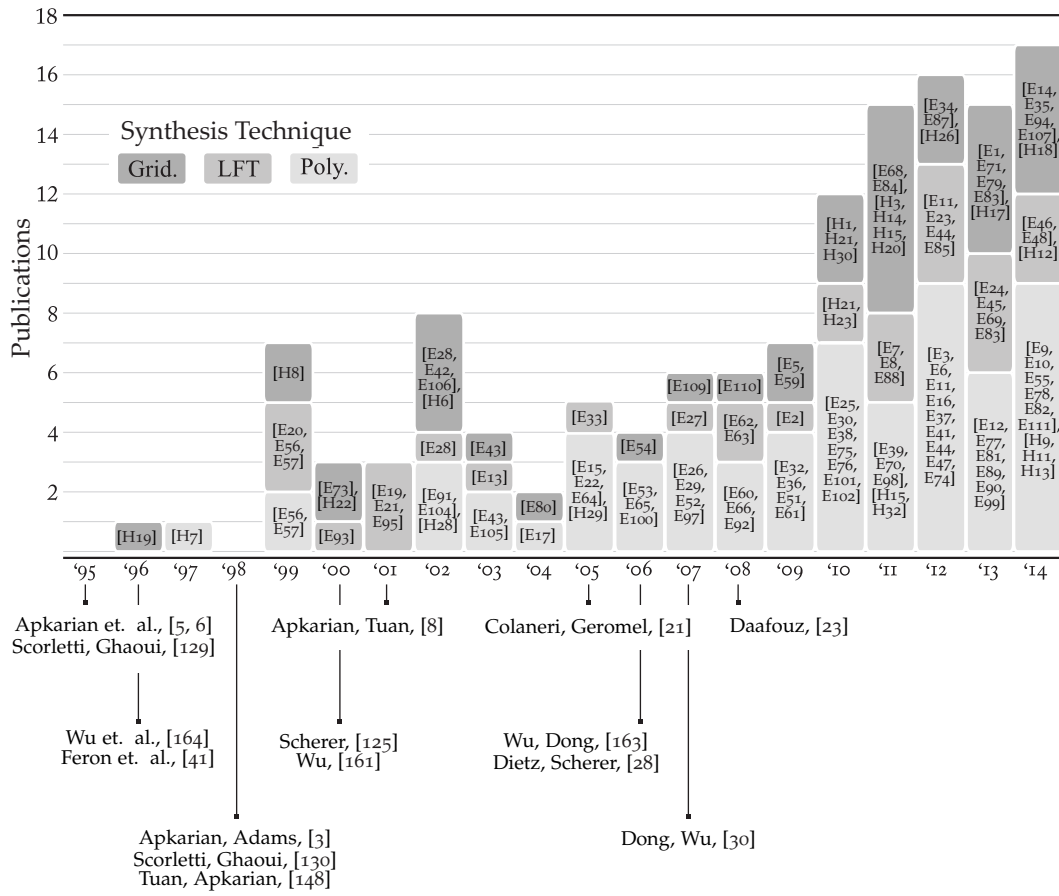
Figure 3.1: Time-line of application results validated by experiments or HiFi simulations and milestones in theoretical LPV research.
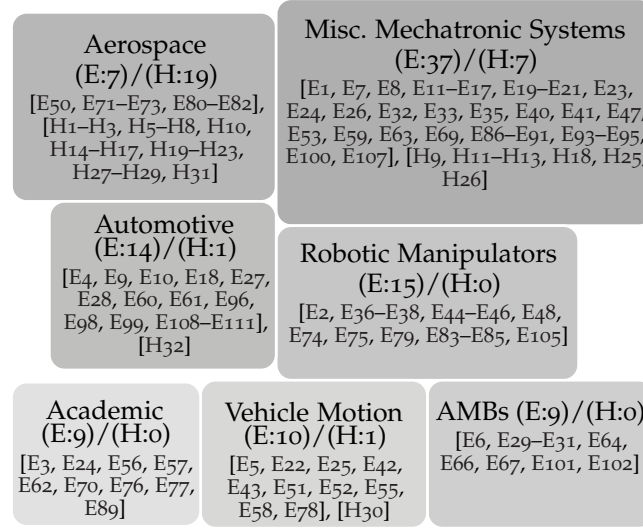
Figure 3.2: LPV control results validated by experiments or HIFI simulations grouped by application type.

simulator developed by the National Renewable Energy Laboratory (NREL)[2] and certified by Germanischer Lloyd Wind Energy[3].

Figure 3.2 proposes a classification of the different types of applications and arranges them by the related number of publications. Especially the field of aerospace applications carries a wide range of different applications, listed in Tab. 3.5. Work on the National Aerospace Association (NASA) HL-20 Re-Entry Vehicle was embedded as a highly nonlinear benchmark system into the LPV Modeling, Analysis and Design (LPVMAD)[4] research project. The project was divided into two phases, where the second phase comprised the validation of data-based modeling and validation tools [96, 144] as well as integral quadratic constraint (IQC)-based analysis and LPV-LFT synthesis methods on a HIFI simulation model [67] and its final results are reported in [H21]. In the first phase, these techniques where tested on simpler simulation models, see, e. g., [94, 96, 108, 150, 152], which are therefore not included in this categorization. A more detailed overview of the project and the challenges of LPV tools in space applications can be found in [95].

Among the miscellaneous mechatronic applications one finds very different systems, listed in Tab. 3.6. Work on active magnetic bearings (AMBs) is listed separately in Fig. 3.2 due to the extensive line of research. The academic examples include the items listed in Tab. 3.7.

The first HIFI simulation-based validations of LPV controllers is reported in 1996 [H19], whereas the first experimental validations date back to 1999 [E20, E56]. In [E56] both polytopic and small-gain theorem-based LFT-LPV controller synthesis techniques are applied to the well-known academic example of an arm-driven in-

Table 3.5: Aerospace applications.

- Airplanes [E80–E82], [H2, H3, H5, H7, H8, H14, H19, H22, E73, H23, H28, H29]
- Hypersonic Vehicles [H24, H27]
- Re-Entry and Launch Vehicles [H21]
- Satellites [E34, E50]
- Turbofan Engines [H6]
- Unmanned Aerial Vehicles (UAVs) [E72]

Table 3.6: Mechatronic applications.

- Wind Energy [H11, H12, H18, H25, H26]
- Agricultural Open Canal Systems [E15], [H9]
- Active Vision Systems [E93]
- CD Players [E20, E21]
- Control Moment Gyroscopes [E1, E94]
- Drilling Systems [E53, E58]
- Electro-Hydraulic Servo Systems [E100]
- Electro-Magnetic Actuators [E26]
- Flexible Ball Screw Drives [E35]
- Magneto-Rheological Dampers [E68, E86, E87], [H13]
- Hydro-Kinetic Turbines [E32]
- Induction Motors/Generators [E13, E95]
- Injection Molding Machines [E91]
- Laser Printers [E17]
- Micro-Systems [E16]
- Active Noise/Vibration Control [E7, E8, E11, E12, E23, E39–E41, E90]
- Container Crane Load Swing [E47, E69]
- Shape Memory Alloys/Ionic Polymer Metal Composites [E59, E63]
- Wafer Scanners [E33]
- Web Server Performance Control [E92]

Table 3.7: Academic examples.

- Active Vibration Control Test Bench [E24, E88, E89]
- Arm-Driven Inverted Pendulum [E56, E57, E62, E70]
- T-Inverted Pendulum [E76]
- Twin Rotor MIMO System [E77]
- Quadruple Tank Process [E3]

verted pendulum, whereas [E20] implements a FBM-based LFT-LPV design on micro-processor hardware for a compact disc player. The underlying theory of LFT-LPV controller synthesis with FBM, however, is first publicly reported in 2000 [124].

In [E73], gridding-based LPV controller synthesis is carried out for the single-input single-output (SISO) pitch control problem of the Vectored thrust Aircraft Advanced flight Control (VAAC) Harrier airplane. The paper focuses less on technical details, but rather on in-flight experience and testing carried out in what was stated to be «one of the most successful first test flights performed by Defence Evaluation and Research Agency (DERA)[5] to date».

Polytopic Approach

Judging from the sheer number of related publications, the polytopic LPV controller synthesis approach is most popular among the three considered here. Accordingly, the range of applications is large, including AMB systems [E6, E29, E30, E64–E66, E101, E102], robotic manipulators [E36–E38, E44, E74, E75, E104, E105], engine control [E60, E61, E99, E111], miscellaneous mechatronic systems [E15–E17, E26, E32, E47, E53, E91, E100], vehicle motion control [E22, E25, E43, E51, E52, E55, E78], academic test benches [E3, E56, E57, E70, E76, E77], noise canceling headsets and vibration control test benches [E9–E12, E24, E39, E41, E89, E90], aerospace flight control [E81, E82] and computer sciences [E92].

Multiplier-Based LFT Approach

At around the time of the first polytopic and small-gain theorem-based LPV controller validations, LFT-LPV synthesis with FBM was successfully applied in [E20], validating simulation results shown in [26]. Even though the number of applications of the multiplier-based LFT-LPV synthesis approach has been relatively small, noteworthy experimental results with industrial relevance were published between 2001 and 2014. These include CD players [E19, E21], induction motors [E13, E95], engines [E27, E28] and a wafer stage [E33]. More recently, the application of LPV techniques in robotics has been considered, both as an example on which to validate methods to handle LPV models of high complexity experimentally [E44–E46, E48] as well as with explicit industrial grade control objectives in mind [E81, E85]. In the field of active noise cancellation headsets and vibration control the LFT approach as per [5] is also followed [E7, E8, E11, E23, E24, E88]. Very recently LFT techniques have also been applied in the control of wind turbines [H12].

Gridding Approach

The gridding-based approach was well-known at least from the publication of [3, 160] and experimental results in flight control [E73] were reported as early as 2000 with impressive results. Aircraft motion control was again considered in [E80] and [E81]. Apart from that, relatively few experimental publications making use of the gridding approach exist, for reasons mentioned above. Among them are automated

---

5 Authors' note: Full meaning of acronym added by the author.

lane guidance [E42], automated driving via visual feedback [E43], robotics [E79, E83, E84, E103], engine control [E54, E109, E110] and the control of a control moment gyroscope [E1, E94]. The comparably high amount of HiFi simulation validated control designs, however, indicates its usefulness in the highly nonlinear aerospace related control problems. Further recent applications include oxygen stochiometry regulation in fuel cells [E14] and wind turbine control [H18].

Examples of Methods Applied for Reduced Scheduling Order

As discussed in from Sect. 3.1, large numbers of scheduling signals/parameters or a large number of repetitions in the parameter block of an LFR induce a high amount of LMI constraints, decision variables, online computational load and memory requirements. The synthesis complexity induced by the scheduling order varies heavily between the major synthesis approaches (polytopic, multiplier-based and gridding). In addition, the complexity incurred strongly depends on the choice of the LPV model, since even within one of the frameworks of polytopic, LFT-based or general LPV models, the representation is most often not unique. For instance, [E48] exploits FBMs, which allow for full/block-diagonal parameter blocks of the plant model's LFR. Without any approximation, this reduces the multiplier size and therefore the number of decision variables in such a degree that the LFT-LPV synthesis method outperforms the other methods in terms of both low synthesis and implementation complexity. In this respect, the number of parameters can only be taken as an indication of the synthesis and implementation complexity involved, but not as a rigorous measure.

Tab. 3.8 categorizes the reported literature in a matrix, comprising the employed synthesis technique and the complexity in terms of the original scheduling order (number of parameters in the polytopic and LFR, or measured signals in the gridding framework) of the original model. The details in the respective references reveal that even though the polytopic approach appears to be capable of dealing with a high scheduling order similar to the LFT-based methods in terms of the number of related publications, approximate models of reduced scheduling order are generally required. In fact, a controller design for a three three-degree of freedom (3-DOF) robotic manipulator reported in [E45] is the only report of a controller affinely scheduled on 16 different parameters without approximation, which is achieved using D/G-S [E21]. In all additional work reported in the polytopic high scheduling order range, approximations are involved.

The gridding approach has not been used for models with a high number of scheduling signals. However, it should be noted that the number of parameters required when turning a general LPV model into an LFT-based or polytopic representation may be much higher than the number of actually measured scheduling signals. A polytopic LPV model of the control moment gyroscope[6] that will be the subject of Sect. 6.2, e.g., requires 15 different parameters, despite being al-

---

6 http://www.ecpsystems.com

Table 3.8: Publications sorted by synthesis technique and number of sched. parameters/signals.

		No. of Scheduling Parameters/Signals		
		Low (1-2)	Medium (3-6)	High (7+)
Synthesis Technique	Poly.	(E:33)/(H:3) [E6, E9, E10, E15–E17, E22, E25, E26, E29, E30, E32, E47, E51–E53, E55–E57, E64–E66, E70, E81, E82, E91, E92, E98–E102], [H7, H11, H15]	(E:15)/(H:4) [E3, E11, E12, E39, E41, E43, E60, E61, E75, E76, E78, E89, E90, E104, E111], [H9, H13, H15, H32]	(E:6)/(H:2) [E36–E38, E44, E74, E77], [H28, H29]
	Grid.	(E:19)/(H:13) [E1, E5, E14, E34, E35, E42, E54, E59, E68, E71, E73, E80, E83, E86, E87, E94, E107, E109, E110], [H2, H3, H6, H8, H14, H15, H18–H22, H26, H30]	(E:5)/(H:1) [E28, E43, E79, E83, E106], [H15]	
	LFT	(E:14)/(H:3) [E13, E19–E21, E24, E33, E56, E57, E63, E69, E83, E85, E93, E95], [H12, H21, H23]	(E:9)/(H:0) [E7, E8, E11, E23, E27, E28, E62, E83, E88]	(E:5)/(H:0) [E2, E44–E46, E48]

Table 3.9: Publications sorted by dynamic order and number of sched. parameters/signals.

		No. of Scheduling Parameters/Signals		
		Low (1-2)	Medium (3-6)	High (7+)
Dynamic Order	Low (1-3)	(E:18)/(H:4) [E4, E13, E15, E26, E32, E47, E54, E55, E59, E72, E92, E95, E98, E100, E107–E110], [H6, H8, H14, H23]	(E:2)/(H:2) [E60, E61], [H9, H32]	(E:1)/(H:0) [E2]
	Medium (4-9)	(E:41)/(H:15) [E1, E14, E19–E22, E29–E31, E34, E35, E42, E51–E53, E56, E57, E63–E71, E73, E80–E83, E85–E87, E91, E93, E94, E99, E101, E102, E111], [H2, H3, H7, H8, H10–H12, H15, H18–H22, H25, H26]	(E:20)/(H:2) [E3, E7, E8, E11, E12, E23, E27, E39–E41, E43, E75, E76, E78, E79, E83, E88, E90, E104, E106], [H13, H15]	(E:9)/(H:2) [E36–E38, E44–E46, E48, E74, E77], [H28, H29]
	High (10+)	(E:5)/(H:1) [E6, E9, E10, E24, E33], [H30]	(E:11)/(H:0) [E7, E8, E11, E12, E23, E28, E39, E41, E88–E90]	(E:2)/(H:0) [E45, E46]

ready considerably simplified by freezing some signals and a linearization of the nonlinear model about a moving operating point, [E1]. The number of scheduling signals eventually used in real-time experiments is then reduced to two by the above-mentioned approach which is justified by a significant increase in performance, although stability and performance guarantees are rendered void. In [E79], a choice of affine scheduling parameters is made, s. t. for frozen parameters the state space model represents two decoupled second order systems and two synthesis problems are solved in a two loop configuration with only a single and two scheduling parameters, respectively. The gridding approach is used, despite the low number of affine scheduling parameters.

In some works, such as [E36, E37, E44–E46], on the control of a robotic manipulator the complexity issues arising due to a high number of polytopic or LFT scheduling parameters are tackled by employing the principle component analysis (PCA)-based reduction of the parameter set [79] detailed in Sect. 2.1.4. The resulting approximate model is then used for designing the controller with tremendously reduced synthesis complexity. In [E45], this is combined with multiplier-based synthesis methods for models with affine parameter-dependence. D/G-Ss are used to cope with the otherwise intractable synthesis complexity and to achieve a low implementation complexity. For the controller synthesized based on the approximate model, stability and performance guarantees are established via *a posteriori* analysis performed in the LFT framework, [E37, E44–E46], i. e., by applying the FBSP on the closed-loop analysis LMI condition. In [E45], both full scheduling order and reduced scheduling order controller designs with guarantees are presented and compared in terms of their implementation complexity. In [E85] only the base axis of an industrial manipulator is considered, whereas in [E81] it is physically motivated to design separate LPV controllers for axis one and the axis pair two/three, comprising only a single and three scheduling parameters, respectively.

In other complex mechanical structures, such as a twin-rotor multiple-input multiple-output (MIMO) system [E77], parameters that are only slightly varying are simply fixed based on physical insight and exploratory experiments. State feedback synthesis is performed, which remains tractable even for eight polytopic scheduling parameters. In [H23] approximations based on physical insight are used to reduce the scheduling block's size of the LFR from 201×201 to 7×7.

The modeling of harmonic multi-sine disturbances in the generalized plant framework usually introduces two LPV scheduling parameters per frequency [E12, E90], which can lead to a very high number of scheduling parameters if many disturbance modes are superimposed. In [E12, E90] it is assumed that the disturbance frequencies are harmonically related and a second order Taylor expansion of sine and cosine terms are used as an approximation to reduce the number of independent scheduling parameters to two, independent of the number of frequencies considered. Despite the approximation, the closed-loop performance shows an effective reduction of noise.

The gain-scheduled controller design in [E34] for the in-orbit control of the engineering test satellite (ETS-VIII) spacecraft is based on a simplified LPV model and preliminary work is presented in [48]. Near symmetry in the singular values is observed and accordingly only half the parameter range is considered. A residual model covering the high frequency modes is then regarded as an additive uncertainty. Novel matrix inequalities are formulated that allow the Lyapunov variable to be constrained on a finer grid than that of the synthesis LMIs. This results in only two controllers to be interpolated. The underlying ideas are a restriction of the closed-loop PDLFs to a special form, where the $(2,1)$, $(2,2)$ and $(1,2)$ blocks are all identical, a parameter-independent controller input matrix, dilated LMIs and spline approximations [103] to reduce the LMI to a finite number.

Tab. 3.9 categorizes the reported results in a matrix comprising the dynamic order (number of states) and the scheduling order of the original model. Considering the low number of publications, it becomes evident that the synthesis of LPV gain-scheduled controllers for plants of both high dynamic and high scheduling order is a field for future research.

4

COMPACT LFT-LPV MODELING

≪We shape our tools and afterwards our tools shape us.≫

Marshall McLuhan

THE previous chapter has shown most of the LPV controller synthesis and implementation complexity is induced by properties of the model. This chapter investigates methods to arrive at equivalent LPV model representations with properties that are more favorable w. r. t. controller design. For this purpose, Sects. 4.1 and 4.2 first provide the problem formulations and the special model class that are dealt with in this chapter:

(i) The derivation of LPV representations from nonlinear ordinary differential equations (ODEs) (Sect. 4.3),

(ii) Optimal rational or affine parameterization of LPV representations (Sect. 4.4 and 4.5).

The chapter is concluded with the novel modeling tools being applied to two nonlinear plant models of moderate and high complexity, respectively. First, Sect. 4.6 deals with the LPV model generation of a 3-DOF robotic manipulator of type Thermo CRS A465. Then, LPV models of various complexity levels are derived for a control moment gyroscope (CMG).

4.1 Problem Formulation

It is well known that representing nonlinear systems in the LPV framework is highly non-unique. This non-uniqueness mostly arises from multiple options of turning arbitrary nonlinear implicit system representations of the form

$$0 = f(\dot{x}, x, u), \tag{4.1}$$
$$y = g(x, u), \tag{4.2}$$

into system (differential) equations linear in the states and inputs. However, even in the case that a—potentially even unique—solution to this task is obtained, the introductory chapters have illustrated that the choice of LPV modeling framework and associated synthesis methods as well as the parameterization approach within such a framework introduces further options.

Consequently, the following two problems can be formulated.

Problem 4.1 (LPV System from Nonlinear Implicit System)
Based on the implicit nonlinear ODE (4.1) and the output equation (4.2), find a general LPV system representation. □

Problem 4.2 (LPV System Parameterization)
Based on a general LPV system representation, find a parameter set admitting a rational or affine LPV system parameterization with a minimal number of parameters. □

In the following sections, the above two distinct problems are investigated separately and solutions are proposed that aim for a systematic modeling approach using full parameter blocks in an LFT-LPV controller synthesis approach. Combining both solution approaches to Probs. 4.1 and 4.2 is aiming at reducing the amount of ambiguity in the derivation of LPV models suitable for efficient controller synthesis. As a standing assumption, LPV models of reduced complexity are desired to render controller synthesis tractable and possibly less conservative. The issue of finding LPV realizations optimal w. r. t. conservatism is only touched.

Problem 4.1 is discussed building on tools developed in [146, Sect. 7.4.2, p. 187] and specializing them for the case of nonlinear mechanical systems. Subsequently, Prob. 4.2 is considered, assuming that a general non-singular descriptor LPV representation has been derived based on a solution of Prob. 4.1.

4.2 Mechanical LPV Systems

An automated tool for generating and assessing affine LPV models is proposed in [77]. The algorithm directly identifies all possible affine representations and assesses the incurred overbounding and the number of parameters as a means of ranking models in terms of their supposed suitability for synthesis.

In contrast, the algorithm proposed in [146, Sect. 7.4.2, p. 187] translates first principle nonlinear differential equations into so-called LPV kernel representations (LPV-KRs) of the form

$$\sum_{i=0}^{n} A_i\left(t, q, \dot{q}, \ddot{q}, \dots\right) \frac{d^i}{dt^i} q = 0, \tag{4.3}$$

which are closely related to descriptor forms.

In this chapter, the class of systems governed by a nonlinear differential equation of the form

$$J(q, t)\ddot{q} + k(\dot{q}, q, t) = g(\dot{q}, q, t) + T(q, t)u, \tag{4.4}$$

is considered, where $J(q, t) \in \mathbb{R}^{n_q \times n_q}$ with $J(q, t) \succ 0$ is the generalized mass matrix, $k(\dot{q}, q, t) \in \mathbb{R}^{n_q}$ is the vector of generalized Coriolis, centrifugal and gyroscopic forces and $g(\dot{q}, q, t) \in \mathbb{R}^{n_q}$ is the vector of applied forces. The control forces and torques are collected in $u \in \mathbb{R}^{n_u}$, which are projected onto the directions of generalized coordinates q by $T(q, t) \in \mathbb{R}^{n_q \times n_u}$.

Remark 4.1 *So-called scleronomic systems are systems devoid of an explicit dependence on the time* t *[131]. The system description (4.5) also covers the non-scleronomic case, since the time may be hidden in the parameters.*

Under the assumption that both q and $\dot{q}$ are measurable signals, it is the goal to rewrite system (4.4) in a compact LFT-based LPV representation. The dependence of the generalized forces and the generalized mass matrix on the state variables q and $\dot{q}$ as well as the explicit time dependence in (4.4) can be considered as parameters collected in $\rho(t) \in \mathcal{F}_\rho^\sigma$.

$$J(\rho)\ddot{q} + k(\rho) = g(\rho) + T(\rho)u, \qquad \rho(t) \in \mathcal{F}_\rho^\sigma. \tag{4.5}$$

Using the shorthand notation $\tilde{k}(\rho) = k(\rho) - g(\rho)$, (4.5) is commonly rewritten as a system of first order differential equations, i.e., as a nonlinear state space model in the form

$$\mathcal{G}_\rho^\sigma : \begin{cases} \begin{bmatrix} \dot{q} \\ \ddot{q} \\ y \end{bmatrix} = \begin{bmatrix} \dot{q} \\ -J^{-1}(\rho)\tilde{k}(\rho) + J^{-1}(\rho)T(\rho)u \\ q \end{bmatrix} \\ \rho(t) \in \mathcal{F}_\rho^\sigma. \end{cases} \tag{4.6}$$

In order to render (4.6) linear in the state—and therefore an LPV representation—a factorization

$$\tilde{k}(\rho) = D(\rho)\dot{q} + K(\rho)q \qquad (4.7)$$

needs to be found. If obtained, the nonlinear differential equation reads as

$$J(\rho)\ddot{q} + D(\rho)\dot{q} + K(\rho)q = T(\rho)u, \qquad \rho(t) \in \mathcal{F}_\rho^\sigma \qquad (4.8)$$

and a general LPV representation can be written as

$$\mathcal{G}_\rho^\sigma : \begin{cases} \begin{bmatrix} \dot{q} \\ \ddot{q} \\ y \end{bmatrix} = \begin{bmatrix} 0 & I & 0 \\ -J^{-1}(\rho)K(\rho) & -J^{-1}(\rho)D(\rho) & J^{-1}(\rho)T(\rho) \\ I & 0 & 0 \end{bmatrix} \begin{bmatrix} q \\ \dot{q} \\ u \end{bmatrix} \\ \rho(t) \in \mathcal{F}_\rho^\sigma. \end{cases} \qquad (4.9)$$

Such differential equations arise in the modeling of holonomic dynamic multibody systems in tree structure [131, Chap. 2, p. 18] or any kind of systems that, e. g., by the electrical-mechanical analogy, are modeled by generalized inertia, damping and stiffness and whose states and inputs correspond to quantities of generalized forces, velocities, displacements [15, Sect. II].

Using physical insight—which is already essential during first principles modeling—heuristic algorithms, as well as rigorous mathematical tools, the purpose of this chapter is to present a systematic approach to obtaining compact LFRs of nonlinear mechanical systems. As opposed to the methods proposed in [77, 146], some aspects of physical insight alleviate the ambiguities when obtaining LPV models based on (4.4). Furthermore, the techniques proposed in Sects. 4.4 and 4.5 of this chapter will allow systematic rational as well as affine LPV parameterization with a minimum number of parameters and an immediate option to approximate based on model coefficients only.

In fact, due to a novel PCA-based approach to obtaining a set of LPV parameters proposed in Sect. 4.5, once a parameter block of a suitable LFR has been extracted, the ambiguities in LPV modeling are mainly reduced to the factorization (4.7). Since the term $J(\rho)\ddot{q}$ turns out naturally from first principles modeling, maintaining the maximal order of derivatives is not an issue, as opposed to the algorithm proposed in [146, Sect. 7.4.2, p. 191]. An attempt at representing also all of the lower time derivatives of the generalized coordinates then boils down to populating $K(\rho)$ and $D(\rho)$ as fully as possible. Such a heuristic will possibly result in a better representation of the inherent coupling at the cost of a larger number of LPV parameters. A trade-off can be found by only applying this heuristic on rows of the system matrices which the control input does not enter directly.

4.3 Factorization of the Vector of Generalized Forces

In this section, an algorithm is proposed to obtain a factorization—or rather a set of candidate factorizations—as in (4.7). The following assumptions are made

(A4.1) The vector $\tilde{k}(\rho)$ is polynomial in $\dot{q}$, q and transcendental terms.

Ass. (A4.1) is justified for mechanical systems represented by the form of the Newton-Euler Equations and their projections onto the generalized coordinates q via D'Alembert's principle, which eliminates reaction forces and torques as well as coordinate transformations by rotation. I. e., any rational parameter dependency is assumed to be easily covered by functions, in which $\tilde{k}(\rho)$ is polynomial. The transcendental terms in q raise the issue of so-called non-factorizable terms, for which the solutions proposed in [146, Sect. 7.4.3], are adopted to render $\tilde{k}(\rho)$ polynomial in q:

- Substitution of $\sin(q) = \mathrm{sinc}(q)q$,

- Taylor approximation and elimination of constant terms.

Under the Ass. (A4.1) the multiple possibilities of factorizing $\tilde{k}(\rho)$ essentially reduce to the various options of pulling out a generalized coordinate q_i or velocity $\dot{q}_i$ from the individual monomial terms into the state vector, while the remainder of the monomials is turned into a parameter-dependent matrix entry in $K(\rho)$ and $D(\rho)$, respectively.

4.3.1 *Constructing All Possible Factorizations*

For the purpose of factorizing

$$\tilde{k}(\rho) = \begin{bmatrix} K(\rho) & D(\rho) \end{bmatrix} \begin{bmatrix} q \\ \dot{q} \end{bmatrix} \tag{4.10}$$

first construct a decomposition in terms of a monomial basis $m_x(x) : \mathbb{R}^{n_x} \mapsto \mathbb{R}^{n_{m_x}}$ in the states $x = \begin{bmatrix} q^\top & \dot{q}^\top \end{bmatrix}^\top \in \mathbb{R}^{n_x}$ with the required degree. Separate the vector of monomials into univariate and multivariate monomials, $m_x^u(x)$ and $m_x^m(x)$, respectively.

$$m_x^u(x) = \begin{bmatrix} m_{x,1}^u(x) \\ m_{x,2}^u(x) \\ \vdots \\ m_{x,n_{m_x^u}}^u(x) \end{bmatrix}, \quad m_x^m(x) = \begin{bmatrix} m_{x,1}^m(x) \\ m_{x,2}^m(x) \\ \vdots \\ m_{x,n_{m_x^m}}^m(x) \end{bmatrix}.$$

---

which reads as

$$\tilde{k}(\rho) = \begin{bmatrix} \tilde{k}_1(\rho) \\ \vdots \\ \tilde{k}_{n_q}(\rho) \end{bmatrix} = \begin{bmatrix} \underline{\tilde{k}}^u(\rho) & \underline{\tilde{k}}^m(\rho) \end{bmatrix} \begin{bmatrix} m_x^u(q) \\ m_x^m(q) \end{bmatrix},$$

$$\underline{\tilde{k}}^m(\rho) = \begin{bmatrix} \underline{\tilde{k}}_1^m(\rho) \\ \vdots \\ \underline{\tilde{k}}_{n_q}^m(\rho) \end{bmatrix} = \begin{bmatrix} \tilde{k}_{11}^m(\rho) & \tilde{k}_{12}^m(\rho) & \cdots & \tilde{k}_{1n_{m_x^m}}^m(\rho) \\ \vdots & & \ddots & \vdots \\ \tilde{k}_{n_q 1}^m(\rho) & \tilde{k}_{n_q 2}^m(\rho) & \cdots & \tilde{k}_{n_q n_{m_x^m}}^m(\rho) \end{bmatrix} \in \mathbb{R}^{n_q \times n_{m_x^m}},$$

and an identically structured $\underline{\tilde{k}}^u(\rho) \in \mathbb{R}^{n_q \times n_{m_x^u}}$. Note that the required maximum degree of monomials can be reduced, if substitutions similar to $\sin(q) = \mathrm{sinc}(q_i)q_i$ are only performed, where otherwise the term would not be factorizable, i. e., when no generalized coordinate or velocity is part of the product. This, however, also forecloses factorization options.

With respect to mechanical systems, this reasoning is somewhat related to the preference of pulling out generalized velocity coordinates $\dot{q}$ as opposed to generalized position coordinates q. Consequently, the majority of parameter-dependent terms will appear in the generalized damping matrix $D(\rho)$. Such a preference may be justified by the following arguments:

(i) Since usually position measurements are less corrupted by noise or in some applications are more readily available than velocity measurements that may require numerical differentiation, the fundamental requirement of exact knowledge of the LPV parameters during online computation is more likely to be fulfilled.

(ii) The number of possible matrix/state vector factorizations of the vector of generalized forces is reduced. This, however, comes at the risk of not enumerating potentially well suited parameterizations.

Collecting the different possible factorizations (4.10) can now first be treated on the level of each vector coefficient/monomial pair for each row i

$$\left(\tilde{k}_{ij}^m(\rho), m_{x,j}^m(x) \right), \quad (i,j) \in \{1, \ldots, n_q\} \times \{1, \ldots, n_{m_x^m}\}.$$

For each of these pairs, the options result from possibilities to pull out a single state variable x_k, $k \in \{1, 2, \ldots, n_x\}$, contained in $m_{x,j}^m(x)$ and multiplying the remaining monomial into the coefficient

$$\tilde{k}_{ijk}^m(\rho) \triangleq \tilde{k}_{ij}^m(\rho) \frac{m_{x,j}^m(x)}{x_k}, \quad k \in \{1, 2, \ldots, n_x\}. \tag{4.11}$$

Accordingly, $\tilde{k}_{ijk}^m(\rho)$ can be a summand in the $(i,k)^{\mathrm{th}}$ entry of $\begin{bmatrix} K(\rho) & D(\rho) \end{bmatrix}$. For the coefficients associated with the univariate monomials, there exists only a single

obvious factorization—the one based on the single state variable the respective monomial is composed from.

For a formalized discussion on the construction of a possible factorizations with regard to the multivariate terms, consider the notation

$$\left\lfloor \frac{m_{x,j}^m(x)}{x_k} \right\rfloor = \begin{cases} \frac{m_{x,j}^m(x)}{x_k}, & \text{if } x_k \text{ is a factor of } m_{x,j}^m(x), \\ 0 & \text{otherwise.} \end{cases}$$

Denote the number of admissible combinations n_c, s.t. $l \in \{1, 2, \ldots, n_c\}$ and introduce selector vectors associated with choice l, the ith row and j^{th} monomial,

$$c_{ij}^{(l)} = \left[c_{ij1}^{(l)} \; c_{ij2}^{(l)} \; \ldots \; c_{ijn_x}^{(l)} \right], \qquad \mathfrak{C}_{ij}^{(l)} \triangleq \operatorname*{diag}_{k=1}^{n_x} \left(c_{ijk}^{(l)} \right),$$

with

$$\sum_{k=1}^{n_x} c_{ijk}^{(l)} = \operatorname{tr}\left(\mathfrak{C}_{ij}^{(l)} \right) = 1. \quad c_{ijk}^{(l)} = 0, \text{ if } \left\lfloor \frac{m_{x,j}^m(x)}{x_k} \right\rfloor = 0. \tag{4.12}$$

Note that by this construction

$$\begin{aligned} m_{x,j}^m(x) &= \sum_{k=1}^{n_x} c_{ijk}^{(l)} \left\lfloor \frac{m_{x,j}^m(x)}{x_k} \right\rfloor x_k \\ &= \left[\left\lfloor \frac{m_{x,j}^m(x)}{x_1} \right\rfloor \left\lfloor \frac{m_{x,j}^m(x)}{x_2} \right\rfloor \cdots \left\lfloor \frac{m_{x,j}^m(x)}{x_{n_x}} \right\rfloor \right] \mathfrak{C}_{ij}^{(l)} x \\ &= \left\lfloor \frac{m_{x,j}^m(x)}{x} \right\rfloor \mathfrak{C}_{ij}^{(l)} x, \end{aligned}$$

where the following shorthand is used:

$$\left\lfloor \frac{m_{x,j}^m(x)}{x} \right\rfloor \triangleq \left[\left\lfloor \frac{m_{x,j}^m(x)}{x_1} \right\rfloor \left\lfloor \frac{m_{x,j}^m(x)}{x_2} \right\rfloor \cdots \left\lfloor \frac{m_{x,j}^m(x)}{x_{n_x}} \right\rfloor \right].$$

Consequently, the ith row is parameterized by the selector matrix via

$$\tilde{k}_i^m(\rho) = \sum_{j=1}^{n_{m_x^m}} \tilde{k}_{ij}^m(\rho) \left\lfloor \frac{m_{x,j}^m(x)}{x} \right\rfloor \mathfrak{C}_{ij}^{(l)} x = \tilde{k}_i^m(\rho) \left\lfloor \frac{m_x^m(x)}{x} \right\rfloor \mathfrak{C}_i^{(l)} x \tag{4.13}$$

$$\text{where } \left\lfloor \frac{m_x^m(x)}{x} \right\rfloor \triangleq \operatorname*{diag}_{j=1}^{n_{m_x^m}} \left(\left\lfloor \frac{m_{x,j}^m(x)}{x} \right\rfloor \right),$$

$$\mathfrak{C}_i^{(l)} \triangleq \operatorname*{col}_{j=1}^{n_{m_x^m}} \left(\mathfrak{C}_{ij}^{(l)} \right).$$

By taking into account constraint (4.12), the matrix $\mathfrak{C}_i^{(l)}$ thus yields the decision variables to construct any possible factorization of the ith row $\tilde{k}_i^m(\rho)$.
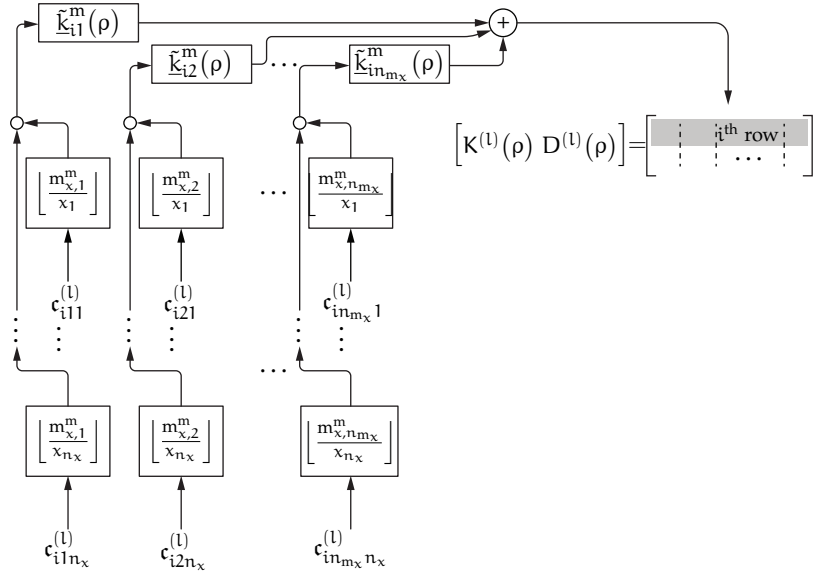
Figure 4.1: Composition tree for constructing the ith row of $\left[K(\rho) \quad D(\rho)\right]$ resulting from multivariate monomials.

Figure 4.1 illustrates the decomposition of $\tilde{k}(\rho)$ in terms of selector gains $c_{ijk}^{(l)}$ the column coefficients $\tilde{k}_{ij}(\rho)$ and the factored monomials $\left\lfloor \dfrac{m_{x,j}^{m}(x)}{x_k} \right\rfloor$.

Consider Exs. 4.1 and 4.2 for illustration.

Example 4.1 (Van der Pol Oscillator)

For illustration, consider the Van der Pol Oscillator [71] a stable oscillator usually described by a state dependent damping coefficient and an exciting stiffness term. The governing differential equations can be written in the form

$$\ddot{q} + \tilde{k} = u, \qquad \tilde{k}(q, \dot{q}) = b(1 - q^2)\dot{q} - q.$$

The monomial decomposition of vector $\tilde{k}$ reads as

$$\tilde{k}(q, \dot{q}) = b(1 - q^2)\dot{q} - q = \begin{bmatrix} -1 & b & \vdots & -b \end{bmatrix} \begin{bmatrix} q \\ \dot{q} \\ q^2\dot{q} \end{bmatrix}.$$

From this, only $-bq^2\dot{q}$ contains a multivariate monomial that results in multiple options for factorization. Parameterizing this multivariate term in terms of the selector matrix as per (4.13) yields

$$\tilde{k}^m(q, \dot{q}) = -b \begin{bmatrix} q\dot{q} & q^2 \end{bmatrix} \begin{bmatrix} c_{111}^{(l)} & \\ & c_{112}^{(l)} \end{bmatrix} \begin{bmatrix} q \\ \dot{q} \end{bmatrix}, \qquad c_{111}^{(l)} + c_{112}^{(l)} = 1.$$

Due to the constraint $c_{111}^{(l)} + c_{112}^{(l)} = 1$, all LPV factorizations can thus be parameterized by a scalar $c = c_{111}^{(l)} \in [0, 1]$, resulting in

$$\begin{bmatrix} \dot{q} \\ \ddot{q} \end{bmatrix} + \begin{bmatrix} 0 & -1 \\ -1 - bq\dot{q}c & b - bq^2(1 - c) \end{bmatrix} \begin{bmatrix} q \\ \dot{q} \end{bmatrix} = \begin{bmatrix} 0 \\ 1 \end{bmatrix} u.$$

$\square$

Example 4.2 (Pendulum With Variable Length)

For illustration consider a container crane that is essentially modeled as a pendulum with variable length [E69]. The pendulum length and angle are denoted x *and* q*, respectively. The pendulum length* x *has first order dynamics, s.t. the resulting governing differential equations can be written in the form*

$$
\begin{bmatrix} x & \\ & b_3 \end{bmatrix} \begin{bmatrix} \ddot{q} \\ \ddot{x} \end{bmatrix} + \tilde{k} = \begin{bmatrix} 0 \\ u \end{bmatrix}, \qquad \tilde{k}(\rho) = \begin{bmatrix} b_1 \sin(q) + b_2 \dot{q}x + 2\dot{q}\dot{x} \\ \dot{x} \end{bmatrix}.
$$

Before constructing the monomial decomposition, the sine term is factored as $\mathrm{sinc}(q)q$*, which results in*

$$
\tilde{k}(\rho) = \begin{bmatrix} b_1\mathrm{sinc}(q) & 0 & \vdots & b_2 & 2 \\ 0 & 1 & \vdots & 0 & 0 \end{bmatrix} \begin{bmatrix} q \\ \dot{x} \\ \dot{q}x \\ \dot{q}\dot{x} \end{bmatrix}.
$$

Parameterizing these multivariate terms in terms of the selector matrix as per (4.13) yields

$$
\tilde{k}^m(\rho) = \begin{bmatrix} b_2 & 2 \\ 0 & 0 \end{bmatrix} \begin{bmatrix} 0 \; x \; \dot{q} \; 0 & \vdots \\ \vdots & 0 \; \dot{x} \; 0 \; \dot{q} \end{bmatrix} \begin{bmatrix} 0 & & & \\ & c_{112}^{(l)} & & \\ & & c_{113}^{(l)} & \\ & & & 0 \\ 0 & & & \\ & c_{122}^{(l)} & & \\ & & 0 & \\ & & & c_{124}^{(l)} \end{bmatrix} \begin{bmatrix} q \\ \dot{q} \\ x \\ \dot{x} \end{bmatrix}.
$$

Due to the constraints $c_{112}^{(l)} + c_{113}^{(l)} = 1$ *and* $c_{122}^{(l)} + c_{124}^{(l)} = 1$*, all LPV factorizations can thus be parameterized by scalars* $c_1 = c_{112}^{(l)} \in [0, 1]$ *and* $c_2 = c_{122}^{(l)} \in [0, 1]$*, resulting in*

$$
\begin{bmatrix} 1 & & & \\ & x & & \\ & & 1 & \\ & & & b_3 \end{bmatrix} \begin{bmatrix} \dot{q} \\ \ddot{q} \\ \dot{x} \\ \ddot{x} \end{bmatrix} + \begin{bmatrix} 0 & -1 & 0 & 0 \\ b_1\mathrm{sinc}(q) & b_2 c_1 x + 2 c_2 \dot{x} & b_2(1 - c_1)\dot{q} & 2(1 - c_2)\dot{q} \\ 0 & 0 & 0 & -1 \\ 0 & 0 & 0 & 1 \end{bmatrix} \begin{bmatrix} q \\ \dot{q} \\ x \\ \dot{x} \end{bmatrix} = \begin{bmatrix} 0 \\ 0 \\ 0 \\ u \end{bmatrix}.
$$

$\square$

4.3.2 *Evaluating Factorizations*

The above parameterization yields infinitely many factorizations due to the degrees of freedom in choosing $c_{ijk}^{(l)}$. In fact, due to the constraint (4.12), for the ith row and j^{th} monomial, n_x the allowed coefficients $c_{ijk}^{(l)}$ yield the part in the positive quadrat of the surface of the unit sphere in an n_x-dimensional space associated with the vector 1-norm, illustrated in Fig. 4.2a for the three-dimensional case.

When strengthening the constraint (4.12), by additionally requiring

$$c_{ijk}^{(l)} \in \{1, 0\}, \tag{4.14}$$

the decision set becomes a finite set, as illustrated in Fig. 4.2b.

(a) Exemplary decision set of the $c_{ijk}^{(l)}$ as the positive quadrat of the surface of the unit sphere associated with the vector 1-norm in a 3-dimensional space.

(b) Exemplary decision set of the $c_{ijk}^{(l)}$ as the extremal points of the surface of the unit sphere associated with the vector 1-norm in the positive quadrat in a 3-dimensional space.
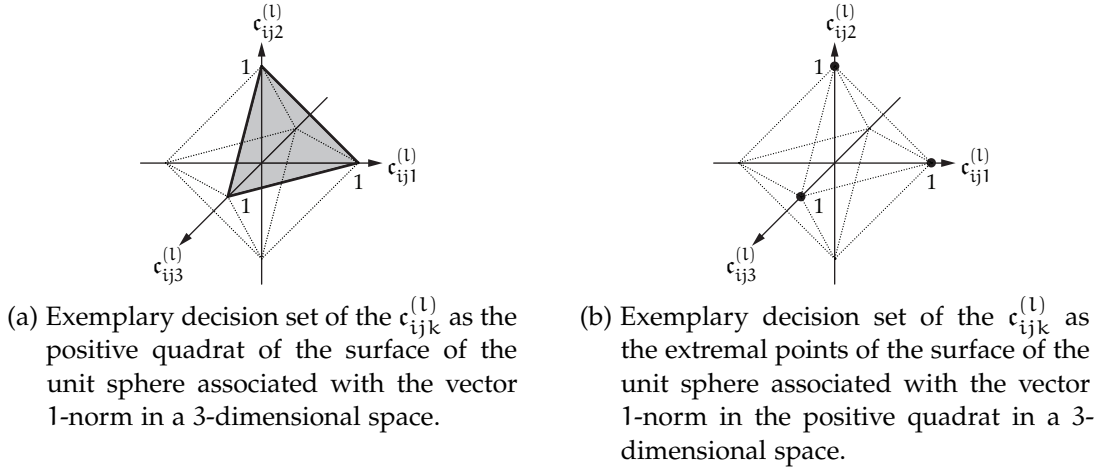
Figure 4.2: Illustration of decision sets in the LPV factorization process.

While in [77], possible overbounding in the parameter range incurred by a particular LPV parameterization is used as the major selective property for affine LPV models, the algorithm in [146, Sect. 7.4.2] priorizes the resulting number of LPV parameters and preservation of dynamic order for each row of the nonlinear differential equation. The last aspect corresponds to the aforementioned priority of pulling higher order derivatives w. r. t. each degree of freedom into the state vector instead of having them as a parameter in the $K(\rho)$ and $D(\rho)$ matrices.

Based on some such heuristic rules, the introduction a further weighting matrix

$$W_i = \operatorname*{diag}_{j=1}^{n_{m_x^m}}\left(\begin{bmatrix} a_{ij1} & a_{ij2} & \dots & a_{ijn_x} \end{bmatrix}\right),$$

$$\text{with } a_{ijk} = \begin{cases} a_{ijk} \in \mathbb{R}, & \text{if } \left\lfloor \dfrac{m_{x,j}^m(x)}{x_k} \right\rfloor \neq 0 \\ 0, & \text{otherwise,} \end{cases} \tag{4.15}$$

can yield a framework for an *a priori* specification of an objective measure. By taking the product, one has the matrix

$$
W_i \mathfrak{C}_i^{(l)} = \begin{bmatrix} a_{i11} c_{i11}^{(l)} & a_{i12} c_{i12}^{(l)} & \cdots & a_{i1n_x} c_{i1n_x}^{(l)} \\ a_{i21} c_{i21}^{(l)} & a_{i22} c_{i22}^{(l)} & \cdots & a_{i2n_x} c_{i2n_x}^{(l)} \\ \vdots & & \ddots & \vdots \\ a_{in_{m_x^m}1} c_{in_{m_x^m}1}^{(l)} & a_{in_{m_x^m}2} c_{in_{m_x^m}2}^{(l)} & \cdots & a_{in_{m_x^m}n_x} c_{in_{m_x^m}n_x}^{(l)} \end{bmatrix},
$$

which inherits the sparsity pattern from W_i, cf. (4.15).

The coefficients a_{ijk} can be perceived as design parameters that under some objective measure incur a penalty for a particular entry in row i and column k. The following objective measures are proposed:

PENALIZE SPARSITY, FINITE DECISIONS
Following the heuristic that fully populated plant matrices increase the capability of a representation to represent couplings for frozen parameter values, sparsity in the resulting factorization is penalized. For this purpose define L as a $n_{m_x^m} \times n_{m_x^m}$ lower left triangular matrix full of ones. This matrix is used to penalize terms accumulating in a certain column by producing a cumulative sum of the rows of $W_i \mathfrak{C}_i^{(l)}$. Summing over both columns and rows yields a single objective measure. If decisions are constrained by (4.14), the lowest objective measure indicates the desired factorization.

The corresponding optimization problem can be formulated as

$$
\min_{c_{ijk}^{(l)}} \mathbf{1}_{n_{m_x^m}}^{\top} \left(L W_i \mathfrak{C}_i^{(l)} \right) \mathbf{1}_{n_x}, \quad \text{s.t.} \quad (4.14). \tag{4.16}
$$

PENALIZE SPARSITY, INFINITE DECISIONS
For the case of infinitely many combinations of coefficients according to constraint (4.12), the number of factorizations can no longer be enumerated and assigned to an objective measure. In this case, the largest singular value of $W_i \mathfrak{C}_i^{(l)}$, subject to (4.12) can be taken as a measure of the uniformity by which coefficients are distributed due to the factorization. For illustration, consider $a_{ijn_x} = 1$, $\forall (j, n_x) \in \{1, \ldots, n_{m_x^m}\} \times \{1, \ldots, n_x\}$. Then,

The corresponding optimization problem can be formulated as

$$
\min_{c_{ijk}^{(l)}} \overline{\sigma} \left(W_i \mathfrak{C}_i^{(l)} \right), \quad \text{s.t.} \quad (4.12). \tag{4.17}
$$

PROMOTE SPARSITY
In case, coupling terms are already sufficiently represented by the nominal system matrices, penalizing sparsity can lead to unnecessary complex LPV representations. In such situations, the usual decision constraint (4.14), [77, 146], is superior to reduce the number of parameter-dependent terms.

Thus, the following optimization problem is proposed

$$\max_{\mathfrak{c}^{(l)}_{ijk}} 1^\top_{n_{mm}^m} \left(LW_i \mathfrak{c}^{(l)}_i \right) 1_{n_x}, \quad \text{s.t.} \quad (4.14).$$ (4.18)

Consider Ex. 4.3 for illustration.

Example 4.3 (Pendulum With Variable Length, cont'd)

Reconsider Ex. 4.2 on p. 110. In the spirit of [E47, E69], the angular velocity $\dot{q}$ and angle q is to be regulated to zero.

$$\begin{bmatrix} 1 & & & \\ & x & & \\ & & 1 & \\ & & & b_3 \end{bmatrix} \begin{bmatrix} \dot{q} \\ \ddot{q} \\ \dot{x} \\ \ddot{x} \end{bmatrix} + \begin{bmatrix} 0 & -1 & 0 & 0 \\ b_1 \operatorname{sinc}(q) & b_2 \mathfrak{c}_1 x + 2\mathfrak{c}_2 \dot{x} & b_2(1-\mathfrak{c}_1)\dot{q} & 2(1-\mathfrak{c}_2)\dot{q} \\ 0 & 0 & 0 & -1 \\ 0 & 0 & 0 & 1 \end{bmatrix} \begin{bmatrix} q \\ \dot{q} \\ x \\ \dot{x} \end{bmatrix} = \begin{bmatrix} 0 \\ 0 \\ 0 \\ u \end{bmatrix}.$$

If both $\mathfrak{c}_1 = \mathfrak{c}_2 = 1$ are chosen, the angular mode is always decoupled from the pendulum length.

$$\begin{bmatrix} 1 & & & \\ & x & & \\ & & 1 & \\ & & & b_3 \end{bmatrix} \begin{bmatrix} \dot{q} \\ \ddot{q} \\ \dot{x} \\ \ddot{x} \end{bmatrix} + \begin{bmatrix} 0 & -1 & 0 & 0 \\ b_1 \operatorname{sinc}(q) & b_2 x + 2\dot{x} & 0 & 0 \\ 0 & 0 & 0 & -1 \\ 0 & 0 & 0 & 1 \end{bmatrix} \begin{bmatrix} q \\ \dot{q} \\ x \\ \dot{x} \end{bmatrix} = \begin{bmatrix} 0 \\ 0 \\ 0 \\ u \end{bmatrix}.$$

On the other hand, if both $\mathfrak{c}_1 = \mathfrak{c}_2 = 0$ are chosen

$$\begin{bmatrix} 1 & & & \\ & x & & \\ & & 1 & \\ & & & b_3 \end{bmatrix} \begin{bmatrix} \dot{q} \\ \ddot{q} \\ \dot{x} \\ \ddot{x} \end{bmatrix} + \begin{bmatrix} 0 & -1 & 0 & 0 \\ b_1 \operatorname{sinc}(q) & 0 & b_2 \dot{q} & 2\dot{q} \\ 0 & 0 & 0 & -1 \\ 0 & 0 & 0 & 1 \end{bmatrix} \begin{bmatrix} q \\ \dot{q} \\ x \\ \dot{x} \end{bmatrix} = \begin{bmatrix} 0 \\ 0 \\ 0 \\ u \end{bmatrix}.$$

the pendulum appears as undamped for frozen parameter values. Consequently, to preserve coupling through $\dot{x}$ in the (2,4)-term, sparsity in the resulting factorization has to be penalized. However, as $x > 0$, it is also desirable to penalize sparsity to the extent that local damping in q via the (2,2)-term is maintained. For this purpose, a high penalty $a_{1j3} = 1$ may be imposed on the third column for all monomials, whereas a particularly low penalty $a_{1j4} = 0.1$ is imposed on the fourth. The remaining penalties for the second column are set to $a_{1j2} = 0.5$. From

$$W_1 \mathfrak{c}^{(l)}_1 = \begin{bmatrix} 0 & a_{112} & a_{113} & 0 & \vdots & & & \\ & & & & 0 & a_{122} & 0 & a_{124} \end{bmatrix} \begin{bmatrix} 0 \\ \mathfrak{c}_1 \\ (1-\mathfrak{c}_1) \\ & & 0 \\ \cdots \\ 0 \\ & \mathfrak{c}_2 \\ & & 0 \\ & & & (1-\mathfrak{c}_2) \end{bmatrix},$$

one therefore has when following the optimization problem (4.16)

$$1_{n_{m_{\tilde{x}}^m}}^\top \left(LW_1 \mathfrak{c}_1^{(l)} \right) 1_{n_x}$$

$$= \begin{bmatrix} 1 & 1 \end{bmatrix} \begin{bmatrix} 1 & 0 \\ 1 & 1 \end{bmatrix} \begin{bmatrix} 0 & a_{112}\mathfrak{c}_1 & a_{113}(1-\mathfrak{c}_1) & 0 \\ 0 & a_{122}\mathfrak{c}_2 & 0 & a_{124}(1-\mathfrak{c}_2) \end{bmatrix} \begin{bmatrix} 1 \\ 1 \\ 1 \\ 1 \end{bmatrix}$$

$$= \begin{bmatrix} 2 & 1 \end{bmatrix} \begin{bmatrix} a_{112}\mathfrak{c}_1 + a_{113}(1-\mathfrak{c}_1) \\ a_{122}\mathfrak{c}_2 + a_{124}(1-\mathfrak{c}_2) \end{bmatrix}$$

$$= 2a_{112}\mathfrak{c}_1 + 2a_{113}(1-\mathfrak{c}_1) + a_{122}\mathfrak{c}_2 + a_{124}(1-\mathfrak{c}_2).$$

$$= \mathfrak{c}_1 + 2(1-\mathfrak{c}_1) + \frac{1}{2}\mathfrak{c}_2 + \frac{1}{10}(1-\mathfrak{c}_2).$$

The minimizing solution is obviously $\mathfrak{c}_1 = 1$ and $\mathfrak{c}_2 = 0$. For more complex problems such an optimization can also be performed by the Matlab function «fmincon». Note, that this factorization has been used effectively in real-time, experimental active damping control of a container crane test rig [E47, E69].

With equal weights $a_{ijk} = 1$, optimization (4.17) returns $\mathfrak{c}_1 = \mathfrak{c}_2 = {}^1/3$ using «fmincon». This solution reflects an equal distribution of monomial terms: Two terms weighted by $^1/_3$ in the second column and one term each weighted $^2/_3$ in the third and fourth column. While not necessarily resulting in the best control performance, such factorizations of high complexity preserve both coupling and damping/stiffness terms and can be used to check feasibility of a control problem as a preliminary step. □

4.3.3 Further Considerations

The above approaches are only heuristics, intended to help systematize the tedious and error prone factorization procedure. Based on the above factorization, further heuristics—or possibly even rigorous methods—can be developed. As mentioned in [146], obtaining a tractable number of LPV terms is only one dimension of the LPV parameterization issue. It appears, however, difficult to rigorously connect more control-oriented objective measures, such as stabilizability and detectablility for all frozen parameter values.

As an initial step towards this direction, consider the following condition on stabilizability of an LTI system in non-singular, i.e., E_{xx} is invertible, descriptor form

$$P: \begin{bmatrix} E_{xx} & 0 \\ 0 & I \end{bmatrix} \begin{bmatrix} \dot{x} \\ y \end{bmatrix} = \begin{bmatrix} F_{xx} & F_{xu} \\ C_y & D_{yu} \end{bmatrix} \begin{bmatrix} x \\ u \end{bmatrix}. \tag{4.19}$$

Lemma 4.1 (Stabilizability of a Descriptor LTI System [88])
The system P *from (4.19) is stabilizable iff*

$$\begin{bmatrix} sE_{xx} - F_{xx} & F_{xu} \end{bmatrix} \quad \textit{has full row rank } \forall s \in \mathbb{C}^+. \tag{4.20}$$

$\square$

Proof: The proof follows immediately from premultiplying the well-known condition

$$\begin{bmatrix} sI - A & B_u \end{bmatrix} \quad \text{has full row rank } \forall s \in \mathbb{C}^+$$

by E_{xx} and the fact that $\text{rank}(MN) = \text{rank}(N)$ for all matrices M of full column rank. $\blacksquare$

By «local stabilizability», we will denote the fact that all LTI systems, resulting from all possible frozen parameter values of an LPV system, are stabilizable.

Formally, we have for the LPV plant

$$\mathcal{P}_\rho^\sigma : \begin{cases} \begin{bmatrix} E_{xx}(\rho) & 0 \\ 0 & I \end{bmatrix} \begin{bmatrix} \dot{x} \\ y \end{bmatrix} = \begin{bmatrix} F_{xx}(\rho) & F_{xu}(\rho) \\ C_y(\rho) & D_{yu}(\rho) \end{bmatrix} \begin{bmatrix} x \\ u \end{bmatrix}, \\ \rho(t) \in \mathcal{F}_\rho^\sigma \end{cases} \tag{4.21}$$

the following definition.

Definition 4.1 (Local Stabilizability of LPV Systems)
The LPV *system* $\mathcal{P}_\rho^\sigma$ *from (4.21) is said to be* locally stabilizable, *if it is stabilizable for all fixed* $\rho \in \boldsymbol{\rho}$.

Consequently, one can formulate the following corollary.

Remark 4.2 *Unlike the gridded evaluation of stability conditions on the basis of matrix inequality conditions, common as an* a posteriori *check in the gridding* LPV *synthesis approach, continuity arguments do not prevail with respect to rank conditions, which are discontinuous.*

Corollary 4.1 (Local Stabilizability of a Descriptor LPV System)
The system $\mathcal{P}_\rho^\sigma$ *from (4.21) is locally stabilizable iff*

$$\begin{bmatrix} sE_{xx}(\rho) - F_{xx}(\rho) & F_{xu}(\rho) \end{bmatrix}$$
$$\textit{has full row rank } \forall\, (s, \rho) \in \mathbb{C}^+ \times \boldsymbol{\rho}. \tag{4.22}$$

$\square$

Analogously, one may define «local detectability» as follows.

Definition 4.2 (Local Detectability of LPV Systems)
The LPV *system* $\mathcal{P}_\rho^\sigma$ *from (4.21) is said to be* locally detectable, *if it is detectable for all fixed* $\rho \in \boldsymbol{\rho}$.

Formally, the following corollary provides a rank condition to check for local detectability.

Corollary 4.2 (Local Detectability of a Descriptor LPV System)
The system $\mathcal{P}_\rho^\sigma$ from (4.21) is locally detectable iff

$$\begin{bmatrix} sE_{xx}(\rho) - F_{xx}(\rho) \\ C_y(\rho) \end{bmatrix}$$

has full column rank $\forall (s, \rho) \in \mathbb{C}^+ \times \boldsymbol{\rho}$. (4.23)

$\square$

The conditions of Cors. 4.1 and 4.2 may be difficult to check in general, but for practical purposes, it may often be sufficient to evaluate it on a sufficiently dense grid for a constant $s = 0$.

The descriptor-like form of the rank conditions may further simplify the evaluation by avoiding rational terms.

4.4 A Full-Block Linear Fractional Transformation-Based Linear Parameter-Varying Parameterization of Descriptor Models

In the following, explicit LFRs of general LPV models will be derived based on a non-singular descriptor form. These LFT-LPV model representations are developed making use of full LFT parameter blocks as opposed to diagonal ones usually assumed in the literature, e. g., [5, 161, 163].

Potential benefits of full parameter blocks have been hinted at in [53, Chap. 4.4, p. 58] and [125]. Their usefulness in synthesis will be explored in Chap. 5, whereas the following sections of this chapter focus on LFRs of small size. The next chapter will continue with the automated rational or affine parameterization of the resulting full parameter blocks by a minimal number of parameters.

4.4.1 *Non-Singular LPV Descriptor Representation*

Consider models of physical plants governed by an LPV differential equation in non-singular descriptor form

$$
\mathcal{G}_\rho^\sigma : \begin{cases} \begin{bmatrix} E_{xx}(\rho) & E_{xy}(\rho) \\ E_{yx}(\rho) & E_{yy}(\rho) \end{bmatrix} \begin{bmatrix} \dot{x} \\ y \end{bmatrix} = \begin{bmatrix} F_{xx}(\rho) & F_{xu}(\rho) \\ F_{yx}(\rho) & F_{yu}(\rho) \end{bmatrix} \begin{bmatrix} x \\ u \end{bmatrix}, \\ \rho(t) \in \mathcal{F}_\rho^\sigma \end{cases}
\tag{4.24}
$$

where

$$
E(\rho) \triangleq \begin{bmatrix} E_{xx}(\rho) & E_{xy}(\rho) \\ E_{yx}(\rho) & E_{yy}(\rho) \end{bmatrix} \in \mathbb{R}^{(n_x+n_y)\times(n_x+n_y)},
$$

$$
F(\rho) \triangleq \begin{bmatrix} F_{xx}(\rho) & F_{xu}(\rho) \\ F_{yx}(\rho) & F_{yu}(\rho) \end{bmatrix} \in \mathbb{R}^{(n_x+n_y)\times(n_x+n_u)},
$$

with $E(\rho)$ non-singular. Both matrices have arbitrary dependency on $\rho \in \mathcal{F}_\rho^\sigma$. Consider Ex. 4.4 to appreciate nonlinear mechanical LPV systems as a special case of system representation (4.24).

Remark 4.3 *The attribute «non-singular» is derived from restricting* $E(\rho)$ *to invertible matrices only and therefore prohibiting any kinds of algebraic constraints.*

Example 4.4 (Mechanical Descriptor LPV System)
Clearly, mechanical LPV systems as introduced in the previous sections are a special case of (4.24) when written in the form

$$
\mathcal{G}^\sigma_\rho : \begin{cases} \begin{bmatrix} I & 0 & 0 \\ 0 & J(\rho) & 0 \\ 0 & 0 & I \end{bmatrix} \begin{bmatrix} \dot{q} \\ \ddot{q} \\ y \end{bmatrix} = \begin{bmatrix} 0 & I & 0 \\ -K(\rho) & -D(\rho) & T(\rho) \\ I & 0 & 0 \end{bmatrix} \begin{bmatrix} q \\ \dot{q} \\ u \end{bmatrix}, \\ \rho(t) \in \mathcal{F}^\sigma_\rho, \end{cases} \tag{4.25}
$$

with $q \in \mathbb{R}^{n_q}$, $\dot{q} \in \mathbb{R}^{n_q}$, $u \in \mathbb{R}^{n_u}$. □

Introduce LFRs for the parameter-dependent matrices $E(\rho)$ and $F(\rho)$ of the form

$$
E(\rho) = E_0(\rho) + \tilde{\Delta}_E(\rho) = \Delta_E(\rho) \star \begin{bmatrix} 0 & W_E(\rho) \\ V(\rho) & E_0(\rho) \end{bmatrix}, \tag{4.26}
$$

$$
F(\rho) = F_0(\rho) + \tilde{\Delta}_F(\rho) = \Delta_F(\rho) \star \begin{bmatrix} 0 & W_F(\rho) \\ V(\rho) & F_0(\rho) \end{bmatrix}. \tag{4.27}
$$

The masking matrices $V(\rho)$, $W_E(\rho)$ and $W_F(\rho)$ can be used to select parameter-dependent blocks $\Delta_E(\rho)$ and $\Delta_F(\rho)$ that are potentially smaller in size than their nominal matrices $E_0(\rho)$ and $F_0(\rho)$, respectively. For generality, the nominal matrices remain parameter-dependent and even the masking matrices could contain parameters, consequently allowing a combined gridding and multiplier-based synthesis approach as per [161], if, e.g., some parameters are difficult to treat in the LFT framework.

Define

$$
\Upsilon(\rho) \triangleq \left[\Delta_E(\rho), \Delta_F(\rho) \right], \quad \Upsilon(\rho) \in \mathbb{R}^{n_{q\Upsilon} \times n_{p\Upsilon}} \tag{4.28}
$$

and require the following assumptions to hold.

(**A**4.2) A parameterization is chosen that satisfies $0 \in \{ \Upsilon(\rho) \mid \rho \in \boldsymbol{\rho} \}$.

(**A**4.3) The matrix $E_0(\rho)$ is non-singular for all $\rho \in \boldsymbol{\rho}$.

Ass. (A4.2) is required for multiplier-based synthesis as per [125]. It guarantees that the inertia hypotheses on the multipliers as from Lma. 2.4 lead to the existence of an explicit formula for the parameter block of the controller given in Lma. 2.5 on page 69. Consequently, consider an admissible nominal operating point $\rho_0 \in \boldsymbol{\rho}$, for which $\Upsilon(\rho_0) \neq 0$. Then clearly

$$
\Upsilon(\rho) = \left(\Upsilon(\rho) - \Upsilon(\rho_0) \right) + \Upsilon(\rho_0),
$$

where $\left(\Upsilon(\rho) - \Upsilon(\rho_0)\right)$ defines the new block $\Upsilon(\rho)$ and $\Upsilon(\rho_0)$ can be shifted into the nominal system matrices $E_0(\rho)$ and $F_0(\rho)$.

In the case that Ass. (A4.2) cannot be satisfied for any physically admissible parameter $\rho \in \boldsymbol{\rho}$, the compact set of admissible parameters may be extended at the cost of introducing overbounding and consequently conservatism in controller synthesis. It can therefore be assumed that Ass. (A4.2) holds. Ass. (A4.3) restricts the class of descriptor systems to not include algebraic constraints, s. t. a standard state space representation can always be derived.

4.4.2 *Compact Rational LFT-LPV Parameterization*

From compact LFRs associated with coprime factor representations [44], an LFR of

$$G_\rho(\rho) \triangleq E^{-1}(\rho)F(\rho) = \left(E_0 + \tilde{\Delta}_E(\rho)\right)^{-1}\left(F_0 + \tilde{\Delta}_F(\rho)\right)$$

can be found as

$$G_\rho(\rho) = \left[\tilde{\Delta}_E(\rho)\ \tilde{\Delta}_F(\rho)\right] \star \left[\begin{array}{c:cc} -E_0{}^{-1} & -E_0{}^{-1}F_0 \\ \hdashline 0 & I \\ \hdashline E_0{}^{-1} & E_0{}^{-1}F_0 \end{array}\right].$$ (4.29)

Using (4.29), it is straightforward to obtain the system representation (4.31) as an LFR with non-square parameter block $\Upsilon(\rho)$.

$$\mathcal{G}_\rho^\sigma : \begin{cases} \begin{bmatrix} \dot{x} \\ \hdashline p_\Upsilon \\ y \end{bmatrix} = \begin{bmatrix} A & B_\Upsilon & B_u \\ \hdashline C_\Upsilon & D_{\Upsilon\Upsilon} & D_{\Upsilon u} \\ C_y & D_{y\Upsilon} & D_{yu} \end{bmatrix} \begin{bmatrix} x \\ \hdashline q_\Upsilon \\ u \end{bmatrix} \\ \qquad q_\Upsilon = \Upsilon(\rho)p_\Upsilon, \quad \rho(t) \in \mathcal{F}_\rho^\sigma, \end{cases}$$ (4.30)

$$\begin{bmatrix} D_{\Upsilon\Upsilon} & C_\Upsilon & D_{\Upsilon u} \\ \hdashline B_\Upsilon & A & B_u \\ D_{y\Upsilon} & C_y & D_{yu} \end{bmatrix} = \begin{bmatrix} -W_E E_0{}^{-1}V & -W_E E_0{}^{-1}F_0 \\ \hdashline 0 & W_F \\ E_0{}^{-1}V & E_0{}^{-1}F_0 \end{bmatrix},$$ (4.31)

$$\mathcal{G}_\rho^\sigma : \begin{cases} \begin{bmatrix} \dot{x} \\ \hdashline p_\Lambda \\ y \end{bmatrix} = \begin{bmatrix} A & B_\Lambda & B_u \\ \hdashline C_\Lambda & 0 & D_{\Lambda u} \\ C_y & D_{y\Lambda} & D_{yu} \end{bmatrix} \begin{bmatrix} x \\ \hdashline q_\Lambda \\ u \end{bmatrix} \\ \qquad q_\Lambda = \Lambda(\rho)p_\Lambda, \quad \rho(t) \in \mathcal{F}_\rho^\sigma, \end{cases}$$ (4.32)

$$\begin{bmatrix} 0 & C_\Lambda & D_{\Lambda u} \\ \hdashline B_\Lambda & A & B_u \\ D_{y\Lambda} & C_y & D_{yu} \end{bmatrix} = \begin{bmatrix} 0 & C_\Lambda & D_{\Lambda u} \\ \hdashline B_\Upsilon & A & B_u \\ D_{y\Upsilon} & C_y & D_{yu} \end{bmatrix}.$$ (4.33)

Example 4.5 (Mechanical Descriptor LPV System, cont'd)

For the special case (4.25), introduce LFRs *for the parameter-dependent matrices* $J(\rho)$, $K(\rho)$, $D(\rho)$ *and* $T(\rho)$ *of the form*

$$J(\rho) = J_0(\rho) + \tilde{\Delta}_J(\rho) = \Delta_J(\rho) \star \begin{bmatrix} 0 & W_J \\ \hline V_J & J_0(\rho) \end{bmatrix}, \tag{4.34}$$

$$K(\rho) = K_0(\rho) + \tilde{\Delta}_K(\rho) = \Delta_K(\rho) \star \begin{bmatrix} 0 & W_K \\ \hline V_J & K_0(\rho) \end{bmatrix}, \tag{4.35}$$

$$D(\rho) = D_0(\rho) + \tilde{\Delta}_D(\rho) = \Delta_D(\rho) \star \begin{bmatrix} 0 & W_D \\ \hline V_J & D_0(\rho) \end{bmatrix}, \tag{4.36}$$

$$T(\rho) = T_0(\rho) + \tilde{\Delta}_T(\rho) = \Delta_T(\rho) \star \begin{bmatrix} 0 & W_T \\ \hline V_J & T_0(\rho) \end{bmatrix}. \tag{4.37}$$

Define

$$V = \begin{bmatrix} 0 \\ V_J \\ 0 \end{bmatrix}, \qquad W_E = \begin{bmatrix} 0 & W_J & 0 \end{bmatrix},$$

$$W_F = \mathrm{diag}(W_K, W_D, W_T),$$

$$E_0(\rho) = \begin{bmatrix} I & 0 & 0 \\ 0 & J_0(\rho) & 0 \\ 0 & 0 & I \end{bmatrix}, \quad F_0(\rho) = \begin{bmatrix} 0 & I & 0 \\ -K_0(\rho) & -D_0(\rho) & T_0(\rho) \\ I & 0 & 0 \end{bmatrix},$$

$$\Delta_E(\rho) = \Delta_J(\rho), \quad \Delta_F(\rho) = \begin{bmatrix} -\Delta_K(\rho) & -\Delta_D(\rho) & \Delta_T(\rho) \end{bmatrix}.$$

$\square$

4.4.3 *Compact Affine LFT-LPV Parameterization*

An alternative representation can be derived by considering the parameter block $\Lambda(\rho) \in \mathbb{R}^{n_{q_\Lambda} \times n_{p_\Lambda}}$, with

$$\Lambda(\rho) \stackrel{\triangle}{=} \Upsilon(\rho) \star W_\Lambda = \Upsilon(\rho) \star \begin{bmatrix} D_{\Upsilon\Upsilon} & W_{\Lambda 12} \\ \hline I & 0 \end{bmatrix}, \tag{4.38}$$

where, in order to minimize n_{p_Λ}, a case distinction should be made:

$$W_{\Lambda 12} \stackrel{\triangle}{=} \begin{cases} \begin{bmatrix} C_\Upsilon & D_{\Upsilon u} \end{bmatrix} W(\rho) & \text{if} \quad n_u + n_x \leqslant n_{p_\Upsilon} \\ I_{n_{p_\Upsilon}} & \text{if} \quad n_u + n_x > n_{p_\Upsilon}. \end{cases}$$

Using this for an alternative compact representation yields the system description (4.33), which is affinely dependent on the compact non-square matrix $\Lambda(\rho)$. Accordingly, in the system matrices, make the case distinction

$$\begin{bmatrix} C_\Lambda & D_{\Lambda u} \end{bmatrix} \triangleq \begin{cases} W^\top(\rho) & \text{if} \quad n_u + n_x \leqslant n_{p_\Upsilon} \\ \begin{bmatrix} C_\Upsilon & D_{\Upsilon u} \end{bmatrix} & \text{if} \quad n_u + n_x > n_{p_\Upsilon}. \end{cases} \tag{4.39}$$

The matrix $W(\rho) \in \mathbb{R}^{(n_u+n_x) \times n_{p_\Lambda}}$ contains an orthogonal basis of the space complementary to $\ker \begin{bmatrix} C_\Lambda & D_{\Lambda u} \end{bmatrix}$ and satisfies $W(\rho) W^\top(\rho) = I_{(n_u+n_x)}$. This construction allows to generate parameter blocks $\Lambda(\rho)$ with $n_{p_\Lambda} < n_u + n_x$ for the case that columns of the system matrix $G_\rho(\rho)$ are parameter-independent. For the typical case that all plant parameters are located within $\Delta_E(\rho)$ and $\Delta_F(\rho)$, s. t. all masking and nominal matrices are constant, the construction of W is a simple task.

In contrast to (4.33), the representation (4.31) is rational in $\Upsilon(\rho)$. In view of mechanical model structures as shown in (4.25), the block $\Upsilon(\rho)$ clearly separates generalized inertia, stiffness, damping and input gains, which facilitates a systematic affine or rational parameterization of $\Upsilon(\rho)$ by inspection. Due to the relation of both parameter blocks made explicit in (4.38), this also gives rise to a rational parameterization of $\Lambda(\rho)$ in terms of parameters in which $\Upsilon(\rho)$ is affine or rational. A fully affine parameterization can be derived based on the reformulation of Eq. (4.38) as

$$\Lambda(\rho) = \left(I + \Delta_E(\rho) W_E E_0^{-1} V \right)^{-1} \Upsilon(\rho) W_{\Lambda 12} \tag{4.40}$$

obtained by simple manipulations. Using

$$\Lambda(\rho) = \frac{1}{d(\rho)} \tilde{\Lambda}(\rho) \tag{4.41}$$

with

$$d(\rho) \triangleq \det \left(I + \Delta_E(\rho) W_E E_0^{-1} V \right) \tag{4.42}$$

and where

$$\tilde{\Lambda}(\rho) = \text{adj} \left(I + \Delta_E(\rho) W_E E_0^{-1} V \right) \Upsilon(\rho) W_{\Lambda 12}, \tag{4.43}$$

the term $d(\rho)$ can be identified as a common denominator and the problem reduces to parameterizing $\tilde{\Lambda}(\rho)$. The next section will formally introduce such a systematic approach of parameterizing LPV models.

Figures 4.3a–4.3c illustrate the parameterizations of the LPV system and their relation. Note that the sizes of the parameter blocks $\Upsilon(\rho)$ and $\Lambda(\rho)$ may differ. For the special case of mechanical systems, consider Ex. 4.6 for illustration.

(a) LFT-LPV plant as an interconnection of the general LPV plant $G_\Lambda(\rho)$ and the parameter block $\Lambda(\rho)$.

(b) LFT-LPV plant as an interconnection of the general LPV plant $G_\Upsilon(\rho)$ and the parameter block $\Upsilon(\rho)$.

(c) LFT-LPV plant as an interconnection of the general LPV plant $G_\Lambda(\rho)$ and the parameter block $\Lambda(\rho)$ represented as an LFR in the block $\Upsilon(\rho)$ and the parameter-dependent matrix $W_\Lambda(\rho)$.
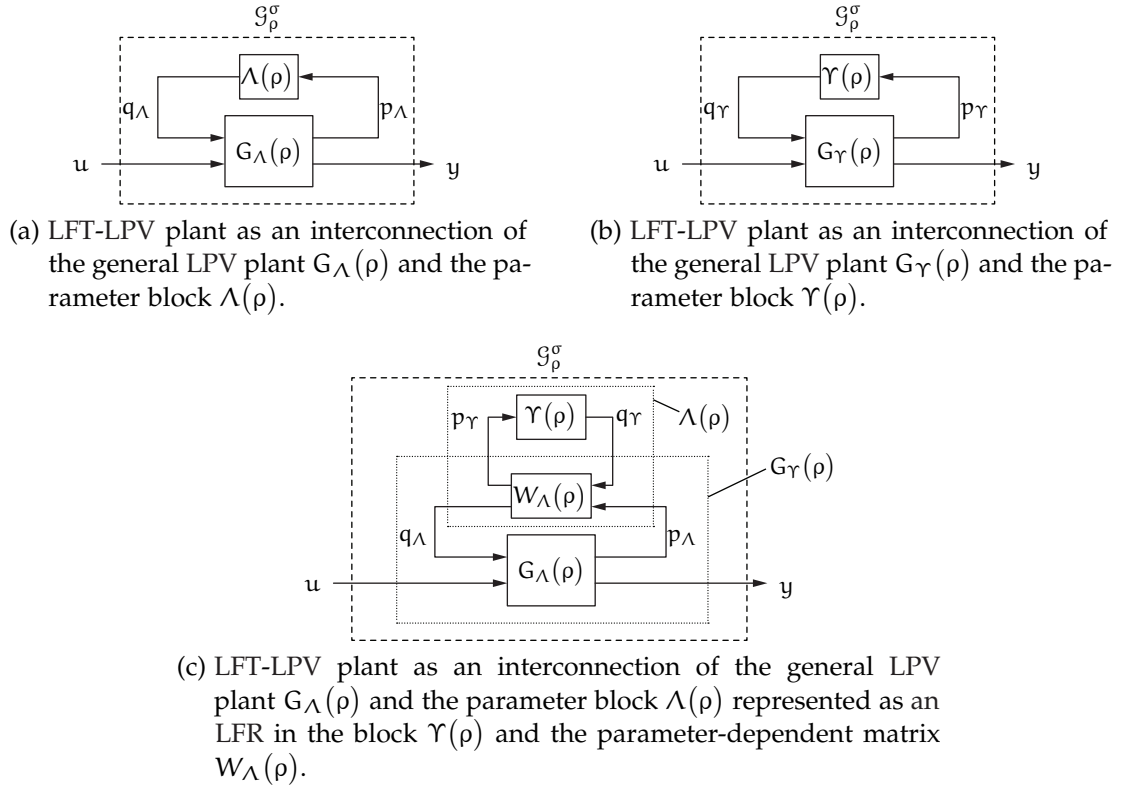
Figure 4.3: LFT-LPV plant model representations with compact parameter blocks.

Example 4.6 (Mechanical Descriptor LPV System, cont'd)
For the special case (4.25), and LFRs *for the parameter-dependent system matrices introduced as in Ex. 4.5, note that the worst-case sizes of the parameter blocks $\Upsilon(\rho)$ and $\Lambda(\rho)$ as obtained from Eq. 4.28 and 4.38, respectively, are*

$$\Upsilon(\rho) \in \mathbb{R}^{n_q \times (3n_q + n_u)}, \quad \Lambda(\rho) \in \mathbb{R}^{n_q \times (2n_q + n_u)},$$

where $q \in \mathbb{R}^{n_q}$. For constant input gains, e.g., $\mathsf{T}(\rho) = I_{n_q}$, both parameter blocks attain the same size: $n_q \times 3n_q$. □

4.5 SEMI-AUTOMATED PARAMETERIZATION

THE parameter blocks $\Upsilon(\rho)$ and $\Lambda(\rho)$ have thus far been considered in terms of their dependency on the general LPV parameters ρ, which are usually considered to consist of the directly measurable signals, cf. Sect. 2.1.1. For their use in multiplier-based LFT-LPV synthesis approaches, parameter sets in which the parameter blocks are rational are required.

4.5.1 *Usage in an LFT-LPV Synthesis Approach*

From Lmas. 2.2 and 2.5, i. e., under the inertia hypotheses on full multiplier blocks, the multiplier conditions encountered in Thms. 2.15 and 2.17 can be evaluated on the vertices of matrix polytopes conv $(\boldsymbol{\Upsilon})$ and conv $(\boldsymbol{\Lambda})$, respectively, where

$$\boldsymbol{\Upsilon} \stackrel{\triangle}{=} \left\{ \Upsilon(\rho) \mid \rho \in \boldsymbol{\rho} \right\}, \tag{4.44}$$

$$\boldsymbol{\Lambda} \stackrel{\triangle}{=} \left\{ \Lambda(\rho) \mid \rho \in \boldsymbol{\rho} \right\}. \tag{4.45}$$

In practice, the vertices of the matrix polytopes are derived from a set of parameters in which the respective parameter block is affine. Such an approach allows fully populated parameter blocks, such as $\Lambda(\rho)$ or $\Upsilon(\rho)$ derived above. Therefore, methods to systematically parameterize $\Upsilon(\rho)$ or $\Lambda(\rho)$ affinely are required.

Since the number of vertices usually grow exponentially with the number of parameters, synthesis complexity may be rendered intractable for large numbers of affine parameters. Chap. 5 will detail methods that benefit from the use of compact full parameter blocks, while also using knowledge on their underlying rational parameterization.

4.5.2 *Affine and Rational Parameterizations*

Parameterizations of the blocks $\Upsilon(\rho)$ and $\Lambda(\rho)$ in LFR form with standard diagonal parameter blocks are developed to maintain the underlying rational parameter-dependency. In this regard, consider a mapping from measurable parameters to a parameter set that renders $\Upsilon(\delta)$ polynomial in δ, denoted

$$f^{\rho \to \delta} \in \mathcal{C}^1(\boldsymbol{\rho}, \mathbb{R}^{n_\delta}), \quad \rho(t) \mapsto f^{\rho \to \delta}\big(\rho(t)\big) \stackrel{\triangle}{=} \delta(t),$$

Preliminary results of this section have been previously published in [60]. The results are extended by a more comprehensive parameterization algorithm.

It allows for a parameterization of $\Lambda(\rho)$ rational in δ, which yields

$$\Upsilon(\delta) = \Delta_\Upsilon(\delta) \star \left[\begin{array}{c|c} W_{\Delta 11} & W_{\Delta 12} \\ \hline W_{\Delta 21} & W_{\Delta 22} \end{array}\right] = \Delta_\Upsilon(\delta) \star W_\Delta, \tag{4.46}$$

$$\Delta_\Upsilon(\delta) = \operatorname*{diag}_{i=1}^{n_\delta}\left(\delta_i(t)I_{r^\Upsilon_{\delta,i}}\right)$$

$$\Lambda(\delta) = \Delta_\Lambda(\delta) \star \left[\begin{array}{c|c} V_{\Delta 11} & V_{\Delta 12} \\ \hline V_{\Delta 21} & V_{\Delta 22} \end{array}\right] = \Delta_\Lambda(\delta) \star V_\Delta, \tag{4.47}$$

$$\Delta_\Lambda(\delta) = \operatorname*{diag}_{i=1}^{n_\delta}\left(\delta_i(t)I_{r^\Lambda_{\delta,i}}\right),$$

Note that due to (4.38) $\Delta_\Lambda(\delta) = \Delta_\Upsilon(\delta)$.

In order to develop affine parameterizations, a mapping

$$f^{\rho \to \theta} \in \mathcal{C}^1(\boldsymbol{\rho}, \mathbb{R}^{n_\theta}), \quad \rho(t) \mapsto f^{\rho \to \theta}(\rho(t)) \stackrel{\triangle}{=} \theta(t),$$

which renders $\Lambda(\rho)$ affine in the parameters θ and a further mapping rendering $\Upsilon(\rho)$ affine in the parameters υ,

$$f^{\rho \to \upsilon} \in \mathcal{C}^1(\boldsymbol{\rho}, \mathbb{R}^{n_\upsilon}), \quad \rho(t) \mapsto f^{\rho \to \upsilon}(\rho(t)) \stackrel{\triangle}{=} \upsilon(t),$$

is required. Such mappings allow to construct LFRs of the form

$$\Upsilon(\upsilon) = \Upsilon_\Upsilon(\upsilon) \star \left[\begin{array}{c|c} 0 & W_{\Upsilon 12} \\ \hline W_{\Upsilon 21} & W_{\Upsilon 22} \end{array}\right] = \Upsilon_\Upsilon(\upsilon) \star W_\Upsilon, \tag{4.48}$$

$$\Upsilon_\Upsilon(\upsilon) = \operatorname*{diag}_{i=1}^{n_\upsilon}(\upsilon_i(t)I_{r_{\upsilon,i}}).$$

$$\Lambda(\theta) = \Theta_\Lambda(\theta) \star \left[\begin{array}{c|c} 0 & V_{\Theta 12} \\ \hline V_{\Theta 21} & V_{\Theta 22} \end{array}\right] = \Theta_\Lambda(\theta) \star V_\Theta, \tag{4.49}$$

$$\Theta_\Lambda(\theta) = \operatorname*{diag}_{i=1}^{n_\theta}(\theta_i(t)I_{r_{\theta,i}})$$

Figures 4.4a and 4.4c show decompositions that choose the rational plant representation based on $\Upsilon(\rho)$ as a starting point. Figure 4.4a illustrates the case, where a parameterization $\Upsilon(\upsilon)$ is found by means of a mapping $\upsilon \stackrel{\triangle}{=} f^{\rho \to \upsilon}(\rho)$ that renders the parameter block affine in the parameters υ. Pulling out these parameters into standard LFR with diagonal blocks is performed using (4.48). Figure 4.4c depicts the case, where $\Upsilon(\delta)$ is rationally parameter dependent and (4.46) is employed to generate a diagonal feedback block $\Delta_\Upsilon(\delta)$.

Figures 4.4b and 4.4d illustrate the same ideas for decompositions that choose the affine plant representation based on $\Lambda(\rho)$ instead.
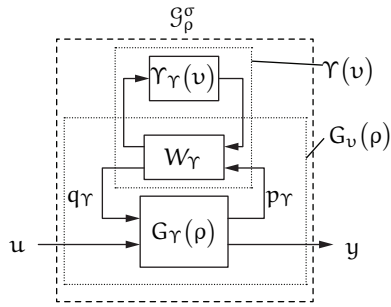
(a) LFT-LPV plant $G_\Upsilon(\rho)$ in interconnection with the affinely parameterized parameter block $\Upsilon(\upsilon)$. The block $\Upsilon(\upsilon)$ in turn is decomposed by the LFT $\Upsilon(\upsilon) = \Upsilon_\Upsilon(\upsilon) \star W_\Upsilon$.
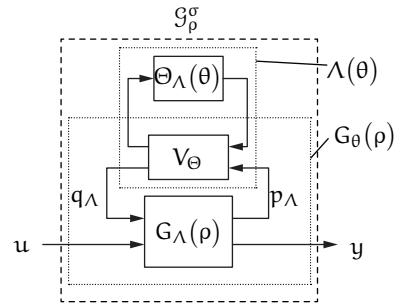
(b) LFT-LPV plant $G_\Lambda(\rho)$ in interconnection with the affinely parameterized parameter block $\Lambda(\theta)$. The block $\Lambda(\theta)$ in turn is decomposed by the LFT $\Lambda(\theta) = \Theta_\Lambda(\theta) \star V_\Theta$.
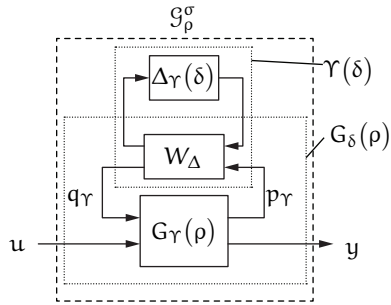
(c) LFT-LPV plant $G_\Upsilon(\rho)$ in interconnection with the polynomially parameterized parameter block $\Upsilon(\delta)$. The block $\Upsilon(\delta)$ in turn is decomposed by the LFT $\Upsilon(\delta) = \Delta_\Upsilon(\delta) \star W_\Delta$.
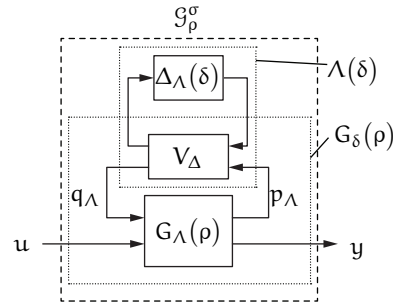
(d) LFT-LPV plant $G_\Lambda(\rho)$ in interconnection with the rationally parameterized parameter block $\Lambda(\delta)$. The block $\Lambda(\delta)$ in turn is decomposed by the LFT $\Lambda(\delta) = \Delta_\Lambda(\delta) \star V_\Delta$.

Figure 4.4: LFT-LPV plant models with full parameter blocks parameterized as LFRs with diagonal parameter blocks.

4.5.3 Tools for Automated Parameterization

To automate the process of parameterization, consider the following lemma as the main tool for the subsequent discussion.

Lemma 4.2 (Polynomial Basis)
Consider a function

$$N : \delta \to \mathbb{R}^{n_1 \times n_2}, \delta \mapsto N(\delta)$$

with polynomial dependence on the parameter vector

$$\delta = \begin{bmatrix} \delta_1 \ \delta_2 \ \dots \ \delta_{n_\delta} \end{bmatrix}^\top \in \delta.$$

Let the vector of monomials $m(\delta) = \begin{bmatrix} m_1(\delta) \ m_2(\delta) \ \dots \ m_{n_m}(\delta) \end{bmatrix}^\top$ *occurring in* $N(\delta)$
admit the decomposition

$$N(\delta) = \underline{N} \left(m(\delta) \otimes I_{n_2} \right) \tag{4.50}$$

$$\underline{N} = \begin{bmatrix} N_1 & N_2 & \dots & N_{n_m} \end{bmatrix} \in \mathbb{R}^{n_1 \times n_m n_2},$$

$$N_i = \begin{bmatrix} n_{i,1} & n_{i,2} & \dots & n_{i,n_2} \end{bmatrix} \in \mathbb{R}^{n_1 \times n_2},$$

$$n_{i,j} \in \mathbb{R}^{n_1}, \ i \in \{1, 2, \dots, n_m\}, \ j \in \{1, 2, \dots, n_2\}.$$

Then a vector $p(\delta) = \begin{bmatrix} p_1(\delta) \ p_2(\delta) \ \dots \ p_{n_p}(\delta) \end{bmatrix}^\top$ *contains a minimal number* n_p *of polynomials that admits a decomposition*

$$N(\delta) = \underline{P} \left(p(\delta) \otimes I_{n_2} \right) \tag{4.51}$$

$$\underline{P} = \begin{bmatrix} P_1 & P_2 & \dots & P_{n_p} \end{bmatrix} \in \mathbb{R}^{n_1 \times n_p n_2},$$

$$P_i = \begin{bmatrix} p_{i,1} & p_{i,2} & \dots & p_{i,n_2} \end{bmatrix} \in \mathbb{R}^{n_1 \times n_2},$$

$$p_{i,j} \in \mathbb{R}^{n_1}, \ i \in \{1, 2, \dots, n_p\}, \ j \in \{1, 2, \dots, n_2\}.$$

with $n_p \leqslant n_m$ *is given by* $p(\delta) = V^\top m(\delta)$, *where* $V \in \mathbb{R}^{n_m \times n_p}$ *and* $\underline{P}$ *are derived from the singular value decomposition (SVD)*

$$n(\delta) \triangleq \begin{bmatrix} n_{1,1} & n_{2,1} & \dots & n_{n_m,1} \\ n_{1,2} & n_{2,2} & \dots & n_{n_m,2} \\ \vdots & & \ddots & \vdots \\ n_{1,n_2} & n_{2,n_2} & \dots & n_{n_m,n_2} \end{bmatrix} m(\delta) = [u \ u_0] \begin{bmatrix} \Sigma & 0 \\ 0 & 0 \end{bmatrix} \begin{bmatrix} V^\top \\ V_0^\top \end{bmatrix} m(\delta)$$

$$= \begin{bmatrix} p_{1,1} & p_{2,1} & \dots & p_{n_p,1} \\ p_{1,2} & p_{2,2} & \dots & p_{n_p,2} \\ \vdots & & \ddots & \vdots \\ p_{1,n_2} & p_{2,n_2} & \dots & p_{n_p,n_2} \end{bmatrix} p(\delta) = U\Sigma p(\delta).$$

$\Box$

Lemma 4.2 essentially provides a systematic way to obtain affine parameterizations of polynomially parameter-dependent parameter blocks. The new affine parameters are simply defined from the polynomial terms. By first normalizing the monomial basis, a polynomial basis derived via Lma. 4.2 will not be biased, since all weights are shifted into the coefficient matrices the PCA relies on. In return, after obtaining a polynomial basis, its normalization facilitates further modeling steps.

Remark 4.4 *An affine decomposition of* $N(\delta)$ *into coefficient matrices* N_i *and monomials* $m_i(\delta)$ *can be easily performed using standard symbolic tools in Matlab.*

The following proposition formalizes the normalization of the monomial basis.

Proposition 4.1 (Normalization of Monomial Basis)
Consider a function

$$N : \delta \to \mathbb{R}^{n_1 \times n_2}, \delta \mapsto N(\delta)$$

with polynomial dependence on the parameter vector $\delta \in \boldsymbol{\delta}$. *Furthermore, consider the decomposition in terms of a monomial basis* $m(\delta)$ *as from Lma. 4.2.*

Let the vector of shifted (e. g., normalized) parameters be given as

$$\delta_N = \begin{bmatrix} \delta_{1N} \\ \delta_{2N} \\ \vdots \\ \delta_{n_\delta N} \end{bmatrix}, \quad \delta_{iN} = \frac{1}{\delta_{iR}} (\delta_i - \delta_{i0}), \ i \in \{1, 2, \ldots, n_\delta\},$$

where in the case of normalization, one has

$$\delta_{iR} = \frac{1}{2} (\overline{\delta}_i - \underline{\delta}_i) \quad and \quad \delta_{i0} = \frac{1}{2} (\overline{\delta}_i + \underline{\delta}_i), \ i \in \{1, 2, \ldots, n_\delta\}.$$

Express the vector of monomials occurring in $N(\delta)$ *as*

$$m(\delta) = M_N m(\delta_N) + m(\delta_0),$$

which admits the decomposition

$$\begin{aligned} N(\upsilon) &= \underline{N} (M_N \otimes I_{n_2}) (m(\delta_N) \otimes I_{n_2}) + \underline{N} (m(\delta_0) \otimes I_{n_2}) \\ &= \underline{N}_N (m(\delta_N) \otimes I_{n_2}) + \underline{N}_0 \end{aligned}$$

$\Box$

Since for the parameterization of parameter blocks $\Upsilon(\bullet)$ or $\Lambda(\bullet)$, each column corresponds to a specific state, state derivative or plant input, it can be appropriate to weight each column with the respective maximum bounds or range of the admissible state or input trajectories. If such information is available *a priori*, it can be used to reduce the bias of the singular value decomposition via the following corollary.

Corollary 4.3 (Weighted Polynomial Basis)
In addition to the conditions of Lma. 4.2, consider an invertible weighting matrix W used to weight the function $N(\delta)$ by right multiplication

$$N_w : \delta \to \mathbb{R}^{n_1 \times n_2}, \delta \mapsto N_w(\delta) = N(\delta) W$$

Due to the decompositon of Lma. 4.2, one may write

$$
\begin{aligned}
N(\delta) &= \underline{N} \left(I_{n_m} \otimes W \right) \left(I_{n_m} \otimes W^{-1} \right) \left(m(\delta) \otimes I_{n_2} \right) \\
&= \underline{N}_w \left(m(\delta) \otimes I_{n_2} \right) w^{-1}
\end{aligned}
\tag{4.52}
$$

and a vector of polynomials $p_w(\delta)$ resulting from the weighted coefficient matrix that admits a decomposition

$$N(\delta) = \underline{P}_w \left(I_{n_p} \otimes W^{-1} \right) \left(p_w(\delta) \otimes I_{n_2} \right) \tag{4.53}$$

is obtained by application of Lma. 4.2 on $N_w(\delta)$. $\qquad\square$

Proof: The application of Lma. 4.2 simply results in

$$N_w(\delta) = \underline{P}_w \left(p_w(\delta) \otimes I_{n_2} \right)$$

which by

$$
\begin{aligned}
N(\delta) &= N_w(\delta) W^{-1} \\
&= \underline{P}_w \left(p_w(\delta) \otimes I_{n_2} \right) W^{-1} \\
&= \underline{P}_w \left(I_{n_p} \otimes W^{-1} \right) \left(p_w(\delta) \otimes I_{n_2} \right)
\end{aligned}
$$

yields the result. $\qquad\blacksquare$

Note that the polynomial basis terms in the vector of polynomials $p(\delta)$ derived from applying Lma. 4.2 to a polynomial matrix are ordered by descending magnitude of the singular values. The following corollary provides an unbiased means to approximate a given matrix polynomial.

Corollary 4.4 (Polynomial Basis Approximation)
Consider the decompositon (4.51) in terms of

$$
p(\delta) = \begin{bmatrix} \hat{p}(\hat{\delta}) \\ \check{p}(\check{\delta}) \end{bmatrix}, \quad \text{where} \quad
\begin{aligned}
\hat{p} &: \hat{\delta} \to \mathbb{R}^{n_{\hat{p}}}, & \hat{\delta} &\mapsto \hat{p}(\hat{\delta}), \\
\check{p} &: \check{\delta} \to \mathbb{R}^{n_p - n_{\hat{p}}}, & \check{\delta} &\mapsto \check{p}(\check{\delta}),
\end{aligned}
$$

$$
\hat{p}(\hat{\delta}) = \begin{bmatrix} p_1(\hat{\delta}) \\ p_2(\hat{\delta}) \\ \vdots \\ p_{n_{\hat{p}}}(\hat{\delta}) \end{bmatrix}, \quad
\check{p}(\check{\delta}) = \begin{bmatrix} p_{n_{\hat{p}}+1}(\check{\delta}) \\ p_{n_{\hat{p}}+2}(\check{\delta}) \\ \vdots \\ p_{n_p}(\check{\delta}) \end{bmatrix}
$$

$$\hat{\delta} \in \hat{\delta} \subset \mathbb{R}^{n_{\delta}}, \quad \check{\delta} \in \check{\delta} \subset \mathbb{R}^{n_{\delta}}, \quad \hat{\delta} \cup \check{\delta} = \delta$$

derived by Lma. 4.2 applied on the decomposition (4.50). Further assume that the monomial basis is normalized according to Prop. 4.1. Then, an approximation

$$\hat{N}: \hat{\delta} \to \mathbb{R}^{n_1 \times n_2}, \hat{\delta} \mapsto \hat{N}(\hat{\delta})$$

of $N(\delta)$ is given by

$$N(\delta) \approx \hat{N}(\hat{\delta}) = \underline{\hat{P}} \left(\hat{p}(\hat{\delta}) \otimes I_{n_2} \right)$$
$$\underline{\hat{P}} = \begin{bmatrix} P_1 & P_2 & \dots & P_{n_{\hat{p}}} \end{bmatrix} \in \mathbb{R}^{n_1 \times n_{\hat{p}} n_2}.$$

$\square$

Proof: Omitting the (insignificant) last $n_p - n_{\hat{p}}$ singular values in the procedure of Lma. 4.2 yields the result. $\blacksquare$

Remark 4.5 *It may happen that the first $n_{\hat{p}}$ polynomials in $p(\delta)$ only depend on a subset of parameters, collected in the vector $\hat{\delta}$, which—in turn—takes only admissible values from $\hat{\delta} \subseteq \delta$.*

4.5.4 *Parameterization Procedure*

In the following, a procedure for parameterizing LFT-LPV systems is proposed. The procedure can be denoted as «semi-automated», because it relies on an initial choice of parameters in which the descriptor system matrices are polynomial. Although this choice may have a non-negligible effect on the resulting complexity and performance, it has to be performed on a level that still offers a high amount of transparency to the engineer and can thus be easily performed manually. The subsequent automated parameterization procedure then provides a guideline in obtaining models and approximations thereof of intermediate to low complexity. This renders the objective of finding a small parameter set in the initial manual definition of polynomial parameters less important, which allows to strengthen the focus on retaining couplings and reducing overbounding by the selection of parameters.

The procedure is first explained in detail, after which it is summarized in Alg. 4.1 and illustrated in a matrix-type classification of the resulting models in Fig. 4.6.

4.5.4.1 *Polynomial Parameterization of $\Upsilon(\rho)$*

The block $\Upsilon(\rho)$ is formed and masking matrices V, W_E and W_F are defined selecting only parameter-dependent blocks. For subsequent application of Lma. 4.2 and Cor. 4.4 with minimum bias, choose equally weighted entries in the masking matrices—preferably identities. The choice of a polynomial parameterization of $\Upsilon(\rho)$ presents the foundation of subsequent rational or affine parameterizations. A parameter set $\tilde{\delta}$ can be selected manually even for complex systems, simply covering all transcendental terms or introducing taylor expansions with sufficient accuracy.

Subsequently, Ass. (A4.2) is satisfied via a shift based on some admissible operating point ρ_0, which also guarantees that the nominal system retains physical meaning.

Therefore, first decompose $\Upsilon(\rho)$ as a linear combination of monomials $m_{\tilde{\delta}}(\tilde{\delta})$,

$$\Upsilon(\tilde{\delta}) = \underline{\tilde{\Upsilon}}\left(m_{\tilde{\delta}}(\tilde{\delta}) \otimes I_{n_{p\Upsilon}}\right), \quad m_{\tilde{\delta}}(\tilde{\delta}) \in \mathbb{R}^{n_{m_{\tilde{\delta}}}},$$

where the parameter vector $\tilde{\delta}$ contains all transcendental and non-transcendental terms from which the monomials are constructed without taking into consideration that each parameter in $\tilde{\delta}$ should be allowed to take zero as a value. Since it is the goal to enable LFT parameterizations of $\Upsilon(\bullet)$ with diagonal parameter blocks, such as those given in Eq. (4.46) that contain zero in their compact set of admissible values, the shift based on ρ_0 should be performed on the level of the parameters $\tilde{\delta}$, rather than on the level of the monomials. Consider Ex. 4.7 for illustration.

Example 4.7 (Admissible Diagonal Parameter Blocks)
Assume that $\rho \triangleq \begin{bmatrix} \rho_1 & \rho_2 \end{bmatrix}$ and $\rho_0 = \begin{bmatrix} 0 & 0 \end{bmatrix}$. Further assume $|\rho| \leqslant \begin{bmatrix} \pi & \pi \end{bmatrix}/4$ and that a particular monomial as part of the matrix $\Upsilon(\rho)$ is

$$\begin{aligned} m(\rho) &= \cos(\rho_1)\cos(\rho_2) \\ &= \left(\cos(\rho_1)-1\right)\left(\cos(\rho_2)-1\right)+\left(\cos(\rho_1)-1\right)+\left(\cos(\rho_2)-1\right)+1. \end{aligned}$$

In view of Ass. (A4.2), an admissible LFR of $m(\rho)$ is

$$m(\rho) = \begin{bmatrix} \delta_1 & \\ & \delta_2 \end{bmatrix} \star \begin{bmatrix} 0 & 1 & 1 \\ 0 & 0 & 1 \\ \hline 1 & 1 & 1 \end{bmatrix}, \quad \begin{bmatrix} \delta_1 \\ \delta_2 \end{bmatrix} \triangleq \begin{bmatrix} \cos(\rho_1)-1 \\ \cos(\rho_2)-1 \end{bmatrix}.$$

On the other hand, the LFR

$$m(\rho) = \begin{bmatrix} \delta_1 & \\ & \delta_2 \end{bmatrix} \star \begin{bmatrix} 0 & 0 & 1 \\ 1 & 0 & 0 \\ \hline 0 & 1 & 0 \end{bmatrix}, \quad \begin{bmatrix} \delta_1 \\ \delta_2 \end{bmatrix} \triangleq \begin{bmatrix} \cos(\rho_1) \\ \cos(\rho_2) \end{bmatrix}.$$

is impractical, since both $\cos(\rho_1)$ and $\cos(\rho_2)$ cannot become zero. Finally, the choice

$$m(\rho) = \delta \star \begin{bmatrix} 0 & 1 \\ \hline 1 & 1 \end{bmatrix}, \quad \delta \triangleq \cos(\rho_1)\cos(\rho_2)-1,$$

may appear attractive, but in the case of multiple occurrences of $\cos(\rho_1)$ and $\cos(\rho_2)$ in other entries of matrices related to $\Upsilon(\rho)$, such a choice can forcefully hide the underlying coupling. □

Consequently, in the monomial vector $m_{\tilde{\delta}}(\tilde{\delta})$, substitute

$$\tilde{\delta}_i(\rho) = \delta_i(\rho) + \tilde{\delta}_i(\rho_0), \quad \delta_i(\rho) \triangleq \tilde{\delta}_i(\rho) - \tilde{\delta}_i(\rho_0), \quad i \in \{1, \dots, n_{\tilde{\delta}}\}.$$

This can yield a larger vector of monomials $m_{\delta}(\delta) \in \mathbb{R}^{n_{m_\delta}}$, $n_{m_\delta} \geqslant n_{m_{\tilde{\delta}}}$, in the shifted parameters and produces a constant term and a modified decomposition

$$m_{\tilde{\delta}}(\tilde{\delta}) = M_0 m_{\delta}(\delta) + m_{\tilde{\delta}}(\tilde{\delta}(\rho_0)), \quad M_0 \in \mathbb{R}^{n_{m_{\tilde{\delta}}} \times n_{m_\delta}}.$$

$$\Upsilon(\delta) = \underline{\Upsilon}\left(m_{\delta}(\delta) \otimes I_{n_{p\Upsilon}}\right) + \underline{\Upsilon}_0,$$

where $\underline{\Upsilon} = \tilde{\underline{\Upsilon}}\left(M_0 \otimes I_{n_{p\Upsilon}}\right)$, $\underline{\Upsilon}_0 = \tilde{\underline{\Upsilon}}\left(m_{\tilde{\delta}}(\tilde{\delta}(\rho_0)) \otimes I_{n_{p\Upsilon}}\right)$. Attribute the offset $\underline{\Upsilon}_0$ to the nominal system matrices E_0 and F_0, which then guarantees

$$0 \in \left\{\Upsilon(\delta) \mid \delta(\rho) = f^{\rho \to \delta}(\rho), \ \rho \in \boldsymbol{\rho}\right\}.$$

Example 4.8 (Shifting of a Monomial Vector)
Consider the nonlinear term

$$m(\rho) = \cos(\rho_1)\cos(\rho_2) + \sin(\rho_1)\cos(\rho_2),$$

and its decomposition into constant coefficients and monomial vector

$$m(\rho) = \tilde{\underline{\Upsilon}} m_{\tilde{\delta}}(\tilde{\delta}) = \begin{bmatrix} 1 & 1 \end{bmatrix} \begin{bmatrix} \tilde{\delta}_1 \tilde{\delta}_2 \\ \tilde{\delta}_2 \tilde{\delta}_3 \end{bmatrix}, \quad \begin{bmatrix} \tilde{\delta}_1 \\ \tilde{\delta}_2 \\ \tilde{\delta}_3 \end{bmatrix} \triangleq \begin{bmatrix} \cos(\rho_1) \\ \cos(\rho_2) \\ \sin(\rho_1) \end{bmatrix}.$$

With $\rho_0 = \begin{bmatrix} \rho_{1,0} & \rho_{2,0} \end{bmatrix}^\top = \begin{bmatrix} 0 & 0 \end{bmatrix}^\top$, one obtains

$$\delta \triangleq \begin{bmatrix} \delta_1 \\ \delta_2 \\ \delta_3 \end{bmatrix} = \begin{bmatrix} \tilde{\delta}_1 - \tilde{\delta}_{1,0} \\ \tilde{\delta}_2 - \tilde{\delta}_{2,0} \\ \tilde{\delta}_3 - \tilde{\delta}_{3,0} \end{bmatrix}, \quad \tilde{\delta}(\rho_0) = \begin{bmatrix} \tilde{\delta}_{1,0} \\ \tilde{\delta}_{2,0} \\ \tilde{\delta}_{3,0} \end{bmatrix} = \begin{bmatrix} 1 \\ 1 \\ 0 \end{bmatrix}.$$

$$m(\rho) = \begin{bmatrix} 1 & 1 \end{bmatrix} \left(\begin{bmatrix} \tilde{\delta}_{2,0} & \tilde{\delta}_{1,0} & 0 & 1 & 0 \\ 0 & 0 & \tilde{\delta}_{2,0} & 0 & 1 \end{bmatrix} \begin{bmatrix} \delta_1 \\ \delta_2 \\ \delta_3 \\ \delta_1 \delta_2 \\ \delta_2 \delta_3 \end{bmatrix} + \begin{bmatrix} \tilde{\delta}_{1,0} \tilde{\delta}_{2,0} \\ \tilde{\delta}_{2,0} \tilde{\delta}_{3,0} \end{bmatrix} \right)$$

$$= \begin{bmatrix} \tilde{\delta}_{2,0} & \tilde{\delta}_{1,0} & \tilde{\delta}_{2,0} & 1 & 1 \end{bmatrix} m_{\delta}(\delta) + \tilde{\delta}_{2,0}(\tilde{\delta}_{1,0} + \tilde{\delta}_{3,0}) = \underline{\Upsilon} m_{\delta}(\delta) + \tilde{\underline{\Upsilon}} m_{\tilde{\delta}}(\tilde{\delta}(\rho_0)).$$

$\square$

Performing a normalization instead of a shift about some nominal operating point $\rho_0 \in \boldsymbol{\rho}$ may be tempting at this stage, but in many cases this will result in the constant offset $\underline{\Upsilon}_0$ and therefore the nominal system matrices will not correspond to a physically admissible system in terms of the compact set of general parameters $\boldsymbol{\rho}$. This is unavoidable, but a deliberate choice can be made to keep the offset resulting from normalization performed later in the LFT parameter block instead of shifting it to the nominal system matrices. Consider Ex. 4.9 for illustration.

Example 4.9 (Normalization of a Monomial Vector)

Consider the nonlinear vector-valued function

$$m(\rho) = \begin{bmatrix} \sin(\rho) \\ \cos(\rho) \end{bmatrix}, \quad |\rho| \leqslant \pi/2,$$

and the ranges of the trigonometric terms

$$\sin(\rho) \in [-1, 1], \quad \cos(\rho) \in [0, 1].$$

The normalized new parameters

$$\delta \triangleq \begin{bmatrix} \delta_1(\rho) \\ \delta_2(\rho) \end{bmatrix} = \begin{bmatrix} \sin(\rho) \\ 2(\cos(\rho) - 0.5) \end{bmatrix},$$

produce a constant offset after substitution that does not correspond to any particular $m(\rho_0)$, *where* $\rho_0 \in [-\pi/2, \pi/2]$. *Thus*

$$m(\rho) = \begin{bmatrix} \delta_1(\rho) \\ \frac{1}{2}\delta_2(\rho) \end{bmatrix} + \begin{bmatrix} 0 \\ 0.5 \end{bmatrix}.$$

$\square$

Consequently, for the remainder, it is assumed that such a transformation has been performed and subsequently a normalization according to Prop. 4.1 is applied,

$$\Upsilon(\delta_N) = \underline{\Upsilon}_N \left(m_\delta(\delta_N) \otimes I_{n_{p_\Upsilon}} \right) + \underline{\Upsilon}_{N0}, \tag{4.54}$$

where $\underline{\Upsilon}_{N0}$ now results from the normalization and remains part of the parameter block. In the following, the subscript $_N$ will be dropped for simplicity of notation. The set of parameters δ therefore represents a rational parameterization that admits an LFR of the form (4.46), with a parameter block $\Delta_\Upsilon(\delta)$ that satisfies

$$0 \in \left\{ \Delta_\Upsilon(\delta) \;\middle|\; \delta(\rho) = f^{\rho \to \delta}(\rho), \; \rho \in \boldsymbol{\rho} \right\}.$$

Remark 4.6 *Note that in general an SVD will yield fully populated matrices $V_{\hat{\upsilon}}$ and $V_{\hat{\upsilon}}$ in Eq. (4.55). Thus, the approximate parameter vector $\hat{\upsilon}$ usually depends on the full parameter vector δ. Eliminating entries close to zero in the coefficient matrix $V_{\hat{\upsilon}}$ can yield simpler parametric dependencies $\upsilon(\hat{\delta})$, possibly omitting some general LPV parameters altogether.*

4.5.4.2 *Affine Parameterization of $\Upsilon(\rho)$*

Application of Lma. 4.2 on the normalized monomial decomposition of $\Upsilon(\delta)$ from (4.54)[1] and a subsequent normalization of the polynomials yields a normalized polynomial decomposition based on the vector of polynomials in δ,

$$\upsilon(\delta) \triangleq \begin{bmatrix} V_{\hat{\upsilon}}^{\top} \\ V_{\check{\upsilon}}^{\top} \end{bmatrix} m_{\delta}(\delta) \ \in \mathbb{R}^{n_{\upsilon}}, \tag{4.55}$$

where $V_{\hat{\upsilon}} \in \mathbb{R}^{n_{\hat{\upsilon}} \times n_{m_{\delta}}}$ and $V_{\check{\upsilon}} \in \mathbb{R}^{n_{\check{\upsilon}} \times n_{m_{\delta}}}$ are obtained by Lma. 4.2 and contain the coefficients with which the monomials are linearly combined. The polynomials are defined as the set of parameters υ in which $\Upsilon(\upsilon)$ is affine. The constant offset $\underline{\Upsilon}_0$ remains unchanged and the affine decomposition is

$$\Upsilon(\upsilon) = \underline{\Upsilon}_{\upsilon} \left(\upsilon(\delta) \otimes I_{n_{p_{\Upsilon}}} \right) + \underline{\Upsilon}_0.$$

Using Cor. 4.4, an approximation $\hat{\Upsilon}(\hat{\upsilon})$ can be defined up to a desired accuracy. For this purpose, discard the lower rows of (4.55) corresponding to non-significant singular values according to Cor. 4.4. Let these rows correspond to the coefficient matrix $V_{\check{\upsilon}}$. Then, the vector of approximate parameters is

$$\hat{\upsilon}(\delta) = V_{\hat{\upsilon}}^{\top} m_{\delta}(\delta) \ \in \mathbb{R}^{n_{\hat{\upsilon}}}. \tag{4.56}$$

By resubstitution, an approximation $\hat{\Upsilon}(\hat{\delta})$ can be obtained as well.

4.5.4.3 *Rational Parameterization of $\Lambda(\rho)$*

Due to (4.38), $\Lambda(\delta)$ is directly available. Similarily, approximations $\hat{\Lambda}(\hat{\delta})$ and $\hat{\Lambda}(\hat{\upsilon})$ can be obtained from the respective approximations $\hat{\Upsilon}(\hat{\bullet})$.

4.5.4.4 *Affine Parameterization of $\Lambda(\rho)$*

From (4.41), observe that $\tilde{\Lambda}(\upsilon)$ is polynomial in υ, s. t. a decomposition

$$\Lambda(\upsilon) = \frac{1}{d(\upsilon)} \underline{\Lambda} \left(m_{\upsilon}(\upsilon) \otimes I_{n_{p_{\Lambda}}} \right).$$

can be found. A set of affine parameters is constructed from

$$\theta(\upsilon) = \frac{1}{d(\upsilon)} \begin{bmatrix} V_{\hat{\theta}}^{\top} \\ V_{\check{\theta}}^{\top} \end{bmatrix} m_{\upsilon}(\upsilon) \ \in \mathbb{R}^{n_{\theta}}, \tag{4.57}$$

---

1 Recall that the subscript $_N$ has been dropped.

where the coefficient matrices $V_{\hat{\theta}} \in \mathbb{R}^{n_{\hat{\theta}} \times n_{m_v}}$ and $V_{\check{\theta}} \in \mathbb{R}^{n_{\check{\theta}} \times n_{m_v}}$ are obtained by application of Lma. 4.2 and Cor. 4.4, respectively, on the monomial decomposition without the denominator. By discarding singular values associated with $V_{\check{\theta}}$—possibly due to the reason that they are particularly small—an approximating set of parameters can be obtained via

$$\hat{\theta}(\upsilon) = \frac{1}{d(\upsilon)} V_{\hat{\theta}}^\top m_\upsilon(\upsilon) \ \in \mathbb{R}^{n_{\hat{\theta}}}. \tag{4.58}$$

An alternative approximate, fully affine parameterization can be obtained by applying Lma. 4.2 on $\hat{\Lambda}(\hat{\upsilon})$, which yields yet another parameter set ϕ.

4.5.5 Summary

The procedure described in the previous sections allows to systematically construct a set parameterizations of a plant model with different trade-offs between parameter complexity and incurred overbounding. Based on the results, *a priori* assessments of the incurred synthesis and implementation complexity can be performed, s. t. the most suitable plant representation may be selected for use in, e. g., the LFT-LPV controller synthesis framework as per [125].

Figs. 4.5a and 4.5b illustrate the chain of LFT interconnections for the case that some general LPV parameters have been taken to remain in the masking matrices V, W_E, W_F or the nominal matrices E_0 and F_0.

The diagram shown in Fig. 4.6 presents a summary of the above transformations. The boxes show the respective system descriptions as LFTs of a parameter block and an input-output operator $G_\bullet(\rho)$. The parameter-dependence of the operators arises specifically from possible parameter-dependency of the masking or nominal matrices. However, it is suppressed in the diagram.

The representations are categorized on two axes: The horizontal segments indicate whether the respective LFRs denote rational or affine dependence on the parameter block. The vertical segments categorize the type of parameterizations of the parameter blocks and the structure of the block. For instance, in the representation $\Upsilon(\delta) \star G_\Upsilon$, the parameter block $\Upsilon(\delta)$ is polynomially dependent on δ, while $\Upsilon(\delta) \star G_\Upsilon$ is a rational function in the block $\Upsilon(\delta)$.

The segments that indicate affine dependence of the parameter blocks on some parameters are of particular interest. As mentioned above, affinely parameterized parameter blocks render the evaluation of multiplier conditions as per Lma. 2.2, i. e., based on LMIs in the vertices spanning the corresponding matrix polytopes, applicable. In an LFT-LPV synthesis setting based on PiDLFs, Lma. 2.5 is then applied to construct the controller's scheduling block. Hence, the smaller the affinely parameterized parameter block, the less costly the implementation of the controller, cf. Eq. (3.11). Note, however, that the required number of LMIs increases exponentially with the number of parameters.

When full parameter blocks are considered the commutativity requirements imposed by D/G-S, cf. Lma. 2.3 and Exs. 2.3 and 2.4, introduce a high amount of con-

(a) LFT-LPV plant $G_\Lambda(\rho)$ in interconnection with the parameter block $\Lambda(\delta,\rho)$. The block $\Lambda(\delta,\rho)$ is decomposed by the LFT $\Lambda(\delta,\rho) = (\Delta_\Upsilon(\delta) \star W_\Delta) \star W_\Lambda(\rho)$.

(b) LFT-LPV plant $G_\Lambda(\rho)$ in interconnection with the parameter block $\Lambda(\upsilon,\rho)$. The block $\Lambda(\upsilon,\rho)$ is decomposed by the LFT $\Lambda(\upsilon,\rho) = (\Upsilon_\Upsilon(\upsilon) \star W_\Upsilon) \star W_\Lambda(\rho)$.
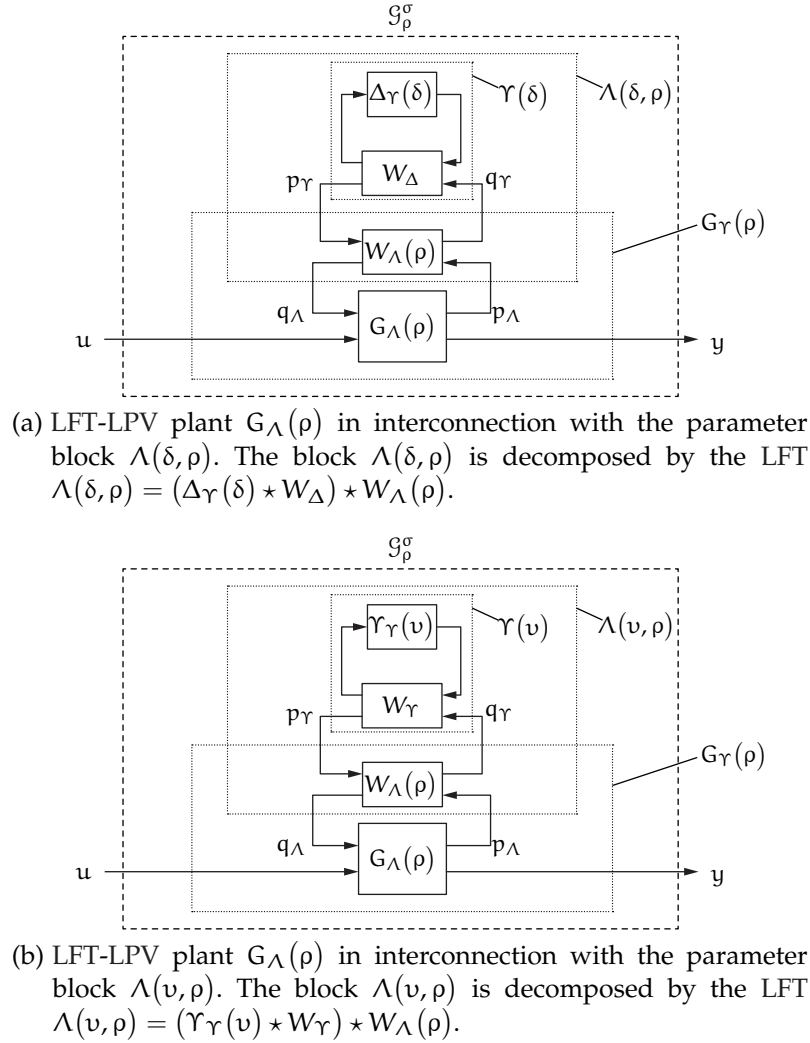
Figure 4.5: LFT-LPV plant models with diagonal parameter blocks and different options in the parameterization hierarchy.

servatism. Recall that by Lma. 2.6, the use of D/G-S constraints permits to choose a copy of the plant's parameter block as the controller's scheduling function. The use of D/G-S constraints is therefore advised only for diagonal affinely parameterized parameter-blocks.

In subsequent sections, it will be shown that the application of the full-block S-Procedure on multiplier conditions—thus introducing an additional so-called multiplier stage—will allow a more efficient approach to controller synthesis with both low implementation and synthesis complexity. By combining compact, full parameter blocks and FBMs in the first multiplier stage with diagonal parameter blocks and D/G-S in a second multiplier stage, low conservatism and compact controller scheduling functions can be achieved without the need to solve a large number of LMIs.

For this purpose, the dash-dotted lines in Fig. 4.6 denote the use of LFRs from Eqs. (4.46), (4.47), (4.48) or (4.49) to arrive at standard parameterizations with diago-
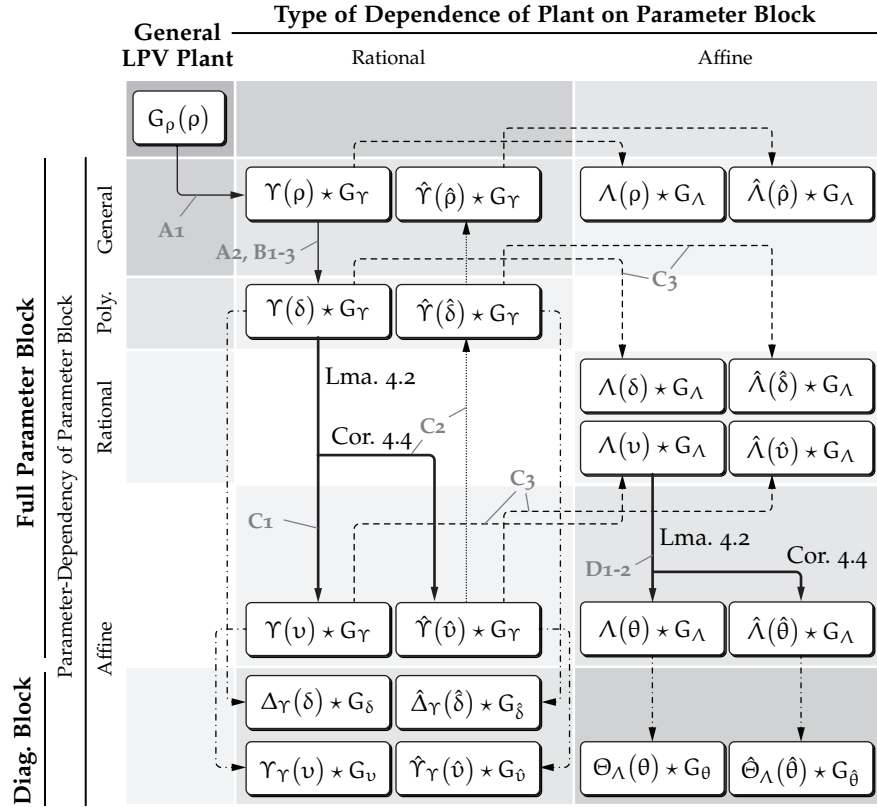
Figure 4.6: Visualization of Alg. 4.1.
(———) Thin solid lines indicate manual operations.
(- - - -) Dashed lines show immediately available transformations via Eq. (4.38).
(-·-·-·) Dash-dotted lines indicate the use of standard Matlab tools to transform an LFR with a full parameter block to an LFR with diagonal parameter block.
(·········) Dotted lines indicate a resubstitution using the functional dependence of a parameter set on another, e. g., on the measurable parameter set ρ.
(———) Thick solid lines indicate the application of Lma. 4.2 or Cor. 4.4.

nal parameter blocks that are possibly better suited for evaluation in some synthesis LMIs, e. g., to employ an additional multiplier stage as will be detailed in the next chapter.

Finally, Alg. 4.1 summarizes the suggested parameterization procedure detailed in Sect. 4.5.4. The individual phases of the algorithm are indicated in Fig. 4.6.

4.5.6 *Discussion: Relation to Parameter Set Mapping*

The technique presented in Lma. 4.2 and Cor. 4.4 has a close relationship to the parameter set mapping (PSM) technique proposed in [79], cf. Sect. 2.1.4. However, it holds the following advantages.

Algorithm 4.1 Rational and affine full-block/diagonal parameterizations from a general descriptor LPV plant model.

(A) Manual Initialization:

1:    Define V, W_E and W_F:
- Choose param.-dep. rows and columns of $E(\rho)$ and $F(\rho)$.

2:    Define parameters $\tilde{\delta}$ covering all transcendental nonlinear terms.

(B) Automated Nominal Shift and Normalization:

1:    Shift about a nominal operating point ρ_0 by application of Prop. 4.1.

2:    Define E_0 and F_0 with dependence on ρ if desired.

3:    Define $\Upsilon(\delta)$ while normalizing the parameter vector δ.

(C) Automated Rational Parameterization and Approximation:

1:    Define $\Upsilon(\upsilon)$ via Lma. 4.2 and normalization of υ by Prop. 4.1.

2:    Define $\Upsilon(\hat{\upsilon})$ and $\Upsilon(\hat{\delta})$ by application of Cor. 4.4.

3:    Form $\Lambda(\upsilon)$, $\Lambda(\hat{\upsilon})$, $\Lambda(\delta)$ and $\Lambda(\hat{\delta})$ from $\Upsilon(\bullet)$ via Eq. (4.38).

(D) Automated Affine Parameterization and Approximation:

1:    Define $\tilde{\Lambda}(\upsilon)$ and $d(\upsilon)$ by Eq. (4.43) and (4.42).

2:    Define $\tilde{\Lambda}(\theta)$ and $\tilde{\Lambda}(\hat{\theta})$ by applying Lma. 4.2 and Cor. 4.4 on $\tilde{\Lambda}(\upsilon)$:
- First reattach the denominator $d(\upsilon)$ to θ.
- If $\Lambda(\upsilon)$ has constant parts, append $1/d(\upsilon)$ to θ.
- Normalize θ by Prop. 4.1.

4.5.6.1 *Obtaining the Affine Parameter Set*

While the PSM technique has been proposed to approximate a parameter set by a set containing fewer parameters or to rotate the parameter set coordinate basis with the purpose to reduce overbounding, the technique proposed here provides an automated derivation of a new set of parameters ordered by significance in which a polynomial matrix is affine. The typical manual and error prone derivation of affine parameters is thus avoided.

4.5.6.2 *Minimality and Overbounding*

The parameter set derived by application of Lma. 4.2 yields a minimal number of affine parameters, reducing hidden coupling and overbounding. Furthermore, an intimate relation to the rational parameterizations is easily retained by the approach, which will prove useful in extended synthesis conditions detailed in Sect. 5.

4.5.6.3 *Approximation of LFRs*

When PSM is applied to a given parameter set on which a parameter block depends, e. g., affinely, the old parameters are replaced by linear combinations of the new ones. In general, the order of an LFR will therefore increase, which can

sometimes be avoided by setting coefficients to zero that are already very close to zero, cf. Sect. 2.1.4.2. PSM is therefore not an adequate tool for the approximation of LFRs. In contrast, approximations based on Cor. 4.4 do not only reduce the number of parameters a matrix depends on, but also reduce the order of the corresponding LFR with diagonal parameter block. With the novel technique, an approximation of the affine parameter set is as simple as omitting parameters starting from the highest index. This is due to the coordinate basis which is already rotated to reflect parameter directions of decreasing influence. Consequently, when following the parameterization procedure detailed in Sects. 4.4 and 4.5 any approximation based on Cor. 4.4 will yield a plant model with less deviation from the nominal case, ultimately yielding the nominal plant model if the full set of parameters is discarded.

However, the approximating quality of the approach shares the disadvantage with the PSM approach that no guarantees exist that an approximate LPV representation retains the dynamic characteristics relevant for control purposes. These could, e.g., be quantified by the degree of variation in frozen parameter pole locations.

4.5.6.4 *Data Free Approach*

Apart from plant coefficients, the proposed method acts only on the respective parameter block, which represents a deviation from nominal dynamics. This deviation is then efficiently parameterized affinely or approximated based on the influence of monomial terms. In contrast to PSM, the approach therefore completely avoids data generation, which would require gridding the parameter range or recording experimental trajectories.

4.6 Example — Compact LFT-LPV Model of a 3-DOF Robotic Manipulator

$\mathbf{F}$OR illustration, consider the example of a 3-DOF robotic manipulator, where the dynamics of joints one q_1, two q_2 and three q_3 are modeled [E45]. Figure 4.7 illustrates the robot, whereas Fig. 4.8 pictures the joint coordinate frames of interest. From the Denavit-Hartenberg (DH) convention result the joint coordinates q_1, $\tilde{q}_2$ and $\tilde{q}_3$. The so-called «ready position» of the robot is defined as $\tilde{q}_2 = \frac{\pi}{2}$ and $\tilde{q}_3 = -\pi$. The coordinate frame used in the model's nonlinear differential equations are relative to this ready position, while joint three is also adjusted to a fixed reference frame with respect to the horizontal, as follows:

$$q_2 \overset{\triangle}{=} \tilde{q}_2 - \frac{\pi}{2}, \quad q_3 \overset{\triangle}{=} \tilde{q}_3 + \pi + q_2.$$

The angle $q_{3s} \overset{\triangle}{=} \tilde{q}_3 + \pi$ is shown in Fig. 4.8 for illustration. The dimensions of the workspace result from $L_1 = 50\,\mathrm{mm}$, $L_2 = 305\,\mathrm{mm}$ and $L_3 = 330\,\mathrm{mm}$.

Table 4.1: Kinematic limits of the Thermo CRS A465 3-DOF robot.

Angle	Range [°]	Angle	Range [°]	Vel.	Range [° s^{-1}]
q_1	$[-170, \ldots, 170]$	q_1	$[-170, \ldots, 170]$	$\dot{q}_1$	$[-100, \ldots, 100]$
$\tilde{q}_2$	$[0, \ldots, 180]$	q_2	$[-90, \ldots, 90]$	$\dot{q}_2$	$[-80, \ldots, 80]$
$\tilde{q}_3$	$[-235, \ldots, -45]$	q_3	$[-145, \ldots, 225]$	$\dot{q}_3$	$[-150, \ldots, 150]$

(a) DH convention-based coordinate frames.   (b) Modified coordinate frames and angular velocities.

4.6.1 *Nonlinear LPV Model*

Using the Euler-Lagrange formulation, the rigid-body dynamic model of the three-link manipulator is obtained as a 6th-order system with three inputs and three outputs governed by a differential of the form

$$J(\rho)\ddot{q} + \tilde{k}(\rho) + k_c(\rho) = \tau.$$

The vector $k_c(\rho)$ denotes the vector of Coulomb friction terms

$$k_c(\rho) = \begin{bmatrix} b_{18}\mathrm{sign}(\dot{q}_1) \\ b_{19}\mathrm{sign}(\dot{q}_2) \\ b_{20}\mathrm{sign}(\dot{q}_3) \end{bmatrix}, \tag{4.59}$$
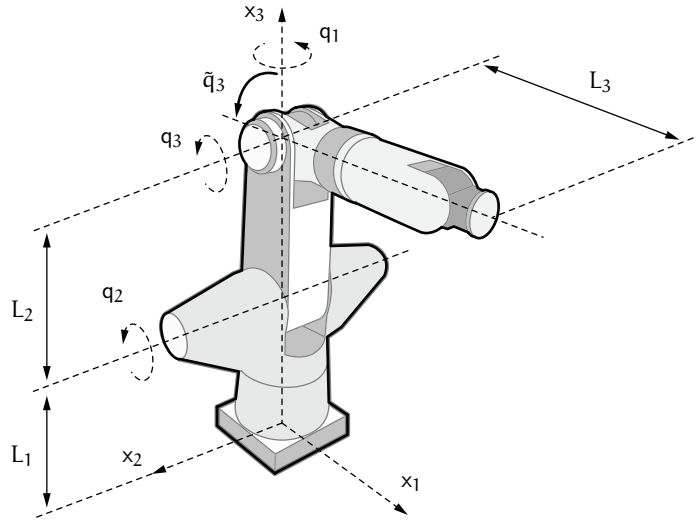
Figure 4.7: Isometric view of the 3-DOF robot model.
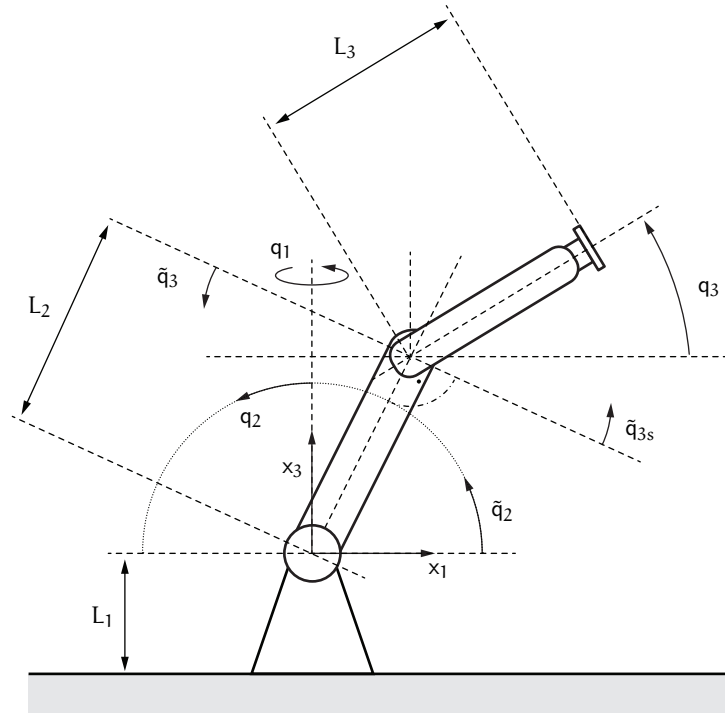
Figure 4.8: Side view of the 3-DOF robot model.

which are neglected in the LPV model and will be compensated for separately in the controller implementation by redefining the inputs as

$$u \stackrel{\triangle}{=} \tau - k_c(\rho) = \begin{bmatrix} \tau_1 \\ \tau_2 \\ \tau_3 \end{bmatrix} - \begin{bmatrix} b_{18}\text{sign}(\dot{q}_1) \\ b_{19}\text{sign}(\dot{q}_2) \\ b_{20}\text{sign}(\dot{q}_3) \end{bmatrix}.$$

The vector of generalized forces is given as

$$\tilde{k}(\rho) = \begin{bmatrix} \tilde{k}_1(\rho) \\ \tilde{k}_2(\rho) \\ \tilde{k}_3(\rho) \end{bmatrix}, \tag{4.60}$$

$$\tilde{k}_1(\rho) = b_1\dot{q}_1 + (b_2s_2c_2 + b_3c_2s_3)\,\dot{q}_1\dot{q}_2 + (b_3s_2c_3 + b_4s_3c_3)\,\dot{q}_1\dot{q}_3$$

$$\tilde{k}_2(\rho) = \left(2b_{11}s_2c_2 + 2b_{12}s_3c_3 - \tfrac{1}{2}b_3\,(s_2c_3 + c_2s_3)\right)\dot{q}_1^2$$
$$+ \tfrac{1}{2}b_3\,(c_2s_3 - s_2c_3)\,\dot{q}_2^2 + b_{10}\dot{q}_2$$
$$+ \tfrac{1}{2}b_3\,(s_2c_3 - c_2s_3)\,\dot{q}_3^2 + b_8s_2 + b_9s_3$$

$$\tilde{k}_2(\rho) = \left(2b_{12}s_3c_3 - \tfrac{1}{2}b_3s_2c_3\right)\dot{q}_1^2 + \tfrac{1}{2}b_3\,(c_2s_3 - s_2c_3)\,\dot{q}_2^2$$
$$- b_{15}\dot{q}_2 + b_{15}\dot{q}_3 + b_9s_3$$

Due to the predominant trigonometric terms and the typical substitution $\sin(\rho) = \mathrm{sinc}(\rho)\rho$, along with a preference to pull out generalized velocities $\dot{q}_i$, $i = 1, 2, 3$ into the state vector, the factorization of the generalized forces is not ambiguous, except for the first row of the generalized damping matrix, which contains multiplications of distinct generalized velocity variables. A factorization rendering $D(\rho)$ fully populated is chosen for increased coupling at frozen operating points leading to the mechanical system of LPV differential equations (4.61).

$$
\begin{aligned}
&\begin{array}{l}\text{Abbreviations:}\\ s_i \overset{\triangle}{=} \sin(q_i)\\ c_i \overset{\triangle}{=} \cos(q_i)\end{array}
\begin{bmatrix} b_3s_2s_3 + b_6c_2^2 + b_7c_3^2 + b_5 & 0 & 0 \\ 0 & \tfrac{1}{2}b_3\,(c_2c_3 + s_2s_3) + b_{13} & \tfrac{1}{2}b_3\,(c_2c_3 + s_2s_3) + b_{14} \\ 0 & \tfrac{1}{2}b_3\,(c_2c_3 + s_2s_3) + b_{17} & b_{16} \end{bmatrix}
\begin{bmatrix} \ddot{q}_1 \\ \ddot{q}_2 \\ \ddot{q}_3 \end{bmatrix} \\[2mm]
&+ \begin{bmatrix} b_1 & (b_2s_2c_2 + b_3c_2s_3)\,\dot{q}_1 & (b_3s_2c_3 + b_4s_3c_3)\,\dot{q}_1 \\ (2b_{11}s_2c_2 + 2b_{12}s_3c_3 - \tfrac{1}{2}b_3\,(s_2c_3 + c_2s_3))\,\dot{q}_1 & \tfrac{1}{2}b_3\,(c_2s_3 - s_2c_3)\,\dot{q}_2 + b_{10} & \tfrac{1}{2}b_3\,(s_2c_3 - c_2s_3)\,\dot{q}_3 \\ (2b_{12}s_3c_3 - \tfrac{1}{2}b_3s_2c_3)\,\dot{q}_1 & \tfrac{1}{2}b_3\,(c_2s_3 - s_2c_3)\,\dot{q}_2 - b_{15} & b_{15} \end{bmatrix}
\begin{bmatrix} \dot{q}_1 \\ \dot{q}_2 \\ \dot{q}_3 \end{bmatrix} \\[2mm]
&+ \begin{bmatrix} 0 & 0 & 0 \\ 0 & b_8s_2/q_2 & b_9s_3/q_3 \\ 0 & 0 & b_9s_3/q_3 \end{bmatrix}
\begin{bmatrix} q_1 \\ q_2 \\ q_3 \end{bmatrix}
= \begin{bmatrix} \tau_1 \\ \tau_2 \\ \tau_3 \end{bmatrix}
- \begin{bmatrix} b_{18}\mathrm{sign}(\dot{q}_1) \\ b_{19}\mathrm{sign}(\dot{q}_2) \\ b_{20}\mathrm{sign}(\dot{q}_3) \end{bmatrix}
= \begin{bmatrix} u_1 \\ u_2 \\ u_3 \end{bmatrix} \tag{4.61}
\end{aligned}
$$

The coefficients b_k, $k \in \{1, \ldots, 20\}$—given in Tab. B.1 in App. B.7 on p. 335—have been estimated experimentally on a real plant and details on the procedure applied to the two-degree of freedom (2-DOF) case are provided in [E37].

4.6.2 *Parameterization*

With the parameters $\tilde{\delta}$ from Tab. 4.3b covering up all transcendental and trigonometric terms, thus rendering the matrices polynomial in $\tilde{\delta}$, the generalized inertia, stiffness and damping matrices are decomposed into parameter-dependent and nominal parts. The nominal operating point $\rho_0 = \begin{bmatrix} 0, 0, 0, 0, 0 \end{bmatrix}^\top$ is chosen, about

Table 4.2: Measurable signals and LPV parameters.

| $\rho_1 \triangleq q_2$ |
| $\rho_2 \triangleq q_3$ |
| $\rho_3 \triangleq \dot{q}_1$ |
| $\rho_4 \triangleq \dot{q}_2$ |
| $\rho_5 \triangleq \dot{q}_3$ |

(a) Measurable signals.

$\tilde{\delta}_1 \triangleq \sin(\rho_1)$	$\tilde{\delta}_6 \triangleq \operatorname{sinc}(\rho_2)$
$\tilde{\delta}_2 \triangleq \sin(\rho_2)$	$\tilde{\delta}_7 \triangleq \rho_3$
$\tilde{\delta}_3 \triangleq \cos(\rho_1)$	$\tilde{\delta}_8 \triangleq \rho_4$
$\tilde{\delta}_4 \triangleq \cos(\rho_2)$	$\tilde{\delta}_9 \triangleq \rho_5$
$\tilde{\delta}_5 \triangleq \operatorname{sinc}(\rho_1)$	

(b) Parameters $\tilde{\delta}$.

$\delta_1 \triangleq 1.0\,\tilde{\delta}_1$	$\delta_6 \triangleq 2.9\,\tilde{\delta}_6 - 1.9$
$\delta_2 \triangleq 1.7\,\tilde{\delta}_2 - 0.7$	$\delta_7 \triangleq 0.6\,\tilde{\delta}_7$
$\delta_3 \triangleq 2.0\,\tilde{\delta}_3 - 1.0$	$\delta_8 \triangleq 0.7\,\tilde{\delta}_8$
$\delta_4 \triangleq 1.2\,\tilde{\delta}_4 - 0.2$	$\delta_9 \triangleq 0.5\,\tilde{\delta}_9$
$\delta_5 \triangleq 5.5\,\tilde{\delta}_5 - 4.5$	

(c) Parameters δ.

which the parameters are shifted to include zero. Therefore, further constant terms are shifted into the nominal matrices, which are then defined as

$$J_0 \triangleq \begin{bmatrix} b_5 + b_6 + b_7 & 0 & 0 \\ 0 & {}^1\!/_2 b_3 + b_{13} & {}^1\!/_2 b_3 + b_{14} \\ 0 & {}^1\!/_2 b_3 + b_{17} & b_{16} \end{bmatrix}, \ K_0 \triangleq \begin{bmatrix} 0 & 0 & 0 \\ 0 & 0 & 0 \\ 0 & 0 & 0 \end{bmatrix}, \ D_0 \triangleq \begin{bmatrix} b_1 & 0 & 0 \\ 0 & b_{10} & 0 \\ 0 & -b_{15} & b_{15} \end{bmatrix}.$$

The constant nominal matrices E_0 and F_0 are thus defined in accordance with Ex. 4.5 and by observing that $T_0 = I$. Similarly, masking matrices are defined to form W_E, W_F and V. Observe that the first column of the generalized stiffness matrix $K(\rho)$ is parameter-independent, which allows to define

$$\Upsilon(\tilde{\delta}) \triangleq \begin{bmatrix} \Delta_E(\tilde{\delta}) & \Delta_F(\tilde{\delta}) \end{bmatrix} \in \mathbb{R}^{3 \times 8}.$$

Subsequently, a normalization is applied, s. t. $|\delta_i| \leqslant 1$, $i = 1, 2, \ldots, 9$. The resulting constant terms that appear due to the offsets associated with the normalization are chosen to remain in the parameter block $\Upsilon(\delta)$ in accordance with Alg. 4.1.

The parameter block $\Upsilon(\delta)$ is then decomposed into a linear combination of 30 monomials in δ. Lemma 4.2 and further normalization according to Prop. 4.1 is then applied to obtain affine dependence of $\Upsilon(\upsilon)$ in $n_\upsilon = 10$ parameters υ. Normalized singular values of the vectorized monomial decomposition are given in Fig. 4.9a.

4.6.3 Approximation and Summary

An approximation is chosen by selecting all normalized singular values greater or equal 6×10^{-2} and a set of the first $n_{\hat{\upsilon}} = 2$ parameters remains, leading to a maximum absolute entry-wise error of 1.41×10^{-2} in the coefficient matrix. It turns out that this approximation renders Δ_E and Δ_K—the part of Δ_F corresponding to the generalized stiffness matrix—parameter-independent, s. t. the approximate parameter block can be reduced to a square 3×3 matrix, $\hat{\Upsilon}(\hat{\upsilon}) \triangleq -\hat{\Delta}_D(\hat{\upsilon})$, in which the plant is now affine.

From this approximation, approximate parameter vectors $\hat{\rho}$ and $\hat{\delta}$ are inferred by resubstituting the respective functions $\hat{\upsilon}(\delta)$ or $\hat{\upsilon}(\rho)$. Accordingly, the approximate plant is only dependent on q_2, q_3 and $\dot{q}_1$.

(a) Singular values of the mono-
    mial decomposition of $\Upsilon(\delta)$.

(b) Singular values of the
    monomial decomposition of
    $d(\upsilon)\Lambda(\upsilon)$.
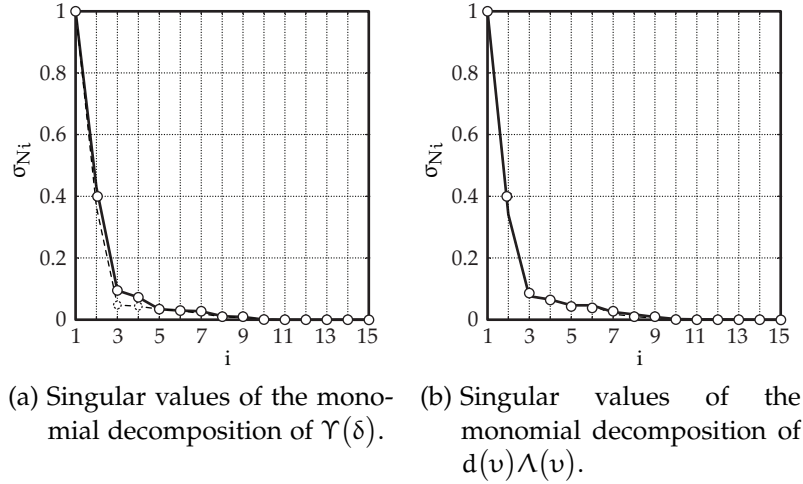
Figure 4.9: Singular values of the monomial decomposition of $\Upsilon(\delta)$ for constructing a rational and an affine robot model.
(——) Weighted normalized singular values (Cor. 4.3);
(-----) Unweighted normalized singular values.

Tab. 4.3 summarizes the resulting parameter blocks and relations. The repetitions of the respective parameters in a diagonal parameter block are given as vectors $r^\bullet$. For the repetitions resulting from approximations the vectors $r^{\hat{\bullet}}$ indicate omissions by zero repetitions. For instance, $r^{\hat{\delta}}$ identifies that $\hat{\Delta}_\Upsilon(\hat{\delta})$ *does not* depend on δ_5, δ_6, δ_8 and δ_9. Thus, according to Tab. 4.3b, angular velocities $\dot{q}_2$ and $\dot{q}_3$ do not need to be measured online for implementation of any controller synthesized based on the approximate model in terms of $\hat{\upsilon}$ or $\hat{\delta}$, respectively.

From the definitions of $\Upsilon(\delta)$, $\Upsilon(\upsilon)$ and $\hat{\Upsilon}(\hat{\upsilon})$, parameterizations $\Lambda(\delta)$, $\Lambda(\upsilon)$ and $\hat{\Lambda}(\hat{\upsilon})$ follow from (4.38). Then, Lma. 4.2 is applied to the polynomial matrix $d(\upsilon)\Lambda(\upsilon)$ by first canceling the common denominator. Fig. 4.9b again shows the corresponding singular values, which leads to $n_\theta = 15$ parameters without approximation.

Choosing the first $n_{\hat{\theta}} = 2$ parameters yields a maximum absolute entry-wise error of 2.91×10^{-2} in the coefficient matrix. It again turns out that this approximation renders Δ_E and Δ_K parameter-independent, and the approximate matrix $\hat{\Lambda}(\hat{\theta}) \overset{\triangle}{=} -\hat{\Delta}_D(\hat{\theta})$ even retains the same sparsity pattern as $\hat{\Upsilon}(\hat{\upsilon})$. Accordingly, controllers based on this latter approximation do not require online measurement of $\dot{q}_2$ and $\dot{q}_3$, as before.

Note that in the work documented in [E45], affine parameterizations of both $\Upsilon(\upsilon)$ and $\Lambda(\theta)$ have been performed by error-prone manual inspection. Furthermore, a fully affine parameterization has previously only been found with 16 parameters.

Table 4.3: Parameter block sizes and no. of repetitions for the 3-DOF robot.

Full Sched. Order	Size	Red. Sched. Order	Size
$\Upsilon(\delta) = \Delta_\Upsilon(\delta) \star W_\Delta$	3×8	$\hat{\Upsilon}(\hat{\delta}) = \hat{\Delta}_\Upsilon(\hat{\delta}) \star \hat{W}_\Delta$	3×3
$\Upsilon(\upsilon) = \Upsilon_\Upsilon(\upsilon) \star W_\Upsilon$	3×8	$\hat{\Lambda}(\hat{\theta}) = \hat{\Theta}_\Lambda(\hat{\theta}) \star \hat{V}_\Theta$	3×3
$\Lambda(\theta) = \Theta_\Lambda(\theta) \star V_\Theta$	3×8	$\hat{\Upsilon}(\hat{\upsilon}) = \hat{\Upsilon}_\Upsilon(\hat{\upsilon}) \star \hat{W}_\Upsilon$	3×3

Diagonal Blocks	Size	Repetitions r_i
$\Upsilon_\Upsilon(\upsilon)$	18×18	$r^\upsilon = [2\,2\,2\,1\,3\,2\,1\,3\,1\,1]$
$\hat{\Upsilon}_\Upsilon(\hat{\upsilon})$	4×4	$r^{\hat{\upsilon}} = [2\,2\,0\,0\,0\,0\,0\,0\,0\,0]$
$\Delta_\Upsilon(\delta)$	31×31	$r^\delta = [3\,6\,8\,7\,1\,1\,3\,1\,1]$
$\hat{\Delta}_\Upsilon(\hat{\delta})$	15×15	$r^{\hat{\delta}} = [3\,3\,3\,3\,0\,0\,3\,0\,0]$
$\Theta_\Lambda(\theta)$	31×31	$r^\theta = [2\,2\,2\,2\,3\,1\,1\,3\,3\,1\,3\,3\,1\,2\,2]$
$\hat{\Theta}_\Lambda(\hat{\theta})$	4×4	$r^{\hat{\theta}} = [2\,2\,0\,0\,0\,0\,0\,0\,0\,0\,0\,0\,0\,0\,0]$

For assessing implementation complexity, Tab. 4.4 lists the number of arithmetic operations to calculate the parameter vectors or blocks from the measurable signals for each of the models. The numbers of operations is enumerated in an optimized way, i.e., by a hierarchical approach it is generally less costly to first compute, e.g., the parameter vector $\upsilon(\rho)$ and insert it into $\Upsilon(\upsilon) = \Upsilon(\upsilon(\rho))$, instead of evaluating $\Upsilon(\rho)$ directly. However, this does not hold true in the case $a[\Lambda(\rho)]$, where it turns out less costly to use the parameterization in terms of υ. Furthermore, the symbolic expressions are first rewritten in Horner scheme to reduce the amount of necessary coefficients and operations. The number of arithmetic operations associated with the diagonal parameter blocks $\Delta_\bullet(\bullet)$ and $\hat{\Delta}_\bullet(\bullet)$ is identical to the number of operations required to evaluate the respective parameter vector, since diagonal concatenation is assumed to not incur additional complexity.

Table 4.4: Number of arithmetic operations for computing and scalar variables for storing parameter blocks and vectors for the robot model.

Parameter Vectors			
	a[•]/(m[•])		a[•]/(m[•])
$\delta(\rho)$	15/(14)	$\hat{\delta}(\hat{\rho})$	7/(8)
$\upsilon(\rho)$	188/(79)	$\hat{\upsilon}(\hat{\rho})$	56/(30)
$\theta(\rho)$	825/(281)	$\hat{\theta}(\hat{\rho})$	174/(48)
Parameter Blocks			
	a[•]/(m[•])		a[•]/(m[•])
$\Upsilon(\rho)$	245/(120)	$\hat{\Upsilon}(\hat{\rho})$	75/(52)
$\Lambda(\rho)$	886/(306)	$\hat{\Lambda}(\hat{\rho})$	90/(57)

4.7 Example — Compact LFT-LPV Model of a 4-DOF Control Moment Gyroscope

Consider the example of a four-degree of freedom (4-DOF) CMG manufactured by ECP Systems[2]. The CMG exhibits strong inherent nonlinear coupling and is a considerably more challenging plant to control than the 3-DOF robotic manipulator considered in the previous section. LTI control methods have thus far been only capable of stabilizing the plant in a limited angular range [89].

The CMG consists of an actuated flywheel $((\dot{q}_1, q_1))$ located in a gimbal mounting. The second gimbal $((\dot{q}_2, q_2))$ is also actuated, while gimbals three $((\dot{q}_3, q_3))$ and four $((\dot{q}_4, q_4))$ are not. The latter two mark the angular outputs to be controlled. Each of the gimbals is linked to its previous by a rotational joint perpendicular to its axis. Figure 4.11 illustrates the kinematic setup.

Previous attempts at applying LPV control methods to the CMG have been based on a model linearized about a moving operating point in terms of the flywheel's angular velocity $\dot{q}_1$, and the angles of both gimbal two and three, q_2 and q_3, respectively [E1, 1, E94]. Validation results for the linearized model indicated a good fit with respect to the full nonlinear model for typical trajectories and both simulation and experimental results revealed very good control performance. However, the purpose of this section is to discuss the application of the systematic modeling and approximation tools detailed in Sects. 4.3 to 4.5 on the basis of the full nonlinear model of the CMG. It is the purpose to illustrate that these tools are applicable to highly nonlinear plants and can yield exact models and good approximations that render both controller synthesis for high performance and low implementation complexity tractable as well as the design of controllers that provide strict stability and performance guarantees.

Table 4.5: Kinematic limits of the CMG.

Angle	Range [°]	Vel.	Range $[\mathrm{rad\,s^{-1}}]$	Accel.	Range $[\mathrm{rad\,s^{-2}}]$
q_1	$[-180,\dots,180]$	$\dot{q}_1$	$[30,\dots,65]$	$\ddot{q}_1$	$[-10,\dots,10]$
q_2	$[-25,\dots,25]$	$\dot{q}_2$	$[-2,\dots,2]$	$\ddot{q}_2$	$[-10,\dots,10]$
q_3	$[-75,\dots,75]$	$\dot{q}_3$	$[-2,\dots,2]$	$\ddot{q}_3$	$[-7.5,\dots,7.5]$
q_4	$[-180,\dots,180]$	$\dot{q}_4$	$[-2,\dots,2]$	$\ddot{q}_4$	$[-7.5,\dots,7.5]$

(a) Angular limits of the CMG. (b) Limits of the angular velocities and accelerations of the CMG.

---

[2] www.ecpsystems.com

Preliminary results of this section have been previously published in [E49]. The results are extended by considering additional models and a more detailed complexity analysis.
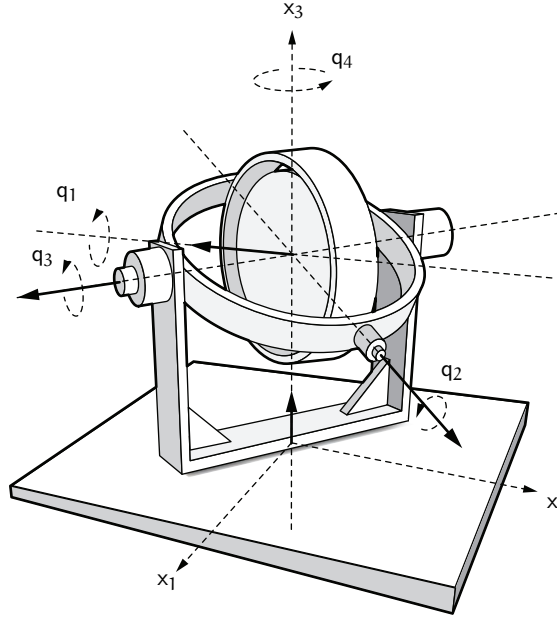
Figure 4.10: Isometric view of the 4-DOF CMG.

4.7.1 *Nonlinear LPV Model*

A set of nonlinear differential equations is obtained via the modeling tool Neweul-M^2 [75] and takes the form of a rigid-body dynamic model of 8th-order with two inputs and two outputs

$$\tilde{J}(\tilde{q})\ddot{\tilde{q}} + \tilde{\bar{k}}(\dot{\tilde{q}}, \tilde{q}) = \tilde{T}(\tilde{q})\tau, \qquad (4.62)$$

where $\tilde{q} \overset{\triangle}{=} \begin{bmatrix} q_1, q_2, q_3, q_4 \end{bmatrix}^\top$. The full model is given in (4.63) below.

Abbreviations:
$s_i \overset{\triangle}{=} \sin(q_i)$
$c_i \overset{\triangle}{=} \cos(q_i)$

$$\begin{bmatrix} b_1 & 0 & b_1 c_2 & b_1 s_2 c_3 \\ 0 & b_3 & 0 & -b_3 s_3 \\ b_1 c_2 & 0 & b_2 s_2^2 + b_4 & -b_2 s_2 c_2 c_3 \\ b_1 s_2 c_3 & -b_3 s_3 & -b_2 s_2 c_2 c_3 & -b_2 s_2^2 c_3^2 + b_5 s_3^2 + b_6 \end{bmatrix} \begin{bmatrix} \ddot{q}_1 \\ \ddot{q}_2 \\ \ddot{q}_3 \\ \ddot{q}_4 \end{bmatrix}$$

$$+ \begin{bmatrix} b_{13}\dot{q}_1 \\ b_{14}\dot{q}_2 \\ b_{15}\dot{q}_3 \\ b_{15}\dot{q}_4 \end{bmatrix} + \begin{bmatrix} \tilde{\bar{k}}_1(\dot{\tilde{q}}, \tilde{q}) \\ \tilde{\bar{k}}_2(\dot{\tilde{q}}, \tilde{q}) \\ \tilde{\bar{k}}_3(\dot{\tilde{q}}, \tilde{q}) \\ \tilde{\bar{k}}_4(\dot{\tilde{q}}, \tilde{q}) \end{bmatrix} = \begin{bmatrix} b_{16} & 0 \\ 0 & b_{17} \\ 0 & 0 \\ 0 & 0 \end{bmatrix} \begin{bmatrix} u_1 \\ u_2 \end{bmatrix}, \qquad (4.63)$$

$$\tilde{\bar{k}}_1(\dot{\tilde{q}}, \tilde{q}) = b_1 \left(c_2 c_3 \dot{q}_2 \dot{q}_4 - s_2 \dot{q}_2 \dot{q}_3 - s_2 s_3 \dot{q}_3 \dot{q}_4 \right),$$

$$\tilde{\bar{k}}_2(\dot{\tilde{q}}, \tilde{q}) = b_1 \left(s_2 \dot{q}_1 \dot{q}_3 - c_2 c_3 \dot{q}_1 \dot{q}_4 \right) + b_2 \left(c_2 c_3^2 s_2 \dot{q}_4^2 - c_2 s_2 \dot{q}_3^2 \right)$$
$$- b_8 c_3 \dot{q}_3 \dot{q}_4 + b_7 (1 - 2s_2^2) c_3 \dot{q}_3 \dot{q}_4 + 2b_9 c_2^2 c_3 \dot{q}_3 \dot{q}_4,$$

$$\tilde{\bar{k}}_3(\dot{\tilde{q}}, \tilde{q}) = b_1 \left(s_2 s_3 \dot{q}_1 \dot{q}_4 - s_2 \dot{q}_1 \dot{q}_2\right) + (b_8 + b_7) c_3 \dot{q}_2 \dot{q}_4 + b_{11} s_3 c_3 \dot{q}_4^2$$
$$+ b_{10} \left(2 c_2^2 c_3 \dot{q}_2 \dot{q}_4 - 2 s_2 c_2 \dot{q}_2 \dot{q}_3 - s_3 c_2^2 c_3 \dot{q}_4^2\right)$$

$$\tilde{\bar{k}}_4(\dot{\tilde{q}}, \tilde{q}) = b_1 \left(c_2 c_3 \dot{q}_1 \dot{q}_2 - s_2 s_3 \dot{q}_1 \dot{q}_3\right) + b_2 s_2 s_3 c_2 \dot{q}_3^2 - 2 b_{11} s_3 c_3 \dot{q}_3 \dot{q}_4$$
$$+ 2 b_{10} \left(c_2^2 c_3 \dot{q}_2 \dot{q}_3 + s_2 c_2 c_3^2 \dot{q}_2 \dot{q}_4 + s_3 c_2^2 c_3 \dot{q}_3 \dot{q}_4\right) + b_{12} c_3 \dot{q}_2 \dot{q}_3,$$
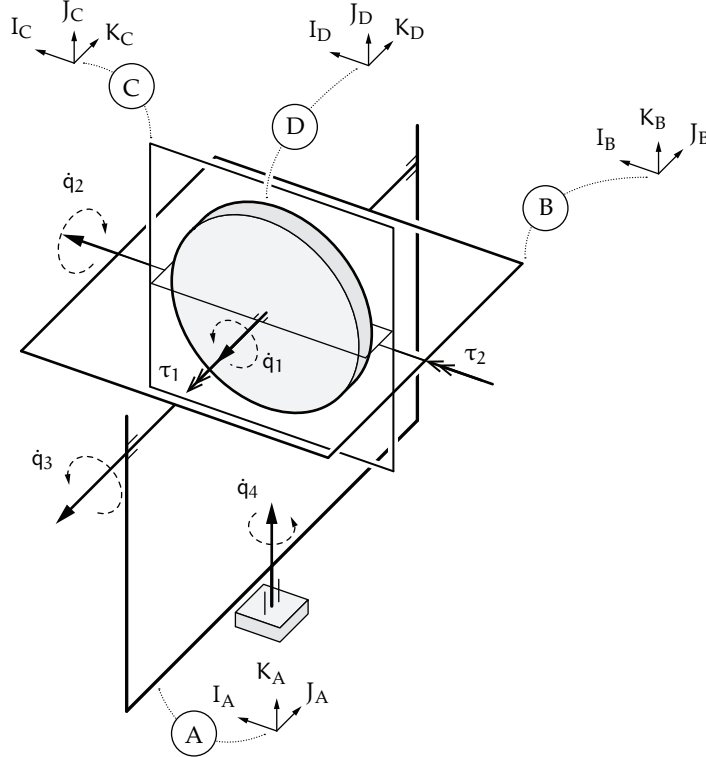
Figure 4.11: Schematic view of the 4-DOF CMG [113].

A schematic overview of the CMG is given in Fig. 4.11. Tab. B.2 in App. B.8 on p. 336 lists the physical and grouped parameters with their respective values. The moments of inertia $I_\bullet$, $J_\bullet$, $K_\bullet$ of bodies A, B, C, D about the directions indicated in Fig. 4.11 have been identified experimentally in [E1].

4.7.1.1 *Full Model Representation*

A gridded analysis of some possible state space representations according to Cor. 4.1 on p. 115 reveals that in certain frozen local joint configurations the system is not locally stabilizable in the sense of Def. 4.1. This forecloses the factorization of the vector of generalized forces $\tilde{\bar{k}}(\dot{\tilde{q}}, \tilde{q})$ into generalized damping and stiffness terms, linear in the states. However, to circumvent the issue of stabilizability, it turns out that eliminating the states connected to the flywheel $(\dot{q}_1, q_1)$, by solving the second differential equation from (4.62) for $\ddot{q}_1$ and substituting into the remaining three, renders the system locally stabilizable. Using the new vector of general-

ized coordinates $q = \begin{bmatrix} q_2, q_3, q_4 \end{bmatrix}^\top$, the resulting nonlinear differential equations are given in (4.64) below.

$$J(q)\ddot{q} + \begin{bmatrix} \tilde{k}_2(\dot{q}, q) \\ \tilde{k}_3(\dot{q}, q) \\ \tilde{k}_4(\dot{q}, q) \end{bmatrix} = T(q)\begin{bmatrix} u_1 \\ u_2 \end{bmatrix} - \begin{bmatrix} 0 \\ b_{13}c_2\dot{q}_1 \\ b_{13}s_2c_3\dot{q}_1 \end{bmatrix}, \tag{4.64}$$

$$\tilde{k}_2(\dot{q}, q) = b_1\,(c_2c_3\dot{q}_1\dot{q}_4 - s_2\dot{q}_1\dot{q}_3) + b_2\left(s_2c_2\dot{q}_3^2 - s_2c_2c_3^2\dot{q}_4^2\right)$$
$$- b_{14}\dot{q}_2 + b_8c_3\dot{q}_3\dot{q}_4 + b_7(2s_2^2 + 1)c_3\dot{q}_3\dot{q}_4 - 2b_9c_2^2c_3\dot{q}_3\dot{q}_4,$$

$$\tilde{k}_3(\dot{q}, q) = b_1\left(s_2\dot{q}_1\dot{q}_2 - s_2c_2\dot{q}_2\dot{q}_3 - s_2s_3\dot{q}_1\dot{q}_4 + c_2^2c_3\dot{q}_2\dot{q}_4 - s_2s_3c_2\dot{q}_3\dot{q}_4\right)$$
$$+ b_{10}\left(s_3c_2^2c_3\dot{q}_4^2 + 2s_2c_2\dot{q}_2\dot{q}_3 - 2c_2^2c_3\dot{q}_2\dot{q}_4\right)$$
$$- b_{15}\dot{q}_3 - b_7c_3\dot{q}_2\dot{q}_4 - b_8c_3\dot{q}_2\dot{q}_4 - b_{11}s_3c_3\dot{q}_4^2,$$

$$\tilde{k}_4(\dot{q}, q) = b_1\left(s_2s_3\dot{q}_1\dot{q}_3 - c_2c_3\dot{q}_1\dot{q}_2 - s_2^2c_3\dot{q}_2\dot{q}_3 + s_2c_2c_3^2\dot{q}_2\dot{q}_4 - s_2^2s_3c_3\dot{q}_3\dot{q}_4\right)$$
$$2b_{10}\left(-c_2^2c_3\dot{q}_2\dot{q}_3 - s_2c_2c_3^2\dot{q}_2\dot{q}_4 - s_3c_2^2c_3\dot{q}_3\dot{q}_4\right)$$
$$- b_{15}\dot{q}_4 - b_{12}c_3\dot{q}_2\dot{q}_3 + 2b_{11}s_3c_3\dot{q}_3\dot{q}_4 - b_2s_2s_3c_2\dot{q}_3^2.$$

The generalized inertia and input matrix are

$$J(q) = \begin{bmatrix} b_3 & 0 & -b_3s_3 \\ 0 & (b_1 + b_2)s_2^2 + b_4 - b_1 & -(b_1 + b_2)s_2c_2c_3 \\ -b_3s_3 & -b_2s_2c_2c_3 & -(b_1 + b_2)(1 - s_3^2)s_2^2 + b_5s_3^2 + b_6 \end{bmatrix},$$

$$T(q) = \begin{bmatrix} 0 & b_{17} \\ -b_{16}c_2 & 0 \\ -b_{16}s_2c_3 & 0 \end{bmatrix}.$$

Terms involving only sine, cosine terms and $\dot{q}_1$ result from the elimination of the flywheel states. These are not factorizable in an LPV sense [146] but lie in the range space of the parameter-dependent input gain matrix, which allows a cancellation by redefinition of the first input as

$$\hat{u}_1 \overset{\triangle}{=} u_1 - \frac{b_{13}}{b_{16}}\dot{q}_1.$$

4.7.1.2 *Partial Feedback Cancellation*

In order to reduce the LFT-LPV model complexity used for synthesis, a partial cancellation of nonlinear terms directly accessible through the control inputs can be performed. For this purpose define

$$u_{1,F} \overset{\triangle}{=} \tilde{k}_1(\dot{q}, \tilde{q}) + u_1,$$
$$u_{2,F} \overset{\triangle}{=} \tilde{k}_2(\dot{q}, \tilde{q}) + u_2. \tag{4.65}$$

Similarly to the full model representation the flywheel states $(\dot{q}_1, q_1)$ are eliminated. The resulting nonlinear differential equations are given in (4.66) below.

$$J(q)\ddot{q} + \begin{bmatrix} 0 \\ \tilde{k}_{3,F}(\dot{q}, q) \\ \tilde{k}_{4,F}(\dot{q}, q) \end{bmatrix} = T(q) \begin{bmatrix} u_{1,F} \\ u_{2,F} \end{bmatrix}, \tag{4.66}$$

$$\tilde{k}_{3,F}(\dot{q}, q) = b_1 \left(s_2 \dot{q}_1 \dot{q}_2 - s_2 s_3 \dot{q}_1 \dot{q}_4 \right) + b_{10} \left(s_3 c_2^2 c_3 \dot{q}_4^2 + 2 s_2 c_2 \dot{q}_2 \dot{q}_3 - 2 c_2^2 c_3 \dot{q}_2 \dot{q}_4 \right)$$
$$- b_{15} \dot{q}_3 - b_7 c_3 \dot{q}_2 \dot{q}_4 - b_8 c_3 \dot{q}_2 \dot{q}_4 - b_{11} s_3 c_3 \dot{q}_4^2,$$

$$\tilde{k}_{4,F}(\dot{q}, q) = b_1 \left(s_2 s_3 \dot{q}_1 \dot{q}_3 - c_2 c_3 \dot{q}_1 \dot{q}_2 \right) + 2 b_{10} \left(-c_2^2 c_3 \dot{q}_2 \dot{q}_3 - s_2 c_2 c_3^2 \dot{q}_2 \dot{q}_4 - s_3 c_2^2 c_3 \dot{q}_3 \dot{q}_4 \right)$$
$$- b_{15} \dot{q}_4 - b_{12} c_3 \dot{q}_2 \dot{q}_3 + 2 b_{11} s_3 c_3 \dot{q}_3 \dot{q}_4 - b_2 s_2 s_3 c_2 \dot{q}_3^2.$$

4.7.1.3 *Linearization About Moving Operating Point*

An approach to simplify the nonlinear differential equations even further is pursued in [E1, 1, E94] by linearizing Eq. (4.62) about a moving operating point given by

$$\bar{q} \triangleq \begin{bmatrix} \bar{q}_1 \\ \bar{q}_2 \\ \bar{q}_3 \\ \bar{q}_4 \end{bmatrix}, \quad \dot{\bar{q}} \triangleq \begin{bmatrix} \dot{\bar{q}}_1 \\ \dot{\bar{q}}_2 \\ \dot{\bar{q}}_3 \\ \dot{\bar{q}}_4 \end{bmatrix} = \begin{bmatrix} \dot{\bar{q}}_1 \\ 0 \\ 0 \\ 0 \end{bmatrix}, \quad \ddot{\bar{q}} \triangleq \begin{bmatrix} \ddot{\bar{q}}_1 \\ \ddot{\bar{q}}_2 \\ \ddot{\bar{q}}_3 \\ \ddot{\bar{q}}_4 \end{bmatrix} = \begin{bmatrix} 0 \\ 0 \\ 0 \\ 0 \end{bmatrix}. \tag{4.67}$$

Denote this operating point $\bar{\zeta} \triangleq \begin{bmatrix} \bar{q}^\top, & \dot{\bar{q}}^\top, & \ddot{\bar{q}}, & \bar{u} \end{bmatrix}$, whereas $\tilde{\zeta} \triangleq \begin{bmatrix} \tilde{q}^\top, & \dot{\tilde{q}}^\top, & \ddot{\tilde{q}}, & u \end{bmatrix}$ collects the state variables and derivatives as well as the inputs. The Jacobian linearization is then derived by

$$\left. \frac{\partial \tilde{J}(\tilde{q})\ddot{\tilde{q}}}{\partial \tilde{\zeta}} \right|_{\bar{\zeta}} \partial\tilde{\zeta} + \left. \frac{\partial \tilde{\tilde{k}}(\dot{\tilde{q}}, \tilde{q})}{\partial \tilde{\zeta}} \right|_{\bar{\zeta}} \partial\tilde{\zeta} = \left. \frac{\partial \tilde{T}(\tilde{q})\tau}{\partial \tilde{\zeta}} \right|_{\bar{\zeta}} \partial\tilde{\zeta}, \tag{4.68}$$

where $\partial\tilde{\zeta} \triangleq \tilde{\zeta} - \bar{\zeta}$. After subsequent elimination of the state deviations with respect to the flywheel $(\partial\dot{q}_1, \partial q_1)$ the differential equations take the form given in (4.69) below.

$$J(\bar{q})\partial\ddot{q} + \left(\begin{bmatrix} b_{14} & 0 & 0 \\ 0 & b_{15} & 0 \\ 0 & 0 & b_{15} \end{bmatrix} + \dot{\bar{q}}_1 b_1 \begin{bmatrix} 0 & s_2 & -c_2 c_3 \\ -s_2 & 0 & s_2 s_3 \\ c_2 c_3 & -s_2 s_3 & 0 \end{bmatrix} \right) \partial\dot{q} = T(\bar{q}) \begin{bmatrix} \partial u_1 \\ \partial u_2 \end{bmatrix}, \quad (4.69)$$

4.7.1.4 *Factorization of the Vector of Generalized Forces*

Each of the parameter dependent terms in the vector of generalized forces has at least a single angular velocity that can be pulled out as a state variable. Consequently, the heuristic approach of preferring generalized velocity variables as a

state is pursued, whereas the remainder of each term is considered an LPV parameter. This reduces the size of the full-block parameter matrix, since only the generalized damping matrix will be populated. Consequently, the resulting descriptor LPV models will take the form

$$
\mathcal{G}_\rho^\sigma : \begin{cases} \begin{bmatrix} I_2 & & \\ & J(\rho) & \\ & & I_2 \end{bmatrix} \begin{bmatrix} \dot{q}_3 \\ \dot{q}_4 \\ \ddot{q}_2 \\ \ddot{q}_3 \\ \ddot{q}_4 \\ y \end{bmatrix} = \begin{bmatrix} 0_{2\times 2} & \begin{bmatrix} 0_{2\times 1} & I_2 \end{bmatrix} & 0 \\ 0_{2\times 2} & -D(\rho) & T(\rho) \\ I_2 & 0 & 0 \end{bmatrix} \begin{bmatrix} q_3 \\ q_4 \\ \dot{q}_2 \\ \dot{q}_3 \\ \ddot{q}_4 \\ u \end{bmatrix} \\ \rho(t) \in \mathcal{F}_\rho^\sigma. \end{cases} \tag{4.70}
$$

For the subsequent factorization, two approaches are chosen from the ones considered in Sect. 4.3.2:

  (i) Penalize sparsity, finite decisions, cf. (4.16) on p. 112,

  (ii) Promote sparsity, finite decisions, cf. (4.18) on p. 113.

More specifically, the selector vector entries $c_{ijk}^{(l)}$ are limited to $\{1, 0\}$ and the objective measure is either (i) minimized or (ii) maximized, according to (4.16) and (4.18), respectively.

Despite the highly nonlinear nature of the plant, approach (ii) is expected to yield adequate results, since in the gridding-based gain-scheduling approach presented in [E94], the synthesis is performed on the strongly simplified plant formulation (4.69) with good control performance. On closer inspection, the model based on a linearization about a moving operating point simply lacks some of the nonlinear terms of the full model representation. Promoting sparsity in the generalized damping matrix will therefore possibly retain the relevant nonlinear coupling terms, while adding the full model description in a way that preserves guarantees as well as induces a significantly lower complexity during synthesis.

On a related note, the application of Lma. 4.2 on p. 126 as introduced in Sect. 4.5 is expected to yield fewer affine parameters derived from the polynomial terms, if sparsity during factorization is promoted.

As a consequence, five model representations are derived:

  1. full model, penalized sparsity (FMax)

  2. full model, promoted sparsity (FMin)

  3. PFC model, penalized sparsity (PFCMax)

  4. PFC model, promoted sparsity (PFCMin)

  5. moving operating point (MOP)

The model matrices are explicitly stated in the Eqs. (4.72) (FMax/FMin), (4.71) (PFCMax/PFCMin) and (4.69) (MOP).

For simplicity, all trigonometric terms are preserved and only after the factorization, they are substituted by polynomial expansions to reduce conservatism, as detailed next.

$$J(q)\ddot{q} + \left(\tilde{D}_{\text{MOP}}(\dot{q}, q) + D_{\text{PFCMax/PFCMin}}(\dot{q}, q)\right)\dot{q} = T(q)\begin{bmatrix} u_{1,F} \\ u_{2,F} \end{bmatrix}, \qquad (4.71)$$

$$\tilde{D}_{\text{MOP}}(\dot{q}, q) = \begin{bmatrix} 0 & 0 & 0 \\ 0 & b_{15} & 0 \\ 0 & 0 & b_{15} \end{bmatrix} + \dot{q}_1 b_1 \begin{bmatrix} 0 & 0 & 0 \\ -s_2 & 0 & s_2 s_3 \\ c_2 c_3 & -s_2 s_3 & 0 \end{bmatrix},$$

$$D_{\text{PFCMin}}(\dot{q}, q) = \begin{bmatrix} 0 & 0 & 0 \\ \dot{q}_4(2b_{10}+b_7+b_8-2b_{10}s_2^2)c_3 \\ -2\dot{q}_3 b_{10}s_2 c_2 & 0 & \dot{q}_4\left(b_{11}-b_{10}(1-s_2^2)\right)s_3 c_3 \\ 2\dot{q}_4 b_{10}s_2 c_2(1-s_3^2) & \begin{matrix}\dot{q}_3 b_2 s_2 s_3 c_2 \\ +2\dot{q}_4\left(b_{10}(1-s_2^2)-b_{11}\right)s_3 c_3 \\ +\dot{q}_2(2b_{10}+b_{12}-2b_{10}s_2^2)c_3\end{matrix} & 0 \end{bmatrix},$$

$$D_{\text{PFCMax}}(\dot{q}, q) = \begin{bmatrix} 0 & 0 & 0 \\ \dot{q}_4(2b_{10}+b_7+b_8-2b_{10}s_2^2)c_3 & -2\dot{q}_2 b_{10}s_2 c_2 & \dot{q}_4\left(b_{11}-b_{10}(1-s_2^2)\right)s_3 c_3 \\ \dot{q}_3(2b_{10}+b_{12}-2b_{10}s_2^2)c_3 & \begin{matrix}\dot{q}_3 b_2 s_2 s_3 c_2 \\ +2\dot{q}_4\left(b_{10}(1-s_2^2)-b_{11}\right)s_3 c_3\end{matrix} & 2\dot{q}_2 b_{10}s_2 c_2(1-s_3^2) \end{bmatrix}.$$

$$J(q)\ddot{q} + \left(D_{\text{MOP}}(\dot{q}, q) + D_{\text{FMax/FMin}}(\dot{q}, q)\right)\dot{q} = T(q)\begin{bmatrix} \hat{u}_1 \\ u_2 \end{bmatrix}, \qquad (4.72)$$

$$D_{\text{MOP}}(\dot{q}, q) = \begin{bmatrix} b_{14} & 0 & 0 \\ 0 & b_{15} & 0 \\ 0 & 0 & b_{15} \end{bmatrix} + \dot{q}_1 b_1 \begin{bmatrix} 0 & s_2 & -c_2 c_3 \\ -s_2 & 0 & s_2 s_3 \\ c_2 c_3 & -s_2 s_3 & 0 \end{bmatrix},$$

$$D_{\text{FMin}}(\dot{q}, q) = \begin{bmatrix} 0 & \begin{matrix}\dot{q}_4\left(2b_9-2(b_7+b_9)s_2^2+b_7-b_8\right)c_3 \\ -\dot{q}_3 b_2 s_2 c_2\end{matrix} & \dot{q}_4 b_2 s_2 c_2(1-s_3^2) \\ \dot{q}_3(b_1-2b_{10})s_2 c_2 & 0 & \begin{matrix}\dot{q}_4\left(b_{11}-b_{10}(1-s_2^2)\right)s_3 c_3 \\ +\dot{q}_3 b_1 s_2 s_3 c_2 \\ +\dot{q}_2\left((2b_{10}-b_1)(1-s_2^2) \\ +b_7+b_8\right)c_3\end{matrix} \\ \dot{q}_4(2b_{10}-b_1)s_2 c_2(1-s_3^2) & \begin{matrix}\dot{q}_4\left(2b_{10}-2b_{11}+(b_1-2b_{10})s_2^2\right)s_3 c_3 \\ +\dot{q}_2\left(2b_{10}+b_{12}+(b_1-2b_{10})s_2^2\right)c_3 \\ +\dot{q}_3 b_2 s_2 s_3 c_2\end{matrix} & 0 \end{bmatrix},$$

$$D_{\text{FMax}}(\dot{q}, q) = \begin{bmatrix} 0 & \begin{matrix}\dot{q}_4\left(2b_9-2(b_7+b_9)s_2^2 \\ +b_7-b_8\right)c_3 \\ -\dot{q}_3 b_2 s_2 c_2\end{matrix} & \dot{q}_4 b_2 s_2 c_2(1-s_3^2) \\ \begin{matrix}\dot{q}_4\left(b_7+b_8+(2b_{10}-b_1)(1-s_2^2)\right)c_3 \\ +\dot{q}_3(b_1-2b_{10})s_2 c_2\end{matrix} & \dot{q}_4 b_1 s_2 s_3 c_2 & \dot{q}_4\left(b_{11}-b_{10}(1-s_2^2)\right)s_3 c_3 \\ \dot{q}_3\left((2b_{10}+b_1)s_2^2+b_{12}\right)c_3 & \begin{matrix}\dot{q}_4\left(2b_{10}-2b_{11} \\ +(b_1-2b_{10})s_2^2\right)s_3 c_3 \\ +\dot{q}_3 b_2 s_2 s_3 c_2\end{matrix} & -\dot{q}_2(b_1-2b_{10})s_2 c_2(1-s_3^2) \end{bmatrix}.$$

4.7.1.5 *Polynomial Expansion of Trigonometric Terms*

Due to the limited angular range, trigonometric terms are considered to be exactly represented in terms of polynomials. For this purpose, sine and cosine functions are developed by polynomials with appropriate degrees and monomials that match a Taylor series expansion. Consequently, the best fit is obtained by the polynomial approximations

$$\sin(q_2) \approx \ \ 0.99078 \, q_2,$$
$$\sin(q_3) \approx -0.15138 \, q_3^3 + 0.99445 \, q_3,$$
$$\cos(q_2) \approx -0.49313 \, q_2^2 + 0.99987 \, q_2,$$
$$\cos(q_3) \approx \ \ 0.03852 \, q_3^4 - 0.49822 \, q_3^2 + 0.99986.$$

Over the considered angular range given in Tab. 4.6a, the average accuracy increases by about a factor of two as indicated in Tab. 4.6 and visualized in Fig. 4.12. In light of the above expansions, squared cosine terms are substituted by their respective squared sine terms, i. e., $\cos^2(\bullet) = 1 - \sin^2(\bullet)$, to allow for fewer repetitions in an LFR.

Table 4.6: Comparison of polynomial expansions of trigonometric terms for the CMG.

Sine/Cosine Term	Avg. Expansion Error	
	Taylor Expansion	Polynomial Fit
$\sin(q_2)$	1.09 %	0.81 %
$\sin(q_3)$	0.60 %	0.25 %
$\cos(q_2)$	0.03 %	0.01 %
$\cos(q_3)$	0.26 %	0.01 %

4.7.2 *Parameterization*

With the parameters $\tilde{\delta}$ from Tab. 4.8a and the polynomial expansion of the trigonometric terms, the matrices are naturally rendered polynomial in the parameters $\tilde{\delta}$, which are identical to the measurable LPV signals ρ. The model (MOP) based on a linearization about a moving operating point is considered to be scheduled by the real-time signals, of which only ρ_1, ρ_2 and ρ_3 remain due to the approximation.

The generalized inertia, stiffness and damping matrices are decomposed into parameter-dependent and nominal parts after performing a shift about the nominal operating point $\rho_0 = \begin{bmatrix} 0, 0, 45, 0, 0, 0 \end{bmatrix}^\top$, about which the parameters are shifted to include zero. The constant nominal matrices $\bar{E}$ and $\bar{F}$ are thus defined in accordance
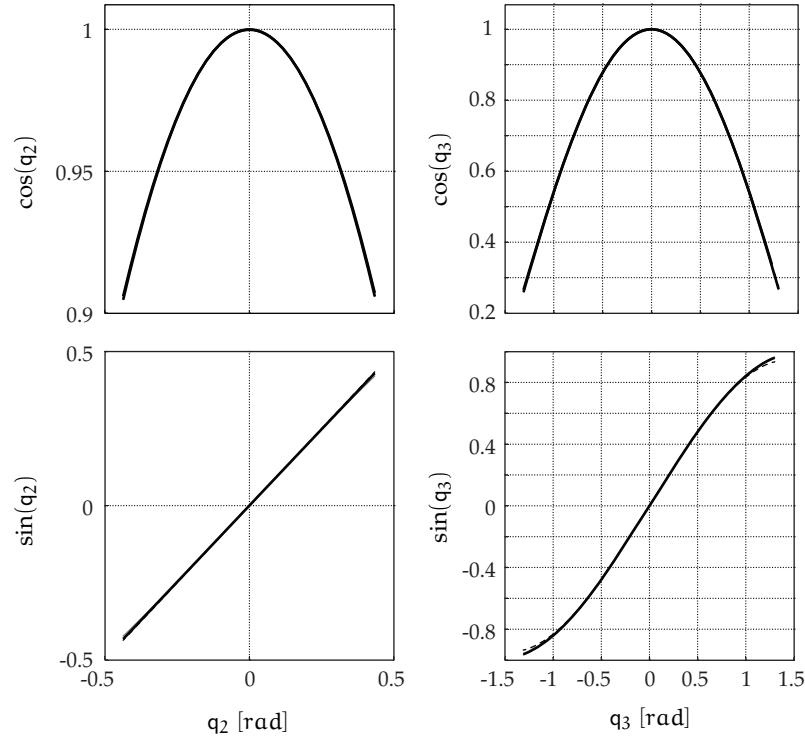
Figure 4.12: Polynomial approximations of cosine and sine terms.
    (——) Polynomial approximation;
    (- - - -) exact trigonometric function.

with Ex. 4.5. Similarly, masking matrices are defined to form W_E, W_F and V.

Subsequently, a normalization is applied, s.t., $|\delta_i| \leqslant 1$, $i = 1, 2, \ldots, 6$. The resulting constant terms that appear due to the offsets associated with the normalization are chosen to remain in the parameter block $\Upsilon(\delta)$ in accordance with Alg. 4.1 on p. 137. The resulting set of parameters is defined in Tab. 4.8b.

The parameter block $\Upsilon(\delta)$ is then decomposed into a linear combination of monomials in δ for each of the modeling options. Lemma 4.2 and further normalization according to Prop. 4.1 are then applied to obtain affine dependence of $\Upsilon(\upsilon)$ in the new parameters υ. The normalized singular values of the vectorized monomial decompositions of each modeling option are given in Fig. 4.13. Cor. 4.3 is applied to weight the columns with the expected maximum magnitude of the respective states. For comparison, the unweighted normalized singular values are also shown.

As evident from Fig. 4.13, the differences resulting from promoting or penalizing sparsity in the generalized damping matrix mostly reside in the maximum number of affine parameters. Furthermore, the set of singular values resulting from model (MOP) closely resembles the ones of the models (PFCMax) and (PFCMin). The latter three models appear to be already quite accurately modeled by only a single parameter υ if a weighted singular value decomposition according to Cor. 4.3 is used.

Table 4.7: Measurable signals and LPV parameters for the CMG.

$$\rho_1 = \tilde{\delta}_1 \overset{\triangle}{=} q_2 \qquad\qquad \delta_1 \overset{\triangle}{=} 2.29\,\tilde{\delta}_1$$

$$\rho_2 = \tilde{\delta}_2 \overset{\triangle}{=} q_3 \qquad\qquad \delta_2 \overset{\triangle}{=} 0.76\,\tilde{\delta}_2$$

$$\rho_3 = \tilde{\delta}_3 \overset{\triangle}{=} \dot{q}_1 \qquad\qquad \delta_3 \overset{\triangle}{=} 0.07\,\tilde{\delta}_3 - 3.0$$

$$\rho_4 = \tilde{\delta}_4 \overset{\triangle}{=} \dot{q}_2 \qquad\qquad \delta_4 \overset{\triangle}{=} 1.00\,\tilde{\delta}_4$$

$$\rho_5 = \tilde{\delta}_5 \overset{\triangle}{=} \dot{q}_3 \qquad\qquad \delta_5 \overset{\triangle}{=} 0.50\,\tilde{\delta}_5$$

$$\rho_6 = \tilde{\delta}_6 \overset{\triangle}{=} \dot{q}_4 \qquad\qquad \delta_6 \overset{\triangle}{=} 0.50\,\tilde{\delta}_6$$

(a) Measurable signals.   (b) Parameters δ.

4.7.3 *Approximation and Summary*

An approximation is chosen by selecting the two largest normalized singular values each, since a significant drop in magnitude is observed below. The maximum absolute entry-wise errors range between 1.851×10^{-1} and 2.15×10^{-1} in the coefficient matrices of the respective models. In contrast to the approximation resulting from truncating polynomials in case of the 3-DOF robot detailed in Sect. 4.6, the remaining two parameters contribute to generalized inertia, damping and input gain matrices, s. t., the resulting parameter blocks are reduced in size, but the overall plant parameterization remains rational.

Table 4.8: Parameter block sizes for the CMG model.

Full Sched. Order	Size	Red. Sched. Order	Size	
			F/MOP	PFC
$\Upsilon(\delta) = \Delta_\Upsilon(\delta) \star W_\Delta$	3×7	$\hat{\Upsilon}(\hat{\delta}) = \hat{\Delta}_\Upsilon(\hat{\delta}) \star \hat{W}_\Delta$	3×6	2×6
$\Upsilon(\upsilon) = \Upsilon_\Upsilon(\upsilon) \star W_\Upsilon$	3×7	$\hat{\Lambda}(\hat{\upsilon}) = \hat{\Upsilon}_\Upsilon(\hat{\upsilon}) \star \hat{W}_\Lambda$	3×4	2×4
$\Lambda(\upsilon) = \Upsilon_\Upsilon(\upsilon) \star W_\Lambda$	3×5	$\hat{\Upsilon}(\hat{\upsilon}) = \hat{\Upsilon}_\Upsilon(\hat{\upsilon}) \star \hat{W}_\Upsilon$	3×6	2×6

From the approximations, the approximate parameter vector $\hat{\delta}$ is inferred by resubstituting the function $\hat{\upsilon}(\delta)$. It is observed that in both of the cases where sparsity is penalized (FMAX, PFCMAX), the plant matrices become independent of $\dot{q}_2$.

Tab. 4.8 and Tab. 4.9 summarize the resulting parameter block properties in terms of size and repetitions given as vectors $r^\bullet$. Again, for the repetitions resulting from approximations the vectors $r^{\hat{\bullet}}$ indicate omissions by zero repetitions. As evident from the tables, the numbers of repetitions for the approximate parameter blocks represented in terms of the parameters δ increase. Note that the commonly available tools for the exact reduction of LFRs of Matlab [149] as well as the n-D (Kalman

Table 4.9: Parameter block information for the CMG models.

Model	Block	Size	Par. No.	Repetitions r_i
FMAX	$\Upsilon_\gamma(\upsilon)$	31×31	$n_\upsilon = 13$	$r^\upsilon = [3,\ \ 2, 3, 2, 3, 3, 2, 3, 3, 1, 3, 2, 1]$
	$\hat{\Upsilon}_\gamma(\hat{\upsilon})$	5×5	$n_{\hat{\upsilon}} = 2$	$r^{\hat{\upsilon}} = [3,\ \ 2, 0, 0, 0, 0, 0, 0, 0, 0, 0, 0, 0]$
	$\Delta_\gamma(\delta)$	59×59	$n_\delta = 6$	$r^\delta = [9, 41, 3, 1, 2, 3]$
	$\hat{\Delta}_\gamma(\hat{\delta})$	80×80	$n_{\hat{\delta}} = 5$	$r^{\hat{\delta}} = [9, 57, 5, 0, 4, 5]$
FMIN	$\Upsilon_\gamma(\upsilon)$	29×29	$n_\upsilon = 11$	$r^\upsilon = [3,\ \ 2, 3, 2, 3, 3, 2, 3, 3, 3, 2]$
	$\hat{\Upsilon}_\gamma(\hat{\upsilon})$	5×5	$n_{\hat{\upsilon}} = 2$	$r^{\hat{\upsilon}} = [3,\ \ 2, 0, 0, 0, 0, 0, 0, 0, 0, 0]$
	$\Delta_\gamma(\delta)$	62×62	$n_\delta = 6$	$r^\delta = [9, 42, 3, 2, 3, 3]$
	$\hat{\Delta}_\gamma(\hat{\delta})$	80×80	$n_{\hat{\delta}} = 6$	$r^{\hat{\delta}} = [9, 57, 5, 2, 2, 5]$
PFCMAX	$\Upsilon_\gamma(\upsilon)$	24×24	$n_\upsilon = 11$	$r^\upsilon = [2,\ \ 2, 2, 2, 2, 2, 2, 2, 2, 2, 2]$
	$\hat{\Upsilon}_\gamma(\hat{\upsilon})$	4×4	$n_{\hat{\upsilon}} = 2$	$r^{\hat{\upsilon}} = [2,\ \ 2, 0, 0, 0, 0, 0, 0, 0, 0, 0]$
	$\Delta_\gamma(\delta)$	55×55	$n_\delta = 6$	$r^\delta = [6, 39, 3, 2, 2, 3]$
	$\hat{\Delta}_\gamma(\hat{\delta})$	56×56	$n_{\hat{\delta}} = 5$	$r^{\hat{\delta}} = [6, 38, 5, 0, 5, 2]$
PFCMIN	$\Upsilon_\gamma(\upsilon)$	18×18	$n_\upsilon = 9$	$r^\upsilon = [2,\ \ 2, 2, 2, 2, 2, 2, 2, 2]$
	$\hat{\Upsilon}_\gamma(\hat{\upsilon})$	4×4	$n_{\hat{\upsilon}} = 2$	$r^{\hat{\upsilon}} = [2,\ \ 2, 0, 0, 0, 0, 0, 0, 0]$
	$\Delta_\gamma(\delta)$	52×52	$n_\delta = 6$	$r^\delta = [6, 37, 3, 1, 2, 3]$
	$\hat{\Delta}_\gamma(\hat{\delta})$	65×65	$n_{\hat{\delta}} = 6$	$r^{\hat{\delta}} = [6, 45, 5, 2, 2, 5]$
MOP	$\Upsilon_\gamma(\upsilon)$	22×22	$n_\upsilon = 8$	$r^\upsilon = [3,\ \ 2, 3, 2, 3, 3, 3, 2]$
	$\hat{\Upsilon}_\gamma(\hat{\upsilon})$	5×5	$n_{\hat{\upsilon}} = 2$	$r^{\hat{\upsilon}} = [3,\ \ 2, 0, 0, 0, 0, 0, 0]$
	$\Delta_\gamma(\delta)$	34×34	$n_\delta = 3$	$r^\delta = [8, 23, 3]$
	$\hat{\Delta}_\gamma(\hat{\delta})$	44×44	$n_{\hat{\delta}} = 3$	$r^{\hat{\delta}} = [6, 33, 5]$

(a) FMAX.

(b) FMIN.

(c) PFCMAX.

(d) PFCMIN.

(e) PFCMAX.
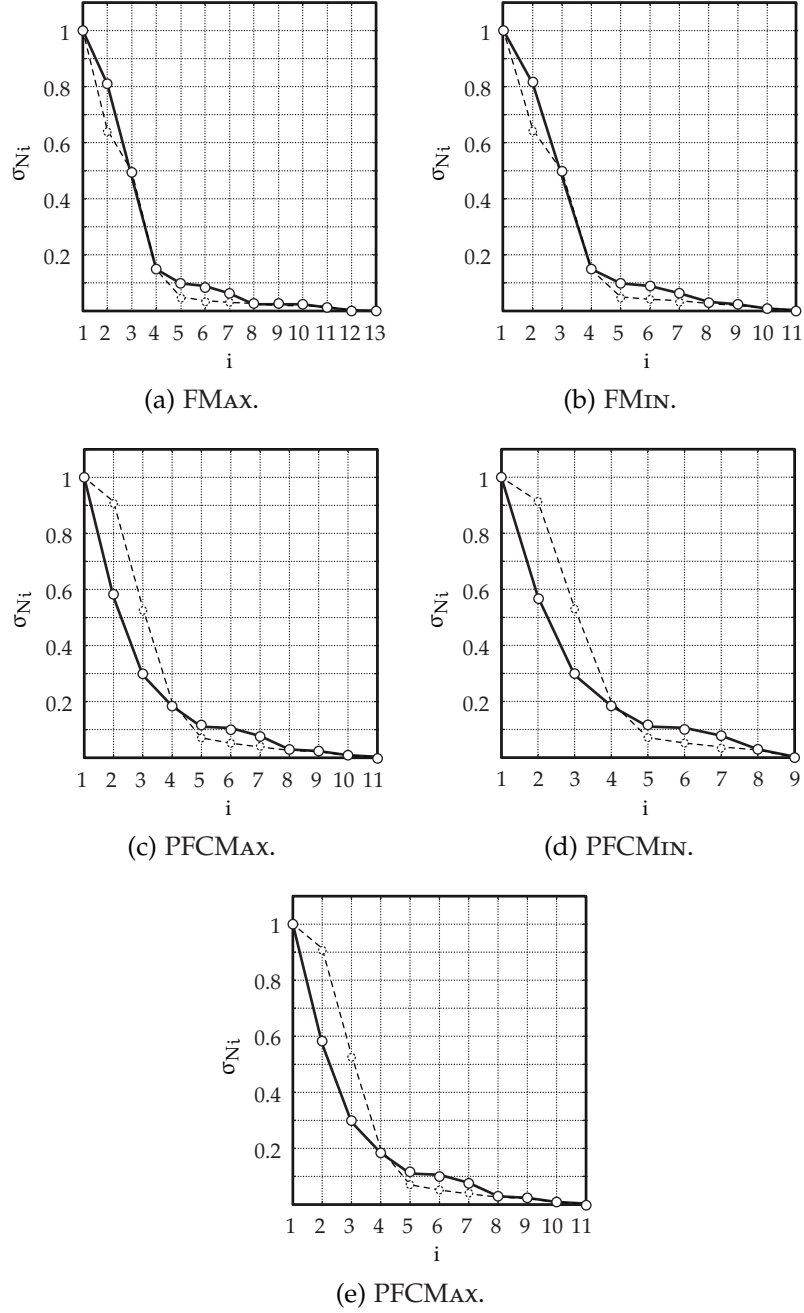
Figure 4.13: Singular values of the monomial decomposition of $\Upsilon(\delta)$ for the respective CMG models.
(——) Weighted normalized singular values (Cor. 4.3);
(-----) Unweighted normalized singular values.

like) decomposition or the generalized Gramian approach [13, 14, 25, 93] available through the ONERA LFR Toolbox, do not yield any further reduction in repetitions than the ones reported in Tab. 4.9.

For assessing implementation complexity, Tab. 4.10 lists the number of arithmetic operations to calculate the parameter vectors or blocks from the measurable signals

for each of the models. The numbers of operations is enumerated in an optimized way, i. e., by a hierarchical approach it is generally less costly to first compute, e. g., the parameter vector $\upsilon(\rho)$ and insert it into $\Upsilon(\upsilon) = \Upsilon(\upsilon(\rho))$, instead of evaluating $\Upsilon(\rho)$ directly. The number of arithmetic operations associated with the diagonal parameter blocks $\Delta_\bullet(\bullet)$ and $\hat{\Delta}_\bullet(\bullet)$ is identical to the number of operations required to evaluate the respective parameter vector, since diagonal concatenation is assumed to not incur additional complexity.

Table 4.10: Number of arithmetic operations for computing and scalar variables for storing parameter blocks and vectors for the CMG model.

Parameter Vectors					
	a[•]/(m[•]) by Model				
	PFC		F		MOP
	Min	Max	Min	Max	
$\delta(\rho)$	6/(7)	6/(7)	6/(7)	6/(7)	4/(4)
$\hat{\delta}(\hat{\rho})$	6/(7)	6/(7)	6/(7)	6/(7)	4/(4)
$\upsilon(\rho)$	477/(160)	477/(153)	572/(186)	637/(204)	197/(73)
$\hat{\upsilon}(\hat{\rho})$	126/(51)	126/(43)	141/(47)	143/(47)	60/(22)
Parameter Blocks					
$\Upsilon(\rho)$	537/(196)	537/(193)	652/(237)	718/(256)	254/(112)
$\hat{\Upsilon}(\hat{\rho})$	138/(62)	138/(55)	156/(62)	156/(60)	75/(37)

5

SYNTHESIS OF LINEAR PARAMETER-VARYING CONTROLLERS FOR COMPLEX SYSTEMS USING MULTIPLIER-BASED SYNTHESIS

≪Any product of the mind is a reaction of the past, a synthesis of what is old.≫

Barry Long

I N the previous chapter the derivation of descriptor LPV plant representations with small-in-size LFT parameter blocks and automated parameterization was investigated. The purpose of this chapter is to exploit this modeling framework, in order to reduce both synthesis and implementation complexity of LPV controllers.

In light of this, a two-stage multiplier approach to LFT-LPV synthesis is introduced in Sect. 5.1 as an effective method to evaluate multiplier conditions associated with the small-in-size LFT parameter blocks by finitely many LMIs irrespective of the underlying type of parameterization. Using this approach, implementation complexity remains constant and it is discussed in which cases it is lower than the one incurred by standard approaches.

Furthermore, improved LFT-LPV state-feedback controller synthesis conditions are derived in Sect. 5.2 that make use of the descriptor framework. As a consequence, decision variables are reduced and the evaluation of FBM-based conditions is simplified.

5.1 A Multi-Stage Multiplier Approach to LFT-LPV Synthesis

AFTER the proposition of parameterizations for an LPV plant in Sect. 4.5, the following result is introduced to facilitate the discussion on their efficient use in synthesis. For this purpose, the application of Lma. 2.1 on primal and dual multiplier conditions occurring in the context of LFT-LPV synthesis is made explicit.

Corollary 5.1 (Two-Stage FBSP)
Consider a matrix-valued function $\Delta(\rho, \delta)$ represented via the LFR

$$\Delta(\rho, \delta) = \Delta_\Delta(\delta) \star \begin{bmatrix} W_{11}(\rho) & W_{12}(\rho) \\ \hline W_{21}(\rho) & W_{22}(\rho) \end{bmatrix} \in \mathcal{C}^0(\boldsymbol{\rho} \times \boldsymbol{\delta}, \, \mathbb{R}^{(n_{q_\Delta} \times n_{p_\Delta})}),$$

where the parameter vectors ρ and δ are confined to compact sets, s. t. $\rho \in \boldsymbol{\rho} \subset \mathbb{R}^{n_\rho}$ and $\delta \in \boldsymbol{\delta} \subset \mathbb{R}^{n_\delta}$, and where $\Delta_\Delta(\delta) \in \mathcal{C}^0(\boldsymbol{\delta}, \, \mathbb{R}^{(n_{q_{\Delta\Delta}} \times n_{p_{\Delta\Delta}})})$. Further, let $M \in \mathbb{S}^{(n_{q_\Delta} + n_{p_\Delta})}$, $N \in \mathbb{S}^{(n_{q_\Delta} + n_{p_\Delta})}$. The quadratic matrix inequalities

$$\begin{bmatrix} \bullet \\ \bullet \end{bmatrix}^\top M \begin{bmatrix} I \\ \hline \Delta(\rho, \delta) \end{bmatrix} \succ 0, \quad \forall (\rho, \delta) \in \boldsymbol{\rho} \times \boldsymbol{\delta} \tag{5.1}$$

$$\begin{bmatrix} \bullet \\ \bullet \end{bmatrix}^\top N \begin{bmatrix} -\Delta^\top(\rho, \delta) \\ \hline I \end{bmatrix} \prec 0, \quad \forall (\rho, \delta) \in \boldsymbol{\rho} \times \boldsymbol{\delta} \tag{5.2}$$

hold iff there exist $\check{M} \in \mathbb{S}^{(n_{q_{\Delta\Delta}} + n_{p_{\Delta\Delta}})}$, $\check{N} \in \mathbb{S}^{(n_{q_{\Delta\Delta}} + n_{p_{\Delta\Delta}})}$ that satisfy

$$\begin{bmatrix} \bullet \\ \bullet \end{bmatrix}^\top \begin{bmatrix} \check{M} & \\ & M \end{bmatrix} \begin{bmatrix} W_{11}(\rho) & W_{12}(\rho) \\ I & 0 \\ \hline 0 & I \\ W_{21}(\rho) & W_{22}(\rho) \end{bmatrix} \succ 0, \, \forall \rho \in \boldsymbol{\rho} \tag{5.3}$$

$$\begin{bmatrix} \bullet \\ \bullet \end{bmatrix}^\top \check{M} \begin{bmatrix} I \\ \hline \Delta_\Delta(\delta) \end{bmatrix} \prec 0, \, \forall \delta \in \boldsymbol{\delta} \tag{5.4}$$

$$\begin{bmatrix} \bullet \\ \bullet \end{bmatrix}^\top \begin{bmatrix} \check{N} & \\ & N \end{bmatrix} \begin{bmatrix} W_{11}^\top(\rho) & W_{21}^\top(\rho) \\ I & 0 \\ \hline -W_{12}^\top(\rho) & -W_{22}^\top(\rho) \\ 0 & I \end{bmatrix} \succ 0, \, \forall \rho \in \boldsymbol{\rho} \tag{5.5}$$

$$\begin{bmatrix} \bullet \\ \bullet \end{bmatrix}^\top \check{N} \begin{bmatrix} I \\ \hline \Delta_\Delta^\top(\delta) \end{bmatrix} \succ 0, \, \forall \delta \in \boldsymbol{\delta}. \tag{5.6}$$

Preliminary results of this section have been previously published in [57, E46, E48, 60]. The results are extended by a more comprehensive treatment of the complexity reduction achieved.

□

Proof: Observe that

$$
\begin{bmatrix} I \\ \Delta(\rho,\delta) \end{bmatrix} = \Delta_\Delta(\delta) \star \begin{bmatrix} W_{11}(\rho) & W_{12}(\rho) \\ 0 & I \\ W_{21}(\rho) & W_{22}(\rho) \end{bmatrix},
$$

$$
\begin{bmatrix} -\Delta^\top(\rho,\delta) \\ I \end{bmatrix} = \Delta_\Delta^\top(\delta) \star \begin{bmatrix} W_{11}^\top(\rho) & W_{21}^\top(\rho) \\ -W_{12}^\top(\rho) & -W_{22}^\top(\rho) \\ 0 & I \end{bmatrix}.
$$

The equivalence follows from Lma. 2.1 applied to Conds. (5.1) and (5.2). ■

Here, the application of Cor. 5.1 is proposed in conjunction with LFT-LPV-based controller synthesis using PIDLFs and an LMI-based construction of controller variables. Reconsider the comparison of D/G-S- and FBM-based synthesis in Tab. 2.1 on p. 72 and recall that in this framework, the scheduling policy of the controller is essentially determined by the type of multiplier constraints that are used:

- D/G-scalings allow to choose the controller's parameter block as a copy of the plant's parameter block as per Lma. 2.6 on page 70.

- FBMs require the online computation of the controller's parameter block as per Lma. 2.5 on page 69.

Essentially, Cor. 5.1 can be applied for two distinct reasons that may also be exploited in combination:

1. REDUCTION OF SYNTHESIS AND IMPLEMENTATION COMPLEXITY
   Despite the more elaborate computation of the controller's parameter block, compact LFT-LPV plant parameterizations with full parameter blocks can yield controllers that are less costly to implement. However, FBM-based synthesis conditions may yield intractable synthesis conditions. Corollary 5.1 can be used to recover the benefits of D/G-S-based synthesis listed in Tab. 2.1 on p. 72, by employing FBM in the first and D/G-S in the second multiplier stage.

2. REDUCTION OF CONSERVATISM
   In case the use of either D/G-S constraints or FBMs in the first multiplier stage is prescribed, e.g., if reduced implementation complexity is required or the online computation of matrix inverses is to be avoided, underlying parameterizations can be used to reduce overbounding associated with the parameterization in the first multiplier stage.

The following sections provide details on the above reasons.

5.1.1 Reduction of Implementation Complexity via Full-Block Multipliers and Full Parameter Blocks

One of the benefits of applying Cor. 5.1 becomes apparent by noticing that only the first multiplier stage determines the construction of the controller's parameter block.

Therefore, appreciate that the more involved computation of the controller's parameter block $\Delta^K(\Delta^P(\delta))$ as an LFT of the plant's parameter block $\Delta^P(\delta)$ due to the choice of FBMs, may in fact be computationally less expensive than the standard LFT-LPV-based controller synthesis using a plant parameterization with a diagonal parameter block. A prerequisite for this to happen, is a sufficiently compact size of the plant's parameter block.

For this purpose, let the parameter block of the plant be denoted $\Delta^P(\delta)$ and let there exist an LFR

$$\Delta^P(\delta) = \Delta^P_\Delta(\delta) \star \left[\begin{array}{c|c} W_{11} & W_{12} \\ \hline W_{21} & W_{22} \end{array}\right] \in \mathcal{C}^0(\delta,\ \mathbb{R}^{(n_{q^P_\Delta} \times n_{p^P_\Delta})}), \tag{5.7}$$

with a diagonal parameter block $\Delta^P_\Delta(\delta) \in \mathcal{C}^0(\delta,\ \mathbb{R}^{(n^P_\Delta \times n^P_\Delta)})$. Provided the incurred conservatism is not prohibitively excessive, it is clear that the parameter block $\Delta^P_\Delta(\delta)$ may be used directly in a D/G-S-based synthesis approach, rendering the controller's parameter block $\Delta^K(\delta) \stackrel{\triangle}{=} \Delta^P_\Delta(\delta)$. As an alternative, assume that the synthesis multiplier conditions can also be solved using $\Delta^P(\delta)$ and FBMs directly.

We now aim at comparing the implementation complexities following from the two plant parameterizations and multiplier constraints denoted by both

$$\mathsf{a}\big[K_{\text{D/G-S}}(\delta)\big] \quad \text{and} \quad \mathsf{a}\big[K_{\text{FBM}}(\delta)\big]$$

that yield the total number of arithmetic operations required to compute the state space matrices of the respective controller in each time instant, as derived from Eq. (3.8) on page 80.

Consequently, in the case of D/G-S, it remains to evaluate

$$\mathsf{a}\big[K_{\text{D/G-S}}(\delta)\big] \leqslant \left(n^P_\Delta\left(2n^P_\Delta-1\right)+2n^P_\Delta(n_x+n_u)\right)(n_x+n_y)$$
$$+ \mathsf{a}\big[\Psi^K_{\text{D/G-S}}(\delta)\big]$$

with $\mathsf{a}\big[\Psi^K_{\text{D/G-S}}(\delta)\big] \leqslant 2n^{P\,2}_\Delta\left(2n^P_\Delta-1\right)+n^P_\Delta\left(\tfrac{2}{3}n^{P\,2}_\Delta+1\right)$ and where

$$\Psi^K_{\text{D/G-S}}(\delta) = \Delta^P_\Delta(\delta)\left(I - D^{K_{\text{D/G-S}}}_{\Delta\Delta}\Delta^P_\Delta(\delta)\right)^{-1}.$$

In contrast, when using FBMs the complexity indicator $\mathsf{a}\big[K_{\text{FBM}}(\delta)\big]$ takes the form of the full set of Eqs. (3.8), (3.9) and (3.11), where the size of the controller's parameter block takes on the size of the plant's parameter block, $n^K_{q_\Delta} = n^P_{q_\Delta}$ and $n^K_{p_\Delta} = n^P_{p_\Delta}$.

Example 5.1 illustrates—for the special case of square mechanical LPV plants—that even for moderately sized diagonal parameter blocks, the implementation of scheduling functions resulting from FBM-based synthesis can be less costly.

Example 5.1 (Impl. Complexity for Square Mechanical LPV Plants)
Consider the case of LPV control of a mechanical system as developed throughout Exs. 4.4 and 4.5 with n_q degrees of freedom, $n_u = n_y = n_q$ and a standard S/KS weighting scheme with parameter-independent first order shaping filters, s.t. $n_x = 4n_q$. If second order shaping filters are used, we have $n_x = 6n_q$, while a standard four-block problem with first order input disturbance and reference filters yields $n_x = 8n_q$.

Let the modeling approach detailed in Chap. 4 yield generalized inertia, stiffness, damping and input matrices, $J(\rho)$, $K(\rho)$, $D(\rho)$ and $T(\rho)$, fully populated with parameter-dependent entries. Such a setup yields a worst-case full non-square parameter block of size $n_q \times 3n_q$, which is derived from the case distinction given in Eq. 4.39 on page 121 and illustrated in Ex. 4.6.

Take as a decision variable

$$\xi(n_q, n_\Delta^P) \triangleq \operatorname{sign}\left(a\left[K_{D/G\text{-}S}(\delta)\right] - a\left[K_{FBM}(\delta)\right]\right), \tag{5.8}$$

where for some value pair (n_q, n_Δ^P), $\xi(n_q, n_\Delta^P) = 1$ indicates that FBM-based synthesis yields controllers that are less costly to implement than D/G-S-based controllers scheduled on the diagonal parameter block and the value $\xi(n_q, n_\Delta^P) = -1$ means the opposite. Then Fig. 5.1 illustrates the decision for all value pairs (n_q, n_Δ^P) with

$$n_q \in \{1, 2, \ldots, 24\} \quad \text{and} \quad n_\Delta^P \in \{1, 2, \ldots, 50\}.$$

As indicated, the slope of the decision border increases if more elaborate sensitivity shaping schemes are employed. The particular pairs $(n_q = 3, n_\Delta^P = 31)$ and $(n_q = 3, n_\Delta^P = 18)$ lie in the vicinity of the LFT-LPV modeling example of a 3-DOF robotic manipulator presented in Sect. 4.6, indicated by a black box, cf. Tab. 4.3 on p. 144. Grey boxes indicate the approximate models that have been derived. The drastic reduction of diagonal parameter block sizes due to the approximation results in D/G-S-based controllers to be actually less costly during implementation.

$\square$

Remark 5.1 *Note that the assumptions made in Ex. 5.1 are conservative: If a diagonal parameter block of small size can be found, chances are that the system matrices are also not fully populated with parameter-dependent entries and thus even smaller full parameter blocks can be found by using masking matrices.*

In order to compare the potential benefits of using the full-block parameterization in conjunction with the parameter-block $\Lambda(\bullet)$ with the full-block representation in terms of $\Upsilon(\bullet)$, consider the following example.
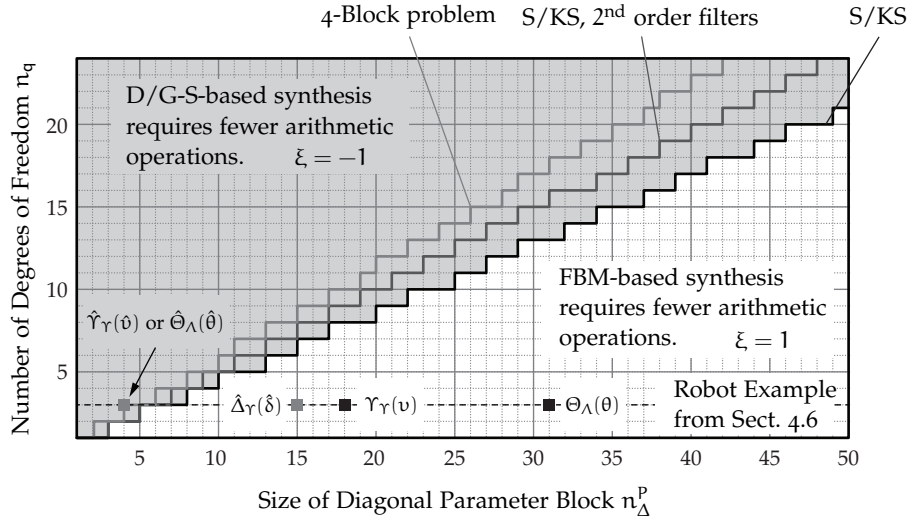
Figure 5.1: Comparison of implementation complexity for a square mechanical LPV plant: D/G-S using diagonal parameter blocks vs. FBMs using full non-square parameter blocks against increasing size of the diagonal parameter block and increasing number of degrees of freedom.

Example 5.2 (Impl. Complexity for Square Descriptor LPV Plants)

Consider the case of LPV control of a physical general descriptor system as developed from Eq. (4.24) with n_x physical states, $n_u = n_y = n_x$ and a standard S/KS weighting scheme with parameter-independent first order shaping filters, s. t. $n_x = 3n_x$.

Let the modeling approach detailed in Chap. 4 yield matrices, $E(\rho)$ and $F(\rho)$ fully populated with parameter-dependent entries. Such a setup yields a worst-case parameter block $\Lambda(\bullet)$ of size $2n_x \times 2n_x$. Alternatively, the block $\Lambda(\bullet)$ with size $2n_x \times 3n_x$ on which the plant depends rationally can be used.

Take again (5.8) as the decision variable. Figure 5.2 illustrates the potential benefit of using the parameterization in terms of $\Lambda(\bullet)$ for the first FBM-based multiplier stage. The grey line indicates the border line above which D/G-S-based synthesis yields controllers with less implementation complexity, when $\Lambda(\bullet)$ is used. The black line corresponds to $\Upsilon(\bullet)$, which in this example is larger and thus leads to a lowered border line for the decision.

A comparison with Fig. 5.1 from Ex. 5.1 in turn illustrates the potential of using the masking matrices to pull out only parameter-dependent parts into the parameter block.

<div style="text-align: right">□</div>

Recall that from Lma. 2.5 on p. 69 the parameter block $\Delta^K\big(\Delta^P(\delta)\big)$ can be written as an LFT

$$\Delta^K\big(\Delta^P(\delta)\big) = \begin{bmatrix} \widetilde{W}_{11} & \widetilde{W}_{12} \\ \widetilde{W}_{21} & \widetilde{W}_{22} \end{bmatrix} \star \begin{bmatrix} & \Delta^{P\top}(\delta) \\ \Delta^P(\delta) & \end{bmatrix} = \widetilde{W} \star \widetilde{\Delta}^P(\delta),$$
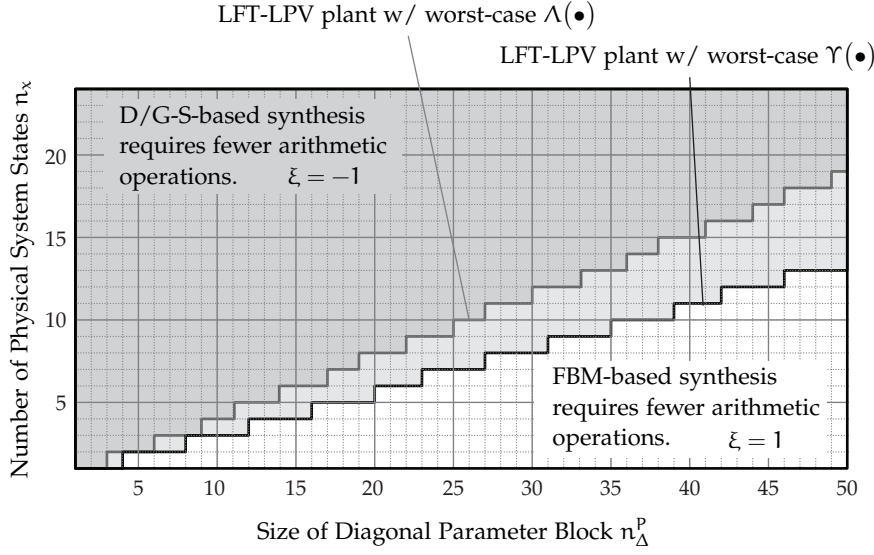
Figure 5.2: Comparison of implementation complexity for a square descriptor LPV plant: D/G-S using diagonal parameter blocks vs. FBMs using full non-square parameter blocks against increasing size of the diagonal parameter block and increasing number of degrees of freedom.

while it is in fact more efficiently evaluated in the form (2.162). Instead of computing $\Delta^K(\Delta^P(\delta))$ and the LFT of the controller state space matrices separately, the controller matrices can also be expressed as an LFT in terms of $\widetilde{\Delta}^P(\delta)$ directly, as illustrated by Fig. 5.3. Defining $n_{\widetilde{\Delta}}^P \triangleq n_{q_\Delta}^P + n_{p_\Delta}^P$ the resulting cost of implementation can be assessed by

$$a\left[\widetilde{K}_{FBM}(\delta)\right] \leqslant \left(n_{\widetilde{\Delta}}^P\left(2n_{\widetilde{\Delta}}^P-1\right)+2n_{\widetilde{\Delta}}^P(n_x+n_u)\right)(n_x+n_y)$$
$$+ a\left[\Psi^{\widetilde{K}}_{FBM}(\delta)\right]$$

with $a\left[\Psi^{\widetilde{K}}_{FBM}(\delta)\right] \leqslant 2n_{\widetilde{\Delta}}^{P\,2}\left(2n_{\widetilde{\Delta}}^P-1\right)+n_{\widetilde{\Delta}}^P\left(\tfrac{2}{3}n_{\widetilde{\Delta}}^{P\,2}+1\right)$ and where

$$\Psi^{\widetilde{K}}_{FBM}(\delta) = \widetilde{\Delta}^P(\delta)\left(I-D_{\Delta\Delta}^{\widetilde{K}_{FBM}}\widetilde{\Delta}^P(\delta)\right)^{-1}.$$

5.1.2 *Rendering Full-Block Multiplier-Based Synthesis Tractable*

Sect. 5.1.1 showed that in many cases FBM-based LFT-LPV synthesis yields controllers that are less costly to implement, given a sufficiently compact parameter block can be found. However, solving FBM-based multiplier conditions in the vertices may not always be tractable. In this case Cor. 5.1 can be applied in conjunction with an LFR of the full parameter block, parameterized via a diagonal parameter block, of the form (5.7).

(a) LPV control loop with LFT-LPV controller $K_{FBM}(\delta)$ in interconnection with FBM-based parameter block $\Delta^K(\Delta^P(\delta))$ expanded as an LFT $\widetilde{W} \star \widetilde{\Delta}^P(\delta)$.

(b) LPV control loop with LFT-LPV controller $K_{FBM}(\delta)$ represented as $\widetilde{K}_{FBM}(\delta) = K_{FBM}(\delta) \star \widetilde{W}$.
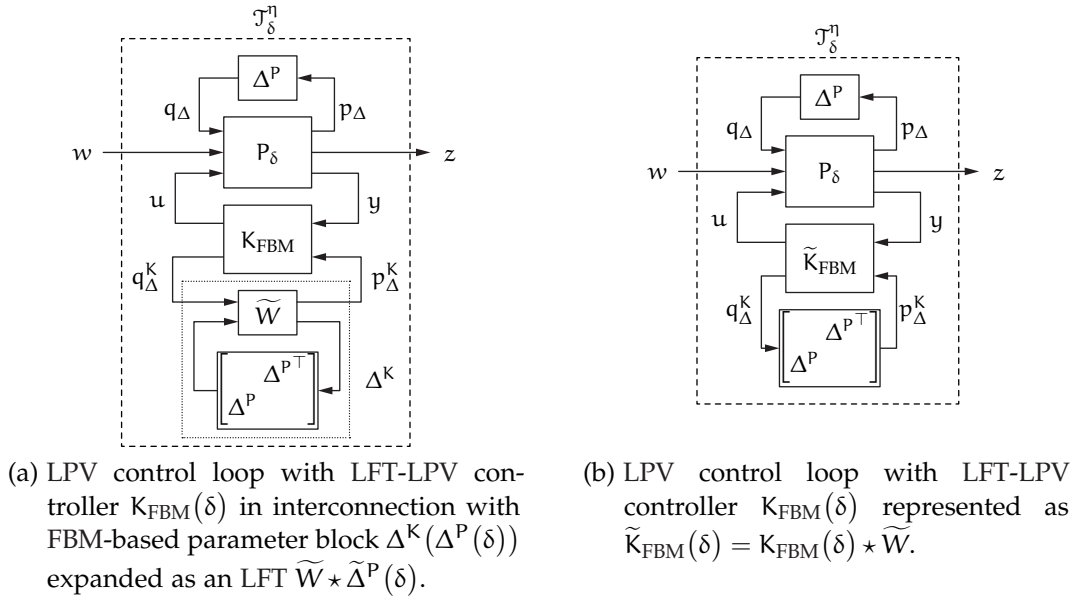
Figure 5.3: LPV control loop with LFT-LPV controller $K(\delta)$ in interconnection with FBM-based parameter block $\Delta^K(\Delta^P(\delta))$.

In such a case, the results of Chap. 4, more specifically those of Sect. 4.5, provide a range of parameterization options to choose from for use in the second D/G-S-based multiplier stage. Proper normalization allows to use the standard non-shifted D/G-S-constraints, which render the multiplier conditions trivially fulfilled.

5.1.3 Reduction of Conservatism

The use of D/G-S-constraints in the first or second multiplier stage is conservative in general. Examples 5.1 and 5.2 also illustrate the adverse effects of large diagonal parameter blocks on the implementation complexity. The case of FBM-based synthesis with the corresponding parameter block of the controller not being considered prohibitively complex *a priori* is discussed first.

5.1.3.1 Overcoming the Limits of Affine Parameterization of Full Parameter Blocks

In standard LFT-LPV synthesis with diagonal parameter blocks, the choice between different rational parameterizations is affected by a trade-off between implementation complexity and conservatism. In contrast, the implementation complexity due to the use of full parameter-blocks of constant dimensions is not dependent on the complexity of rational parameter-dependent terms occurring in such a block. More specifically, the implementation complexity resulting from a block $\Upsilon(\bullet)$ remains a constant, independent of the choice of parameterizations $\Upsilon(\delta)$ from (4.46) or $\Upsilon(\upsilon)$ from (4.48) on pp. 124. Sect. 5.1.2 showed that such parameterizations can be used to omit the formulation of multiplier conditions in vertices of the matrix polytope, in order to render FBMs tractable.

As long as the incurred synthesis complexity permits, the second multiplier stage should therefore be based on a parameterization of the compact full parameter block that exhibits the least amount of overbounding. In LFT parameterizations, such a choice often results in the least amount of parameters with the largest amount of repetitions. In such cases, it might even happen that controller synthesis based on a compact parameter block and FBM-based multiplier constraints solved in the vertices of a matrix polytope derived from an affine parameterization of the parameter block, turns out to be more conservative than using a rational parameterization with very little overbounding and D/G-S in the second (or first) stage.

Practical examples of parameterizations that incur a high amount of overbounding are sine and cosine terms of a common angle that need to be separately covered by newly introduced affine parameters, even though a Taylor expansion of sufficient accuracy can be found. The Taylor expansion approach might yield a high order polynomial in a single variable, while the repetitions of two different affine parameters are few. Clearly, in the affine parameterization the information on the common argument of the sine and cosine terms is lost and might incur excessive converatism, while, in turn, a diagonal parameter block of the Taylor expansion might lead to intractable implementation complexity using first stage D/G-S-constraints. The solution to such a kind of problem resides in moving the D/G-S-based multiplier conditions with the Taylor expansion parameterization to the second stage, in order to reduce conservatism, while retaining the small-in-size FBM-based first multiplier stage, for the purpose of keeping implementation complexity as low as possible.

5.1.3.2 *Avoiding Online Inverses by Diagonal Affine Parameterization in the First Multiplier Stage*

In practice, hardware restrictions may often permit the implementation of controllers that require the computation of a matrix inverse online. In such cases, it is mandatory to obtain a particularly simple scheduling law, such as an affinely scheduled controller. In order to obtain such an affinely scheduled controller using LFT-LPV controller synthesis methods, the following steps need to be taken:

(i) Affinely parameterize the LPV plant, e. g., by using the methods described in Sect. 4.5.4.4, or Alg. 4.1, respectively.

(ii) Obtain an LFR with a diagonal parameter block $\Theta_\Lambda(\theta)$ that contains the affine parameters θ from (4.49).

(iii) Perform D/G-S-based LFT-LPV controller synthesis. According to [161], a controller scheduled affinely on $\Theta_\Lambda(\theta)$ is guaranteed to exist, if the controller existence conditions are satisfied. As an alternative, designs may also be based on approximate parameter blocks.

However, as mentioned earlier, affine parameterizations usually involve an increased number of LPV parameters that are handled as independent and therefore incur overbounding. It is thus desirable to evaluate the synthesis conditions based on underlying rational parameterizations, which may incur a much tighter compact set with respect to the physically admissible range. For this purpose, resubstitute the affine parameters θ by their functional dependence on, e.g., the parameter set δ using the mapping

$$f^{\delta \to \theta} \in \mathcal{C}^1(\delta, \mathbb{R}^{n_\theta}), \quad \delta(t) \mapsto f^{\delta \to \theta}\big(\delta(t)\big) \overset{\triangle}{=} \theta(t).$$

This leads to an LFR

$$\Theta_\Lambda(\theta) = \Delta_\Theta^P(\delta) \star \begin{bmatrix} U_{\Delta 11} & U_{\Delta 12} \\ \hline U_{\Delta 21} & U_{\Delta 22} \end{bmatrix} \in \mathcal{C}^0(\delta, \ \mathbb{R}^{(n_{q_\Theta^P} \times n_{p_\Theta^P})}), \tag{5.9}$$

$$= \Delta_\Theta^P(\delta) \star U_\Delta,$$

$$\Delta_\Theta^P(\delta) = \operatorname*{diag}_{i=1}^{n_\delta}\big(\delta_i(t) I_{r_{\delta,i}^\Theta}\big),$$

with which Cor. 5.1 can be applied.

5.1.4 *Summary*

The introduction of a second multiplier stage is a particular way to provide an exact relaxation, in order to evaluate the multiplier condition of the first stage. Or relaxations—exact or possibly approximate ones—, such as sum-of-squares (SOS)-based methods can be employed [27, 63]. However, the use of the FBSP appears to be attractive due to its simplicity. The application examples of Chap. 6 will provide insight on the conservatism and complexity incurred.

5.2 Improved LFT-LPV State Feedback Synthesis Conditions

$\mathbf{F}$IRSTLY, FBSP-based methods to turn LPV state-feedback controller synthesis as per Thm. 5.1 into a convex optimization problem are reviewed.

5.2.1 *Standard LFT-LPV State Feedback Synthesis Conditions*

Theorem 5.1 (SF Controller Synthesis, extended from [160])
Under Ass. (A2.1) and (A2.4)–(A2.7), there exists a state-feedback controller gain $F(\delta)$ *given by Eq. (2.127) on p. 2.127, i.e.,*

$$F(\delta) = -\left(D_{pu}^\top(\delta)D_{pu}(\delta)\right)^{-1}\left(\gamma B_u^\top(\delta)S^{-1}(\delta) + D_{pu}^\top(\delta)C_p(\delta)\right),$$

that renders the closed-loop system $\mathfrak{T}_\delta^\eta$ *as defined in (2.20) asymptotically stable over* $\delta \times \eta$ *with an induced* $\mathcal{L}_2$-*norm from* $w \to z$ *bounded from above by* $\gamma > 0$, *if there exist* $N \in \mathbb{S}^{(n_{p_\Delta}^B + n_{q_\Delta}^B)}$, $P \in \mathbb{S}^{(n_{p_\Delta}^S + n_{q_\Delta}^S)}$ *and for the quadratic function*

$$S(\delta) = Q^\top(\delta)SQ(\delta) \in \mathcal{C}^1(\delta, \mathbb{S}^{n_x}), \quad S(\delta) \succ 0\ \forall \delta \in \boldsymbol{\delta},$$

with

$$Q(\delta) = \Delta_Q(\delta) \star \left[\begin{array}{c|c} Q_{11} & Q_{12} \\ \hline Q_{21} & Q_{22} \end{array}\right] \in \mathcal{C}^1(\delta, \mathbb{R}^{n_S \times n_x})$$

there exists $S \in \mathbb{S}^{n_S}$ *and* $\gamma > 0$ *that satisfy*

$$\mathcal{L}_N = \begin{bmatrix} \bullet \\ \bullet \end{bmatrix}^\top \begin{bmatrix} N & & \\ & \begin{matrix} 0\ S \\ S\ 0 \end{matrix} & \\ & & \Gamma^{-1} \end{bmatrix} \begin{bmatrix} I & 0 \\ B_{11} & B_{12} \\ \hline B_{21} & B_{22} \end{bmatrix} \succ 0, \tag{5.10}$$

$$\mathcal{L}_P = \begin{bmatrix} \bullet \\ \bullet \end{bmatrix}^\top \begin{bmatrix} P & \\ & S \end{bmatrix} \begin{bmatrix} Q_{11} & Q_{12} \\ I & 0 \\ \hline Q_{21} & Q_{22} \end{bmatrix} \succ 0, \tag{5.11}$$

$$\mathcal{L}_N(\delta, \eta) = \begin{bmatrix} \bullet \\ \bullet \end{bmatrix}^\top N \begin{bmatrix} \Delta_B(\delta, \eta) \\ \hline I \end{bmatrix} \prec 0,\ \forall\, (\delta, \eta) \in (\boldsymbol{\delta} \times \boldsymbol{\eta}) \tag{5.12}$$

$$\mathcal{L}_P(\delta) = \begin{bmatrix} \bullet \\ \bullet \end{bmatrix}^\top P \begin{bmatrix} I \\ \hline \Delta_Q(\delta) \end{bmatrix} \prec 0,\ \forall \delta \in \boldsymbol{\delta} \tag{5.13}$$

Preliminary results of this section have been previously published in [E49].

where

$$B(\delta, \eta) = U(\delta, \eta) G(\delta) = \Delta_B(\delta, \eta) \star \left[\begin{array}{c|c} B_{11} & B_{12} \\ \hline B_{21} & B_{22} \end{array}\right]$$

$$U(\delta, \eta) = \left[\begin{array}{cc:c} Q(\delta) & \partial Q(\delta, \eta) & \\ 0 & Q(\delta) & \\ \hdashline & & I\ 0 \\ & & 0\ I \end{array}\right] = \Delta_U(\delta, \eta) \star \left[\begin{array}{c|c} U_{11} & U_{12} \\ \hline U_{21} & U_{22} \end{array}\right]$$

$$\Delta_B(\delta, \eta) = \left[\begin{array}{cc} \Delta_U(\delta, \eta) & \\ & \Delta_G(\delta) \end{array}\right]$$

$$G(\delta) = \left[\begin{array}{cc} -A^\top(\delta) & -C_p^\top(\delta) \\ I & 0 \\ \hdashline -B_p^\top(\delta) & 0 \\ 0 & I \end{array}\right] \quad N_S(\delta) = \Delta_G(\delta) \star \left[\begin{array}{c|c} G_{11} & G_{12} \\ \hline G_{21} & G_{22} \end{array}\right]$$

$$N_S(\delta) = \ker\left(\left[\begin{array}{cc} B_u^\top(\delta) & D_{pu}^\top(\delta) \end{array}\right]\right)$$

$$\left[\begin{array}{c|c} B_{11} & B_{12} \\ \hline B_{21} & B_{22} \end{array}\right] = \left[\begin{array}{cc|c} U_{11} & U_{12}G_{21} & U_{12}G_{22} \\ 0 & G_{11} & G_{12} \\ \hline U_{21} & U_{22}G_{21} & U_{22}G_{22} \end{array}\right] \tag{5.14}$$

□

Theorem 5.1 presents verifiable conditions to synthesize the state-feedback gain from Eq. (2.127). By essentially following [163], i.e., in order to construct the LFR of the outer factor $B(\delta)$, LFRs of the Lyapunov basis functions $U(\delta)$ via Eq. (B.3) on p. 327, the nullspace $N_S(\delta)$ via Lma. A.4 on p. 319 and subsequently $G(\delta)$ by multiplication of LFRs via Eq. (A.2) on p. 318 need to be obtained. For descriptor LPV systems, however, the complexity incurred by this construction can be reduced.

5.2.2 *LFT-LPV State Feedback Synthesis Conditions for Descriptor LPV Systems*

The following proposition presents an alternative construction based on a class of descriptor LFT-LPV systems. For this purpose, first recall the considered class of physical plant models given in Eq. (4.24) on page 117. Ass. (A2.7) and (A2.5) on an associated generalized plant configuration imply the following conditions on the physical plant model.

(**A**5.1) The full set of physical states is measurable, i.e., the plant model $\mathcal{G}_\rho^\sigma$ from Eq. (4.24) fulfills

$$E(\rho) \triangleq \begin{bmatrix} E_{xx}(\rho) & E_{xy}(\rho) \\ 0 & I \end{bmatrix} \in \mathbb{R}^{(n_x+n_y)\times(n_x+n_y)},$$

$$F(\rho) \triangleq \begin{bmatrix} F_{xx}(\rho) & F_{xu}(\rho) \\ I & 0 \end{bmatrix} \in \mathbb{R}^{(n_x+n_y)\times(n_x+n_u)}.$$

(**A**5.2) The plant matrix $E_{xy}(\rho)$ fulfills $E_{xy}(\rho) = 0$.

Ass. (A5.1) yields a strictly proper state space representation with identity as the output gain.

$$\mathcal{G}_\rho^\sigma : \begin{cases} \begin{bmatrix} \dot{x} \\ y \end{bmatrix} = \begin{bmatrix} E_{xx}^{-1}(\rho) & 0 \\ 0 & I \end{bmatrix} \begin{bmatrix} (F_{xx}(\rho) - E_{xy}(\rho)) & F_{xu}(\rho) \\ I & 0 \end{bmatrix} \begin{bmatrix} x \\ u \end{bmatrix}, \\ \rho(t) \in \mathcal{F}_\rho^\sigma \end{cases} \tag{5.15}$$

W.l.o.g., Ass. (A5.2) can be fulfilled by redefining $F_{xx}(\rho)$ as the difference occurring in (5.15).

Within this setup and under the otherwise standard state-feedback setting completed by Ass. (A2.6) and (A2.7), the generalized plant

$$\mathcal{P}_\rho^\sigma : \begin{cases} \begin{bmatrix} \dot{x} \\ z \\ y \end{bmatrix} = \begin{bmatrix} A(\rho) & B_p(\rho) & B_u(\rho) \\ C_p(\rho) & D_{pp}(\rho) & D_{pu}(\rho) \\ C_y(\rho) & D_{yp}(\rho) & D_{yu}(\rho) \end{bmatrix} \begin{bmatrix} x \\ w \\ u \end{bmatrix} \\ \rho(t) \in \mathcal{F}_\rho^\sigma, \end{cases}$$

can be written as

$$\mathcal{P}_\rho^\sigma : \begin{cases} \begin{bmatrix} E_{xx}(\rho) & 0 & 0 \\ 0 & I & 0 \\ 0 & 0 & I \end{bmatrix} \begin{bmatrix} \dot{x} \\ z \\ y \end{bmatrix} = \begin{bmatrix} F_{xx}(\rho) & F_p(\rho) & F_{xu}(\rho) \\ C_p(\rho) & 0 & D_{pu}(\rho) \\ I & 0 & 0 \end{bmatrix} \begin{bmatrix} x \\ w \\ u \end{bmatrix} \\ \rho(t) \in \mathcal{F}_\rho^\sigma, \end{cases} \tag{5.16}$$

where $x \in \mathbb{R}^{n_x}$, $u \in \mathbb{R}^{n_u}$, $y \in \mathbb{R}^{n_x}$, $w \in \mathbb{R}^{n_w}$, $z \in \mathbb{R}^{n_z}$.

W.l.o.g., in the generalized plant description (5.16), the performance channel input gain matrix $B_p(\rho)$ is restricted to a descriptor-like structure $E_{xx}^{-1}(\rho)F_p(\rho)$. For standard sensitivity shaping schemes, e.g., the S/KS configuration, such an assumption can be made, since, if the matrix E_{xx} is really only a source of the physical plant being modeled in a descriptor framework, one has $E_{xx}^{-1}(\rho)F_p(\rho) = F_p(\rho)$. In such a case, the entries in $B_p(\rho)$ denote input gains to prefilters of the reference or output disturbance low-pass filter, which are required due to Ass. (A2.6), and which will not be affected by the physical inertia. In a four-block shaping scheme,

in turn, input disturbances are usually supposed to directly act on the plant inputs. Then, the descriptor representation appears quite naturally. In any case, if so required, the input gain can be defined as $F_P(\rho) = E_{xx}(\rho)\widetilde{F}_P(\rho)$, in order to eliminate the effect of the inertia.

Proposition 5.1 (Compact Full-Block LFT Parameterization)
For the generalized plant representation given in Eq. (5.16) and parameter-dependent plant matrices of the form

$$E_{xx}(\rho) = E_{xx0}(\rho) + \tilde{\Delta}_E(\rho) = \Delta_E(\rho) \star \begin{bmatrix} 0 & W_E(\rho) \\ \hline V(\rho) & E_{xx0}(\rho) \end{bmatrix}, \tag{5.17}$$

$$F_{xx}(\rho) = F_{xx0}(\rho) + \tilde{\Delta}_{F,x}(\rho) = \Delta_{F,x}(\rho) \star \begin{bmatrix} 0 & W_{F,x}(\rho) \\ \hline V(\rho) & F_{xx0}(\rho) \end{bmatrix}, \tag{5.18}$$

$$F_P(\rho) = F_{P0}(\rho) + \tilde{\Delta}_{F,p}(\rho) = \Delta_{F,p}(\rho) \star \begin{bmatrix} 0 & W_{F,p}(\rho) \\ \hline V(\rho) & F_{P0}(\rho) \end{bmatrix}, \tag{5.19}$$

with $\Delta_F(\rho) = \begin{bmatrix} \Delta_{F,x}(\rho), & \Delta_{F,p}(\rho) \end{bmatrix}$, $W_F(\rho) = \mathrm{diag}(W_{F,x}(\rho), W_{F,p}(\rho))$, the conditions of Thm. 5.1 can be written with the LFR in terms of $\Delta_E(\rho)$ and $\Delta_F(\rho)$ of the outer factor $G(\rho)$

$$G(\rho) = \Delta_G(\rho) \star \begin{bmatrix} 0 & G_{12}(\rho) \\ \hline G_{21}(\rho) & G_{22}(\rho) \end{bmatrix}, \qquad \Delta_G(\rho) = \begin{bmatrix} \Delta_F^\top(\rho) \\ \Delta_E^\top(\rho) \end{bmatrix}$$

$$G_{21}(\rho) = \begin{bmatrix} -I & 0 & 0 \\ 0 & 0 & I \\ \hline 0 & -I & 0 \\ 0 & 0 & 0 \end{bmatrix} \begin{bmatrix} W_F^\top(\rho) & 0 \\ 0 & W_E^\top(\rho) \end{bmatrix}$$

$$G_{12}(\rho) = V^\top(\rho) \begin{bmatrix} I & 0 \end{bmatrix} N_{S,F}(\rho)$$

$$G_{22}(\rho) = \begin{bmatrix} -F_{xx0}^\top(\rho) & -C_P^\top(\rho) \\ E_{xx0}^\top(\rho) & 0 \\ \hline -F_{P0}^\top(\rho) & 0 \\ 0 & I \end{bmatrix} N_{S,F}(\rho)$$

$$N_{S,F}(\rho) = \ker\left(\begin{bmatrix} F_{xu}^\top(\rho) & D_{pu}^\top(\rho) \end{bmatrix}\right).$$

□

Proof: First observe that a parameter-dependent kernel representation of $N_S(\rho)$ in Eq. (2.134) on page 60 can be found in

$$N_S(\rho) = \ker\left(\begin{bmatrix} B_u^\top(\rho) & D_{pu}^\top(\rho) \end{bmatrix}\right)$$

$$= \begin{bmatrix} E_{xx}^\top(\rho) & 0 \\ 0 & I \end{bmatrix} \ker\left(\begin{bmatrix} F_{xu}^\top(\rho) & D_{pu}^\top(\rho) \end{bmatrix}\right)$$

due to the non-singularity of $E_{xx}(\rho)$. This results in the outer factor

$$
\begin{bmatrix}
-A^\top(\rho) & -C_p^\top(\rho) \\
\hdashline
I & 0 \\
-B_p^\top(\rho) & 0 \\
0 & I
\end{bmatrix}
\begin{bmatrix}
E_{xx}^\top(\rho) & 0 \\
0 & I
\end{bmatrix}
N_{S,F}(\rho)
$$

$$
=
\begin{bmatrix}
-F_{xx}^\top(\rho) & -C_p^\top(\rho) \\
E_{xx}^\top(\rho) & 0 \\
\hdashline
-F_p^\top(\rho) & 0 \\
0 & I
\end{bmatrix}
N_{S,F}(\rho),
\tag{5.20}
$$

which is affine in $\Delta_G(\rho)$ for which then an LFR can be easily constructed. This concludes the proof. ∎

Proposition 5.1 provides means to more compactly define the outer factors in Thm. 5.1 for use with full-block multipliers, while still separating the parameter blocks $\Delta_E(\rho)$ and $\Delta_F(\rho)$. In contrast, directly constructing the LFT parameterization of the nullspace $N_S(\rho)$ along the lines of [163], i.e., by application of Lma. A.4 on p. 319, results in an LFR of higher order, as the inverse of $F_{xx}(\rho)$ needs to be considered. Compared to that, the approach proposed in Prop. 5.1 merely requires an LFR of $\ker\left(\begin{bmatrix} F_{xu}^\top(\rho), & D_{pu}^\top(\rho) \end{bmatrix}\right)$, which for many mechanical systems may even be constant.

Due to the diagonal concatenation, it is also expected that the approach of [163] leads to a larger parameter block when converted to a diagonal parameter block.

5.2.3 *Summary*

The above results provide a simple method to effectively exploit descriptor models with non-singular generalized inertias. They do not easily extend to cover the singular case, see, e.g., [102]. However, compared to other methods for non-singular descriptor models, for which a detailed overview is presented in [0], the methods provide benefits simply due to the manipulation of the synthesis conditions and involve no modification during implementation.

The above methods are also enabling a simplified use of full-block multipliers: As the outer factors are linear in both the parameter blocks Δ_E and Δ_F, an affine parameterization of these blocks is sufficient to allow for a small-in-size multiplier condition that is checked in the vertices spanning the convex hull of the parameter range. This potentially reduces overbounding and the number of decision variables over the standard approach using diagonal parameter blocks and D/G-scalings.

An extension to the output-feedback case is obvious, since the projections used in the primal LMI do not even involve the inverse of the generalized inertia. Thus, no improvement is to be expected.

6

APPLICATION EXAMPLES

≪Tell me, I'll forget.
Show me, I'll remember.
Involve me, I'll understand.≫

Chinese Proverb

THIS chapter presents two case studies for the LPV control of complex plants with both low synthesis and implementation complexity. Reduced as well as full scheduling order control approaches are presented for:

(i) The low-complexity output-feedback LPV control of a robotic manipulator (Sect. 6.1),

(ii) Experimental real-time state-feedback and output-feedback LPV control of a control moment gyroscope (Sect. 6.2).

The two case studies build on the modeling framework introduced in Chap. 4 and the improved synthesis tools derived in Chap. 5 and illustrate the obtained benefits.

With respect to the robotic manipulator, high-performance full scheduling order control is rendered tractable with low implementation complexity further reduced over previous results, [E45]. A controller for the CMG is synthesized based on the exact model for the first time, while the novel approximation scheme results in a state-feedback control scheme of particularly low complexity.

6.1 A Three-Degrees-of-Freedom Robotic Manipulator

In the following, a case study in LPV control of the Thermo CRS A465 robotic manipulator is conducted. Sect. 6.1.1 outlines the problem setup and Sect. 6.1.2 briefly introduces a computed torque control (CTC) reference design. Sects. 6.1.3 and 6.1.4 illustrate the improvements obtained by employing a two-stage multiplier approach to PIDLF-based output-feedback (OF) LFT-LPV controller synthesis techniques w.r.t. both synthesis and implementation complexity associated with full and reduced scheduling order models. A summary is provided in Sect. 6.1.5.

6.1.1 Problem Setup

Position control of rigid robotic manipulators is widely considered a problem for which satisfactory industry-standard, high-performance solutions exist [128, 140]. Cost efficiency has sparked research pursuing high performance control of flexible manipulators, e.g., [E83]. The latter is an ongoing field of research and while LPV control has already been successfully implemented even for such an advanced control problem, the purpose of considering LPV control for a rigid robotic manipulator in this thesis is less based on a desire to compete with the standard approaches, but to showcase the ability of the LFT-LPV control framework to cope with a system of high complexity. Furthermore, the advances in reducing implementation complexity of LFT-LPV controllers will be emphasized. In light of this, feedforward compensation is deliberately omitted at this point. Regardless, a CTC design will be presented first for reference.

Remark 6.1 *Experimental results with two-stage multiplier approaches using a slightly less advanced modeling approach have been presented in [E48]. The results presented here use a four-block sensitivity shaping design and significantly faster reference trajectories over [E48, 60] to highlight the capabilities of the controller designs.*

6.1.1.1 Choice of Reference Trajectories

The reference trajectories are chosen to drive the robotic manipulator of type Thermo CRS A465 to its allowed specified limits in terms of the angles and an-

---

Preliminary results of this section have been previously published in [E48, 60]. The results are extended by benchmarking against a computed torque control design and an improved tuning as well as a more detailed complexity analysis. The methods introduced in Sect. 5.1 have been validated experimentally in [E48].

gular velocities with a ten percent safety margin. For this purpose, the reference trajectories are essentially designed by sinusoids

$$r_{q_i}(t) \overset{\triangle}{=} \alpha_i(t)\bar{q}_i \sin(\omega_i t),$$
$$\omega_1 = 1\,s^{-1},\ \omega_2 = 2\,s^{-1},\ \omega_3 = 2\,s^{-1},$$
$$\bar{q}_1 = 150°,\ \bar{q}_2 = 80°,\ \bar{q}_3 = 170°.$$

For smooth initial and final parts of the trajectories, the amplitude is multiplied by ramp signals shown in Fig. 6.1. The trajectories are further modified in order to satisfy

$$\cos\left(\frac{\pi}{180°}r_{q_2}\right) L_2 + \sin\left(\frac{\pi}{180°}r_{q_3}\right) L_3 > L_1.$$

Cf. Fig. 4.8 on p. 140 for reference to the lengths involved. Finally a low-pass filter is applied.
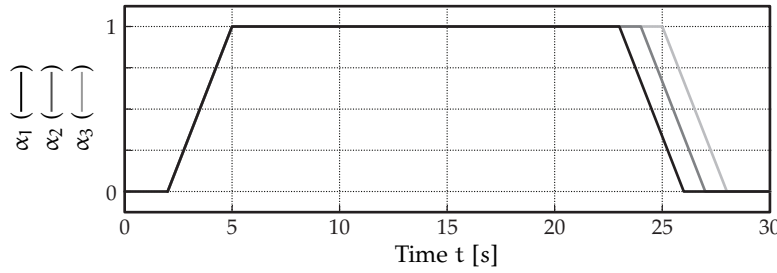
Figure 6.1: Reference trajectory phase-in factors α_i for the robot.

6.1.2 *Computed Torque Reference Controller Design*

The CTC reference design is based on the results summarized in [20], where the particular control law—commonly referred to as «computed torque feedback control» [20]—takes the form of a particular parameter-dependent state-feedback (SF) control law

$$u_{\text{CTC, FB}} = J(\rho)\,(\ddot{r} + u_{\text{FB}}) + D(\rho)\dot{q} + K(\rho)q. \tag{6.1}$$

Due to the fact that all nonlinear generalized damping and stiffness terms are directly accessible through the input, they are effectively being canceled if they are known accurately enough.

Under the assumption of perfect cancellation of nonlinear terms, the system is reduced to a double integrator system

$$\ddot{q} - \ddot{r} = u_{\text{FB}}, \tag{6.2}$$

where the sole purpose of the remaining feedback control action u_{FB} consists in rejecting potential deviations from the reference trajectory. CTC in the form of (6.1) is a feedback control law, as opposed to the case, where generalized velocities and positions are precomputed and therefore form a feedforward control law

$$u_{CTC,\,FF} = J(\rho_r)\,(\ddot{r} + u_{FB}) + D(\rho_r)\dot{r} + K(\rho_r)r. \tag{6.3}$$

Here, $\rho_r(t)$ denotes the precomputed trajectory of the scheduling parameters associated with the planned reference trajectory $r(t)$. The design choices, advantages and disadvantages associated with implementing a CTC controller in either feedforward or feedback configuration have been discussed extensively in the literature, see, e. g., [20, 92, E83, 145]. For the purpose of this thesis, the feedback configuration is chosen for better a comparison with the LPV reference control scheme.

6.1.2.1 LTI-$\mathcal{H}_\infty$ Controller Design

The control input u_{FB} can take many forms, such as proportional integral derivative (PID) control

$$u_{FB} = K_P e + K_D \dot{e} + K_I \int^t e\, d\tau. \tag{6.4}$$

However, for the purpose of this thesis, an LTI-$\mathcal{H}_\infty$ controller design is used that employs the same shaping scheme as the one that will be used for the subsequent LPV controller designs. The robot model is considered exact and no further uncertainty modeling is performed.

The generalized plant configuration depicted in Fig. 6.2 is used throughout the section, with shaping filters defined as

$$
\begin{aligned}
W_S(s) &= \operatorname*{diag}_{i=1}^{3}(W_{Si}), & W_{KS}(s) &= \operatorname*{diag}_{i=1}^{3}(W_{KSi}), \\
W_{Si}(s) &= \tfrac{3333}{s^2+2s+1},\ i \in \{1,2\}, & W_{KSi}(s) &= 50\tfrac{s^2+40s+400}{s^2+4\cdot10^4 s+4\cdot10^8}, \\
W_{S3}(s) &= \tfrac{8333}{s^2+2s+1}, \\
V_d(s) &= \operatorname*{diag}_{i=1}^{3}(V_{di}), & V_r(s) &= \operatorname*{diag}_{i=1}^{3}(V_{ri}), \\
V_{di}(s) &= \tfrac{1}{5s+10}, & V_{ri}(s) &= \tfrac{5}{s+5},\ i \in \{1,3\}, \\
& & V_{r2}(s) &= \tfrac{10}{s+10}.
\end{aligned}
$$

The synthesis results and implementation complexity of the CTC reference controller will be listed in the following enumerations for the respective LPV controller designs for comparison. Band-limited white noise with a power matching the experimental setup is added to the feedback signals, in order to assess the noise attenuation of the controllers.
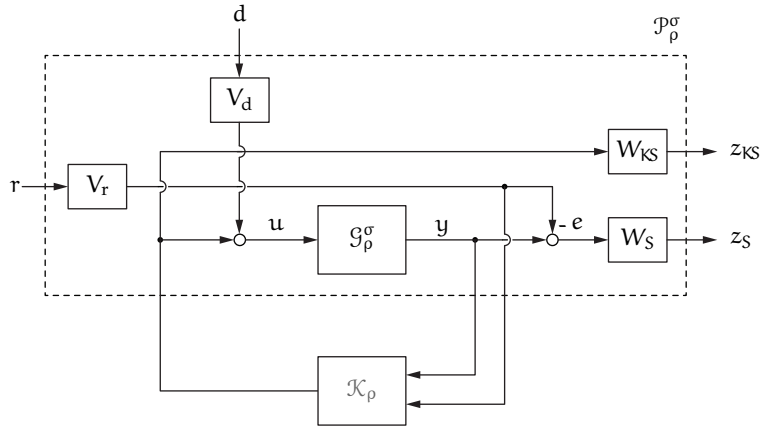
Figure 6.2: Generalized plant configuration for OF controller synthesis for the robot.

6.1.3 *Full Scheduling Order Output-Feedback Linear Parameter-Varying Control*

The purpose of the following full scheduling order OF LPV controller designs is to showcase the ability of the modeling framework presented in Chap. 4 and the modified two-stage multiplier LFT-LPV synthesis methods presented in Chap. 5, Sect. 5.1 to handle LPV plants of high scheduling complexity, while achieving low implementation complexity.

The generalized plant configuration including the shaping filters used during synthesis is adopted from the CTC LTI-$\mathcal{H}_\infty$ controller design, cf. Fig. 6.2.

Controller designs are carried out via three different approaches:

  (i) **FBMs:** PIDLF-based OF LPV controller synthesis as per Thm. 2.17 on p. 66 using FBMs in a single multiplier stage,

 (ii) **FBMs + D/G-Ss:** PIDLF-based OF LPV controller synthesis as per Thm. 2.17 using FBMs in the first and D/G-Ss in the second multiplier stage via the application of Cor. 5.1 on p. 160,

(iii) **D/G-Ss:** PIDLF-based OF LPV controller synthesis as per Thm. 2.17 using D/G-Ss in a single multiplier stage.

FBMs require the construction of a controller parameter block Δ^K according to Lma. 2.5 on p. 69, which incurs additional online computations, whose complexity needs to be assessed. In contrast, D/G-Ss allow the controller to be scheduled by a copy of the plant's parameter block according to Lma. 2.6 on p. 70. Here, method (ii) is used to combine the benefits of FBMs and D/G-Ss from Tab. 2.1 on p. 72 in terms of synthesis complexity and the possibility to consider fully populated parameter blocks of small size. Method (i) is used to illustrate the achieved benefits and method (iii) acts as the standard reference method for LFT-based LPV controller synthesis.

6.1.3.1 *Synthesis and Simulation Results*

Tab. 6.1 lists synthesis, simulation and complexity results for full scheduling order control of the robotic manipulator. The method and the associated parameter blocks—introduced in Sect. 4.6, Tab. 4.3 on p. 144—are indicated in the left columns. The diagonal parameter block used in the second multiplier stage can be inferred from Tab. 4.3 or the argument of the respective parameter block. The RMSEs for each joint as well as their average is given. The control effort is quantified via

$$E_u \triangleq \frac{1}{T} \int_0^T \sum_{i=1}^3 u_i^2 \, dt.$$

Synthesis complexity is reported in terms of the synthesis time $t[\bullet]$, number of decision variables $d[\bullet]$ and total size of the LMI $s[\bullet]$ for both the controller existence conditions and the LMI-based synthesis of the controller parameters (in parentheses).

Table 6.1: OF controller synthesis options for the robot models with various full scheduling order parameterizations.
$\bullet/(\bullet)$: The first value indicates quantities associated with the LMI-based existence conditions, cf. Thm. 2.17, p. 66, using—in some cases—a two-stage multiplier approach, cf. Cor. 5.1, p. 160, whereas values in parentheses indicate quantities associated with the LMI-based derivation of controller parameters.

			RMSE [°]				**Synthesis Complexity**			
Syn.	**Blk.**	γ	q_1	q_2	q_3	Avg.	E_u	$t[\bullet]$	$d[\bullet]$	$s[\bullet]$
FBMs	$\Upsilon(\upsilon)$	0.91	0.064	0.040	0.061	0.055	2.60	374.4 s/(26.5 s)	733/(1157)	11 468/(131)
FBMs + D/G-Ss	$\Upsilon(\delta)$	0.93	0.054	0.039	0.056	0.050	2.60	16.5 s/(17.2 s)	1075/(1157)	452/(131)
	$\Lambda(\delta)$	0.90	0.051	0.039	0.052	0.047	2.60	16.3 s/(20.4 s)	1075/(1157)	452/(131)
	$\Upsilon(\upsilon)$	0.88	0.059	0.039	0.058	0.052	2.60	10.0 s/(27.9 s)	809/(1157)	348/(131)
	$\Lambda(\upsilon)$	0.87	0.059	0.039	0.057	0.052	2.60	10.7 s/(17.6 s)	809/(1157)	348/(131)
	$\Lambda(\theta)$	1.32	0.083	0.074	0.062	0.073	2.60	12.8 s/(29.1 s)	883/(1157)	452/(131)
D/G-Ss	$\Delta_\Upsilon(\delta)$	0.94	0.058	0.062	0.074	0.065	2.60	17.3 s/(736.9 s)	943/(3540)	408/(233)
	$\Upsilon_\Upsilon(\upsilon)$	1.08	0.070	0.077	0.079	0.075	2.61	8.3 s/(114.4 s)	677/(2162)	304/(181)
	$\Theta_\Lambda(\theta)$	2.10	0.129	0.175	0.139	0.148	2.61	16.5 s/(372.4 s)	751/(3540)	408/(233)
CTC	$\Upsilon(\rho)$	1.00	0.058	0.053	0.086	0.066	2.64	3.5 s	300/(810)	84/(54)

As apparent from Tab. 6.1, controllers based on a parameterization in terms of δ or υ perform slightly better than the CTC controller at mildly reduced control effort. A deterioration of performance is visible for controllers based on the fully affine parameterization in terms of θ. The based parameterization in terms of δ

has a slight advantage over the automated parameterization rendering Υ affine in υ. Differences in performance are more clearly revealed in D/G-S-based synthesis, while the use of FBM appears to alleviate some of the conservatism.

In all LPV control cases, the two-stage multiplier approach achieves the fastest total synthesis time (below $42\,\mathrm{s}$), whereas the other approaches show significantly increased synthesis complexity at reduced or comparable performance levels.

6.1.3.2 *Implementation Complexity*

Tab. 6.2 lists the implementation complexity of each synthesized controller in terms of the required arithmetic operations a[•] and scalar variables m[•] to be stored. The complexity is divided into computing/storing the plant's parameter block (Blk.), the controller's parameter block $\hat{\Delta}^{K}(\,\bullet\,)$ as a function of the former, the operations to perform the LFT of the controller parameter block with the constant state space system matrix (LFT), as well as the remaining operations to compute the controller's time-varying state space matrices (Matrices) together with the memory requirements of the controller parameters. The number of arithmetic operations a[•] and memory requirements m[•] for the respective blocks are listed in Tab. 4.4 on p. 144. In each case, the most effective implementation is chosen. Therefore, the choice of parameterization in the second multiplier stage has no effect on the resulting implementation complexity. The complexity of the CTC controller is approximated by computing/storing the parameter block $\Upsilon(\rho)$ and storing the state space matrices from LTI-$\mathcal{H}_{\infty}$ synthesis. As obvious from Tab. 6.2, the CTC controller implementation is the least costly. Some additional computations are incurred due to the use of the parameter block $\Lambda(\bullet)$, despite the fact that the LFT is not required, since the controller can be synthesized to be affine in its parameter block. However, in conclusion, the use of FBMs in conjunction with small-in-size fully populated parameter blocks has a significant advantage over the conventional D/G-S-based synthesis approach.

Figure 6.3 shows the simulation results of reference tracking control of the robotic manipulator using a full scheduling order OF LPV controller synthesized by a two-stage multiplier approach using the parameterization via $\Lambda(\delta)$ (method (ii)). When compared to the results obtained by CTC the controller outputs appear less aggressive. In fact, a close zoom-in on the trajectories and controller outputs, cf. Fig. 6.4, indicates slightly reduced deviations from the reference command as well as fewer oscillations in the control signals. The comparison also includes an OF LPV controller synthesized by a standard single-stage D/G-S approach using the affine parameterization via $\Lambda(\theta)$.

Table 6.2: Implementation complexity for OF controllers synthesized on full scheduling order robot models.

| | | No. of Arith. Ops./Mem. Req. | | | | | | | | |
| | | Blk. | | $\Delta^K(\bullet)$ | | LFT | Matrices | | Total | |
Syn.	**Blk.**	a[•]	m[•]	a[•]	a[•]	m[•]	a[•]	m[•]	a[•]	m[•]
FBMs	$\Upsilon(\upsilon)$	245	120	3311	924	276	6210	1140	10 042	2184
FBMs + D/G-Ss	$\Upsilon(\bullet)$	245	120	3311	924	276	6210	1140	10 042	2184
	$\Lambda(\bullet)$	886	306	3311	924	—	6210	1140	10 407	2370
D/G-Ss	$\Delta_\Upsilon(\delta)$	15	14	—	—	137 130	106 950	3538	244 095	3552
	$\Upsilon_\Upsilon(\upsilon)$	188	79	—	—	26 586	48 060	2160	74 834	2239
	$\Theta_\Lambda(\theta)$	825	281	—	—	—	51 057	3538	51 882	3819
CTC	$\Upsilon(\rho)$	245	120	—	—	—	—	810	245	930
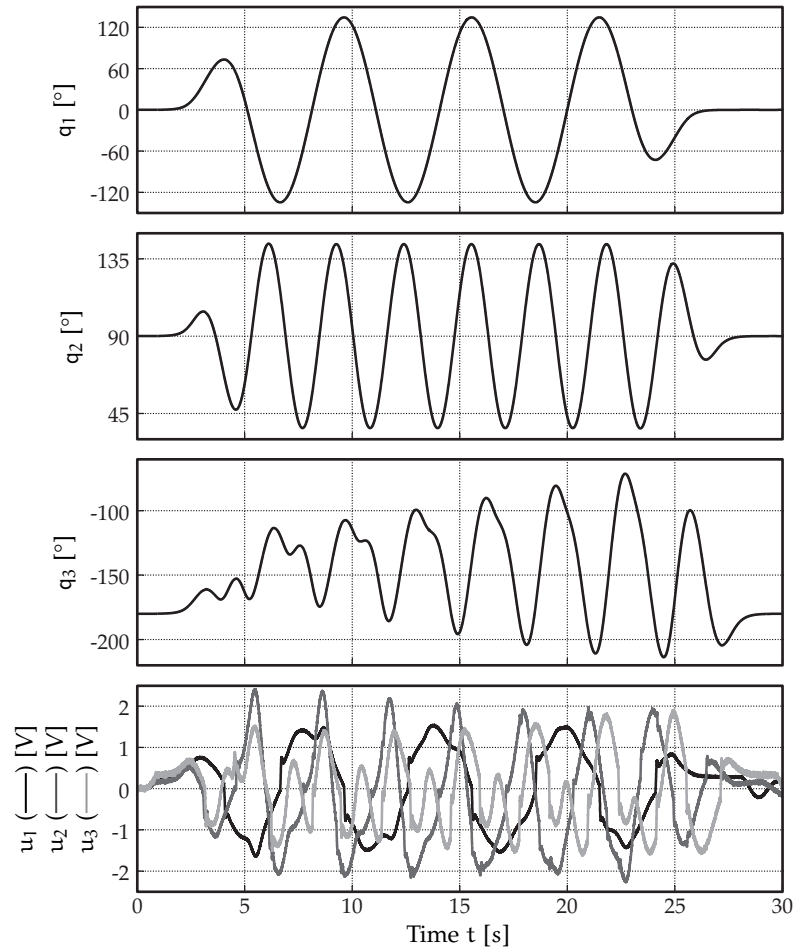
Figure 6.3: Simulation results of reference tracking control of the robotic manipulator using a full scheduling order OF LPV controller synthesized by a two-stage multiplier approach using the parameterization via $\Lambda(\delta)$.
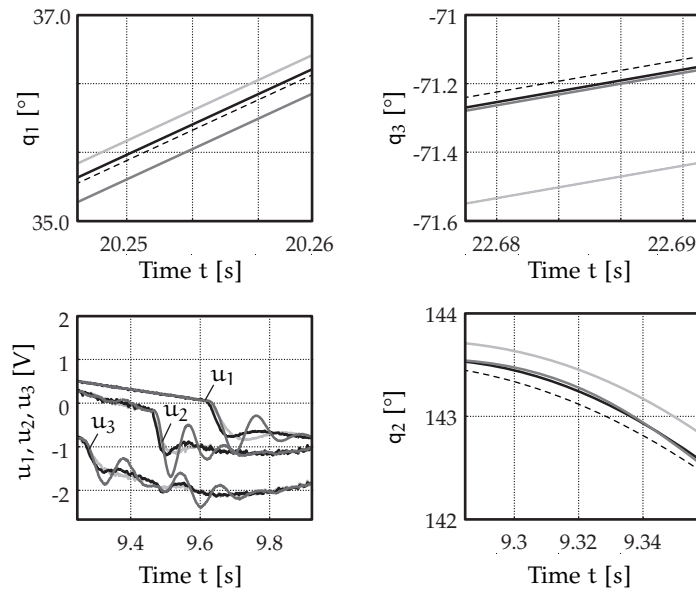
Figure 6.4: Comparison of simulation results of reference tracking control of the robotic manipulator using full scheduling order controllers.

(——) OF LPV controller synthesized by a two-stage multiplier approach using the parameterization via $\Lambda(\delta)$.

(——) Combined CTC-OF LTI-$\mathcal{H}_\infty$ controller.

(——) OF LPV controller synthesized by a standard single-stage D/G-S approach using the affine parameterization via $\Lambda(\theta)$.

(-----) Dashed lines indicate the reference trajectory.

6.1.4 *Reduced Scheduling Order Output-Feedback Linear Parameter-Varying Control*

The purpose of the following reduced scheduling order OF LPV controller designs is to showcase the ability of the modeling framework presented in Chap. 4 and the modified two-stage multiplier LFT-LPV synthesis methods presented in Chap. 5, Sect. 5.1 to approximate LPV plants of high scheduling complexity with simpler ones, while achieving low implementation complexity and maintain high control performance. The synthesis methods (i)–(iii) from Sect. 6.1.3 are again applied and evaluated.

6.1.4.1 *Synthesis and Simulation Results*

Tab. 6.3 lists synthesis, simulation and complexity results for reduced scheduling order control of the robotic manipulator. The associated approximate models with their respective parameter blocks are derived in Sect. 4.6 and listed in Tab. 4.3 on p. 144. The data for the evaluation of control performance, synthesis and implementation complexity follows the figures detailed in Sect. 6.1.3.

Table 6.3: OF controller synthesis options for the robot models with various reduced scheduling order parameterizations.
$\bullet/(\bullet)$: The first value indicates quantities associated with the LMI-based existence conditions using—in some cases—a two-stage multiplier approach, cf. Thm. 2.17, p. 66, and Cor. 5.1, p. 160, whereas values in parentheses indicate quantities associated with the LMI-based derivation of controller parameters.

| | | | **OF Control/Synth. Performance** | | | | | | | |
| | | | RMSE [°] | | | | | Synthesis Complexity | | |
Syn.	**Blk.**	γ	q_1	q_2	q_3	Avg.	E_u	$t[\bullet]$	$d[\bullet]$	$s[\bullet]$
FBMs	$\hat{\Upsilon}(\hat{v})$	0.50	0.031	0.029	0.034	0.031	2.62	5.4 s/(14.8 s)	643/(992)	376/(121)
FBMs + D/G-Ss	$\hat{\Upsilon}(\hat{\delta})$	0.50	0.027	0.022	0.031	0.027	2.62	6.3 s/(17.8 s)	733/(992)	304/(121)
	$\hat{\Upsilon}(\hat{v})$	0.48	0.022	0.030	0.034	0.029	2.64	6.9 s/(28.6 s)	659/(992)	216/(121)
D/G-Ss	$\hat{\Delta}_\Upsilon(\hat{\delta})$	0.51	0.025	0.072	0.060	0.052	2.60	20.3 s/(117.9 s)	691/(1892)	280/(169)
	$\hat{\Upsilon}_\Upsilon(\hat{v})$	0.48	0.023	0.054	0.051	0.042	2.65	6.2 s/(20.2 s)	617/(1056)	192/(125)
CTC	$\Upsilon(\rho)$	1.00	0.058	0.053	0.086	0.066	2.64	3.5 s	300/(810)	84/(54)

The FBM-based controllers of reduced scheduling order achieve significantly improved performance over the full scheduling order controllers at only slightly elevated control effort. All reduced scheduling order LPV controllers perform better than the CTC design at reduced or lower control effort. The figures indicating the synthesis complexity are still consistently higher than the LTI-$\mathcal{H}_\infty$ CTC design. However, they are reduced over the full scheduling order cases.

Differences between the parameterizations in terms of $\hat{\delta}$ and $\hat{\upsilon}$ appear to show improved performance for the latter. When visualizing the amount of overbounding induced by the respective parameterizations, cf. Fig. 6.5, it becomes obvious that evaluating $\hat{\upsilon}$ over all admissible δ incurs a larger amount of overbounding than evaluating $\hat{\upsilon}$ over all admissible υ. The reason resides in the fact that in the course of the automated parameterization as per Alg. 4.1 on p. 137 in Sect. 4.5, the extrema of each newly introduced set of parameters are determined via a dense gridding of the measurable set of signals. Due to this approach, the conservatism introduced initially by covering transcendental terms as parameters δ is slightly amended.
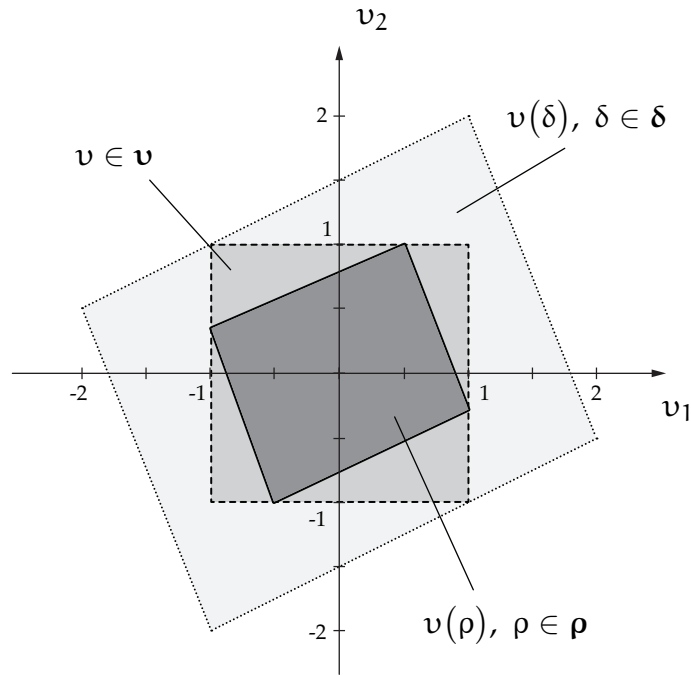
Figure 6.5: Compact sets of admissible values of the parameters υ_1 and υ_2 resulting from different parameterizations of $\upsilon(\bullet)$.

6.1.4.2 *Implementation Complexity*

Tab. 6.4 lists the implementation complexity of each synthesized controller in terms of the required arithmetic operations $\mathsf{a}[\bullet]$ and scalar variables $\mathsf{m}[\bullet]$ to be stored. The reduced number of arithmetic operations and memory requirements for the respective approximate blocks is again taken from Tab. 4.4 on p. 144.

By selecting a D/G-Ss-based reduced scheduling order controller synthesized via the parameterization in terms of the parameter block $\hat{\Upsilon}_\Upsilon(\hat{\upsilon})$, the implementation complexity is reduced to about a third of that of the least costly full scheduling order controller. The CTC design still requires significantly less implementation effort, but results in twice the average root mean square error (RMSE).

Table 6.4: Implementation complexity for OF controllers synthesized on reduced scheduling order robot models.

		No. of Arith. Ops./Mem. Req.								
		Blk.		$\hat{\Delta}^K(\bullet)$		LFT	Matrices		Total	
Syn.	**Blk.**	a[•]	m[•]	a[•]	a[•]	m[•]	a[•]	m[•]	a[•]	m[•]
FBMs (+ D/G-Ss)	$\hat{\Upsilon}(\dot{\bullet})$	75	52	468	294	111	5310	990	5679	1336
D/G-Ss	$\hat{\Delta}_\Upsilon(\hat{\delta})$	7	8	—	—	15 315	37 350	1890	52 972	383
	$\hat{\Upsilon}_\Upsilon(\hat{v})$	56	30	—	—	—	3294	924	3350	954
CTC	$\Upsilon(\rho)$	245	120	—	—	—	—	810	245	930

6.1.5 *Summary and Discussion*

LPV controller synthesis for both full and reduced scheduling order plant representations is successfully conducted yielding very good performance. The two-stage multiplier approach for PIDLF-based OF LPV controller synthesis as per Thm. 2.17 using FBMs in the first and D/G-Ss in the second multiplier stage via the application of Cor. 5.1 on p. 160 significantly reduces the implementation and synthesis complexity in almost all cases.

FULL SCHEDULING ORDER CONTROL
The application of systematic modeling tools from Chap. 4 for exact, low complexity model representations makes it possible to synthesize controllers that can provide closed-loop stability and performance guarantees. In a previous publication [E37], this was considered impractical. Furthermore, the conservatism introduced through the automated affine parameterization of the block $\Upsilon(\bullet)$ is seemingly reduced over the manual parameterization approach presented in [E48].

The proposed methods reduce the number of arithmetic operations for online implementation by 96 % from 244 095 to 10 407, when comparing the best performing controllers synthesized via the standard D/G-S-based LFT-LPV approach to the novel two-stage multiplier approach. Control performance is maintained (even slightly improved), while the respective associated total time consumed during synthesis is reduced by 95 % from 754.2 s to 36.7 s.

In conclusion, the option for full scheduling order synthesis with the best performance, synthesis and implementation complexity is found to be an OF LPV controller synthesized by a two-stage multiplier approach using the parameterization in terms of $\Lambda(\delta)$. The synthesis and complexity analysis results clearly show a disadvantage of fully affine parameterizations and a synthesis approach that aims for affine scheduling via D/G-Ss for plants with a high number of parameters. The benefits in implementation complexity due to the small-in-size full parameter block

representations render the seemingly more intutitive gains from affine scheduling void.

Reduced Scheduling Order Control

The application of systematic modeling tools from Chap. 4 and novel approximation methods introduced in Sect. 4.5 yield approximate, low complexity model representations that appear to maintain relevant plant information for high performance control. The conservatism of the design is reduced, which may be either a result of the truncation of scheduling parameters that are less relevant for the control problem or better numerical conditions due to the reduction of the synthesis complexity.

The implementation complexity of the FBMs-based controllers is reduced by about a half over the full scheduling order case. However, the conventional D/G-S-based LFT-LPV synthesis using the parameterization in terms of the automatically derived affine parameters $\hat{v}$ is now less costly to implement. This is mainly a consequence of the approximation rendering the generalized inertia matrix parameter-independent, thus resulting in a fully affine plant parameterization.

The loss of closed-loop stability and performance guarantees can be amended by recovery via an *a posteriori* analysis along the lines of [E46]. In this work, an iterative approach at solving the associated bilinear matrix inequalities (BMIs) for performance optimization has been performed successfully for the case that only 2-DOF are controlled. The method of parameter set mapping [79] was used to obtain an approximate plant model. Due to the fact that the performance using the novel approximation in the venue of Sect. 4.5 does in fact yield improved control performance, such an iteration is not expected to result in further improvements without the use of PDLFs. In light of this, the proposed methods can be regarded as an efficient tool to synthesize high performance, low complexity initial controllers for structured LPV control with a pre-specified scheduling policy.

Tab. 6.5 summarizes the above-mentioned synthesis options and compares experimental control performance, synthesis complexity in terms of the total solver time as well as implementation complexity for online computation of the controllers' state space matrices. The results are grouped by full/reduced scheduling order and ordered by increasing performance.

The state-of-the-art CTC design outperforms all LPV controllers in terms of implementation complexity. It is assumed that by some retuning, the performance disadvantage may be reduced. However, the proposed LPV control methodology can also be applied for plants, in which only a partial cancellation of nonlinear terms via feedback or feedforward control is possible. In light of this, the methods achieve a significant improvement in terms of both synthesis complexity and implementation complexity that approaches the CTC methodology. A combination of both approaches to the extent possible therefore promises to result in an efficient high performance controller design methodology. The CMG is a plant that allows such an approach and will be considered in the next section.

Table 6.5: Summary of synthesis results obtained for the robot model. Tracking accuracy from simulation results, solver time and implementation complexities ares shown.

Sched. Order	Block	Syn.	Perf.		Syn.	Impl.	
			RMSE [°]	E_u	$t[\bullet]$	$a[\bullet]$	$m[\bullet]$
Full	$\Delta_\gamma(\delta)$	OF-PIDLF, FBM+D/G-S	0.050	2.60	33.7 s	10 042	2184
Red.	$\hat{\Upsilon}_\gamma(\hat{\upsilon})$	OF-PIDLF, D/G-S	0.042	2.65	26.4 s	3350	954
	$\hat{\Upsilon}(\hat{\delta})$	OF-PIDLF, FBM+D/G-S	0.027	2.62	24.1 s	5679	1336

6.2 A Four-Degrees-of-Freedom Control Moment Gyroscope

IN the following, experimental real-time LPV control of a laboratory scale control moment gyroscope will be investigated. Sect. 6.2.1 will outline the problem setup and matters of investigation. Sects. 6.2.2 and 6.2.3 consider the application of SF LPV control techniques on both full and reduced scheduling order models, whereas Sect. 6.2.4 considers OF LPV control based on the reduced scheduling order models. A summary is provided in Sect. 6.2.5.

6.2.1 *Problem Setup*

Reconsider the LPV model representations of the CMG derived in Sect. 4.7, pp. 145 for use in both OF as well as SF control settings.

Throughout the sections, the controller designs are based on the following control objectives:

(i) Guaranteed closed-loop performance and stability,

(ii) Fast reference tracking in gimbals three and four,

(iii) Fast input disturbance rejection,

(iv) Low synthesis and implementation complexity.

Item (i) will only be strictly guaranteed for synthesis results based on the full scheduling order models under the assumption that the models are exact. However, the suitability of the controllers synthesized based on the reduced scheduling order for *a posteriori* analysis in the venue of [E45] will be discussed. In connection to items (ii) to (iv), the CMG will prove an illustrative example of a trade-off between potentially conservative full scheduling order control and high performance reduced scheduling order control. W. r. t. synthesis complexity, a comparison between standard LFT-LPV-based state-feedback and improved conditions derived in Sect. 5.2 that exploit a descriptor-style LPV model representation will illustrate significant advantages. However, the best performance is still achieved by reduced scheduling order controllers.

Tab. 6.6 provides an overview about the respectively synthesis options that will be conducted. Each of these can in turn be performed on one of the factorization/-modeling options FMAX/FMIN, PFCMAX/PFCMIN and MOP.

Table 6.6: Synthesis options conducted on the CMG models.

Sched. Order	Model	Block	OF		SF			
			D/G-S	FBM	Std., Thm. 5.1		Impr'd., Prop. 5.1	
			PıDLF	PıDLF	PıDLF	PDLF	PıDLF	PDLF
Full	FMax	$\Delta_\gamma(\delta)$	×	×	×	✓	×	✓
	FMin	$\Delta_\gamma(\delta)$	×	×	×	✓	×	✓
	PFCMax	$\Delta_\gamma(\delta)$	×	×	×	✓	×	✓
	PFCMin	$\Delta_\gamma(\delta)$	×	×	×	✓	×	✓
Red.	PFCMin	$\hat{\Upsilon}(\hat{v})$	×	✓	×	×	×	×
	PFCMin	$\hat{\Upsilon}_\gamma(\hat{v})$	✓	×	✓	✓	✓	✓
	MOP	$\bar{\Delta}_\gamma(\bar{\delta})$	×	×	×	✓	×	✓

Quantitative performance criteria assessed in the following will consist of the rise times in both gimbals three and four, t_{rq_3} and t_{rq_4}, respectively, as well as the total average RMSE. In addition, the control effort will be accounted for by

$$E_u \stackrel{\triangle}{=} \frac{1}{T} \int_0^T \sum_{i=1}^2 u_i^2 \, dt.$$

6.2.2 *Full Scheduling Order State-Feedback Linear Parameter-Varying Control*

State-feedback controller synthesis is considered for the full scheduling order plant model of the CMG. I. e., synthesis will be based on the exact plant representations FMax/FMin and PFCMax/PFCMin. For minimum conservatism, parameterizations in terms of the respective blocks $\Delta(\delta)$ are used.

6.2.2.1 *Generalized Plant Configuration and Controller Implementation*

A standard S/KS weighting scheme—borrowed from [E94]—is employed for the generalized plant in state-feedback configuration, which is depicted in Fig. 6.6. The shaping filters

$$W_S(s) = \begin{bmatrix} W_{S3} & \\ & W_{S4} \end{bmatrix}, \qquad W_{KS}(s) = \begin{bmatrix} W_{KS1} & \\ & W_{KS2} \end{bmatrix},$$
$$W_{S3}(s) = 4.5\tfrac{1}{s}, \qquad W_{KS1}(s) = 5 \cdot 10^5 \tfrac{s+0.83}{s+4.59\cdot10^5},$$
$$W_{S4}(s) = 4.0\tfrac{1}{s}, \qquad W_{KS2}(s) = 5 \cdot 10^5 \tfrac{s+0.23}{s+2.31\cdot10^5},$$

are used, which have been derived after fine tuning.

The augmentation of the CMG plant model by dynamic weighting filters requires the implementation of these filters as part of a dynamic controller of which only
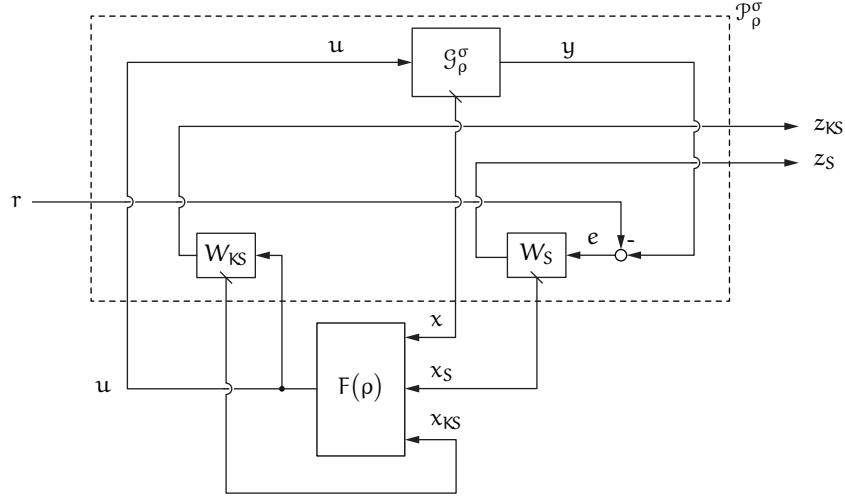
Figure 6.6: Generalized plant configuration of the SF gain controller synthesis for the CMG.

the time-varying state-feedback gain $F(\delta)$ is synthesized by convex optimization. For implementation, the shaping filters' output gains are set to identity, s.t. their respective states are fed to the state-feedback gain. Consequently, the resulting state-feedback-based dynamic controller is implemented as indicated in Fig. 6.7.

The access to the state vector of a dynamic system is indicated by the diagonal line crossing the border of the block.
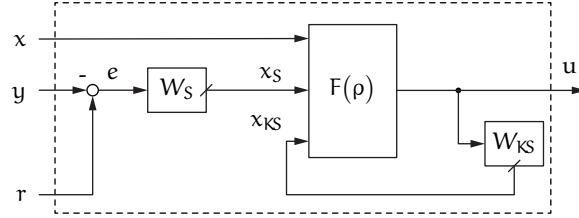
Figure 6.7: Implementation scheme of the SF gain controller for the CMG.

6.2.2.2 *Design of the Parameter-Dependent Lyapunov Function*

Based on prior attempts at controlling the CMG [E94], a PDLF is expected to be required. Indeed, the attempt of synthesizing a state-feedback controller with a PIDLF based on the exact plant models fails and is discarded. The following basic parameterization of the Lyapunov matrix is used.

$$
\begin{aligned}
S(\delta) = Q^\top(\delta)SQ(\delta) &\in \mathcal{C}^1(\delta, \mathbb{S}^{n_x}), \quad S(\delta) \succ 0 \; \forall \delta \in \delta, \\
&= S_{00} + \sum_{i=1}^{3}\left(\delta_i\left(\begin{bmatrix} S_{i0} \\ 0 \end{bmatrix} + \begin{bmatrix} S_{i0}^\top & 0 \end{bmatrix} + \sum_{j=1}^{3}\frac{\delta_j}{2}\begin{bmatrix} \left(S_{ij}+S_{ij}^\top\right) & 0 \\ 0 & 0 \end{bmatrix}\right)\right)
\end{aligned}
\tag{6.5}
$$

This structure is achieved by the factorization

$$Q(\delta) \triangleq \begin{bmatrix} \delta_1 I_{n_x^G \times n_x^P} \\ \delta_2 I_{n_x^G \times n_x^P} \\ \delta_3 I_{n_x^G \times n_x^P} \\ I_{n_x^P} \end{bmatrix} = \begin{bmatrix} \delta_1 \begin{bmatrix} I_{n_x^G} & 0 \end{bmatrix} \\ \delta_2 \begin{bmatrix} I_{n_x^G} & 0 \end{bmatrix} \\ \delta_3 \begin{bmatrix} I_{n_x^G} & 0 \end{bmatrix} \\ I_{n_x^P} \end{bmatrix}, \quad S \triangleq \begin{bmatrix} S_{11} & S_{12} & S_{13} & S_{10} \\ \bullet & S_{22} & S_{23} & S_{20} \\ \bullet & \bullet & S_{33} & S_{30} \\ \bullet & \bullet & \bullet & S_{00} \end{bmatrix}, \qquad (6.6)$$

$$\text{where } S_{ij} \in \begin{cases} \mathbb{R}^{n_x^G \times n_x^P}, & i \in \{1,2,3\}, j = 0, \\ \mathbb{R}^{n_x^G \times n_x^G}, & i,j \in \{1,2,3\}, i \neq j, \\ \mathbb{S}^{n_x^G \times n_x^G}, & i = j \in \{1,2,3\}, \\ \mathbb{S}^{n_x^P \times n_x^P}, & i = j = 0 \end{cases}.$$

Tests on possible parameter-dependencies of the Lyapunov function are performed based on the model PFCMIN with full scheduling order and a state-feedback synthesis performed by improved LMI conditions as per Prop. 5.1. During synthesis D/G-scalings are used to render the synthesis problem tractable. In each case, the parameter-dependency is restricted to the part of the Lyapunov matrix corresponding to the physical states, as defined in (6.6). Figure 6.8 illustrates the results in terms of the achieved performance indices γ versus all combinations of including the parameters δ_i, $i \in \{1,2,3\}$ in a PDLF of the form (6.6). Here, e.g., $\neg\delta_i$ indicates that δ_i is not included. It turns out that parameters $\rho_1 = q_2$, $\rho_2 = q_3$ and $\rho_3 = \dot{q}_1$, cf. Tab. 4.7 on p. 154, contribute significantly to an improved performance, which is in accordance to the findings in [E94], where the approximate plant model based on a linearization about a MOP is considered.

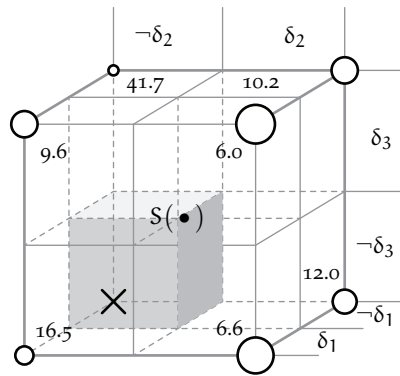Figure 6.8: SF synthesis results in terms of the achieved performance index γ for different PDLF parameterizations for the CMG PFCMIN plant model with full scheduling order.

Based on these findings, the effects of considering only the part of the Lyapunov matrix that corresponds to the physical states and the inclusion of mixed/quadratic terms is further investigated. The results are presented in Tab. 6.7.

Table 6.7: SF synthesis results using the improved synthesis conditions from Prop. 5.1 in terms of the achieved performance index γ for different PDLF parameterizations for the CMG PFCMin plant model with full scheduling order.

Mixed/Quadr. Terms	Gen. Plant States	SF Control/Synth. Performance							
		γ	t_{rq_3}	t_{rq_4}	RMSE	E_u	$t[\bullet]$	$d[\bullet]$	$s[\bullet]$
✓	✓	5.7	3.3 s	2.4 s	17.8	1.6	15.1 min	5100	342
	✗	6.0	3.5 s	2.6 s	18.2	1.4	2.5 min	3099	248
✗	✓	7.1	4.2 s	2.9 s	19.5	1.3	12.1 min	4080	342
	✗	7.1	4.2 s	2.9 s	19.5	1.3	2.8 min	2979	284

As apparent from Tab. 6.7 the inclusion of quadratic and mixed terms has a strong beneficial effect on the control performance without significantly affecting the synthesis time or number of decision variables. This is in contrast to the claim mentioned in [E94], which may be explained by the additional conservatism induced by D/G-scalings that is alleviated through a more complex PDLF parameterization. In fact, the increase in decision variables is only small compared to the number incurred by the multiplier-based synthesis technique.

Moreover, the benefit of including parameter-dependencies in the portions of the PDLF that correspond to generalized plant filter states is negligible compared to the strongly increased synthesis complexity. W. r. t. the implementation complexity assessed by the evaluation of the number of arithmetic operations $a\lceil F(\delta) \rceil$ necessary to compute the state-feedback gain in each time instant, the restriction of the PDLF according to (6.6) is negligible.

6.2.2.3 *Improved vs. Standard State-Feedback Synthesis*

Throughout the above-shown sets of synthesis data (Tab. 6.7), SF synthesis conditions improved for descriptor LPV systems according to Prop. 5.1 have already been used. To indicate the potential in reducing the number of decision variables, size of LMIs and, consequently, synthesis time, various SF controller synthesis options are compared in Tab. 6.8. For this purpose, the PDLF is selected as (6.6) and D/G-Ss are used to evaluate multiplier conditions.

As expected, control performance is not affected by the use of the improved conditions. Synthesis complexity, however, is strongly reduced. Tab. 6.9 lists the relative reductions, revealing that in average the number of decision variables, size of LMIs and synthesis time is reduced by 43.4 %, 17.6 % and 88.9 %, respectively.

Tab. 6.10 lists synthesis data for the cases that a PDLF with mixed/quadratic terms and parameter-dependency w. r. t. all generalized plant states is used in conjunction with the PFCMin CMG model. Even though, the major part of the synthe-

Table 6.8: PDLF-based SF controller synthesis options for the various CMG models of full scheduling order.

Synth.	Model	PDLF	SF Control/Synth. Performance							
			γ	t_{rq_3}	t_{rq_4}	RMSE	E_u	$t[\bullet]$	$d[\bullet]$	$s[\bullet]$
Prop. 5.1	FMAX $\Delta_\gamma(\delta)$ ✓		6.1	3.5 s	2.9 s	18.3	1.3	4.6 min	3495	260
	FMIN							5.1 min	3604	266
	PFCMAX $\Delta_\gamma(\delta)$ ✓		6.0	3.5 s	2.6 s	17.2	1.5	3.1 min	3294	254
	PFCMIN							2.5 min	3099	248
Thm. 5.1	FMAX $\Delta_\gamma(\delta)$ ✓		6.1	3.5 s	2.9 s	18.3	1.3	39.2 min	6459	320
	FMIN							46.7 min	6610	326
	PFCMAX $\Delta_\gamma(\delta)$ ✓		6.0	3.5 s	2.6 s	17.2	1.5	28.3 min	5745	304
	PFCMIN							22.7 min	5214	294

Table 6.9: Reduction in synthesis complexity due to application of Prop. 5.1 for the PDLF-based SF controller synthesis for various full scheduling order CMG models .

Model	Block	Relative Reduction		
		$d[\bullet]$	$s[\bullet]$	$t[\bullet]$
FMAX	$\Delta_\gamma(\delta)$	45.9 %	19.8 %	88.4 %
FMIN	$\Delta_\gamma(\delta)$	44.5 %	18.4 %	89.1 %
PFCMAX	$\Delta_\gamma(\delta)$	42.7 %	16.5 %	89.1 %
PFCMIN	$\Delta_\gamma(\delta)$	40.6 %	15.6 %	88.9 %
Average		43.4 %	17.6 %	88.9 %

sis complexity is incurred through the use of fully parameterized Lyapunov matrix, the improvements still amount to 68.4 % reduction in synthesis time.

Table 6.10: Comparison of SF controller synthesis options for the PFCMIN CMG model of full scheduling order with fully PDLF.

Model Block		SF Synth. Performance		Reduction
		Std., Thm. 5.1	Impr'd., Prop. 5.1	
PFCMIN $\Delta_\gamma(\delta)$	γ	5.7	5.7	
	$t[\bullet]$	47.7 min	15.1 min	68.4 %
	$d[\bullet]$	7549	5100	32.4 %
	$s[\bullet]$	388	342	11.9 %

6.2.2.4 *Implementation Complexity*

Due to the generalized plant configuration and model structure, most of the generalized plant matrices are parameter-independent and it remains to compute

$$F(\delta) = - \left(D_{pu}^\top D_{pu} \right)^{-1} \left(\gamma B_u^\top(\delta) S^{-1}(\delta) + D_{pu}^\top C_p \right). \tag{6.7}$$

The input gain matrix $B_u(\delta)$ only contains non-zero entries in the third to fifth row. The leading term $- \left(D_{pu}^\top D_{pu} \right)^{-1}$ amounts to a constant, scalar gain and the term $D_{pu}^\top C_p$ is zero except for a diagonal 2×2 matrix in the last two columns. The implementation complexity is therefore approximately assessed by considering $a[F(\rho)] \approx a[S^{-1}(\rho)]$.

A look-up table (LUT)-based implementation can trade the number of arithmetic operations against memory. It turns out that storing the state-feedback gain in 45 different grid points (810 scalar variables) from taking three for δ_1 and δ_2, as well as five for δ_3, respectively, results in consistent control performance, although rigorous closed-loop guarantees are rendered void.

In order to further reduce the memory requirements, the SF controller synthesis using a PDLF dependent on δ_1 and δ_2 only can also be considered. As indicated in Fig. 6.8, the drop in performance by omitting δ_3 from the Lyapunov matrix parameterization is not severe. At the cost of increased synthesis effort, a PDLF with parameter-dependence included also in portions associated with the generalized plant states may partially recover the performance deterioration. Tab. 6.11 indicates that by this reasoning a performance index of $\gamma = 6.17$ is attained and rise times lower accordingly. Consequently, storing the SF gain in 9 different grid points (162 scalar variables) from taking three for δ_1 and δ_2, results in adequate performance.

Tab. 6.12 provides a comprehensive list of both required arithmetic operations and stored scalar variables for the full scheduling order SF controllers. Both the cases when the parameter-dependent Lyapunov matrix is constructed and inverted online (Comp.), as well as a look-up table-based implementation (LUT) are considered. The inversion of the 9×9 Lyapunov matrix requires 486 operations not considering positive definiteness. Due to mixed/quadratic parameter-dependencies in

the matrices, an additional 495 (for a PDLF dependent on δ_1, δ_2 and δ_3) and 225 (for a PDLF dependent on δ_1 and δ_2 only) operations are required for the construction of the matrix to be inverted.

In conclusion, controllers based on the PFCMIN CMG model involve a negligible amount of extra implementation complexity due to the partial feedback cancellation at significantly reduced synthesis effort and slightly improved performance. If a fully parameterized PDLF dependent on δ_1 and δ_2 only is used in conjunction with the PFCMIN CMG model, a slight deterioration in performance is traded against significantly reduced LUT-based implementation complexity.

Table 6.11: SF synthesis result comparison for reduced implementation complexity using the improved synthesis conditions from Prop. 5.1 in terms of the achieved performance index γ for different PDLF parameterizations for the CMG PFCMIN plant model with full scheduling order.

PDLF	Gen. Plant States	SF Control/Synth. Performance							
		γ	t_{rq_3}	t_{rq_4}	RMSE	E_u	$t[\bullet]$	$d[\bullet]$	$s[\bullet]$
$\delta_1, \delta_2, \delta_3$	✓	5.7	3.3 s	2.4 s	17.8	1.6	15.1 min	5100	342
	✗	6.0	3.5 s	2.6 s	18.2	1.4	2.5 min	3099	248
$\delta_1, \delta_2, \neg\delta_3$	✓	6.2	3.6 s	2.8 s	18.7	1.4	9.7 min	4218	270
	✗	6.6	3.8 s	2.9 s	19.0	1.2	2.7 min	2779	208

Table 6.12: Implementation complexity for SF controllers synthesized on full scheduling order CMG models.

Type	PDLF	Model	No. of Arith. Ops./Mem. Req.							
			Parameters		SF Gain		PFC		Total	
			$a[\bullet]$	$m[\bullet]$	$a[\bullet]$	$m[\bullet]$	$a[\bullet]$	$m[\bullet]$	$a[\bullet]$	$m[\bullet]$
Comp.	$\delta_1, \delta_2, \delta_3$	F $\Delta_\gamma(\delta)$	4	4	985	300	—	—	989	304
		PFC $\Delta_\gamma(\delta)$	4	4	985	300	73	6	1062	310
	$\delta_1, \delta_2, \neg\delta_3$	PFC $\Delta_\gamma(\delta)$	2	2	711	378	73	6	786	386
LUT	$\delta_1, \delta_2, \delta_3$	F $\Delta_\gamma(\delta)$	4	2	—	810	—	—	4	812
		PFC $\Delta_\gamma(\delta)$	4	2	—	810	73	6	77	818
	$\delta_1, \delta_2, \neg\delta_3$	PFC $\Delta_\gamma(\delta)$	4	2	—	162	73	6	77	243

6.2.2.5 *Simulation Results*

Figure 6.9 depicts an exemplary closed-loop simulation using a SF controller synthesized based on the full scheduling order CMG PFCMIN model and a PDLF dependent on δ_1, δ_2 and δ_3 in portions associated with the physical states including mixed/quadratic dependence. As apparent from the results, all scheduling parameters remain within the prespecified bounds and the control performance is satisfactory. Further performance data is listed in Tab. 6.8 on p. 195.
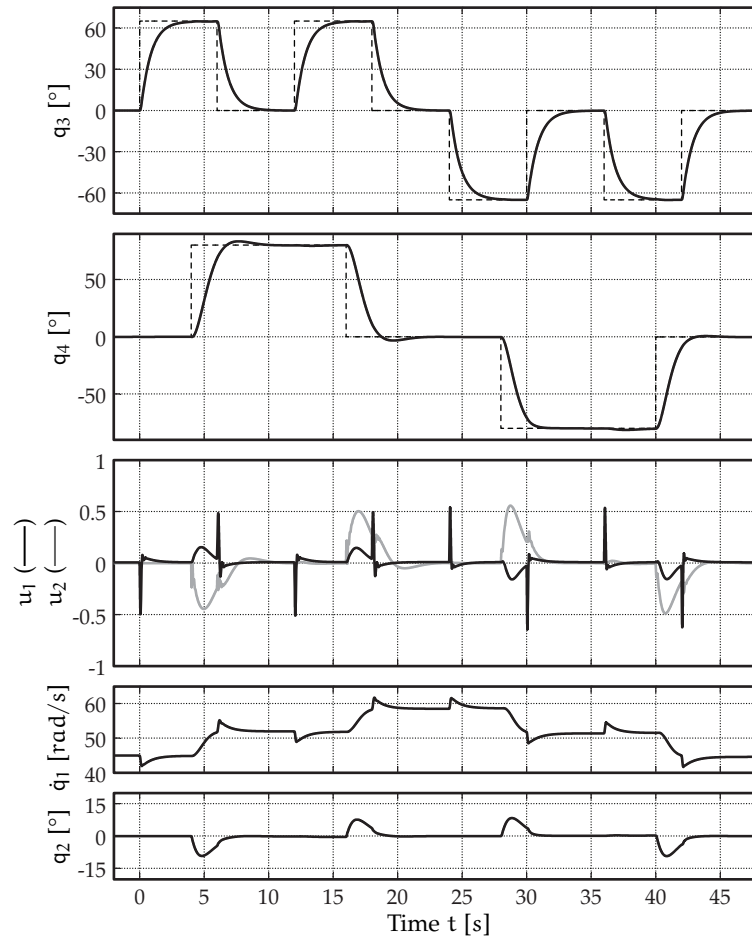

Figure 6.9: Simulation results of reference tracking of the CMG with full scheduling order.
(——) Solid lines indicate signals.
(-----) Dashed lines indicate the reference trajectory.

6.2.2.6 *Experimental Validation*

The SF controllers synthesized via improved LMIs and based on the full scheduling order CMG models PFCMIN and FMIN are tested in real-time experiments, cf. Fig. 6.10. Tab. 6.13 lists the achieved performance indices.

Table 6.13: Experimental performance for SF controllers on the full scheduling order CMG.

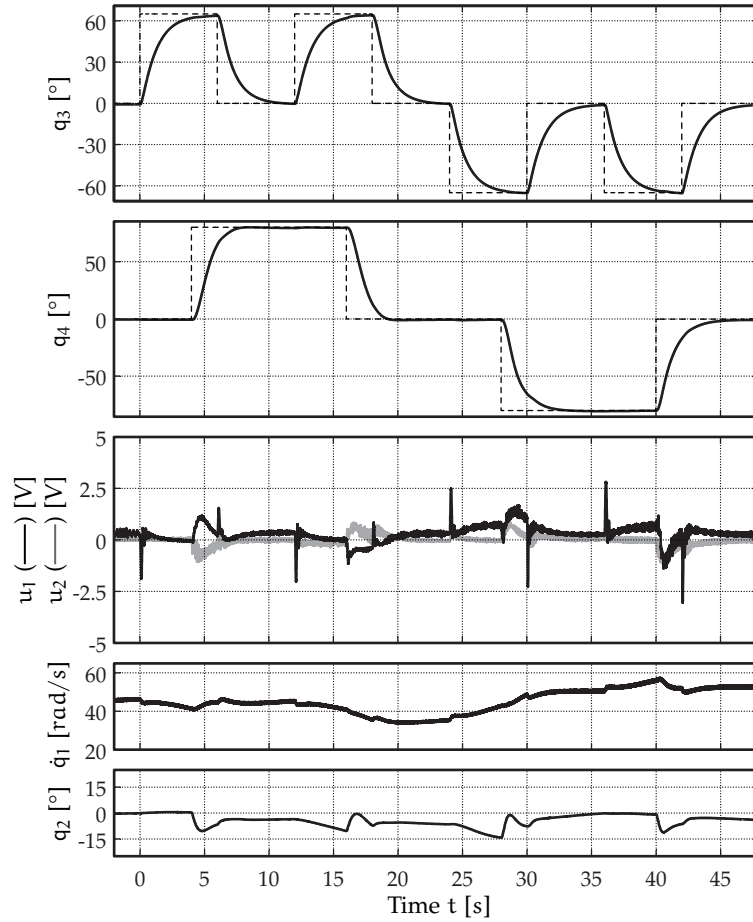| Model	Exp. SF Ctrl. Perf.			
	t_{rq_3}	t_{rq_4}	RMSE	E_u
PFCMIN $\Delta_\gamma(\delta)$	3.46 s	2.63 s	18.1306	2.1659
FMIN $\Delta_\gamma(\delta)$	3.52 s	2.89 s	18.2056	2.1997

Figure 6.10: Experimental results of reference tracking control of the CMG using a SF controller synthesized based on the full scheduling order CMG PFCMIN model.
(——) Solid lines indicate signals.
(- - - - -) Dashed lines indicate the reference trajectory.

6.2.3 *Reduced Scheduling Order State-Feedback Linear Parameter-Varying Control*

The previous section showed that for the CMG satisfactory control performance can be achieved by synthesizing a state-feedback controller based on the full non-approximate plant model. The incurred implementation complexity matches the one obtained in [E94], which used the approximate model obtained through linearization about a moving operating point (MOP) in order to render the gridding-based LPV controller synthesis tractable. As a comparison, in this section LPV controller synthesis is based on the approximate plant model of the CMG derived in Sect. 4.7, p. 145, for the purpose of reducing both synthesis and implementation complexity. In this section state-feedback controller synthesis is considered and a generalized plant configuration identical to the one described in Sect. 6.2.2.1 and depicted in Fig. 6.6 on p. 192 is used.

6.2.3.1 *Choice of Lyapunov Functions and Shaping Filters*

It turns out that the approximate plant model of the CMG derived in Sect. 4.7, p. 145, in terms of $\hat{\Upsilon}_\Upsilon(\hat{v})$ does not require a PDLF during synthesis to achieve feasibility and good performance. Thus, besides reducing the synthesis effort by an approximate plant model, the implementation complexity of the resulting controller is also reduced. However, the shaping filters have been retuned to

$$
W_S(s) = \begin{bmatrix} W_{S3} & \\ & W_{S4} \end{bmatrix}, \qquad W_{KS}(s) = \begin{bmatrix} W_{KS1} & \\ & W_{KS2} \end{bmatrix},
$$
$$
W_{S3}(s) = 14\tfrac{1}{s}, \qquad\qquad W_{KS1}(s) = 3 \cdot 10^3 \tfrac{s+0.77}{s+9295},
$$
$$
W_{S4}(s) = 14\tfrac{1}{s}, \qquad\qquad W_{KS2}(s) = 1 \cdot 10^4 \tfrac{s+0.57}{s+7559},
$$

in order to achieve the best control performance.

Due to the low complexity of the reduced scheduling order model, a PDLF is expected to not incur strongly increased synthesis complexity. Consequently, the following parameterization is chosen

$$
Q(v) \triangleq \begin{bmatrix} \delta_1 I_{n_x^G \times n_x^P} \\ \delta_2 I_{n_x^G \times n_x^P} \\ I_{n_x^P} \end{bmatrix}, \quad S \triangleq \begin{bmatrix} S_{11} & S_{12} & S_{10} \\ \bullet & S_{22} & S_{20} \\ \bullet & \bullet & S_{00} \end{bmatrix}, \tag{6.8}
$$

$$
\text{where } S_{ij} \in \begin{cases} \mathbb{R}^{n_x^G \times n_x^P}, & i \in \{1,2\}, j = 0, \\ \mathbb{R}^{n_x^G \times n_x^G}, & i,j \in \{1,2\}, i \neq j, \\ \mathbb{S}^{n_x^G \times n_x^G}, & i = j \in \{1,2\}, \\ \mathbb{S}^{n_x^P \times n_x^P}, & i = j = 0 \end{cases}.
$$

Again, a retuning to

$$W_S(s) = \begin{bmatrix} W_{S3} & \\ & W_{S4} \end{bmatrix}, \qquad W_{KS}(s) = \begin{bmatrix} W_{KS1} & \\ & W_{KS2} \end{bmatrix},$$

$$W_{S3}(s) = 5.5\tfrac{1}{s}, \qquad\qquad W_{KS1}(s) = 5 \cdot 10^2 \tfrac{s+1.15}{s+1155},$$

$$W_{S4}(s) = 3.5\tfrac{1}{s}, \qquad\qquad W_{KS2}(s) = 6 \cdot 10^2 \tfrac{s+0.57}{s+695},$$

is performed for optimizing the resulting performance in the cases where a PDLF is used.

The approximate model based on linearization (MOP) requires PDLFs, in order to yield acceptable results [E94]. Therefore, a PDLF dependent on δ_1, δ_2 and δ_3 in portions associated with the physical states including mixed/quadratic dependence as in Sect. 6.2.2 is used. Consequently, implementation of a controller based on the CMG MOP model is as costly as the controllers synthesized based on the full scheduling order models (partial feedback cancellation (PFC)/full model (F)) derived in this thesis. Controller synthesis schemes based on the CMG MOP model therefore serve the purpose of reducing the synthesis complexity.

6.2.3.2 *Synthesis Results and Complexity*

Tab. 6.14 lists data on the synthesis complexity with respect to the models of reduced scheduling order. While synthesis based on the novel approximation takes less than a second due to PIDLFs, synthesis time based on the MOP model is significantly reduced by application of Prop. 5.1. However, the use of PDLF w. r. t. the CMG PFCMIN model also incurs significantly less synthesis complexity than in the case of the CMG MOP model, while the performance characteristics are improved.

Table 6.14: SF controller synthesis options for CMG models of reduced scheduling order.

Synth.	Model		PDLF	SF Control/Synth. Performance							
				γ	t_{rq_3}	t_{rq_4}	RMSE	E_u	$t[\bullet]$	$d[\bullet]$	$s[\bullet]$
Prop. 5.1	PFCMIN	$\hat{\Upsilon}_\Upsilon(\hat{v})$	✓	5.3	2.4 s	2.5 s	17.3	1.6	7.1 s	579	112
			✗	17.4	3.4 s	2.7 s	17.2	1.5	0.7 s	54	32
	MOP	$\bar{\Delta}_\Upsilon(\bar{\delta})$	✓	5.8	3.4 s	2.8 s	18.0	1.3	1.0 min	2033	212
Thm. 5.1	PFCMIN	$\hat{\Upsilon}_\Upsilon(\hat{v})$	✓	5.3	2.4 s	2.5 s	17.3	1.6	7.4 s	579	112
			✗	17.4	3.4 s	2.7 s	17.2	1.5	0.8 s	54	32
	MOP	$\bar{\Delta}_\Upsilon(\bar{\delta})$	✓	5.8	3.4 s	2.8 s	18.0	1.3	5.8 min	3597	256

6.2.3.3 *Implementation Complexity*

For PIDLFs, no inverse is required for the computation of the state-feedback gain

$$F(\delta) = - \left(D_{pu}^{\top} D_{pu} \right)^{-1} \left(\gamma B_{u}^{\top}(\delta) S^{-1} + D_{pu}^{\top} C_{p} \right).$$ (6.9)

Consequently, a symbolic expression can be found that requires a minimum number of arithmetic operations during online implementation. The SF gain resulting from PIDLF-based synthesis w. r. t. the reduced scheduling order model PFCMIN is

$$F(\upsilon) = \begin{bmatrix} 1.10 & 0.00 & 0.00 & 0.12 & 0.00 & -0.23 & 0.00 & 2.10 & 0.00 \\ 0.00 & 0.34 & -0.04 & 0.00 & 0.11 & 0.00 & -0.07 & 0.00 & 0.82 \end{bmatrix}$$
$$+ \frac{\upsilon_2 \cdot 10^{-6}}{3.3 \cdot 10^{-3} \upsilon_2 - 1.0} \begin{bmatrix} -27.0 & 0.0 & 0.0 & -3.0 & 0.0 & 5.5 & 0.0 & 4.1 & 0.0 \\ 0.0 & 0.0 & 0.0 & 0.0 & 0.0 & 0.0 & 0.0 & 0.0 & 0.0 \end{bmatrix}.$$ (6.10)

As apparent from (6.10), the SF gain is nearly constant. In contrast—as mentioned above—implementing the controller synthesized based on the MOP model is as costly as the full scheduling order controllers. Comparable performance is only achieved, if the Lyapunov matrix is chosen to depend on δ_1, δ_2 and δ_3. As before, the controller can be stored in a LUT using 810 scalars. Recall that in constrast to this, the PDLF-based controller synthesized with the reduced scheduling order CMG PFCMIN model is only scheduled on two parameters, υ_1 and υ_2. It turns out that a look-up table implementation with 162 scalars is sufficient for maintaining the controlled response. However, the parameters $\upsilon_1(\rho)$ and $\upsilon_2(\rho)$ need to be computed online, which amounts to $a[\hat{\upsilon}(\rho)] = 126$ arithmetic operations, cf. Tab. 4.10 on p. 157. An additional $a[u_F(\rho)] = 73$ operations are required for the PFC. Tab. 6.15 lists a comprehensive enumeration of both required arithmetic operations and stored scalar variables for the reduced scheduling order SF controllers. Both the cases when the parameter-dependent Lyapunov matrix is constructed and inverted online (Comp.), as well as a look-up table-based implementation (LUT) are considered. The inversion of the 9×9 Lyapunov matrix requires 486 operations not considering positive definiteness. Due to mixed/quadratic parameter-dependencies in the matrices, an additional 495 (MOP) and 225 (MOP) operations are required for the construction of the matrix to be inverted. As before, the number of arithmetic operations required to compute the SF gain is approximated by $a[F(\rho)] \approx a[S^{-1}(\rho)]$ due to the constant performance channel matrices.

In conclusion, a LUT-based implementation is considerably more efficient in all cases. While the PDLF-based online computations in both PFCMIN and MOP cases are within the same order, the LUT-based implementation in the PFCMIN case shows a clear advantage. However, since $\hat{\upsilon}$ is a function of all six measurable signals, a gridding has to be performed in terms of $\hat{\upsilon}_1$ and $\hat{\upsilon}_2$. This prevents further considerations to trade online computations versus LUTs. The PIDLF-based controller with SF gain (6.10) may also be approximated by the nominal constant SF gain for even further reduced implementation complexity (not shown).

Table 6.15: Implementation complexity for SF controllers synthesized on reduced scheduling order CMG models.

Type	PDLF	Model	No. of Arith. Ops./Mem. Req.							
			Parameters		SF Gain		PFC		Total	
			$a[\bullet]$	$m[\bullet]$	$a[\bullet]$	$m[\bullet]$	$a[\bullet]$	$m[\bullet]$	$a[\bullet]$	$m[\bullet]$
Comp.	✗	PFCMin $\hat{\Upsilon}_\Upsilon(\hat{\upsilon})$	126	51	11	16	73	6	210	73
	✓	PFCMin $\hat{\Upsilon}_\Upsilon(\hat{\upsilon})$	126	51	711	190	73	6	910	320
		MOP $\bar{\Delta}_\Upsilon(\bar{\delta})$	4	4	981	300	—	—	985	304
LUT	✗	PFCMin $\hat{\Upsilon}_\Upsilon(\hat{\upsilon})$	126	51	—	54	73	6	199	111
	✓	PFCMin $\hat{\Upsilon}_\Upsilon(\hat{\upsilon})$	126	51	—	162	73	6	199	219
		MOP $\bar{\Delta}_\Upsilon(\bar{\delta})$	4	4	—	810	—	—	4	814

In light of the simulation results and synthesis complexity shown in Tab. 6.14, both PDLF- and PiDLF-based controllers synthesized based on the PFCMin CMG model are superior to the one synthesized based on the MOP CMG model.

6.2.3.4 *Experimental Validation*

Tab. 6.16 lists quantities that indicate the experimental control performance for the respective controllers. From this evaluation, the PDLF-based SF controller synthesized based on the reduced scheduling order CMG PFCMin model performs significantly better than the other controllers, which show similar performance. The experimental results are in accordance with the simulation results shown in Tab. 6.14.

Table 6.16: Experimental performance for SF controllers on the reduced sched. order CMG.

PDLF	Model	Exp. SF Ctrl. Perf.			
		t_{rq_3}	t_{rq_4}	RMSE	E_u
✓	PFCMin $\hat{\Upsilon}_\Upsilon(\hat{\upsilon})$	2.49 s	2.54 s	16.8	2.1
	MOP $\bar{\Delta}_\Upsilon(\bar{\delta})$	3.38 s	2.76 s	17.9	1.9
✗	PFCMin $\hat{\Upsilon}_\Upsilon(\hat{\upsilon})$	3.42 s	2.81 s	17.1	2.1

Figure 6.11 shows experimental results of reference tracking control of the CMG using the PiDLF-based SF controller synthesized based on the reduced scheduling order CMG PFCMin model. For comparison, Fig. 6.12 indicates the improvement in performance via the PDLF-based SF controller synthesized based on the reduced

scheduling order CMG PFCMin model. As apparent, the decreased rise time in q_3 comes at the price of increased cross-coupling effects.

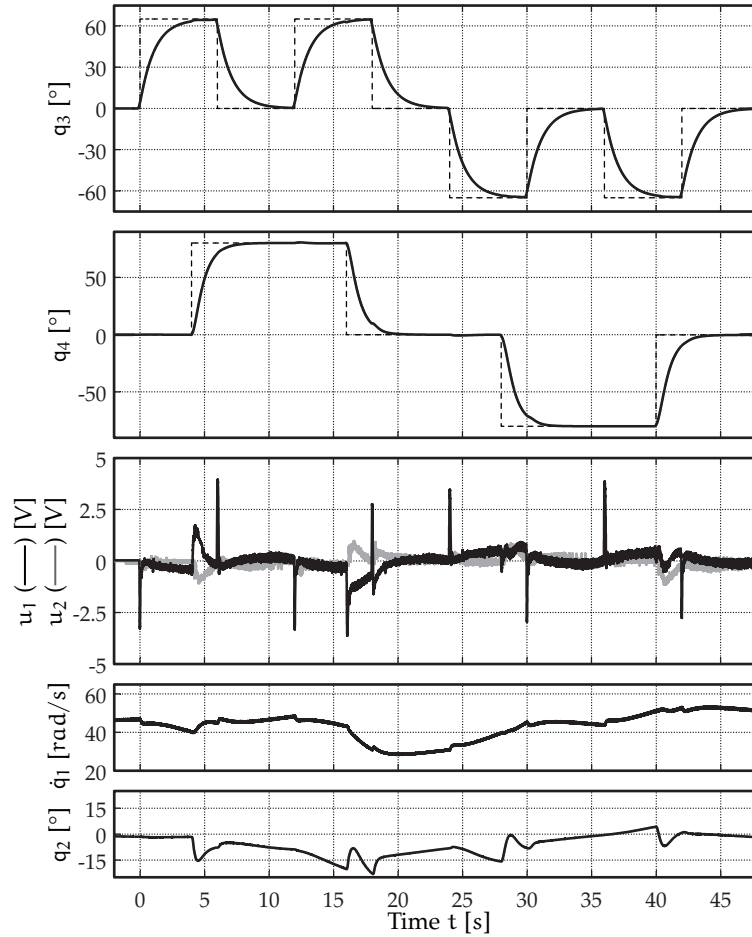Figure 6.11: Experimental results of reference tracking of the CMG using a SF controller synthesized based on the reduced scheduling order CMG PFCMin model.
(——) Solid lines indicate signals.
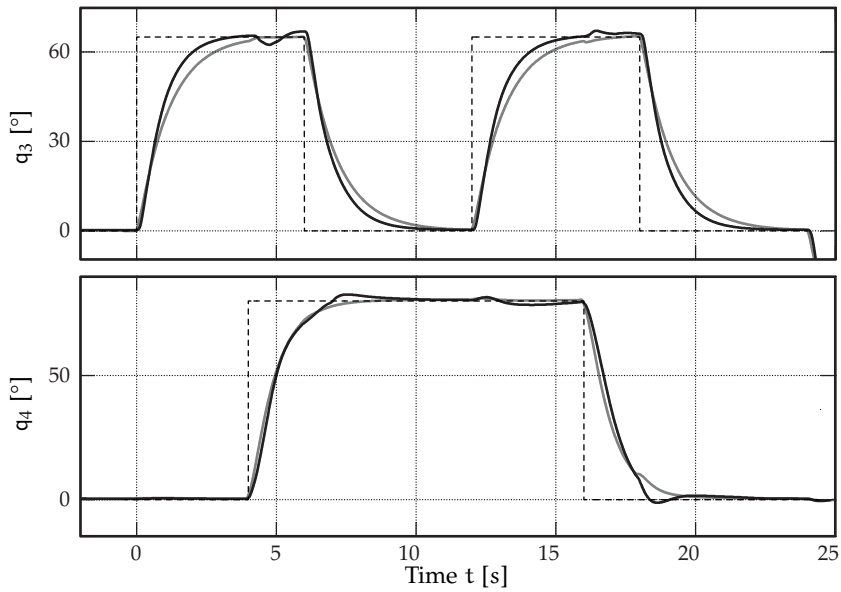(- - - - -) Dashed lines indicate the reference trajectory.

Figure 6.12: PDLF vs. PIDLF: Comparison of experimental results of reference tracking control of the CMG using a SF controller synthesized based on the reduced scheduling order CMG PFCMIN model.
(——) Black lines: PDLF-based SF controller.
(——) Gray lines: PIDLF-based SF controller.
(-----) Dashed lines indicate the reference trajectory.

6.2.4 *Reduced Scheduling Order Output-Feedback Linear Parameter-Varying Control*

The previous sections illustrated the synthesis of SF controllers for both full and reduced scheduling order models. It has been shown that—with tractable effort—SF controllers providing closed-loop guarantees can be designed either by considering exact complex models or by synthesizing controllers that render *a posteriori* analysis for recovering closed-loop stability and performance guarantees particularly simple [E45]. These designs resulted in satisfactory control performance.

The synthesis of OF controllers is more involved, as it generally requires twice the number of LMIs and hence decision variables. Furthermore, implementation complexity is increased in both PIDLF- and PDLF-based synthesis over the SF case. However, OF control schemes are conceptually appealing as they integrate the optimization of state observation and filtering into the controller design process. For this reason, in the following, an OF controller is designed for the CMG PFCMIN and FMIN model.

6.2.4.1 *Generalized Plant Configuration and Implementation Complexity*

The best output-feedback controller synthesis results have been obtained by a four-block design [141], which takes into account input disturbances explicitly and pro-

vides the angular velocity states $x_{\dot{q}} = \begin{bmatrix} \dot{q}_2, \dot{q}_3, \dot{q}_4 \end{bmatrix}^\top$ as additional feedback signals over the controlled variables $y_q = \begin{bmatrix} q_3, q_4 \end{bmatrix}^\top$. The corresponding generalized plant configuration is shown in Fig. 6.13.
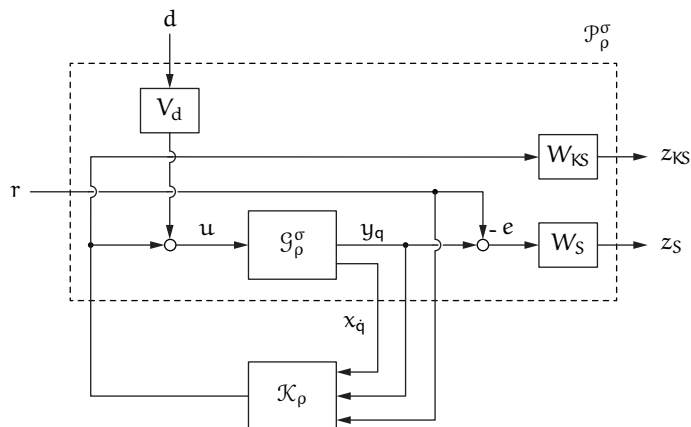

Figure 6.13: Generalized plant configuration for OF controller synthesis for the CMG.

The shaping filters are tuned to

$$W_S(s) = \begin{bmatrix} W_{S3}(s) \\ & W_{S4}(s) \end{bmatrix}, \quad W_{KS}(s) = \begin{bmatrix} W_{KS1}(s) \\ & W_{KS2}(s) \end{bmatrix},$$

$$W_{S3}(s) = \frac{4}{5}\frac{s+7.5}{s+0.006}, \qquad W_{KS1}(s) = 100\frac{s+5.33}{s+666.6},$$

$$W_{S4}(s) = \frac{4}{5}\frac{s+3.0}{s+0.0024}, \qquad W_{KS2}(s) = 100\frac{s+1.33}{s+166.7},$$

$$V_d(s) = \begin{bmatrix} V_{d1}(s) \\ & V_{d2}(s) \end{bmatrix}, \qquad \begin{aligned} V_{d1}(s) &= 5, \\ V_{d2}(s) &= 10. \end{aligned}$$

In contrast to the SF design, the OF controller does not require manual augmentation by dynamic weighting filters and the controller dynamics are explicitly synthesized through convex optimization. The output-feedback controller is synthesized via the LFT-LPV synthesis technique presented in [124] by using FBMs and D/G-S directly due to the low number of parameters in the reduced scheduling order parameter set. Consequently, the controller's scheduling function will vary and be based on the approximate plant's parameter block. Based on the results from Sect. 3.1 the implementation complexity for the OF controllers is assessed *a priori* in Tab. 6.17 for both the CMG PFCMIN and FMIN model. Synthesis complexity is not assessed *a priori*, as it is expected to be tractable for all reduced scheduling order cases. Details and sizes w. r. t. the respective blocks for the CMG PFCMIN and FMIN model are given in Tabs. 4.8 and 4.9 on p. 154.

As apparent from Tab. 6.17, the implementation complexity resulting from OF controllers synthesized based on the CMG PFCMIN model is the lowest. Any controller design based on the CMG FMIN model would therefore have to show increased performance to be preferable.

Table 6.17: Implementation complexity for OF controllers synthesized on reduced scheduling order CMG models.

Syn.	Model	No. of Arith. Ops./Mem. Req.									
		$\hat{\Upsilon}(\hat{\rho})$		$\hat{\Delta}^K(\hat{\Upsilon})$		LFT	Matrices		PFC		Total	
		a[•]	m[•]	a[•]	m[•]	a[•]	a[•]	m[•]	a[•]	m[•]	a[•]	m[•]
D/G-S	FMIN $\hat{\Upsilon}(\hat{v})$	141	47	—	—	538	2480	336	—	—	3159	383
	PFCMIN $\hat{\Upsilon}(\hat{v})$	126	51	—	—	271	1856	300	73	6	2326	357
FBM	FMIN $\hat{\Upsilon}(\hat{v})$	156	62	1764	630	210	1584	308	—	—	3714	1000
	PFCMIN $\hat{\Upsilon}(\hat{v})$	138	62	1277	504	87	1056	286	73	6	2631	858

Note, however, that a LUT-based implementation incurs about the same complexity for each controller. In this case the computation of the reduced scheduling order parameters $\hat{v}$ requires $a[\hat{v}] = 126$ (PFCMIN) or $a[\hat{v}] = 141$ (FMIN), respectively. For each grid point, 176 scalars need to be stored, which amounts to $n_g^{n_{\hat{v}}} \cdot 176$ scalars in total for a regular gridding. Since $n_{\hat{v}} = 2$ and $n_g = 3$ leads to 1584 scalars, while for four grid points the number of scalars to be stored already exceed the number of online arithmetic operations for implementation as the LFT-based controller.

6.2.4.2 *Synthesis Complexity and Simulation Results*

Tab. 6.18 lists data on the synthesis complexity and nonlinear simulation results w. r. t. the reduced scheduling order OF controllers in closed loop with the full nonlinear model[1]. As apparent from the data, synthesis options based on the CMG PFCMIN model perform better with the same multiplier constraints. Furthermore, a significant improvement of FBMs over D/G-Ss can be observed in the case of both models.

6.2.4.3 *Experimental Validation*

Tab. 6.19 lists the experimental results of both OF controllers synthesized based on the reduced scheduling order CMG PFCMIN model with FBMs and D/G-Ss. Some downtuning was required to maintain stable closed-loop behaviour during the experiments, since the high performance achieved in q_3 incurred more pronounced coupling effects than during simulation. The FBM-based controller still achieves a significantly shorter rise time in q_3, whereas differences in $t_{r_{q_4}}$ diminish. The increased RMSE is due to stronger coupling effects. However, the FBM-based con-

---

1 For a fair comparison the shaping filters for all but the FBM PFCMIN case were relaxed to $W_{S3}(s) = \frac{4}{5}\frac{s+3.75}{s+0.003}$, $W_{S4}(s) = \frac{4}{5}\frac{s+1.65}{s+0.00132}$, i. e., allowing for some overshoot that, however, does not occur. This significantly improved the results.

Table 6.18: OF controller synthesis options for CMG models of reduced scheduling order. $\bullet/(\bullet)$: The first value indicates quantities associated with the LMI-based existence conditions, cf. Thm. 2.17, p. 66, whereas values in parentheses indicate quantities associated with the LMI-based derivation of controller parameters.

		OF Control/Synth. Performance							
Syn.	**Model**	γ	t_{rq_3}	t_{rq_4}	RMSE	E_u	$t[\bullet]$	$d[\bullet]$	$s[\bullet]$
D/G-S	FMIN $\hat{\Upsilon}_\gamma(\hat{\upsilon})$	11.1	3.6 s	5.7 s	21.2	1.1	1.1 s/(3.2 s)	117/(338)	102/(120)
	PFCMIN $\hat{\Upsilon}_\gamma(\hat{\upsilon})$	8.9	2.5 s	3.6 s	18.9	1.3	0.9 s/(3.9 s)	107/(302)	94/(112)
FBM	FMIN $\hat{\Upsilon}_\gamma(\hat{\upsilon})$	3.3	2.5 s	2.5 s	16.4	1.7	1.0 s/(3.8 s)	181/(325)	134/(152)
	PFCMIN $\hat{\Upsilon}_\gamma(\hat{\upsilon})$	2.7	0.8 s	2.1 s	15.1	1.9	1.1 s/(5.8 s)	163/(308)	126/(144)

troller shows less excessive control action. This is confirmed in a comparison of the experimental signals in Fig. 6.11.

Table 6.19: Experimental performance for OF controllers on the reduced scheduling order CMG plant.

		Exp. OF Ctrl. Perf.			
Synth.	**Model**	t_{rq_3}	t_{rq_4}	RMSE	E_u
D/G-S	PFCMIN $\hat{\Upsilon}(\hat{\upsilon})$	2.0 s	2.6 s	16.6	2.5
FBM	PFCMIN $\hat{\Upsilon}(\hat{\upsilon})$	1.2 s	2.6 s	15.7	2.1

6.2.5 *Comparison and Summary*

LPV controller synthesis for both full and reduced scheduling order plant representations is successfully conducted yielding satisfactory performance. In all cases the use of the PFCMIN CMG model has resulted in the best or equal performance as well as synthesis and implementation complexity characteristics. In the following, the results of this section are summarized and discussed.

FULL SCHEDULING ORDER STATE-FEEDBACK CONTROL
The application of systematic modeling tools from Chap. 4 for exact, low complexity model representations makes it possible to synthesize controllers that can provide closed-loop stability and performance guarantees. Synthesis complexity is significantly reduced, when the standard synthesis conditions as per Thm. 5.1 are combined with the improved outer factor representations for descriptor LPV systems via Prop. 5.1. In the case of the CMG, the reduction in complexity amounts
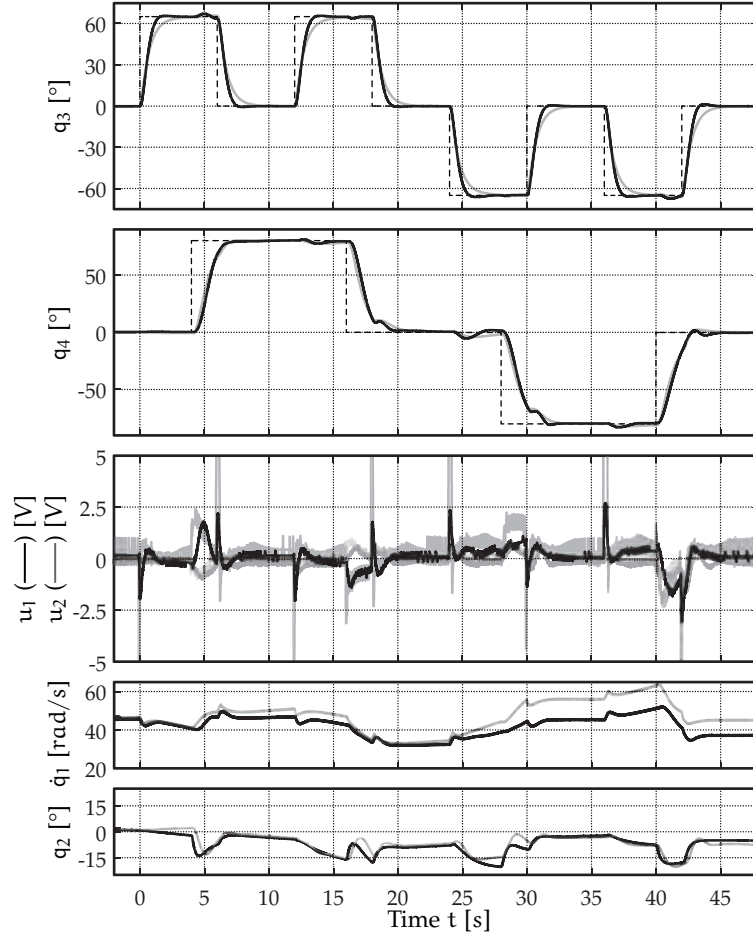
Figure 6.14: Comparison of experimental results of reference tracking control of the CMG using an OF controllers synthesized based on the reduced scheduling order CMG PFCMIN model with FBMs and D/G-Ss (transparent overlay).
(——) Solid lines indicate signals.
(- - - -) Dashed lines indicate the reference trajectory.

to an average of 88.9 % in synthesis time at maintained performance levels. Via the use of PFC and the possibilities of the automated factorization and descriptor LPV modeling framework, the solver time is therefore reduced from a worst case of 46.7 min to 2.5 min. Several PDLFs are investigated and a trade-off between synthesis and implementation complexity at only minor differences in performance is discussed. In conclusion, the best options for full scheduling order synthesis are

(i) **Best Performance/Synthesis Complexity**: SF controller synthesis based on the PFCMIN CMG model with a PDLF parameterized in parts associated with physical plant states in δ_1, δ_2 and δ_3 with mixed/quadratic terms,

(ii) **Best Performance/Implementation Complexity**: SF controller synthesis based on the PFCMin CMG model with a fully parameterized PDLF in δ_1, δ_2 and δ_3 with mixed/quadratic terms.

Reduced Scheduling Order Control

The application of systematic modeling tools from Chap. 4 and novel approximation methods introduced in Sect. 4.5 yield approximate, low complexity model representations that maintain relevant plant information for high performance control. In the case of the CMG, the automated affine parameterization of the small-in-size descriptor LPV parameter blocks yields exact models that appear to be too conservative to be used for synthesis. However, conservatism is reduced in the course of approximation by truncating parameters from parameter blocks that appear to contribute only negligibly to the relevant nonlinear characteristics. Closed-loop stability and performance guarantees are rendered void if these models are used for synthesis, but may be recovered analytically, verified experimentally or via simulations. Synthesis complexity is significantly reduced, which facilitates the tuning process. In the case of the CMG, the reduction in complexity amounts to synthesis times well below $10\,s$ in all cases making use of the novel approximations. In contrast, the quantitative characteristics of synthesis and implementation results using an approximation based on a moving operating point essentially range in the order of the newly obtained full scheduling order results described above, while—strictly speaking—not providing closed-loop guarantees.

The low complexity plant representations permit further design choices in the trade-off between performance versus implementation complexity: While a PiDLF-based SF controller can maintain the performance levels of the full scheduling order controllers at very low synthesis and implementation complexity, both PDLF-based SF and PiDLF-based OF controllers achieve significantly better performance at the cost of increased implementation complexity. The PiDLF-based OF controllers incur an implementation complexity of approximately twice the number of arithmetic operations and stored variables compared to the PDLF-based SF controllers, the use of FBMs results in the best performance of all controllers tested in both simulation and experiments. In conclusion the best options for reduced scheduling order controllers are

(i) **Best Performance/Synthesis Complexity**: OF controller synthesis based on the approximate PFCMin CMG model with a PiDLF and FBMs,

(ii) **Best Performance/Implementation Complexity**: SF controller synthesis based on the approximate PFCMin CMG model with a PiDLF.

Tab. 6.20 summarizes the above-mentioned synthesis options and compares experimental control performance, synthesis complexity in terms of the total solver time as well as implementation complexity for either LUT-based implementation or online computation (Comp.). The results are grouped by full/reduced scheduling order and SF/OF control approaches and ordered by increasing performance.

Table 6.20: Summary of synthesis results obtained for the PFCMin CMG model. Experimentally validated rise times, solver time and implementation complexities are shown.

| Sched. Order | Block | Syn. | Perf. | | Syn. | Impl. Cmplx. | | | |
| | | | t_{rq_3} | t_{rq_4} | $t[\bullet]$ | LUT | | Comp. | |
						$a[\bullet]$	$m[\bullet]$	$a[\bullet]$	$m[\bullet]$
Full	$\Delta\gamma(\delta)$	SF-PDLF, (δ_1, δ_2)	3.6 s	2.8 s	9.7 min	77	243	786	386
	$\Delta\gamma(\delta)$	SF-PDLF, $(\delta_1, \delta_2, \delta_3)$	3.5 s	2.6 s	2.5 min	77	818	1062	310
Red.	$\hat{\Upsilon}_\gamma(\hat{\upsilon})$	SF-PIDLF	3.4 s	2.7 s	0.7 s	199	111	210	73
	$\hat{\Upsilon}_\gamma(\hat{\upsilon})$	SF-PDLF, (υ_1, υ_2)	2.4 s	2.5 s	7.1 s	199	219	910	320
	$\hat{\Upsilon}_\gamma(\hat{\upsilon})$	OF-PIDLF, D/G-Ss	2.0 s	2.6 s	4.8 s	—	—	2326	357
	$\hat{\Upsilon}(\hat{\upsilon})$	OF-PIDLF, FBMs	1.2 s	2.6 s	6.9 s	—	—	2631	858

Part II

CONTROL OF INTERCONNECTED LINEAR PARAMETER-VARYING SYSTEMS

The centralized control of complex systems that are derived from the composition of a multitude of individual subsystems is often susceptible to failures, inefficient or even intractable. The second part of this thesis extends the linear parameter-varying (LPV) control methodology to enable the synthesis of resilient distributed control schemes that can handle heterogeneous LPV subsystem dynamics as well as arbitrary, directed and time-varying interconnection topologies at synthesis complexity levels in the order of a single subsystem.

7

STATE OF THE ART IN INTERCONNECTED SYSTEMS
CONTROL

≪/'kɒmplɛks/,   adjective.
Consisting of many different and
connected parts.≫

Microsoft Bing Search Engine

As an introduction to the extensive field of research on the analysis and control of interconnected systems, this chapter first defines and reviews important terminology, as well as basic graph theoretic fundamentals in Sect. 7.1. Section 7.2 then continues with a brief survey on distributed controller synthesis approaches. Special emphasis is put on classifying literature with respect to *subsystem* and *topology* properties considered as well as specific features of the associated synthesis approach, e. g., scalability.

The informed reader may skip to Tab. 7.1 on p. 228 for a concise summary over the related publications and a rough classification of the present work.

7.1 Interconnected Systems

Many complex systems can be regarded as assemblies of subsystems interconnected through some topology. The entirety of such an interconnected system usually has a high number of states, inputs and outputs, for which classical controller synthesis approaches are intractable. Therefore, the common approach to most methods that can handle interconnected systems resides in the exploitation of the interconnection topology's structure and similarities between subsystems.

As a means of denomination, consider the following terminology.

≪**Distributed System (DS)**≫: A distributed system (DS) is a system with spatial states, such as a system that can be represented by partial differential equations (PDEs).

≪**Interconnected System (IS)**≫: An interconnected system (IS) is a general term for a set of subsystems combined or coupled through some topology.

≪**Multi-Agent System (MAS)**≫: A multi-agent system (MAS) is a subclass of ISs, for which the subsystems are ≪agents≫. Such agents are required to be autonomous in the sense that they are not coupled but incorporate their own actuation and sensing capabilities and usually work towards achieving some goal. Their interconnection serves the purpose of information exchange only.

≪**Spatially Interconnected System (SIS)**≫: A spatially interconnected system (SIS) is a subclass of ISs, for which the subsystems incorporate spatial states inherently or through discretization and there exists coupling in the spatial states.

Remark 7.1 *In a game-theoretic interpretation, agents might also have diverging interests [139].*

In this thesis, the terms ≪information exchange≫ and ≪communication≫ are used to describe the transmission of non-physical data only, as opposed to physical coupling, which allows the exchange of energy and thus interconnection in terms of subsystem states. As such, the author is well aware that information exchange through some sort of wireless networks is usually subject to time-delays. However, time-delays are not covered in this thesis. Figure 7.1 visualizes the possible intersections in the system classes defined above.

Remark 7.2 *Over the available literature, the terminology employed is often inconsistent. E.g., [24], assume regular grid topologies when considering* SIS. *Figure 7.1 provides an attempt to showcase possible extensions.*

For the purpose of modeling ISs and DSs, essentially two approaches have emerged for system representations that are then associated with certain distributed controller synthesis methods.

(i) Systems interconnected through an arbitrary, finite topology,

(ii) Systems interconnected through a regular, infinite or periodic, grid topology.
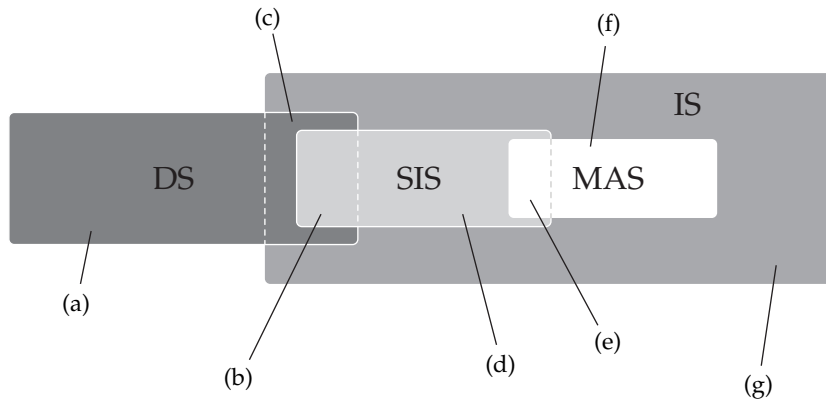
Figure 7.1: Classes of interconnected/distributed systems.

While methods related to systems interconnected through an arbitrary topology usually exploit graph theory to describe the interaction between subsystems, see, e. g., [40, 97], systems that are regularly interconnected over a grid topology are often described using shift operators to maintain information about a subsystem's location in the interconnection array, see, e. g., [24].

7.1.1 *Examples*

In order to develop an almost intuitive understanding of the terminology introduced above, consider the following examples for the respective sets and intersections.

(a) **DS \ IS:** A flexible beam or plate that is considered by continuous, i. e., non-discretized PDEs is an example that is found to be in the set of DSs but is not an IS, cf. Fig. 7.2a.

(b) **DS ∩ SIS:** If such a flexible beam or plate is discretized in space, e. g., based on the positions of piezo patches acting as both actuators and sensors [90], the system can be considered a DS *and* an SIS, cf. Fig. 7.2b.

(c) **(DS ∩ IS) \ SIS:** If a distributed system is not discretized in space, but some other dimension, e. g., time or a different abstract dimension, the system can be considered a DS *and* an IS but *not* an SIS. By slightly abusing terminology, these systems may also be discretized in space, while the actual *distance* is not a matter of interest. Examples can be found in virtual network topologies, or even distributed algorithms, cf. Fig. 7.2c.

(d) **(SIS \ DS) \ MAS:** An example for an SIS that is not modeled from discretizing a DS and does not involve autonomous agents is a train, where only the leading car is powered and the following wagons are connected, e. g., via spring-damper systems, cf. Fig. 7.2d.

(e) **SIS ∩ MAS:** A fleet of quadrotor helicopters that are physically coupled, e. g., via ropes or rigid links can be regarded as an MAS that is also an SIS. Another example can be found in swarm-like algorithms that use virtual agents to solve, e. g., NP-hard problems [64], cf. Fig. 7.2e.

(f) **MAS \ SIS:** A physically decoupled fleet of quadrocopters that exchange information on their position to achieve some formation is a pure MAS, cf. Fig. 7.2f.

(g) **IS \ (DS ∪ SIS ∪ MAS):** An IS that is neither a DS, SIS, or MAS must incorporate entities that are incapable of acting on the environment on their own, are distributed in a non-spatial sense and do not result from the discretization of a continuum. As an example, consider a distributed algorithm with entities that can directly influence another autonomous entity, which amounts to a virtual coupling, cf. Fig. 7.2g.
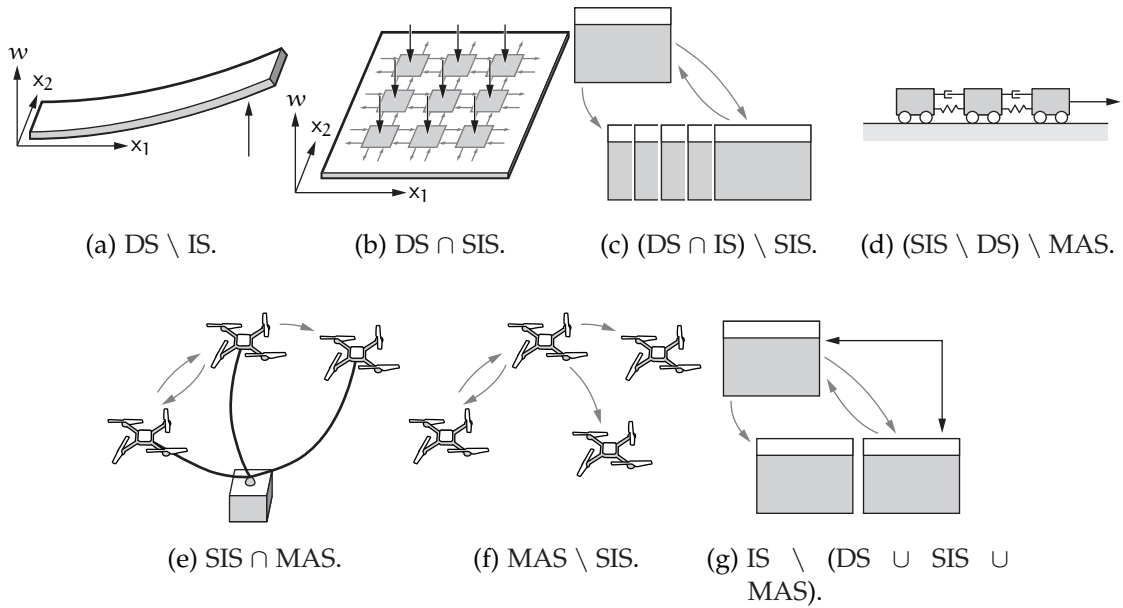

(a) DS \ IS.   (b) DS ∩ SIS.   (c) (DS ∩ IS) \ SIS.   (d) (SIS \ DS) \ MAS.

(e) SIS ∩ MAS.   (f) MAS \ SIS.   (g) IS \ (DS ∪ SIS ∪ MAS).

Figure 7.2: Examples of classes of interconnected/distributed systems.

7.1.2 *Basic Graph Theory*

Graph theory has become a useful tool for the purpose of describing networks among agents [40, 109]. In addition, the framework of «decomposable systems» introduced in [99] as well as the even more general framework introduced in [80], is facilitated by graph representations of the considered interconnections. Only the concepts most relevant for understanding the contents of this thesis are presented here. The interested reader is referred to [109] for an in-depth coverage of graph theory.

7.1.2.1 *Definitions*

First, a set of the most relevant definitions is presented that establishes graph theory as a fundamental mathematical framework to represent interaction between subsystems.

Definition 7.1 (Weighted and Directed Time-Varying Graph)
A weighted and directed time-varying graph (TVG) is defined as a triple

$$\mathcal{G}(t) = (\mathcal{V}, \, \mathcal{E}(t), \, \mathcal{W}(t)),\tag{7.1}$$

consisting of a set of h vertices, $\mathcal{V} = \{v_1, \ldots, v_h\}$, $h \in \mathbf{H} \subseteq \mathbb{N}$, a time-varying set of edges $\mathcal{E}(t) \subset \mathcal{V} \times \mathcal{V}$ and a time-varying set of associated weights $\mathcal{W}(t) \in \mathbb{R}^{\mathrm{card}(\mathcal{E}(t))}$.

In the above definition, the vertices v_k, $k \in \mathbf{H}$, correspond to the subsystems, where the index set $\mathbf{H} = \{1, 2, \ldots, h\}$ collects the indices of all subsystems. An edge $e_{ji} = (v_i, v_j) \in \mathcal{E}(t)$, $(i, j) \in \mathbf{H} \times \mathbf{H}$, indicates a connection *from* subsystem i *to* j with weight $w_{ij}(t) \in \mathcal{W}(t)$. All weights $w_{ij}(t)$ are assumed nonnegative, piecewise continuous and bounded functions of time, i.e., $w_{ij}(t) \in \{0\} \cup [a, b]$, $\forall\, (i, j) \in \mathbf{H} \times \mathbf{H}$, $\forall t \in \mathbb{R}^+$ and $0 < a \leqslant b$. Consequently, $e_{ji} = (v_i, v_j) \in \mathcal{E}(t)$ iff $w_{ij}(t) \geqslant a$. W.l.o.g. self-loops are disallowed.

Remark 7.3 *To formally accommodate cases, in which the number of subsystems may be* unknown *a priori* or time-varying, consider h a number of arbitrary size, already including those subsystems that will eventually join the interconnected system.*

Definition 7.2 (Weighted Adjacency Matrix of a TVG)
A time-varying weighted adjacency matrix $\mathscr{A}(t)$ is associated with a weighted and directed time-varying graph $\mathcal{G}(t)$. It is defined as

$$\mathscr{A}(t) \triangleq \begin{cases} w_{ij}(t), & \textit{if } e_{ji} = (v_i, v_j) \in \mathcal{E}(t), \\ 0, & \textit{otherwise.} \end{cases}\tag{7.2}$$

For each time instant, the weighted adjacency matrix $\mathscr{A}(t)$ completely characterizes a given graph $\mathcal{G}(t)$ and consequently its variation over time. Since permutations of vertices do not alter the spectral properties of the weighted adjacency matrix $\mathscr{A}(t)$, all results of this thesis are invariant over different enumerations of vertices.

A special case of Def. 7.1 is an «undirected» graph.

Definition 7.3 (Weighted and Undirected Time-Varying Graph)
A weighted and undirected TVG is defined as a graph according to Def. 7.1, where

$$w_{ij}(t) = w_{ji}(t), \; \forall\, (i, j) \in \mathbf{H} \times \mathbf{H}, \; \forall t \in \mathbb{R}^+.\tag{7.3}$$

An important observation for undirected graphs consists in the fact that $\mathscr{A}(t) = \mathscr{A}^\top(t)$, $\forall t \in \mathbb{R}^+$. The set of neighbors of a subsystem k at some time $t \in \mathbb{R}^+$ is defined as follows.

Definition 7.4 (Index Set of Neighbors of a Vertex in a TVG)

The set of indices of neighbors of a vertex i at time t is denoted as

$$\mathbf{H}_i(t) \triangleq \{k \in \mathbf{H} \mid w_{ik}(t) \geqslant a\}. \tag{7.4}$$

Consequently, the set of vertices that mark neighbors to vertex k is given by $\mathcal{N}_i(t) \triangleq \{v_k \in \mathcal{V} \mid k \in \mathbf{H}_i(t)\}$. At a particular time instant t, a «directed path» is a sequence of distinct directed edges from $\mathcal{E}(t)$. A directed graph $\mathcal{G}(t)$ is «strongly connected» at time t, if it contains a directed path from every vertex to every other vertex. A «directed spanning tree» is said to exist at time t, if there exists a vertex v_k—denoted the «root»—, from which there is a directed path to every other vertex. «Weak connectedness», in turn, denotes the existence of an *undirected* path from every vertex to every other vertex. A «rooted directed spanning tree» at time t of a graph $\mathcal{G}(t)$, is a subgraph, where every vertex has exactly one parent except for the root, which has no parent, but has a directed path to every other node.

The «in-degree» and «out-degree» of vertex v_k are defined as

$$d_k^{\mathrm{in}}(t) \triangleq \sum_{j=1}^{h} w_{kj}(t), \quad d_k^{\mathrm{out}}(t) \triangleq \sum_{j=1}^{h} w_{jk}(t) \tag{7.5}$$

A graph is called «balanced» at time t if $d_k^{\mathrm{in}}(t) = d_k^{\mathrm{out}}(t)$, $\forall k \in \mathbf{H}$. Consequently, an undirected graph is also a balanced graph for all times.

A diagonal in- and out-degree matrix can be defined as

$$\mathscr{D}^{\mathrm{in}}(t) \triangleq \operatorname*{diag}_{k=1}^{h}\left(d_k^{\mathrm{in}}(t)\right), \quad \mathscr{D}^{\mathrm{out}}(t) \triangleq \operatorname*{diag}_{k=1}^{h}\left(d_k^{\mathrm{out}}(t)\right), \tag{7.6}$$

respectively. For most purposes and if not stated otherwise, the in-degree matrix will be considered and written in short-hand notation as $\mathscr{D}(t) \triangleq \mathscr{D}^{\mathrm{in}}(t)$, as well as $d_k(t) \triangleq d_k^{\mathrm{in}}(t)$, $k \in \mathbf{H}$. Consequently, one may obtain $\mathscr{D}^{\dagger}(t)$ by application of Cor. A.1 on p. 316.

The (combinatorial) graph Laplacian matrix is defined using the in-degree matrix and the adjacency matrix.

Definition 7.5 (Graph Laplacian [109])

The graph Laplacian matrix $\mathscr{I}(t)$ is defined as

$$\mathscr{I}(t) \triangleq \mathscr{D}(t) - \mathscr{A}(t), \tag{7.7}$$

i.e.,

$$\mathscr{I}_{ij}(t) = \begin{cases} \sum_{i=1}^{h} w_{ij}(t), & \textit{if } i = j \textit{ and } \operatorname{card}(\mathcal{N}_i(t)) \neq 0, \\ -w_{ij}(t), & \textit{if } j \in \mathbf{H}_i(t), \\ 0, & \textit{otherwise.} \end{cases} \tag{7.8}$$

The Laplacian matrix can be normalized by various ways. Here, a row normalization by means of the in-degree is presented.

Remark 7.4 *Row-normalizing the Laplacian or adjacency matrix usually requires each subsystem to know the number of incoming signals during implementation. Knowing the number of recipients on the other hand is generally undesired.*

Definition 7.6 (Normalized Graph Laplacian [154])
The normalized graph Laplacian matrix $\mathscr{L}_N(t)$ is defined as

$$\mathscr{L}_N(t) \triangleq \mathscr{D}^\dagger(t)(\mathscr{D}(t) - \mathscr{A}(t)), \tag{7.9}$$

i. e.,

$$\mathscr{L}_{Nij}(t) = \begin{cases} 1, & \text{if } i = j \text{ and } \operatorname{card}(\mathcal{N}_i(t)) \neq 0, \\ -\operatorname{card}(\mathcal{N}_i(t))^{-1}, & \text{if } j \in \mathcal{N}_i(t), \\ 0, & \text{otherwise.} \end{cases} \tag{7.10}$$

As a consequence, define the row-normalized adjacency matrix as $\mathscr{A}_N(t) \triangleq \mathscr{D}^\dagger(t)\mathscr{A}(t)$. Note that for undirected graphs, the adjacency matrix $\mathscr{A}(t)$ is symmetric, whereas symmetry is lost after normalization. This also holds true for the Laplacian and its row-normalized version.

Furthermore, for graphs where the in-degree of each vertex is nonzero, $\mathscr{D}^\dagger(t)\mathscr{D}(t) = I_h$, s. t. in this case

$$\mathscr{L}_N(t) = I_h - \mathscr{A}_N(t), \qquad \mathscr{A}_N(t) = I_h - \mathscr{L}_N(t). \tag{7.11}$$

Let the symbols $\mathscr{A}(\mathcal{G}(t))$, $\mathscr{A}_N(\mathcal{G}(t))$, $\mathscr{L}(\mathcal{G}(t))$ and $\mathscr{L}_N(\mathcal{G}(t))$ denote the sets of all admissible (row-normalized) adjacency and Laplacian matrices associated with a given time-varying graph $\mathcal{G}(t)$, respectively. In the following, the association with the graph will be dropped in notation, despite the fact that a particular graph relevant to some specific problem formulation needs to be considered.

7.1.2.2 *Spectral Properties*

Denote the set $\mathbb{A}(A(t))$ as the union of the sets of momentary eigenvalues $\lambda(A(t))$ of a time-varying matrix $A(t) \in \mathbb{C}^{n \times n}$, $\forall t \geqslant 0$. By construction, the row sums of the combinatorial and row-normalized Laplacian are zero, from which it follows that 1_k is their right-hand eigenvector corresponding to the zero eigenvalue.

By Geršgorin's circle theorem [43], the spectrum of the normalized Laplacian matrix fulfills

$$\mathbb{A}(\mathscr{L}_N(t)) \subset \{\lambda \in \mathbb{C} \mid |\lambda - 1| \leqslant 1\}, \tag{7.12}$$

whereas, in the case of graphs with all vertices having non-zero in-degree, one has due to (7.11)

$$\mathbb{A}\big(\mathscr{A}_N(t)\big) \subset \{\lambda \in \mathbb{C} \mid |\lambda| \leqslant 1\}. \tag{7.13}$$

For the combinatorial graph Laplacian, however, one has

$$\mathbb{A}\big(\mathscr{L}(t)\big) \subset \left\{\lambda \in \mathbb{C} \;\middle|\; |\lambda - \overline{d^{in}}| \leqslant \overline{d^{in}}, \; \overline{d^{in}} = \max_{k \in \mathbf{H}, \; t \in \mathbb{R}^+} d_k^{in}(t)\right\}, \tag{7.14}$$

and for the unnormalized adjacency matrix

$$\mathbb{A}\big(\mathscr{A}(t)\big) \subset \left\{\lambda \in \mathbb{C} \;\middle|\; |\lambda| \leqslant \overline{d^{in}}, \; \overline{d^{in}} = \max_{k \in \mathbf{H}, \; t \in \mathbb{R}^+} d_k^{in}(t)\right\}. \tag{7.15}$$

For undirected graphs, the above statements (7.14) and (7.15) apply when restricting the spectrum to be real, $\lambda \in \mathbb{R}$.

7.2 DISTRIBUTED CONTROLLER SYNTHESIS APPROACHES

Iɴ the following distributed controller synthesis approaches are surveyed. First a classification is introduced that allows to relate the existing literature to the contributions of this thesis.

7.2.1 *Classification*

An overview of some existing approaches for the synthesis of distributed controllers is presented. The overview does not claim to be exhaustive, but covers the most prominent work, while neglecting certain extensions.

An attempt to classify the achievements in terms of their applicability to certain classes of distributed control problems is made. Such a classification can only be regarded as a crude outline and is restricted to the actual results stated in the respective publications, rather than the potential outlined or implied. The latter are therefore considered open research directions, some of which are catered to in this thesis.

The classification is divided into three main categories that regard admissible properties of the *subsystems*, of the *topology* through which these are interconnected and specific features of the respective *synthesis approach*. In the following, the categories and subcategories are briefly discussed.

7.2.1.1 *Subsystem Properties*

Admissible subsystem properties are evaluated based on whether nonlinear subsystems can be handled (mostly in LPV form). It is distinguished between the admissible type of LPV parameter-dependence, i. e., polytopic (Poly.) or LFT-based. It is further indicated, whether subsystems are allowed to incorporate «heterogeneous system dynamics» (HD) and/or may be «heterogeneously scheduled» (HS). Heterogeneous dynamics refer to differences in the state space system matrices, whereas heterogeneous scheduling (HS) refers to different LPV scheduling policies. A system may be allowed to also have both heterogeneous subsystem dynamics and scheduling (HDS). Furthermore, it is considered whether or not subsystem interaction may be restricted to be purely virtual as, e. g., in most MAS setups, or may exhibit physical coupling.

7.2.1.2 *Topology Properties*

Admissible topologies are categorized based on directedness, graph structure and time-variance. Topologies may be allowed to be fully directed (Full) or directed under the restriction of diagonalizability (Diag.). Furthermore, topologies may also be limited to be directed only between prespecified groups of subsystems (Grp.). The limiting case, when groups are considered to consist of single subsystems is discussed below.

The allowed structure of the topologies is distinguished between arbitrary (Arb.) structures usually based on graph representations and the tools from graph theory and regular (Reg.) structures that make use of shift operators to represent mostly infinite or periodic interconnections.

The time-varying nature of topologies is classified by the way, in which allowable sets of topologies are defined. Graph representations may be allowed to range within a set that is implicitly (Impl.) described, e. g., by the range of eigenvalues of the interconnection matrix. Alternatively, topologies may be allowed to explicitly (Expl.) range within a specific predetermined set of distinct graphs.

7.2.1.3 *Properties of the Synthesis Method*

The synthesis method is classified by the kind of feedback (FB) considered, namely output-feedback (OF) or state-feedback (SF). Depending on whether nonlinear subsystems are covered by the respective method, the classification also indicates whether the synthesis method is considered in a gain-scheduling (GS) or robust (RB) control fashion.

After synthesis, the guarantees available through the synthesis algorithm are listed as stability (Stab.) and performance (Perf.) guarantees separately. Finally, the degree of scalability of the approaches are estimated in the sense as how much synthesis complexity increases with the number of subsystems. Here, (−−) indicates that synthesis complexity scales at least polynomially with h, while (−) indicates a linear increase. A single plus (+) indicates synthesis complexity scales favorably with increasing number of subsystems, while ultimately the consideration of arbitrarily many subsystems will still lead to complexity issues. While the latter certainly also holds true for the evaluation with two plusses (++), in these cases the respective priors of the method allow for virtually infinite subsystems.

7.2.2 *Survey*

The following brief survey aims to highlight noteworthy research in the area of both multi-agent systems and interconnected systems.

7.2.2.1 *Multi-Agent Systems-Related Work*

Fax and Murray [40] consider homogeneous interconnected linear time-invariant (LTI) subsystems, interconnected by a time-invariant interconnection topology. They make use of graph theory by modeling the interconnection by the graph Laplacian. A signal transformation in the form of a Schur transformation is applied that turns the graph Laplacian into upper triangular form, which eventually allows to analyze cooperative control loops for their stability by conditions that incorporate the complexity of only a single agent. Thus, stability can be analyzed for h decoupled systems, each of the dimension of a single agent differing only

in the graph Laplacian eigenvalues. After transformation, the approach therefore essentially consists in a robust controller synthesis problem.

Seyboth, Schmidt, and Allgöwer [132] present a similar approach, modified for homogeneous interconnected LPV systems. The idea of the signal transformation is applied here for the case of homogenous scheduling to decouple the system, s. t. analysis and distributed scheduled controller synthesis for achieving consensus can be done for h decoupled systems. The work of [132] does not, however, present convexly verifiable conditions for heterogeneous scheduling and limits the heterogeneously scheduled parts of the agents' system matrix to those that do not contribute to the interaction. Neither Fax and Murray nor Seyboth et al. consider performance in their conditions and consequently do not reveal the fact that lower and upper performance bounds, in terms of the $\mathcal{H}_\infty$-/induced $\mathcal{L}_2$-gain, depend on the condition number of the signal transformation matrix [34, 100].

In [117], analysis results for general interconnected systems with infinite interconnection time-delays is presented based on an $\mathcal{L}_1$-norm condition. This is extended to controller synthesis in [116].

Non-holonomically constrained subsystems may be encountered in MASs, e. g., when the agent network consists of wheeled vehicles or jet planes. A variety of publications consider the case of interconnected non-holonomic agents and present specialized solutions that do not draw from a general framework, [29, 31, 101]. In [165] the framework of LPV systems is used to model non-holonomic agents, while a similar LPV formulation is already successfully applied in the distributed control framework of [54] in [107].

7.2.2.2 *Interconnected Systems-Related Work*

Bamieh et al. [11] consider homogeneous regularly interconnected LTI subsystems that can be described as PDEs. A Fourier transform is used to block diagonalize the systems from a regular array interconnection. Thus, the infinite dimensional control problem can be solved by finite algebraic riccati equations (AREs), parameterized over frequency. The resulting controller does not necessarily inherit the interconnection of the plant, but the influence decays exponentially with spatial distance. Thus, by spatial truncation a desired degree of decentralization can be traded off against a loss in optimality.

The framework of ≪decomposable systems≫ has been introduced by Massioni and Verhaegen [99]. Homogeneous interconnected LTI subsystems are considered, interconnected by a time-invariant and diagonalizable interconnection topology. Using a signal transformation, similar to [40], a diagonalization of the interconnection matrix is achieved that allows to render the synthesis particularly efficient, as it can be reduced to the complexity of the order of only a single subsystem. However, this results in a restriction to time-invariant topologies. Controllers are not only synthesized for stabilization, but performance is considered in an $\mathcal{H}_\infty$-norm optimal framework via the Bounded Real Lemma (BRL), cf. Thm. 2.6 on p. 38. Furthermore, interconnections are allowed with respect to all signals of the generalized plant,

effectively enabling to consider physically coupled system. Solutions are given in terms of Riccati equations [99] as well as linear matrix inequalities (LMIs) [100], the latter of which are derived by the full-block 𝒮-Procedure (FBSP), cf. Thm. 2.4 on p. 34. This results in convex conditions for distributed state-feedback controller synthesis for interconnected homogeneous LTI subsystems with low complexity. An extension to heterogeneous subsystems has been proposed and conceived by Massioni in [98] simultaneously and independently to the present thesis and related associated research [55, 56, 61]. The authors' modeling framework remains confined to the class of decomposable systems, but instead of a signal transformation, a singular value decomposition (SVD) of the interconnection matrix is considered. Possibly conservatively, the proposed approach guarantees stability and performance through the use of D-scaling (D-S) constraints for scalar repeated time-varying interconnection matrices $\ell(t)$ and it is discussed that the involved multiplier condition holds for both $\ell(t)$ and $-\ell(t)$. The method is developed in the discrete-time LTI case.

A more general framework is proposed by Langbort, Chandra, and D'Andrea [80], where distributed output-feedback controller synthesis is considered for interconnected heterogeneous LTI subsystems on the basis of individual interconnection operators, assembled in a diagonal linear fractional transformation (LFT)-based feedback block with possible repetitions. This allows arbitrary, directed and time-varying interconnection topologies at the price of high synthesis complexity. Although not explicitly stated, nonlinear subsystems can be represented by exploiting self-loops, effectively resulting in LFT-LPV subsystem descriptions. By structural constraints on Lyapunov and multiplier matrices, the synthesis conditions can be decoupled into conditions for each subsystem. As stated in [80], large scale systems may result in intractable conditions as complexity increases quickly with the number of subsystems.

Stemming from the field of SIS, [24] presents a special case of the work detailed in [80], where instead of heterogeneous LTI systems homogeneous ones are considered. Furthermore, the interconnection is restricted to regularly structured ones. The representation of the interconnection as an LFT with diagonal block as in [80] and with the same structural constraints on the Lyapunov and multipliers leads again to a decoupling of the synthesis conditions. Due to the homogenous nature of the subsystems and the regular interconnection, only a single set of conditions of the complexity of a single subsystem needs to be solved. Langbort et al. [81] extend [24] to regularly structured but finite interconnections, e. g., finite grid structures. For this purpose, boundary conditions are introduced. It is proven that in case of spatially reversible boundary conditions, the analysis and synthesis conditions for the finite system are equivalent to the infinite case, s. t. the results from [24] can be applied.

Dullerud et al. and Wu, [32, 162], extend [24] to heterogeneous interconnected subsystems with regularly structured interconnections. While in [32] general heterogeneous interconnected subsystems are considered, [162] restricts the subsys-

tems to be heterogeneously scheduled LPV subsystems. The latter work has recently been extended by reducing conservatism through parameter-dependent Lyapunov functions (PDLFs) and D/G-scaling (D/G-S) in [90, 91].

7.2.2.3 *Contributions*

The contents of Part II of this thesis mainly draw from the publications [54–56, 61]. The objective of the research, whose results are presented in the following, consists in extending the ideas presented in [97] to provide and allow for

- LPV subsystems that are both heterogeneously scheduled and have heterogeneous dynamics,

- arbitrary directed and switching interconnection topologies,

- a high degree of scalability,

- synthesis conditions that are posed as a convex optimization problem in terms of LMIs, providing guaranteed upper bounds on the achievable control performance and guaranteed stability,

- physical and virtual interconnections.

As a result, the presented methods are applicable to the general class of ISs, while exploiting graph theory to render synthesis conditions significantly less complex than the comparably general techniques presented in [80]. In addition, they are not restricted to regularly structured interconnection topologies as in [90, 162]. By combining the results of this thesis with work published in [38], also explicit topology models can be taken into account.

7.2.3 *Summary*

Tab. 7.1 provides an overview of selected distributed controller synthesis approaches. This thesis' contributions are listed at the bottom for comparison[1].

---

1 The subsystem property HS of the work [132] is provided by necessary and sufficient conditions that can be checked *a posteriori* only. All other indicators are assessed in terms of what properties and guarantees are provided immediately after the proposed synthesis algorithm.

Table 7.1: Overview about distributed synthesis approaches.

	Subsystems			Topologies					Synthesis				
	NL	Het.	Cpl'd.	Direct.	Struct.		TV		Meth.		Guarant.		Scal.
					Arb.	Reg.	Impl.	Expl.	FB	GS	Stab.	Perf.	
Bamieh et al., [11]	✗	✗	✓	Full	✗	✓	✗	✗	SF	LTI	✗	✗	+
Wu, [162]	LFT	HS	✓	Full	✗	✓	✗	✗	OF	GS	✓	✓	++
Liu et al., [90]	LFT	HS	✓	Full	✗	✓	✗	✗	OF	GS	✓	✓	++
D'Andrea et al., [24]	✗	✗	✓	Full	✗	✓	✗	✗	OF	LTI	✓	✓	++
Dullerud et al., [32]	✗	HD	✓	Full	✗	✓	✗	✗	OF	LTI	✓	✓	++
Langbort et al., [80]	LFT	HDS	✓	Full	✓	✓	✓	✓	OF	GS	✓	✓	−−
Massioni, [97]	✗	✗	✓	Diag.	✓	✓	✗	✗	SF	LTI	✓	✗	+
Massioni, [98]	✗	HD	✓	Full	✓	✓	✓	✗	SF/OF	LTI	✓	✓	++
Seyboth et al., [132]	Poly.	HS*	✗	Diag.	✓	✓	✗	✗	SF	GS	✗	✗	+
Pilz et al., [116]	✗	✗	✗	Full	✓	✓	✓	✗	OF	LTI	✓	✓	+
Eichler et al., [38]	LFT	✗	✓	Full	✓	✓	✗	✓	OF	RB	✓	✗	+
Hoffmann et al., [54]	LFT	HS	✓	✗	✓	✓	✓	✗	OF	GS	✓	✓	+
Hoffmann et al., [55, 56]	LFT	HDS	✓	Grp.	✓	✓	✓	✗	OF	GS	✓	✓	+
Present Work, [61]	LFT	HDS	✓	Full	✓	✓	✓	✓	OF	GS	✓	✓	++

Legend

Subsystems	NL	nonlinear (NL) subsystem dynamics allowed by type: LFT-LPV, polytopic LPV
	Het.	heterogeneous subsystem dynamics (HD), scheduling (HS) or both (HDS) allowed
	Cpl'd.	Physically coupled subsystems allowed
Directed topology	Full	Fully directed topologies allowed
	Diag.	Only diagonalizable directed topologies allowed
	Grp	Directed topologies between groups of subsystems allowed
Structured topology	Arb.	Arbitrary topologies allowed
	Reg.	Regularly structured topologies allowed
TV topology	Impl.	Time-varying topologies are implicitly (conservatively) allowed
	Expl.	Time-varying topologies can be explicitly (less conservatively) considered
Synthesis method	FB	output-feedback (OF) or state-feedback (SF) synthesis method
	GS	gain-scheduling (GS), robust (RB)-LTI or LTI controller
Guarantees	Stab.	Stability guaranteed after synthesis
	Perf.	Performance guaranteed after synthesis
Scalability		Degree in which synthesis complexity scales with the number of subsystems

8

A COMPACT MODELING FRAMEWORK FOR INTERCONNECTED LINEAR PARAMETER-VARYING SYSTEMS

> ≪*Entities must not be multiplied beyond necessity.*≫

> John Punch, 1639,
> ≪*lex parsimoniae*≫,
> or ≪*Occam's Razor*≫

THE contents of this chapter are devoted to establish a compact framework for the modeling of a rather general class of interconnected LPV subsystems. Sect. 8.1 introduces this framework by formally defining heterogeneous LPV subsystem representations and their interconnection (Sect. 8.1.1), the interconnected closed-loop (Sect. 8.1.2) and considered classes of interconnections (Sect. 8.1.3), followed by a note on the density of diagonalizable matrices (Sect. 8.1.4).

The chapter continues with a discussion on special cases of the general framework in Sect. 8.2, most notably the class of ≪*decomposable systems*≫ [97] and some extensions.

8.1 General Interconnected Linear Parameter-Varying Systems

$\mathbf{F}$or the purpose of aligning the framework of interconnected LPV system representations with results presented in the subsequent sections, an MAS with the sets $\mathbf{G}_1$ and $\mathbf{G}_2$ as groups of leaders and followers, respectively, will be considered for motivation. The framework will naturally extend to both a larger number of groups as well as the special case of a single group of interconnected subsystems. Despite the motivational MAS setup, physical interconnection between the subsystems is explicitly allowed within the framework.

In the following, each subsystem's dynamics will be defined within the LPV framework, as well as the entirety of the systems interconnected through an operator $\mathscr{L}$.

8.1.1 *Interconnected Linear Parameter-Varying System Representation*

Define $\mathbf{G}$ as a partition of the set of subsystem indices $\mathbf{H}$, i. e., $\mathbf{G} = \{\mathbf{G}_1, \mathbf{G}_2, \ldots, \mathbf{G}_g\}$ contains pairwise disjoint sets with $\bigcup_{f=1}^{g} (\mathbf{G}_f) = \mathbf{H}$ and cardinalities $\mathrm{card}\,(\mathbf{H}) = h$ and $\mathrm{card}\,(\mathbf{G}_f) = h_f, \forall f = 1, \ldots, g,\ g \leqslant h$. The set $\mathbf{G}_f \subset \mathbf{H}$ contains the indices of subsystems belonging to group number $f \in \mathbb{N}$. For further notational purposes, define the column vector

$$e_f \triangleq \operatornamewithlimits{col}_{k=1}^{h}(\delta_f(k)), \text{ with } \delta_f(k) = \begin{cases} 1, & k \in \mathbf{G}_f \\ 0, & \text{otherwise} \end{cases}, \ \mathbf{G}_f \subset \mathbf{H},$$

i. e., a vector with ones in the rows corresponding to the indices in $\mathbf{G}_f$ and zeros otherwise. Associate the matrix E_f via $E_f \triangleq \mathrm{diag}(e_f)$.

Consider Ex. 8.1 as the above-mentioned leader-follower configuration.

Remark 8.1 *Choosing a virtual agent as a leader is an intuitive way to impose a reference for the center of gravity of a formation.*

Example 8.1 (MAS with Two Groups of Agents)
Consider an example, cf. Fig. 8.1, where $\mathbf{G} = \{\mathbf{G}_1, \mathbf{G}_2\} = \{\{1, 2, 3\}, \{4, 5, 6, 7\}\}$. Note that particular to this configuration, subsystems are interconnected with directed signal flow between and undirected communication within the groups. Further, observe that from the definitions, one has

$$e_1 = \begin{bmatrix} 1_{3\times 1} \\ 0_{4\times 1} \end{bmatrix}, \quad E_1 = \begin{bmatrix} I_3 & 0 \\ 0 & 0_4 \end{bmatrix} \quad e_2 = \begin{bmatrix} 0_{3\times 1} \\ 1_{4\times 1} \end{bmatrix}, \quad E_2 = \begin{bmatrix} 0_3 & 0 \\ 0 & I_4 \end{bmatrix}.$$
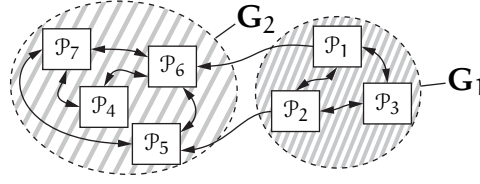
$\square$

Figure 8.1: Exemplary interconnection of two groups of agents.

Consider LPV subsystems $\mathcal{P}_k$, $k \in \mathbf{G}_f$, whose state space models depend on the respective group of subsystems $\mathbf{G}_f$ to which the subsystem index k belongs. That means, for all $k \in \mathbf{G}_f$, $\mathcal{P}_k$ is described by the following state space representation

$$
\mathcal{P}_k : \begin{cases} \begin{bmatrix} \dot{x}_k \\ p_k \\ d_k \\ z_k \\ y_k \end{bmatrix} = \begin{bmatrix} A_f & B_{f,\Delta} & B_{f,i} & B_{f,p} & B_{f,u} \\ C_{f,\Delta} & D_{f,\Delta\Delta} & D_{f,\Delta i} & D_{f,\Delta p} & D_{f,\Delta u} \\ C_{f,i} & D_{f,i\Delta} & D_{f,ii} & D_{f,ip} & D_{f,iu} \\ C_{f,p} & D_{f,p\Delta} & D_{f,pi} & D_{f,pp} & D_{f,pu} \\ C_{f,y} & D_{f,y\Delta} & D_{f,yi} & D_{f,yp} & 0 \end{bmatrix} \begin{bmatrix} x_k \\ q_k \\ v_k \\ w_k \\ u_k \end{bmatrix} = P_f \begin{bmatrix} x_k \\ q_k \\ v_k \\ w_k \\ u_k \end{bmatrix}, \\ q_k = \underline{\Delta}_f\big(\delta_k(t)\big) p_k, \qquad \delta_k(t) \in \boldsymbol{\mathcal{F}}^{\eta}_{\delta,k}, \end{cases}
$$
(8.1)

where $x_k \in \mathbb{R}^{n_{f,x}}$, $p_k \in \mathbb{R}^{n_{f,p}}$, $q_k \in \mathbb{R}^{n_{f,q}}$, $d_k \in \mathbb{R}^{n_{f,d}}$, $v_k \in \mathbb{R}^{n_{f,v}}$, $z_k \in \mathbb{R}^{n_{f,z}}$, $w_k \in \mathbb{R}^{n_{f,w}}$, $y_k \in \mathbb{R}^{n_{f,y}}$, $u_k \in \mathbb{R}^{n_{f,u}}$ and $\delta_k \in \mathbb{R}^{n_{f,\delta}}$ is the LPV parameter vector. Within each group, the signal sizes are identical. For the purpose of simpler notation, introduce for each subsystem symbols associated with channel sizes $n_{\bullet_k} = n_{f,\bullet}$, $\forall k \in \mathbf{G}_f$, where $\bullet$ represents the respective channel.

The scheduling parameters of the kth subsystem are collected in a vector $\delta_k(t) = \underset{i=1}{\overset{n_{f,\delta}}{\text{col}}}(\delta_{k,i}(t))$ with all admissible parameter values and rates ranging in compact sets $\boldsymbol{\delta}_f$ and $\boldsymbol{\eta}_f$, $\forall f \in \{1, \ldots, g\}$, respectively. The parameter block Δ_k is an analytic matrix-valued function of the scheduling signal vector

$$
\Delta_k(t) = \underline{\Delta}_f\big(\delta_k(t)\big) : \mathbb{R}^{n_{f,\delta}} \mapsto \mathbb{R}^{n_{f,q} \times n_{f,p}}
$$

and may typically assume either a block-diagonal form

$$
\Delta_k(t) = \underset{i=1}{\overset{n_{f,\delta}}{\text{diag}}}\big(\delta_{k,i}(t) I_{r_{f,i}}\big), \quad k \in \mathbf{G}_f,
$$

or a general full parameter block as considered in Part I. The framework therefore does not preclude the consideration of complex LPV subsystems, as the synthesis methods based on full block parameterizations and the resulting efficient LFT-LPV controller implementation will apply on a subsystem level. A block diagram of a single LPV subsystem is shown in Fig. 8.2.

Recall that the state space model matrix P_f from (8.1) is related to the symbol representing the dynamic LTI system as $P_k = \frac{1}{s} I_{n_{f,x}} \star P_f$, $k \in \mathbf{G}_f$. As before, the symbol $\mathcal{P}_k$, in turn, represents the LPV system as an input-output map given by $\mathcal{P}_k = \Delta_k(t) \star P_k$, $\delta_k(t) \in \boldsymbol{\delta}_k$ $k \in \mathbf{H}$.
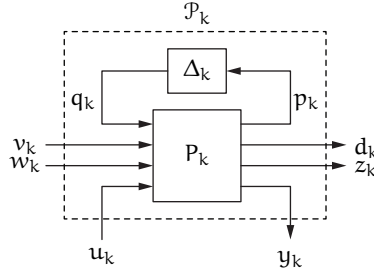
Figure 8.2: LPV subsystem representation.

The interconnected LPV system in its general form can be considered as being «heterogeneous» in two distinct ways:

HETEROGENEOUS SCHEDULING: Within each group f, the parameter block retains the same structure, i. e., functional dependence on the scheduling parameters $\delta_k \in \boldsymbol{\delta}_f$ via $\underline{\Delta}_f(\delta_k)$. Furthermore, the parameter values are confined to the same compact sets $\boldsymbol{\delta}_f$ for all entities in the group. In contrast, the scheduling parameters $\delta_k(t)$ may be elements of individual admissible trajectories $\mathcal{F}^{\eta}_{\delta,k}$, and may therefore take individual values at time instant t for different subsystems k from the set of all subsystems $\mathbf{H}$. This local dependence of each subsystem on its individual parameters will be denoted «heterogeneous scheduling».

HETEROGENEOUS DYNAMICS: The fact that the system descriptions in terms of the state space matrices P_f may vary between groups will be considered as «heterogeneous dynamics» of the LPV subsystems.

The entirety of the subsystems is regarded as a system of h interconnected subsystems as shown in Fig. 8.3a, denoted

$$
\mathscr{P}:
\begin{cases}
\begin{bmatrix} \dot{x} \\ p \\ d \\ z \\ y \end{bmatrix}
=
\left[
\begin{array}{c:cccc}
A & B_{\Delta} & B_i & B_p & B_u \\ \hdashline
C_{\Delta} & D_{\Delta\Delta} & D_{\Delta i} & D_{\Delta p} & D_{\Delta u} \\
C_i & D_{i\Delta} & D_{ii} & D_{ip} & D_{iu} \\
C_p & D_{p\Delta} & D_{pi} & D_{pp} & D_{pu} \\
C_y & D_{y\Delta} & D_{yi} & D_{yp} & 0
\end{array}
\right]
\begin{bmatrix} x \\ q \\ v \\ w \\ u \end{bmatrix}
= P
\begin{bmatrix} x \\ q \\ v \\ w \\ u \end{bmatrix}, \\[4em]
\quad q = \Delta p, \qquad v = \mathscr{L}(d), \qquad \delta(t) \in \mathcal{F}^{\eta}_{\delta}, \qquad \mathscr{L}(t) \in \mathcal{F}_{\mathscr{L}},
\end{cases}
\tag{8.2}
$$

where

$$x = \operatorname*{col}_{k=1}^{h}(x_k) \in \mathbb{R}^{n_x}, \qquad p = \operatorname*{col}_{k=1}^{h}(p_k) \in \mathbb{R}^{n_p}, \quad q = \operatorname*{col}_{k=1}^{h}(q_k) \in \mathbb{R}^{n_q},$$

$$d = \operatorname*{col}_{k=1}^{h}(d_k) \in \mathbb{R}^{n_d}, \qquad v = \operatorname*{col}_{k=1}^{h}(v_k) \in \mathbb{R}^{n_v}, \quad z = \operatorname*{col}_{k=1}^{h}(z_k) \in \mathbb{R}^{n_z},$$

$$w = \operatorname*{col}_{k=1}^{h}(w_k) \in \mathbb{R}^{n_w}, \qquad y = \operatorname*{col}_{k=1}^{h}(y_k) \in \mathbb{R}^{n_y}, \quad u = \operatorname*{col}_{k=1}^{h}(u_k) \in \mathbb{R}^{n_u},$$

$$\Delta = \operatorname*{diag}_{k=1}^{h}(\Delta_k) \in \mathbb{R}^{n_p \times n_q}.$$

(a) Interconnected LPV system composed of LPV subsystems.

(b) Interconnected LPV system in compact representation.

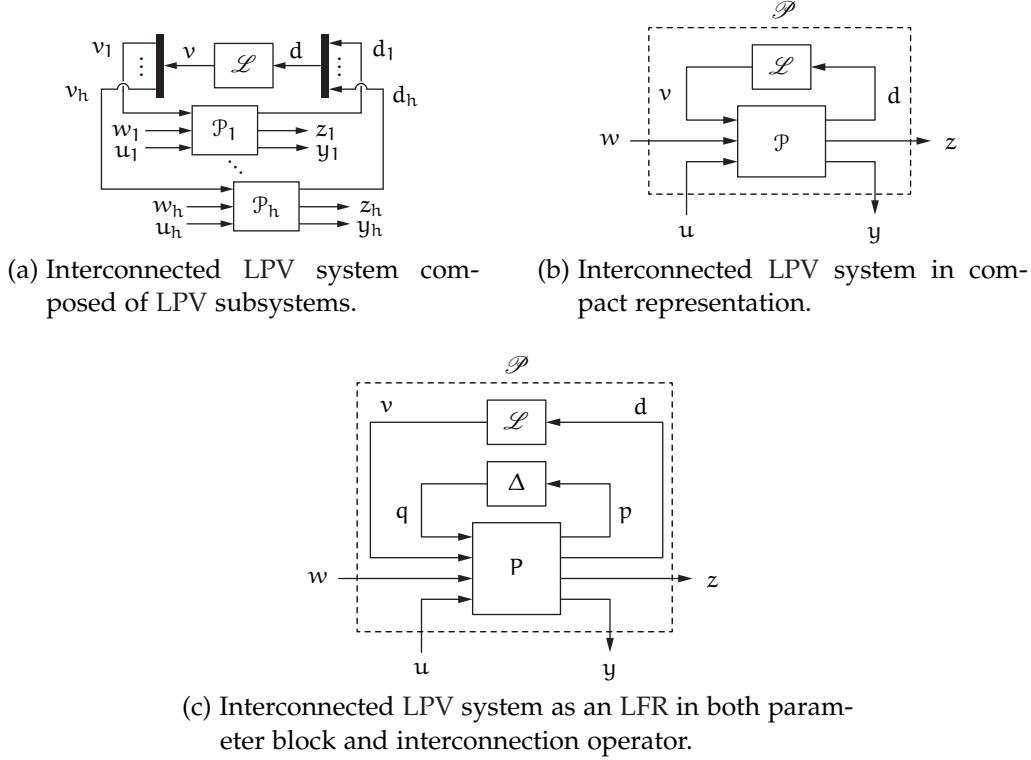(c) Interconnected LPV system as an LFR in both parameter block and interconnection operator.

Figure 8.3: The interconnected LPV system.

Via the above signal definitions, it can be inferred that the state space matrices of (8.2) consist of block-diagonally concatenated subsystem matrices from (8.1). Due to the heterogeneity in the subsystem dynamics, each matrix A, B_Δ, $\ldots$, in (8.2) can be written in the form

$$M = \sum_{f=1}^{g} (E_f \otimes M_f)$$

Any coupling between the subsystems is therefore solely represented by the interconnection signals d_k and v_k, $\forall k \in \mathbf{H}$ and an interconnection operator $\mathscr{L}$. In analogy to the LPV representation related notation, the interconnection operator can be regarded as both an element of a function space of admissible «topology variations» $\mathscr{L}(t) \in \mathcal{F}_{\mathscr{L}}$ as well as being confined to a compact set of admissible operator values, i.e., $\mathscr{L} \in \mathbf{\mathscr{L}}$, which may be, e.g., real-valued matrices, s.t. $\mathbf{\mathscr{L}} \subseteq \mathbb{R}^{n_v \times n_d}$.

Remark 8.2 *In this thesis, the introduction of bounds on the rate of change of the interconnection matrix is dispensed with, as the focus of the developed methods is on switching topologies.*

Definition 8.1 (Topology Variation Set)
Given a compact set $\mathbf{\mathscr{L}}$, the topology variation set $\mathcal{F}_{\mathscr{L}}$ denotes a set of piecewise continuous functions, mapping $\mathbb{R}^+$ into $\mathbf{\mathscr{L}}$ with a finite number of discontinuities in any interval.

Note that, even though the coupling information is represented by an LFT comprising an interconnection operator and respective signals, such an interconnection needs not be solely virtual, i. e., a communication of information over networks. In fact, the system representation allows state, input and output signals to be included in the interconnection, which enables the modeling of physical couplings as well.

Again, denote the dynamic LTI system $P = \frac{1}{s} I_{n_x} \star P$ and the LPV representation $\mathcal{P} = \Delta(t) \star P$. Further, the interconnected LPV system is denoted $\mathscr{P} = \mathscr{L} \star \mathcal{P}$. The scheduling parameters are collected in a vector $\delta(t) = \operatorname*{col}_{k=1}^{h}(\delta_k(t))$ with all admissible parameter values and rates ranging in the compact sets

$$\delta = \delta_1 \times \delta_2 \times \ldots \times \delta_g \triangleq \bigtimes_{f=1}^{g} (\delta_f), \quad \eta = \eta_1 \times \eta_2 \times \ldots \times \eta_g \triangleq \bigtimes_{f=1}^{g} (\eta_f).$$

Accordingly, the admissible trajectories are ranging in the set

$$\mathcal{F}_\delta^\eta = \mathcal{F}_{\delta,1}^\eta \times \mathcal{F}_{\delta,2}^\eta \times \ldots \times \mathcal{F}_{\delta,g}^\eta \triangleq \bigtimes_{f=1}^{g} \left(\mathcal{F}_{\delta,f}^\eta \right).$$

Several block diagram representations of the entire interconnected system (8.2) are depicted in Fig. 8.3 for illustration.

8.1.2 *The Interconnected Closed-Loop System*

Consider controllers associated with $\mathcal{P}_k$ given by $K_k = \frac{1}{s} I_{n_{f,x}^K} \star K_f$, $\mathcal{K}_k = \Delta_k^K(t) \star K_k$, $k \in \mathbf{G}_f$, with

$$
\mathcal{K}_k : \begin{cases}
\begin{bmatrix} \dot{x}_k^K \\ u_k \\ d_k^K \\ p_k^K \end{bmatrix} = \left[\begin{array}{c|ccc} A_f^K & B_{f,y}^K & B_{f,i}^K & B_{f,\Delta}^K \\ \hline C_{f,u}^K & D_{f,uy}^K & D_{f,ui}^K & D_{f,u\Delta}^K \\ C_{f,i}^K & D_{f,iy}^K & D_{f,ii}^K & D_{f,i\Delta}^K \\ C_{f,\Delta}^K & D_{f,\Delta y}^K & D_{f,\Delta i}^K & D_{f,\Delta\Delta}^K \end{array} \right] \begin{bmatrix} x_k^K \\ y_k \\ v_k^K \\ q_k^K \end{bmatrix} = K_f \begin{bmatrix} x_k^K \\ y_k \\ v_k^K \\ q_k^K \end{bmatrix}, \\
q_k^K = \Delta_k^K p_k^K, \qquad \delta_k(t) \in \mathcal{F}_{\delta,f}^\eta,
\end{cases}
\tag{8.3}
$$

where $x_k^K \in \mathbb{R}^{n_{f,x}^K}$, $p_k^K \in \mathbb{R}^{n_{f,p}^K}$, $q_k^K \in \mathbb{R}^{n_{f,q}^K}$, $d_k^K \in \mathbb{R}^{n_{f,d}^K}$, $v_k^K \in \mathbb{R}^{n_{f,v}^K}$, $k \in \mathbf{G}_f$ and concatenated signals

$$
\begin{aligned}
x^K &= \operatorname*{col}_{k=1}^{h} \left(x_k^K \right) \in \mathbb{R}^{n_x^K}, & p^K &= \operatorname*{col}_{k=1}^{h} \left(p_k^K \right) \in \mathbb{R}^{n_p^K}, \\
q^K &= \operatorname*{col}_{k=1}^{h} \left(q_k^K \right) \in \mathbb{R}^{n_q^K}, & d^K &= \operatorname*{col}_{k=1}^{h} \left(d_k^K \right) \in \mathbb{R}^{n_d^K}, \\
v^K &= \operatorname*{col}_{k=1}^{h} \left(v_k^K \right) \in \mathbb{R}^{n_v^K}, & \Delta^K &= \operatorname*{diag}_{k=1}^{h} \left(\Delta_k^K \right) \in \mathbb{R}^{n_p^K \times n_q^K}.
\end{aligned}
$$

Each controlled subsystem is described by $\mathcal{P}_k \star \mathcal{K}_k$. The entirety of interconnected controllers is denoted

$$
\mathcal{K} : \begin{cases}
\begin{bmatrix} \dot{x}^K \\ u \\ d^K \\ p^K \end{bmatrix} = \left[\begin{array}{c|ccc} A^K & B_y^K & B_i^K & B_\Delta^K \\ \hline C_u^K & D_{uy}^K & D_{ui}^K & D_{u\Delta}^K \\ C_i^K & D_{iy}^K & D_{ii}^K & D_{i\Delta}^K \\ C_\Delta^K & D_{\Delta y}^K & D_{\Delta i}^K & D_{\Delta\Delta}^K \end{array} \right] \begin{bmatrix} x^K \\ y \\ v^K \\ q^K \end{bmatrix} = K \begin{bmatrix} x^K \\ y \\ v^K \\ q^K \end{bmatrix}, \\[2em]
\quad q^K = \Delta^K p^K, \quad v^K = \mathscr{L}^K(d^K), \quad \delta^K \in \mathcal{F}_\delta^\eta, \quad \mathscr{L}^K \in \mathcal{F}_{\mathscr{L}}^K.
\end{cases}
\tag{8.4}
$$

Again, denote the dynamic LTI system $K = \frac{1}{s} I_{n_x^K} \star K$ and the LPV representation $\mathcal{K} = \Delta^K(t) \star K$. The interconnected LPV controller is denoted $\mathscr{K} = \mathscr{L}^K \star \mathcal{K}$.

The complete interconnected system is simply formed by $\mathscr{T} = \mathscr{P} \star \mathscr{K}$, such that after permutation of channels one may write

$$
\mathscr{T} : \begin{cases}
\begin{bmatrix} \dot{\mathfrak{r}} \\ \mathfrak{p} \\ \mathfrak{d} \\ z \end{bmatrix} = \underbrace{\left[\begin{array}{c|ccc} \mathcal{A} & \mathcal{B}_\Delta & \mathcal{B}_i & \mathcal{B}_p \\ \hline \mathcal{C}_\Delta & \mathcal{D}_{\Delta\Delta} & \mathcal{D}_{\Delta i} & \mathcal{D}_{\Delta p} \\ \mathcal{C}_i & \mathcal{D}_{i\Delta} & \mathcal{D}_{ii} & \mathcal{D}_{ip} \\ \mathcal{C}_p & \mathcal{D}_{p\Delta} & \mathcal{D}_{pi} & \mathcal{D}_{pp} \end{array} \right]}_{T = T_0 + WKV} \begin{bmatrix} \mathfrak{r} \\ q \\ \mathfrak{v} \\ w \end{bmatrix}, \\[3em]
\quad q = \Delta p, \qquad v = \mathscr{L}(d), \qquad\qquad \delta \in \mathcal{F}_\delta^\eta \\[0.5em]
\quad q^K = \Delta^K p^K, \quad v^K = \mathscr{L}^K(d^K) \quad (\mathscr{L}, \mathscr{L}^K) \in \mathcal{F}_{\mathscr{L}} \times \mathcal{F}_{\mathscr{L}}^K,
\end{cases}
\tag{8.5}
$$

where

$$
\mathfrak{r} = \begin{bmatrix} x \\ x^K \end{bmatrix} \in \mathbb{R}^{n_\mathfrak{r}}, \quad \mathfrak{p} = \begin{bmatrix} p \\ p^K \end{bmatrix} \in \mathbb{R}^{n_\mathfrak{p}}, \quad q = \begin{bmatrix} q \\ q^K \end{bmatrix} \in \mathbb{R}^{n_q},
$$

$$
\mathfrak{d} = \begin{bmatrix} d \\ d^K \end{bmatrix} \in \mathbb{R}^{n_\mathfrak{d}}, \quad \mathfrak{v} = \begin{bmatrix} v \\ v^K \end{bmatrix} \in \mathbb{R}^{n_\mathfrak{v}}.
$$

Ultimately, it is the goal to synthesize a set of interconnected controllers that use only local information and a communication topology $\mathscr{L}^K$ to achieve a certain global objective. Irrespective of any potential physical couplings between the subsystems, the interaction between the controllers will turn out purely virtual, i. e., it will consist of information that will be communicated among the respective controllers. In most applications, e. g., when the topology is determined by communication links limited by maximum transmission distance—consider, e. g., a proximity graph—the controllers should inherit the topology of the plant, i. e., $\mathscr{L}^K = \mathscr{L}$, $\mathcal{F}_{\mathscr{L}}^K \equiv \mathcal{F}_{\mathscr{L}}$ and consequently $\mathscr{L}^K \equiv \mathscr{L}$, which is assumed in the following.

For strictly proper plants $\mathcal{P}$, the closed-loop state space model matrices are linear in the controller:

$$
T = T_0 + WKV = \left[\begin{array}{c|ccc} \mathcal{A} & \mathcal{B}_\Delta & \mathcal{B}_i & \mathcal{B}_p \\ \hline \mathcal{C}_\Delta & \mathcal{D}_{\Delta\Delta} & \mathcal{D}_{\Delta i} & \mathcal{D}_{\Delta p} \\ \mathcal{C}_i & \mathcal{D}_{i\Delta} & \mathcal{D}_{ii} & \mathcal{D}_{ip} \\ \mathcal{C}_p & \mathcal{D}_{p\Delta} & \mathcal{D}_{pi} & \mathcal{D}_{pp} \end{array} \right]
\tag{8.6}
$$

$$
T = \begin{bmatrix} A & 0 & B_\Delta & 0 & B_i & 0 & B_p \\ 0 & 0 & 0 & 0 & 0 & 0 & 0 \\ C_\Delta & 0 & D_{\Delta\Delta} & 0 & D_{\Delta i} & 0 & D_{\Delta p} \\ 0 & 0 & 0 & 0 & 0 & 0 & 0 \\ C_i & 0 & D_{i\Delta} & 0 & D_{ii} & 0 & D_{ip} \\ 0 & 0 & 0 & 0 & 0 & 0 & 0 \\ C_p & 0 & D_{p\Delta} & 0 & D_{pi} & 0 & D_{pp} \end{bmatrix} + \begin{bmatrix} 0 & B_u & 0 & 0 \\ I & 0 & 0 & 0 \\ 0 & D_{\Delta u} & 0 & 0 \\ 0 & 0 & 0 & I \\ 0 & D_{iu} & 0 & 0 \\ 0 & 0 & I & 0 \\ 0 & D_{pu} & 0 & 0 \end{bmatrix}
$$

$$
\times \begin{bmatrix} A^K & B_y^K & B_i^K & B_\Delta^K \\ C_u^K & D_{uy}^K & D_{ui}^K & D_{u\Delta}^K \\ C_i^K & D_{iy}^K & D_{ii}^K & D_{i\Delta}^K \\ C_\Delta^K & D_{\Delta y}^K & D_{\Delta i}^K & D_{\Delta\Delta}^K \end{bmatrix} \begin{bmatrix} 0 & I & 0 & 0 & 0 & 0 & 0 \\ C_y & 0 & D_{y\Delta} & 0 & D_{yi} & 0 & D_{yp} \\ 0 & 0 & 0 & 0 & 0 & I & 0 \\ 0 & 0 & 0 & I & 0 & 0 & 0 \end{bmatrix}, \tag{8.7}
$$

The interconnected closed-loop configuration is visualized in Figs. 8.4a–8.4c.

8.1.3 *Classes of Interconnections*

The subsystems are interconnected by an interconnection topology, modeled by the operator $\mathscr{L}$ as shown in Fig. 8.3. Denoting $\mathscr{L}$ a general interconnection operator allows for a wide range of different system theoretic, structural and graph theoretic properties. In the following, the discussion will be limited to specific subclasses.

8.1.3.1 *System Theoretic Classification*

In general, one may allow $\mathscr{L}$ to be a linear/nonlinear, static/dynamic and time-invariant/-varying operator to encompass all cases considered in [80], as illustrated in Fig. 8.5. The major difference to the present work is a structural one: It resides in the fact that the interconnection operator $\mathscr{L}$ is not restricted to be diagonally structured, consequently allowing a more compact interconnected system representation. Thus note that the above formulation of interconnected LPV systems includes the one proposed in [80].

However, the discussion will be limited to the cases, when $\mathscr{L}$ is static, linear, real-valued and possibly time-varying, as indicated by the gray box in Fig. 8.5. Formally, the following assumption is made.

(A8.1) **Real-Valued, Static, Linear and Time-Varying Interconnection:**
The interconnection operator $\mathscr{L}$ is static, linear, time-varying and ranges in a compact set, i. e.,

$$
\mathscr{L}(t, d) : \mathbb{R}^+ \times \mathbb{R}^{n_d} \to \mathbb{R}^{n_v}, \quad (t, d) \mapsto v \overset{\triangle}{=} \mathscr{L}(t)d,
$$

where $\mathscr{L}(t) : \mathbb{R}^+ \to \mathscr{L} \subset \mathbb{R}^{n_v \times n_d}, \forall t \in \mathbb{R}^+$.

However, the modeling framework—and to some extent the results discussed below—also apply to a wider class. For instance, nonlinear operators can also be
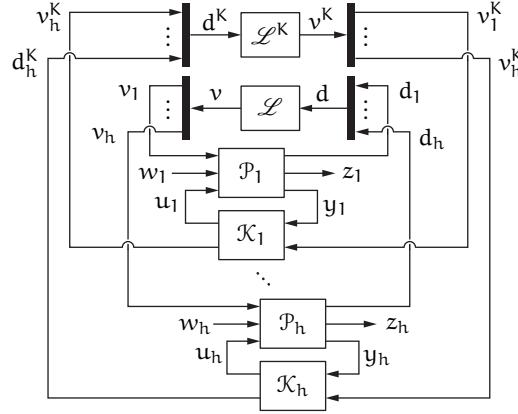
(a) Interconnected closed-loop LPV system composed from LPV subsystems.
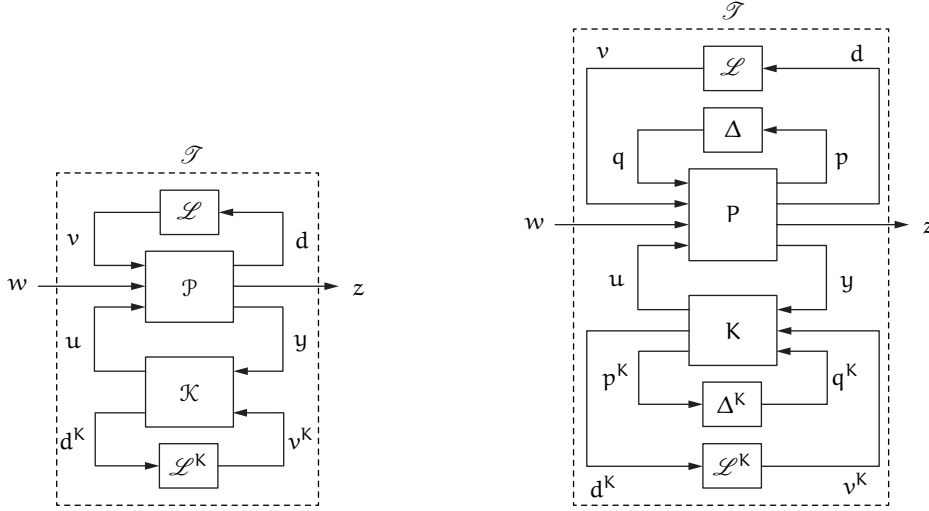
(b) Interconnected closed-loop LPV system in compact representation.

(c) Interconnected closed-loop LPV system as LFRs in both parameter block and interconnection operator.

Figure 8.4: The interconnected closed-loop LPV system.

treated in a quasi-linear parameter-varying (Q-LPV)-fashion by considering the interconnection operator a function of the interconnection input or output signals, v or d, respectively. Certain (potentially nonlinear) operators that can be modeled by integral quadratic constraints (IQCs) and handled by multipliers in the form of D/G-S [80, 104] can already be considered by the techniques presented in this thesis, as well. Furthermore, along the lines of [36], the interconnection operator can sometimes be factorized, s.t. a real-valued matrix $\mathscr{L} \in \boldsymbol{\mathscr{L}}$ emerges as the essential item to bear information on connectivity, while other operators incorporate dynamics, such as time delays.

For brevity of notation, time dependency will often be dropped.
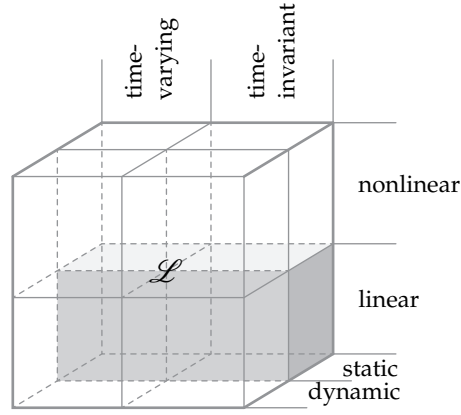
Figure 8.5: Classes of interconnection operators.

8.1.3.2 *Structural Classification*

Restricting the interconnection operator to exhibit special structural properties is the key to considerably reduce the complexity of the synthesis approach presented later on—more specifically—by imposing similar structural properties on multiplier decision variables.

For this purpose, first assume that the operator $\mathscr{L}(t)$ can be partitioned as

$$
\mathscr{L}(t) = \begin{bmatrix} \mathscr{L}_{11}(t) & \mathscr{L}_{12}(t) & \cdots & \mathscr{L}_{1h}(t) \\ \mathscr{L}_{21}(t) & \mathscr{L}_{22}(t) & \cdots & \mathscr{L}_{2h}(t) \\ \vdots & & \ddots & \vdots \\ \mathscr{L}_{h1}(t) & \mathscr{L}_{h2}(t) & \cdots & \mathscr{L}_{hh}(t) \end{bmatrix},
\tag{8.8}
$$

with $\mathscr{L}_{ij}(t) : \mathbb{R}^+ \to \boldsymbol{\mathscr{L}}_{ij} \subseteq \mathbb{R}^{n_{v_i} \times n_{d_j}}$, $(i,j) \in \mathbf{H} \times \mathbf{H}$.

The following structural properties of the interconnection are assumed.

(A8.2) Square Interconnection Operators $\mathscr{L}_{ij}$:
An invariant number of interconnection in- and output channels is assumed, i. e., $n_{\mathscr{L}} \overset{\triangle}{=} n_{f,d} = n_{f,v}$, $f = 1,\ldots,g$.

(A8.3) Scalar Repeated Interconnection Operators:
A single scalar interconnection operator $\ell_{ij}(t)$ encodes each connection between two subsystems, i. e., $\mathscr{L}_{ij}(t) = \ell_{ij}(t)I_{n_{\mathscr{L}}}$, with $\ell_{ij}(t) : \mathbb{R}^+ \to \boldsymbol{\ell}_{ij} \subseteq \mathbb{R}$.

Under the Ass. (A8.2) and (A8.3), one can write

$$
\mathscr{L}(t) = \ell(t) \otimes I_{n_{\mathscr{L}}}, \text{ with } \ell(t) = \begin{bmatrix} \ell_{11}(t) & \ell_{12}(t) & \cdots & \ell_{1h}(t) \\ \ell_{21}(t) & \ell_{22}(t) & \cdots & \ell_{2h}(t) \\ \vdots & & \ddots & \vdots \\ \ell_{h1}(t) & \ell_{h2}(t) & \cdots & \ell_{hh}(t) \end{bmatrix},
$$

$$
\ell(t) : \mathbb{R}^+ \to \boldsymbol{\ell} \subseteq \mathbb{R}^{h \times h}.
\tag{8.9}
$$

The compactness of the set $\mathscr{L}$ is implied by the compactness of a set $\boldsymbol{\ell}$, in which the real-valued, time-varying matrix $\ell(t)$ remains for all times.

8.1.3.3 *Graph Theoretic Classification*

The fundamental graph theoretic property used for classification in this thesis resides in «directedness». Methods that can cover matrix representations $\mathscr{L}(t)$ of directed or undirected graphs will be developed. More specifically, assume scalar repeated interconnection operators according to (A8.3) and a partitioning of $\ell(t)$ based on the definition of subsystem groups

$$\ell(t) = \begin{bmatrix} \ell_{G_1 G_1}(t) & \ell_{G_1 G_2}(t) & \cdots & \ell_{G_1 G_g}(t) \\ \ell_{G_2 G_1}(t) & \ell_{G_2 G_2}(t) & \cdots & \ell_{G_2 G_g}(t) \\ \vdots & & \ddots & \vdots \\ \ell_{G_g G_1}(t) & \ell_{G_g G_2}(t) & \cdots & \ell_{G_g G_g}(t) \end{bmatrix}, \tag{8.10}$$
$$\ell_{G_i G_j}(t) : \mathbb{R}^+ \to \boldsymbol{\ell}_{G_i G_j} \subseteq \mathbb{R}^{h_i \times h_j}.$$

The transformation of matrix inequalities that allow to arrive at conditions with a complexity in the order of a single subsystem usually require the interconnection matrix to be diagonalizable or normal as technical assumptions. For this purpose, introduce the following notation.

(A8.4) **Diagonalizable Matrix, $\ell \in \boldsymbol{\ell}_D^{h \times h}$:**
A real diagonalizable $h \times h$ matrix is an element of the set

$$\boldsymbol{\ell}_D^{h \times h} \triangleq \left\{ \ell \in \mathbb{R}^{h \times h} \mid \exists F, \text{ s.t. } F^{-1} \ell F = \Lambda \text{ is diagonal} \right\}.$$

(A8.5) **Normal Matrix, $\ell \in \boldsymbol{\ell}_N^{h \times h}$:**
A real normal $h \times h$ matrix is an element of the set

$$\boldsymbol{\ell}_N^{h \times h} \triangleq \left\{ \ell \in \mathbb{R}^{h \times h} \mid \exists F, \ F^{-1} = F^*, \text{ s.t. } F^* \ell F = \Lambda \text{ is diagonal} \right\}.$$

The definition of sets that regard the matrix representations of the interconnection topologies as elements of function spaces then follows as:

(A8.6) **Arbitrary Interconnection, $\ell(t) \in \mathscr{F}_{\boldsymbol{\ell}, \mathbb{R}}^{h \times h}$:**
A matrix representation of an arbitrary time-varying (TV) topology is an element of the set

$$\mathscr{F}_{\boldsymbol{\ell}, \mathbb{R}}^{h \times h} \triangleq \left\{ \ell(t) \mid \ell(t) : \mathbb{R}^+ \to \mathbb{R}^{h \times h} \right\}.$$

(A8.7) **Symmetric Interconnection, $\ell(t) \in \mathscr{F}_{\boldsymbol{\ell}, S}^{h \times h}$:**
A matrix representation of a symmetric TV topology is an element of the set

$$\mathscr{F}_{\boldsymbol{\ell}, S}^{h \times h} \triangleq \left\{ \ell(t) \mid \ell(t) : \mathbb{R}^+ \to S^{h \times h} \right\}.$$

(A8.8) Skew-Symmetric Interconnection, $\ell(t) \in \mathcal{F}_{\boldsymbol{\ell},\mathbb{AS}}^{h \times h}$:

A matrix representation of an anti-symmetric topology is an element of the set

$$\mathcal{F}_{\boldsymbol{\ell},\mathbb{AS}}^{h \times h} \triangleq \left\{ \ell(t) \,\middle|\, \ell(t) : \mathbb{R}^+ \to \mathbb{AS}^{h \times h} \right\}.$$

(A8.9) Groupwise Symmetric Interconnection, $\ell(t) \in \mathcal{F}_{\boldsymbol{\ell},\mathrm{G,S}}^{h \times h}$:

A matrix representation of a topology that is symmetric within groups is an element of the set

$$\mathcal{F}_{\boldsymbol{\ell},\mathrm{G,S}}^{h \times h} \triangleq \left\{ \ell(t) \text{ partitioned as (9.11)} \,\middle|\right.$$
$$\left. \ell_{\mathrm{G_f G_f}}(t) \in \mathcal{F}_{\boldsymbol{\ell},\mathrm{S}}^{h_f \times h_f}, \; \forall f = 1, \ldots, g \right\}.$$

It is obvious that a TV topology that is undirected can be written as an element of the set $\mathcal{F}_{\boldsymbol{\ell},\mathrm{S}}^{h \times h}$. As a relaxation, a topology that is undirected within and potentially directed between groups can be written as an element of the set $\mathcal{F}_{\boldsymbol{\ell},\mathrm{G,S}}^{h \times h}$. In this case, it will be shown that one may always rewrite the interconnection as a fully symmetric matrix by the introduction of virtual interconnection channels. However, even for undirected topologies, symmetry is lost after (row-) normalization of the corresponding Laplacian or adjacency matrix. In distributed formation control, the use of the (row-) normalized Laplacian matrix in distributed formation control problems is attractive from the point of view of an *a priori* knowledge on the eigenvalue locations being within a circle with radius one about the point $1 + j0$, the Perron disc, irrespective of the number of subsystems involved. In light of this, the definition of the further following sets will be useful.

(A8.10) Diagonalizable Interconnection, $\ell(t) \in \mathcal{F}_{\boldsymbol{\ell},\mathrm{D}}^{h \times h}$:

The matrix representation of a diagonalizable topology is an element of the set

$$\mathcal{F}_{\boldsymbol{\ell},\mathrm{D}}^{h \times h} \triangleq \left\{ \ell(t) \,\middle|\, \ell(t) : \mathbb{R}^+ \to \boldsymbol{\ell}_{\mathrm{D}}^{h \times h} \right\}.$$

(A8.11) Normal Interconnection, $\ell(t) \in \mathcal{F}_{\boldsymbol{\ell},\mathrm{N}}^{h \times h}$:

The matrix representation of a unitarily diagonalizable (normal) topology is an element of the set

$$\mathcal{F}_{\boldsymbol{\ell},\mathrm{N}}^{h \times h} \triangleq \left\{ \ell(t) \,\middle|\, \ell(t) : \mathbb{R}^+ \to \boldsymbol{\ell}_{\mathrm{N}}^{h \times h} \right\}.$$

Note that $\mathcal{F}_{\boldsymbol{\ell},\mathrm{S}}^{h \times h} \subset \mathcal{F}_{\boldsymbol{\ell},\mathrm{G,S}}^{h \times h} \subset \mathcal{F}_{\boldsymbol{\ell},\mathrm{N}}^{h \times h} \subset \mathcal{F}_{\boldsymbol{\ell},\mathrm{D}}^{h \times h}$. The sets $\mathcal{F}_{\mathscr{L},\mathrm{S}}^{h \times h}$, $\mathcal{F}_{\mathscr{L},\mathrm{G,S}}^{h \times h}$, $\mathcal{F}_{\mathscr{L},\mathrm{N}}^{h \times h}$, $\mathcal{F}_{\mathscr{L},\mathrm{D}}^{h \times h}$, and $\mathcal{F}_{\mathscr{L},\mathbb{R}}^{h \times h}$ are defined accordingly, implying scalar repeated interconnection operators with an interconnection channel width $n_{\mathscr{L}}$. When clear from the context, the superscript indicating the matrix dimensions is omitted.

8.1.3.4 *Summary*

After having established the fundamental constraints to linear, static, scalar repeated interconnection operators, the remaining classes are found to consist in dynamic/nonlinear interconnections. Of these, time-delayed interconnections are of special interest, for which preliminary work is presented in [36].

The representation developed above is more compact than the one in [80], since the operator $\mathscr{L}$ is not required to be (block-)diagonal. In cases where a subsystem's output signals are received by different subsystems, or linear combinations of several subsystems' output signals are received via a single input channel by another subsystem, this effectively decreases the size of the system matrices. Otherwise, output and input signals would have to occur repeatedly in d and v.

8.1.4 *On the Density of Diagonalizable Matrices over the Set of Complex Matrices*

While the set of diagonalizable (or simple) matrices $\boldsymbol{\ell}_D^{h \times h}$ is dense over the set of complex-valued matrices $\mathbb{C}^{h \times h}$, [50], the set of normal matrices $\boldsymbol{\ell}_N^{h \times h}$ is not dense due to the requirement on the existence of a unitary transformation, or equivalently

$$\ell \in \boldsymbol{\ell}_N^{h \times h} \equiv \left\{ \ell \in \boldsymbol{\ell}_D^{h \times h} \; \middle| \; \ell^* \ell = \ell \ell^* \right\}.$$

Density in the mathematical sense means that the Lebesgue measure of the respective complementary set is zero. With respect to the question of density of diagonalizable matrices, loosely speaking, this means that from a large set of random matrices, the probability that a matrix is non-diagonalizable is zero. Even more practically, this means that any given matrix in $\mathbb{C}^{h \times h}$ can be approximated arbitrarily closely by a diagonalizable matrix. Similar to popular lines of reasoning with respect to non-singular matrices, which are also dense over $\mathbb{C}^{h \times h}$ [51] a perturbation argument could thus be employed to assume diagonalizability of any interconnection matrix w. l. o. g.

Most approaches use some kind of transformation on the interconnection matrix to reduce the complexity of the analysis or synthesis problem. While for stability analysis, it may be sufficient to consider, e. g., a Schur decomposition, [40], which always exists, the consideration of performance in an efficient analysis/synthesis problem of low complexity requires some form of diagonalization, see, e. g., [54, 56, 97]. The approach presented in [97] makes use of a signal transformation to decouple subsystems. However, even if such an argument on the density of diagonalizable matrices would be employed, the signal transformation method used in [97] would possibly suffer from arbitrary large deteriorations in the tightness of the performance bounds, which are determined by the condition number of the associated transformation matrix. Close to non-diagonalizability, such a transformation may become ill-conditioned.

In subsequent sections, results will be presented that employ a transformation on multiplier conditions associated with the interconnection. Such a transformation

on an LMI dispenses with the idea of a signal transformation, while maintaining both a guaranteed upper bound on the performance level and further also allowing time-varying interconnections. This transformation is required to be a congruence transformation to preserve the symmetry of the LMI. As a congruence transformation consists of unitary matrices, the interconnection matrix is therefore required to be normal. It will be shown that by the introduction of virtual interconnection channels, this can always be achieved.

8.2 Special Cases and Extensions

THE rather general framework for representing interconnected LPV subsystems is motivated by exploiting graph theory for a compact representation of the interconnection similar to the work of [97], while maintaining the flexibility of the LFT-based modeling approach presented in [80]. As such, «decomposable systems» emerge as a natural special case of the proposed modeling framework. Systems with regular grid topologies will also be shown to be a special case.

Remark 8.3 *In [97, 99, 100], diagonalizability of a constant ℓ is assumed, instead of considering a Schur decomposition as in, e.g., [40], for the purpose of including performance optimization in addition to stability as a synthesis objective.*

8.2.1 *Decomposable Systems*

Massioni et al. [99] introduced the notion of «decomposable systems» in the context of an interconnected LTI system, whose system matrices are structured as a decentralized and an interconnected part. In order not to introduce unnecessary limitations, the notion of «decomposable systems» is straightforwardly extended to cover time-varying interconnections. For this purpose, first consider the following definition.

Definition 8.2 (Decomposable Matrix [99])
Given a TV *diagonalizable topology* $\ell(t) \in \mathcal{F}_{\ell}^{h \times h} \subseteq \mathcal{F}_{\ell, D}^{h \times h}$, *a matrix* $\check{M}(t) : \mathbb{R}^+ \to \mathbb{R}^{hn \times hm}$ *is said to be «decomposable», if for all* $t \in \mathbb{R}^+$ *there exist* $M^d, M^i \in \mathbb{R}^{n \times m}$, *s.t.*

$$\check{M}(t) = I_h \otimes M^d + \ell(t) \otimes M^i. \tag{8.11}$$

Superscripts $\bullet^d$ and $\bullet^i$ identify the local and the interconnected portions of a decomposable matrix. While being slightly informal, the notation $\check{\bullet}$ will indicate that a matrix is decomposable. The special case when the interconnected part is zero is included in that notation.

Due to the assumption that $\ell(t)$ is diagonalizable for all $t \in \mathbb{R}^+$, one may find a time-varying, invertible matrix $F(t)$, s.t.

$$(F(t) \otimes I_n)^{-1} \check{M}(t) (F(t) \otimes I_m) = I_h \otimes M^d + \Lambda(t) \otimes M^i. \tag{8.12}$$

As a straightforward extension from [99], consider the following definition of a «decomposable LFT-LPV system».

Definition 8.3 (Decomposable LFT-LPV System, extended from [99])
Consider the system

$$
\mathscr{\check{P}}:\begin{cases}
\begin{bmatrix}\dot{\check{x}}\\ \check{p}\\ \check{z}\\ \check{y}\end{bmatrix}=\begin{bmatrix}\check{A}(t) & \check{B}_\Delta(t) & \check{B}_p(t) & \check{B}_u(t)\\ \check{C}_\Delta(t) & \check{D}_{\Delta\Delta}(t) & \check{D}_{\Delta p}(t) & \check{D}_{\Delta u}(t)\\ \check{C}_p(t) & \check{D}_{p\Delta}(t) & \check{D}_{pp}(t) & \check{D}_{pu}(t)\\ \check{C}_y(t) & \check{D}_{y\Delta}(t) & \check{D}_{yp}(t) & 0\end{bmatrix}\begin{bmatrix}\check{x}\\ \check{q}\\ \check{w}\\ \check{u}\end{bmatrix}=P_d\begin{bmatrix}\check{x}\\ \check{q}\\ \check{w}\\ \check{u}\end{bmatrix},\\
\check{q}=\check{\Delta}\check{p}, \qquad \delta\in\boldsymbol{\delta}.
\end{cases}
\tag{8.13}
$$

System (8.13) is called «decomposable», iff all of its system matrices $\check{A}(t)$, $\check{B}_\Delta(t)$, ..., are decomposable matrices.

The approach presented in [97, 99, 100] exploits the so-called «decomposition property» by introducing signal transformations of the form $\check{x} = (F(t) \otimes I)\hat{x}$ to obtain a modal decomposition of system (8.13). As an immediate consequence, a time-varying transformation $F(t)$ would lead to the introduction of its time derivative into the system description. A signal transformation approach thus precludes time-varying interconnections. Furthermore, the same signal transformation (now considered constant) on the LFT-LPV parameter channel requires homogeneous scheduling as

$$
\hat{q} = (F \otimes I)^{-1}\check{\Delta}(F \otimes I)\hat{p} = \check{\Delta}\hat{p},
$$

where it has been assumed that the interconnected part of $\check{\Delta}$, is zero, $\Delta^i = 0$.

However, in order to identify the system representation (8.13) as a special case of (8.2), first consider a reordering of the system signals to obtain

$$
\check{P} = I_h \otimes P^d + \ell(t) \otimes P^i = \Psi_y P_d \Psi_u,
$$

$$
\Psi_u \zeta_u = \begin{bmatrix}\dot{\check{x}}\\ \check{q}\\ \check{w}\\ \check{u}\end{bmatrix}, \quad \Psi_y^\top \zeta_y = \begin{bmatrix}\dot{\check{x}}\\ \check{p}\\ \check{z}\\ \check{y}\end{bmatrix}.
\tag{8.14}
$$

Such a permutation can be derived by means of Lma. A.3 on p. 317. As a result, the interconnection matrix can be extracted via an LFT, s. t. the system can be rewritten as

$$
\mathscr{\check{P}}:\begin{cases}
\begin{bmatrix}\zeta_y\\ d\end{bmatrix}=\begin{bmatrix}I_h \otimes P^d & I_h \otimes P^i\\ I & 0\end{bmatrix}\begin{bmatrix}\zeta_u\\ v\end{bmatrix},\\
\check{q}=\check{\Delta}\check{p}, \quad \delta\in\boldsymbol{\delta}, \quad v=(\ell(t)\otimes I_{n_{\mathscr{L}}})d, \quad \ell(t)\in\mathcal{F}_\ell.
\end{cases}
\tag{8.15}
$$

Since usually not all signals contribute to the interconnection of the entire system and consequently some, if not many, system matrices will have an interconnected part equal to zero, the dimension of the interconnection channel $n_{\mathscr{L}}$ can often be drastically reduced. When reverting the signal permutation (8.14) in (8.15) a special case of the interconnected LFT-LPV system (8.2) is obtained in the sense that

- the subsystems have homogeneous dynamics,

- the interconnection is of scalar repeated nature according to Ass. (A8.3).

Apart from that, the results in subsequent sections will show that by avoiding the above-mentioned signal transformation

- the subsystems may be heterogeneously scheduled,
  i.e., $\check{\Delta} = \overset{h}{\underset{k=1}{\mathrm{diag}}}(\Delta_k)$,

- the interconnection may be time-varying.

Furthermore, by dispensing with the rather artificially restricted notion of «decomposable systems», i.e., by directly formulating the interconnected system within an LFT framework via concatenation of individual subsystems, heterogeneous dynamics may be allowed in the modeling stage. As it turns out, heterogeneity in both dynamics and scheduling can be easily handled also in the analysis and synthesis conditions.

8.2.2 *Systems Interconnected Through a Regular Grid Topology*

Regular grid topologies in n_g dimensions can be modeled by choosing ℓ accordingly from an interconnection of $h = \prod_{i=1}^{n_g} h_{x_i}$ subsystems, where h_{x_1} to $h_{x_{n_g}}$ are the numbers of subsystems in the—possibly virtual—x_i directions, $i \in \{1, 2, \ldots, n_g\}$, respectively. Consequently, an undirected grid graph $\mathcal{G}_g$ can be regarded as a graph Cartesian product, cf. Fig. 8.6,

$$\mathcal{G}_g = \mathcal{G}_1 \times \mathcal{G}_2 \times \ldots \mathcal{G}_{n_g} \tag{8.16}$$

of n_g undirected path graphs $\mathcal{G}_i$ of lengths h_{x_i}, $i \in \{1, 2, \ldots, n_g\}$ [49]. The spectra
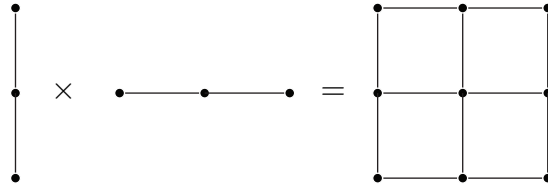
Figure 8.6: Graph Cartesian product of two path graphs to form a grid graph.

of the combinatorial graph Laplacian and the adjacency matrix of a path graph $\mathcal{G}_i$ are [18]

$$\Lambda\left(\mathscr{L}(\mathcal{G}_i)\right) = \left\{\lambda \in \mathbb{R} \;\middle|\; \lambda_j = 2 - 2\cos\left(\pi\frac{j}{h_i}\right), \; j \in \{1, 2, \ldots, h_i - 1\}\right\},$$

$$\Lambda\left(\mathscr{A}(\mathcal{G}_i)\right) = \left\{\lambda \in \mathbb{R} \;\middle|\; \lambda_j = 2\cos\left(\pi\frac{j}{h_i + 1}\right), \; j \in \{1, 2, \ldots, h_i\}\right\}.$$

For simplicity, consider a two-dimensional grid array, $n_g = 2$ and $h_1 = h_2 = h_g$. Then, the adjacency matrix of the grid topology can be computed by [70]

$$\mathscr{A}(\mathcal{G}_g) = \mathscr{A}(\mathcal{G}_1) \otimes I_{h_2} + I_{h_1} \otimes \mathscr{A}(\mathcal{G}_2) \tag{8.17}$$

For $\lambda_{1,i}$ and $\lambda_{2,j}$ denoting the eigenvalues of $\mathscr{A}(\mathcal{G}_1)$ and $\mathscr{A}(\mathcal{G}_2)$, respectively, the corresponding spectrum of $\mathscr{A}(\mathcal{G}_g)$ is then given by

$$\mathbb{A}(\mathscr{A}(\mathcal{G}_g)) = \left\{ \lambda \in \mathbb{R} \mid \lambda_g = \lambda_{1,i}\lambda_{2,j}, \ i \in \{1, \ldots, h_1\}, \ j \in \{1, \ldots, h_2\} \right\},$$

from which the maximum and minimum eigenvalue can be easily inferred. Subsequent normalization of the Laplacian or adjacency matrix, however, recovers the immediate knowledge of the eigenloci to reside inside the unit, or Perron disc, respectively.

8.2.3 *Multi-Topology Systems*

Multi-topology systems can simply be realized by relaxing Ass. (A8.3) to the more general case of multiple scalar interconnection operators

(A8.12) **Multiple Scalar Repeated Interconnection Operators:**
Multiple scalar interconnection operators $\ell_{ij_l}(t)$ encode each connection between two subsystems, i.e.,

$$\mathscr{L}_{ij}(t) = \operatorname*{diag}_{l=1}^{n_{\mathscr{L}}} \left(\ell_{ij_l}(t) \right), \text{with } \ell_{ij_l}(t) : \mathbb{R}^+ \to \mathbb{R}.$$

A reordering of the interconnection channels then yields a block diagonal interconnection operator. Such a framework may be useful for the following cases, amongst others:

- A combination of representing physical coupling as well as communication interaction in scenarios, such as (d) and (e), shown in Figs. 7.2d and 7.2e on p. 218,

- Separate topologies for formation control and general distance keeping (collision avoidance) in MAS settings,

- Fault-diagnosis and isolation for systems with redundant interconnection channels.

9

SYNTHESIS OF DISTRIBUTED LINEAR PARAMETER-VARYING CONTROLLERS FOR INTERCONNECTED HETEROGENEOUS SUBSYSTEMS

≪The welfare of each is bound up in the welfare of all.≫

Helen Keller

THIS chapter aims at developing a capable framework for the synthesis of distributed LPV controllers for heterogeneous systems interconnected through arbitrary directed and time-varying topologies.

In Sect. 9.1, it will be shown how directed topologies can be normalized, i. e., time-varying, directed interconnection matrices can be represented as a combination of matrices with the property of being diagonalizable by a unitary transformation. This requires the introduction of virtual interconnection channels, which do not contribute to the control objectives, but allow to pull out a symmetrized[1]—or more generally, normalized—interconnection matrix in an LFR.

In Sect. 9.2, this technique is applied in the context of multiplier-based synthesis conditions.

---

[1] In the publications [55, 56] the term ≪symmetrification≫ was adopted initially. The authors noticed only later that the proper english term is ≪symmetrization≫, a notion encountered in various mathematical publications and—in its core—related to the idea presented in this thesis.

Preliminary results of this chapter have been previously published in [54–56, 61].

9.1 Symmetrization and Normalization of Directed Interconnection Topologies

The interconnection operator $\mathscr{L}$ will be considered as a parameter block within an LFT-LPV robust gain-scheduling analysis and controller synthesis framework. Within that framework the use of D/G-S [E21] allows to copy the plant's parameter block to the controller as described in Lma. 2.6 and Cor. 2.3 on pp. 70 and 70, respectively. Symmetry of the parameter block and its commutativity with the scalings are necessary conditions for this. This allows to let the synthesized distributed controllers inherit the interconnection topology from the plant representation. Furthermore, normal real-valued interconnection matrices provide a guarantee for the existence of a diagonalizing transformation and real eigenvalues of $\mathscr{L}$, s. t. the synthesis problem can eventually be transformed to an LFT-LPV controller synthesis problem with a diagonal parameter block, cf. Sect. 9.2. More generally, a real-valued interconnection matrix is required to be «normal», thus diagonalizable, for such a diagonalizing transformation to exist. If an appropriate structure is imposed on the multiplier matrix variables and in addition, the Lyapunov matrices are chosen to be structured as well, the synthesis complexity can be reduced to be of the order of a single subsystem. In order to guarantee stability and performance in the face of time-varying interconnection topologies, knowledge about the admissible range of eigenvalues of the normalized interconnection matrix is required. Furthermore, the masking matrix structure due to the normalization is required to be invariant.

For this purpose, consider a real-valued, static, linear and possibly time-varying interconnection operator that is given by the matrix $\ell(t)$ derived from a scalar repeated structure. Further, let $\ell(t)$ represent a directed topology, i.e., $\ell(t) \in \mathcal{F}_{\ell,\mathbb{R}}^{h \times h}$. It is the objective to find a representation

$$\ell(t) = V_\ell \tilde{\ell}(t) W_\ell = \tilde{\ell}(t) \star \left[\begin{array}{c|c} 0 & W_\ell \\ \hline V_\ell & 0 \end{array} \right], \text{ where } \tilde{\ell}(t) \in \mathcal{F}_{\ell,N}^{\tilde{h} \times \tilde{h}}, \tag{9.1}$$

$$\text{with } V_\ell W_\ell = I_h \tag{9.2}$$

and $V_\ell W_\ell = I_h$. In general $\tilde{h} \geqslant h$. Consequently, one has

$$\mathscr{L}(t) = V_\mathscr{L} \tilde{\mathscr{L}}(t) W_\mathscr{L} = \tilde{\mathscr{L}}(t) \star \left[\begin{array}{c|c} 0 & W_\mathscr{L} \\ \hline V_\mathscr{L} & 0 \end{array} \right], \tag{9.3}$$

where $\tilde{\mathscr{L}}(t) \in \mathcal{F}_{\mathscr{L},N}^{h \times h} \triangleq \mathcal{F}_{\mathscr{L},N}^{\tilde{h} \times \tilde{h}}$ and $V_\mathscr{L} W_\mathscr{L} = I_{hn_\mathscr{L}}$, $V_\mathscr{L} = V_\ell \otimes I_{n_\mathscr{L}}$, $W_\mathscr{L} = W_\ell \otimes I_{n_\mathscr{L}}$. Denote λ and $\tilde{\lambda}$ the sets of unique admissible eigenvalues of the possibly time-varying interconnection matrices (unnormalized and normalized) and let the sets be defined by the respective union of the sets of unique momentary eigenvalues $\mathbb{A}(\ell(t))$ and $\mathbb{A}(\tilde{\ell}(t))$ for all time instants. I. e.,

$$\lambda \triangleq \bigcup_{\forall t \in \mathbb{R}^+} \mathbb{A}(\ell(t)), \qquad \tilde{\lambda} \triangleq \bigcup_{\forall t \in \mathbb{R}^+} \mathbb{A}(\tilde{\ell}(t)). \tag{9.4}$$

Note that in general $\boldsymbol{\lambda} \neq \tilde{\boldsymbol{\lambda}}$, whereas due to the scalar repeated structure of the interconnection

$$\boldsymbol{\lambda} = \boldsymbol{\Lambda} \triangleq \bigcup_{\forall t \in \mathbb{R}^+} \mathbb{A}\big(\mathscr{L}(t)\big), \qquad \tilde{\boldsymbol{\lambda}} = \tilde{\boldsymbol{\Lambda}} \triangleq \bigcup_{\forall t \in \mathbb{R}^+} \mathbb{A}\big(\tilde{\mathscr{L}}(t)\big). \tag{9.5}$$

Analogously, consider set $\boldsymbol{\sigma}$ of unique admissible singular values of the possibly time-varying interconnection matrix and let it be defined by the union of the set of unique momentary singular values $\boldsymbol{\Sigma}\big(\ell(t)\big)$ for all time instants. I. e.,

$$\boldsymbol{\sigma} \triangleq \bigcup_{\forall t \in \mathbb{R}^+} \boldsymbol{\Sigma}\big(\ell(t)\big) = \bigcup_{\forall t \in \mathbb{R}^+} \mathbb{A}\big(\ell^\top(t)\ell(t)\big) \tag{9.6}$$

$$\boldsymbol{\sigma} = \boldsymbol{\Sigma} \triangleq \bigcup_{\forall t \in \mathbb{R}^+} \boldsymbol{\Sigma}\big(\mathscr{L}(t)\big) = \bigcup_{\forall t \in \mathbb{R}^+} \mathbb{A}\big(\mathscr{L}^\top(t)\mathscr{L}(t)\big). \tag{9.7}$$

With regard to the question of finding a time-varying normalized interconnection matrix $\tilde{\ell}(t)$ in accordance with the time-invariant transformation given in (9.1) with the constraint (9.2), the following problem is formulated.

Problem 9.1 (Normalization of an Interconnection Matrix)
For an interconnection operator $\mathscr{L}(t) = \ell(t) \otimes I_{n_{\mathscr{L}}}$, i. e., satisfying Ass. (A8.1), (A8.3), with $\ell(t) \in \mathcal{F}_{\ell,\mathbb{R}}^{h \times h}$, find a representation (9.1), satisfying (9.2). $\qquad\square$

The usefulness of the identity condition (9.2) will become clear in Sect. 9.2. As a prerequisite, the transformation given in (9.1) is first attributed to the constant state space matrices of the LFR of the closed-loop system, illustrated by Fig. 9.1. In conjunction with assuming that the controller inherits the interconnection topology, i. e., $\mathscr{L}^K = \mathscr{L}$, a normalization of the form (9.3) allows to define augmented closed-loop matrices by

$$\tilde{T} = \tilde{T}_0 + \tilde{W}\tilde{K}\tilde{V} = W_{\mathscr{L}}\left(T_0 + WKV\right)V_{\mathscr{L}},$$

or more specifically

$$\tilde{T} = \begin{bmatrix} \mathcal{A} & \mathcal{B}_\Delta & \tilde{\mathcal{B}}_i & \mathcal{B}_p \\ \mathcal{C}_\Delta & \mathcal{D}_{\Delta\Delta} & \tilde{\mathcal{D}}_{\Delta i} & \mathcal{D}_{\Delta p} \\ \tilde{\mathcal{C}}_i & \tilde{\mathcal{D}}_{i\Delta} & \tilde{\mathcal{D}}_{ii} & \tilde{\mathcal{D}}_{ip} \\ \mathcal{C}_p & \mathcal{D}_{p\Delta} & \tilde{\mathcal{D}}_{pi} & \mathcal{D}_{pp} \end{bmatrix} = \underbrace{\begin{bmatrix} I & & & \\ & I & & \\ & & I_2 \otimes W_{\mathscr{L}} & \\ & & & I \end{bmatrix}}_{W_{\mathscr{L}}} T \underbrace{\begin{bmatrix} I & & & \\ & I & & \\ & & I_2 \otimes V_{\mathscr{L}} & \\ & & & I \end{bmatrix}}_{V_{\mathscr{L}}}.$$

This is illustrated in Fig. 9.1. The interconnected closed-loop system, augmented by a normalized interconnection matrix is therefore defined as

$$
\tilde{\mathscr{T}} : \begin{cases}
\begin{bmatrix} \dot{\mathfrak{x}} \\ \mathfrak{p} \\ \tilde{\mathfrak{d}} \\ z \end{bmatrix} = \underbrace{\left[\begin{array}{c|ccc} \mathcal{A} & \mathcal{B}_\Delta & \tilde{\mathcal{B}}_i & \mathcal{B}_p \\ \hline \mathcal{C}_\Delta & \mathcal{D}_{\Delta\Delta} & \tilde{\mathcal{D}}_{\Delta i} & \mathcal{D}_{\Delta p} \\ \tilde{\mathcal{C}}_i & \tilde{\mathcal{D}}_{i\Delta} & \tilde{\mathcal{D}}_{ii} & \tilde{\mathcal{D}}_{ip} \\ \mathcal{C}_p & \mathcal{D}_{p\Delta} & \tilde{\mathcal{D}}_{pi} & \mathcal{D}_{pp} \end{array}\right]}_{\tilde{T}=\tilde{T}_0+\tilde{W}\tilde{K}\tilde{V}} \begin{bmatrix} \mathfrak{x} \\ \mathfrak{q} \\ \tilde{\mathfrak{v}} \\ w \end{bmatrix}, \\[3em]
\quad \mathfrak{q} = \Delta\mathfrak{p}, \qquad \tilde{\mathfrak{v}} = \mathscr{L}\tilde{\mathfrak{d}}, \qquad \delta \in \mathcal{F}_\delta^\eta \\[0.5em]
\quad \mathfrak{q}^K = \Delta^K\mathfrak{p}^K, \quad \tilde{v}^K = \mathscr{L}\tilde{\mathfrak{d}}^K, \quad \mathscr{L} \in \mathcal{F}_{\mathscr{L},N}^{\tilde{\hbar}\times\tilde{\hbar}},
\end{cases}
\tag{9.8}
$$

where

$$
\tilde{\mathfrak{d}} = \begin{bmatrix} \tilde{\mathfrak{d}} \\ \tilde{\mathfrak{d}}^K \end{bmatrix} \in \mathbb{R}^{n_{\tilde{\mathfrak{d}}}}, \quad \tilde{\mathfrak{v}} = \begin{bmatrix} \tilde{v} \\ \tilde{v}^K \end{bmatrix} \in \mathbb{R}^{n_{\tilde{\mathfrak{v}}}},
$$

and

$$
\tilde{T} = \tilde{T}_0 + \tilde{W}\tilde{K}\tilde{V} = \left[\begin{array}{c|ccc} \mathcal{A} & \mathcal{B}_\Delta & \tilde{\mathcal{B}}_i & \mathcal{B}_p \\ \hline \mathcal{C}_\Delta & \mathcal{D}_{\Delta\Delta} & \tilde{\mathcal{D}}_{\Delta i} & \mathcal{D}_{\Delta p} \\ \tilde{\mathcal{C}}_i & \tilde{\mathcal{D}}_{i\Delta} & \tilde{\mathcal{D}}_{ii} & \tilde{\mathcal{D}}_{ip} \\ \mathcal{C}_p & \mathcal{D}_{p\Delta} & \tilde{\mathcal{D}}_{pi} & \mathcal{D}_{pp} \end{array}\right]
\tag{9.9}
$$

$$
T = \left[\begin{array}{cc|cc|cc|c} A & 0 & B_\Delta & 0 & \tilde{B}_i & 0 & B_p \\ 0 & 0 & 0 & 0 & 0 & 0 & 0 \\ \hline C_\Delta & 0 & D_{\Delta\Delta} & 0 & \tilde{D}_{\Delta i} & 0 & D_{\Delta p} \\ 0 & 0 & 0 & 0 & 0 & 0 & 0 \\ \tilde{C}_i & 0 & \tilde{D}_{i\Delta} & 0 & \tilde{D}_{ii} & 0 & \tilde{D}_{ip} \\ 0 & 0 & 0 & 0 & 0 & 0 & 0 \\ \hline C_p & 0 & D_{p\Delta} & 0 & \tilde{D}_{pi} & 0 & D_{pp} \end{array}\right] + \left[\begin{array}{ccc} 0 & B_u & 0 & 0 \\ I & 0 & 0 & 0 \\ 0 & D_{\Delta u} & 0 & 0 \\ 0 & 0 & 0 & I \\ 0 & \tilde{D}_{iu} & 0 & 0 \\ 0 & 0 & I & 0 \\ 0 & D_{pu} & 0 & 0 \end{array}\right]
$$

$$
\times \left[\begin{array}{c|ccc} A^K & B_y^K & \tilde{B}_i^K & B_\Delta^K \\ C_u^K & D_{uy}^K & \tilde{D}_{ui}^K & D_{u\Delta}^K \\ \tilde{C}_i^K & \tilde{D}_{iy}^K & \tilde{D}_{ii}^K & \tilde{D}_{i\Delta}^K \\ C_\Delta^K & D_{\Delta y}^K & \tilde{D}_{\Delta i}^K & D_{\Delta\Delta}^K \end{array}\right] \left[\begin{array}{cc|cc|cc|c} 0 & I & 0 & 0 & 0 & 0 & 0 \\ C_y & 0 & D_{y\Delta} & 0 & \tilde{D}_{yi} & 0 & D_{yp} \\ 0 & 0 & 0 & 0 & 0 & I & 0 \\ 0 & 0 & 0 & I & 0 & 0 & 0 \end{array}\right].
\tag{9.10}
$$

For the purpose of reordering the interconnected system according to the heterogeneous subsystem dynamics, one can find further permutations, s. t.

$$
\check{T} = \Psi_{T,1}\tilde{T}\Psi_{T,2}^\top = \sum_{f=1}^{g} \mathsf{E}_f \otimes \left[\begin{array}{c|ccc} \mathcal{A}_f & \mathcal{B}_{f,\Delta} & \check{\mathcal{B}}_{f,i} & \mathcal{B}_{f,p} \\ \hline \mathcal{C}_{f,\Delta} & \mathcal{D}_{f,\Delta\Delta} & \check{\mathcal{D}}_{f,\Delta i} & \mathcal{D}_{f,\Delta p} \\ \check{\mathcal{C}}_{f,i} & \check{\mathcal{D}}_{f,i\Delta} & \check{\mathcal{D}}_{f,ii} & \check{\mathcal{D}}_{f,ip} \\ \mathcal{C}_{f,p} & \mathcal{D}_{f,p\Delta} & \check{\mathcal{D}}_{f,pi} & \mathcal{D}_{f,pp} \end{array}\right] = \sum_{f=1}^{g} \mathsf{E}_f \otimes \check{T}_f,
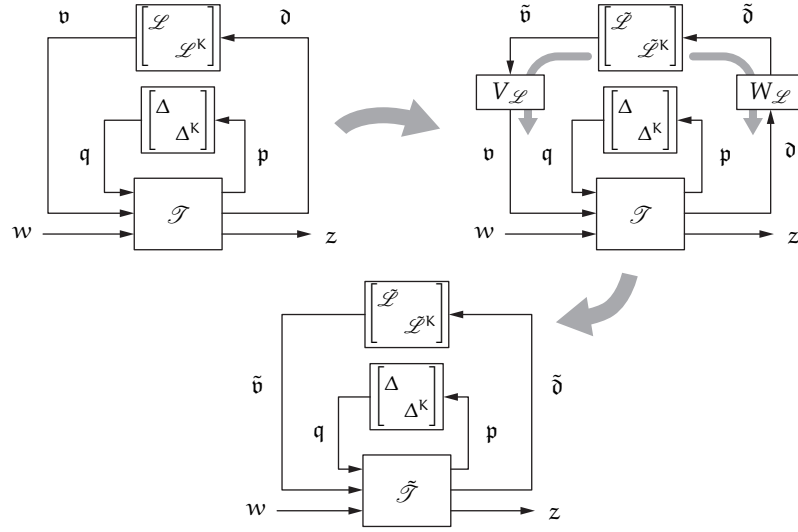$$

Figure 9.1: Interconnected LPV system structure with normalized interconnection topology.

with

$$
\check{T}_{\mathrm{f}} = \underbrace{\begin{bmatrix} I & & & \\ & I & & \\ & & I_2 \otimes W_{\mathscr{L}_{\mathrm{f}}} & \\ & & & I \end{bmatrix}}_{W_{\mathscr{L}_{\mathrm{f}}}} \underbrace{\begin{bmatrix} \mathcal{A}_{\mathrm{f}} & \mathcal{B}_{\mathrm{f},\Delta} & \mathcal{B}_{\mathrm{f},\mathrm{i}} & \mathcal{B}_{\mathrm{f},\mathrm{p}} \\ \mathcal{C}_{\mathrm{f},\Delta} & \mathcal{D}_{\mathrm{f},\Delta\Delta} & \mathcal{D}_{\mathrm{f},\Delta\mathrm{i}} & \mathcal{D}_{\mathrm{f},\Delta\mathrm{p}} \\ \mathcal{C}_{\mathrm{f},\mathrm{i}} & \mathcal{D}_{\mathrm{f},\mathrm{i}\Delta} & \mathcal{D}_{\mathrm{f},\mathrm{ii}} & \mathcal{D}_{\mathrm{f},\mathrm{ip}} \\ \mathcal{C}_{\mathrm{f},\mathrm{p}} & \mathcal{D}_{\mathrm{f},\mathrm{p}\Delta} & \mathcal{D}_{\mathrm{f},\mathrm{pi}} & \mathcal{D}_{\mathrm{f},\mathrm{pp}} \end{bmatrix}}_{T_{\mathrm{f}}} \underbrace{\begin{bmatrix} I & & & \\ & I & & \\ & & I_2 \otimes V_{\mathscr{L}_{\mathrm{f}}} & \\ & & & I \end{bmatrix}}_{V_{\mathscr{L}_{\mathrm{f}}}}.
$$

Note that since **G** contains only pairwise disjoint sets, using suitable permutations $\Psi_{\mathrm{K},2}^{\top}\Psi_{\mathrm{K},1} = I$ one can write

$$
\check{T}_{\mathrm{f}} = \left(\Psi_{\mathrm{T},1}\tilde{T}_0\Psi_{\mathrm{T},2}^{\top}\right) + \left(\Psi_{\mathrm{T},1}\tilde{W}\Psi_{\mathrm{K},2}^{\top}\right)\left(\Psi_{\mathrm{K},1}\tilde{K}\Psi_{\mathrm{K},2}^{\top}\right)\left(\Psi_{\mathrm{K},1}\tilde{V}\Psi_{\mathrm{T},2}^{\top}\right),
$$

$$
= \sum_{\mathrm{f}=1}^{g} \mathsf{E}_{\mathrm{f}} \otimes \left(W_{\mathscr{L}_{\mathrm{f}}}\underbrace{(T_{\mathrm{f},0} + W_{\mathrm{f}}K_{\mathrm{f}}V_{\mathrm{f}})}_{T_{\mathrm{f}}}V_{\mathscr{L}_{\mathrm{f}}}\right).
$$

In the above equations, $W_{\mathscr{L}_{\mathrm{f}}}$ and $V_{\mathscr{L}_{\mathrm{f}}}$ denote corresponding portions of the masking matrices $W_{\mathscr{L}}$ and $V_{\mathscr{L}}$ introduced during normalization.

9.1.1 *Symmetrization of Groupwise Directed Topologies*

When considering groups of subsystems with undirected interconnections within and directed between the groups, one can find a symmetrized representation of the scalar interconnection operator ℓ as follows:

Proposition 9.1 (Groupwise Symmetrization [55, 56])
Let the interconnection operator $\mathscr{L}(\mathrm{t}) = \ell(\mathrm{t}) \otimes I_{n_{\mathscr{L}}}$ be real-valued, static, linear and

possibly time-varying, of scalar repeated structure according to Ass. (A8.1) and (A8.3) on p. 236 as well as subdivided into blocks corresponding to groups as in (9.11) on p. 254. I.e., $\ell(t) \in \mathcal{F}_{\boldsymbol{\ell},G,S}^{h \times h}$ satisfies Ass. (A8.9) on p. 240. From the partition $\mathbf{G} = \{\mathbf{G}_1, \mathbf{G}_2, \ldots, \mathbf{G}_g\}$ of $\mathbf{H}$, this means

$$\ell(t) = \begin{bmatrix} \ell_{G_1 G_1}(t) & \ell_{G_1 G_2}(t) & \cdots & \ell_{G_1 G_g}(t) \\ \ell_{G_2 G_1}(t) & \ell_{G_2 G_2}(t) & \cdots & \ell_{G_2 G_g}(t) \\ \vdots & & \ddots & \vdots \\ \ell_{G_g G_1}(t) & \ell_{G_g G_2}(t) & \cdots & \ell_{G_g G_g}(t) \end{bmatrix}, \tag{9.11}$$

$$\ell_{G_i G_j}(t) : \mathbb{R}^+ \to \boldsymbol{\ell}_{G_i G_j} \subseteq \mathbb{R}^{h_i \times h_j}.$$

Then one can find operators $\ell_f(t) \in \mathcal{F}_{\boldsymbol{\ell},S}^{h \times h}$ with W_{ℓ_f}, V_{ℓ_f}, s.t.

$$\ell(t) = \tilde{\ell}(t) \star \left[\begin{array}{c|c} 0 & W_\ell \\ \hline V_\ell & 0 \end{array} \right], \quad \tilde{\ell}(t) = \sum_{f=1}^g \mathcal{E}_f \otimes \ell_f(t), \tag{9.12}$$

with $V_\ell W_\ell = I_h$, $V_\ell = \sum_{f=1}^g V_{\ell_f}$, $W_\ell = \sum_{f=1}^g W_{\ell_f}$, and where $\tilde{h} = gh$ and masking matrices $\mathcal{E}_f \in \mathbb{R}^{g \times g}$ indicate the block-matrix position of the operator ℓ_f on the diagonal. Consequently, $\tilde{\ell}(t) \in \mathcal{F}_{\boldsymbol{\ell},S}^{\tilde{h} \times \tilde{h}}$. $\qquad\square$

Proof: The proof follows by mathematical induction. Dependence on time is omitted for brevity.

Basis

Assume $g = 2$. A possible symmetrization can then be derived as

$$\ell = \left[\begin{array}{c|c} \ell_{G_1 G_1} & \ell_{G_1 G_2} \\ \hline \ell_{G_2 G_1} & \ell_{G_2 G_2} \end{array} \right] = \tilde{\ell} \star \left[\begin{array}{c|c} 0 & W_\ell \\ \hline V_\ell & 0 \end{array} \right] = \begin{bmatrix} \ell_1 & \\ & \ell_2 \end{bmatrix} \star \left[\begin{array}{c|c} 0 & \begin{matrix} I_h \\ I_h \end{matrix} \\ \hline E_1 \; E_2 & 0 \end{array} \right], \tag{9.13}$$

$$\text{where } \ell_1 = \ell_1^\top = \left[\begin{array}{c|c} \ell_{G_1 G_1} & \ell_{G_1 G_2} \\ \hline \ell_{G_1 G_2}^\top & \bullet \end{array} \right], \quad \ell_2 = \ell_2^\top = \left[\begin{array}{c|c} \bullet & \ell_{G_2 G_1}^\top \\ \hline \ell_{G_2 G_1} & \ell_{G_2 G_2} \end{array} \right].$$

Note that $V_\ell W_\ell = I_h$.

Inductive Step

Assume that for g groups a symmetrization has already been derived as

$$\ell = \tilde{\ell} \star \left[\begin{array}{c|c} 0 & W_\ell \\ \hline V_\ell & 0 \end{array} \right], \quad \begin{array}{l} \tilde{\ell} \in \mathcal{F}_{\boldsymbol{\ell},S}^{\tilde{h} \times \tilde{h}} \\ \ell_f \in \mathcal{F}_{\boldsymbol{\ell},S}^{h \times h} \end{array}, \tag{9.14}$$

with $\tilde{h} = gh$ and $V_\ell W_\ell = I_h$. Consider a further group, s.t. there are $g+1$ groups in the interconnection matrix ℓ_+ containing an additional $h_{(g+1)}$ subsystems, i.e., $h_{1:(g+1)} = h + h_{(g+1)}$. Then, one can write

$$
\ell_+ = \left[\begin{array}{ccc|c} & & & \ell_{G_1 G_{(g+1)}} \\ & \tilde{\ell} \star \begin{bmatrix} 0 & W_\ell \\ \hline V_\ell & 0 \end{bmatrix} & & \ell_{G_2 G_{(g+1)}} \\ & & & \vdots \\ & & & \ell_{G_g G_{(g+1)}} \\ \hline \ell_{G_{(g+1)} G_1} & \ell_{G_{(g+1)} G_2} \cdots \ell_{G_{(g+1)} G_g} & & \ell_{G_{(g+1)} G_{(g+1)}} \end{array} \right]
$$

$$
= \left[\begin{array}{c|c} \ell & \ell_{G_{1:g} G_{g+1}} \\ \hline \ell_{G_{g+1} G_{1:g}} & \ell_{G_{g+1} G_{g+1}} \end{array} \right].
$$

Rewrite this as

$$
\ell_+ = \begin{bmatrix} V_\ell & 0 \\ \hline 0 & I_{h_{(g+1)}} \end{bmatrix} \begin{bmatrix} \tilde{\ell} & W_\ell \ell_{G_{1:g} G_{g+1}} \\ \hline \ell_{G_{g+1} G_{1:g}} V_\ell & \ell_{G_{g+1} G_{g+1}} \end{bmatrix} \begin{bmatrix} W_\ell & 0 \\ \hline 0 & I_{h_{(g+1)}} \end{bmatrix}
$$

and observe that a symmetrization exists in

$$
\ell_+ = \begin{bmatrix} \ell_{+,1} & \\ & \ell_{+,2} \end{bmatrix} \star \left[\begin{array}{c|c} 0 & \begin{bmatrix} I_h \\ I_h \end{bmatrix} \begin{bmatrix} W_\ell & 0 \\ 0 & I_{h_{(g+1)}} \end{bmatrix} \\ \hline \begin{bmatrix} V_\ell & 0 \\ 0 & I_{h_{(g+1)}} \end{bmatrix} \begin{bmatrix} \sum_{f=1}^{g} E_f \; E_{(g+1)} \end{bmatrix} & 0 \end{array} \right]
$$

$$
= \begin{bmatrix} \ell_{+,1} & \\ & \ell_{+,2} \end{bmatrix} \star \left[\begin{array}{c|c} 0 & \begin{matrix} W_\ell & 0 \\ 0 & I_{h_{(g+1)}} \\ W_\ell & 0 \\ 0 & I_{h_{(g+1)}} \end{matrix} \\ \hline \begin{matrix} V_\ell\, 0\, 0 & 0 \\ 0\, 0\, 0\, I_{h_{(g+1)}} & 0 \end{matrix} & \begin{matrix} 0 \\ 0 \end{matrix} \end{array} \right]
$$

Consequently, one may employ the short-hand notation

$$
\ell_+ = \tilde{\ell}_+ \star \begin{bmatrix} 0 & W_{\ell_+} \\ \hline V_{\ell_+} & 0 \end{bmatrix}
$$

$$
\text{where } \ell_{+,1} = \ell_{+,1}^\top = \begin{bmatrix} \tilde{\ell} & W_\ell \ell_{G_{1:g} G_{g+1}} \\ \hline \ell_{G_{1:g} G_{g+1}}^\top W_\ell^\top & \bullet \end{bmatrix}
$$

$$
\ell_{+,2} = \ell_{+,2}^\top = \begin{bmatrix} \bullet & V_\ell^\top \ell_{G_{g+1} G_{1:g}}^\top \\ \hline \ell_{G_{g+1} G_{1:g}} V_\ell & \ell_{G_{g+1} G_{g+1}} \end{bmatrix}.
$$

Note that as before $V_{\ell_+} W_{\ell_+} = I_{h_{1:(g+1)}}$. $\blacksquare$

Remark 9.1 *It will become clear in Sect. 9.2.3.1 that the technical assumption $V_\ell W_\ell = I_h$ is due to Lma. A.9 and Cor. A.2 in the appendix.*

By observing

$$\tilde{\mathscr{L}} = \sum_{f=1}^{g} (1_{g \times g} \otimes \ell_f) \circledast (\mathcal{E}_f \otimes I_{n_{\mathscr{L}}}) \tag{9.15}$$

Accordingly, we have

$$\mathscr{L} = \Psi_i \tilde{\mathscr{L}} \Psi_i^\top = \Psi_i \left(\sum_{f=1}^{g} \mathcal{E}_f \otimes \mathscr{L}_f \right) \Psi_i^\top$$

$$= \Psi_i \left(\sum_{f=1}^{g} \mathcal{E}_f \otimes (\ell_f \otimes I_{n_{\mathscr{L}}}) \right) \Psi_i^\top = \sum_{f=1}^{g} \ell_f \otimes (\mathcal{E}_f \otimes I_{n_{\mathscr{L}}}).$$

$$V_{\mathscr{L}} \Psi_i^\top = \sum_{f=1}^{g} E_f \otimes (v_{\ell_f} \otimes I_{n_{\mathscr{L}}}) = \sum_{f=1}^{g} E_f \otimes V_{\mathscr{L}_f} \tag{9.16}$$

$$\Psi_i W_{\mathscr{L}} = \sum_{f=1}^{g} E_f \otimes (w_{\ell_f} \otimes I_{n_{\mathscr{L}}}) = \sum_{f=1}^{g} E_f \otimes W_{\mathscr{L}_f}. \tag{9.17}$$

9.1.2 *Optimal Symmetrization and Conservatism*

Note that the symmetrization, i. e., the choice of both the masking matrices W_ℓ and V_ℓ and the symmetric virtual interconnection operators ℓ_f is not unique.

Example 9.1 (Leader-Follower Setup I)
In a leader-follower configuration where communication is undirected within, but directed between both groups $\mathbf{G} = \{\mathbf{G}_1, \mathbf{G}_2\}$, *a 2×2 block partition for the interconnection operator may be imposed, which can be decomposed as*

$$\ell = \begin{bmatrix} \ell_{G_1G_1} & \ell_{G_1G_2} \\ \ell_{G_2G_1} & \ell_{G_2G_2} \end{bmatrix} = \begin{bmatrix} \ell_1 & \\ & \ell_2 \end{bmatrix} \star \begin{bmatrix} 0 & I_h \\ & I_h \\ \hline E_1 \ E_2 & 0 \end{bmatrix}, \tag{9.18}$$

where $\ell_1 = \ell_1^\top = \begin{bmatrix} \ell_{G_1G_1} & \ell_{G_1G_2} \\ \ell_{G_1G_2}^\top & \bullet \end{bmatrix}, \quad \ell_2 = \ell_2^\top = \begin{bmatrix} \bullet & \ell_{G_2G_1}^\top \\ \ell_{G_2G_1} & \ell_{G_2G_2} \end{bmatrix}.$

Here $\ell_{G_1G_1}$, $\ell_{G_2G_2}$ *encode undirected communication among leaders or followers, respectively. The off-diagonal blocks encode directed communication between groups. In this case, one has* $\mathcal{E}_1 = \begin{bmatrix} 1 \\ 0 \end{bmatrix}$, $\mathcal{E}_2 = \begin{bmatrix} 0 \\ 1 \end{bmatrix}$, $w_{\ell_1} = \begin{bmatrix} 1 \ 1 \end{bmatrix}^\top$, $w_{\ell_2} = \begin{bmatrix} 1 \ 1 \end{bmatrix}^\top$, $v_{\ell_1} = \begin{bmatrix} 1 \ 0 \end{bmatrix}$ *and* $v_{\ell_2} = \begin{bmatrix} 0 \ 1 \end{bmatrix}$. *Note that matrix entries given by* $\bullet$ *denote symmetric block matrices that drop out.* □

Example 9.2 (Leader-Follower Setup II)
As for the agents depicted in Fig. 8.1 on p. 231, communication from followers to leaders is now disallowed. With scalar repeated identity interconnection operators one has

$$
\ell = \begin{bmatrix} 0 & 1 & 1 & 0 & 0 & 0 & 0 \\ 1 & 0 & 1 & 0 & 0 & 0 & 0 \\ 1 & 1 & 0 & 0 & 0 & 0 & 0 \\ 0 & 0 & 0 & 0 & 0 & 1 & 1 \\ 0 & 1 & 0 & 0 & 0 & 1 & 1 \\ 1 & 0 & 0 & 1 & 1 & 0 & 1 \\ 0 & 0 & 0 & 1 & 1 & 1 & 0 \end{bmatrix} = \begin{bmatrix} \ell_{G_1 G_1} & 0 \\ \ell_{G_2 G_1} & \ell_{G_2 G_2} \end{bmatrix}, \quad \ell_1 = \begin{bmatrix} \ell_{G_1 G_1} & \ell_{G_2 G_1}^\top \\ \ell_{G_2 G_1} & \ell_{G_2 G_2} \end{bmatrix},
$$

$$
\mathcal{L} = \begin{bmatrix} \ell_1 \otimes I_{n_\mathcal{L}} & \\ & \ell_1 \otimes I_{n_\mathcal{L}} \end{bmatrix} \star \begin{bmatrix} 0 & 0 & I_h \otimes I_{n_\mathcal{L}} \\ 0 & 0 & E_1 \otimes I_{n_\mathcal{L}} \\ E_2 \otimes I_{n_\mathcal{L}} & E_1 \otimes I_{n_\mathcal{L}} & 0 \end{bmatrix}
$$

Here, one has $w_{\ell_1} = \begin{bmatrix} 1 & 1 \end{bmatrix}^\top$, $w_{\ell_2} = \begin{bmatrix} 1 & 0 \end{bmatrix}^\top$, $v_{\ell_1} = \begin{bmatrix} 0 & 1 \end{bmatrix}$ and $v_{\ell_2} = \begin{bmatrix} 1 & 0 \end{bmatrix}$. □

The degrees of freedom during symmetrization should be used to minimize conservatism, by using as few as possible different virtual symmetric interconnection operators ℓ_f. Note that in Ex. 9.2 only a single virtual interconnection operator is necessary with two repetitions. This allows for fewer multiplier constraints in the LMI conditions and consequently less conservatism. Furthermore, the completion of the virtual symmetric interconnection operators should not extend the range of eigenvalues. In fact, an LMI optimization problem can be formulated for minimizing the range of eigenvalues of any virtual interconnection operator $\ell_f(\Xi)$ over the resp. symmetrically completing entries collected in the decision variable matrix Ξ, where $\ell_f(\Xi)$ is linear in Ξ and is otherwise known *a priori*.

$$
\min_{\Xi} \overline{\lambda} - \underline{\lambda} \succ 0, \quad \text{s.t.} \quad \underline{\lambda} I_h \prec \ell_f(\Xi) \prec \overline{\lambda} I_h. \tag{9.19}
$$

If all possible topologies are known, between which there occurs switching, the optimization problem (9.19) can be solved in each of these *independently*.

Note that in the leader-follower setup, the bounds on the eigenvalues can always be preserved. To see this, recall that for symmetric matrices $\ell_f \in \mathbb{S}^{h \times h}$ one has $|\lambda_i(\ell_f)| = \sigma_i(\ell_f)$, with $i = 1, \dots, h$. The problem can therefore be posed as a norm-preserving matrix dilation problem. Again, symmetrically completing entries are collected in Ξ and one has [166]

$$
\min_{\Xi} \overline{\sigma} \left(\begin{bmatrix} 0 & \ell_{G_2 G_1}^\top \\ \ell_{G_2 G_1} & \ell_{G_2 G_2} \end{bmatrix} + \begin{bmatrix} I \\ 0 \end{bmatrix} \Xi \begin{bmatrix} I & 0 \end{bmatrix} \right) = \overline{\sigma} \left(\begin{bmatrix} \ell_{G_2 G_1}^\top \\ \ell_{G_2 G_2} \end{bmatrix} \right).
$$

9.1.3 *Normalization of General Directed Topologies*

When considering unstructured subsystems with directed interconnections, one can find a symmetrized representation of the scalar interconnection operator ℓ as follows:

Proposition 9.2 (Normalization I)
Let the arbitrary interconnection operator $\mathscr{L}(t) = \ell(t) \otimes I_{n_{\mathscr{L}}}$, with $\ell(t) \in \mathcal{F}_{\ell,\mathbb{R}}^{h \times h}$ be real-valued, static, linear and possibly time-varying as well as of scalar repeated structure according to Ass. (A8.1) and (A8.3) on p. 236.
Then one can find matrices W_ℓ, V_ℓ, s. t. with the operators

$$\ell(t) = \tilde{\ell}(t) \star \left[\begin{array}{c|c} 0 & W_\ell \\ \hline V_\ell & 0 \end{array}\right], \quad \tilde{\ell}(t) = \begin{bmatrix} \ell(t) & -\ell^\top(t) \\ \ell^\top(t) & \ell(t) \end{bmatrix} \in \mathcal{F}_{\ell,N}^{\tilde{h} \times \tilde{h}}, \tag{9.20}$$

with $V_\ell W_\ell = I_h$, $\tilde{h} = 2h$. □
 Proof: For each $\ell \in \boldsymbol{\ell}$, the matrix $\tilde{\ell}$ is normal, since $\tilde{\ell}\tilde{\ell}^\top = \tilde{\ell}^\top \tilde{\ell}$. In fact, it is easy to check that if a parameterization is introduced, such as

$$\tilde{\ell} = \begin{bmatrix} c_S \ell & -c_{AS} \ell^\top \\ \tilde{c}_S \ell^\top & \tilde{c}_{AS} \ell \end{bmatrix},$$

from the normality condition it follows that $c_S = \tilde{c}_S = c_{AS} = \tilde{c}_{AS}$. A particular choice with $v_S, v_{AS}, w_S, w_{AS} \in \mathbb{R}$ is

$$V_\ell = \begin{bmatrix} v_S I_h & v_{AS} I_h \end{bmatrix}, \quad W_\ell = \begin{bmatrix} w_S I_h \\ w_{AS} I_h \end{bmatrix}, \tag{9.21}$$

which requires

$$v_S w_S + v_{AS} w_{AS} = 1, \tag{9.22}$$

and yields

$$\begin{aligned} \ell &= \begin{bmatrix} v_S I_h & v_{AS} I_h \end{bmatrix} \begin{bmatrix} \ell & -\ell^\top \\ \ell^\top & \ell \end{bmatrix} \begin{bmatrix} w_S I_h \\ w_{AS} I_h \end{bmatrix} \\ &= v_S w_S \ell - v_S w_{AS} \ell^\top + v_{AS} w_S \ell^\top + v_{AS} w_{AS} \ell, \end{aligned}$$

which in addition to (9.22) requires

$$v_{AS} w_S - v_S w_{AS} = 0. \tag{9.23}$$

By setting $w_S = v_S$ and $w_{AS} = v_{AS}$, (9.22) is the sole constraint. Let $w_{AS} = v_{AS} = 0$ to simply introduce virtual zero channels. ∎

Proposition 9.3 (Normalization II)
Let the arbitrary interconnection operator $\mathscr{L}(t) = \ell(t) \otimes I_{n_{\mathscr{L}}}$, with $\ell(t) \in \mathcal{F}_{\ell,\mathbb{R}}^{h \times h}$ be real-valued, static, linear and possibly time-varying as well as of scalar repeated structure according to Ass. (A8.1) and (A8.3) on p. 236.

Then one can find matrices W_ℓ, V_ℓ, s.t. with the operators

$$\ell_S(t) = \ell_S^\top(t) \overset{\triangle}{=} c_S \left(\ell(t) + \ell^\top(t) \right), \tag{9.24}$$

$$\ell_{AS}(t) = -\ell_{AS}^\top(t) \overset{\triangle}{=} c_{AS} \left(\ell(t) - \ell^\top(t) \right), \tag{9.25}$$

where $c_S, c_{AS} \in \mathbb{R}$, one has

$$\ell(t) = \tilde{\ell}(t) \star \begin{bmatrix} 0 & W_\ell \\ \hline V_\ell & 0 \end{bmatrix}, \quad \tilde{\ell}(t) = \begin{bmatrix} \ell_S(t) & \\ & \ell_{AS}(t) \end{bmatrix} \in \mathcal{F}_{\ell,N}^{\tilde{h} \times \tilde{h}}, \tag{9.26}$$

with $V_\ell W_\ell = I_h$, $\tilde{h} = 2h$. $\qquad\square$

Proof: Firstly, since for each $\ell \in \boldsymbol{\ell}$, $\tilde{\ell} \in \boldsymbol{\ell}_N^{\tilde{h} \times \tilde{h}} \subseteq \boldsymbol{\ell}_D^{\tilde{h} \times \tilde{h}}$, $\tilde{\ell}(t) \in \mathcal{F}_{\ell,N}^{\tilde{h} \times \tilde{h}}$. A particular choice with $v_S, v_{AS}, w_S, w_{AS} \in \mathbb{R}$ is

$$V_\ell = \begin{bmatrix} v_S I_h & v_{AS} I_h \end{bmatrix}, \quad W_\ell = \begin{bmatrix} w_S I_h \\ w_{AS} I_h \end{bmatrix}, \tag{9.27}$$

which requires

$$v_S w_S + v_{AS} w_{AS} = 1, \tag{9.28}$$

and yields

$$\ell = \begin{bmatrix} v_S I_h & v_{AS} I_h \end{bmatrix} \begin{bmatrix} \ell_S & \\ & \ell_{AS} \end{bmatrix} \begin{bmatrix} w_S I_h \\ w_{AS} I_h \end{bmatrix}$$
$$= v_S w_S c_S \left(\ell + \ell^\top \right) + v_{AS} w_{AS} c_{AS} \left(\ell - \ell^\top \right).$$

From the required conditions

$$v_S w_S c_S + v_{AS} w_{AS} c_{AS} = 1,$$
$$v_S w_S c_S - v_{AS} w_{AS} c_{AS} = 0,$$

follows $v_S w_S c_S = v_{AS} w_{AS} c_{AS} = \frac{1}{2}$ and with (9.28), it follows that $c_{AS} = \frac{c_S}{2c_S - 1}$. $\qquad\blacksquare$

It is possible that only particular portions of the interconnection matrix are non-symmetric and require normalization. In such a case, the normalization can be chosen such as not to overly increase the size of the virtual interconnection matrix over the actual one.

Definition 9.1 (Degree of Asymmetry [87])
Given an interconnection matrix ℓ, define the «degree of asymmetry» as the maximum singular value of $\ell_{AS} \overset{\triangle}{=} \frac{1}{2} \left(\ell - \ell^\top \right)$, i.e., as

$$\overline{\sigma}_{AS} \overset{\triangle}{=} \overline{\sigma}(\ell_{AS}) = \sup_{\|x\|=1} \|\ell_{AS} x\|_2 \tag{9.29}$$

By defining $\ell_S \triangleq \frac{1}{2}\left(\ell + \ell^\top\right)$, note that

$$\ell = \ell_S + \ell_{\mathbb{AS}} \quad \text{and} \quad \ell^\top = \ell_S - \ell_{\mathbb{AS}}.$$

According to [87], $\ell_{\mathbb{AS}}$ thus captures the difference between ℓ and $\ell^\top$.

9.2 Application of Standard Multiplier-Based Gain-Scheduling Techniques Through Problem Transformation

In the following, it is assumed that an an arbitary interconnection topology is present, i. e., $\ell(t) \in \mathcal{F}_{\ell,\mathbb{R}}^{h \times h}$ according to Ass. (A8.6). It is assumed that Prob. 9.1 has been solved. If ℓ is normal in the first place, i. e., $\ell \in \boldsymbol{\ell}_{N}^{h \times h}$, the trivial transformation $V_\ell = W_\ell = I_h$, $h = \tilde{h}$ is used and the state space system matrices remain unchanged, i. e., $\tilde{T} = T$. Note that in any case, $\tilde{\mathcal{T}}$ and $\mathcal{T}$ exhibit identical input-output behavior.

The following theorem is a rewritten version of the FBSP-based parameter-dependent Bounded Real Lemma (PDBRL) with parameter-independent Lyapunov function (PIDLF) for interconnected LPV systems.

Theorem 9.1 (Analysis of Interconnected LPV Systems [55])
The system $\mathcal{T}$ as defined in (8.5) is asymptotically stable over $\boldsymbol{\delta}$ and for all admissible interaction topologies $\mathscr{L} \in \mathbf{\mathcal{F}}_{\mathscr{L}} \subseteq \mathbf{\mathcal{F}}_{\mathscr{L},\mathbb{R}}$ normalized according to a solution to Prob. 9.1, s. t. $\tilde{\mathscr{L}}(t) \in \mathbf{\mathcal{F}}_{\tilde{\mathscr{L}},N}$, with $\mathcal{L}_2$ gain on the channel $w \to z$ bounded from above by

$$\gamma \leqslant \overset{g}{\underset{f=1}{\max}}(\gamma_f), \quad \gamma_f > 0, \ f = 1, \ldots, g$$

if there exist $\mathcal{M}_X \in \mathbb{S}^{n_r}$, $\mathcal{M}_p \in \mathbb{S}^{n_z + n_w}$, $\mathcal{M}_\Delta \in \mathbb{S}^{n_p + n_q}$ and $\tilde{\mathcal{M}}_i \in \mathbb{S}^{n_{\tilde{\delta}} + n_{\tilde{\upsilon}}}$ that satisfy

$$\begin{bmatrix} \bullet \\ \bullet \\ \bullet \\ \bullet \end{bmatrix}^\top \begin{bmatrix} \mathcal{M}_X & & & \\ & \mathcal{M}_\Delta & & \\ & & \tilde{\mathcal{M}}_i & \\ & & & \mathcal{M}_p \end{bmatrix} \begin{bmatrix} \mathcal{A} & \mathcal{B}_\Delta & \tilde{\mathcal{B}}_i & \mathcal{B}_p \\ I & 0 & 0 & 0 \\ \hdashline \mathcal{C}_\Delta & \mathcal{D}_{\Delta\Delta} & \tilde{\mathcal{D}}_{\Delta i} & \mathcal{D}_{\Delta p} \\ 0 & I & 0 & 0 \\ \hdashline \tilde{\mathcal{C}}_i & \tilde{\mathcal{D}}_{i\Delta} & \tilde{\mathcal{D}}_{ii} & \tilde{\mathcal{D}}_{ip} \\ 0 & 0 & I & 0 \\ \hdashline \mathcal{C}_p & \mathcal{D}_{p\Delta} & \tilde{\mathcal{D}}_{pi} & \mathcal{D}_{pp} \\ 0 & 0 & 0 & I \end{bmatrix} \prec 0, \tag{9.30}$$

$$\begin{bmatrix} \bullet \\ \bullet \\ \bullet \end{bmatrix}^\top \tilde{\mathcal{M}}_i \begin{bmatrix} I & \\ & I \\ \hdashline \tilde{\mathscr{L}} & \\ & \tilde{\mathscr{L}}^K \end{bmatrix} \succ 0, \quad \forall \left(\tilde{\mathscr{L}}, \tilde{\mathscr{L}}^K \right) \in \tilde{\mathscr{L}} \times \tilde{\mathscr{L}}^K, \tag{9.31}$$

$$\begin{bmatrix} \bullet \\ \bullet \\ \bullet \end{bmatrix}^\top \mathcal{M}_\Delta \begin{bmatrix} I & \\ & I \\ \hdashline \Delta & \\ & \Delta^K \end{bmatrix} \succ 0, \quad \forall \delta \in \boldsymbol{\delta}, \tag{9.32}$$

$$\mathcal{M}_p = \sum_{f=1}^{g} (I_2 \otimes E_f) \circledast \mathcal{M}_{f,p}, \quad \mathcal{M}_{f,p} = \begin{bmatrix} \frac{1}{\gamma_f} I & 0 \\ 0 & -\gamma_f I \end{bmatrix}, \tag{9.33}$$

$\square$

Proof: Following [125], the theorem simply states a closed-loop analysis condition for the complete interconnected system, in which both the LPV parameter block, as well as the interconnection matrix have been taken into account via respective full-block multiplier conditions and in which each of the respective different heterogeneous subsystem dynamics is associated with a performance index γ_f. ∎

The following corollary is a useful ingredient for obtaining the controller parameters with the proper sparsity structure imposed by a normalization in accordance to Prob. 9.1. It relies on the fact that imposed matrix structure can be reverted by considering the respective matrix inequalities on a certain subspace.

Corollary 9.1 (IS Analysis Restricted to a Subspace [55])
Under the assumption that there exist $\mathcal{M}_X \in \mathbb{S}^{n_{\mathfrak{x}}}$, $\mathcal{M}_p \in \mathbb{S}^{n_z+n_w}$, $\mathcal{M}_\Delta \in \mathbb{S}^{n_p+n_q}$ and $\tilde{\mathcal{M}}_i \in \mathbb{S}^{n_{\mathfrak{d}}+n_{\mathfrak{v}}}$ that satisfy Cond. (9.30) of Thm. 9.1, the conditions

$$
\begin{bmatrix} \bullet \\ \hline \bullet \\ \hline \bullet \\ \hline \bullet \end{bmatrix}^\top
\begin{bmatrix} \mathcal{M}_X & & & \\ & \mathcal{M}_\Delta & & \\ & & \mathcal{M}_i & \\ & & & \mathcal{M}_p \end{bmatrix}
\begin{bmatrix} \mathcal{A} & \mathcal{B}_\Delta & \mathcal{B}_i & \mathcal{B}_p \\ I & 0 & 0 & 0 \\ \hdashline \mathcal{C}_\Delta & \mathcal{D}_{\Delta\Delta} & \mathcal{D}_{\Delta i} & \mathcal{D}_{\Delta p} \\ 0 & I & 0 & 0 \\ \hdashline \mathcal{C}_i & \mathcal{D}_{i\Delta} & \mathcal{D}_{ii} & \mathcal{D}_{ip} \\ 0 & 0 & I & 0 \\ \hdashline \mathcal{C}_p & \mathcal{D}_{p\Delta} & \mathcal{D}_{pi} & \mathcal{D}_{pp} \\ 0 & 0 & 0 & I \end{bmatrix} \prec 0,
\tag{9.34}
$$

$$
\begin{bmatrix} \bullet \\ \hline \bullet \end{bmatrix}^\top \mathcal{M}_i
\begin{bmatrix} I & & \\ & I & \\ \hdashline \mathscr{L} & & \\ & & \mathscr{L}^K \end{bmatrix} \succ 0, \quad \forall \left(\mathscr{L}, \mathscr{L}^K \right) \in \boldsymbol{\mathscr{L}} \times \boldsymbol{\mathscr{L}}^K,
\tag{9.35}
$$

hold true. □

Proof: Condition (9.34) is merely Cond. (9.30) restricted to the subspace spanned by $W_{\mathscr{L}}$, while Cond. (9.35) is Cond. (9.37) restricted to the subspace spanned by $(I_2 \otimes V_{\mathscr{L}})$. More explicitly, one has

$$
(I_2 \otimes V_{\mathscr{L}}^\top) \begin{bmatrix} \bullet \\ \hline \bullet \end{bmatrix}^\top \tilde{\mathcal{M}}_i
\begin{bmatrix} I & & \\ & I & \\ \hdashline \tilde{\mathscr{L}} & & \\ & & \tilde{\mathscr{L}}^K \end{bmatrix} (I_2 \otimes V_{\mathscr{L}}) \succ 0, \quad \forall \left(\mathscr{L}, \mathscr{L}^K \right) \in \tilde{\boldsymbol{\mathscr{L}}} \times \tilde{\boldsymbol{\mathscr{L}}}^K,
$$

with $\mathcal{M}_i = \begin{bmatrix} \bullet \end{bmatrix}^\top \tilde{\mathcal{M}}_i \, \mathrm{diag}((I_2 \otimes V_{\mathscr{L}}), (I_2 \otimes W_{\mathscr{L}}))$ and

$$
W_{\mathscr{L}}^\top
\begin{bmatrix} \bullet \\ \vdots \\ \bullet \\ \vdots \\ \bullet \\ \bullet \end{bmatrix}^\top
\begin{bmatrix} \mathcal{M}_X & & & \\ & \mathcal{M}_\Delta & & \\ & & \tilde{\mathcal{M}}_i & \\ & & & \mathcal{M}_p \end{bmatrix}
\begin{bmatrix}
\mathcal{A} & \mathcal{B}_\Delta & \tilde{\mathcal{B}}_i & \mathcal{B}_p \\
I & 0 & 0 & 0 \\
\hdashline
\mathcal{C}_\Delta & \mathcal{D}_{\Delta\Delta} & \tilde{\mathcal{D}}_{\Delta i} & \mathcal{D}_{\Delta p} \\
0 & I & 0 & 0 \\
\hdashline
\tilde{\mathcal{C}}_i & \tilde{\mathcal{D}}_{i\Delta} & \tilde{\mathcal{D}}_{ii} & \tilde{\mathcal{D}}_{ip} \\
0 & 0 & I & 0 \\
\hdashline
\mathcal{C}_p & \mathcal{D}_{p\Delta} & \tilde{\mathcal{D}}_{pi} & \mathcal{D}_{pp} \\
0 & 0 & 0 & I
\end{bmatrix}
W_{\mathscr{L}} \prec 0.
$$

Conds. (9.34) and (9.35) are obtained, due to $V_{\mathscr{L}} W_{\mathscr{L}} = I_{hn_{\mathscr{L}}}$. For a general formulation of this result, consult Cor. A.2 on p. 322 in the appendix. $\blacksquare$

9.2.1 *Reduction of Analysis and Synthesis Complexity via Structural Constraints on the Multipliers*

In Theorem 9.1 the analysis of an interconnected LPV system is considered via matrix inequality constraints of the size of the entire interconnected system. Such problems may be tractable for interconnected systems, where only a few subsystems are involved. By imposing particular constraints on the structures of both multipliers and Lyapunov variables, the complexity of the analysis conditions can be drastically reduced. If the subsystems involved are allowed to be heterogeneous, this amounts to a separation into several conditions only slightly coupled via the interconnection multiplier. By using the formalism to distinguish between groups of subsystems that share common dynamics introduced in (8.1) in Sect. 8.1.1 on p. 8.1.1 redundant conditions are revealed and can be eliminated.

Theorem 9.2 (Analysis of Het. Grps. of LPV Systems [55])
The system $\mathcal{T}$ as defined in (8.5) is asymptotically stable over δ and for all admissible interaction topologies $\mathscr{L}(t) \in \mathcal{F}_{\mathscr{L}} \subseteq \mathcal{F}_{\mathscr{L},\mathbb{R}}$ normalized according to a solution to Prob. 9.1, s.t. $\tilde{\mathscr{L}}(t) \in \mathcal{F}_{\tilde{\mathscr{L}},N}$, with $\mathcal{L}_2$ gain on the channel $w \to z$ bounded from above by

$$
\gamma \leqslant \max_{f=1}^{g}(\gamma_f), \quad \gamma_f > 0, \ f = 1, \ldots, g
$$

if there exist $\mathcal{M}_{f,X} \in \mathbb{S}^{n_{f,x}}$, $\mathcal{M}_{f,p} \in \mathbb{S}^{n_{f,z}+n_{f,w}}$, $\mathcal{M}_{f,\Delta} \in \mathbb{S}^{n_{f,p}+n_{f,q}}$ *and* $\tilde{\mathcal{M}}_{f,i} \in \mathbb{S}^{n_{f,\tilde{\delta}}+n_{f,\tilde{v}}}$ *that satisfy for all* $f = 1, \ldots, g$

$$
\begin{bmatrix} \bullet \\ \bullet \\ \bullet \\ \bullet \end{bmatrix}^\top
\begin{bmatrix} \mathcal{M}_{f,X} & & & \\ & \mathcal{M}_{f,\Delta} & & \\ & & \tilde{\mathcal{M}}_{f,i} & \\ & & & \mathcal{M}_{f,p} \end{bmatrix}
\begin{bmatrix}
\mathcal{A}_f & \mathcal{B}_{f,\Delta} & \tilde{\mathcal{B}}_{f,i} & \mathcal{B}_{f,p} \\
I & 0 & 0 & 0 \\
\hdashline
\mathcal{C}_{f,\Delta} & \mathcal{D}_{f,\Delta\Delta} & \tilde{\mathcal{D}}_{f,\Delta i} & \mathcal{D}_{f,\Delta p} \\
0 & I & 0 & 0 \\
\hdashline
\tilde{\mathcal{C}}_{f,i} & \tilde{\mathcal{D}}_{f,i\Delta} & \tilde{\mathcal{D}}_{f,ii} & \tilde{\mathcal{D}}_{f,ip} \\
0 & 0 & I & 0 \\
\hdashline
\mathcal{C}_{f,p} & \mathcal{D}_{f,p\Delta} & \tilde{\mathcal{D}}_{f,pi} & \mathcal{D}_{f,pp} \\
0 & 0 & 0 & I
\end{bmatrix} \prec 0,
\tag{9.36}
$$

$$
\begin{bmatrix} \bullet \\ \bullet \end{bmatrix}^\top \tilde{\mathcal{M}}_i
\begin{bmatrix}
I & & \\
& I & \\
\hdashline
\tilde{\mathscr{L}} & & \\
& & \tilde{\mathscr{L}}^K
\end{bmatrix} \succ 0, \quad \forall \left(\tilde{\mathscr{L}}, \tilde{\mathscr{L}}^K \right) \in \tilde{\boldsymbol{\mathscr{L}}} \times \tilde{\boldsymbol{\mathscr{L}}}^K,
\tag{9.37}
$$

$$
\begin{bmatrix} \bullet \\ \bullet \end{bmatrix}^\top \mathcal{M}_{f,\Delta}
\begin{bmatrix}
I & & \\
& I & \\
\hdashline
\Delta_k & & \\
& & \Delta_k^K
\end{bmatrix} \succ 0, \quad \forall \delta_k \in \boldsymbol{\delta}_f,
\tag{9.38}
$$

where

$$
\tilde{\mathcal{M}}_i = \sum_{f=1}^{g} (1_{4 \times 4} \otimes E_f) \circledast \tilde{\mathcal{M}}_{f,i},
\tag{9.39}
$$

$$
\mathcal{M}_{f,X} =
\begin{bmatrix}
& & X_f & X_f^{12} \\
& & X_f^{12^\top} & X_f^2 \\
\hdashline
X_f & X_f^{12} & & \\
X_f^{12^\top} & X_f^2 & &
\end{bmatrix}, \quad
\tilde{\mathcal{M}}_{f,i} =
\begin{bmatrix}
R_{f,i} & R_{f,i}^{12} & S_{f,i}^\top & S_{f,i}^{12^\top} \\
R_{f,i}^{12^\top} & R_{f,i}^2 & S_{f,i}^{21^\top} & S_{f,i}^{2^\top} \\
\hdashline
S_{f,i} & S_{f,i}^{21} & Q_{f,i} & Q_{f,i}^{12} \\
S_{f,i}^{12} & S_{f,i}^2 & Q_{f,i}^{12^\top} & Q_{f,i}^2
\end{bmatrix},
$$

$$
\mathcal{M}_{f,\Delta} =
\begin{bmatrix}
R_{f,\Delta} & R_{f,\Delta}^{12} & S_{f,\Delta}^\top & S_{f,\Delta}^{12^\top} \\
R_{f,\Delta}^{12^\top} & R_{f,\Delta}^2 & S_{f,\Delta}^{21^\top} & S_{f,\Delta}^{2^\top} \\
\hdashline
S_{f,\Delta} & S_{f,\Delta}^{21} & Q_{f,\Delta} & Q_{f,\Delta}^{12} \\
S_{f,\Delta}^{12} & S_{f,\Delta}^2 & Q_{f,\Delta}^{12^\top} & Q_{f,\Delta}^2
\end{bmatrix}, \quad
\mathcal{M}_{f,p} =
\begin{bmatrix}
\frac{1}{\gamma_f} I & 0 \\
0 & -\gamma_f I
\end{bmatrix}.
$$

$\square$

Proof: By imposing the multiplier structures

$$\mathcal{M}_p = \sum_{f=1}^{g} (I_2 \otimes E_f) \circledast \mathcal{M}_{f,p}, \tag{9.40}$$

$$\mathcal{M}_X = \sum_{f=1}^{g} (1_{4\times4} \otimes E_f) \circledast \mathcal{M}_{f,X}, \tag{9.41}$$

$$\mathcal{M}_\Delta = \sum_{f=1}^{g} (1_{4\times4} \otimes E_f) \circledast \mathcal{M}_{f,\Delta}, \tag{9.42}$$

and (9.39) on the conditions of Thm. 9.1 and suitable permutations—cf. Lma. A.3 on p. 317— Cond. (9.30) of Thm. 9.1 on p. 261 can be written in the form of (9.43) below.

$$\begin{bmatrix} \vdots \\ \vdots \\ \vdots \\ \bullet \end{bmatrix}^{\top} \left\{ \sum_{f=1}^{g} \left(E_f \otimes \begin{bmatrix} \mathcal{M}_{f,X} & & & \\ & \mathcal{M}_{f,\Delta} & & \\ & & \tilde{\mathcal{M}}_{f,i} & \\ & & & \mathcal{M}_{f,p} \end{bmatrix} \right) \right\} \tag{9.43}$$

$$\times \left\{ \sum_{f=1}^{g} \left(E_f \otimes \begin{bmatrix} \mathcal{A}_f & \mathcal{B}_{f,\Delta} & \tilde{\mathcal{B}}_{f,i} & \mathcal{B}_{f,p} \\ I & 0 & 0 & 0 \\ \hline \mathcal{C}_{f,\Delta} & \mathcal{D}_{f,\Delta\Delta} & \tilde{\mathcal{D}}_{f,\Delta i} & \mathcal{D}_{f,\Delta p} \\ 0 & I & 0 & 0 \\ \hline \tilde{\mathcal{C}}_{f,i} & \tilde{\mathcal{D}}_{f,i\Delta} & \tilde{\mathcal{D}}_{f,ii} & \tilde{\mathcal{D}}_{f,ip} \\ 0 & 0 & I & 0 \\ \hline \mathcal{C}_{f,p} & \mathcal{D}_{f,p\Delta} & \tilde{\mathcal{D}}_{f,pi} & \mathcal{D}_{f,pp} \\ 0 & 0 & 0 & I \end{bmatrix} \right) + I_h \otimes \begin{bmatrix} 0 & 0 & 0 & 0 \\ I & 0 & 0 & 0 \\ 0 & 0 & 0 & 0 \\ 0 & I & 0 & 0 \\ 0 & 0 & 0 & 0 \\ 0 & 0 & I & 0 \\ 0 & 0 & 0 & 0 \\ 0 & 0 & 0 & I \end{bmatrix} \right\} \prec 0.$$

Condition (9.43) decouples into h independent conditions, of which g are distinct by construction of the multiplier variables. Each of these is of the form shown in Lemma A.9, Eq. (A.12) in the appendix. ∎

Theorem 9.2 provides analysis conditions that are attractive due to a significant reduction in complexity—at the price of increase conservatism. The conditions are of the size of single LPV subsystems coupled via the interconnection multiplier condition. In Thm. 9.2 each group of distinct subsystem dynamics is explicitly allowed to be analyzed in terms of a group specific multiplier $\tilde{\mathcal{M}}_{f,i}$ associated with the interconnection. Cond. (9.37) remains of the size associated with the entire interconnected system, constituting the coupling.

Eichler et al. [38] elaborate on the application of the FBSP on the interconnection multiplier condition along the lines of Cor. 5.1[2]. This allows to consider explicit LFT-based models for the interconnection matrix $\mathscr{L}(t)$ and a more explicit definition of admissible topologies. In these cases, the complexity of both synthesis and analysis scales strongly with the number of subsystems. However, further structural

---

2 The result of Cor. 5.1 has been developed in cooperation with A. Eichler as a straightforward extension. Its application has been investigated simultaneously in the field of interconnected systems by A. Eichler and in the field of LPV control by C. Hoffmann.

constraints on the second multiplier stage amend this and rather large numbers of subsystems can be considered at the price of some conservatism. The interested reader is referred to [38] for details, whereas this thesis focuses on maintaining scalability of analysis and synthesis conditions under time-varying interconnection topologies.

9.2.2 Diagonalizing Transformation on Multiplier Matrix Inequalities

In the following, two lemmas are presented that allow to consider arbitrary interconnection topologies in analysis and synthesis problems of reduced complexity. The reduction is achieved by straightforward structural assumptions on multipliers associated with the interconnection. The results are presented in a rather general context, whereas their usefulness to further reduce the analysis complexity associated with Thm. 9.2 is formalized afterwards.

Lemma 9.1 (Diagonalizing Transformation)
Let the normal interconnection topology $\mathscr{L}(t) = \ell(t) \otimes I_{n_{\mathscr{L}}}$, with $\ell(t) \in \mathcal{F}_{\ell,N}^{h \times h}$ be real-valued, static, linear and possibly time-varying as well as of scalar repeated structure according to Ass. (A8.1) and (A8.3) on p. 236. Further consider the associated compact set of admissible interconnection matrices $\ell \in \boldsymbol{\ell} \subseteq \boldsymbol{\ell}_N$ and the associated set of admissible eigenvalues (9.4)

$$\boldsymbol{\lambda} \overset{\triangle}{=} \bigcup_{\forall t \in \mathbb{R}^+} \mathbb{A}\big(\ell(t)\big),$$

i.e., for each time instant $\ell(t)$ has eigenvalues $\lambda_k \in \boldsymbol{\lambda} \subseteq \mathbb{C}$, $k = 1, \ldots, h$. Then the following two inequalities are equivalent

(i) $\begin{bmatrix} \bullet \\ \bullet \end{bmatrix}^{\top} \begin{bmatrix} I_h \otimes R & I_h \otimes S^{\top} \\ I_h \otimes S & I_h \otimes Q \end{bmatrix} \begin{bmatrix} I_{hn_{\mathscr{L}}} \\ \mathscr{L} \end{bmatrix} \succ 0, \; \forall \ell \in \boldsymbol{\ell}$

(ii) $\begin{bmatrix} \bullet \\ \bullet \end{bmatrix}^{*} \begin{bmatrix} R & S^{\top} \\ S & Q \end{bmatrix} \begin{bmatrix} I_{n_{\mathscr{L}}} \\ \lambda I_{n_{\mathscr{L}}} \end{bmatrix} \succ 0, \; \forall \lambda \in \boldsymbol{\lambda}.$

$\square$

Proof: Consider a unitary diagonalizing transformation $F^* \ell F = \Lambda$, which is guaranteed to exist, since $\ell \in \boldsymbol{\ell} \subset \boldsymbol{\ell}_N^{h \times h}$, for all $t \in \mathbb{R}^+$. Note also that $F^* \ell^{\top} F = \Lambda^*$. Thus for each $\ell \in \boldsymbol{\ell}$ with $Z = F \otimes I_{n_{\mathscr{L}}}$, one has that (i) is equivalent to

$$Z^* \begin{bmatrix} \bullet \\ \bullet \end{bmatrix}^{\top} \begin{bmatrix} Z \\ & Z \end{bmatrix} \begin{bmatrix} Z \\ & Z \end{bmatrix}^{*} \begin{bmatrix} I_h \otimes R & I_h \otimes S^{\top} \\ I_h \otimes S & I_h \otimes Q \end{bmatrix} \begin{bmatrix} Z \\ & Z \end{bmatrix} \begin{bmatrix} Z \\ & Z \end{bmatrix}^{*} \begin{bmatrix} I_{hn_{\mathscr{L}}} \\ \ell \otimes I_{n_{\mathscr{L}}} \end{bmatrix} Z \succ 0.$$

Due to $F^* = F^{-1}$, the inner matrices Z cancel after commuting with the structured multiplier. Consequently,

$$Z^* \begin{bmatrix} \bullet \\ \bullet \end{bmatrix}^\top \begin{bmatrix} Z \\ & Z \end{bmatrix} \begin{bmatrix} I_h \otimes R & I_h \otimes S^\top \\ I_h \otimes S & I_h \otimes Q \end{bmatrix} \begin{bmatrix} Z \\ & Z \end{bmatrix}^* \begin{bmatrix} I_{h n_{\mathscr{L}}} \\ \ell \otimes I_{n_{\mathscr{L}}} \end{bmatrix} Z \succ 0,$$

$$\iff \begin{bmatrix} \bullet \\ \bullet \end{bmatrix}^* \begin{bmatrix} I_h \otimes R & I_h \otimes S^\top \\ I_h \otimes S & I_h \otimes Q \end{bmatrix} \begin{bmatrix} I_{h n_{\mathscr{L}}} \\ \Lambda \otimes I_{n_{\mathscr{L}}} \end{bmatrix} \succ 0.$$

Since $\Lambda = \operatorname*{diag}_{k=1}^{h}(\lambda_k)$, the last inequality is equivalent to

$$\begin{bmatrix} \bullet \\ \bullet \end{bmatrix}^* \begin{bmatrix} R & S^\top \\ S & Q \end{bmatrix} \begin{bmatrix} I_{n_{\mathscr{L}}} \\ \lambda_k I_{n_{\mathscr{L}}} \end{bmatrix} \succ 0, \ k = 1, \ldots, h,$$

which is the same as satisfying (ii). $\blacksquare$

Remark 9.2 *As discussed in Sect. 8.1.4, the set of normal matrices is not dense over $\mathbb{C}^{h \times h}$ and therefore poses a non-negligible restriction on the allowable interconnection matrices. This necessitates the application of Props. 9.1, 9.3 or 9.2.*

The arguments of Lma. 9.1 fail for the more general case of diagonalizable matrices $\ell \in \boldsymbol{\ell} \subset \boldsymbol{\ell}_D^{h \times h}$, since the diagonalizing transformation would then amount to a similarity transformation $F^{-1} \ell F = \Lambda$, rather than a congruence transformation. Accordingly, one would have $F^* \ell^\top F^{-*} = \Lambda^*$. The congruence transformation is required, however, to maintain the hermitian nature of the matrix inequality. In the way, the proof is formulated above, the issue becomes most obvious when considering the transformed multiplier

$$\begin{bmatrix} Z \\ & Z \end{bmatrix}^* \begin{bmatrix} I_h \otimes R & I_h \otimes S^\top \\ I_h \otimes S & I_h \otimes Q \end{bmatrix} \begin{bmatrix} Z \\ & Z \end{bmatrix} = \begin{bmatrix} F^* F \otimes R & F^* F \otimes S^\top \\ F^* F \otimes S & F^* F \otimes Q \end{bmatrix}$$

$$\neq \begin{bmatrix} I_h \otimes R & I_h \otimes S^\top \\ I_h \otimes S & I_h \otimes Q \end{bmatrix}.$$

Corollary 9.2 *For the case of $\boldsymbol{\lambda} \subset \mathbb{R}$, necessity in Lma. 9.1 is lost, if only the extrema of $\boldsymbol{\lambda}$ are checked.* $\square$

Corollary 9.3 *For the case of $\boldsymbol{\lambda} \subset \mathbb{C}$, necessity in Lma. 9.1 is lost, if vertices of the convex hull* conv $(\boldsymbol{\lambda})$ *of $\boldsymbol{\lambda}$ are checked.* $\square$

Lemma 9.1 can be applied to interconnected systems, for which a solution of Prob. 9.1 has been used to obtain the system representation (9.8) with a normalized scalar repeated interconnection matrix $\tilde{\mathscr{L}}(t) = \tilde{\ell}(t) \otimes I_{n_{\mathscr{L}}}$ in LFT-based feedback. It is an extension of the lemma proposed in [55, 56], in which only symmetric interconnection matrices have been considered that, e. g., are the result of the application of Prop. 9.1.

An alternative to the normalization of interconnection matrices along the lines of Prob. 9.1—or more specifically Props. 9.1, 9.3 and 9.2—has been proposed by Massioni in [98]. At the price of limiting the multipliers associated with the interconnection matrix to D-scalings, an SVD-based diagonalization technique does not require the introduction of virtual interconnection channels.

Lemma 9.2 (Diagonalizing Transformation via SVD [98])
Let the arbitrary interconnection topology $\mathscr{L}(t) = \ell(t) \otimes I_{n_{\mathscr{L}}}$, with $\ell(t) \in \mathcal{F}_{\ell,\mathbb{R}}^{h \times h}$ be real-valued, static, linear and possibly time-varying as well as of scalar repeated structure according to Ass. (A8.1) and (A8.3) on p. 236. Further consider the associated compact set of admissible interconnection matrices $\ell \in \boldsymbol{\ell} \subseteq \ell_{\mathbb{R}}^{h \times h}$ and the associated set of admissible singular values (9.6)

$$\boldsymbol{\sigma} \triangleq \bigcup_{\forall t \in \mathbb{R}^+} \Sigma\big(\ell(t)\big)$$

i.e., for each time instant $\ell(t)$ has singular values $\sigma_k \in \boldsymbol{\sigma} \subseteq \mathbb{R}$, $k = 1, \ldots, h$. Then the following two inequalities are equivalent

(i) $\begin{bmatrix} \bullet \\ \bullet \end{bmatrix}^\top \begin{bmatrix} I_h \otimes R & 0 \\ 0 & I_h \otimes Q \end{bmatrix} \begin{bmatrix} I_{hn_{\mathscr{L}}} \\ \mathscr{L} \end{bmatrix} \succ 0, \, \forall \ell \in \boldsymbol{\ell}$

(ii) $\begin{bmatrix} \bullet \\ \bullet \end{bmatrix}^\top \begin{bmatrix} R & 0 \\ 0 & Q \end{bmatrix} \begin{bmatrix} I_{n_{\mathscr{L}}} \\ \sigma I_{n_{\mathscr{L}}} \end{bmatrix} \succ 0, \, \forall \sigma \in \boldsymbol{\sigma}.$

$\square$

Proof: For each $\ell \in \boldsymbol{\ell}$, consider an SVD $\ell = U\Sigma V^\top$, where $V^\top V = I$, $U^\top U = I$. Thus with $Z_U = U \otimes I_{n_{\mathscr{L}}}$ and $Z_V = V \otimes I_{n_{\mathscr{L}}}$, one has that (i) is equivalent to

$$\begin{bmatrix} \bullet \\ \bullet \end{bmatrix}^\top \begin{bmatrix} I_h \otimes R & 0 \\ 0 & I_h \otimes Q \end{bmatrix} \begin{bmatrix} I_{hn_{\mathscr{L}}} \\ U\Sigma V^\top \otimes I_{n_{\mathscr{L}}} \end{bmatrix} \succ 0.$$

By application of a congruence transformation $Z_V = V \otimes I_{n_{\mathscr{L}}}$, it follows that

$$\begin{bmatrix} \bullet \\ \bullet \end{bmatrix}^\top \begin{bmatrix} Z_V & \\ & Z_U \end{bmatrix}^\top \begin{bmatrix} I_h \otimes R & 0 \\ 0 & I_h \otimes Q \end{bmatrix} \begin{bmatrix} Z_V & \\ & Z_U \end{bmatrix} \begin{bmatrix} I_{hn_{\mathscr{L}}} \\ \Sigma \otimes I_{n_{\mathscr{L}}} \end{bmatrix} \succ 0,$$

$$\iff \begin{bmatrix} \bullet \\ \bullet \end{bmatrix}^\top \begin{bmatrix} I_h \otimes R & 0 \\ 0 & I_h \otimes Q \end{bmatrix} \begin{bmatrix} I_{hn_{\mathscr{L}}} \\ \Sigma \otimes I_{n_{\mathscr{L}}} \end{bmatrix} \succ 0.$$

Since $\Sigma = \operatorname*{diag}_{k=1}^{h}(\sigma_k)$, the last inequality is equivalent to

$$\begin{bmatrix} \bullet \\ \bullet \end{bmatrix}^\top \begin{bmatrix} R & 0 \\ 0 & Q \end{bmatrix} \begin{bmatrix} I_{n_{\mathscr{L}}} \\ \sigma_k I_{n_{\mathscr{L}}} \end{bmatrix} \succ 0, \, k = 1, \ldots, h,$$

which is the same as satisfying (ii). $\blacksquare$

Corollary 9.4 *Necessity in Lma. 9.2 is lost, if only the extrema of σ are checked.* □

A possible significant disadvantageous effect of the limitation to D-scalings in Lma. 9.2 exists in the fact that any multiplier shiftings as per Lma. 2.3, or Cor. 2.4 for use in synthesis, respectively, are disallowed. D-Ss without shifts therefore require to consider ball-shaped regions about the origin, which may be potentially very conservative.

In contrast, Props. 9.3 in conjunction with Lma. 9.1 separates the real and imaginary parts of eigenvalues associated with interconnection matrices and fully allows the use of D/G-scalings and D/G*-scalings—introduced in Cor. 2.2 on p. 54—, respectively. Proposition 9.2 does not introduce such a separation via symmetric and skew-symmetric parts, but offers a general normalization. The resulting complex eigenvalues could then be covered by D-scalings shifted along the real axis. It has to be investigated, whether the introduction of virtual channels or the change in eigenvalue locations due to any method aligned with Prob. 9.1 introduces further conservatism than the method proposed by [98], given in Lma. 9.2.

Further advantages and disadvantages with respect to the separate methods will be considered in the examples.

By application of Lma. 9.1 on the conditions of Thm. 9.2, conditions can be formulated, whose purpose resides in turning the multiplier condition (9.37) of Thm. 9.2 on p. 263, formulated on the entirety of the interconnected subsystems, into a smaller one by restricting the multiplier $\tilde{\mathcal{M}}_{f,i} = \tilde{\mathcal{M}}_{0,i}$, $\forall f \in \{1, 2, \ldots, g\}$, i.e., rendering it the same for all of the different subsystems.

The following theorem formalizes this fact.

Theorem 9.3 (Efficient Analysis of Het. Grps. of LPV Systems [55])
The system $\mathscr{T}$ as defined in (8.5) is asymptotically stable over δ and for all admissible interaction topologies $\mathscr{L}(t) \in \mathcal{F}_{\mathscr{L}} \subseteq \mathcal{F}_{\mathscr{L},\mathbb{R}}$, $\mathscr{L}^K(t) \in \mathcal{F}_{\mathscr{L}}^K \subseteq \mathcal{F}_{\mathscr{L},\mathbb{R}}^K$ normalized according to a solution to Prob. 9.1, s.t. $\tilde{\mathscr{L}}(t) \in \mathcal{F}_{\tilde{\mathscr{L}},N}$, $\tilde{\mathscr{L}}^K(t) \in \mathcal{F}_{\tilde{\mathscr{L}},N}^K$, with $\mathcal{L}_2$ gain on the channel $w \to z$ bounded from above by

$$\gamma \leqslant \max_{f=1}^{g}(\gamma_f), \quad \gamma_f > 0, \ f = 1, \ldots, g$$

if there exist $\mathcal{M}_{f,X} \in \mathbb{S}^{n_{f,x}}$, $\mathcal{M}_{f,p} \in \mathbb{S}^{n_{f,z}+n_{f,w}}$, $\mathcal{M}_{f,\Delta} \in \mathbb{S}^{n_{f,p}+n_{f,q}}$ and $\tilde{\mathcal{M}}_{0,i} = \tilde{\mathcal{M}}_{f,i} \in \mathbb{S}^{n_{f,\delta}+n_{f,\tilde{\delta}}}$, structured as in Thm. 9.2, that satisfy for all $f = 1, \ldots, g$, Conds. (9.36) and (9.38), as well as

$$\begin{bmatrix} \bullet \\ \hline \bullet \end{bmatrix}^\top \tilde{\mathcal{M}}_{0,i} \begin{bmatrix} I & & \\ & I & \\ \hline \tilde{\lambda}I & & \\ & & \tilde{\lambda}^K I \end{bmatrix} \succ 0, \quad \forall \left(\tilde{\lambda}, \tilde{\lambda}^K \right) \in \tilde{\boldsymbol{\lambda}} \times \tilde{\boldsymbol{\lambda}}^K, \tag{9.44}$$

□

Proof: Follows immediately from Lma. 9.1. ∎

Similarly, the application of Lma. 9.2 on the conditions of Thm. 9.2 leads to conditions reduced in complexity based on the singular values associated with the interconnection matrix. In this case, no normalization is required.

Theorem 9.4 (SVD-Based Analysis of Het. Grps. of LPV Systems)

The system $\mathscr{T}$ as defined in (8.5) is asymptotically stable over δ and for all admissible interaction topologies $\mathscr{L}(t) \in \boldsymbol{\mathcal{F}_{\mathscr{L}}} \subseteq \boldsymbol{\mathcal{F}_{\mathscr{L},\mathbb{R}}}$, $\mathscr{L}^K(t) \in \boldsymbol{\mathcal{F}_{\mathscr{L}}^K} \subseteq \boldsymbol{\mathcal{F}_{\mathscr{L},\mathbb{R}}^K}$ with $\mathcal{L}_2$ gain on the channel $w \to z$ bounded from above by

$$\gamma \leqslant \overset{g}{\underset{f=1}{\max}}(\gamma_f), \quad \gamma_f > 0, \ f = 1, \ldots, g$$

if there exist $\mathcal{M}_{f,X} \in \mathbb{S}^{n_{f,x}}$, $\mathcal{M}_{f,p} \in \mathbb{S}^{n_{f,z}+n_{f,w}}$, $\mathcal{M}_{f,\Delta} \in \mathbb{S}^{n_{f,p}+n_{f,q}}$ structured as in Thm. 9.2 and $\tilde{\mathcal{M}}_{0,i} = \tilde{\mathcal{M}}_{f,i} \in \mathbb{S}^{n_{f,\tilde{\delta}}+n_{f,\tilde{v}}}$ structured as

$$\tilde{\mathcal{M}}_{0,i} = \begin{bmatrix} R_{0,i} & R_{0,i}^{12} & 0 & 0 \\ R_{0,i}^{12^\top} & R_{0,i}^2 & 0 & 0 \\ \hdashline 0 & 0 & Q_{0,i} & Q_{0,i}^{12} \\ 0 & 0 & Q_{0,i}^{12^\top} & Q_{0,i}^2 \end{bmatrix},$$

that satisfy for all $f = 1, \ldots, g$, Conds. (9.36) and (9.38), where $V_\ell = I_h$ and $W_\ell = I_h$, as well as

$$\begin{bmatrix} \bullet \\ \bullet \end{bmatrix}^\top \tilde{\mathcal{M}}_{0,i} \begin{bmatrix} I & & & \\ & I & & \\ \hdashline \sigma I & & & \\ & & & \sigma^K I \end{bmatrix} \succ 0, \quad \forall \left(\sigma, \sigma^K\right) \in \boldsymbol{\sigma} \times \boldsymbol{\sigma}^K, \tag{9.45}$$

$\square$

Proof: Follows immediately from Lma. 9.2. $\blacksquare$

9.2.3 *Interconnected Controller Synthesis*

Pursuing the transition from analysis to conditions for the synthesis of interconnected LPV controllers is straightforward: Starting with the conditions of Thm. 9.3, a dualization and subsequent elimination of the controller via Lmas. A.7 and A.8 on p. 321, respectively, yields matrix inequalities that are essentially of the form shown in Thm. 2.17 on p. 66. These conditions are the standard PiDLF/FBSP-based LFT-LPV controller synthesis conditions [124, 125], which offer a novel gain-scheduling perspective on the synthesis of interconnected LPV controllers. For completeness, the resulting synthesis conditions are presented in the following.

Theorem 9.5 (Interconnected Controller Existence Conditions)

There exists a distributed controller $\mathscr{K}$ that renders the closed-loop system $\mathscr{T}$ as defined in (8.5) asymptotically stable over δ and for all admissible interaction topologies $\mathscr{L}(t) \in \boldsymbol{\mathcal{F}_{\mathscr{L}}} \subseteq \boldsymbol{\mathcal{F}_{\mathscr{L},\mathbb{R}}}$ normalized according to a solution to Prob. 9.1, s.t. $\tilde{\mathscr{L}}(t) \in \boldsymbol{\mathcal{F}_{\tilde{\mathscr{L}},N}}$, with $\mathcal{L}_2$ gain on the channel $w \to z$ bounded from above by

$$\gamma \leqslant \overset{g}{\underset{f=1}{\max}}(\gamma_f), \quad \gamma_f > 0, \ f = 1, \ldots, g$$

if there exist the primal multipliers $M_{f,X} \in \mathbb{S}^{n_{f,x}}$, $M_{f,p} \in \mathbb{S}^{n_{f,z}+n_{f,w}}$, $M_{f,\Delta} \in \mathbb{S}^{n_{f,p}+n_{f,q}}$ *and* $\tilde{M}_{f,i} \in \mathbb{S}^{n_{f,\tilde{d}}+n_{f,\tilde{v}}}$, *as well as the dual multipliers* $N_{f,X} \in \mathbb{S}^{n_{f,x}}$, $N_{f,p} \in \mathbb{S}^{n_{f,z}+n_{f,w}}$, $N_{f,\Delta} \in \mathbb{S}^{n_{f,p}+n_{f,q}}$ *and* $\tilde{N}_{f,i} \in \mathbb{S}^{n_{f,\tilde{d}}+n_{f,\tilde{v}}}$, *with*

$$M_{f,p} = \begin{bmatrix} \frac{1}{\gamma_f}I & 0 \\ 0 & -\gamma_f I \end{bmatrix}, \quad N_{f,p} = \begin{bmatrix} \gamma_f I & 0 \\ 0 & -\frac{1}{\gamma_f}I \end{bmatrix},$$

that satisfy for all $f = 1, \ldots, g$,

$$N_M^\top \begin{bmatrix} \bullet \\ \bullet \\ \bullet \\ \bullet \end{bmatrix}^\top \begin{bmatrix} M_{f,X} & & & \\ & M_{f,\Delta} & & \\ & & \tilde{M}_{f,i} & \\ & & & M_{f,p} \end{bmatrix} \begin{bmatrix} A_f & B_{f,\Delta} & \tilde{B}_{f,i} & B_{f,p} \\ I & 0 & 0 & 0 \\ \hdashline C_{f,\Delta} & D_{f,\Delta\Delta} & \tilde{D}_{f,\Delta i} & D_{f,\Delta p} \\ 0 & I & 0 & 0 \\ \hdashline \tilde{C}_{f,i} & \tilde{D}_{f,i\Delta} & \tilde{D}_{f,ii} & \tilde{D}_{f,ip} \\ 0 & 0 & I & 0 \\ \hdashline C_{f,p} & D_{f,p\Delta} & \tilde{D}_{f,pi} & D_{f,pp} \\ 0 & 0 & 0 & I \end{bmatrix} N_M \prec 0,$$

$$N_N^\top \begin{bmatrix} \bullet \\ \bullet \\ \bullet \\ \bullet \end{bmatrix}^\top \begin{bmatrix} N_{f,X} & & & \\ & N_{f,\Delta} & & \\ & & \tilde{N}_{f,i} & \\ & & & N_{f,p} \end{bmatrix} \begin{bmatrix} I & 0 & 0 & 0 \\ -A_f^\top & -C_{f,\Delta}^\top & -\tilde{C}_{f,i}^\top & -C_{f,p}^\top \\ \hdashline 0 & I & 0 & 0 \\ -B_{f,\Delta}^\top & -D_{f,\Delta\Delta}^\top & -\tilde{D}_{f,i\Delta}^\top & -D_{f,p\Delta}^\top \\ \hdashline 0 & 0 & I & 0 \\ -\tilde{B}_{f,i}^\top & -\tilde{D}_{f,\Delta i}^\top & -\tilde{D}_{f,ii}^\top & -\tilde{D}_{f,pi}^\top \\ \hdashline 0 & 0 & 0 & I \\ -B_{f,p}^\top & -D_{f,\Delta p}^\top & -\tilde{D}_{f,ip}^\top & -D_{f,pp}^\top \end{bmatrix} N_N \prec 0,$$

$$\begin{bmatrix} \bullet \\ \bullet \end{bmatrix}^\top \tilde{M}_i \begin{bmatrix} I \\ \hdashline \mathscr{L} \end{bmatrix} \succ 0, \quad \begin{bmatrix} \bullet \\ \bullet \end{bmatrix}^\top \tilde{N}_i \begin{bmatrix} -\mathscr{L}^\top \\ \hdashline I \end{bmatrix} \succ 0, \quad \forall \mathscr{L} \in \boldsymbol{\mathscr{L}}, \tag{9.46}$$

$$\begin{bmatrix} \bullet \\ \bullet \end{bmatrix}^\top M_{f,\Delta} \begin{bmatrix} I \\ \hdashline \Delta_k \end{bmatrix} \succ 0, \quad \begin{bmatrix} \bullet \\ \bullet \end{bmatrix}^\top N_{f,\Delta} \begin{bmatrix} -\Delta_k^\top \\ \hdashline I \end{bmatrix} \prec 0, \quad \forall \delta_k \in \delta_f, \tag{9.47}$$

$$\tilde{M}_i = \sum_{f=1}^{g} (1_{2\times2} \otimes E_f) \circledast \tilde{M}_{f,i}, \quad \tilde{N}_i = \sum_{f=1}^{g} (1_{2\times2} \otimes E_f) \circledast \tilde{N}_{f,i},$$

where

$$\tilde{M}_{f,i} = \begin{bmatrix} M_{f,i}^{11} & M_{f,i}^{12} \\ M_{f,i}^{12^\top} & M_{f,i}^{22} \end{bmatrix}, \quad \tilde{N}_{f,i} = \begin{bmatrix} N_{f,i}^{11} & N_{f,i}^{12} \\ N_{f,i}^{12^\top} & N_{f,i}^{22} \end{bmatrix},$$

and further

$$N_M = \ker\left(\left[C_{f,y}\; D_{f,y\Delta}\; \tilde{D}_{f,yi}\; D_{f,yp}\right]\right),$$
$$N_N = \ker\left(\left[B_{f,u}^\top\; D_{f,\Delta u}^\top\; \tilde{D}_{f,iu}^\top\; D_{f,pu}^\top\right]\right).$$

$\square$

Proof: The proof follows from application of the Parameter Elimination Lemma A.8 on p. 321 on the conditions of Thm. 9.2 and its dual [125]. $\blacksquare$

Conditions 9.46 can be reduced in size by application of either Lma. 9.1 or Lma. 9.2 at the cost of coupling the matrix inequalities by the same multiplier associated with the interconnection. Alternatively, two-stage multiplier approaches can be applied for explicitly modeled time-varying interconnection matrices [38]. In the following, only the result following the from diagonalization of a normalized interconnection according to Lma. 9.1 is presented.

Theorem 9.6 (Efficient Intercon. Controller Existence Conds.)
There exists a distributed controller $\mathcal{K}$ that renders the closed-loop system $\mathcal{T}$ as defined in (8.5) asymptotically stable over δ and for all admissible interaction topologies $\mathcal{L}(t) \in \mathcal{F}_{\mathcal{L}} \subseteq \mathcal{F}_{\mathcal{L},\mathbb{R}}$ normalized according to a solution to Prob. 9.1, s.t. $\tilde{\mathcal{L}}(t) \in \mathcal{F}_{\tilde{\mathcal{L}},N}$, with $\mathcal{L}_2$ gain on the channel $w \to z$ bounded from above by

$$\gamma \leqslant \max_{f=1}^{g}(\gamma_f), \quad \gamma_f > 0,\; f = 1,\ldots,g$$

if there exist the primal multipliers $M_{f,X} \in \mathbb{S}^{n_{f,x}}$, $M_{f,p} \in \mathbb{S}^{n_{f,z}+n_{f,w}}$, $M_{f,\Delta} \in \mathbb{S}^{n_{f,p}+n_{f,q}}$ and $\tilde{M}_{0,i} = \tilde{M}_{f,i} \in \mathbb{S}^{n_{f,\tilde{d}}+n_{f,\tilde{v}}}$, as well as the dual multipliers $N_{f,X} \in \mathbb{S}^{n_{f,x}}$, $N_{f,p} \in \mathbb{S}^{n_{f,z}+n_{f,w}}$, $N_{f,\Delta} \in \mathbb{S}^{n_{f,p}+n_{f,q}}$ and $\tilde{N}_{0,i} = \tilde{N}_{f,i} \in \mathbb{S}^{n_{f,\tilde{d}}+n_{f,\tilde{v}}}$, structured as in Thm. 9.5, that satisfy for all $f = 1,\ldots,g$, all the Conds. of Thm. 9.5, except for Cond. (9.46) exchanged by

$$\begin{bmatrix}\bullet\\\vdots\\\bullet\end{bmatrix}^\top \tilde{M}_{0,i}\begin{bmatrix}I\\\vdots\\\lambda I\end{bmatrix} \succ 0, \quad \begin{bmatrix}\bullet\\\vdots\\\bullet\end{bmatrix}^\top \tilde{N}_{0,i}\begin{bmatrix}-\lambda^* I\\\vdots\\I\end{bmatrix} \succ 0, \quad \forall \lambda \in \boldsymbol{\lambda}, \tag{9.48}$$

$\square$

Proof: Follows immediately from Lma. 9.1. $\blacksquare$

9.2.3.1 *A Convex Solution to Special Structured Controller Synthesis Problems*

In comparison to the standard PıDLF/FBSP-based LFT-LPV controller synthesis conditions, a subtle technical difference appears in the way, the controller needs to be constructed. To begin with, the use of multiplier constraints like, for instance, D/G-Ss, is prescribed that allow the controller to receive a copy of the plant's parameter block—and hence inherit the interconnection topology—according to Lma. 2.6 on p. 70. A symmetrization or normalization along the lines of Props. 9.1

9.3 or 9.2, however, alters the parameter block that is copied to the virtual symmetrized or normalized one. In order to be able to revert the symmetrization or normalization for the controller, structural constraints on the controller's state space matrices need to be imposed, which take the form of a repeated sparsity structure in the controller matrices. Such structural constraints would normally render the problem non-convex. However, Cor. 9.1 on p. 262 already provides the solution. The insight that the existence of a controller of this particular structure is guaranteed is based on Lma. A.9 in the appendix on p. 322. It turns out that the null spaces used for eliminating the controller variables in Thm. 9.5 indeed take the form shown in Lma. A.9. By Cor. A.2 (appendix, p. 322), the conditions of Cor. 9.1 with a modified multiplier associated with the interconnection emerge and the controller parameters can be obtained by convex optimization.

9.2.3.2 *Alternative Controller Constructions — Shaping the Topology*

As noted earlier, it is from Lma. A.9 and Cor. A.2 that the technical assumption $W_{\mathscr{L}}V_{\mathscr{L}} = I$ arises. If this assumption and consequently the approach to revert the symmetrization or normalization w. r. t. the controller's interconnection topology is dispensed with, the interconnection topology to be implemented with the distributed control scheme can be shaped by the control designer. For instance, assume that a normalization according to Prop. 9.2 has been constructed. Then a controller can be synthesized that inherits the interconnection matrix

$$\ell^{K}(t) \overset{\triangle}{=} \tilde{\ell}(t) = \begin{bmatrix} \ell(t) & -\ell^{\top}(t) \\ \ell^{\top}(t) & \ell(t) \end{bmatrix}.$$

As long as a symmetrized or normalized topology is constructed from operators that carry interpretable meaning, such as $\ell(t)$ or $\ell^{\top}(t)$, the actual real-time distributed controller implementation is tractable. For this purpose, the controller parameters are derived for the augmented channel widths, i. e., in this case twice the interconnection channel size. From

$$\ell^{K}(t) = \begin{bmatrix} \ell(t) & -\ell^{\top}(t) \\ \ell^{\top}(t) & \ell(t) \end{bmatrix} = \begin{bmatrix} I & 0 & 0 & -I \\ 0 & I & I & 0 \end{bmatrix} \begin{bmatrix} \ell(t) & & & \\ & \ell(t) & & \\ & & \ell^{\top}(t) & \\ & & & \ell^{\top}(t) \end{bmatrix} \begin{bmatrix} I & 0 \\ 0 & I \\ I & 0 \\ 0 & I \end{bmatrix},$$

it is obvious that the distributed controller implements an undirected interconnection topology even for possibly directed topologies in the interconnected plant representation.

9.2.4 *Discussion*

In essence, the above results offer a convex solution to the synthesis of distributed LPV controllers for heterogeneous LPV subsystems interconnected through arbitrary topologies. The essential tools stem from a shift in perspective that allow the

exploitation of well-known LFT-LPV gain-scheduling controller synthesis methods. The output-feedback case is discussed, but, e. g., [98] shows that state-feedback synthesis is easily possible, as well. In fact, while in [98] output-feedback synthesis is still handled iteratively, but with small-in-size representations of the interconnection, in [80] output-feedback synthesis is performed by convex optimization, but with large-scale interconnected system representations. Therefore, the present work can be regarded as a combination of the advantages of both works.

In the next chapter, the benefits of the novel alternatives to handle arbitrary and time-varying interconnections will be assessed in application examples.

10

APPLICATION EXAMPLES

≪We are all dependent on one another, every soul of us on earth.≫

George Bernhard Shaw

A FTER establishing the theory for the efficient synthesis of distributed controllers, the following chapter presents application examples for the synthesis of distributed controllers via the methods developed in this thesis:

(i) The distributed control of a heterogeneous marginally stable LTI system (Sect. 10.1),

(ii) The leader-follower formation control and reference tracking problem using nonlinear quadrotor helicopter models, (Sect. 10.2).

The first example illustrates the applicability of the methods for unstable systems as well as showing the relatively little conservatism that may be introduced through a distributed control scheme as compared to a centralized one. Furthermore, it is shown that the novel methods can be less conservative than existing ones available for LTI systems. The second example highlights new capabilities: Formation control of nonlinear LPV models are considered using directed and switching topologies in a scalable framework is synthesized using convex optimization.

Preliminary results of this chapter have been previously published in [45, 61].

10.1 A Distributed Heterogeneous Marginally Stable System

An academic example is borrowed from [98].[1] In the following, the setup of the numerical example is detailed in Sect. 10.1.1 and achievable performances in distributed control is analyzed in Sect. 10.1.2.

10.1.1 *Setup of the Numerical Example*

The original example is posed in a discrete-time state space representation and can be found in the appendix in Sect. C.1. For the purpose of alignment with the continuous-time presentation of the results of this thesis, the example has been converted by a bilinear transformation—known as the Tustin approximation—assuming a sampling time of $0.1\,\mathrm{s}$. The resulting distributed LTI system is composed from two groups of systems—a system containing an integrator and a system in the form of an undamped oscillator.

The subsystems have the form

$$
P_k : \begin{cases} \begin{bmatrix} \dot{x}_k \\ d_k \\ z_k \\ y_k \end{bmatrix} = \left[\begin{array}{c|ccc} A_f & B_{f,i} & B_{f,p} & B_{f,u} \\ \hline C_{f,i} & D_{f,ii} & D_{f,ip} & D_{f,iu} \\ C_{f,p} & D_{f,pi} & D_{f,pp} & D_{f,pu} \\ C_{f,y} & D_{f,yi} & D_{f,yp} & 0 \end{array} \right] \begin{bmatrix} x_k \\ v_k \\ w_k \\ u_k \end{bmatrix} \end{cases},
\tag{10.1}
$$

where $x_k \in \mathbb{R}^2$, $d_k \in \mathbb{R}^3$, $v_k \in \mathbb{R}^3$, $z_k \in \mathbb{R}^3$, $w_k \in \mathbb{R}^5$, $y_k \in \mathbb{R}^4$, $u_k \in \mathbb{R}^2$. The respective matrices are

$$
A_1 = \begin{bmatrix} 0 & 0 \\ 10.26 & -0.51 \end{bmatrix}, \ A_2 = \begin{bmatrix} 0 & 9.27 \\ -9.27 & 0 \end{bmatrix},
$$

$$
B_{1,i} = \begin{bmatrix} 0 & 0 & 10 \\ 10.26 & 0 & -5.17 \end{bmatrix}, \ B_{2,i} = \begin{bmatrix} -4.64 & 0 & 9.27 \\ 9.27 & 0 & 4.64 \end{bmatrix},
$$

$$
B_{1,p} = \begin{bmatrix} 10 & 0 & 0 & 0 & 0 \\ -5.17 & 0 & 0 & 0 & 0 \end{bmatrix}, \ B_{2,p} = \begin{bmatrix} 9.27 & 0 & 0 & 0 & 0 \\ 4.63 & 0 & 0 & 0 & 0 \end{bmatrix},
$$

$$
B_{1,u} = \begin{bmatrix} 10 & 0 \\ -5.17 & 0 \end{bmatrix}, \ B_{2,u} = \begin{bmatrix} 9 & 0 \\ 4.64 & 0 \end{bmatrix},
$$

and for $f = 1, 2$,

$$
C_{f,i} = \begin{bmatrix} 1 & 0 \\ 0 & 1 \\ 0 & 0 \end{bmatrix}, \ C_{f,p} = \begin{bmatrix} 0 & 1 \\ 0 & 0 \\ 0 & 0 \end{bmatrix}, \ C_{f,y} = \begin{bmatrix} 1 & 0 \\ 0 & 1 \\ 0 & 0 \\ 0 & 0 \end{bmatrix},
$$

$$
D_{f,ii} = O_3, \ D_{f,ip} = O_{3\times5}, \ D_{f,iu} = O_{3\times2},
$$

---

1 The explicit set of system matrices is not provided in [98], but it has been kindly provided in its entirety by Paolo Massioni upon request.

$$D_{f,pi} = O_{3\times3}, \; D_{f,pp} = O_{3\times5}, \; D_{f,pu} = \begin{bmatrix} 0 & 0 \\ 1 & 0 \\ 0 & 1 \end{bmatrix},$$

$$D_{f,yi} = \begin{bmatrix} 0 & 0 & 0 \\ 0 & 0 & 0 \\ 1 & 0 & 0 \\ 0 & 1 & 0 \end{bmatrix}, \; D_{f,yp} = 0.1 \begin{bmatrix} 0 & 1 & 0 & 0 & 0 \\ 0 & 0 & 1 & 0 & 0 \\ 0 & 0 & 0 & 1 & 0 \\ 0 & 0 & 0 & 0 & 1 \end{bmatrix},$$

$$D_{f,yu} = O_{4\times2}.$$

Note that due to the conversion to continuous-time, the heterogeneity in the system matrices over the original discrete-time versions presented in the appendix in Sect. C.1 increases.

Each group is assumed to consist of h_f agents, s.t. $h = h_1 + h_2$ and $\mathbf{H} = \{1, 2, \ldots, h\}$, $\mathbf{G} = \{\mathbf{G}_1, \mathbf{G}_2\}$, with $\mathbf{G}_1 = \{1, 2, \ldots, h_1\}$ and $\mathbf{G}_2 = \{h_1 + 1, \ldots, h_2\}$. The complete interconnected system P is thus composed from block-diagonal matrices of the form

$$M = \sum_{f=1}^{g} (E_f \otimes M_f).$$

In [98], $h_1 = h_2 = 5$ is imposed, consequently rendering P a 20th order system with 20 inputs and 40 outputs.

An interconnection matrix derived from scalar-repeated, real-valued, directed and row-normalized Laplacian matrices is considered, s.t.

$$\mathscr{L}(t) \overset{\triangle}{=} \mathscr{I}_N(t) \otimes I_3.$$

Due to Geršgorin's circle theorem [43], the spectrum is known *a priori* to be confined to the Perron disc given in (7.12) on p. 221 for an arbitary number of subsystems.

10.1.2 *Performance Comparison: Distributed Vs. Centralized Control*

The following example is based on a preliminary study published in [56]. The discussion will be extended in various ways:

- Comparison of distributed control performances against achievable performance through centralized control,

- Comparison of performances for the methods to normalize arbitrary directed interaction topologies,

- Comparison with recent results published in [98].

10.1.2.1 *Centralized Reference Controller Design*

As a reference, centralized $\mathcal{H}_\infty$-norm optimal controllers are computed for varying sizes of the respective groups $h_1 = \text{card}(\mathbf{G}_1) = h_2 = \text{card}(\mathbf{G}_2) \in \{1, 2, \ldots, 10\}$ and 100 randomly generated interconnection matrices each, in order to serve as an indication of potential loss in performance versus an increasing number of subsystems. The overall system order thus ranges between four and 40. A centralized control strategy achieves a relatively constant control performance ranging in the interval $[1.0031, 1.0444]$. Figure 10.1 depicts the resulting performance indices over the number of subsystems in each group.
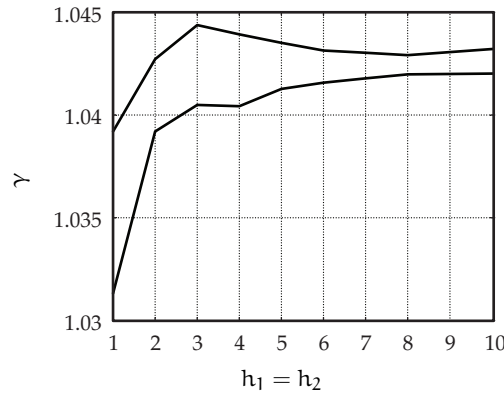
Figure 10.1: Centralized control performance index in terms of the achieved closed-loop $\mathcal{H}_\infty$-norm.

10.1.2.2 *Normalization*

In the following, the distributed formation control system's performance will be evaluated under the different cases that

(i) Normalization, as per Prop. 9.2,

(ii) Normalization, as per Prop. 9.3,

(iii) Direct SVD-based diagonalization as per Lma. 9.2 [98]

is used. Normalization, as per Prop. 9.2 is performed by defining

$$\ell(t) \triangleq \mathscr{I}_N(t) = \begin{bmatrix} I_h & 0 \end{bmatrix} \begin{bmatrix} \mathscr{I}_N(t) & -\mathscr{I}_N(t)^\top \\ \mathscr{I}_N(t)^\top & \mathscr{I}_N(t) \end{bmatrix} \begin{bmatrix} I_h \\ 0 \end{bmatrix}.$$

Normalization, as per Prop. 9.3 is performed by defining

$$\ell(t) \triangleq \mathscr{I}_N(t) = \begin{bmatrix} \tfrac{1}{2}I_h & \tfrac{1}{2}I_h \end{bmatrix} \begin{bmatrix} \mathscr{I}_N(t) + \mathscr{I}_N(t)^\top & 0 \\ 0 & \mathscr{I}_N(t) - \mathscr{I}_N(t)^\top \end{bmatrix} \begin{bmatrix} I_h \\ I_h \end{bmatrix}.$$

Tab. 10.1 lists the ranges of eigenvalues and singular values of the interconnection matrices versus normalization and SVD-based diagonalization obtained from $10,000$ randomly generated interconnection matrices for the cases of $h_1 = h_2 \in [2,\ldots,30]$.

Table 10.1: Ranges of eigenvalues and singular values of the interconnection matrices and versus normalization and SVD-based diagonalization in the numerical example borrowed from [98].

	Eigenvalues		Sing. values
	Re $(\bullet)$	Im $(\bullet)$	
Row-normalized Laplacian $\mathscr{I}_N(t)$	$[0.000, 2.000]$	$[-1.000, 1.000]$	$[0.000, 2.750]$
Method			
(ii) Normalization, Prop. 9.2	$[-1.100, 2.650]$	$[-2.650, 2.650]$	$[0.000, 3.750]$
(iii) Normalization, Prop. 9.3	$[-1.200, 5.000]$	$[-2.250, 2.250]$	$[0.000, 4.550]$
(iv) SVD-based, Lma. 9.2			$[0.000, 2.750]$

(a) (i) Normalization, Prop. 9.2.

(b) (ii) Normalization, Prop. 9.3.
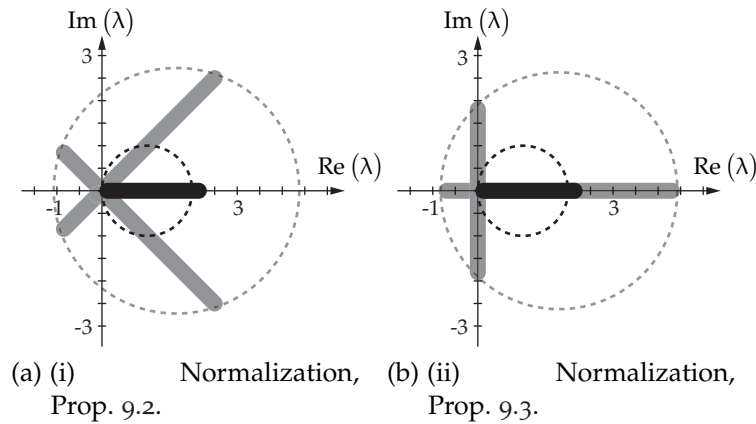
Figure 10.2: Ranges of eigenvalues and singular values in the complex plane for the original and the respective normalizedinterconnection matrices.
(━━) Black lines indicate the original range of singular values.
(-----) Dashed black lines indicates the Perron disc..
(▬) Fat grey lines indicate the range of eigenvalues of the normalizedinterconnection matrices.

10.1.2.3 *Distributed Controller Synthesis Results*

Tab. 10.2 lists the achieved performance indices for the respectively groups versus the methods applied to render the distributed controller synthesis problem effi-

ciently solvable according to the results presented in Chap. 9. The employed controller synthesis machinery essentially relies on the analysis results of Thm. 9.3 for the cases (i)–(iii) and Thm. 9.4 for case (iv) and the respective extension to synthesis made explicit in Thm. 9.6 for the cases (i)–(iii).

Table 10.2: Achieved performance indices in the numerical example versus normalization and SVD-based diagonalization.

Method	Performance γ_f		Rel. Perf. Loss $\frac{\gamma_1}{\gamma_c}$
	$f = 1$	$f = 2$	
Centralized controller	$\gamma_c = 1.0444$		
(i) Normalization, Prop. 9.2	1.0562	1.0346	1.1 %
(ii) Normalization, Prop. 9.3	1.0675	1.0467	2.2 %
(iii) SVD-based, Lma. 9.2	1.0928	1.0766	4.6 %

For reference, Tab. 10.2 states the worst case performance achieved by a centralized controller and the respectively relative loss in performance due to the distributed control approach. The relative loss is considered w. r. t. the performance indices of the first subsystem type, γ_1, since it is consistently larger than γ_2 in all methods (i)–(iii). Note that in contrast to the distributed controllers, the centralized controller does not provide guarantees for time-varying interconnection topologies.

As evident from Tab. 10.7, the best performance is achieved by normalization method (i) (Prop. 9.2), where the virtual interconnection channel is set to zero. No difference is observed, if the virtual channel is constructed via the choice $W_\ell = \frac{1}{2} \begin{bmatrix} I_h, & I_h \end{bmatrix}^\top$ and $V_\ell = \begin{bmatrix} I_h, & I_h \end{bmatrix}$. Normalization method (ii) (Prop. 9.3), which separates real and imaginary eigenvalues by splitting the interconnection matrix into two virtual interconnection matrices—one symmetric, one skew-symmetric—, results in a drop in performance by a factor of 2, while with the SVD-based method (iii) (Lma. 9.2) [98] the performance drops by a factor of 4.2. Overall, the considered methods appear to involve only mild conservatism w. r. t. the present problem.

10.1.2.4 *Comparison of Achieved Performance for Specific Topologies*

In the present example, relatively little conservatism is introduced by using a distributed control approach with synthesis complexity on a subsystem level, which allows for time-varying interconnection matrices. In the following, it will be investigated how the achieved performance of the respective approaches (i)-(iii) correlates to the data for specific interconnection matrices.

A configuration with $h_1 = h_2 = 5$ is considered with 55 randomly generated, directed, row-normalized Laplacian matrices representing the interconnection topologies. The results are depicted in Figs. 10.3
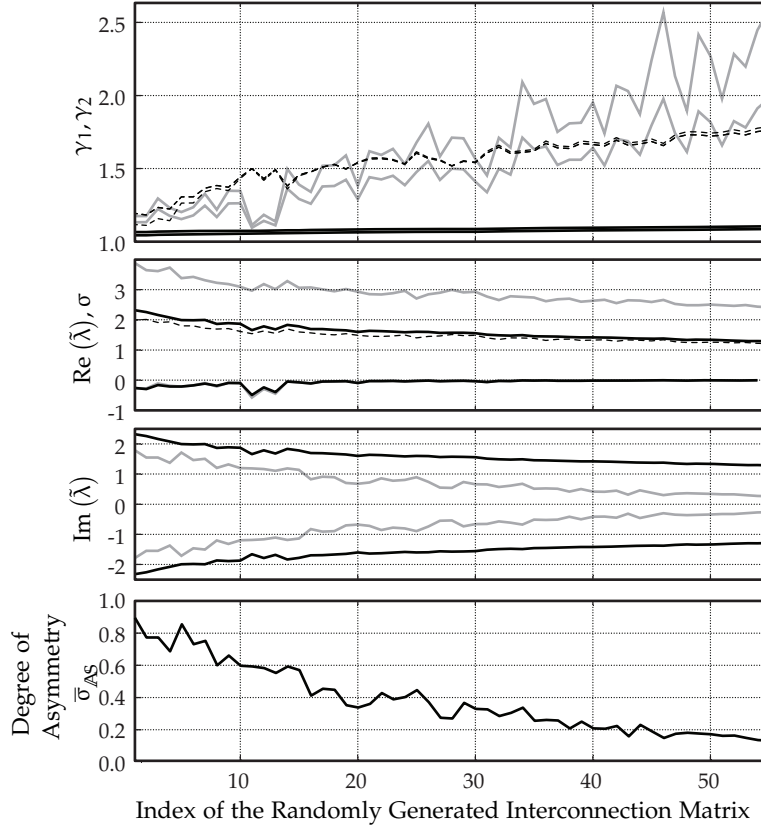
Figure 10.3: Performance indices γ_1 and γ_2, max/min real and imaginary parts of the normalized interconnection matrices vs. the index of the randomly generated Laplacians ordered by performance achieved by method (i), Prop. 9.2.
(——) Black solid lines: Method (i), Prop. 9.2.
(——) Grey solid lines: Method (ii), Prop. 9.3.
(-----) Black dashed lines: Method (iii), Lma. 9.2. Instead of the real part, the maximum singular value is indicated.

For each of the interconnection matrices $\tilde{\ell}$ normalized by methods (i) or (ii), i.e., according to Props. 9.2 or 9.3, respectively, both the maximum and minimum real and imaginary parts of the eigenvalues are presented. With respect to method (iii), only the maximum singular value is provided. The performance index achieved for subsystem type 1 is consistently larger than the one for type 2, i.e., $\gamma_1 > \gamma_2$. In addition Fig. 10.3 shows the degree of asymmetry as defined in Def. 9.1 on p. 259.

10.1.3 *Discussion*

The numerical example indicates that the method of normalization has the potential of introducing less conservatism than the SVD-based method proposed in [98]. The latter is employed in this thesis in the framework of a *convex* optimization problem for the synthesis of distributed output-feedback controllers by the use of D-

scalings. In [98], at the time of publication, the author admits to not have knowledge about a convex solution to the distributed output-feedback problem and an iterative approach for the solution of bilinear matrix inequalities (BMIs) is followed. The published results state an increase by 6 % in terms of the performance index of a distributed output-feedback controller w. r. t. the performance achieved by the centralized controller, which is roughly in accordance with the figure of 4.6 % stated in this thesis. Presumably, the difference can be attributed to the iterative approach, the discrete-to-continuous-time conversion and LMI solver settings, resulting in slight numerical inconsistencies.

For the normalization method (i) (Prop. 9.3) D-scalings are required due to the complex eigenvalues of the virtual interconnection matrix resulting from normalization. The ball in which the eigenvalues may reside can be shifted about the real axis. The fact that the normalization allows the diagonalization according to Lma. 9.1, which relies on a unitary transformation, explicitly allows for non-zero off-diagonal blocks in the multiplier resulting from such a shift. In contrast, Lma. 9.2 relies on the SVD and therefore prescribes zero off-diagonal blocks under all circumstances. Consequently, the multiplier conditions are posed in such a way that not only the range from zero to the maximum singular value, but also the reflection to the negative real axis is considered [98]. Presumably, this is the reason for the stronger decrease in distributed control performance of the SVD-based method (iii) (Lma. 9.2).

The comparison of the respectively methods for specific interconnection matrices documented in Fig. 10.3 reveals that method (i) is consistently providing lower performance indices that methods (ii) and (iii). Figure 10.3 depicts almost constant performance indices $\gamma_1 \approx \gamma_2$ in the case of method (i). While method (iii) also provides almost equal performance for both subsystem types, the performance indices vary much stronger with method (ii). The index γ_1 achieved by method (ii) is in some cases larger and in some cases smaller than the one achieved by method (iii). All methods, however, show a relatively consistent decrease in performance with decreasing real and imaginary eigenvalue ranges. Furthermore, there appears to be a reciprocal correlation between the achieved performance indices and the degree of asymmetry, which is in accordance with [127]. In this work, performance improvements via asymmetric weights on interconnections are discussed. The data presented here suggests that method (i) is more resilient to drops in performance that are due to symmetric interconnections. Method (ii) on the other hand involves a part of the virtual interconnection that is always symmetric, which may account for the stronger deterioration in performance.

10.2 A Leader-Follower Formation of Quadrocopters

As an example that draws from MASs—an important subclass of interconnected systems control that can be handled with the proposed framework and tools—the leader-follower formation control and reference tracking control problem is investigated for a fleet of nonlinear quadrotor helicopter models and a virtual leader agent. The problem is thus posed as the synthesis of an interconnected control scheme considering heterogeneous LPV subsystem dynamics.

The nonlinear LPV model is first derived in Sect. 10.2.1, after which achievable performances in distributed formation control is analyzed in Sect. 10.2.2.

10.2.1 *LPV Modeling of a Quadrotor Helicopter*

Quadrotor helicopters are frequently employed in MASs-based research as they provide a platform for testing cooperative control schemes that is often associated with a multitude of real world applications. The quadrocopters' dynamics are not subject to non-holonomic constraints—a research field that is interesting in its own right. In fact, some of the methods proposed in this thesis, including symmetrization as per Prop. 9.1, have already been successfully applied in [107] to cooperative ground vehicle control, in which a rolling disc acts as a simple agent model with non-holonomic constraints.

Linearized quadrocopter models are often used in publications associated with MASs, as smooth and steady formation flight does often not involve aggressive maneuvers. In [0, 46], however, the potential of gain-scheduled LPV control for quadrocopters has been demonstrated. In this section, an LFT-LPV model of a quadrocopter is developed for use in conjunction with the methods presented in Chap. 9 in a cooperative control setting. Despite the fact that the afore-mentioned methods can easily handle physical couplings, the focus on the subsequent simulation examples will be on the demonstration of including LPV subsystem dynamics into the distributed synthesis problem, as well as offering a «gain-scheduling perspective» on the synthesis of formation control schemes.

10.2.1.1 *Nonlinear* LPV *Model*

Consider the quadrocopter model illustrated in Fig. 10.4. In this thesis, the angular limits shown in Tab. 10.3 will be considered. In [0, 46], it was shown that enlarging the angular limits up to 60° strongly benefits from PDLFs and improved agility via high-performance LPV controllers can be achieved. As the methods presented in this thesis are currently limited to PiDLFs, or static multipliers, respectively, smaller angular limits are considered.

A set of nonlinear differential equations is taken from [16], where the generalized coordinates are identified as the position (x, y, z) and the orientation (q_1, q_2, q_3) in standard yaw-pitch-roll convention. The inertial coordinate system is denoted (x_1, x_2, x_3), whereas the body coordinate system is denoted (X_1, X_2, X_3). The direc-

Table 10.3: Angular limits of the Quadrocopter.

Angle	Range [°]
q_1	$[-40, \ldots, 40]$
q_2	$[-40, \ldots, 40]$
q_3	$[-180, \ldots, 180]$
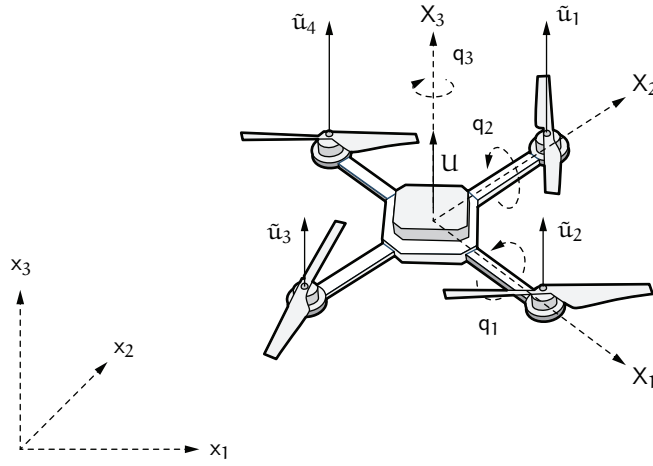
Figure 10.4: Isometric view of a quadrocopter.

tions of both of the angles q_2 and q_3 do not correspond to the axis directions—a convention which has been adopted from the definitions of the commercial quadrocopter Hummingbird designed by Astec. As mentioned in [0, 46], the hub forces and moments defined in [16] are omitted due to their small magnitude and the difficulty involved in their experimental identification.

The force in the inertial frame can be calculated as

$$u = R_{X_1}(q_1) R_{X_2}(q_2) R_{X_3}(q_3) U, \quad U = \sum_{i=1}^{4} u_i,$$

with

$$R_{X_1}(q_1) = \begin{bmatrix} 1 & 0 & 0 \\ 0 & \cos(q_1) & -\sin(q_1) \\ 0 & \sin(q_1) & \cos(q_1) \end{bmatrix}, \quad R_{X_2}(q_2) = \begin{bmatrix} \cos(q_2) & 0 & \sin(q_2) \\ 0 & 1 & 0 \\ -\sin(q_2) & 0 & \cos(q_2) \end{bmatrix},$$

$$R_{X_3}(q_3) = \begin{bmatrix} \cos(q_3) & -\sin(q_3) & 0 \\ \sin(q_3) & \cos(q_3) & 0 \\ 0 & 0 & 1 \end{bmatrix}.$$

The resulting nonlinear differential equations of the dynamic model of 12$^{\text{th}}$-order with four inputs is given in (10.2) below.

Abbreviations:
$s_i \triangleq \sin(q_i)$
$c_i \triangleq \cos(q_i)$

$$
\begin{bmatrix}
m & 0 & 0 & 0 & 0 & 0 \\
0 & m & 0 & 0 & 0 & 0 \\
0 & 0 & m & 0 & 0 & 0 \\
0 & 0 & 0 & J_{11} & 0 & 0 \\
0 & 0 & 0 & 0 & J_{22} & 0 \\
0 & 0 & 0 & 0 & 0 & J_{33}
\end{bmatrix}
\begin{bmatrix}
\ddot{x}_1 \\ \ddot{x}_2 \\ \ddot{x}_3 \\ \ddot{q}_1 \\ \ddot{q}_2 \\ \ddot{q}_3
\end{bmatrix}
$$

$$
+
\begin{bmatrix}
0 \\
0 \\
0 \\
(J_{22} - J_{33})\dot{q}_2\dot{q}_3 \\
(J_{33} - J_{11})\dot{q}_1\dot{q}_3 \\
(J_{11} - J_{22})\dot{q}_2\dot{q}_2 - mg
\end{bmatrix}
=
\begin{bmatrix}
-(c_1 s_2 c_3 + s_1 s_3) & 0 & 0 & 0 \\
(c_1 s_2 s_3 - s_1 c_3) & 0 & 0 & 0 \\
(c_1 c_2) & 0 & 0 & 0 \\
0 & 1 & 0 & 0 \\
0 & 0 & 1 & 0 \\
0 & 0 & 0 & 1
\end{bmatrix}
\begin{bmatrix}
\tilde{u}_1 \\ \tilde{u}_2 \\ \tilde{u}_3 \\ \tilde{u}_4
\end{bmatrix} ,
$$

(10.2)

The moments of inertia $I_{\bullet\bullet}$ and mass m are taken from [122] to reflect realistic values for the Hummingbird quadrocopter model. Tab. 10.4 lists the identified values.

Table 10.4: Physical and grouped parameters of the quadrocopter [122].

Parameter	Value	Parameter	Value
m	$0.640\,00\,\text{kg}$	$b_1 = m$	0.64000
J_{11}	$0.004\,20\,\text{kg}\,\text{m}^2$	$b_2 = J_{11} = J_{22}$	0.00420
J_{22}	$0.004\,20\,\text{kg}\,\text{m}^2$	$b_3 = mg$	6.27840
J_{33}	$0.008\,15\,\text{kg}\,\text{m}^2$	b_4 not used	
g	$9.810\,00\,\text{kg}\,\text{m/s}^2$		
l	$0.280\,00\,\text{m}$		

10.2.1.2 *Input Transformation and LPV Model Representation*

Define the input vector as

$$
u \triangleq \begin{bmatrix} u_1 & u_2 & u_3 & u_4 \end{bmatrix}
$$
$$
= \begin{bmatrix} U + mg, & l(\tilde{u}_1 - \tilde{u}_3), & l(\tilde{u}_2 - \tilde{u}_4), & b_4(-\tilde{u}_1 + \tilde{u}_2 - \tilde{u}_3 + \tilde{u}_4) \end{bmatrix} ,
$$

where u_2, u_3, u_4 represent torques about the axis q_1, q_2 and q_3, respectively, and l is the distance from the quadrocopter's center of gravity to a rotor. A shift in the first input direction about the gravitational force is suggested in [82] to make $u_1 = 0$ the input associated with steady hovering. In the LFT-LPV model derived in the following, it also makes couplings between states explicit [0, 46].

By making the assumption that the inertial coordinate system rotates on the x_3 axis along with the quadrocopter, one can set $q_3 = 0$. The rotation around the

$x_{3,k}$ axis is further assumed to be controlled by some other control loop, which eventually reduces the quadrocopter model to 10 states and 3 inputs. Consequently, the nonlinear differential equations simplify to (10.3) below.

$$
\begin{bmatrix} m & 0 & 0 & 0 & 0 \\ 0 & m & 0 & 0 & 0 \\ 0 & 0 & m & 0 & 0 \\ 0 & 0 & 0 & J_{11} & 0 \\ 0 & 0 & 0 & 0 & J_{22} \end{bmatrix} \begin{bmatrix} \ddot{x}_1 \\ \ddot{x}_2 \\ \ddot{x}_3 \\ \ddot{q}_1 \\ \ddot{q}_2 \end{bmatrix} = \begin{bmatrix} -c_1 s_2 & 0 & 0 \\ -s_1 & 0 & 0 \\ c_1 c_2 & 0 & 0 \\ 0 & 1 & 0 \\ 0 & 0 & 1 \end{bmatrix} \begin{bmatrix} u_1 + mg \\ u_2 \\ u_3 \end{bmatrix} - \begin{bmatrix} mg \\ 0 \\ 0 \end{bmatrix} , \tag{10.3}
$$

An LFT-LPV model is obtained by employing the Taylor approximations

$$
\sin(q) \approx q - \frac{1}{6}q^3, \quad \cos(q) \approx 1 - \frac{1}{2}q^2.
$$

In [0, 46], relative modeling errors of the magnitude of the differential equations in $\ddot{x}_1$, $\ddot{x}_2$ and $\ddot{x}_3$ w.r.t. the magnitude of u_1 of about 5 % at the angular limits are reported.

As it turns out, control performance for a single quadrocopter increases by choosing a factorization approach that penalizes sparsity, according to Sect. 4.3.2 [0, 46]. The model is simple enough to perform a manual factorization, instead of solving the problem given in (4.17) on p. 112. Since a maximum of two states are multiplied with each other, weights of $\frac{1}{2}$ are chosen to introduce as many coupling terms as possible.

The resulting rational model can be represented in general LPV form as given in (10.4) below. For simplicity, a motor model is not included.

$$
\begin{bmatrix} b_1 & 0 & 0 & 0 & 0 \\ 0 & b_1 & 0 & 0 & 0 \\ 0 & 0 & b_1 & 0 & 0 \\ 0 & 0 & 0 & b_2 & 0 \\ 0 & 0 & 0 & 0 & b_2 \end{bmatrix} \begin{bmatrix} \ddot{x}_1 \\ \ddot{x}_2 \\ \ddot{x}_3 \\ \ddot{q}_1 \\ \ddot{q}_2 \end{bmatrix} + b_3 \begin{bmatrix} 0 & 0 & 0 & \frac{1}{4}q_1 q_2 & \left(\frac{1}{4}q_1^2 - 1\right) \\ 0 & 0 & 0 & -1 & 0 \\ 0 & 0 & 0 & \left(\frac{1}{8}q_2^2 - \frac{1}{2}\right)q_1 & \left(\frac{1}{8}q_1^2 - \frac{1}{2}\right)q_2 \\ 0 & 0 & 0 & 0 & 0 \\ 0 & 0 & 0 & 0 & 0 \end{bmatrix} \begin{bmatrix} x_1 \\ x_2 \\ x_3 \\ q_1 \\ q_2 \end{bmatrix}
$$
$$
= \begin{bmatrix} \left(\frac{1}{2}q_1^2 - 1\right)q_2 & 0 & 0 \\ -q_1 & 0 & 0 \\ 1 - \frac{1}{2}q_1^2 - \frac{1}{2}q_2^2 + \frac{1}{4}q_1^2 q_2^2 & 0 & 0 \\ 0 & 1 & 0 \\ 0 & 0 & 1 \end{bmatrix} \begin{bmatrix} u_1 \\ u_2 \\ u_3 \end{bmatrix} , \tag{10.4}
$$

10.2.1.3 *Parameterization*

With the parameters δ from Tab. 10.6a and the polynomial expansion of the trigonometric terms, the matrices are naturally rendered polynomial in δ. Even though a full-block LFT-LPV parameterization detailed in Sect. 4.4 would result in a parameter block of size 3×3 and hence would reduce the computational burden online, a standard parameterization with a diagonal parameter block is used. The diagonal parameter block turns out to be of size 8×8 with repetitions listed in Tab. 10.6b.

Note that the commonly available tools for the exact reduction of LFRs of Matlab [149] as well as the n-D (Kalman like) decomposition or the generalized Gramian approach [13, 14, 25, 93] available through the ONERA LFR Toolbox do not yield any further reduction in repetitions than the ones reported in Tab. 10.6a.

Table 10.5: Measurable signals and LPV parameter block information for the quadrocopter.

$$\delta_1 \overset{\triangle}{=} q_1$$
$$\delta_2 \overset{\triangle}{=} q_2$$

(a) Measurable signals.

Block	Size	Par. No.	Repetitions r_i
$\Delta(\delta)$	8×8	$n_\delta = 2$	$r^\delta = [3, 5]$

(b) Parameter block information for the quadro-copter model.

10.2.2 A Leader-Follower Formation Control and Reference Tracking Problem

The following example is based on a preliminary study published in [56]. The discussion will be extended in various ways:

- Consideration of a high-fidelity LPV agent model,

- Comparison of performances for the methods to normalize arbitrary directed interaction topologies,

- Comparison with recent results published in [98].

10.2.2.1 Problem Setup

Consider a leader-follower setup with a single leader and five followers. Agent 1 assumes the role of the virtual leader with an integrator model $H_1(s) = {}^1\!/_s\,I_3$ in each of the three degrees of freedom with state space model detailed in (10.5). However, to simplify, the reference for the altitude, i. e., the $x_{3,k}$ direction will be held constant at 0.

$$
H_1 : \left\{ \begin{bmatrix} \dot{y}_1 \\ y_1 \end{bmatrix} = \begin{bmatrix} 0_{3\times3} & I_{3\times3} \\ I_{3\times3} & 0_{3\times3} \end{bmatrix} \begin{bmatrix} y_1 \\ u_1 \end{bmatrix} \right. .
\tag{10.5}
$$

The agents' model $\mathcal{H}_k$, $k = 2, 3, \ldots, 6$ is taken as the LFT-LPV quadrocopter model from the previous Sect. 10.2.1. The positions are to be controlled in a distributed fashion and the individual agents' coordinates are denoted

$$
y_k = \begin{bmatrix} x_{1,k}, & x_{2,k}, & x_{3,k} \end{bmatrix}^\top, \quad q_k = \begin{bmatrix} q_{1,k}, & q_{2,k} \end{bmatrix}^\top
$$

for the position and orientation, respectively. Figure 10.5 shows the generalized plants used for synthesis. Shaping filters

$$
W_S = \frac{5}{s + 0.05} I_3, \quad \text{and} \quad W_{KS,k} = \frac{s + 0.1}{s + 10000} I_3
$$

are used to consider tracking and to penalized the control input.

The interconnection matrix is chosen as

$$
\ell(t) = \begin{bmatrix} 0 & 0 \\ \ell_{G_2 G_1}(t) & \ell_{G_2 G_2}(t) \end{bmatrix} .
$$

In the following, the distributed formation control system's performance will be evaluated under the different cases that

(i) Normalization, as per Prop. 9.2,

(ii) Normalization, as per Prop. 9.3,

(a) Leader, $k = 1$.　　　(b) Followers, $k \in \{2, \ldots, 6\}$.
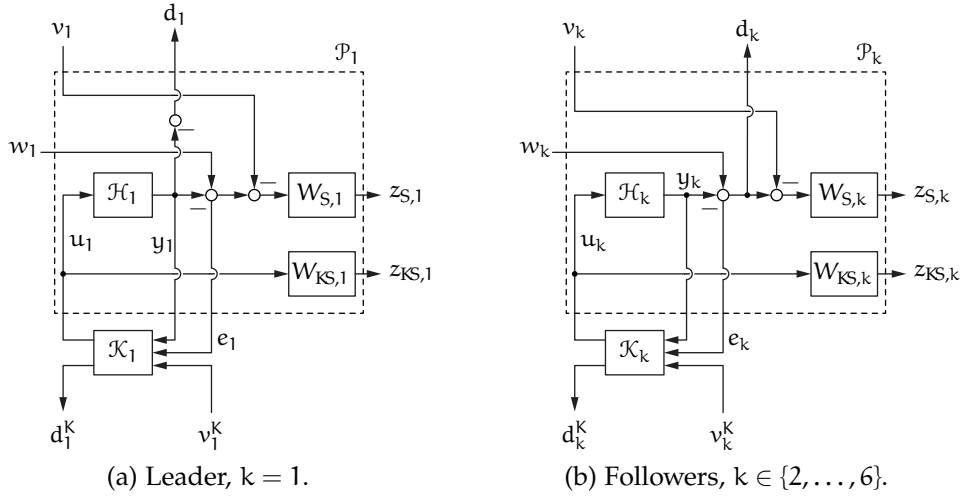
Figure 10.5: Generalized plant configuration for the leader-follower distributed control configuration of a group of quadrocopters with virtual leader.

(iii) Direct SVD-based diagonalization as per Lma. 9.2 [98]

is used.

As a practical consideration, it is assumed that the position information of each agent is simply broadcasted, which implies that the individual agents have no knowledge about the number of recipients. In contrast to this, each agent has information about the number of incoming transmissions to process. In terms of a graph theoretical interpretation, this means that the interconnection matrix may be row-normalized, but not column-normalized. In [56], simultaneous row- and column-normalization is considered to allow the use of symmetrization. However, in order to maintain scalability this technique is not considered.

Consequently, the interconnection $\ell(t)$ is constructed as a time-varying row-normalized adjacency matrix $\mathscr{A}_N(t)$, where $\ell_{G_2 G_1}(t)$ is chosen, s.t. the leader is either sending information to the first two or last three followers and the matrix $\ell_{G_2 G_2}(t)$ is time-varying and ensures connectedness between the followers. The interconnection is set to randomly switch every $5\,\mathrm{s}$.

10.2.2.2 *Normalization*

Tab. 10.6 lists the ranges of eigenvalues and singular values of the interconnection matrices versus normalization and SVD-based diagonalization obtained from randomly generated interconnection matrices. As in the previous Sect. 10.1, Normalization, as per Prop. 9.2 is performed by defining

$$\ell(t) \overset{\triangle}{=} \mathscr{A}_N(t) = \begin{bmatrix} I_h & 0 \end{bmatrix} \begin{bmatrix} \mathscr{A}_N(t) & -\mathscr{A}_N(t)^\top \\ \mathscr{A}_N(t)^\top & \mathscr{A}_N(t) \end{bmatrix} \begin{bmatrix} I_h \\ 0 \end{bmatrix}.$$

Normalization, as per Prop. 9.3 is performed by defining

$$\ell(t) \stackrel{\triangle}{=} \mathscr{A}_N(t) = \begin{bmatrix} \frac{1}{2}I_h & \frac{1}{2}I_h \end{bmatrix} \begin{bmatrix} \mathscr{A}_N(t) + \mathscr{A}_N(t)^\top & 0 \\ 0 & \mathscr{A}_N(t) - \mathscr{A}_N(t)^\top \end{bmatrix} \begin{bmatrix} I_h \\ I_h \end{bmatrix}.$$

Table 10.6: Ranges of eigenvalues and singular values of the interconnection matrices and versus symmetrization/normalization and SVD-based diagonalization in the quadrocopter formation control problem.

	Eigenvalues		Sing. values
	Re $(\bullet)$	Im $(\bullet)$	
$\ell(t)$	$[-1.000, 1.000]$	$[\ \ 0.000, 0.000]$	$[0.000, 1.600]$
Method			
(i) Normalization, Prop. 9.2	$[-1.000, 1.125]$	$[-1.125, 1.125]$	$[0.000, 1.600]$
(ii) Normalization, Prop. 9.3	$[-2.000, 2.000]$	$[-1.000, 1.000]$	$[0.000, 2.000]$
(iii) SVD-based, Lma. 9.2			$[0.000, 1.600]$

(a) (i) Normalization, Prop. 9.2.

(b) (ii) Normalization, Prop. 9.3.

(c) (iii) SVD-based, Lma. 9.2.
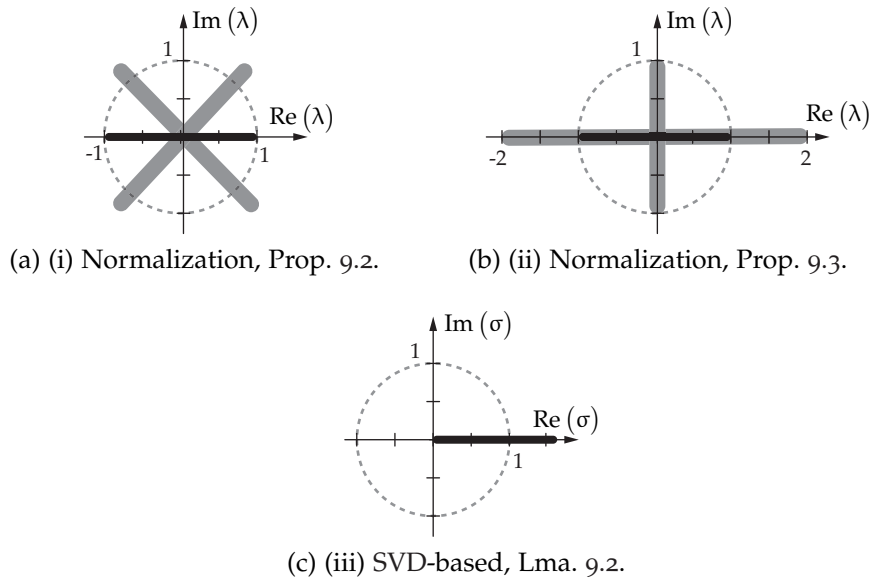
Figure 10.6: Ranges of eigenvalues and singular values in the complex plane for the original and the respective normalizedinterconnection matrices.
(━━) Black lines indicate the original range of eigenvalues/singular values.
(▬▬) Fat grey lines indicate the range of eigenvalues of the normalized interconnection matrices.

10.2.2.3 *Distributed Controller Synthesis*

Tab. 10.7 lists the achieved performance indices for the respectively groups versus the methods applied to render the distributed controller synthesis problem efficiently solvable according to the results presented in Chap. 9. The employed controller synthesis machinery essentially relies on the analysis result of Thm. 9.3 for the cases (i) and (ii) and the respective extensions to synthesis made explicit in Thm. 9.6. Case (iii) relies on Thm. 9.4 and its respective extension to synthesis.

Table 10.7: Achieved performance indices versus symmetrization/normalization and SVD-based diagonalization in the quadrocopter formation control problem.

Method	Performance	
	$f = 1, k = 1$	$f = 2, k = 2, 3, \ldots, 6$
(i) Normalization, Prop. 9.2	1.126	3.299
(ii) Normalization, Prop. 9.3	1.791	4.158
(iii) SVD-based, Lma. 9.2	4.824	7.059

As evident from Tab. 10.7, the best performance by the normalization method (i) (Prop. 9.2), where the virtual interconnection channel is zero. If the virtual channel is constructed via the choice $W_\ell = \frac{1}{2} \begin{bmatrix} I_h, & I_h \end{bmatrix}^\top$ and $V_\ell = \begin{bmatrix} I_h, & I_h \end{bmatrix}$, the performance index drops to 3.0176. Normalization method (ii) (Prop. 9.3), which separates real and imaginary eigenvalues by splitting the interconnection matrix into two virtual interconnection matrices—one symmetric, one skew-symmetric—, already shows a significant deterioration in performance, while the SVD-based method (iii) (Lma. 9.2) [98] results in an even stronger loss of performance.

10.2.2.4 *Simulation Results*

A formation reference $w_k(t) = r(t)r_k$, for $k \in \{2, \ldots, 6\}$ is fed to the followers with $r_2 = [1\ 1\ 0]^\top$, $r_3 = [-1\ -1\ 0]^\top$, $r_4 = [-1\ 1\ 0]^\top$, $r_5 = [1\ -1\ 0]^\top$, $r_6 = [0\ 1\ 0]^\top$. It is deactivated when the leader is not to be tracked ($r(t) = 0$), in order to let the followers perform a rendezvous maneuver. The response of the interconnected system $[x_{1,k}(t)\ x_{2,k}(t)]^\top$ is shown in Fig. 10.8 for controllers synthesized based on normalization method (i) (Prop. 9.2). It can be observed, that in the interval $[35, 45]$ s, the followers stop tracking the leader and rendezvous. For comparison the simulation results for controllers synthesized with the SVD-based method (iii) (Lma. 9.2) are shown in dotted lines. As apparent from the plot, the tracking accuracy deteriorates significantly as a result of the higher performance index. Finally, Fig. 10.7 shows the position of the subsystems in Cartesian coordinates.
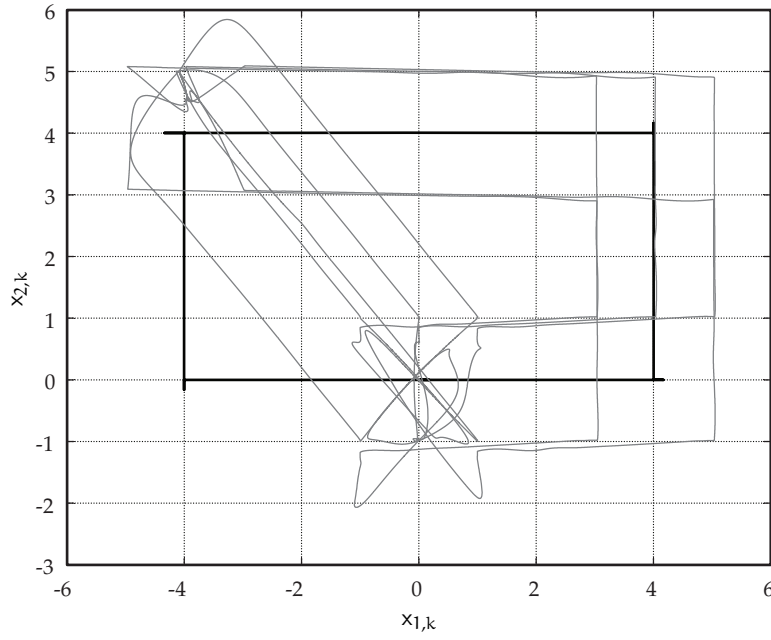
Figure 10.7: Interconnected system response in Cartesian coordinates. Leader-follower configuration of a virtual leader and LPV quadrocopter models. Coordinates $[x_{1,k}(t)\ x_{2,k}(t)]^\top$.
(———) Virtual leader agent, normalization method (i) (Prop. 9.2).
(———) LPV quadrocopter follower agents, normalization method (i) (Prop. 9.2).
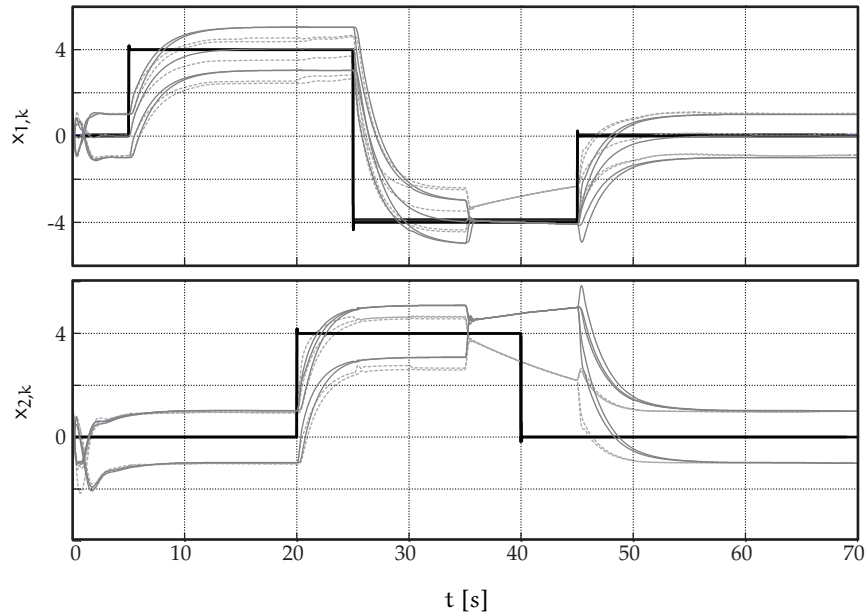
Figure 10.8: Interconnected system response. Leader-follower configuration of a virtual leader and LPV quadrocopter models. Coordinates $[x_{1,k}(t)\ x_{2,k}(t)]^\top$.
(———) Virtual leader agent, normalization method (i) (Prop. 9.2).
(———) LPV quadrocopter follower agents, normalization method (i) (Prop. 9.2).
(·········) LPV quadrocopter follower agents, SVD-based method (iii) (Lma. 9.2).

10.2.3 *Discussion*

10.2.3.1 *Decomposition Methods*

The normalization method (i) (Prop. 9.2) strongly benefits from the potential to render the newly introduced virtual interconnection channel completely zero. D-scalings are required due to the complex eigenvalues of the virtual interconnection matrix resulting from normalization. The ball in which the eigenvalues may reside can be shifted about the real axis. The fact that the normalization allows the diagonalization according to Lma. 9.1, which relies on a unitary transformation, explicitly allows for off-diagonal blocks in the multiplier resulting from such a shift. In contrast, Lma. 9.2 used in method (iii) relies on the SVD and therefore prescribes zero off-diagonal blocks under all circumstances. Consequently, the multiplier conditions are posed in such a way that not only the range from zero to the maximum singular value, but also the reflection to the negative real axis is considered [98]. Presumably, this is the reason for the relatively bad performance of the SVD-based method (iii) (Lma. 9.2).

The separation of real and imaginary eigenvalues in normalization method (ii) (Prop. 9.3) requires the application of both D/G-Ss and D/G*-scalings (D/G*-Ss) for the symmetric and skew-symmetric virtual interconnection matrix, respectively. This results in a sparsity structure of the interconnection multiplier that is similar to the D-Ss required in normalization method (i) without a shift. In method (ii), however, only the D/G-S can be shifted. The ball, in which the union of the sets of real and imaginary eigenvalues is inscribed, is therefore a larger one, which may account for the slight loss in performance. However, it may be possible to achieve better performance by adjusting the coefficients involved in the normalization.

10.2.3.2 *Comparison with Standard Approaches*

The example illustrates that a formation control problem with arbitrary, time-varying topologies and with LPV agents can be efficiently solved as a convex optimization problem, whereas existing approaches, e. g., [115], essentially consider non-convex robust controller synthesis. It is in light of this that the «gain-scheduling perspective» on the synthesis of distributed formation controllers is stressed.

As depicted in Fig. 10.9c, in the novel formation control configuration, the controller is provided with an additional channel that corresponds to communication between the subsystem controllers. The generalized plant configuration is posed in such a way that the formation error e_f is not a direct feedback signal received by the controller. This is in contrast to the configuration shown in Fig. 10.9a, which corresponds to a robust formation control framework [115].

In the present thesis, controller coefficients synthesized via LMIs determine what information is exchanged in-between controllers. This configuration is chosen in

the present example, as can be inferred by inspecting the generalized plant from Fig. 10.5.

While this makes for a less transparent control scheme, it allows to synthesize distributed controllers using convex optimization, instead of by, e. g., iterative techniques, such as μ-synthesis [10]. The essential—and frankly, simple—ingredient consists in the introduction of a dedicated interconnection channel for the controller. One may, however, still provide e_f as a direct feedback signal as depicted in Fig. 10.9b. Such a configuration might aid in improving the performance of the formation control loop, but results in twice the information to be processed for interaction.
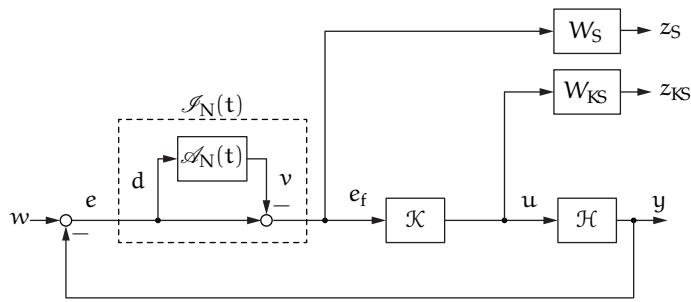
(a) Closed-loop configuration for robust interconnected controller synthesis.
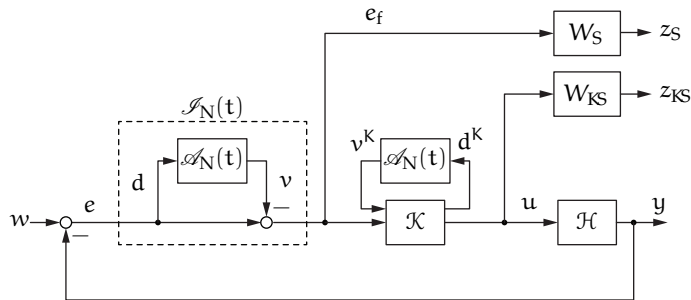
(b) Closed-loop configuration for «gain-scheduled» interconnected controller synthesis *with* direct feedback of the formation error.
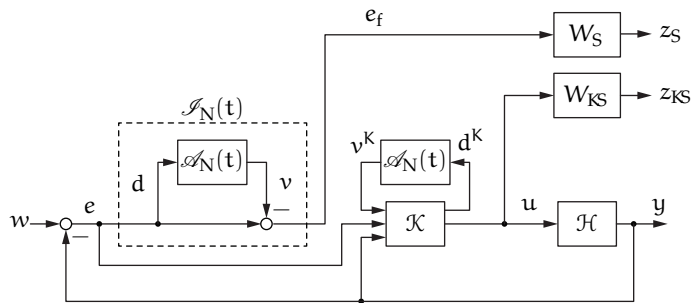
(c) Closed-loop configuration for «gain-scheduled» interconnected controller synthesis *without* direct feedback of the formation error.

Figure 10.9: Closed-loop configurations for cooperative control of MASs.

Part III

SUMMARY, CONCLUSIONS AND OUTLOOK

The novel methods detailed in Part I and II have been shown to be effective and lead to more efficient controller designs for complex non-linear systems. This part summarizes the results, draws conclusions and presents further possible research opportunities.

11

SUMMARY AND CONCLUSIONS

IN this work the analysis and control of systems of high complexity by means of techniques taken and extended from the field of linear parameter-varying (LPV) control is examined. In particular, the items considered that induce «complexity» into a system are twofold:

- A lumped system is complex in the sense that a number of nonlinear effects leads to an LPV representation with many parameters, rendering standard synthesis approaches as well as controller implementations costly and/or time consuming.

- An interconnected system is complex in the sense that it consists of a potentially large number of interconnected subsystems that may be nonlinear and heterogeneous in their dynamics, rendering centralized control schemes as well as synthesis conditions that scale with the number of subsystems inefficient or intractable.

As the items are divided into areas with regard to the modeling of and controller synthesis for complex lumped and interconnected systems, the results of this thesis will first be summarized separately in Sect. 11.1. After that, conclusions are drawn in Sect. 11.2.

11.1 Summary

T HE following provides a brief overview about the advances and proposed methods of this thesis.

11.1.1 *Part I—LPV Control of Complex Lumped Systems*

Figure 1.2 in Sect. 1.2 on p. 4 marked a first attempt at a decision tree guiding control designers to the successful synthesis of LPV controllers for the cases in which model and implementation complexity is an issue. This perspective once again illustrates that many of the obstacles still present in LPV theory have their source in the domain of modeling and realization [E60, 146]. An analysis of the synthesis and implementation complexity induced by the respective modeling approaches, complemented by an extensive survey on practical applications in Chap. 3, comprises both quantitative and empirical evidence of the complexity issues in the field of LPV control. As a result, a set of tools derived from an elaborate enumeration of quantifiers for implementation and synthesis complexity allows the *a priori* assessment of the most suitable combination of modeling and synthesis techniques for a given problem. Such complexity figures are easily derived if all types of model representations—general, linear fractional transformation (LFT)-based and affine— are available. This preliminary research culminates in the summaries given in Tables 3.1 and 3.2 on pp. 83 and 84 as well as Tabs. 3.3 and 3.4 on pp. 89 and 90, for implementation and synthesis complexities, respectively.

Modeling is often the most time consuming aspect of controller design, This issue has sparked the development of a semi-automated modeling framework. Motivated by challenging examples in the form of a three-degree of freedom robotic manipulator and a four-degree of freedom control moment gyroscope, a novel modeling framework for systems governed by systems of nonlinear, second order ordinary differential equations (ODEs) is first derived in Chap. 4. This tool heavily draws from descriptor representation approaches and the possibility to exploit these in multiplier-based synthesis frameworks using the full-block S-Procedure (FBSP). An approach for automated factorization into LPV form presented in Sect. 4.3.1 and Alg. 4.1 on p. 137 that provides semi-automated rational or affine parameterizations are inspired by previous research and issues that remained unsolved in [E60, 146]. A particular open question has consisted in the necessity for data-free approximation tools, for which a solution is proposed in this thesis in terms of a singular value decomposition (SVD)-based approximation of the coefficients associated with a monomial basis of the parameter block of the model. These developments have essentially been driven by Prop. 4.2 on p. 126.

In light of the possibilities of multiplier-based LPV synthesis tools—especially in conjunction with the use of full-block multipliers (FBMs)—Chap. 5 introduces techniques that exploit the novel modeling framework, in order to reduce complexity in synthesis and implementation for both parameter-independent Lyapunov function-

based output-feedback and parameter-dependent Lyapunov function-based state-feedback controller synthesis. Two key enablers are responsible for these improvements. Corollary 5.1 on p. 160 is used as a means to convexly evaluate small-in-size, FBMs-based scaling constraints to keep implementation complexity low in LFT-LPV output-feedback (OF) controller synthesis. Proposition 5.1 on p. 172 significantly reduces multiplier sizes in cases where the generalized inertia matrices incorporate complex parameter-dependency.

Application examples are thoroughly discussed in Chap. 6 that reveal reductions in synthesis time of up to 90 %, while maintaining full closed-loop stability and performance guarantees in case of the control moment gyroscope (CMG) due to proper application of the novel and improved methods. Even without the improved synthesis conditions, the novel modeling framework allows the synthesis of controllers based on an exact model of the CMG. Such a controller design has not been reported before. Similar achievements are obtained for the robotic manipulator in an OF control setting, while for both plants the novel approximation method results not only in reduced synthesis and implementation complexity, but also significantly improves the control performance.

11.1.2 *Part II—Control of Interconnected LPV Systems*

Part II of this thesis first provides an overview about the associated synthesis techniques for interconnected system control in Chap. 7. This part furthermore illustrates the results of this work as a synthesis of ideas from multiplier-based distributed controller design [80] and graph theory [109]. The combination is facilitated by an embedding into a compact modeling framework in Chap. 8 that encompasses known subclasses, such as «decomposable systems» [99].

By rigorously exploiting degrees of freedom in the multiplier-based analysis and synthesis conditions, Chap. 9 provides efficient synthesis conditions for the design of distributed control schemes for virtually and/or physically coupled, heterogenenous and nonlinear LPV subsystems interconnected through arbitrary directed and switching topologies. The tools rely on imposing structural constraints on multipliers only where necessary, in order to keep the induced conservatism low. At the heart of these methods are proposed solutions to Prob. 9.1 posed on p. 251. A particular one is Prop. 9.2 on p. 258, which formulates the method to introduce virtual interconnection channels in order to arrive at a normal interconnection matrix. Such matrices are unitarily diagonalizable, which allows the application of congruence transforms directly on the matrix inequalities that constrain the interconnection multiplier, see Lma. 9.1 on p. 266. This approach is an alternative to more restrictive methods proposed in the literature, e. g., [100], and circumvents issues that require topologies to be constant and undirected as well as subsystems to be homogeneous. For the novel methods to be effective, full advantage of preliminary research on the choice of scalings and the consequences for the controller's

parameter block in an LFT-LPV control setting has to be taken. This background is provided in-depth in Sects. 2.2.5 and 2.3.5.

Chap. 10 presents simulation examples illustrating that the novel methods introduce less conservatism than the ones proposed in [98]. While the first example consists in a fictitious system of marginally stable plants with interconnections in the states, the second one is a nonlinear multi-agent system setting purely set up with only communcation interconnections. In the literature, such problems are seldomly solved using essentially the same set of methods as distributed control problems, but are often tackled by dedicated techniques. The implications of this unification will be discussed in the concluding remarks.

11.2 Concluding Remarks

THE proposed methods of this thesis and achievements in the corresponding examples have various implications for the respective fields. In what follows, the relevancy and impact of this thesis is discussed.

11.2.1 A Set of Tools for Efficient LPV Synthesis

LPV synthesis techniques have been shown to be of high relevance for control problems that require a capable framework for performance specifications and rigorous closed-loop guarantees. Such guarantees only hold in so far as the model can be deemed to be exact, which in turn often induces high levels of complexity. This thesis provides elegant methods to directly use such exact models in a streamlined and coherent modeling and synthesis framework with tractable effort. The scope of plants for which LPV methods can be applied is therefore significantly broadened, which opens new control opportunities for researchers from a variety of disciplines, such as the chemical and process industry.

Furthermore, the degree of automation within the proposed modeling and parameterization framework is dramatically increased. This lowers the level of ambiguity within the LPV paradigm and reduces the amount of manual errors as well as the involved modeling effort. The underlying mathematical tools are surprisingly simple, such that further extensions and combinations with optimization criteria appear feasible and lead to future research directions.

11.2.2 A Novel Decision Tree for LPV Modeling

The initial decision tree depicted in Fig. 1.2, Sect. 1.2 on p. 4 is revised in Fig. 11.1. As part of the integrated approach of modeling and synthesis—most notably—the decision tree now includes *feedback*, or more precisely, the visualization of iterations in the design phase. Decisions, as required due to the heuristic factorization algorithm, can be revised in cases of excessive model complexity. With the underlying descriptor structure in mind, parameter dependence is kept polynomial or affine in the generalized inertia and system matrices. The coherent framework allows approximations for each type of parameter-dependency, which is an option in the case of excessive conservatism or implementation complexity.

In conclusion, the synthesis and modeling methods proposed in this thesis have mostly replaced the traditional LFT-LPV formulations using diagonal parameter blocks for complex systems by the more compact full parameter block representations. Retaining models in the latter form until the eventual controller synthesis has been proven to enhance the number of design options and «tuning knobs» for the control designer. Polytopic representations are rendered nonpreferential alltogether, while gridding-based synthesis retains justification due to the ability to consider non-convex parameter regions. However, in the case of many parameters

to be measured, it is ruled out. LPV controller design is thus rendered both more straightforward and more flexible at the same time.
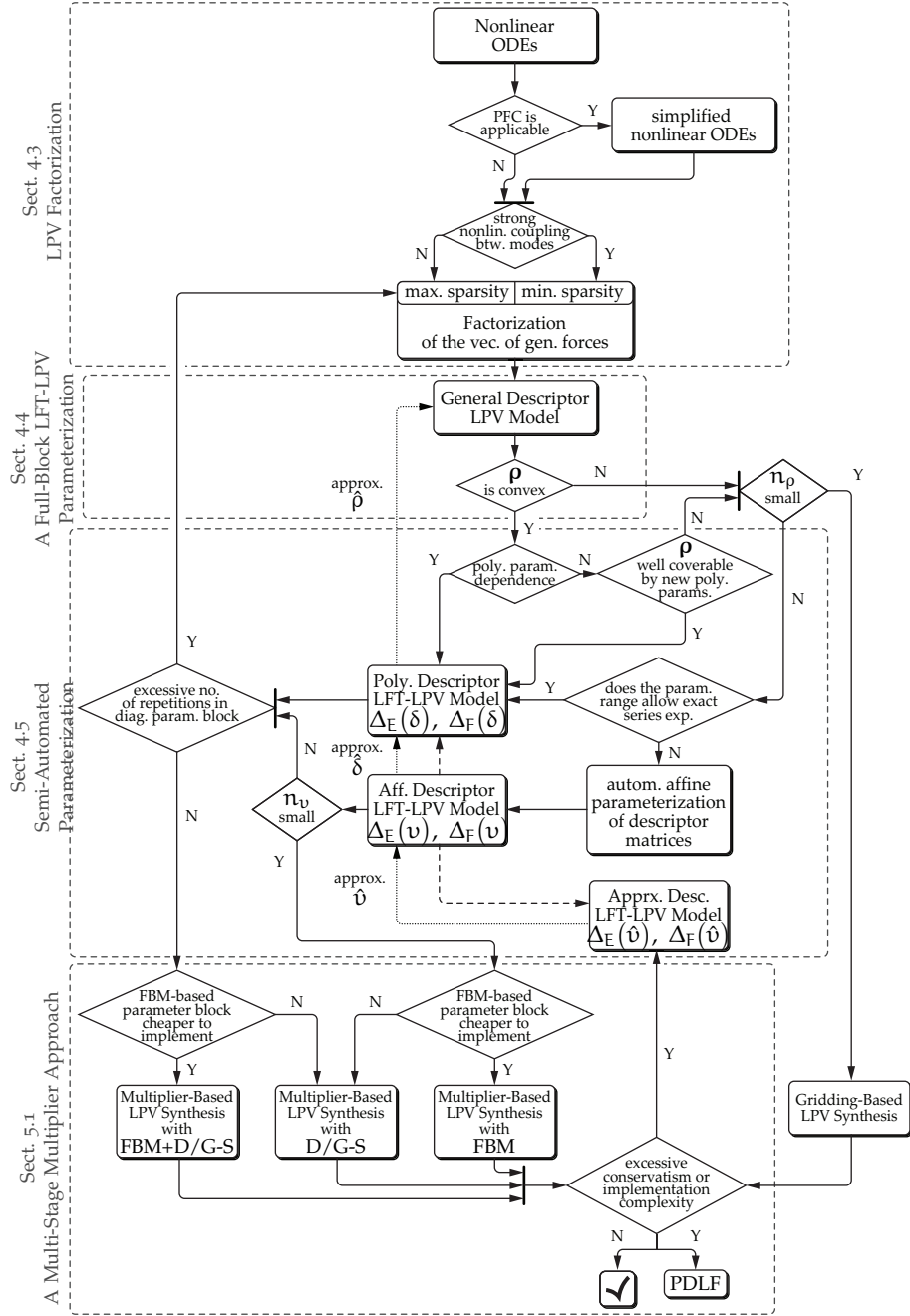

Figure 11.1: An updated decision tree for LPV modeling and controller synthesis for complex LPV systems.
(-----) Directly available through the tools of this thesis.
(⸺) Block may be replaced by its approximate version.

11.2.3 *Convexification of a Robust Control Problem*

In Part II of this thesis, distributed controller synthesis is elegantly posed as a problem solvable via standard LPV techniques. A leader-follower-based formation control scheme provides further insight into the implications of the generality of the proposed framework: A change in perspective leads to the conclusion that a formation control algorithm can be perceived as a «scheduled» controller instead of as a robust one. The «scheduling» in this instance takes the form of the interconnection topology—an entity that does not need to be known explicitly, but happens to allow controllers equipped with an additional interconnection channel to communicate among each other by broadcasting. If proper care is taken in the problem formulation, i.e., for instance the topology is modeled via a row-normalized adjacency matrix, the distributed formation algorithm is scalable in the sense that agents might be added at any time.

The implications of this convexification are possibly quite large and the effectiveness in further distributed control scenarios is currently under investigation.

12

OUTLOOK

THE results of this thesis lead to a wealth of further research opportunities, some of which are described below. The items are divided into ideas with regard to the modeling of and controller synthesis for complex lumped and interconnected systems.

12.1 Part I—LPV Control of Complex Lumped Systems

A PART from the natural need for further experimental validation of the techniques proposed in this thesis on additional plants, such as, e. g., a copolymerization reactor [2], the following items appear to be promising directions that may lead to significant improvements.

Optimization-Based LPV Factorizations

The formalism for characterizing all LPV factorizations via selector coefficients introduced in Sect. 4.3 may be the first step towards optimization-based derivations of LPV models. For instance, for plants of moderate complexity, yet difficult-to-factorize nonlinear ODEs, cf. Ex. 4.2 on p. 110, such a set of selector coefficients can be used as decision variables directly in LPV controller synthesis algorithms—an idea loosely based on [19, H25]. Such synthesis conditions turn out non-convex in the form of bilinear matrix inequalities (BMIs). However, non-smooth optimization techniques [7] may be employed. The results might provide further insight into the conservatism incurred by the non-uniqueness of LPV factorizations and may mark a first step from heuristics towards more rigorous methods.

Utilization of the Coprime Factor Structure

The exploitation of coprime factorization-like structures used in Props. A.1 and A.2 in the appendix on p. 319 for the modeling tools proposed in this thesis proved to be vital for the reduction of synthesis and implementation complexity. It also suggests a deeper mathematical connection to existing model order reduction techniques, e. g., [86], and further ways to utilize them. While it is relatively straightforward to add those parts omitted by the parameter block approximation procedure as unstructured uncertainties for use in a mixed gain-scheduled robust controller synthesis framework, or in less computationally expensive *a posteriori* stability and performance tests, more sophisticated methods may be developed that provide *a priori* guarantees for closed-loop stability and performance, for instance, based on the so-called ν-gap [157].

Automated Coprime Factorization

For general LPV plants in which the coprime factorization does not emerge naturally from the explicit knowledge of the generalized inertia matrix, an automated algorithm for deriving a coprime factorization may be developed, based on [12]. Such an approach might further increase the degree of automation and reduce the amount of ambiguities in the LPV modeling phase, while extending the applicability to an even wider class of systems that is not restricted to second order nonlinear ODEs. Together with an optimization-based LPV factorization as described above, such an approach could yield fully automated and efficient LPV modeling and synthesis tools that are attractive for use in industry and challenging control problems in research.

Approximate Relaxations on Multiplier Conditions

An aspect that has not been explicitly explored in this thesis—although the SVD-based approximation of parameter blocks can be viewed as such—is the approximate relaxation of the multiplier conditions for use in synthesis. Crude approaches could consider the evaluation of vertices spanned by only some of the parameters in which the parameters are affine, followed by an *a posteriori* check (gridded or vertex based) of only the multiplier condition. Further approaches can involve sum-of-squares (SOS) or Pólya's relaxations for polynomial matrix inequalities [27].

Improved Output-Feedback Synthesis

Based on the results of Sect. 5.2, the dual problem of designing (gain-scheduled) observers for LPV plants can be explicitly worked out in a similarly improved manner. As pointed out in [E83], observer-based state-feedback control makes for a highly structured, systematic output-feedback controller design process. The findings from this thesis suggest that such an approach is also beneficial both in terms of synthesis and implementation complexity when compared to parameter-dependent Lyapunov function (PDLF)-based OF controller synthesis as per [163]. However, the fully improved PDLF-based OF controller synthesis conditions making use of the plant's descriptor structure as in Prop. 5.1 on p. 172 can be worked out and applied straightforwardly for further investigation.

Dynamic Multiplier-Based Output-Feedback Synthesis

The use of dynamic D/G-scalings (D/G-Ss) promises to significantly reduce the amount of conservatism in gain-scheduled output-feedback controller synthesis at the cost of a significantly increased controller order [126]. The usefulness of the two-stage multiplier approach presented in this thesis mainly draws from the possibility to use FBMs in the first stage, which allows for small-in-size scheduling blocks of the controller. As both a theoretically and mathematically demanding question, it is still unclear how to solve gain-scheduling problems with dynamic FBMs. However, it may be of interest to investigate to which degree the use of dynamic D/G-Ss in a second multiplier stage can reduce conservatism without affecting implementation complexity. More straightforwardly, it is interesting to assess the increase in implementation complexity due to the methods proposed in [126] and compare these with the standard PDLFs-based methods.

12.2 Part II—Control of Interconnected LPV Systems

In addition to the obvious experimental validation of the techniques proposed in this thesis, the following items appear as attractive directions for future research.

Validation for Distributed Systems

The methods for interconnected LPV controller synthesis developed in this thesis have been validated via a fictitious numerical and a realistic multi-agent system (MAS)-based simulation example. While showing promising results in both cases, an evaluation on a distributed control setting, such as the vibration control of a beam or plate, should be performed. The results can then be benchmarked against methods specialized for regular-grid topologies, e. g., [90, 162]. Since the latter are well-advanced in the sense that they have been extended to employ PDLFs [90] further research might be required. Some examples are given below.

Dynamic Multiplier-Based Synthesis

The effectiveness and applicability of dynamic D-scalings and D/G-scalings [126] for distributed controller synthesis can be investigated using diagonalization techniques based on normalization. A significant improvement in performance is expected in scenarios in which the interconnection topology is known to be fixed. This is often the case in the above-mentioned regular-grid topology-based formulations of distributed systems resulting from spatial discretization. In this line of research, the drawback of the proposed method to always implicitly consider switching topologies can be alleviated and a rigorous comparison with tools based on PDLFs that are limited to fixed regular-grid topologies can be performed.

Shaping the Controllers' Interconnection Topology

In this thesis, a technical assumption on the masking matrices is imposed that guarantees the normalization to be revertible and consequently allows the synthesis of controllers that inherit the interconnection topology from the plant. If this technical assumption on the masking matrices is dispensed with, alternatives to the normalization techniques of Props. 9.2 and 9.3 can be developed that shape the interconnection topology of the controller in desired ways, cf. Sect. 9.2.3.2—a question that has been raised in [155]. As indicated in the comparison performed in Sect. 10.1.2.2 on p. 280, the conservatism incurred may vary and needs to be assessed systematically, in order to show the benefits of, e. g., an undirected controller interaction as opposed to the inherited directed one.

Design of LPV Information Flow Filters

The methods developed in this thesis have been applied on the illustrative example of gain-scheduled formation control of a fleet of quadrotor helicopters. For MASs, the information flow filter (IFF) approach [115] is often preferable, since the design of consensus-based formation and local reference tracking control of the agents

can be separated. However, such a separation is only an approximation for the case of agents subject to non-holonomic constraints. Research is already underway to integrate the non-holonomically constrained dynamics within an LPV representation using a simple rolling disc model [106, 107]. Such an approach can be used to design formation controllers that take into account the constraints via the methods developed in this thesis, while high-performance, potentially PDLF-based local agent controllers are designed separately. As a result, the formation control of airplanes and cars can be considered and efficiently implemented, hence individual control loops can be maintained separately.

Interconnection Time-Delays

In interconnected systems control, communication links are often subject to variable time-delays, due to transport delays or non-ideal networking structures [111]. By employing an integral quadratic constraint (IQC) framework, based on [36], further research can yield synthesis algorithms that extend the work of this thesis to explicitly consider time-delays in the interconnection with known upper bounds. The synthesis framework presented in [151] appears to be straightforward to adapt, while a collection of IQC multiplier parameterizations for time-delays is presented in [114, 153].

APPENDIX

The appendix contains auxiliary mathematical tools and technical material, as well as detailed proofs.

A

AUXILIARY MATHEMATICAL MATERIAL

A.1 GENERAL NOTATION

The symbol $1_{n \times m}$ denotes an $n \times m$ matrix of ones; $1_n \triangleq 1_{n \times 1}$ and $I_n \triangleq \operatorname{diag}(1_n)$.

Vertical and horizontal concatenation of matrices with conformable dimensions is denoted by

$$\operatorname*{col}_{k=1}^{h}(M_k) = \begin{bmatrix} M_1^\top \ \dots \ M_h^\top \end{bmatrix}^\top, \quad \operatorname*{row}_{k=1}^{h}(M_k) = \begin{bmatrix} M_1 \ \dots \ M_h \end{bmatrix}.$$

A.2 ALGEBRAIC TOOLS AND MATRIX CALCULUS

Lemma A.1 (2×2 Block Matrix Inversion [166])
Consider a non-singular square matrix M of the form

$$M = \begin{bmatrix} M_{11} & M_{12} \\ M_{21} & M_{22} \end{bmatrix}, \ M_{11} \in \mathbb{C}^{n \times n}, \ M_{22} \in \mathbb{C}^{m \times m}$$

Then with

$$N = \left(M_{22} - M_{21} M_{11}^{-1} M_{12} \right)^{-1},$$

$$L = \left(M_{11} - M_{12} M_{22}^{-1} M_{21} \right)^{-1},$$

one has

$$M^{-1} = \begin{bmatrix} M_{11}^{-1} + M_{11}^{-1} M_{12} N M_{21} M_{11}^{-1} & -M_{11}^{-1} M_{12} N \\ -N M_{21} M_{11}^{-1} & N \end{bmatrix}$$

$$= \begin{bmatrix} L & -L M_{12} M_{22}^{-1} \\ -M_{22}^{-1} M_{21} L & M_{22}^{-1} + M_{22}^{-1} M_{21} L M_{12} M_{22}^{-1} \end{bmatrix}$$

$\square$

Lemma A.2 (Derivative of a Matrix Inverse [166])
Consider a matrix-valued function $M(t): \mathbb{R} \mapsto \mathbb{C}^{n \times n}$. The derivative of its inverse is given by

$$\frac{dM^{-1}(t)}{dt} = -M^{-1}(t) \frac{dM(t)}{dt} M^{-1}(t). \tag{A.1}$$

□

Definition A.1 (Moore-Penrose Pseudoinverse [166])
Consider a matrix $M \in \mathbb{C}^{m \times n}$. Its Moore-Penrose Pseudoinverse (pseudoinverse) $M^\dagger$ is unique and fulfills the following conditions

(i) $\quad MM^\dagger M = M,$

(ii) $\quad M^\dagger MM^\dagger = M^\dagger,$

(iii) $\quad (MM^\dagger)^* = MM^\dagger,$

(iv) $\quad (M^\dagger M)^* = M^\dagger M.$

It can be defined via

$$M^\dagger \triangleq \lim_{\varepsilon \to 0}(M^*M + \varepsilon I)^{-1}M^* = \lim_{\varepsilon \to 0} M^*(MM^* + \varepsilon I)^{-1}$$

Corollary A.1 (Pseudoinverse for Singular Diagonal Matrices)
From Def. A.1, it follows that the pseudoinverse of a singular diagonal matrix $M = \operatorname{diag}_{i=1}^{n}(m_{ii})$ is given by

$$M^\dagger = \operatorname*{diag}_{i=1}^{n}\left(m_{ii}^\dagger\right), \quad m_{ii}^\dagger \triangleq \begin{cases} 0, & \text{if } m_{ii} = 0, \\ m_{ii}^{-1}, & \text{otherwise.} \end{cases}$$

□

A.2.1 *The Kronecker and Khatri-Rao Product*

The operator $\otimes$ denotes the Kronecker product. I.e., with $A = [a_{ij}] \in \mathbb{C}^{n^A \times m^A}, a_{ij} \in \mathbb{C}$ and block-matrix structures

$$A = [A_{ij}] \in \mathbb{C}^{n^A \times m^A}, \quad A_{ij} \in \mathbb{C}^{n_i^A \times m_j^A},$$
$$B = [B_{ij}] \in \mathbb{C}^{n^B \times m^B}, \quad B_{ij} \in \mathbb{C}^{n_i^B \times m_j^B},$$
$$A \otimes B = \begin{bmatrix} a_{11}B \cdots a_{1m}B \\ \vdots \quad \ddots \quad \vdots \\ a_{n1}B \cdots a_{nm}B \end{bmatrix}.$$

The operator $\circledast$ denotes the Khatri-Rao product.

$$A \circledast B = \begin{bmatrix} A_{11} \otimes B_{11} \cdots A_{1m} \otimes B_{1m} \\ \vdots \quad \ddots \quad \vdots \\ A_{n1} \otimes B_{n1} \cdots A_{nm} \otimes B_{nm} \end{bmatrix}.$$

Lemma A.3 (Kronecker/Khatri-Rao Permutation)

Let a matrix N *and a pair of permutation matrices* Ψ_p *and* Ψ_q *be given, such that*

$$N = \begin{bmatrix} \mathscr{L} \otimes M_{11} \cdots \mathscr{L} \otimes M_{1q} \\ \vdots \quad \ddots \quad \vdots \\ \mathscr{L} \otimes M_{p1} \cdots \mathscr{L} \otimes M_{pq} \end{bmatrix} = (1_{p \times q} \otimes \mathscr{L}) \circledast \begin{bmatrix} M_{11} \cdots M_{1q} \\ \vdots \ddots \vdots \\ M_{p1} \cdots M_{pq} \end{bmatrix},$$

$$\Psi_p N \Psi_q^\top = \mathscr{L} \otimes \begin{bmatrix} M_{11} \cdots M_{1q} \\ \vdots \ddots \vdots \\ M_{p1} \cdots M_{pq} \end{bmatrix},$$

where $M_{ij} \in \mathbb{C}^{p_i \times q_j}$, $\mathscr{L} \in \mathbb{C}^{h \times h}$. *Then* Ψ_p, Ψ_q *are given by*

$$\Psi_f = \mathop{\mathrm{row}}_{j=1}^{f} \left(\mathop{\mathrm{diag}}_{1}^{h} \left(\begin{bmatrix} \delta_{f_1 f_j} I_{f_1 \times f_j} \\ \vdots \\ \delta_{f_p f_j} I_{f_p \times f_j} \end{bmatrix} \right) \right), f \in \{p, q\}$$

where δ_{ij} *is the Kronecker delta and*

$$I_{i \times j} = \begin{cases} \begin{bmatrix} I_{i \times i} & 0 \end{bmatrix} & \text{,if } i < j, \\[2mm] \begin{bmatrix} I_{i \times i} \\ 0 \end{bmatrix} & \text{,if } i > j, \\[2mm] \begin{bmatrix} I_{i \times i} \end{bmatrix} & \text{,if } i = j \end{cases}$$

$\square$

Remark A.1 *Lemma A.3 can be understood as transforming a particular Khatri-Rao product, i.e. one where the left factor is a block matrix with identical blocks, into an equivalent Kronecker product.*

A.3 Linear Fractional Transformations

Definition A.2 (Upper linear fractional transformation (LFT) [166])

Let M *be a matrix partitioned as*

$$M = \begin{bmatrix} M_{11} & M_{12} \\ M_{21} & M_{22} \end{bmatrix} \in \mathbb{C}^{(n_{z,1}+n_{z,2}) \times (n_{w,1}+n_{w,2})}$$

Then an upper linear fractional transformation with respect to $\Delta \in \mathbb{C}^{n_{w,1} \times n_{z,1}}$ *is defined as the map*

$$\mathcal{M}(\Delta) = \Delta \star M : \mathbb{C}^{n_{z,1} \times n_{w,1}} \mapsto \mathbb{C}^{n_{z,2} \times n_{w,2}}$$

with

$$\mathcal{M}(\Delta) = \Delta \star M = \Delta \star \left[\begin{array}{c|c} M_{11} & M_{12} \\ \hline M_{21} & M_{22} \end{array} \right] = M_{22} + M_{21}\Delta(I - M_{11}\Delta)^{-1}M_{12},$$

provided that the inverse of $(I - M_{11}\Delta)$ *exists.*

Definition A.3 (Lower LFT [166])
Let M *partitioned as in Def. A.2. Then a lower linear fractional transformation with respect to* $\Delta \in \mathbb{C}^{n_{w,2} \times n_{z,2}}$ *is defined as the map*

$$\mathcal{M}(\Delta) = M \star \Delta : \mathbb{C}^{n_{z,2} \times n_{w,2}} \mapsto \mathbb{C}^{n_{z,1} \times n_{w,1}}$$

with

$$\mathcal{M}(\Delta) = M \star \Delta = \begin{bmatrix} M_{11} & M_{12} \\ M_{21} & M_{22} \end{bmatrix} \star \Delta = M_{11} + M_{12}\Delta(I - M_{22}\Delta)^{-1}M_{21},$$

provided that the inverse of $(I - M_{22}\Delta)$ *exists.*

Figures A.1a and A.1b provide graphical representations of both upper and lower LFTs.

(a) Upper LFTs.   (b) Lower LFTs.
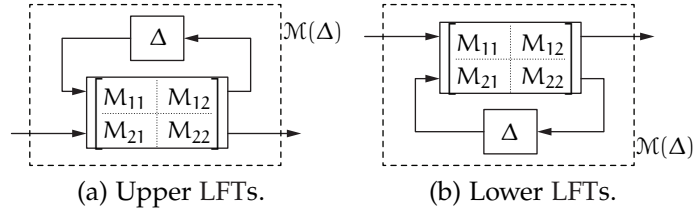
Figure A.1: Linear fractional transformations.

Remark A.2 *Compact graphical representations for* LFTs *are commonly employed. The respective channel sizes can then be inferred from the context.*

(a) Upper LFTs.   (b) Lower LFTs.
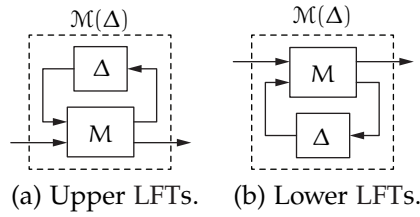
Figure A.2: Compact representations of linear fractional transformations.

Often, the feedback interconnection shown in Figs. A.1a and A.1b is made with a time dependent matrix $\Delta(t)$. For simplicity of notation, time dependence is regularly dropped, e. g., $\Delta = \Delta(t)$.
A multiplication of two LFTs is another LFT [166]

$$(\Delta_M \star M)(\Delta_N \star N) = \left(\Delta_M \star \begin{bmatrix} M_{11} & M_{12} \\ M_{21} & M_{22} \end{bmatrix}\right)\left(\Delta_N \star \begin{bmatrix} N_{11} & N_{12} \\ N_{21} & N_{22} \end{bmatrix}\right)$$

$$= \begin{bmatrix} \Delta_M & 0 \\ 0 & \Delta_N \end{bmatrix} \star \begin{bmatrix} M_{11} & M_{12}N_{21} & M_{12}N_{22} \\ 0 & N_{11} & N_{12} \\ M_{21} & M_{22}N_{21} & M_{22}N_{22} \end{bmatrix}, \tag{A.2}$$

where Δ_M, Δ_N as well as M, N have appropriate dimensions.

The inverse of an LFT [166] can be computed by

$$\left(\Delta \star \begin{bmatrix} M_{11} & M_{12} \\ M_{21} & M_{22} \end{bmatrix} \right)^{-1}$$
$$= \Delta \star \begin{bmatrix} M_{11} - M_{12}M_{22}^{-1}M_{21} & -M_{12}M_{22}^{-1} \\ M_{22}^{-1}M_{21} & M_{22}^{-1} \end{bmatrix}, \qquad (A.3)$$

while it is assumed that the inverse of M_{22} exists.

Lemma A.4 (Nullspace of a linear fractional representation (LFR) [163])
Consider an LFR *in the form*

$$\mathcal{M}(\Delta) = \Delta \star M = \Delta \star \begin{bmatrix} M_{11} & M_{12} \\ M_{21} & M_{22} \end{bmatrix},$$

where $M_{11} \in \mathbb{C}^{n_{z,1} \times n_{w,1}}$, $M_{12} \in \mathbb{C}^{n_{z,1} \times n_{w,2}}$, $M_{21} \in \mathbb{C}^{n_{z,2} \times n_{w,1}}$, $M_{22} \in \mathbb{C}^{n_{z,2} \times n_{w,2}}$. *Assume that* M_{22} *has rank* $n_{z,2} \leqslant n_{w,2}$, *s.t.*

$$M_{22} = U \begin{bmatrix} \Sigma & 0 \end{bmatrix} V^*.$$

Partition $V = \begin{bmatrix} V_1 & V_2 \end{bmatrix}$, *with* $V_1 \in \mathbb{C}^{n_{z,2} \times n_{z,2}}$, $V_2 \in \mathbb{C}^{n_{w,2} \times (n_{w,2}-n_{z,2})}$. *Then, the nullspace of* $\mathcal{M}(\Delta)$ *is* [1]

$$\ker(\mathcal{M}(\Delta)) = \mathrm{im} \left(\Delta \star \begin{bmatrix} M_{11} - M_{12}V_1\Sigma^{-1}U^*M_{21} & M_{12}V_2 \\ -V_1\Sigma^{-1}U^*M_{21} & V_2 \end{bmatrix} \right)$$

$\square$

Compact LFRs can be derived for matrices parameterized reminiscent of coprime factor uncertainty representations [44].

Proposition A.1 (Left Coprime Factor LFR)
For matrices M_0, N_0, Δ_M, $\Delta_N \in \mathbb{C}^{n \times n}$ *with* M_0 *non-singular, the term* $(M_0+\Delta_M)^{-1}(N_0+\Delta_N)$ *can be written as an* LFR *as*

$$(M_0+\Delta_M)^{-1}(N_0+\Delta_N) = \begin{bmatrix} \Delta_M & \Delta_N \end{bmatrix} \star \begin{bmatrix} -M_0^{-1} & -M_0^{-1}N_0 \\ 0 & I \\ M_0^{-1} & M_0^{-1}N_0 \end{bmatrix}. \qquad (A.4)$$

$\square$

---

[1] Note that there is a sign error in [163], which leads to the $(2,1)$ entry of the LFT matrix to be $V_1\Sigma^{-1}U^*M_{21}$.

Proposition A.2 (Right Coprime Factor LFR)

For matrices M_0, N_0, Δ_M, $\Delta_N \in \mathbb{C}^{n \times n}$ with N_0 non-singular, the term $(M_0 + \Delta_M)(N_0 + \Delta_N)^{-1}$ can be written as an LFR as

$$(M_0 + \Delta_M)(N_0 + \Delta_N)^{-1} = \begin{bmatrix} \Delta_N \\ \Delta_M \end{bmatrix} \star \begin{bmatrix} -N_0^{-1} & 0 & N_0^{-1} \\ -M_0 N_0^{-1} & I & M_0 N_0^{-1} \end{bmatrix}. \tag{A.5}$$
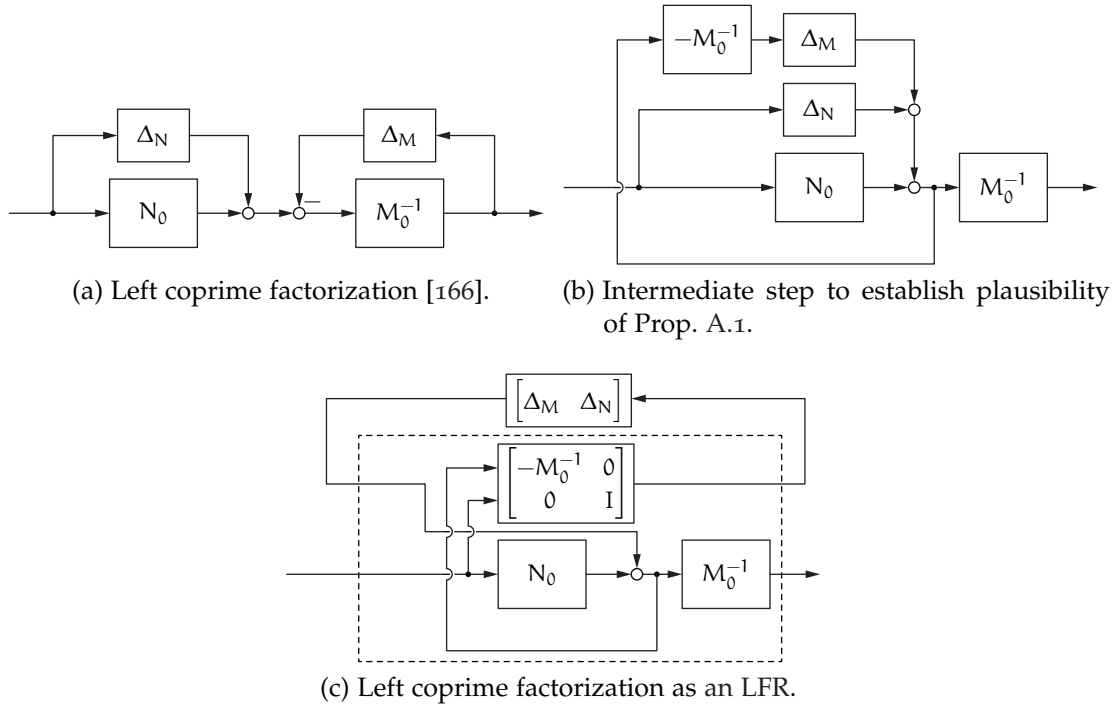
□

Figure A.3 establishes a block diagram interpretation of Prop. A.1.

(a) Left coprime factorization [166].

(b) Intermediate step to establish plausibility of Prop. A.1.

(c) Left coprime factorization as an LFR.

Figure A.3: Left coprime factorization. Transformation into LFR.

A.4 Manipulation of Matrix Inequalities

The symmetric/hermitian completion of blocks of a matrix M partitioned into $n \times n$ blocks is denoted by $\bullet$, s.t.

$$\begin{bmatrix} M_{11} & M_{12} & \cdots & M_{1n} \\ M_{12}^* & M_{22} & & M_{2n} \\ \vdots & & \ddots & \vdots \\ M_{1n}^* & M_{2n}^* & \cdots & M_{nn} \end{bmatrix} = \begin{bmatrix} M_{11} & M_{12} & \cdots & M_{1n} \\ \bullet & M_{22} & & M_{2n} \\ \vdots & & \ddots & \vdots \\ \bullet & \bullet & \cdots & M_{nn} \end{bmatrix}.$$

The notation $\text{sym}(M)$ denotes $M + M^\top$, $\text{herm}(M)$ denotes $M + M^*$, respectively.

For a matrix M to be positive (semi-)definite, we write

$$M \succ 0, \quad \text{or} \quad M \succeq 0, \quad \text{and} \quad M \prec 0, \quad \text{or} \quad M \preceq 0$$

for M to be negative (semi-)definite.

Lemma A.5 (Complex Matrix Inequalities)
For a complex-valued hermitian matrix $L \in \mathbb{H}^{n \times n}$, *the following two matrix inequalities are equivalent*

$$\text{(i)} \quad L = \text{Re}\,L + j\,\text{Im}\,L \succ 0 \qquad\qquad \text{(ii)} \quad \begin{bmatrix} \text{Re}\,L & -\text{Im}\,L \\ \text{Im}\,L & \text{Re}\,L \end{bmatrix} \succ 0 \qquad\qquad \text{(A.6)}$$

$\square$

Lemma A.6 (Dualization Lemma [125])
Assume R *is a nonsingular matrix and* $\mathcal{S}$ *a subspace with* $\text{in}_0 R|_{\mathcal{S}} = 0$, *i.e.,* $S^\top R S$ *is nonsingular for any basis* S *of* $\mathcal{S}$. *Then* $\text{in}\,(R|_{\mathcal{S}}) + \text{in}\left(R^{-1}|_{\mathcal{S}^\perp}\right) = \text{in}\,(R)$. $\square$

Lemma A.7 (Dual Quadratic Inequalities [125])
Consider the matrix inequality in K

$$\begin{bmatrix} I_m \\ T + W^\top K V \end{bmatrix}^\top R \begin{bmatrix} I_m \\ T + W^\top K V \end{bmatrix} \prec 0 \qquad\qquad \text{(A.7)}$$

with $A \in \mathbb{R}^{n \times m}$, $\text{in}(R) = (m, 0, n)$. *Therefore* $S = R^{-1}$ *exists. Then, due to Lma. A.6 on page 321, (A.7) is equivalent to*

$$\begin{bmatrix} -(T + W^\top K V)^\top \\ I_n \end{bmatrix}^\top S \begin{bmatrix} -(T + W^\top K V)^\top \\ I_n \end{bmatrix} \succ 0 \qquad\qquad \text{(A.8)}$$

$\square$

Lemma A.8 (Parameter Elimination Lemma [125])
Inequality (A.7) is solvable iff

$$V^{\perp\top} \begin{bmatrix} I_m \\ T \end{bmatrix}^\top R \begin{bmatrix} I_m \\ T \end{bmatrix} V^\perp \prec 0, \qquad\qquad \text{(A.9)}$$

$$\text{and} \quad W^{\perp\top} \begin{bmatrix} -T^\top \\ I_n \end{bmatrix}^\top S \begin{bmatrix} -T^\top \\ I_n \end{bmatrix} W^\perp \succ 0, \qquad\qquad \text{(A.10)}$$

with $R = S^{-1}$. $\square$

The next lemma follows from the Elimination Lemma [125], cf. Lma. A.8, and can be regarded as a particular solution to the problem of recovering eliminated parameters for structured problems.

Lemma A.9 (Parameter Elimination for Structured Problems [56])
The quadratic matrix inequality

$$\begin{bmatrix} I \\ W(A^\top XB + C)V \end{bmatrix}^\top M \begin{bmatrix} I \\ W(A^\top XB + C)V \end{bmatrix} \prec 0. \tag{A.11}$$

in the unknown X is solvable iff

$$\begin{bmatrix} WB^\perp & V^\perp \end{bmatrix}^\top \begin{bmatrix} I \\ WCV \end{bmatrix}^\top M \begin{bmatrix} I \\ WCV \end{bmatrix} \begin{bmatrix} WB^\perp & V^\perp \end{bmatrix} \prec 0,$$

$$\begin{bmatrix} V^\top A^\perp & W^{\top\perp} \end{bmatrix}^\top \begin{bmatrix} -(WCV)^\top \\ I \end{bmatrix}^\top M^{-1} \begin{bmatrix} -(WCV)^\top \\ I \end{bmatrix} \begin{bmatrix} V^\top A^\perp & W^{\top\perp} \end{bmatrix} \succ 0.$$

where $VW = I$, W, $V^\top$ *have full column rank and* $B^\perp = \ker(B)$, $A^\perp = \ker(A)$, $V^\perp = \ker(V)$, $W^{\top\perp} = \ker(W^\top)$. □

Corollary A.2 (Solution on Subspace [56])
Assume $VW = I$ *and* W, $V^\top$ *have full column rank. The feasibility of the quadratic matrix inequality*

$$\begin{bmatrix} I \\ W(A^\top XB + C)V \end{bmatrix}^\top M \begin{bmatrix} I \\ W(A^\top XB + C)V \end{bmatrix} \prec 0. \tag{A.12}$$

in the unknown X, implies the feasibility of

$$[\bullet]^\top \begin{bmatrix} I \\ A^\top XB + C \end{bmatrix}^\top \begin{bmatrix} W & 0 \\ 0 & W \end{bmatrix}^\top M \begin{bmatrix} W & 0 \\ 0 & W \end{bmatrix} \begin{bmatrix} I \\ A^\top XB + C \end{bmatrix} \prec 0. \tag{A.13}$$

□

Proof: Definiteness on a subspace is implied by definiteness on the entire space. Thus (A.13) is simply (A.12) pre- and postmultiplied by $W^\top$ and W, respectively. ■

A.5 Estimates for Computational Costs

The big $\mathcal{O}$ notation is used to describe complexities. More specifically, $a[f(x)] \in \mathcal{O}(g(x))$ means that there exists $m > 0$ and x_0, such that $|a[f(x)]| \leqslant m|g(x)|, \forall x > x_0$.

Tab. A.1 lists upper bounds on the number of arithmetic computations, denoted by $a[\cdot]$, for elementary matrix operations. Similarly, the number of scalar variables to be stored $m[\cdot]$, which is used as a measure for the memory requirements, is displayed in Tab. A.2.

Table A.1: Complexity of matrix operations.

Operation		Sizes	$a[A]$
Multiplication	$A = BC$	$B \in \mathbb{R}^{n \times m}$, $C \in \mathbb{R}^{m \times p}$	$n(2m-1)p$
Scaling	$A = \underset{i=1}{\overset{n}{\text{diag}}}(b_i)\, C$	$b_i \in \mathbb{R}$, $\quad C \in \mathbb{R}^{n \times m}$	nm
Addition	$A = B + C$	$B \in \mathbb{R}^{n \times m}$, $C \in \mathbb{R}^{n \times m}$	nm
Inversion*	$A = B^{-1}$	$B \in \mathbb{R}^{n \times n}$,	$\frac{2}{3}n^3$

Gauss elimination provides an upper bound for the cost.

Table A.2: Memory requirements of matrix types.

Matrix structure		Sizes	$m[A]$
Full	A	$A \in \mathbb{R}^{n \times m}$,	nm
Symmetric	$A = A^{\top}$	$A \in \mathbb{R}^{n \times n}$,	$\sum_{k=1}^{n+1} k = n(n+1)/2$
Skew-sym.	$A = -A^{\top}$	$A \in \mathbb{R}^{n \times n}$,	$\sum_{k=1}^{n-1} k = n(n-1)/2$

a.6 Barycentric Coordinates for Polytopic Models

For determining the barycentric coordinates $\alpha_l, \forall l \in \{1, \ldots, n_v\}$ for a parameter vector $\theta(t)$ ranging in a *simple* polytope is given by [158]

$$\alpha_l(\theta) = \frac{\tilde{\alpha}_l(\theta(t))}{\sum_{l=1}^{n_v} \tilde{\alpha}_l(\theta(t))}, \quad \tilde{\alpha}_l(\theta) = \frac{\left| \det \left(\underset{k \in J_l}{\text{row}}(v_k) \right) \right|}{\prod_{k \in J_l} (v_k^\top (\theta_{v,l} - \theta(t)))}, \tag{A.14}$$

where J_l denotes the set of indices k, such that the facet normal to v_k contains vertex $\theta_{v,l}$ and $\underset{k \in J_l}{\text{row}}(v_k)$ denotes the horizontal concatenation of the respective vectors.

Remark A.3 *A «simple polytope» is a polytope whose vertices are adjacent to a number of edges or facets that is exactly the dimension of the space the polytope is defined in, e. g., card* $(J_l) = n_\theta$ *[158].*

(a) Barycentric coordinates from parameter.

(b) A hypercube resulting from three parameters.
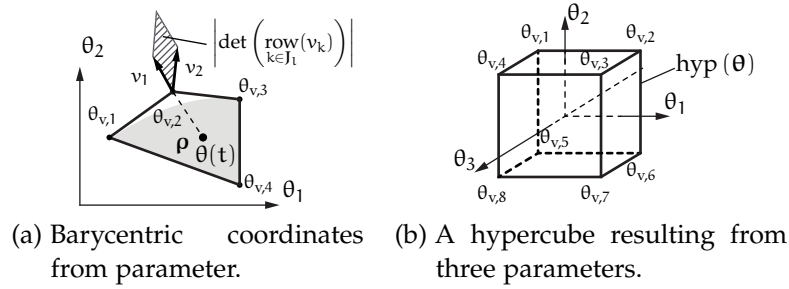
Figure A.4: Examples of barycentric coordinates.

Figure A.4a shows an example and a geometric interpretation. Fig. A.4b shows an exemplary hyperbox of eight vertices resulting from three parameters.

Under the assumption that the parameters are taken to reside in the hyperbox $\text{hyp}(\theta)$, the computation of the barycentric coordinates can be performed more efficiently. In the Matlab function polydec this is performed iteratively according to Alg. A.1.

Algorithm A.1 Barycentric coordinates from parameter $\theta(t)$ varying in a hypercube $\text{hyp}(\theta)$.

    Initialization:

1:     Define $c_0 \triangleq 1$.

    Iteration: $i \leftarrow 1$, number of iterations n_θ

2:     Compute $t_i = \frac{\theta_i(t) - \underline{\theta}_i}{\overline{\theta}_i - \underline{\theta}_i}$, $\quad c_i = \left[c_{i-1}(1 - t_i), \quad c_{i-1} t_i \right]$.

    Return:

3:     Extract barycentric coordinates from $c_{n_\theta} = \left[\alpha_1, \alpha_2, \cdots, \alpha_{n_v} \right]$.

AUXILIARY MATERIAL FROM PART I

B.1 AUXILIARY MATERIAL FOR THEOREM 2.8

Quadratic LFR of Lyapunov Matrices

The result for an LFR of the outer blocks in a quadratic parameter-dependent Lyapunov function (PDLF) shown in [163] is given without proof. The following shows how the result is obtained. Observe that for

$$\mathcal{X}(\delta) = \mathcal{Q}(\delta)^\top \mathcal{X} \mathcal{Q}(\delta)$$

factorizations of the matrix blocks related to the Lyapunov matrices occurring in the Bounded Real Lemma can be obtained as

$$\begin{bmatrix} \partial\mathcal{X}(\delta,\eta) & \mathcal{X}(\delta) \\ \mathcal{X}(\delta) & 0 \end{bmatrix} = \begin{bmatrix} \mathcal{Q}(\delta) & 0 \\ \partial\mathcal{Q}(\delta,\eta) & \mathcal{Q}(\delta) \end{bmatrix}^\top \begin{bmatrix} 0 & \mathcal{X} \\ \mathcal{X} & 0 \end{bmatrix} \begin{bmatrix} \mathcal{Q}(\delta) & 0 \\ \partial\mathcal{Q}(\delta,\eta) & \mathcal{Q}(\delta) \end{bmatrix}$$

$$\begin{bmatrix} 0 & \mathcal{X}(\delta) \\ \mathcal{X}(\delta) & \partial\mathcal{X}(\delta,\eta) \end{bmatrix} = \begin{bmatrix} \mathcal{Q}(\delta) & \partial\mathcal{Q}(\delta,\eta) \\ 0 & \mathcal{Q}(\delta) \end{bmatrix}^\top \begin{bmatrix} 0 & \mathcal{X} \\ \mathcal{X} & 0 \end{bmatrix} \begin{bmatrix} \mathcal{Q}(\delta) & \partial\mathcal{Q}(\delta,\eta) \\ 0 & \mathcal{Q}(\delta) \end{bmatrix}$$

Then, given

$$\mathcal{Q}(\delta) = \Delta \star \begin{bmatrix} \mathcal{Q}_{11} & \mathcal{Q}_{12} \\ \mathcal{Q}_{21} & \mathcal{Q}_{22} \end{bmatrix} = \mathcal{Q}_{22} + \mathcal{Q}_{21}\Delta\left(I - \mathcal{Q}_{11}\Delta_\mathcal{Q}\right)^{-1}\mathcal{U}_{12},$$

and using (A.1) one has for

$$\frac{\mathrm{d}}{\mathrm{dt}}\mathcal{Q}(\delta) = \mathcal{Q}_{21}\left(\dot\Delta + \Delta\left(I - \mathcal{Q}_{11}\Delta\right)^{-1}\mathcal{Q}_{11}\dot\Delta\right)\left(I - \mathcal{Q}_{11}\Delta\right)^{-1}\mathcal{Q}_{12}$$

$$= \mathcal{Q}_{21}\left(I - \Delta\mathcal{Q}_{11}\right)^{-1}\dot\Delta\left(I - \mathcal{Q}_{11}\Delta\right)^{-1}\mathcal{Q}_{12},$$

which gives

$$\partial\mathcal{Q}(\delta,\eta) = \mathcal{Q}_{21}\left(I - \Delta\mathcal{Q}_{11}\right)^{-1}\partial\Delta\left(I - \mathcal{Q}_{11}\Delta\right)^{-1}\mathcal{Q}_{12} \tag{B.1}$$

Using

$$
Q_{21} \left(I - \Delta Q_{11}\right)^{-1} = Q_{21} \left(\Delta \star \begin{bmatrix} 0 & -Q_{11} \\ I & I \end{bmatrix}\right)^{-1} = \Delta \star \begin{bmatrix} Q_{11} & Q_{11} \\ Q_{21} & Q_{21} \end{bmatrix}
$$

$$
\left(I - Q_{11}\Delta\right)^{-1} Q_{12} = \left(\Delta \star \begin{bmatrix} 0 & I \\ -Q_{11} & I \end{bmatrix}\right)^{-1} Q_{12} = \Delta \star \begin{bmatrix} Q_{11} & Q_{12} \\ Q_{11} & Q_{12} \end{bmatrix}
$$

and by (A.2), one can obtain

$$
\partial Q(\delta,\eta) = \begin{bmatrix} \partial\Delta & & \\ & \Delta & \\ & & \Delta \end{bmatrix} \star \begin{bmatrix} 0 & 0 & Q_{11} & Q_{12} \\ Q_{11} & Q_{11} & 0 & 0 \\ 0 & 0 & Q_{11} & Q_{12} \\ Q_{21} & Q_{21} & 0 & 0 \end{bmatrix}
$$

From here it is easy to see that

$$
\begin{bmatrix} Q(\delta) & 0 \\ \partial Q(\delta,\eta) & Q(\delta) \end{bmatrix} = \begin{bmatrix} \partial\Delta & & \\ & \Delta & \\ & & \Delta \end{bmatrix} \star \begin{bmatrix} 0 & 0 & Q_{11} & Q_{12} & 0 \\ Q_{11} & Q_{11} & 0 & 0 & Q_{12} \\ 0 & 0 & Q_{11} & Q_{12} & 0 \\ 0 & 0 & Q_{21} & Q_{22} & 0 \\ Q_{21} & Q_{21} & 0 & 0 & Q_{22} \end{bmatrix}
$$

$$
\begin{bmatrix} Q(\delta) & \partial Q(\delta,\eta) \\ 0 & Q(\delta) \end{bmatrix} = \begin{bmatrix} \partial\Delta & & \\ & \Delta & \\ & & \Delta \end{bmatrix} \star \begin{bmatrix} 0 & 0 & Q_{11} & 0 & Q_{12} \\ Q_{11} & Q_{11} & 0 & Q_{12} & 0 \\ 0 & 0 & Q_{11} & 0 & Q_{12} \\ Q_{21} & Q_{21} & 0 & Q_{22} & 0 \\ 0 & 0 & Q_{21} & 0 & Q_{22} \end{bmatrix}
$$

Compact LFR of Lyapunov Matrices

A more compact LFR of the outer blocks in a quadratic PDLF than those shown in [163] can be obtained as follows. First observe that

$$
\partial Q(\delta,\eta) = \begin{bmatrix} 0 & \Delta \\ \Delta & \partial\Delta \end{bmatrix} \star \begin{bmatrix} 0 & Q_{11} & 0 \\ Q_{11} & 0 & Q_{12} \\ 0 & Q_{21} & 0 \end{bmatrix}.
$$

From here, the LFR of the outer factor of the quadratic PDLF can be written compactly as

$$
\begin{bmatrix} Q(\delta) & 0 \\ \partial Q(\delta,\eta)Q(\delta) \end{bmatrix} = \begin{bmatrix} 0 & \Delta \\ \Delta & \partial\Delta \end{bmatrix} \star \begin{bmatrix} 0 & Q_{11} & 0 & Q_{12} \\ Q_{11} & 0 & Q_{12} & 0 \\ Q_{21} & 0 & Q_{22} & 0 \\ 0 & Q_{21} & 0 & Q_{22} \end{bmatrix}. \tag{B.2}
$$

To see this, expand

$$
\begin{bmatrix} \mathcal{Q}(\delta) & 0 \\ \partial\mathcal{Q}(\delta,\eta)\mathcal{Q}(\delta) \end{bmatrix} = \begin{bmatrix} \mathcal{Q}_{22} & 0 \\ 0 & \mathcal{Q}_{22} \end{bmatrix} + \begin{bmatrix} \mathcal{Q}_{21} & 0 \\ 0 & \mathcal{Q}_{21} \end{bmatrix} \begin{bmatrix} 0 & \Delta \\ \Delta & \partial\Delta \end{bmatrix}
$$

$$
\times \begin{bmatrix} I-\mathcal{Q}_{11}\Delta & -\mathcal{Q}_{11}\partial\Delta \\ 0 & I-\mathcal{Q}_{11}\Delta \end{bmatrix}^{-1} \begin{bmatrix} 0 & \mathcal{Q}_{12} \\ \mathcal{Q}_{12} & 0 \end{bmatrix}
$$

$$
= \begin{bmatrix} \mathcal{Q}_{22} & 0 \\ 0 & \mathcal{Q}_{22} \end{bmatrix} + \begin{bmatrix} 0 & \mathcal{Q}_{21}\Delta \\ \mathcal{Q}_{21}\Delta & \mathcal{Q}_{21}\partial\Delta \end{bmatrix}
$$

$$
\times \begin{bmatrix} (I-\mathcal{Q}_{11}\Delta)^{-1} & (I-\mathcal{Q}_{11}\Delta)^{-1}\mathcal{Q}_{11}\partial\Delta(I-\mathcal{Q}_{11}\Delta)^{-1} \\ 0 & (I-\mathcal{Q}_{11}\Delta)^{-1} \end{bmatrix}
$$

$$
\times \begin{bmatrix} 0 & \mathcal{Q}_{12} \\ \mathcal{Q}_{12} & 0 \end{bmatrix},
$$

which—considering (B.1)—yields the proof. Similarly, one can show that

$$
\begin{bmatrix} \mathcal{Q}(\delta)\partial\mathcal{Q}(\delta,\eta) \\ 0 & \mathcal{Q}(\delta) \end{bmatrix} = \begin{bmatrix} \partial\Delta & \Delta \\ \Delta & 0 \end{bmatrix} \star \begin{bmatrix} 0 & \mathcal{Q}_{11} & 0 & \mathcal{Q}_{12} \\ \mathcal{Q}_{11} & 0 & \mathcal{Q}_{12} & 0 \\ \hline \mathcal{Q}_{21} & 0 & \mathcal{Q}_{22} & 0 \\ 0 & \mathcal{Q}_{21} & 0 & \mathcal{Q}_{22} \end{bmatrix}. \tag{B.3}
$$

B.2 PROOF OF THEOREM 2.14

First observe that from

$$
N_R(\rho) = \ker\left(\begin{bmatrix} I & 0 \end{bmatrix}\right) = \begin{bmatrix} 0 \\ I \end{bmatrix}
$$

Condition (2.122) simply reduces to the requirement $\gamma > 0$ and just the dual Cond. (2.123) remains. Note that a parameter-dependent kernel representation $N_S(\rho)$ can be found in

$$
N_S(\rho) = \ker\left(\begin{bmatrix} B_u^\top(\rho) & D_{pu}^\top(\rho) \end{bmatrix}\right)
$$

$$
= \begin{bmatrix} I & -\left(B_u^\top(\rho)\right)^\dagger D_{pu}^\top(\rho) \\ -\left(D_{pu}^\top(\rho)\right)^\dagger B_u^\top(\rho) & I \end{bmatrix}
$$

$$
= \begin{bmatrix} I & N_{S,2}(\rho) \\ N_{S,1}(\rho) & I \end{bmatrix}.
$$

Observe that $N_{S,1}(\rho)N_{S,2}(\rho) = I$ and define

$$
W = W^\top = N_{S,1}^\top(\rho)N_{S,1}(\rho)
$$

$$
= B_u(\rho)\left(D_{pu}^\top(\rho)D_{pu}(\rho)\right)^{-1}B_u^\top(\rho).
$$

Using this representation of the kernel, expand Cond. (2.134) to obtain

$$
\begin{bmatrix} \bullet \\ \cdots \\ \bullet \end{bmatrix}^{\top}
\left[\begin{array}{cc:c} 0 & S(\rho) & \\ S(\rho) & \partial S(\rho,\sigma) & \\ \hdashline & & \Gamma^{-1} \end{array}\right]
\tag{B.4}
$$

$$
\times
\left[\begin{array}{c:c} -A^{\top}(\rho) - C_{\mathrm{p}}^{\top}(\rho)N_{S,1}(\rho) & -A^{\top}(\rho)N_{S,2}(\rho) - C_{\mathrm{p}}^{\top}(\rho) \\ I & N_{S,2}(\rho) \\ \hdashline -B_{\mathrm{p}}^{\top}(\rho) & -B_{\mathrm{p}}^{\top}(\rho)N_{S,2}(\rho) \\ N_{S,1}(\rho) & I \end{array}\right] \succ 0,
$$

From the state-feedback gain

$$
F(\rho) = - \left(D_{\mathrm{pu}}^{\top}(\rho) D_{\mathrm{pu}}(\rho) \right)^{-1} \\
\times \left(\gamma B_{\mathrm{u}}^{\top}(\rho) S^{-1}(\rho) + D_{\mathrm{pu}}^{\top}(\rho) C_{\mathrm{p}}(\rho) \right),
$$

one has

$$
D_{\mathrm{pu}}(\rho) F(\rho) = \gamma N_{S,1}(\rho) S(\rho)^{-1} - C_{\mathrm{p}}(\rho), \\
B_{\mathrm{u}}(\rho) F(\rho) = -\gamma W S(\rho)^{-1} + N_{S,1}^{\top}(\rho) C_{\mathrm{p}}(\rho).
$$

Thus, inserting the closed-loop matrices into Cond. (2.70) yields

$$
\begin{bmatrix} \bullet \\ \cdots \\ \bullet \end{bmatrix}^{\top}
\left[\begin{array}{cc:c} 0 & S(\rho) & \\ S(\rho) & \partial S(\rho,\sigma) & \\ \hdashline & & \Gamma^{-1} \end{array}\right]
\tag{B.5}
$$

$$
\times
\left[\begin{array}{c:c} -A^{\top}(\rho) - C_{\mathrm{p}}^{\top}(\rho)N_{S,1}(\rho) + \gamma S(\rho)^{-1} W & -\gamma S(\rho)^{-1} N_{S,1}^{\top}(\rho) \\ I & 0 \\ \hdashline -B_{\mathrm{p}}^{\top}(\rho) & 0 \\ 0 & I \end{array}\right] \succ 0.
$$

In order to show equivalence between Conds. (B.4) and (B.5), apply a congruence transformation by multiplying (B.5) from the right by

$$
T_S(\rho) = \begin{bmatrix} I & N_{S,2}(\rho) \\ N_{S,1}(\rho) & I \end{bmatrix}
$$

and from the left by $T_S^{\top}(\rho)$, respectively. This concludes a simple sketch of the proof.

B.3 Auxiliary Material for Theorem 2.15

$$B_R(\delta) = U_R(\delta) G_R(\delta) N_R(\delta) = \Delta_{B_R} \star \begin{bmatrix} B_{R,11} & B_{R,12} \\ B_{R,21} & B_{R,22} \end{bmatrix}, \quad \Delta_{B_R} \in \mathbb{R}^{(n^R_{q_\Delta} \times n^R_{p_\Delta})}$$

$$U_R(\delta) = \begin{bmatrix} Q_R(\delta) & 0 & \\ \partial Q_R(\delta, \eta) & Q_R(\delta) & \\ & & I \ 0 \\ & & 0 \ I \end{bmatrix} = \Delta_{u_R} \star \begin{bmatrix} U_{R,11} & U_{R,12} \\ U_{R,21} & U_{R,22} \end{bmatrix}$$

$$\Delta_{B_R} = \begin{bmatrix} \Delta_{u_R} & & \\ & \Delta^P & \\ & & \Delta^P \end{bmatrix}$$

$$G_R(\delta) = \begin{bmatrix} I & 0 \\ A(\delta) & B_p(\delta) \\ 0 & I \\ C_p(\delta) & D_{pp}(\delta) \end{bmatrix} = \Delta^P \star \begin{bmatrix} G_{R,11} & G_{R,12} \\ G_{R,21} & G_{R,22} \end{bmatrix},$$

$$\begin{bmatrix} G_{R,11} & G_{R,12} \\ G_{R,21} & G_{R,22} \end{bmatrix} = \begin{bmatrix} D_{\Delta\Delta} & C_\Delta & D_{\Delta p} \\ 0 & I & 0 \\ B_\Delta & A & B_p \\ 0 & 0 & I \\ D_{p\Delta} & C_p & D_{pp} \end{bmatrix}, \tag{B.6}$$

$$N_R(\delta) = \ker\left(\begin{bmatrix} C_y(\delta) & D_{yp}(\delta) \end{bmatrix}\right) = \Delta^P \star \begin{bmatrix} N_{R,11} & N_{R,12} \\ N_{R,21} & N_{R,22} \end{bmatrix},$$

$$\begin{bmatrix} B_{R,11} & B_{R,12} \\ B_{R,21} & B_{R,22} \end{bmatrix} = \begin{bmatrix} U_{R,11} & U_{R,12}G_{R,21} & U_{R,12}G_{R,22}N_{R,21} & U_{R,12}G_{R,22}N_{R,22} \\ 0 & G_{R,11} & G_{R,12}N_{R,21} & G_{R,12}N_{R,22} \\ 0 & 0 & N_{R,11} & N_{R,12} \\ U_{R,21} & U_{R,22}G_{R,21} & U_{R,22}G_{R,22}N_{R,21} & U_{R,22}G_{R,22}N_{R,22} \end{bmatrix},$$

$$B_S(\delta) = U_S(\delta) G_S(\delta) N_S(\delta) = \Delta_{B_S} \star \begin{bmatrix} B_{S,11} & B_{S,12} \\ B_{S,21} & B_{S,22} \end{bmatrix}, \quad \Delta_{B_S} \in \mathbb{R}^{(n^S_{q_\Delta} \times n^S_{p_\Delta})} \tag{B.7}$$

$$U_S(\delta) = \begin{bmatrix} Q_S(\delta) & \partial Q_S(\delta, \eta) & \\ 0 & Q_S(\delta) & \\ & & I \ 0 \\ & & 0 \ I \end{bmatrix} = \Delta_{u_S} \star \begin{bmatrix} U_{S,11} & U_{S,12} \\ U_{S,21} & U_{S,22} \end{bmatrix}$$

$$\Delta_{B_S} = \begin{bmatrix} \Delta_{u_S} & & \\ & -\Delta^{P\top} & \\ & & \Delta^{P\top} \end{bmatrix}$$

$$G_S(\delta) = \left[\begin{array}{cc} -A^\top(\delta) & -C_p^\top(\delta) \\ I & 0 \\ \hdashline -B_p^\top(\delta) & -D_{pp}^\top(\delta) \\ 0 & I \end{array}\right] = -\Delta^{P^\top} \star \left[\begin{array}{c|c} G_{S,11} & G_{S,12} \\ \hline G_{S,21} & G_{S,22} \end{array}\right],$$

$$\left[\begin{array}{c|c} G_{S,11} & G_{S,12} \\ \hline G_{S,21} & G_{S,22} \end{array}\right] = \left[\begin{array}{c|cc} -D_{\Delta\Delta}^\top & -B_\Delta^\top & -D_{p\Delta}^\top \\ \hdashline -C_\Delta^\top & -A^\top & -C_p^\top \\ 0 & I & 0 \\ \hdashline -D_{\Delta p}^\top & -B_p^\top & -D_{pp}^\top \\ 0 & 0 & I \end{array}\right] \tag{B.8}$$

$$N_S(\delta) = \ker\left(\left[B_u^\top(\delta)\ D_{pu}^\top(\delta)\right]\right) = \Delta^{P^\top} \star \left[\begin{array}{c|c} N_{S,11} & N_{S,12} \\ \hline N_{S,21} & N_{S,22} \end{array}\right],$$

$$\left[\begin{array}{c|c} B_{S,11} & B_{S,12} \\ \hline B_{S,21} & B_{S,22} \end{array}\right] = \left[\begin{array}{ccc|c} U_{S,11} & U_{S,12}G_{S,21} & U_{S,12}G_{S,22}N_{S,21} & U_{S,12}G_{S,22}N_{S,22} \\ 0 & G_{S,11} & G_{S,12}N_{S,21} & G_{S,12}N_{S,22} \\ 0 & 0 & N_{S,11} & N_{S,12} \\ \hline U_{S,21} & U_{S,22}G_{S,21} & U_{S,22}G_{S,22}N_{S,21} & U_{S,22}G_{S,22}N_{S,22} \end{array}\right]$$

$$B_{RS}(\delta) = \left[\begin{array}{cc} Q_R(\delta) & 0 \\ 0 & Q_S(\delta) \\ \hdashline I & 0 \\ 0 & I \end{array}\right] = \Delta_{B_{RS}} \star \left[\begin{array}{c|c} B_{RS,11} & B_{RS,12} \\ \hline B_{RS,21} & B_{RS,22} \end{array}\right],$$

$$\Delta_{B_{RS}} = \mathrm{diag}(\Delta_R, \Delta_S) \in \mathbb{R}^{(n_{q_\Delta}^{RS} \times n_{p_\Delta}^{RS})}$$

$$\left[\begin{array}{c|c} B_{RS,11} & B_{RS,12} \\ \hline B_{RS,21} & B_{RS,22} \end{array}\right] = \left[\begin{array}{cc|cc} Q_{R,11} & 0 & Q_{R,12} & 0 \\ 0 & Q_{S,11} & 0 & Q_{S,12} \\ \hline Q_{R,21} & 0 & Q_{R,22} & 0 \\ 0 & Q_{S,21} & 0 & Q_{S,22} \\ 0 & 0 & I & 0 \\ 0 & 0 & 0 & I \end{array}\right],$$

B.4 Controller Construction for Theorem 2.16

Theorem B.1 (Mixed General/Affine LFT-LPV Controller [161])
Under Ass. (A2.1)–(A2.6), and given that the conditions of Thm. 2.16 are satisfied for a mixed general/LFT-linear parameter-varying (LPV) plant,

- *affine in the parameters $\delta(t)$, i.e., $D_{\Delta\Delta}(\rho) = 0$,*

- *with performance channel independent of $\delta(t)$, i.e., $D_{\Delta p}(\rho) = 0$, $D_{p\Delta}(\rho) = 0$, and*

- $\begin{bmatrix} D_{\Delta u}(\rho) \\ D_{pu}(\rho) \end{bmatrix}$ and $\begin{bmatrix} D_{y\Delta}(\rho) & D_{yP}(\rho) \end{bmatrix}$ *full column and row rank, respectively,* $\forall \rho \in \boldsymbol{\rho}$,

and given a reconstructed closed-loop multiplier $\mathcal{M}$ *according to Lma. 2.4, there exists a controller* $\mathcal{K}^{\sigma,\eta}_{\rho,\delta}$ *affine in the parameter block* $\Delta^K(\Delta^P)$ *constructed via the following steps*

(i) *Let* $M(\rho)N^\top(\rho) = I - S(\rho)R(\rho)$

(ii) *Solve for* $\hat{B}^K(\rho)$ *and* $\hat{C}^K(\rho)$

$$
\begin{bmatrix} 0 & D_{\Gamma_1}(\rho) \\ D_{\Gamma_1}^\top(\rho) & \mathcal{M}_\Gamma \end{bmatrix} \begin{bmatrix} \hat{B}^{K^\top}(\rho) \\ \bullet \end{bmatrix} = - \begin{bmatrix} C_y(\rho) \\ 0 \\ B_\Delta^\top(\rho)R(\rho) \\ 0 \\ B_P^\top(\rho)R(\rho) \\ C_P(\rho) \end{bmatrix}, \tag{B.9}
$$

$$
\begin{bmatrix} 0 & D_{\Gamma_2}(\rho) \\ D_{\Gamma_2}^\top(\rho) & \mathcal{M}_\Gamma \end{bmatrix} \begin{bmatrix} \hat{C}^K(\rho) \\ \bullet \end{bmatrix} = - \begin{bmatrix} B_u^\top(\rho) \\ 0 \\ B_P^\top(\rho) \\ C_\Delta(\rho)S(\rho) \\ 0 \\ C_P(\rho)S(\rho) \end{bmatrix} \tag{B.10}
$$

$$
D_{\Gamma_1}(\rho) = \begin{bmatrix} D_{y\Delta}(\rho) & 0 & D_{yP}(\rho) & 0 \\ 0 & I & 0 & 0 \end{bmatrix}, \quad D_{\Gamma_2}(\rho) = \begin{bmatrix} 0 & D_{\Delta u}^\top(\rho) & 0 & D_{pu}^\top(\rho) \\ 0 & 0 & I & 0 \end{bmatrix},
$$

$$
\mathcal{M}_\Gamma = \begin{bmatrix} \mathcal{M}_{22}^{-1} & 0 & \mathcal{M}_{12}\mathcal{M}_{11}^{-1} & 0 \\ 0 & -\gamma I & 0 & 0 \\ \mathcal{M}_{11}^{-1}\mathcal{M}_{12}^\top & 0 & -\mathcal{M}_{11}^{-1} & 0 \\ 0 & 0 & 0 & -\gamma I \end{bmatrix}
$$

(iii) *Set*

$$
\hat{A}^K(\rho,\sigma) = R(\rho)\partial S(\rho) + N(\rho)\partial M^\top(\rho) - A^\top(\rho) \tag{B.11}
$$

$$
+ \Bigg(R(\rho) \begin{bmatrix} B_\Delta(\rho) & 0 & B_P(\rho) \end{bmatrix}
$$

$$
+ \hat{B}^K(\rho) \begin{bmatrix} D_{y\Delta}(\rho) & 0 & D_{yP}(\rho) \\ 0 & I & 0 \end{bmatrix} \begin{bmatrix} C_\Delta^\top(\rho) & 0 & C_P^\top(\rho) \end{bmatrix} \Bigg)
$$

$$
\times \mathcal{M}_\Gamma^{-1} \Bigg(\begin{bmatrix} B_\Delta(\rho) & 0 & B_P(\rho) \end{bmatrix} \quad S(\rho) \begin{bmatrix} C_\Delta^\top(\rho) & 0 & C_P^\top(\rho) \end{bmatrix}
$$

$$
+ \hat{C}^{K^\top}(\rho) \begin{bmatrix} D_{\Delta u}^\top(\rho) & 0 & D_{pu}^\top(\rho) \\ 0 & I & 0 \end{bmatrix} \Bigg)^\top
$$

$$A^K(\rho, \sigma) = N^{-1}(\rho) \left(\hat{A}^K(\rho, \sigma) - R(\rho) \begin{bmatrix} B_u(\rho) & 0 \end{bmatrix} \hat{C}^K(\rho) \right. \tag{B.12}$$

$$\left. - \hat{B}^K(\rho) \begin{bmatrix} C_y(\rho) \\ 0 \end{bmatrix} S(\rho) - R(\rho)A(\rho)S(\rho) \right) M^{-\top}(\rho),$$

$$\begin{bmatrix} B_y^K(\rho) & B_\Delta^K(\rho) \end{bmatrix} = N^{-1}(\rho)\hat{B}^K(\rho), \tag{B.13}$$

$$\begin{bmatrix} C_u^K(\rho) \\ C_\Delta^K(\rho) \end{bmatrix} = \hat{C}^K(\rho)M^{-\top}(\rho), \tag{B.14}$$

$$\begin{bmatrix} D_{uy}^K(\rho) & D_{u\Delta}^K(\rho) \\ D_{\Delta y}^K(\rho) & D_{\Delta\Delta}^K(\rho) \end{bmatrix} = 0. \tag{B.15}$$

$\square$

$\blacksquare$

Proof: Details of the proof can be found in [161].

B.5 Proof of Lemma 2.5

The extension is derived based on the requirement that the closed-loop multiplier condition and its dual should be fulfilled.

$$\begin{bmatrix} I \\ \Delta(\delta) \end{bmatrix}^* \mathcal{M} \begin{bmatrix} I \\ \Delta(\delta) \end{bmatrix} \succ 0, \ \forall \delta \in \boldsymbol{\delta}, \tag{B.16}$$

$$\begin{bmatrix} -\Delta^*(\delta) \\ I \end{bmatrix}^* \mathcal{N} \begin{bmatrix} -\Delta^*(\delta) \\ I \end{bmatrix} \prec 0, \ \forall \delta \in \boldsymbol{\delta}.$$

Additional inertia requirements on the closed-loop multiplier are given as

$$\mathcal{M}_{22} \prec 0, \quad \mathcal{N}_{11} \succ 0. \tag{B.17}$$

Note that due to the requirement $0 \in \{\Delta(\delta) \mid \delta \in \boldsymbol{\delta}\}$, $\mathcal{M}_{11} \succ 0$ and $\mathcal{N}_{22} \prec 0$ are implied.

However, as opposed to the reconstruction of the Lyapunov matrix, the positivity and negativity constraints are more involved. From the inertia hypotheses one has

$$\begin{bmatrix} \bullet \\ \bullet \end{bmatrix}^\top \left(\begin{bmatrix} I \\ & T^\top \end{bmatrix} \begin{bmatrix} M & I \\ I & (M - N^{-1})^{-1} \end{bmatrix} \begin{bmatrix} I \\ & T \end{bmatrix} \right) \begin{bmatrix} I_{n_\Delta} & 0 \\ 0 & 0 \\ 0 & I_{n_\Delta} \\ 0 & 0 \end{bmatrix} \succ 0,$$

$$\begin{bmatrix} \bullet \\ \bullet \end{bmatrix}^\top \left(\begin{bmatrix} I \\ & T^\top \end{bmatrix} \begin{bmatrix} M & I \\ I & (M - N^{-1})^{-1} \end{bmatrix} \begin{bmatrix} I \\ & T \end{bmatrix} \right) \begin{bmatrix} 0 & 0 \\ I_{n_\Delta} & 0 \\ 0 & 0 \\ 0 & I_{n_\Delta} \end{bmatrix} \prec 0,$$

from which by application of Schur complements (2.160) and (2.161) follow.

To construct the controller's parameter block observe that

$$\begin{bmatrix} I \\ \Delta(\delta) \end{bmatrix}^* \begin{bmatrix} \mathcal{M}_{11} & \mathcal{M}_{12} \\ \mathcal{M}_{12}^\top & \mathcal{M}_{22} \end{bmatrix} \begin{bmatrix} I \\ \Delta(\delta) \end{bmatrix} \succ 0, \ \forall \delta \in \boldsymbol{\delta},$$

is equivalent to

$$\begin{bmatrix} \mathcal{M}_{11} + \mathcal{M}_{12}\Delta(\delta) + \Delta^*(\delta)\mathcal{M}_{12}^\top & \Delta^*(\delta) \\ \Delta(\delta) & -\mathcal{M}_{22}^{-1} \end{bmatrix} \succ 0, \ \forall \delta \in \boldsymbol{\delta}.$$

A congruence transform results in

$$\begin{bmatrix} I & 0 \\ -\mathcal{M}_{12} & I \end{bmatrix}^\top \begin{bmatrix} \mathcal{M}_{11} + \mathcal{M}_{12}\Delta(\delta) + \Delta^*(\delta)\mathcal{M}_{12}^\top & \Delta^*(\delta) \\ \Delta(\delta) & -\mathcal{M}_{22}^{-1} \end{bmatrix} \begin{bmatrix} I & 0 \\ -\mathcal{M}_{12} & I \end{bmatrix}$$

$$= \begin{bmatrix} \mathcal{M}_{11} - \mathcal{M}_{12}\mathcal{M}_{22}^{-1}\mathcal{M}_{12}^\top & \Delta^*(\delta) + \mathcal{M}_{12}\mathcal{M}_{22}^{-1} \\ \Delta(\delta) + \mathcal{M}_{22}^{-1}\mathcal{M}_{12}^\top & -\mathcal{M}_{22}^{-1} \end{bmatrix}$$

$$= \begin{bmatrix} \mathcal{U} & \Delta^*(\delta) + \mathcal{W}^\top \\ \Delta(\delta) + \mathcal{W} & \mathcal{V} \end{bmatrix} \succ 0$$

$$= \begin{bmatrix} \mathcal{U}_{11} & \mathcal{U}_{12} & \mathcal{W}_{11}^\top + \Delta^{P*} & \mathcal{W}_{21}^\top \\ \mathcal{U}_{12}^\top & \mathcal{U}_{22} & \mathcal{W}_{12}^\top & \mathcal{W}_{22}^\top + \Delta^{K*} \\ \hdashline \mathcal{W}_{11} + \Delta^P & \mathcal{W}_{12} & \mathcal{V}_{11} & \mathcal{V}_{12} \\ \mathcal{W}_{21} & \mathcal{W}_{22} + \Delta^K & \mathcal{V}_{12}^\top & \mathcal{V}_{22} \end{bmatrix} \succ 0$$

Applying the permutation Ψ yields

$$\begin{bmatrix} \mathcal{U}_{11} & \mathcal{W}_{11}^\top + \Delta^{P*} & \mathcal{U}_{12} & \mathcal{W}_{21}^\top \\ \mathcal{W}_{11} + \Delta^P & \mathcal{V}_{11} & \mathcal{W}_{12} & \mathcal{V}_{12} \\ \hdashline \mathcal{U}_{12}^\top & \mathcal{W}_{12}^\top & \mathcal{U}_{22} & \mathcal{W}_{22}^\top + \Delta^{K*} \\ \mathcal{W}_{21} & \mathcal{V}_{12}^\top & \mathcal{W}_{22} + \Delta^K & \mathcal{V}_{22} \end{bmatrix} \succ 0,$$

while a further Schur complement results in

$$\begin{bmatrix} \mathcal{U}_{22} & \mathcal{W}_{22}^\top + \Delta^{K*} \\ \mathcal{W}_{22} + \Delta^K & \mathcal{V}_{22} \end{bmatrix}$$

$$- \begin{bmatrix} \mathcal{U}_{12}^\top & \mathcal{W}_{12}^\top \\ \mathcal{W}_{21} & \mathcal{V}_{12}^\top \end{bmatrix} \begin{bmatrix} \mathcal{U}_{11} & \mathcal{W}_{11}^\top + \Delta^{P*} \\ \mathcal{W}_{11} + \Delta^P & \mathcal{V}_{11} \end{bmatrix}^{-1} \begin{bmatrix} \mathcal{U}_{12} & \mathcal{W}_{21}^\top \\ \mathcal{W}_{12} & \mathcal{V}_{12} \end{bmatrix} \succ 0.$$

In order to render this inequality fulfilled by eliminating the off-diagonal blocks, choose (2.162).

b.6 Proof of Lemma 2.6

Define

$$N^{-1} = \begin{bmatrix} \tilde{N}_{11} & \tilde{N}_{12} \\ \tilde{N}_{12}^\top & \tilde{N}_{22} \end{bmatrix},$$

Consider the $(1,1)$ and $(2,2)$ blocks of

$$M - N^{-1} = \begin{bmatrix} M_{11} - \tilde{N}_{11} & M_{12} - \tilde{N}_{12} \\ \bullet & M_{22} - \tilde{N}_{22} \end{bmatrix},$$

and observe that due to (2.163)

$$M_{11} - \left(N_{11} - N_{12} N_{22}^{-1} N_{12}^\top \right)^{-1} \succcurlyeq M_{11} - N_{11}^{-1} \succ 0,$$

$$M_{22} - \left(N_{22} - N_{12}^\top N_{11}^{-1} N_{12} \right)^{-1} \preccurlyeq M_{22} - N_{22}^{-1} \prec 0.$$

This results in

$$\mathcal{M}_{11} = \begin{bmatrix} M_{11} & M_{11} - \tilde{N}_{11} \\ M_{11} - \tilde{N}_{11} & M_{11} - \tilde{N}_{11} \end{bmatrix} \succ 0,$$

$$\mathcal{M}_{22} = \begin{bmatrix} M_{22} & M_{22} - \tilde{N}_{22} \\ M_{22} - \tilde{N}_{22} & M_{22} - \tilde{N}_{22} \end{bmatrix} \prec 0,$$

which can be shown by Schur complements leading to the equivalent conditions $\tilde{N}_{11} \succ 0$ and $\tilde{N}_{22} \prec 0$, which are true due to the dual of Cond. (2.154). Inserting the reconstructed closed-loop multiplier into Cond. (2.158) gives

$$\begin{bmatrix} \bullet \\ \bullet \end{bmatrix}^* \begin{bmatrix} M & M - N^{-1} \\ M - N^{-1} & M - N^{-1} \end{bmatrix} \begin{bmatrix} I \\ \Delta^P(\delta) \\ \hline & I \\ & \Delta^K(\delta) \end{bmatrix} \succ 0, \ \forall \delta \in \boldsymbol{\delta},$$

which by choosing $\Delta^K(\delta) = \Delta^P(\delta)$ and (2.164) allows the application of a Schur complement to obtain

$$\begin{bmatrix} \bullet \\ \bullet \end{bmatrix}^* N^{-1} \begin{bmatrix} I \\ \Delta^P(\delta) \end{bmatrix} \succ 0, \ \forall \delta \in \boldsymbol{\delta},$$

which holds by assumption.

B.7 Parameters of the Robotic Manipulator

The grouped parameters of the 3-DOF robotic manipulator model used in Sect. 4.6 and Sect. 6.1 are taken from [47] and are listed in Tab. B.1. Here, $I_{11,n}$, $I_{22,n}$ and $I_{33,n}$ are the moments of inertia, m_n and a_n are the mass and length, $M_{1,n}$ and $M_{2,n}$ are the first moments of inertia in direction of the respective axis $O_n - x_{1n}$ and $O_n - x_{2n}$, where O_n is the origin, and $I_{m,n}$ and $f_{v,n}$ are the motor moment of inertia and viscous friction coefficient of the nth link respectively. The notation is in accordance with the modified Denavit-Hartenberg convention. More information on base parameters of manipulators can be found in [72].

Table B.1: Estimated inertial and friction parameters of the 3-DOF robotic manipulator (with non-SI units) [47].

Parameter	Value
$b_1 = f_{v,1}$	0.4701
$b_2 = 2(m_3 a_2^2 - I_{11,2} + I_{22,2})$	0.1094
$b_3 = M_{2,3} a_2$	0.0151
$b_4 = 2(I_{11,3} - I_{22,3})$	0.0591
$b_5 = m_3 a_2^2 + I_{11,3} + I_{22,2} + I_{33,1}$	0.0626
$b_6 = I_{11,2} - I_{22,2} - m_3 a_2^2$	0.0229
$b_7 = I_{22,3} - I_{11,3}$	-0.0054
$b_8 = -(M_{x,2} + a_2 m_3)g$	-0.0051
$b_9 = -M_{2,3}g$	0.0097
$b_{10} = f_{v,2}$	0.7741
$b_{11} = \frac{1}{2}(I_{11,2} - I_{22,2} - m_3 a_2^2)$	0.2345
$b_{12} = \frac{1}{2}(I_{22,3} - I_{11,3})$	0.0731
$b_{13} = m_3 a_2^2 + I_{33,2}$	0.1991
$b_{14} = I_{33,2}$	0.0603
$b_{15} = f_{v,3}$	0.7218
$b_{16} = I_{33,3} + I_{m,3}$	0.1033
$b_{17} = -I_{m,3}$	0.0906
$b_{18} = f_{c,1}$	0.2814
$b_{19} = f_{c,2}$	0.1610
$b_{20} = f_{c,3}$	0.3249

B.8 Parameters of the Control Moment Gyroscope

The physical and grouped parameters of the 4-DOF control moment gyroscope (CMG) listed in Tab. B.2 and used in Sect. 4.7 and Sect. 6.2 are kindly provided by the authors of [1].

Table B.2: Physical and grouped parameters of the CMG.

Parameter	Value	Parameter	Value
K_A	$0.0670 \, \text{kg m}^2$	$b_1 = J_D$	0.0273
I_B	$0.0119 \, \text{kg m}^2$	$b_2 = I_D - J_C - J_D + K_C$	-0.0135
J_B	$0.0178 \, \text{kg m}^2$	$b_3 = I_C + I_D$	0.0240
K_B	$0.0297 \, \text{kg m}^2$	$b_4 = J_B + J_C + J_D$	0.0681
I_C	$0.0092 \, \text{kg m}^2$	$b_5 = I_B + I_C - K_B - K_C$	-0.0306
J_C	$0.0230 \, \text{kg m}^2$	$b_6 = I_D + K_A + K_B + K_C$	0.1335
K_C	$0.0220 \, \text{kg m}^2$	$b_7 = I_D - J_D$	-0.0125
I_D	$0.0148 \, \text{kg m}^2$	$b_8 = I_C - J_C + K_C + I_D$	0.0230
J_D	$0.0273 \, \text{kg m}^2$	$b_9 = K_C - J_C$	-0.0010
K_D	$0.0148 \, \text{kg m}^2$	$b_{10} = J_C - K_C - I_D + J_D$	0.0135
$f_{v,1}$	$0.000\,187 \, \text{N m s/rad}$	$b_{11} = J_C - I_C - I_D - I_B + J_D + K_B$	0.0441
$f_{v,2}$	$0.0118 \, \text{N m s/rad}$	$b_{12} = K_C - J_C - J_D - I_C$	-0.0375
$f_{v,3}$	$0.0027 \, \text{N m s/rad}$	$b_{13} = f_{v,1}$	
$f_{v,4}$	$0.0027 \, \text{N m s/rad}$	$b_{14} = f_{v,2}$	
$\bar{\tau}_1$	$0.666 \, \text{N m}$	$b_{15} = f_{v,3}$	
$\bar{\tau}_2$	$2.440 \, \text{N m}$	$b_{16} = \bar{\tau}_1$	
		$b_{17} = \bar{\tau}_2$	

C

AUXILIARY MATERIAL FROM PART II

c.1 Discrete-Time Numerical Example for Sect. 10.1

In [98], Massioni proposed a numerical example for a distributed linear time-invariant (LTI) system composed from two groups of systems—a system containing an integrator and a system in the form of an undamped oscillator. The original system is proposed in discrete-time and the full matrices have been provided upon request. For completeness, they are reproduced here.

The subsystems have the form

$$
P_k : \begin{cases} \begin{bmatrix} x_k(n+1) \\ d_k(n) \\ z_k(n) \\ y_k(n) \end{bmatrix} = \begin{bmatrix} A_f & B_{f,i} & B_{f,p} & B_{f,u} \\ C_{f,i} & D_{f,ii} & D_{f,ip} & D_{f,iu} \\ C_{f,p} & D_{f,pi} & D_{f,pp} & D_{f,pu} \\ C_{f,y} & D_{f,yi} & D_{f,yp} & 0 \end{bmatrix} \begin{bmatrix} x_k(n) \\ v_k(n) \\ w_k(n) \\ u_k(n) \end{bmatrix} \end{cases}, \tag{C.1}
$$

where $x_k \in \mathbb{R}^2$, $d_k \in \mathbb{R}^3$, $v_k \in \mathbb{R}^3$, $z_k \in \mathbb{R}^3$, $w_k \in \mathbb{R}^5$, $y_k \in \mathbb{R}^4$, $u_k \in \mathbb{R}^2$ and $n \in \mathbb{N}$ is the discrete time instant as a multiple of the sampling time T_s, i.e., $t = nT_s$. The respective matrices are

$$
A_1 = \begin{bmatrix} 1 & 0 \\ 1 & 0.95 \end{bmatrix}, \quad A_2 = \begin{bmatrix} 0.6 & 0.8 \\ -0.8 & 0.6 \end{bmatrix},
$$

and for $f = 1, 2$,

$$
B_{f,i} = \begin{bmatrix} 0 & 0 & 1 \\ 1 & 0 & 0 \end{bmatrix}, \quad B_{f,p} = \begin{bmatrix} 1 & 0 & 0 & 0 & 0 \\ 0 & 0 & 0 & 0 & 0 \end{bmatrix}, \quad B_{f,u} = \begin{bmatrix} 1 & 0 \\ 0 & 0 \end{bmatrix},
$$

$$
C_{f,i} = \begin{bmatrix} 1 & 0 \\ 0 & 1 \\ 0 & 0 \end{bmatrix}, \quad C_{f,p} = \begin{bmatrix} 0 & 1 \\ 0 & 0 \\ 0 & 0 \end{bmatrix}, \quad C_{f,y} = \begin{bmatrix} 1 & 0 \\ 0 & 1 \\ 0 & 0 \\ 0 & 0 \end{bmatrix},
$$

$$D_{f,ii} = O_3, \ D_{f,ip} = O_{3\times5}, \ D_{f,iu} = O_{3\times2},$$

$$D_{f,pi} = O_{3\times3}, \ D_{f,pp} = O_{3\times5}, \ D_{f,pu} = \begin{bmatrix} 0 & 0 \\ 1 & 0 \\ 0 & 1 \end{bmatrix},$$

$$D_{f,yi} = \begin{bmatrix} 0 & 0 & 0 \\ 0 & 0 & 0 \\ 1 & 0 & 0 \\ 0 & 1 & 0 \end{bmatrix}, \ D_{f,yp} = 0.1 \begin{bmatrix} 0 & 1 & 0 & 0 & 0 \\ 0 & 0 & 1 & 0 & 0 \\ 0 & 0 & 0 & 1 & 0 \\ 0 & 0 & 0 & 0 & 1 \end{bmatrix},$$

$$D_{f,yu} = O_{4\times2}.$$

The matrix $D_{f,pu}$ has been scaled by $\frac{1}{100}$, in order to shift the lower bound on the achievable $\mathcal{H}_\infty$-norm to 1.

ACRONYMS AND INITIALISMS

LIST OF SYMBOLS

LINEAR ALGEBRA

$\Delta \star M$	Upper LFT.
$M \star \Delta$	Lower LFT.
$M \succ 0$, $M \succcurlyeq 0$	Positive (semi-)definiteness.
$M \prec 0$, $M \preccurlyeq 0$	Negative (semi-)definiteness.
$1_{n \times m}$ $1_n \triangleq 1_{n \times 1}$	Matrix of ones with dimensions $n \times m$.
$I_n \triangleq \mathrm{diag}(1_n)$	Identity matrix of dimensions $n \times n$.
$A \otimes B$	Kronecker product.
$A \circledast B$	Khatri-Rao product.
$\mathrm{Re}\,(a)$	Real part of some complex number $a \in \mathbb{C}$.
$\mathrm{Im}\,(a)$	Imaginary part of some complex number $a \in \mathbb{C}$.
$\mathrm{tr}(M)$	Trace of matrix M.
$\mathrm{adj}(M)$	Adjoint of matrix M.
$\mathrm{rank}\,(M)$	Rank of matrix M.
$\dim\,(M)$	Dimensions of matrix M, s. t. if $M \in \mathbb{C}^{n \times m}$, $\dim\,(M) = (n, m)$.
$\mathrm{in}\,(M)$	Inertia of a matrix M, s. t. if with n_-, n_0, n_+ being the eigenvalues with negative, zero and positive real part, respectively, $\mathrm{in}\,(M) = (n_-, n_0, n_+)$.
Π	Projection.
λ	Eigenvalue.
σ, Σ	Singular value and matrix of singular values, s. t. an SVD of a matrix M yields $M = U\Sigma V^*$.
$\mathbb{\Lambda}(M)$	Spectrum of matrix M.
$\mathbb{\Sigma}(M)$	Set of singular values of matrix M.
$M^\top, M^*$	Transpose and conjugate transpose of a matrix.
$M^{-1}, M^\dagger$	Inverse and pseudo-inverse of a matrix.

MATRICES

A, B, C, D / $\mathcal{A}, \mathcal{B}, \mathcal{C}, \mathcal{D}$ / $\mathscr{A}, \mathscr{B}, \mathscr{C}, \mathscr{D}$

$\qquad$ System, input, output and feed-through matrix of an open-loop/closed-loop/specially denoted state space model, respectively.

$\overset{i=1}{\underset{n}{\operatorname{diag}}}(M_i)$ $\qquad$ Diagonal concatenation of matrices $M_1, M_2, \ldots, M_n$.

$\overset{i=1}{\underset{n}{\operatorname{col}}}(M_i)$ $\qquad$ Vertical concatenation of $M_1, M_2, \ldots, M_n$, s.t. M_1 is on top.

$\overset{i=1}{\underset{n}{\operatorname{row}}}(M_i)$ $\qquad$ Horizontal concatenation of $M_1, M_2, \ldots, M_n$, s.t. M_1 is left-most.

SPACES, SETS AND MAPPINGS

$\mathbb{N}$, $\mathbb{N}^+$	Set of whole numbers $\{0, 1, 2, 3, \ldots\}$ and set of whole numbers without zero.
$\mathbb{Z}$	Set of integers, i.e., set of whole numbers with additive inverses.
$\mathbb{R}^{n \times m}$	Set of real-valued $n \times m$ matrices.
$\mathbb{R}^+$	Set of non-negative real-valued scalars.
$\mathbb{C}^{n \times m}$	Set of complex-valued $n \times m$ matrices.
$\mathbb{S}^n$	Set of real-valued symmetric $n \times n$ matrices.
$\mathbb{H}^n$	Set of complex-valued hermitian $n \times n$ matrices.
$\mathbb{AS}^n$	Set of real-valued skew-symmetric $n \times n$ matrices.
$\mathbb{AH}^n$	Set of complex-valued skew-hermitian $n \times n$ matrices.
$j\mathbb{R}^{n \times m}$	Set of purely imaginary-valued $n \times m$ matrices.
$\mathcal{C}^0(\mathbb{F}_1, \mathbb{F}_2)$	Set of continuous functions mapping from some field $\mathbb{F}_1$ into another $\mathbb{F}_2$.
$\mathcal{C}^k(\mathbb{F}_1, \mathbb{F}_2)$	Set of k-times continuously differentiable functions mapping from some field $\mathbb{F}_1$ into another $\mathbb{F}_2$.
$\mathcal{A}$	Typical typeset for a set.
$\mathcal{A} \times \mathcal{B}$	Cartesian product of the sets $\mathcal{A}$ and $\mathcal{B}$.
$\operatorname{conv}(\mathcal{A})$	Convex hull of the set $\mathcal{A}$, i.e., a set $\operatorname{conv}(\mathcal{A}) \supseteq \mathcal{A}$ containing $\mathcal{A}$, but enlarged to form the smallest possible convex set.
$\operatorname{hyp}(\mathcal{A})$	Hyperbox of the set $\mathcal{A}$, i.e., a set $\operatorname{hyp}(\mathcal{A}) \supseteq \mathcal{A}$ containing $\mathcal{A}$, but enlarged to form a convex set that contains all combinations of maximum and minimum values of independent dimensions.

SPACES, SETS AND MAPPINGS, CONT'D

$\mathrm{im}(M)$	Image or column space of a matrix M. Instead of a space, it can also denote a matrix containing a basis of the image space, i. e., if $N = \mathrm{im}(M) \in \mathbb{C}^{n \times m}$, then $\exists \alpha \in \mathbb{C}^m$, s. t. $M = N\alpha$.
$\mathrm{ker}(M)$	Kernel or null space of a matrix M. Instead of a space, it can also denote a matrix containing a basis of the null space, i. e., if $N = \mathrm{ker}(M)$, then $MN = 0$.

SIGNALS AND SYSTEMS

$\mathcal{P}$, P, P	Generalized plant—LPV system, input-output operator, system matrix.
$\mathcal{T}$, T, T	Closed-loop plant—LPV system, input-output operator, system matrix.
$\mathcal{K}$, K, K	Controller—LPV system, input-output operator, system matrix.
$\mathcal{G}$, G, G	Physical plant model—LPV system, input-output operator, system matrix.
$\mathcal{G}^\sigma_\rho$, G^σ_ρ, G^σ_ρ	Physical plant model associated with the parameter set and rates (ρ, σ)—LPV system, input-output operator, system matrix.
$G = \left[\begin{array}{c\|c} A & B \\ \hline C & D \end{array}\right]$	Rosenbrock notation. $G(s) = D + C(sI - A)^{-1}B$.

(ρ,σ), (δ,η), (θ,ν), (ϕ,ψ), (υ,ζ) —————

LPV scheduling signals and associated rates of change. Typically denoting parameters (from left to right) that incur general, rational or affine parameter dependency. The last tupel denotes parameters in which a system's inertia, damping and stiffness matrix is affine.

$(\boldsymbol{\rho},\boldsymbol{\sigma})$, $(\boldsymbol{\delta},\boldsymbol{\eta})$, $(\boldsymbol{\theta},\boldsymbol{\nu})$, $(\boldsymbol{\phi},\boldsymbol{\psi})$, $(\boldsymbol{\upsilon},\boldsymbol{\zeta})$ —————

Compact set of admissible values of the signal $\rho(t)$ and compact set of admissible values of the rates of change $\sigma(t)$ of the signal $\rho(t)$ as well as for parameters $\delta(t)$, $\theta(t)$, $\phi(t)$, $\upsilon(t)$ and associated rates $\eta(t)$, $\nu(t)$, $\psi(t)$, $\zeta(t)$.

$\mathcal{F}_\rho, \mathcal{F}_\delta, \mathcal{F}_\theta, \mathcal{F}_\phi, \mathcal{F}_\upsilon, \mathcal{F}^\sigma_\rho, \mathcal{F}^\eta_\delta, \mathcal{F}^\nu_\theta, \mathcal{F}^\psi_\phi, \mathcal{F}^\zeta_\upsilon$ —————

Set of admissible trajectories of the signal $\rho(t)$, or parameter $\delta(t)$, $\theta(t)$, $\phi(t)$ or $\upsilon(t)$, respectively, and with bounds on the respective rates $\eta(t)$, $\nu(t)$, $\psi(t)$ or $\zeta(t)$.

$s = \sigma + j\omega$	Complex frequency variable, Laplace operator.
σ, ω	Real part of complex frequency variable σ and frequency ω .
$\mathcal{L}^n_2$	Space of n-dimensional signals square integrable over $t \in [-\infty, \infty]$.
$\|\cdot\|_p$	Vector p-norm. If $p = 2$, $\|\cdot\|_2 = \|\cdot\|$.
$\|\cdot\|_2$	Induced $\mathcal{L}_2$-norm.
$x(t)$	State vector.
$\mathfrak{x}(t)$	Closed-loop state vector.
$u(t)$	Input vector.
$y(t)$	Output vector.

Signals and Systems, cont'd

$w(t)$	Performance input vector.
$z(t)$	Performance output vector.
$q_\bullet(t)$	LFT input vector w. r. t. the parameter block associated with $\bullet \in \{\Delta, \Theta, \Phi, \Upsilon, \Lambda\}$.
$p_\bullet(t)$	LFT output vector w. r. t. the parameter block associated with $\bullet \in \{\Delta, \Theta, \Phi, \Upsilon, \Lambda\}$.
$v(t)$	Interconnection input vector.
$d(t)$	Interconnection output vector.
$\bar{x}(t)$	Equilibrium of signal $x(t)$.
$\partial x(t)$	Deviation $\partial x(t) \triangleq x(t) - \bar{x}(t)$ of signal $x(t)$ from the equilibrium $\bar{x}(t)$.

Miscellaneous Symbols

$m(\bullet), m_j(\bullet)$	Vector of monomials $m(\bullet)$ and j^{th} monomial $m_j(\bullet)$ as the jth entry.
$p(\bullet), p_j(\bullet)$	Vector of polynomials $p(\bullet)$ and j^{th} polynomial $p_j(\bullet)$ as the jth entry.
$\underline{\tilde{k}}(\bullet), \tilde{k}_{ij}(\bullet)$	Matrix $\underline{\tilde{k}}(\bullet)$ resulting from factoring out a monomial vector from the vector of generalized forces. Matrix entry $\tilde{k}_{ij}(\bullet)$ for i^{th} row and j^{th} monomial.
$\tilde{k}_{ijk}(\bullet)$	Matrix entry $\tilde{k}_{ijk}(\bullet)$ of LPV representation, resulting from multiplication of $\tilde{k}_{ij}(\bullet)$ with the kth state.
$c_{ijk}^{(l)}, c_{ij}^{(l)}$	Selector coefficient $c_{ijk}^{(l)}$ of the lth choice for the ith row, j^{th} monomial and k^{th} state. Selector coefficient vector $c_{ij}^{(l)} \triangleq \operatorname*{row}_{k=1}^{n_x}\left(c_{ijk}^{(l)}\right)$.
$\mathfrak{C}_{ij}^{(l)}, \mathfrak{C}_{i}^{(l)}$	Selector coefficient matrix $\mathfrak{C}_{ij}^{(l)} \triangleq \operatorname*{diag}_{k=1}^{n_x}\left(c_{ijk}^{(l)}\right)$ of the lth choice for the ith row and j^{th} monomial. Selector coefficient matrix $\mathfrak{C}_{i}^{(l)} \triangleq \operatorname*{diag}_{j=1}^{n_m}\left(\mathfrak{C}_{ij}^{(l)}\right)$ of the lth choice for the ith row.
$\left\lfloor \frac{a}{b} \right\rfloor$	$\left\lfloor \frac{a}{b} \right\rfloor \triangleq \begin{cases} a/b, & \text{if } b \text{ is a factor of } a \\ 0, & \text{otherwise.} \end{cases}$
$\dot{x}(t)$	Time derivative of signal $x(t)$, i. e., $\dot{x}(t) \triangleq \frac{dx(t)}{dt}$.

Complexity

$a[M]$	Number of arithmetic operations necessary to calculate M.
$m[M]$	Number of scalar variables necessary to store M.
$d[\mathcal{L}]$	Number of decision variables in LMI $\mathcal{L}$.
$s[\mathcal{L}]$	Size of LMI $\mathcal{L}$.
$t[K]$	Synthesis time associated with the controller K.

Interconnected Systems

$\mathcal{G}(t)$	Time-varying graph $\mathcal{G}(t) = (\mathcal{V}, \mathcal{E}(t), \mathcal{W}(t))$ defined as a tupel of a vertex set $\mathcal{V}$, a time-varying edge set $\mathcal{E}(t)$ and a time-varying set of weights $\mathcal{W}(t)$.
$\mathbf{H}$	Set of subsystem indices.
$\mathbf{H}_k$	Index set of neighboring subsystems to subsystem k.
$\mathcal{N}_k$	Vertex set of neighboring subsystems to subsystem k.
$\mathbf{G}$	Partition $\mathbf{G} = \{\mathbf{G}_1, \mathbf{G}_2, \ldots, \mathbf{G}_g\}$ of subsystem indices. The index sets $\mathbf{G}_f$, $f = 1, \ldots, g$, associate some subsystem index $k \in \mathbf{H}$ with a group index f.
d_k	In-degree matrix.
e_f	Column vector with zeros everywhere and ones in the entries, whose indices correspond to the ones in the set $\mathbf{G}_f$.
E_f	Matrix with zeros everywhere and ones in the entries on the diagonal, whose indices corresponds to the ones in the set $\mathbf{G}_f$. Formal definition: $E_f \stackrel{\triangle}{=} \operatorname{diag}(e_f)$.
$\mathscr{L}, \tilde{\mathscr{L}}$	Interconnection matrix or operator and its normalized version, respectively.
$\ell, \tilde{\ell}$	Interconnection matrix with scalar entries, s.t. $\mathscr{L} = \ell \otimes I$ and its normalized version, respectively.
$\mathscr{A}, \mathscr{A}_N$	Adjacency matrix; row-normalized adjacency matrix.
$\mathscr{I}, \mathscr{I}_N$	Graph Laplacian; row-normalized graph Laplacian.
$\mathscr{A}(\mathcal{G}(t)), \mathscr{A}_N(\mathcal{G}(t)), \mathscr{I}(\mathcal{G}(t)), \mathscr{I}_N(\mathcal{G}(t))$	
	Sets of admissible (row-normalized) adjacency and Laplacian matrices associated with a time-varying graph $\mathcal{G}(t)$.
$\mathscr{L}, \ell$	
	Compact sets of admissible interconnection operator values.
$\mathcal{F}_{\mathscr{L}}, \mathcal{F}_\ell$	
	Sets of admissible topology variations.
$\ell_D^{h \times h}, \ell_N^{h \times h}$	
	Sets of diagonalizable and normal matrices of size $h \times h$, respectively.
$\mathcal{F}_{\ell, \mathbb{R}}^{h \times h}, \mathcal{F}_{\ell, S}^{h \times h}, \mathcal{F}_{\ell, \mathbb{AS}}^{h \times h}, \mathcal{F}_{\ell, G, S}^{h \times h}, \mathcal{F}_{\ell, D}^{h \times h}, \mathcal{F}_{\ell, N}^{h \times h},$	
	Sets of admissible topology variations, where the time ($\mathbb{R}^+$) is mapped into arbitrary, symmetric, skew-symmetric, groupwise-symmetric, diagonalizable and normal matrices of size $h \times h$, respectively.
$\check{M}$	Decomposable matrix.
F	Diagonalizing transformation.

INTERCONNECTED SYSTEMS, CONT'D

$\lambda\ (\Lambda),\ \tilde{\lambda}\ (\tilde{\Lambda})$	Range of admissible eigenvalues of a possibly time-varying interconnection matrix $\ell\ (\mathscr{L})$ and its normalized version, respectively.
$\sigma\ (\Sigma)$	Range of admissible singular values of a possibly time-varying interconnection matrix $\ell\ (\mathscr{L})$.
$d,\ \eth,\ \tilde{d},\ \tilde{\eth},\ \nu,\ \upsilon,\ \tilde{\nu},\ \tilde{\upsilon}$	
	Interconnection output and input channels for the open- and closed-loop system and their counterparts due to normalization.
$\overline{\sigma}_{\mathbb{AS}}$	Degree of asymmetry.

MATRIX INEQUALITIES

$\mathcal{L}$	LMI identifier.
N	Matrix containing the basis of a null space.
$V,\ \partial V$	Lyapunov function and derivative along a trajectory.
$X,\ \partial X,\ \mathcal{X},\ \partial\mathcal{X}$	Open- and closed-loop Lyapunov matrix X and $\mathcal{X}$ as well as their derivatives along a trajectory.
$Y,\ \partial Y,\ \mathcal{Y},\ \partial\mathcal{Y}$	Dual open- and closed-loop Lyapunov matrix Y and $\mathcal{Y}$ as well as their derivatives along a trajectory.
$R,\ S$	Lyapunov matrices R and S of primal and dual projected BRL matrix inequality conditions, respectively.
$Q_R(\bullet),$	Parameter-dependent outer factor $Q(\bullet)$ of quadratically parameter-dependent Lyapunov matrix $R(\bullet) = Q_R^\top(\bullet)RQ_R(\bullet)$.
$U(\bullet)$	Parameter-dependent outer factor of some quadratically parameter-dependent matrix inequality.
Γ	Performance multiplier/IQC coefficient matrix.
$M,\ \mathcal{M}$	Multiplier in primal matrix inequality condition. The notation $\mathcal{M}$ refers to a closed-loop analysis condition.
$N,\ \mathcal{N}$	Multiplier in dual matrix inequality condition. The notation $\mathcal{N}$ refers to a closed-loop analysis condition.
$P,\ \mathcal{P}$	Multiplier in parameter-dependent Lyapunov matrix positive-definiteness condition. The notation $\mathcal{P}$ refers to a closed-loop analysis condition.
$\check{M},\ \check{N}$	Higher-stage multipliers in primal/dual matrix inequality conditions.
$R,\ S,\ Q$	Block-matrices of multipliers.
$\bullet$	Symmetric completion in a symmetric matrix, i.e., $\begin{bmatrix} M_{11} & M_{12} \\ \bullet & M_{12} \end{bmatrix} = \begin{bmatrix} M_{11} & M_{12} \\ M_{12}^\top & M_{22} \end{bmatrix}$ and $\begin{bmatrix} \bullet \end{bmatrix}^\top QN = N^\top QN$.

LIST OF SUB-/SUPERSCRIPTS AND MODIFIERS

cl, ol	Closed-loop, open-loop.
p	Performance channel.
u	Input channel.
y	Output channel.
$\Delta, \Theta, \Phi, \Upsilon, \Lambda$	LFT-LPV channel w. r. t. the parameter block Δ, Θ, Φ, Υ or Λ.
e	Error signal channel.
r	Reference signal channel.
i	Interconnection signal channel.
v	Vertex.
g	Grid.
0	Nominal value.
N	Normalized value.
w	Weighted value.
$m^u(\bullet), m^m(\bullet)$	Monomial vector with univariate and multivariate monomials.
$\hat{x}, \hat{P}, \hat{\Delta}$	Approximated signal x, system P or matrix Δ.

BIBLIOGRAPHY

[1] H. S. Abbas, A. Ali, S. M. Hashemi, and H. Werner. «LPV State-Feedback Control of a Control Moment Gyroscope.» In: *Contr. Eng. Prac.* 24 (2014), pp. 129–137. ISSN: 09670661 (cit. on pp. 145, 149, 336).

[2] H. S. Abbas, S. Rahme, N. Meskin, C. Hoffmann, R. Toth, and J. Mohammadpour. «Linear Parameter-Varying Control of a Copolymerization Reactor.» In: *1st IFAC Workshop LPV Syst.* 2015 (cit. on pp. 308, 378).

[3] P. Apkarian and R. J. Adams. «Advanced Gain-Scheduling Techniques for Uncertain Systems.» In: *IEEE Trans. Contr. Syst. Technol.* 6.1 (1998), pp. 21–32. ISSN: 1063-6536. DOI: 10.1109/87.654874 (cit. on pp. 4, 6, 17, 34, 58, 61, 92, 95).

[4] P. Apkarian, G. Becker, P. Gahinet, and H. Kajiwara. *LMI Techniques in Control Engineering from Theory to Practice.* 1996 (cit. on pp. 29, 38).

[5] P. Apkarian and P. Gahinet. «A Convex Characterization of Gain-Scheduled H-Infinity Controllers.» In: *IEEE Trans. Automat. Contr.* (1995), pp. 853–864. ISSN: 0018-9286 (cit. on pp. 4, 20, 46, 92, 95, 117).

[6] P. Apkarian, P. Gahinet, and G. Becker. «Self-Scheduled H-Infinity Control of Linear Parameter-varying Systems: a Design Example.» In: *Automatica* 31.9 (1995), pp. 1251–1261. ISSN: 00051098 (cit. on pp. 4, 6, 62, 92).

[7] P. Apkarian and D. Noll. «Nonsmooth H-Infinity-Synthesis.» In: *IEEE Trans. Automat. Contr.* 51.1 (2006), pp. 71–86. ISSN: 0018-9286 (cit. on p. 308).

[8] P. Apkarian and H. D. Tuan. «Parameterized LMIs in Control Theory.» In: *SIAM J. Control & Opt.* 38.4 (2000), pp. 1241–1265. ISSN: 0363-0129 (cit. on p. 92).

[9] K. J. Astrøm and P. R. Kumar. «Control: A Perspective.» In: *Automatica* 50.1 (2014), pp. 3–43. ISSN: 00051098. DOI: 10.1016/j.automatica.2013.10.012 (cit. on pp. 1, 7).

[10] G. J. Balas, J. C. Doyle, K. Glover, A. K. Packard, and R. S. Smith. m-*Analysis and Synthesis Toolbox.* 4, Release 13. The MathWorks, Inc, 2002 (cit. on p. 296).

[11] B. Bamieh, F. Paganini, and M. A. Dahleh. «Distributed Control of Spatially Invariant Systems.» In: *IEEE Trans. Automat. Contr.* 47.7 (2002), pp. 1091–1107. ISSN: 0018-9286. DOI: 10.1109/TAC.2002.800646 (cit. on pp. 225, 228).

[12] C. L. Beck. «Coprime Factors Reduction Methods for Linear Parameter Varying and Uncertain Systems.» In: *Syst. & Contr. Letters* 55 (2006), pp. 199–213. ISSN: 0167-6911 (cit. on p. 308).

[13] C. L. Beck and R. D'Andrea. «Computational Study And Comparisons Of LFT Reducibility Methods.» In: *Proc. Amer. Control Conf.* 1998 (cit. on pp. 156, 288).

[14] C. L. Beck and J. C. Doyle. «A Necessary and Sufficient Minimality Condition for Uncertain Systems.» In: *IEEE Trans. Automat. Contr.* 44.10 (1999), pp. 1802–1813. ISSN: 0018-9286. DOI: 10.1109/9.793720 (cit. on pp. 156, 288).

[15] R. H. Bishop, ed. *The Mechatronics Handbook.* The Electrical Engineering Handbook Series. Boca Raton, Fla: CRC Press, 2002. ISBN: 0849300665 (cit. on p. 104).

[16] S. Bouabdallah. «Design and Control of Quadrotors With Application to Autonomous Flying.» Ph.D. Thesis. Lausanne, France: Ecole Polytechnique Federale De Lausanne, 2007. URL: http://www.es.ele.tue.nl/education/5HC99/wiki/images/3/39/EPFL_TH3727.pdf (cit. on pp. 285, 286).

[17] S. P. Boyd, L. El Ghaoui, E. Feron, and V. Balakrishnan. *Linear Matrix Inequalities in System and Control Theory*. Vol. 15. Studies in Applied Mathematics. 1994. ISBN: 089871334X (cit. on pp. 32, 37).

[18] A. E. Brouwer and W. H. Haemers. *Spectra of Graphs*. Universitext. Springer, 2011. ISBN: 9781461419389 (cit. on p. 245).

[19] F. Bruzelius, S. Pettersson, and C. Breitholtz. «Linear Parameter-Varying Descriptions of Nonlinear Systems.» In: *Proc. Amer. Control Conf.* 2004, pp. 1374–1379 (cit. on p. 308).

[20] P. Chiaccio, L. Sciaviccio, and B. Siciliano. «The Potential of Model-Based Control Algorithms for Improving Industrial Robot Tracking Performance.» In: *Proc. Int. Workshop Intell. Motion Contr.* 1990 (cit. on pp. 177, 178).

[21] P. Colaneri and J. C. Geromel. «Parameter-Dependent Lyapunov Functions for Time Varying Polytopic Systems.» In: *Proc. Amer. Control Conf.* 2005, pp. 604–608. DOI: 10.1109/ACC.2005.1470023 (cit. on p. 92).

[22] Costa, Oswaldo Luiz do Valle, M. D. Fragoso, and M. G. Todorov. *Continuous-Time Markov Jump Linear Systems*. Probability and its applications. Berlin and London: Springer, 2013. ISBN: 9783642341007 (cit. on p. 3).

[23] J. Daafouz, J. Bernussou, and J. C. Geromel. «On Inexact LPV Control Design of Continuous–Time Polytopic Systems.» In: *IEEE Trans. Automat. Contr.* 53.7 (2008), pp. 1674–1678. ISSN: 0018-9286. DOI: 10.1109/TAC.2008.928119 (cit. on p. 92).

[24] R. D'Andrea and G. E. Dullerud. «Distributed Control Design for Spatially Interconnected Systems.» In: *IEEE Trans. Automat. Contr.* 48.9 (2003), pp. 1478–1495. ISSN: 0018-9286. DOI: 10.1109/TAC.2003.816954 (cit. on pp. 9, 216, 217, 226, 228).

[25] R. D'Andrea and S. Khatri. «Kalman Decomposition of Linear Fractional Transformation Representations and Minimality.» In: *Proc. Amer. Control Conf.* 1997 (cit. on pp. 156, 288).

[26] M. Dettori and C. W. Scherer. «Gain Scheduling Control for a CD Player Mechanism Using LPV Techniques.» In: *Proc. Mediterranean Conf. Contr. & Syst.* 1998 (cit. on p. 95).

[27] S. G. Dietz. «Analysis and Control of Uncertain Systems by Using Robust Semi-Definite Programming.» Ph.D. Thesis. Delft, Netherlands: Delft University of Technology, 2008 (cit. on pp. 168, 309).

[28] S. G. Dietz, C. W. Scherer, and W. Huygen. «Linear Parameter-Varying Controller Synthesis Using Matrix Sum-of-Squares Relaxations.» In: *XVI Brazilian Automat. Conf.* 2006 (cit. on p. 92).

[29] D. V. Dimarogonas and K. J. Kyriakopoulos. «On the Rendezvous Problem for Multiple Nonholonomic Agents.» In: *IEEE Trans. Automat. Contr.* 52.5 (2007), pp. 916–922. ISSN: 0018-9286. DOI: 10.1109/TAC.2007.895897 (cit. on p. 225).

[30] K. Dong and F. Wu. «Robust and Gain-Scheduling Control of LFT Systems Through Duality and Conjugate Lyapunov Functions.» In: *Int. J. Contr.* 80.4 (2007), pp. 555–568. ISSN: 0020-7179. DOI: 10.1080/00207170601080213 (cit. on p. 92).

[31] W. Dong and J. A. Farrell. «Cooperative Control of Multiple Nonholonomic Mobile Agents.» In: *IEEE Trans. Automat. Contr.* 53.6 (2008), pp. 1434–1448. ISSN: 0018-9286. DOI: 10.1109/TAC.2008.925852 (cit. on p. 225).

[32] G. E. Dullerud and R. D'Andrea. «Distributed Control of Heterogeneous Systems.» In: *IEEE Trans. Automat. Contr.* 49.12 (2004), pp. 2113–2128. ISSN: 0018-9286. DOI: 10.1109/TAC.2004.838499 (cit. on pp. 226, 228).

[33] A. Eichler, C. Hoffmann, and H. Werner. «Design of Tutorial Activities and Homework Assignments for a Large-Enrollment Introductory Course in Control Systems.» In: *Proc. IFAC Symp. on Advances in Control Education*. University of Sheffield, 2013, pp. 43–48 (cit. on p. 379).

[34] A. Eichler, C. Hoffmann, and H. Werner. «Robust Control of Decomposable LPV Systems Under Time-Invariant and Time-Varying Interconnection Topologies (Part 1).» In: *Proc. 52nd IEEE Conf. Decision Control*. 2013 (cit. on pp. 225, 379).

[35] A. Eichler, C. Hoffmann, and H. Werner. «Robust Control of Decomposable LPV Systems Under Time-Invariant and Time-Varying Interconnection Topologies (Part 2).» In: *Proc. 52nd IEEE Conf. Decision Control*. 2013 (cit. on p. 379).

[36] A. Eichler, C. Hoffmann, and H. Werner. «Robust Stability Analysis of Interconnected Systems with Uncertain Time-Varying Time Delays via IQCs.» In: *Proc. 52nd IEEE Conf. Decision Control*. 2013 (cit. on pp. 229, 237, 241, 311, 379).

[37] A. Eichler, C. Hoffmann, and H. Werner. «Conservatism of Analysis and Controller Synthesis of Decomposable Systems.» In: *Proc. 19th IFAC World Congr.* 2014 (cit. on p. 378).

[38] A. Eichler, C. Hoffmann, and H. Werner. «Robust Control of Decomposable LPV Systems.» In: *Automatica* 50.12 (2014), pp. 3239–3245. ISSN: 00051098. DOI: 10.1016/j.automatica.2014.10.046 (cit. on pp. 227, 228, 265, 266, 272, 378).

[39] Fan, Michael K. H., A. L. Tits, and J. C. Doyle. «Robustness in the Presence of Mixed Parametric Uncertainty and Unmodeled Dynamics.» In: *IEEE Trans. Automat. Contr.* 36.1 (1991), pp. 25–38. ISSN: 0018-9286 (cit. on p. 48).

[40] J. A. Fax and R. M. Murray. «Information Flow and Cooperative Control of Vehicle Formations.» In: *IEEE Trans. Automat. Contr.* 49.9 (2004), pp. 1465–1476. ISSN: 0018-9286. DOI: 10.1109/TAC.2004.834433 (cit. on pp. 217, 218, 224, 225, 241, 243).

[41] E. Feron, P. Apkarian, and P. Gahinet. «Analysis and Synthesis of Robust Control Systems via Parameter-Dependent Lyapunov Functions.» In: *IEEE Trans. Automat. Contr.* 41.7 (1996), pp. 1041–1046. ISSN: 0018-9286. DOI: 10.1109/9.508913 (cit. on p. 92).

[42] P. Gahinet, P. Apkarian, and M. Chilali. «Affine Parameter-Dependent Lyapunov Functions and Real Parametric Uncertainty.» In: *IEEE Trans. Automat. Contr.* 41.3 (1996), pp. 436–442. ISSN: 0018-9286. DOI: 10.1109/9.486646 (cit. on pp. 6, 62).

[43] S. Geršgorin. «Über die Abgrenzung der Eigenwerte einer Matrix.» In: *Bulletin de l'Académie des Sciences de l'URSS* 6 (1931), pp. 749–754 (cit. on pp. 221, 279).

[44] K. Glover and D. McFarlane. «Robust Stabilization of Normalized Coprime Factor Plant Descriptions with H-Infinity-Bounded Uncertainty.» In: *IEEE Trans. Automat. Contr.* 34.8 (1989), pp. 821–830. ISSN: 0018-9286 (cit. on pp. 119, 319).

[45] P. S. Gonzalez Cisneros, C. Hoffmann, M. Bartels, and H. Werner. «Linear Parameter-Varying Controller Design for a Nonlinear Quad-Rotor Helicopter Model for Use in Distributed Formation Control Schemes.» In: *Proc. 54th IEEE Conf. Decision Control*. 2015 (cit. on p. 277).

[46] P. S. Gonzalez Cisneros, C. Hoffmann, M. Bartels, and H. Werner. «Linear Parameter-Varying Controller Design for a Nonlinear Quad-Rotor Helicopter Model for High Speed Trajectory Tracking.» In: *Proc. Amer. Control Conf.* 2016 (cit. on pp. 285–288, 378).

[47] U. Gürcüoğlu. «Hybrid Position/Force Control of A Robot Manipulator Using LPV Techniques.» Master's Thesis. 2011 (cit. on p. 335).

[48] Y. Hamada, T. Ohtani, T. Kida, and T. Nagashio. ≪A New Gain Scheduling Controller Synthesis and its Application to Attitude Control Systems of a Large Flexible Satellite.≫ In: *Proc. Int. Conf. Control Applicat.* 2006, pp. 2914–2920 (cit. on p. 99).

[49] F. Harary. *Graph Theory*. Reading, Mass.: Perseus Books, 1999. ISBN: 9780201410334 (cit. on p. 245).

[50] D. J. Hartfiel. ≪Dense Sets of Diagonalizable Matrices.≫ In: *Proc. Amer. Math. Soc.* 123.6 (1995), pp. 1669–1672 (cit. on p. 241).

[51] D. J. Hartfiel. *Matrix Theory and Applications With MATLAB*. Boca Raton, Fla.: CRC Press, 2001. ISBN: 9781584881087 (cit. on p. 241).

[52] S. Hecker, A. Varga, and J.-F. Magni. ≪Enhanced LFR-toolbox for MATLAB and LFT-based gain scheduling.≫ In: *ONERA-DLR Aerospace Symposium*. 2004 (cit. on p. 82).

[53] A. Helmersson. ≪Methods for Robust Gain-Scheduling.≫ Ph.D. Thesis. Sweden: Linköping University, 1995 (cit. on pp. 48, 117).

[54] C. Hoffmann, A. Eichler, and H. Werner. ≪Distributed Control of Linear Parameter-Varying Decomposable Systems.≫ In: *Proc. Amer. Control Conf.* 2013, pp. 2386–2391 (cit. on pp. 225, 227–229, 241, 249, 378).

[55] C. Hoffmann, A. Eichler, and H. Werner. ≪Control of Heterogeneous Groups of LPV Systems Interconnected Through Directed and Switching topologies.≫ In: *Proc. Amer. Control Conf.* 2014, pp. 5156–5161. DOI: 10.1109/ACC.2014.6858631 (cit. on pp. 226–229, 249, 253, 261–263, 267, 269, 378).

[56] C. Hoffmann, A. Eichler, and H. Werner. ≪Control of Heterogeneous Groups of Systems Interconnected Through Directed and Switching Topologies.≫ In: *IEEE Trans. Automat. Contr.* 60.7 (2015), pp. 1904–1909. ISSN: 0018-9286. DOI: 10.1109/TAC.2014.2362595 (cit. on pp. 226–229, 241, 249, 253, 267, 279, 290, 291, 322, 377).

[57] C. Hoffmann, S. M. Hashemi, H. S. Abbas, and H. Werner. ≪Synthesis of LPV Controllers With Reduced Implementation Complexity.≫ In: *Proc. Amer. Control Conf.* 2014, pp. 3766–3771. DOI: 10.1109/ACC.2014.6858716 (cit. on pp. 23, 25, 26, 80, 117, 160, 377).

[58] C. Hoffmann and H. Werner. ≪Complexity of Implementation and Synthesis in Linear Parameter-Varying Control.≫ In: *Proc. 19th IFAC World Congr.* 2014, pp. 11749–11760 (cit. on pp. 19, 76, 377).

[59] C. Hoffmann and H. Werner. ≪A Survey of Linear Parameter-Varying Control Applications Validated by Experiments or High-Fidelity Simulations.≫ In: *IEEE Trans. Contr. Syst. Technol.* 23.2 (2015), pp. 416–433. ISSN: 1063-6536. DOI: 10.1109/TCST.2014.2327584 (cit. on pp. 4, 6, 82, 91, 377).

[60] C. Hoffmann and H. Werner. ≪Compact LFT-LPV Modeling With Automated Parameterization for Efficient LPV Controller Synthesis.≫ In: *Proc. Amer. Control Conf.* 2015 (cit. on pp. 18, 117, 123, 139, 160, 176, 377).

[61] C. Hoffmann and H. Werner. ≪Control of Heterogeneous LPV Subsystems Interconnected through Arbitrary Directed and Switching Topologies.≫ In: *Proc. 54th IEEE Conf. Decision Control*. 2015 (cit. on pp. 226–229, 249, 277, 377).

[62] C. Hoffmann and H. Werner. *Reglerentwurf für verteilte, nicht-lineare, heterogene Systeme bei zeitlich veränderlicher Interaktionstopologie mit Hilfe multiplier-basierter konvexer Optimierungsmethoden*. Boppard, Rheinland-Pfalz, Germany, 2015 (cit. on p. 379).

[63] Hol, C. W. J. and C. W. Scherer. ≪Sum-of-Squares Relaxations for Robust Polynomial Semi-Definite Programs.≫ In: *Proc. 16th IFAC World Congr.* 2005 (cit. on p. 168).

[64] S. Ilie and C. Bădică. «Multi-Agent Distributed Framework for Swarm Intelligence.» In: *Procedia Comput. Sci.* 18 (2013), pp. 611–620. ISSN: 18770509. DOI: 10.1016/j.procs.2013.05.225 (cit. on p. 218).

[65] T. Iwasaki. «LPV System Analysis With Quadratic Separator.» In: *Proc. 37th IEEE Conf. Decision Contr.* Florida and USA, 1998 (cit. on p. 41).

[66] T. Iwasaki and G. Shibata. «LPV System Analysis via Quadratic Separator for Uncertain Implicit Systems.» In: *IEEE Trans. Automat. Contr.* 46.8 (2001), pp. 1195–1208. ISSN: 0018-9286 (cit. on pp. 36, 81).

[67] B. E. Jackson, C. I. Cruz, and W. A. Ragsdale. *Real-Time Simulation Model of the HL-20 Lifting Body: NASA Technical Memorandum.* 1992 (cit. on p. 93).

[68] J. M. Jonkman and Buhl Jr., Marshall L. *FAST Users's Guide.* 2005. URL: http://www.osti.gov/bridge (cit. on p. 91).

[69] G. Kaiser, Q. Liu, C. Hoffmann, M. Korte, and H. Werner. «Torque Vectoring for an Electric Vehicle Using an LPV Drive Controller and a Torque and Slip Limiter.» In: *Proc. 51st IEEE Conf. Decision Control.* 2012, pp. 5016–5021 (cit. on p. 379).

[70] C.-Y. Kao and A. Rantzer. «Robust Stability Analysis of Linear Systems With Time-Varying Delays.» In: *Proc. 16th IFAC World Congr.* 2005 (cit. on p. 246).

[71] H. K. Khalil. *Nonlinear systems.* 3rd ed. Upper Saddle River, N.J.: Prentice Hall, 2002. ISBN: 9780131227408 (cit. on p. 109).

[72] W. Khalil and E. Dombre. *Modeling, Identification and Control of Robots.* Kogan Page Science , UK, 2004. ISBN: 190399666X (cit. on p. 335).

[73] A. Knoblach, M. Assanimoghaddam, H. Pfifer, and F. Saupe. «Robust Performance Analysis: A Review of Techniques for Dealing with Infinite Dimensional LMIs.» In: *Proc. Int. Conf. Control Applicat.* 2013 (cit. on p. 61).

[74] E. Köse and C. W. Scherer. «Gain-Scheduled Control Using Dynamic Integral Quadratic Constraints.» In: *Proc. 5th IFAC Symp. Robust Control Des.* 2006, pp. 220–225 (cit. on p. 70).

[75] T. Kurz and P. Eberhard. «Symbolic Modeling and Analysis of Elastic Multibody Systems.» In: *Intl. Symp. Coupled Methods in Numerical Dyn.* 2009 (cit. on p. 146).

[76] A. Kwiatkowski, J. P. Blath, H. Werner, and M. Schultalbers. «Application of LPV Gain Scheduling to Charge Control of an SI Engine.» In: *Proc. Conf. Comput. Aided Control Syst. Des.* 2006, pp. 2327–2331. DOI: 10.1109/CACSD-CCA-ISIC.2006.4777003 (cit. on p. 25).

[77] A. Kwiatkowski, M. Boll, and H. Werner. «Automated Generation and Assessment of Affine LPV Models.» In: *Proc. 45th IEEE Conf. Decision Control.* 2006, pp. 6690–6695 (cit. on pp. 103, 104, 111, 112).

[78] A. Kwiatkowski and H. Werner. «LPV Control of a 2-DOF Robot Using Parameter Reduction.» In: *Proc. 44th IEEE Conf. Decision Contr.* 2005, pp. 3369–3374 (cit. on p. 19).

[79] A. Kwiatkowski and H. Werner. «PCA-Based Parameter Set Mappings for LPV Models With Fewer Parameters and Less Overbounding.» In: *IEEE Trans. Contr. Syst. Technol.* 16.4 (2008), pp. 781–788. ISSN: 1063-6536. DOI: 10.1109/TCST.2007.903094 (cit. on pp. 6, 18, 25, 26, 98, 136, 188).

[80] C. Langbort, R. S. Chandra, and R. D'Andrea. «Distributed Control Design for Systems Interconnected Over an Arbitrary Graph.» In: *IEEE Trans. Automat. Contr.* 49.9 (2004), pp. 1502–1519. ISSN: 0018-9286. DOI: 10.1109/TAC.2004.834123 (cit. on pp. 8, 11, 218, 226–228, 236, 237, 241, 243, 274, 301).

[81] C. Langbort and R. D'Andrea. «Distributed Control of Spatially Reversible Interconnected Systems with Boundary Conditions.» In: *SIAM J. Control & Opt.* 44.1 (2005), pp. 1–28. ISSN: 0363-0129. DOI: 10.1137/S0363012902415803 (cit. on p. 226).

[82] D. Lara, A. Sanchez, R. Lozano, and P. Castillo. «Real-Time Embedded Control System for VTOL Aircrafts: Application to Stabilize a Quad-Rotor Helicopter.» In: *Proc. Int. Conf. Control Applicat.* 2006 (cit. on p. 287).

[83] D. J. Leith and W. E. Leithead. *Comments On the Prevalence of Linear Parameter Varying Systems: Technical report*. Glasgow, UK, 1999 (cit. on p. 3).

[84] D. J. Leith and W. E. Leithead. «On Formulating Nonlinear Dynamics in LPV Form.» In: *Proc. 39th IEEE Conf. Decision Contr.* 2000, pp. 3526–3527 (cit. on p. 3).

[85] D. J. Leith and W. E. Leithead. «Survey of Gain-Scheduling Analysis & Design.» In: *Int. J. Contr.* 73.11 (2000), pp. 1001–1025. ISSN: 0020-7179 (cit. on p. 3).

[86] L. Li and F. Paganini. «Structured Coprime Factor Model Reduction Based on LMIs.» In: *Automatica* 41.1 (2005), pp. 145–151. ISSN: 00051098. DOI: 10.1016/j.automatica.2004.09.003 (cit. on p. 308).

[87] Y. Li and Z.-L. Zhang. «Random Walks on Digraphs, the Generalized Digraph Laplacian and the Degree of Asymmetry.» In: *Algorithms and Models for the Web-Graph*. Ed. by D. Hutchison, T. Kanade, J. Kittler, J. M. Kleinberg, F. Mattern, J. C. Mitchell, M. Naor, O. Nierstrasz, C. Pandu Rangan, B. Steffen, M. Sudan, D. Terzopoulos, D. Tygar, M. Y. Vardi, G. Weikum, R. Kumar, and D. Sivakumar. Vol. 6516. Lecture Notes in Computer Science. Berlin, Heidelberg: Springer Berlin Heidelberg, 2010, pp. 74–85. ISBN: 9783642180088. DOI: 10.1007/978-3-642-18009-5_8 (cit. on pp. 259, 260).

[88] F. Liao, Z. Ren, M. Tomizuka, and J. Wu. «Preview Control for Impulse-Free Continuous-Time Descriptor Systems.» In: *Int. J. Contr.* 88.6 (2015), pp. 1142–1149. ISSN: 0020-7179. DOI: 10.1080/00207179.2014.996769 (cit. on p. 115).

[89] J. Liceaga and E. Liceaga. «Multivariable Gyroscope Control by Individual Channel Design.» In: *Proc. Int. Conf. Contr. Applicat.* 2005, pp. 785–790. DOI: 10.1109/CCA.2005.1507224 (cit. on p. 145).

[90] Q. Liu, C. Hoffmann, and H. Werner. «Distributed Control of Parameter-Varying Spatially Interconnected Systems Using Parameter-Dependent Lyapunov Functions.» In: *Proc. Amer. Control Conf.* 2013, pp. 3278–3283 (cit. on pp. 217, 227, 228, 310, 379).

[91] Q. Liu, A. Mendez Gonzalez, and H. Werner. «Distributed Control of Spatially-Interconnected Parameter-Invariant and LPV Models for Actuated Beams.» In: *Proc. Amer. Control Conf.* 2014 (cit. on p. 227).

[92] M. Löhning. «Robust Control of Elastic Robots.» Ph.D. Thesis. TUHH, Eissendorfer Str. 40, 21073 Hamburg, Germany, 2011 (cit. on p. 178).

[93] J.-F. Magni. *User Manual of the Linear Fractional Representation Toolbox: Version 2.0*. 2006 (cit. on pp. 156, 288).

[94] A. Mandadzhiev. «Robust Controller Synthesis via the Edge Laplacian.» Project Work. 2010 (cit. on p. 93).

[95] A. Marcos and S. Bennani. «LPV Modeling, Analysis and Design in Space Systems: Rationale, Objectives and Limitations.» In: *Proc. AIAA Guidance, Navigation, Control Conf.* 2009. DOI: 10.2514/6.2009-5633 (cit. on p. 93).

[96] A. Marcos, M. L. Kerr, G. de Zaiacomo, L. Peñin, Z. Szabó, J. Bokor, and G. Rodonyi. «Application of LPV/LFT Modeling and Data-Based Validation to a Re-Entry Vehicle.» In: *Proc. AIAA Guidance, Navigation, Control Conf.* 2009. DOI: 10.2514/6.2009-5634 (cit. on p. 93).

[97] P. Massioni. «Decomposition Methods for Distributed Control and Identification.» PhD. Netherlands: Delft University of Technology, 2010 (cit. on pp. 8, 217, 227–229, 241, 243, 244).

[98] P. Massioni. «Distributed Control for Alpha-Heterogeneous Dynamically Coupled Systems.» In: *Syst. & Contr. Letters* 72 (2014), pp. 30–35. ISSN: 0167-6911. DOI: 10.1016/j.sysconle.2014.08.006 (cit. on pp. 8, 11, 226, 228, 268, 269, 274, 278–284, 290, 291, 293, 295, 302, 337).

[99] P. Massioni and M. Verhaegen. «Distributed Control for Identical Dynamically Coupled Systems: A Decomposition Approach.» In: *IEEE Trans. Automat. Contr.* 54.1 (2009), pp. 124–135. ISSN: 0018-9286. DOI: 10.1109/TAC.2008.2009574 (cit. on pp. 218, 225, 226, 243, 244, 301).

[100] P. Massioni and M. Verhaegen. «A Full Block S-Procedure Application to Distributed Control.» In: *Proc. Amer. Control Conf.* 2010 (cit. on pp. 225, 226, 243, 244, 301).

[101] S. Mastellone, D. M. Stipanovic, C. R. Graunke, K. A. Intlekofer, and M. W. Spong. «Formation Control and Collision Avoidance for Multi-agent Non-Holonomic Systems: Theory and Experiments.» In: *Int. J. Robotics Research* 27.1 (2008), pp. 107–126. DOI: 10.1177/0278364907084441 (cit. on p. 225).

[102] I. Masubuchi. «Synthesis of Output Feedback Controllers for Descriptor Systems Satisfying Closed-Loop Dissipativity.» In: *Proc. 44th IEEE Conf. Decision Contr.* 2005, pp. 5012–5017 (cit. on p. 173).

[103] I. Masubuchi, A. Kume, and E. Shimemura. «Spline-Type Solution to Parameter-Dependent LMIs.» In: *Proc. 37th IEEE Conf. Decision Contr.* Florida and USA, 1998 (cit. on p. 99).

[104] A. Megretski and A. Rantzer. «System Analysis Via Integral Quadratic Constraints.» In: *IEEE Trans. Automat. Contr.* 42.6 (1997). ISSN: 0018-9286 (cit. on pp. 34, 237).

[105] G. Meinsma, Y. Shrivastava, and M. Fu. «A Dual Formulation Of Mixed Mu And On The Losslessness Of (D,G) Scaling.» In: *IEEE Trans. Automat. Contr.* 42.7 (1997), pp. 1032–1036. ISSN: 0018-9286 (cit. on p. 87).

[106] A. Mendez Gonzalez, C. Hoffmann, and H. Werner. «LPV Formation Control for Non-Holonomic Agents with Directed and Switching Communication Topologies.» In: *Proc. 54th IEEE Conf. Decision Control.* 2015 (cit. on pp. 311, 378).

[107] A. Mendez Gonzalez and H. Werner. «LPV Formation Control of Non-Holonomic Multi-Agent Systems.» In: *Proc. 19th IFAC World Congr.* 2014 (cit. on pp. 225, 285, 311).

[108] P. Menon, E. Prempain, I. Postlethwaite, D. Bates, and S. Bennani. «An LPV Loop Shaping Controller Design for the NASA-HL-20 Re-Entry Vehicle.» In: *Proc. AIAA Guidance, Navigation, Control Conf.* 2009. DOI: 10.2514/6.2009-5635 (cit. on p. 93).

[109] M. Mesbahi and M. Egerstedt. *Graph theoretic methods in multiagent networks*. Princeton series in applied mathematics. Princeton and Oxford: Princeton University Press, 2010. ISBN: 9780691140612 (cit. on pp. 8, 218, 220, 301).

[110] T. Oehlschlägel, C. Heise, S. Theil, and T. Steffen. «Stability Analysis of Closed Loops of Non-Linear Systems and LPV Controllers Designed Using Approximated Quasi-LPV Systems.» In: *7th IFAC Symp. Robust Control Des.* 2012 (cit. on p. 25).

[111] R. Olfati-Saber and R. M. Murray. «Consensus Problems in Networks of Agents With Switching Topology and Time-Delays.» In: *IEEE Trans. Automat. Contr.* 49.9 (2004), pp. 1520–1533. ISSN: 0018-9286. DOI: 10.1109/TAC.2004.834113 (cit. on p. 311).

[112] M. C. de Oliveira and R. E. Skelton. «Stability Tests for Constrained Linear Systems.» In: *Perspectives in Robust Control*. Ed. by S. R. Moheimani. Vol. 268. Lecture Notes in Control and Information Sciences. London: Springer London, 2001, pp. 241–257. ISBN: 9781852334529. DOI: 10.1007/BFb0110624 (cit. on pp. 34, 39).

[113] T. R. Parks. *Manual for Model 750 Control Moment Gyroscope*. 1999 (cit. on p. 147).

[114]   H. Pfifer and P. J. Seiler. «An Overview of Integral Quadratic Constraints for Delayed Nonlinear and Parameter-Varying Systems.» In: *arXiv* (2015) (cit. on p. 311).

[115]   U. Pilz, A. Popov, and H. Werner. «An Information Flow Filter Approach to Cooperative Vehicle Control.» In: *Proc. 18th IFAC World Congr.* 2011, pp. 7432–7437. DOI: 10.3182/20110828-6-IT-1002.01102 (cit. on pp. 9, 295, 310).

[116]   U. Pilz and H. Werner. «An H-One Control Approach to Cooperative Control of Multi-Agent Systems.» In: *Proc. 51st IEEE Conf. Decision Control.* 2012. DOI: 10.1109/CDC.2012.6426879 (cit. on pp. 225, 228).

[117]   A. Popov and H. Werner. «Robust Stability of a Multi-Agent System under Arbitrary and Time-Varying Communication Topologies and Communication Delays.» In: *IEEE Trans. Automat. Contr.* 57.9 (2012), pp. 2343–2347. ISSN: 0018-9286. DOI: 10.1109/TAC.2012.2186094 (cit. on p. 225).

[118]   L. Qiu and S. Hara, eds. *Developments in Control Theory Towards Glocal Control.* Vol. v. 76. IET control engineering series. London, UK: Institution of Engineering and Technology, 2012. ISBN: 9781849195348 (cit. on p. 7).

[119]   C. G. Rieger, D. I. Gertman, and M. A. McQueen. «Resilient Control Systems: Next Generation Design Research.» In: *Proc. 2nd Conf. Human Syst. Interact.* 2009, pp. 632–636. DOI: 10.1109/HSI.2009.5091051 (cit. on p. 7).

[120]   M. G. Safonov. «Origins of Robust Control: Early History and Future Speculations.» In: *Annual Rev. Contr.* 36.2 (2012), pp. 173–181. ISSN: 13675788. DOI: 10.1016/j.arcontrol.2012.09.001 (cit. on p. 3).

[121]   Schaft, A. J. van der and J. M. Schumacher. *An Introduction to Hybrid Dynamical Systems.* Vol. 251. Lecture Notes in Control and Information Sciences. London and New York: Springer, 2000. ISBN: 9781852332334 (cit. on p. 3).

[122]   W. Scheibner. «Systemidentifikation und Modellierung eines Quadrokopters.» Bachelor Thesis. 2014 (cit. on p. 287).

[123]   C. W. Scherer. «A Full Block S-Procedure With Applications.» In: *Proc. 36th IEEE Conf. Decision Contr.* Vol. 3. California, 1997, pp. 2602–2607. DOI: 10.1109/CDC.1997.657769 (cit. on pp. 34, 51).

[124]   C. W. Scherer. «Robust Mixed Control and LPV Control with Full Block Scalings.» In: *Advances in Linear Matrix Inequality Methods in Control.* Ed. by L. El Ghaoui and S.-I. Niculescu. Philadelphia, PA: SIAM, 2000. ISBN: 0898714389 (cit. on pp. 4, 21, 36, 46, 66, 69, 70, 81, 92, 95, 206, 270).

[125]   C. W. Scherer. «LPV Control and Full Block Multipliers.» In: *Automatica* 37.3 (2001), pp. 361–375. ISSN: 00051098. DOI: 10.1016/S0005-1098(00)00176-X (cit. on pp. 4, 6, 18, 21, 34–36, 44–47, 65, 66, 68, 70–72, 92, 117, 118, 134, 262, 270, 272, 321).

[126]   C. W. Scherer. «Gain-Scheduling Control With Dynamic Multipliers by Convex Optimization.» In: (2014) (cit. on pp. 309, 310).

[127]   A.-K. Schug, A. Eichler, and H. Werner. «A Decentralized Asymmetric Weighting Approach for Improved Convergence of Multi-Agent Systems with Directed Interaction.» In: *Proc. 19th IFAC World Congr.* 2014 (cit. on p. 284).

[128]   L. Sciavicco and B. Siciliano. *Modelling and Control of Robot Manipulators.* 2nd ed. Advanced textbooks in control and signal processing. London and New York: Springer, 2000. ISBN: 9781852332211 (cit. on p. 176).

[129]   G. Scorletti and L. El Ghaoui. «Improved Linear Matrix Inequality Conditions for Gain Scheduling.» In: *Proc. 34th IEEE Conf. Decision Contr.* Vol. 4. 1995, pp. 3626–3631 (cit. on pp. 4, 92).

[130] G. Scorletti and L. El Ghaoui. «Improved LMI Conditions for Gain Scheduling and Related Control Problems.» In: *Int. J. Robust Nonlinear Contr.* 8 (1998), pp. 845–877. ISSN: 10498923 (cit. on pp. 4, 48, 49, 52, 53, 70, 92).

[131] R. Seifried, ed. *Dynamics of Underactuated Multibody Systems: Modeling, Control and Optimal Design*. Vol. volume 205. Solid Mechanics and its Applications. 2014. ISBN: 9783319012278 (cit. on pp. 103, 104).

[132] G. S. Seyboth, G. S. Schmidt, and F. Allgöwer. «Cooperative Control of Linear Parameter-Varying Systems.» In: *Proc. Amer. Control Conf.* 2012 (cit. on pp. 225, 227, 228).

[133] J. S. Shamma. «Analysis and Design of Gain Scheduled Control Systems.» Ph.D. Thesis. Massachusetts Institute of Technology, 1988 (cit. on pp. 3, 4, 16).

[134] J. S. Shamma. «An Overview of LPV Systems.» In: *Control of Linear Parameter Varying Systems with Applications*. Ed. by J. Mohammadpour and C. W. Scherer. Boston, MA: Springer US, 2012. ISBN: 9781461418337 (cit. on p. 2).

[135] J. S. Shamma and M. Athans. «Analysis of Gain Scheduled Control for Nonlinear Plants.» In: *IEEE Trans. Automat. Contr.* 35.8 (1990), pp. 898–907. ISSN: 0018-9286. DOI: 10.1109/9.58498 (cit. on pp. 3, 4).

[136] J. S. Shamma and M. Athans. «Guaranteed properties of gain scheduled control for linear parameter-varying plants.» In: *Automatica* 27.3 (1991), pp. 559–564. ISSN: 00051098. DOI: 10.1016/0005-1098(91)90116-J (cit. on p. 3).

[137] J. S. Shamma and M. Athans. «Gain Scheduling: Potential Hazards and Possible Remedies.» In: *IEEE Contr. Syst. Mag.* 12.3 (1992), pp. 101–107. ISSN: 0272-1708 (cit. on p. 4).

[138] S. H. Sheth. «PSM Based LPV Modelling and Control of the ECP Model 750 Control Moment Gyroscope.» Project Work. 2012 (cit. on p. 3).

[139] Y. Shoham and K. Leyton-Brown. *Multiagent systems: Algorithmic, game-theoretic, and logical foundations*. Cambridge and New York: Cambridge University Press, 2009. ISBN: 9780521899437 (cit. on p. 216).

[140] B. Siciliano and O. Khatib. *Springer Handbook of Robotics*. Berlin and Heidelberg: Springer, 2008. ISBN: 9783540239574 (cit. on p. 176).

[141] S. Skogestad and I. Postlethwaite. *Multivariable Feedback Control - Analysis and Design*. 2nd. John Wiley & Sons, Ltd, 2005. ISBN: 9780470011683 (cit. on p. 205).

[142] Z. Szabó, Z. Biro, and J. Bokor. «Möbius Transform and Efficient LPV Synthesis.» In: *Proc. 51st IEEE Conf. Decision Control.* 2012 (cit. on p. 70).

[143] Z. Szabó, Z. Biro, P. Gaspar, and J. Bokor. «Controller Scheduling Blocks in Non-Conservative LPV Design.» In: *5th IFAC Symp. Syst. Struct. Control.* 2013, pp. 671–676 (cit. on pp. 47, 70).

[144] Z. Szabó, A. Marcos, D. Mostaza, M. L. Kerr, G. Rodonyi, J. Bokor, and S. Bennani. «Development of an Integrated LPV/LFT Framework: Modeling and Data-Based Validation Tool.» In: *IEEE Trans. Contr. Syst. Technol.* 19.1 (2011), pp. 104–117. ISSN: 1063-6536. DOI: 10.1109/TCST.2010.2072783 (cit. on p. 93).

[145] Tenreiro Machado, J. A., Martins de Carvalho, J. L., and Galhano, Alexandra M. S. F. «Analysis of Robot Dynamics and Compensation Using Classical and Computed Torque Techniques.» In: *IEEE Trans. Educ.* 36.4 (1993), pp. 372–379. ISSN: 0018-9359 (cit. on p. 178).

[146] R. Toth. *Modeling and Identification of Linear Parameter-Varying Systems*. Berlin: Springer Berlin, Heidelberg, New York and Springer, 2010. ISBN: 9783642138126 (cit. on pp. 6, 102–105, 111, 112, 114, 148, 300).

[147] E. J. Townsend. *Functions Of A Complex Variable*. 2009. ISBN: 1110354487 (cit. on p. 19).

[148] H. D. Tuan and P. Apkarian. «Relaxations of Parameterized LMIs With Control Applications.» In: *Proc. 37th IEEE Conf. Decision Contr.* Florida and USA, 1998, pp. 1747–1752. DOI: 10.1109/CDC.1998.758548 (cit. on p. 92).

[149] A. Varga and G. Looye. «Symbolic and Numerical Software Tools for LFT-Based Low Order Uncertainty Modeling.» In: *Proc. Int. Symp. Comput.-Aided Control Syst. Des.* 1999 (cit. on pp. 154, 288).

[150] J. Veenman, H. Köroglu, and C. W. Scherer. «Analysis of the Controlled NASA HL20 Atmospheric Re-Entry Vehicle Based on Dynamic IQCs.» In: *Proc. AIAA Guidance, Navigation, Control Conf.* 2009. DOI: 10.2514/6.2009-5637 (cit. on p. 93).

[151] J. Veenman and C. W. Scherer. «A Synthesis Framework for Robust Gain-Scheduling Controllers.» In: *Automatica* 50.11 (2014), pp. 2799–2812. ISSN: 00051098. DOI: 10.1016/j.automatica.2014.10.002 (cit. on p. 311).

[152] J. Veenman, C. W. Scherer, and H. Köroglu. «IQC-Based LPV Controller Synthesis for the NASA HL20 Atmospheric Re-entry Vehicle.» In: *Proc. AIAA Guidance, Navigation, Control Conf.* 2009. DOI: 10.2514/6.2009-5636 (cit. on p. 93).

[153] J. Veenman, C. W. Scherer, and H. Köroglu. «Robust Stability and Performance Analysis With Integral Quadratic Constraints.» In: *Preprint Series Stuttgart Res. Centre Sim. Technol.* (2015) (cit. on p. 311).

[154] J. J. P. Veerman, G. Lafferriere, J. S. Caughman, and A. Williams. «Flocks and Formations.» In: *J. Stat. Phys.* 121.5-6 (2005), pp. 901–936. ISSN: 0022-4715. DOI: 10.1007/s10955-005-6999-9 (cit. on p. 221).

[155] P. Viccione, C. W. Scherer, and M. Innocenti. «LPV Synthesis with Integral Quadratic Constraints for Distributed Control of Interconnected Systems.» In: *Proc. 6th IFAC Symp. Robust Control Des.* 2009, pp. 13–18. DOI: 10.3182/20090616-3-IL-2002.00003 (cit. on p. 310).

[156] M. Vidyasagar. *Nonlinear Systems Analysis.* 2nd. Classics in Applied Mathematics. 3600 University City Science Center, Philadelphia, PA 19104-2688: SIAM, 2002. ISBN: 0898715261 (cit. on pp. 29–31).

[157] G. Vinniecombe. «A n-Gap Distance for Uncertain and Nonlinear Systems.» In: *Proc. 38th IEEE Conf. Decision Contr.* 1999 (cit. on p. 308).

[158] J. Warren, S. Schaefer, A. N. Hirani, and M. Desbrun. «Barycentric Coordinates for Convex Sets.» In: *Adv. Comput. Math.* 27.3 (2007), pp. 319–338. ISSN: 1019-7168. DOI: 10.1007/s10444-005-9008-6 (cit. on pp. 25, 79, 324).

[159] S. Wollnack, C. Hoffmann, and H. Werner. «Affine LPV Controller Design with Linear Growth of the Number of LMI Constraints.» In: *Proc. Amer. Control Conf.* 2013 (cit. on p. 378).

[160] F. Wu. «Control of Linear Parameter Varying Systems.» Ph.D. Thesis. California and USA: University of Berkeley, 1995 (cit. on pp. 16, 17, 31–34, 38, 60, 61, 95, 169).

[161] F. Wu. «A Generalized LPV System Analysis and Control Synthesis Framework.» In: *Int. J. Contr.* 74.7 (2001), pp. 745–759. ISSN: 0020-7179 (cit. on pp. 4, 22, 36, 43, 44, 59, 64, 65, 67, 92, 117, 118, 167, 330, 332).

[162] F. Wu. «Distributed Control for Interconnected Linear Parameter-Dependent Systems.» In: *IEE Proc., Control Theory Appl.* 150.5 (2003), pp. 518–527. ISSN: 13502379. DOI: 10.1049/ip-cta:20030706 (cit. on pp. 226–228, 310).

[163] F. Wu and K. Dong. «Gain-Scheduling Control of LFT Systems Using Parameter-Dependent Lyapunov Functions.» In: *Automatica* 42.1 (2006), pp. 39–50. ISSN: 00051098. DOI: 10.1016/j.automatica.2005.08.020 (cit. on pp. 4, 6, 36, 41, 42, 58, 59, 63, 64, 92, 117, 170, 173, 309, 319, 325, 326).

[164] F. Wu, X. Yang, A. K. Packard, and G. Becker. «Induced L2-Norm Control for LPV Systems with Bounded Parameter Variation Rates.» In: *Int. J. Robust Nonlinear Contr.* 6.9-10 (1996), pp. 983–998. ISSN: 10498923 (cit. on pp. 4, 92).

[165] T. Yang, Z. Liu, H. Che, and R. Pei. «Distributed Robust Control of Multiple Mobile Robots Formations via Moving Horizon Strategy.» In: *Proc. Amer. Control Conf.* 2006. DOI: 10.1109/ACC.2006.1656654 (cit. on p. 225).

[166] K. Zhou, J. C. Doyle, and K. Glover. *Robust and Optimal Control.* Prentice-Hall, N.J., USA, 1996. ISBN: 0134565673 (cit. on pp. 27, 38, 257, 315–320).

Experimental LPV Control Applications

[E1] H. S. Abbas, A. Ali, S. M. Hashemi, and H. Werner. «LPV Gain-Scheduled Control of a Control Moment Gyroscope.» In: *Proc. Amer. Control Conf.* 2013 (cit. on pp. 92–94, 96–98, 145, 147, 149).

[E2] H. S. Abbas, S. M. Hashemi, and H. Werner. «Decentralized LPV Gain-Scheduled PD Control of a Robotic Manipulator.» In: *Proc. ASME Dyn. Syst. Control Conf.* 2009. DOI: 10.1115/DSCC2009-2651 (cit. on pp. 92, 93, 97).

[E3] A. Abdullah and M. Zribi. «Control Schemes for a Quadruple Tank Process.» In: *Int. J. Comput. Commun.* 7.4 (2012), pp. 594–605. ISSN: 1841-9836 (cit. on pp. 92–95, 97).

[E4] E. Alfieri, A. Amstutz, Onder, Christopher H., and L. Guzzella. «Automatic Design and Parametrization of a Model-Based Controller Applied to the AF-Ratio Control of a Diesel Engine.» In: *5th IFAC Symp. Adv. Automotive Control.* 2007 (cit. on pp. 93, 97).

[E5] D. Andreo, V. Cerone, D. Dzung, and D. Regruto. «Experimental Results on LPV Stabilization of a Riderless Bicycle.» In: *Proc. Amer. Control Conf.* 2009. DOI: 10.1109/ACC.2009.5160397 (cit. on pp. 92, 93, 97).

[E6] H. M. N. K. Balini, J. Witte, and C. W. Scherer. «Synthesis and Implementation of Gain-Scheduling and LPV Controllers for an AMB System.» In: *Automatica* 48.3 (2012), pp. 521–527. ISSN: 00051098. DOI: 10.1016/j.automatica.2011.08.061 (cit. on pp. 92, 93, 95, 97).

[E7] P. Ballesteros and C. Bohn. «A Frequency-Tunable LPV Controller for Narrowband Active Noise and Vibration Control.» In: *Proc. Amer. Control Conf.* 2011 (cit. on pp. 92–95, 97).

[E8] P. Ballesteros and C. Bohn. «Disturbance Rejection through LPV Gain-Scheduling Control with Application to Active Noise Cancellation.» In: *Proc. 18th IFAC World Congr.* 2011 (cit. on pp. 92–95, 97).

[E9] P. Ballesteros, X. Shu, and C. Bohn. «A Discrete-time MIMO LPV Controller for the Rejection of Nonstationary Harmonically Related Multisine Disturbances.» In: *Proc. Amer. Control Conf.* 2014, pp. 4464–4469 (cit. on pp. 92, 93, 95, 97).

[E10] P. Ballesteros, X. Shu, and C. Bohn. «Active Control of Engine-Induced Vibrations in Automotive Vehicles through LPV Gain Scheduling.» In: *SAE Int. J. Passeng. Cars – Electron. Electr. Syst.* 7.1 (2014), pp. 264–272. ISSN: 1946-4622. DOI: 10.4271/2014-01-1686 (cit. on pp. 92, 93, 95, 97).

[E11] P. Ballesteros, X. Shu, W. Heins, and C. Bohn. «LPV Gain-Scheduled Output Feedback for Active Control of Harmonic Disturbances with Time-Varying Frequencies.» In: *Advances on Analysis and Control of Vibrations.* Ed. by M. Zapateiro de la Hoz and F. Pozo. InTech, 2012, pp. 65–86. ISBN: 9789535106999. DOI: 10.5772/50294 (cit. on pp. 92–95, 97).

[E12] P. Ballesteros, X. Shu, W. Heins, and C. Bohn. «Reduced-Order Two-Parameter pLPV Controller for the Rejection of Nonstationary Harmonically Related Multisine Disturbances.» In: *Proc. Europ. Control Conf.* 2013 (cit. on pp. 92–95, 97, 98).

[E13]   J. D. Bendtsen and K. Trangbæk. ≪Discrete-Time LPV Current Control of an Induction Motor.≫ In: *Proc. 42nd IEEE Conf. Decision Contr.* 2003, pp. 5903–5908 (cit. on pp. 92–95, 97).

[E14]   F. D. Bianchi, C. Kunusch, C. Ocampo-Martinez, and R. S. Sanchez-Pena. ≪A Gain-Scheduled LPV Control for Oxygen Stoichiometry Regulation in PEM Fuel Cell Systems.≫ In: *IEEE Trans. Contr. Syst. Technol.* 22.5 (2014), pp. 1837–1844. ISSN: 1063-6536. DOI: 10.1109/TCST.2013.2288992 (cit. on pp. 92, 93, 96, 97).

[E15]   Y. Bolea, V. Puig, J. Blesa, M. Gómez, and J. Rodellar. ≪LPV vs. Multi-Model PI(D) Gain-Scheduling Applied to Canal Control.≫ In: *Proc. 16th IFAC World Congr.* 2005 (cit. on pp. 92–95, 97).

[E16]   M. Boudaoud, Y. Le Gorrec, Y. Haddab, and P. Lutz. ≪Gain Scheduled Control Strategies for a Nonlinear Electrostatic Microgripper: Design and Real Time Implementation.≫ In: *Proc. 51st IEEE Conf. Decision Control*. 2012, pp. 3127–3132. DOI: 10.1109/CDC.2012.6426177 (cit. on pp. 92–95, 97).

[E17]   C.-L. Chen and G.-C. Chiu. ≪Compensating for Spatially Repetitive Disturbance With Linear Parameter Varying Repetitive Control.≫ In: *Proc. Int. Conf. Control Applicat.* 2004, pp. 736–741 (cit. on pp. 92–95, 97).

[E18]   M. Corno, M. Tanelli, S. M. Savaresi, and L. Fabbri. *Design and Validation of a Gain-Scheduled Controller for the Electronic Throttle Body in Ride-by-Wire Racing Motorcycles*. 2011. DOI: 10.1109/TCST.2010.2066565 (cit. on p. 93).

[E19]   M. Dettori. ≪LMI Techniques for Control with Application to a Compact Disc Player Mechanism.≫ Ph.D Thesis. Delft and Netherlands: Delft University of Technology, 2001 (cit. on pp. 31, 33, 38–41, 46, 92, 93, 95, 97).

[E20]   M. Dettori and C. W. Scherer. ≪Design and Implementation of a Gain Scheduled Controller for A Compact Disc Player.≫ In: *Proc. Europ. Control Conf.* 1999 (cit. on pp. 92–95, 97).

[E21]   M. Dettori and C. W. Scherer. ≪LPV Design for a CD Player: An Experimental Evaluation of Performance.≫ In: *Proc. 40th IEEE Conf. Decision Control*. 2001, pp. 4711–4716 (cit. on pp. 4, 69, 71, 80, 81, 92–97, 250).

[E22]   G. A. dos Reis, A. A. G. Siqueira, and M. H. Terra. ≪Nonlinear H-Infinity Control via Quasi-LPV Representation and Game Theory for Wheeled Mobile Robots.≫ In: *Proc. Mediterranean Conf. Contr. & Automat.* 2005 (cit. on pp. 92, 93, 95, 97).

[E23]   F. Duarte, P. Ballesteros, X. Shu, and C. Bohn. ≪Active Control of the Harmonic and Transient Response of Vibrating Flexible Structures with Piezoelectric Actuators.≫ In: *International Conference and Exhibition of New Actuators and Drive Systems*. 2012, pp. 447–450 (cit. on pp. 92–95, 97).

[E24]   F. Duarte, P. Ballesteros, X. Shu, and C. Bohn. ≪An LPV Discrete-Time Controller for the Rejection of Harmonic Time-Varying Disturbances in a Lightweight Flexible Structure.≫ In: *Proc. Amer. Control Conf.* 2013 (cit. on pp. 92–95, 97).

[E25]   P. de Filippi, M. Tanelli, M. Corno, S. M. Savaresi, and L. Fabbri. ≪Design of Steering Angle Observers for the Active Control of Two-Wheeled Vehicles.≫ In: *Proc. Int. Conf. Control Applicat.* 2010, pp. 155–160 (cit. on pp. 92, 93, 95, 97).

[E26]   A. Forrai, T. Ueda, and T. Yumura. ≪Electromagnetic Actuator Control: A Linear Parameter-Varying Approach.≫ In: *IEEE Trans. Ind. Electron.* 54.3 (2007). ISSN: 0278-0046 (cit. on pp. 92–95, 97).

[E27]   C. Gauthier, O. Sename, L. Dugard, and G. Meissonnier. ≪Some Experimental Results of an H-Infinity-LPV Controller Applied to a Diesel Engine Common Rail Injection System.≫ In: *5th IFAC Symp. Adv. Automotive Control*. 2007 (cit. on pp. 92, 93, 95, 97).

[E28] A. U. Genc. «Linear Parameter-Varying Modelling and Robust Control of Variable Cam Timing Engines.» PhD thesis. UK: University of Cambridge, 2002. URL: http://www-control.eng.cam.ac.uk/aug20/thesis.pdf (cit. on pp. 92, 93, 95, 97).

[E29] A. S. Ghersin, R. S. Smith, and R. S. Sánchez-Peña. «Classical, Robust and LPV Control of a Magnetic-bearing Experiment.» In: *Identification and Control*. Ed. by R. S. Sánchez-Peña, J. Quevedo Casín, and V. Puig. [New York]: Springer-Verlag London Limited, 2007, pp. 277–325. ISBN: 9781846288982. DOI: 10.1007/978-1-84628-899-9_10 (cit. on pp. 92, 93, 95, 97).

[E30] A. S. Ghersin, R. S. Smith, and R. S. Sánchez-Peña. «LPV Control of a Magnetic Bearing Experiment.» In: *Latin Amer. Appl. Research* 10 (2010), pp. 303–310 (cit. on pp. 92, 93, 95, 97).

[E31] N. Gibson and G. D. Buckner. «Real-Time Adaptive Control of Active Magnetic Bearings Using Linear Parameter Varying Models.» In: *Proc. SoutheastCon*. 2002, pp. 268–272. DOI: 10.1109/.2002.995603 (cit. on pp. 93, 97).

[E32] V. J. Ginter and J. K. Pieper. «Robust Gain Scheduled Control of a Hydrokinetic Turbine Part 2: Testing.» In: *Proc. Elect. Power & Energy Conf.* 2009, pp. 1–5 (cit. on pp. 92–95, 97).

[E33] M. Groot Wassink, M. van de Wal, C. W. Scherer, and O. Bosgra. «LPV Control for a Wafer Stage: Beyond the Theoretical Solution.» In: *Contr. Eng. Prac.* 13.2 (2005), pp. 231–245. ISSN: 09670661. DOI: 10.1016/j.conengprac.2004.03.008 (cit. on pp. 92–95, 97).

[E34] Y. Hamada, T. Ohtani, T. Kida, T. Nagashio, I. Yamaguchi, T. Kasai, T. Igawa, S. Mitani, K. Sunagawa, and M. Ikeda. «In-orbit Control Experiment on ETS-VIII Spacecraft.» In: *JAXA Res. Develop. Report* (2012), pp. 1–109 (cit. on pp. 92, 94, 97, 99).

[E35] M. Hanifzadegan and R. Nagamune. «Switching Gain-Scheduled Control Design for Flexible Ball-Screw Drives.» In: *J. Dyn. Syst., Meas. Contr.* 136.1 (2014), p. 14503. ISSN: 00220434. DOI: 10.1115/1.4025154 (cit. on pp. 92–94, 97).

[E36] S. M. Hashemi, H. S. Abbas, and H. Werner. «LPV Modelling and Control of a 2-DOF Robotic Manipulator Using PCA-Based Parameter Set Mapping.» In: *Proc. 48th IEEE Conf. Decision Control*. 2009, pp. 7418–7423. DOI: 10.1109/CDC.2009.5400621 (cit. on pp. 25, 92, 93, 95, 97, 98).

[E37] S. M. Hashemi, H. S. Abbas, and H. Werner. «Low-Complexity Linear Parameter-Varying Modeling and Control of a Robotic Manipulator.» In: *Contr. Eng. Prac.* 20 (2012), pp. 248–257. ISSN: 09670661 (cit. on pp. 6, 25, 92, 93, 95, 97, 98, 141, 187).

[E38] S. M. Hashemi and H. Werner. «Gain-Scheduled H-Infinity Control of a Robotic Manipulator With Nonlinear Joint Friction.» In: *Virtual Control Conference*. 2010 (cit. on pp. 92, 93, 95, 97).

[E39] W. Heins, P. Ballesteros, and C. Bohn. «Gain-Scheduled State-Feedback Control for Active Cancellation of Multisine Disturbances with Time-Varying Frequencies.» In: *Conference on Active Noise and Vibration Control Methods*. 2011 (cit. on pp. 92, 94, 95, 97).

[E40] W. Heins, P. Ballesteros, and C. Bohn. «Experimental Evaluation of an LPV-Gain-Scheduled Observer for Rejecting Multisine Disturbances with Time-Varying Frequencies.» In: *Proc. Amer. Control Conf.* 2012 (cit. on pp. 93, 94, 97).

[E41] W. Heins, P. Ballesteros, X. Shu, and C. Bohn. «LPV Gain-Scheduled Observer-Based State Feedback for Active Control of Harmonic Disturbances with Time-Varying Frequencies.» In: *Advances on Analysis and Control of Vibrations*. Ed. by M. Zapateiro de la Hoz and F. Pozo. InTech, 2012, pp. 35–64. ISBN: 9789535106999. DOI: 10.5772/50293 (cit. on pp. 92–95, 97).

[E42] P. Hingwe, H.-S. Tan, A. K. Packard, and M. Tomizuka. «Linear Parameter Varying Controller for Automated Lane Guidance: Experimental Study on Tractor-Trailers.» In: *IEEE Trans. Contr. Syst. Technol.* 10.6 (2002), pp. 793–806. ISSN: 1063-6536. DOI: 10.1109/TCST.2002.804118 (cit. on pp. 92, 93, 96, 97).

[E43]   H. Hirano, Y. Kawi, and M. Fujita. «Automated Driving for an Experimental Vehicle using Visual Feedback Control.» In: *Proc. SICE Annu. Conf.* 2003 (cit. on pp. 92, 93, 95–97).

[E44]   C. Hoffmann, S. M. Hashemi, H. S. Abbas, and H. Werner. «Closed-Loop Stability and Performance Optimization in LPV Control Based on a Reduced Parameter Set.» In: *Proc. 51st IEEE Conf. Decision Control.* 2012, pp. 5146–5151. DOI: 10.1109/CDC.2012.6427053 (cit. on pp. 25, 92, 93, 95, 97, 98, 378).

[E45]   C. Hoffmann, S. M. Hashemi, H. S. Abbas, and H. Werner. «Benchmark Problem — Nonlinear Control of a 3-DOF Robotic Manipulator.» In: *Proc. 52nd IEEE Conf. Decision Control.* 2013, pp. 5534–5539. DOI: 10.1109/CDC.2013.6760761 (cit. on pp. 25, 28, 80, 92, 93, 95–98, 139, 143, 175, 190, 205, 378).

[E46]   C. Hoffmann, S. M. Hashemi, H. S. Abbas, and H. Werner. «Synthesis of LPV Controllers With Low Implementation Complexity Based on a Reduced Parameter Set.» In: *IEEE Trans. Contr. Syst. Technol.* 22.6 (2014), pp. 2393–2398. ISSN: 1063-6536. DOI: 10.1109/TCST.2014.2303397 (cit. on pp. 25, 42, 80, 92, 93, 95, 97, 98, 117, 160, 188, 377).

[E47]   C. Hoffmann, C. Radisch, and H. Werner. «Active Damping of Container Crane Load Swing by Hoisting Modulation - An LPV Approach.» In: *Proc. 51st IEEE Conf. Decision Control.* 2012, pp. 5140–5145. DOI: 10.1109/CDC.2012.6426889 (cit. on pp. 4, 92–95, 97, 113, 114, 378).

[E48]   C. Hoffmann and H. Werner. «Linear Parameter-Varying Control of Complex Mechanical Systems.» In: *Proc. 19th IFAC World Congr.* 2014, pp. 6147–6152 (cit. on pp. 10, 18, 92, 93, 95–97, 117, 160, 176, 187, 377).

[E49]   C. Hoffmann and H. Werner. «LFT-LPV Modeling and Control of a Control Moment Gyroscope.» In: *Proc. 54th IEEE Conf. Decision Control.* 2015 (cit. on pp. 105, 145, 169, 190, 377).

[E50]   S. Houria, N. Shinichi, O. Yoshimasa, and H. Yoshiro. «Orbital Experiments of Linearly Interpolated Gain Scheduling Attitude Controller Using ETS-VIII Spacecraft.» In: *18th IFAC Symp. Automat. Control in Aerospace.* 2010, pp. 193–197 (cit. on pp. 93, 94).

[E51]   R. S. Inoue, A. A. G. Siqueira, and M. H. Terra. «Experimental Results on the Nonlinear H-Infinity Control via Quasi-LPV Representation and Game Theory for Wheeled Mobile Robots.» In: *Robotica* 27.04 (2009), p. 547. DOI: 10.1017/S0263574708004931 (cit. on pp. 92, 93, 95, 97).

[E52]   R. S. Inoue, A. A. G. Siqueira, and M. Terra. «Experimental Results on the Nonlinear H-Infinity Control via Quasi-LPV Representation and Game Theory for Wheeled Mobile Robots.» In: *Proc. Int. Conf. Control Applicat.* 2007, pp. 1456–1461 (cit. on pp. 92, 93, 95, 97).

[E53]   T. Ioki, K. Ohtsubo, H. Kajiwara, W. Koterayama, and M. Nakamura. «On Vibration Control of Flexible Pipes in Ocean Drilling System.» In: *International Offshore and Polar Engineering Conference.* 2006 (cit. on pp. 92–95, 97).

[E54]   M. Jung and K. Glover. «Calibratable Linear Parameter-Varying Control of a Turbocharged Diesel Engine.» In: *IEEE Trans. Contr. Syst. Technol.* 14.1 (2006), pp. 45–62. ISSN: 1063-6536. DOI: 10.1109/TCST.2005.860513 (cit. on pp. 92, 96, 97).

[E55]   G. Kaiser, M. Korte, Q. Liu, C. Hoffmann, and H. Werner. «Torque Vectoring for a Real, Electric Car Implementing an LPV Controller.» In: *Proc. 19th IFAC World Congr.* 2014 (cit. on pp. 92, 93, 95, 97, 378).

[E56]   H. Kajiwara, P. Apkarian, and P. Gahinet. «LPV Techniques for Control of an Inverted Pendulum.» In: *IEEE Contr. Syst. Mag.* 19.1 (1999), pp. 44–54. ISSN: 0272-1708 (cit. on pp. 92–95, 97).

[E57] H. Kajiwara, P. Apkarian, and P. Gahinet. «Wide-Range Stabilization of an Arm-Driven Inverted Pendulum Using Linear Parameter-Varying Techniques.» In: *IEEE Contr. Syst. Mag.* 19 (1999), pp. 44–54. ISSN: 0272-1708 (cit. on pp. 92–95, 97).

[E58] O. Kazuhisa, S. Hidetaka, M. Takahiro, K. Wataru, and K. Hiroyuki. «Experimental Study on Reentry Operation of a Flexible Marine Riser by Gain-scheduled Control.» In: *J. Japan Soc. of Naval Architects and Ocean Eng.* 2 (2005), pp. 49–55 (cit. on pp. 93, 94).

[E59] A. Kilicarslan, G. Song, and K. M. Grigoriadis. «LPV Gain Scheduling Control of Hysteresis on an SMA Wire System.» In: *Proc. ASME Dyn. Syst. Control Conf.* 2009, pp. 419–426. DOI: 10.1115/DSCC2009-2623 (cit. on pp. 92–94, 97).

[E60] A. Kwiatkowski. «LPV Modeling and Application of LPV Controllers to SI Engines.» Ph.D. Thesis. Hamburg, Germany: Hamburg University of Technology, 2008 (cit. on pp. 4, 6, 25, 92, 93, 95, 97, 300).

[E61] A. Kwiatkowski, H. Werner, J. P. Blath, A. Ali, and M. Schultalbers. «Linear Parameter Varying PID Controller Design for Charge Control of a Spark-Ignited Engine.» In: *Contr. Eng. Prac.* 17.11 (2009), pp. 1307–1317. ISSN: 09670661. DOI: 10.1016/j.conengprac.2009.06.005 (cit. on pp. 92, 93, 95, 97).

[E62] N. Lachhab, H. S. Abbas, and H. Werner. «A Neural-Network Based Technique for Modelling and LPV Control of an Arm-Driven Inverted Pendulum.» In: *Proc. 47th IEEE Conf. Decision Control.* 2008, pp. 3860–3865. DOI: 10.1109/CDC.2008.4739222 (cit. on pp. 92–94, 97).

[E63] H.-H. Lin, B.-K. Fang, M.-S. Ju, and C.-C. K. Lin. «Control of Ionic Polymer-Metal Composites for Active Catheter Systems via Linear Parameter-Varying Approach.» In: *J. Intell. Material Syst. Struct.* 20.3 (2008), pp. 273–282. ISSN: 1045-389X. DOI: 10.1177/1045389X08093565 (cit. on pp. 92–94, 97).

[E64] B. Lu, H. Choi, and G. D. Buckner. «LPV Control Design and Experimental Implementation for a Magnetic Bearing System.» In: *Proc. Conf. Ind. Electron. Soc.* 2005, 6 pp. DOI: 10.1109/IECON.2005.1568925 (cit. on pp. 92, 93, 95, 97).

[E65] B. Lu, H. Choi, and G. D. Buckner. «LPV Control Design and Experimental Implementation for a Magnetic Bearing System.» In: *Proc. Amer. Control Conf.* 2006 (cit. on pp. 92, 95, 97).

[E66] B. Lu, H. Choi, G. D. Buckner, and K. Tammi. «Linear Parameter-Varying Techniques for Control of a Magnetic Bearing System.» In: *Contr. Eng. Prac.* 16.10 (2008), pp. 1161–1172. ISSN: 09670661. DOI: 10.1016/j.conengprac.2008.01.002 (cit. on pp. 92, 93, 95, 97).

[E67] F. Matsumura, T. Namerikawa, K. Hagiwara, and M. Fujita. «Application of Gain Scheduled H-Infinity Robust Controllers to a Magnetic Bearing.» In: *IEEE Trans. Contr. Syst. Technol.* 4.5 (1996). ISSN: 1063-6536 (cit. on pp. 93, 97).

[E68] M. Meisami-Azad, F. A. Shirazi, and K. M. Grigoriadis. «Anti-Windup LPV Control Design of MR Dampers for Structural Vibration Suppression.» In: *Proc. ASME Dyn. Syst. Control Conf.* 2011, pp. 189–196. DOI: 10.1115/DSCC2011-6072 (cit. on pp. 92, 94, 97).

[E69] A. Mendez Gonzalez, C. Hoffmann, C. Radisch, and H. Werner. «LPV Observer Design and Damping Control of Container Crane Load Swing.» In: *Proc. Europ. Control Conf.* 2013 (cit. on pp. 4, 82, 92–94, 97, 110, 113, 114, 379).

[E70] A. Mukhtar and H. Werner. «Discrete-Time LPV Controller Synthesis Using Dilated LMIs With Application to an Arm-Driven Inverted Pendulum.» In: *Proc. 18th IFAC World Congr.* 2011, pp. 7708–7712 (cit. on pp. 92–95, 97).

[E71] T. Nagashio, T. Kida, Y. Hamada, and T. Ohtani. ≪Robust Two-Degrees-of-Freedom Attitude Controller Design and Flight Test Result for Engineering Test Satellite-VIII Spacecraft.≫ In: *IEEE Trans. Contr. Syst. Technol.* (2013), p. 1. ISSN: 1063-6536. DOI: 10.1109/TCST.2013.2248009 (cit. on pp. 92, 93, 97).

[E72] F. Niel, Y. Ameho, J.-M. Biannic, F. Defaÿ, and C. Bérard. ≪A Novel Parameter Varying Controller Synthesis Method for Quadrotor Control.≫ In: *Proc. AIAA Guidance, Navigation, Control Conf.* 2013. DOI: 10.2514/6.2013-4534 (cit. on pp. 93, 94, 97).

[E73] G. Papageorgiou, K. Glover, G. D'Mello, and Y. Patel. ≪Taking Robust LPV Control Into Flight on the VAAC Harrier.≫ In: *Proc. 39th IEEE Conf. Decision Contr.* 2000, pp. 4558–4564 (cit. on pp. 92–95, 97).

[E74] C. S. E.-D. Paraiso, S. M. Hashemi, and H. Werner. ≪Black-Box versus Grey-Box LPV Identification to Control a Mechanical System.≫ In: *Proc. 51st IEEE Conf. Decision Control.* 2012 (cit. on pp. 92, 93, 95, 97).

[E75] R. J. Patton and S. Klinkhieo. ≪LPV Fault Estimation and FTC of a Two-Link Manipulator.≫ In: *Proc. Amer. Control Conf.* 2010 (cit. on pp. 92, 93, 95, 97).

[E76] D. Robert, O. Sename, and D. Simon. ≪An H-Infinity LPV Design for Sampling Varying Controllers: Experimentation With a T-Inverted Pendulum.≫ In: *IEEE Trans. Contr. Syst. Technol.* 18.3 (2010). ISSN: 1063-6536 (cit. on pp. 92–95, 97).

[E77] D. Rotondo, F. Nejjari, and V. Puig. ≪Quasi-LPV Modeling, Identification and Control of a Twin Rotor MIMO System.≫ In: *Contr. Eng. Prac.* 21.6 (2013), pp. 829–846. ISSN: 09670661. DOI: 10.1016/j.conengprac.2013.02.004 (cit. on pp. 92–95, 97, 98).

[E78] D. Rotondo, J. Romera, V. Puig, and F. Nejjari. ≪Identification and Switching Quasi-LPV Control of a Four Wheeled Omnidirectional Robot.≫ In: *Proc. Mediterranean Conf. Contr. & Automat.* 2014 (cit. on pp. 92, 93, 95, 97).

[E79] A. Salimi, A. Ramezanifar, J. Mohammadpour, and K. M. Grigoriadis. ≪Gain-Scheduling Control of a Cable-Driven MRI-Compatible Robotic Platform for Intracardiac Interventions.≫ In: *Proc. Amer. Control Conf.* 2013 (cit. on pp. 92, 93, 96–98).

[E80] M. Sato. ≪Robust H-Two Problem for LPV Systems and its Application to Model-Following Controller Design for Aircraft Motions.≫ In: *Proc. Int. Conf. Control Applicat.* 2004, pp. 442–449 (cit. on pp. 92–95, 97).

[E81] M. Sato. ≪Robust Gain-Scheduled Flight Controller Using Inexact Scheduling Parameters.≫ In: *Proc. Amer. Control Conf.* 2013 (cit. on pp. 92–95, 97, 98).

[E82] M. Sato. ≪Discrete-Time Gain-Scheduled Model-Matching Flight Controller Using Inexact Scheduling parameters.≫ In: *Proc. Conf. Control Applicat.* Juan Les Antibes, 2014, pp. 171–176. DOI: 10.1109/CCA.2014.6981347 (cit. on pp. 92–95, 97).

[E83] F. Saupe. ≪Linear Parameter Varying Control Design for Industrial Manipulators.≫ Ph.D. Thesis. Hamburg and Germany: Hamburg University of Technology, 2013 (cit. on pp. 3, 4, 39, 62, 92, 93, 96, 97, 176, 178, 309).

[E84] F. Saupe and H. Pfifer. ≪Applied LPV Control Exploiting the Separation Principle for the Single Axis Positioning of an Industrial Manipulator.≫ In: *Proc. Int. Conf. Control Applicat.* 2011, pp. 1476–1481 (cit. on pp. 62, 92, 93, 96).

[E85] F. Saupe and H. Pfifer. ≪An Observer Based State Feedback LFT LPV Controller for an Industrial Manipulator.≫ In: *7th IFAC Symp. Robust Control Des.* 2012 (cit. on pp. 62, 79, 92, 93, 95, 97, 98).

[E86] F. A. Shirazi, K. M. Grigoriadis, and G. Song. ≪Parameter Varying Control of an MR Damper for Smart Base Isolation.≫ In: *Proc. Amer. Control Conf.* 2011 (cit. on pp. 93, 94, 97).

[E87] F. A. Shirazi, J. Mohammadpour, K. M. Grigoriadis, and G. Song. «Identification and Control of an MR Damper With Stiction Effect and its Application in Structural Vibration Mitigation.» In: *IEEE Trans. Contr. Syst. Technol.* 20.5 (2012), pp. 1285–1301. ISSN: 1063-6536. DOI: 10.1109/TCST.2011.2164920 (cit. on pp. 92–94, 97).

[E88] X. Shu, P. Ballesteros, and C. Bohn. «Active Vibration Control for Harmonic Disturbances with Time-Varying Frequencies through LPV Gain Scheduling.» In: *Proc. 23rd Chin. Control Decision Conf.* 2011 (cit. on pp. 92–95, 97).

[E89] X. Shu, P. Ballesteros, W. Heins, and C. Bohn. «Design of Structured Discrete-Time LPV Gain-Scheduling Controllers through State Augmentation and Partial State Feedback.» In: *Proc. Amer. Control Conf.* 2013 (cit. on pp. 92–95, 97).

[E90] X. Shu, W. Heins, P. Ballesteros, and C. Bohn. «Two-Parameter pLPV Modeling of Nonstationary Harmonically Related Multisine Disturbances for Reduced-Order Gain-Scheduling Control.» In: *International Conference on Modeling, Identification and Control.* 2013, pp. 404–411. DOI: 10.2316/P.2013.794-078 (cit. on pp. 92–95, 97, 98).

[E91] T. Sugiyama and K. Uchida. «Switching from Velocity to Force Control for the Electro-Hydraulic Servosystem Based on LPV System Modeling.» In: *Proc. 15th IFAC World Congr.* 2002 (cit. on pp. 92–95, 97).

[E92] Q. Sun, G. Dai, and W. Pan. «LPV Model and Its Application in Web Server Performance Control.» In: *Proc. Int. Conf. Comput. Sci. Software Eng.* 2008, pp. 486–489 (cit. on pp. 92, 94, 95, 97).

[E93] M. Sznaier, B. Murphy, and O. Camps. «An LPV Approach to Synthesizing Robust Active Vision Systems.» In: *Proc. 39th IEEE Conf. Decision Contr.* 2000, pp. 2545–2550 (cit. on pp. 92–94, 97).

[E94] J. Theis, C. Radisch, and H. Werner. «Self-Scheduled Control of a Gyroscope.» In: *Proc. 19th IFAC World Congr.* 2014, pp. 6129–6134 (cit. on pp. 92–94, 96, 97, 145, 149, 150, 191–194, 200, 201).

[E95] K. Trangbæk. «Linear Parameter Varying Control of Induction Motors.» PhD thesis. Denmark: Aalborg University, 2001. URL: http://www.control.auc.dk/~ktr/Thesis/Thesis.pdf (cit. on pp. 92–95, 97).

[E96] X. Wei. «Advanced LPV Techniques for Diesel Engines.» PhD thesis. Linz, Austria: Johannes Kepler University, 2006 (cit. on p. 93).

[E97] X. Wei and L. del Re. «Gain Scheduled H-Infinity Control for Air Path Systems of Diesel Engines Using LPV Techniques.» In: *IEEE Trans. Contr. Syst. Technol.* 15.3 (2007), pp. 406–415. ISSN: 1063-6536. DOI: 10.1109/TCST.2007.894633 (cit. on p. 92).

[E98] A. P. White, Z. Ren, G. Zhu, and J. Choi. «Mixed H-Two/H-Infinity Observer-Based LPV Control of a Hydraulic Engine Cam Phasing Actuator.» In: *Proc. ASME Dyn. Syst. Control Conf.* 2011, pp. 741–748. DOI: 10.1115/DSCC2011-5937 (cit. on pp. 92, 93, 97).

[E99] A. P. White, Z. Ren, G. Zhu, and J. Choi. «Mixed H-Two/H-Infinity Observer-Based LPV Control of a Hydraulic Engine Cam Phasing Actuator.» In: *IEEE Trans. Contr. Syst. Technol.* 21.1 (2013), pp. 229–238. ISSN: 1063-6536. DOI: 10.1109/TCST.2011.2177464 (cit. on pp. 92, 93, 95, 97).

[E100] F. Wijnheijmer, G. Naus, W. Post, M. Steinbuch, and P. Teerhuis. «Modelling and LPV Control of an Electro-Hydraulic Servo System.» In: *Proc. Int. Conf. Control Applicat. Comput. Aided Control Syst. Design.* 2006, pp. 3116–3121 (cit. on pp. 92–95, 97).

[E101] J. Witte, H. M. N. K. Balini, and C. W. Scherer. «Experimental Results With Stable and Unstable LPV Controllers for Active Magnetic Bearing Systems.» In: *Proc. Int. Conf. Control Applicat.* 2010, pp. 950–955. DOI: 10.1109/CCA.2010.5611087 (cit. on pp. 92, 93, 95, 97).

[E102] J. Witte, B. Harimohan N. M. K., and C. W. Scherer. ≪Robust and LPV Control of an AMB System.≫ In: *Proc. Amer. Control Conf.* 2010 (cit. on pp. 92, 93, 95, 97).

[E103] Z. Yu, H. Chen, and P.-Y. Woo. ≪Gain Scheduled LPV H-Infinity Control Based on LMI Approach for a Robotic Manipulator.≫ In: *J. Robotic Syst.* 19.12 (2002), pp. 585–593. ISSN: 0741-2223 (cit. on p. 96).

[E104] Z. Yu, H. Chen, and P.-Y. Woo. ≪Gain Scheduled LPV H-Infinity LMI Approach for a Robotic Manipulator.≫ In: *J. Robotic Syst.* 19.12 (2002), pp. 585–593. ISSN: 0741-2223 (cit. on pp. 92, 95, 97).

[E105] Z. Yu, H. Chen, and P.-Y. Woo. ≪Polytopic Gain Scheduled H-Infinity Control for Robotic Manipulators.≫ In: *Robotica* 21.5 (2003), pp. 495–504 (cit. on pp. 92, 93, 95).

[E106] Z. Yu, H. Chen, and P.-Y. Woo. ≪Conservativeness-Reduced Design of a Gain Scheduled H-Infinity Controller for a Robotic Manipulator.≫ In: *Proc. Int. Conf. on Robotics and Automat.* 2002 (cit. on pp. 92, 97).

[E107] K. Zavari, G. Pipeleers, and J. Swevers. ≪Gain-Scheduled Controller Design: Illustration on an Overhead Crane.≫ In: *IEEE Trans. Ind. Electron.* 61.7 (2014), pp. 3713–3718. ISSN: 0278-0046. DOI: 10.1109/TIE.2013.2270213 (cit. on pp. 92, 93, 97).

[E108] F. Zhang, K. M. Grigoriadis, M. Franchek, and I. Makki. ≪Transient Lean Burn Air-fuel Ratio Control Using Input Shaping Method Combined with Linear Parameter-Varying Control.≫ In: *Proc. 44th IEEE Conf. Decision Contr.* 2005, pp. 3290–3295 (cit. on pp. 93, 97).

[E109] F. Zhang, K. M. Grigoriadis, M. A. Franchek, and I. H. Makki. ≪Linear Parameter-Varying Lean Burn Air-Fuel Ratio Control for a Spark Ignition Engine.≫ In: *J. Dyn. Syst., Meas. Contr.* 129.4 (2007), p. 404. ISSN: 00220434. DOI: 10.1115/1.2745849 (cit. on pp. 92, 93, 96, 97).

[E110] F. Zhang, K. M. Grigoriadis, M. A. Franchek, and I. H. Makki. ≪Transient Lean Burn Air-Fuel Ratio Linear Parameter-Varying Control Using Input Shaping.≫ In: *Int. J. Model., Ident. Contr.* 3.3 (2008), p. 318. ISSN: 1746-6172. DOI: 10.1504/IJMIC.2008.020129 (cit. on pp. 92, 93, 96, 97).

[E111] S. Zhang, J. J. Yang, and G. Zhu. ≪LPV Gain-Scheduling Control of an Electronic Throttle with Experimental Validation.≫ In: *Proc. Amer. Control Conf.* 2014, pp. 190–195 (cit. on pp. 92, 93, 95, 97).

HiFi-Simulation-Validated LPV Control Applications

[H1] D. J. Alvarez and B. Lu. ≪Comparison of Classical, H-Infinity, and LPV Flight Control Design Methods, Part I: Desktop Analysis.≫ In: *Proc. AIAA Atmospheric Flight Mechanics Conf.* 2010. DOI: 10.2514/6.2010-7940 (cit. on pp. 91–93).

[H2] D. J. Alvarez and B. Lu. ≪Comparison of Classical, H-Infinity, and LPV Flight Control Design Methods, PART II: Piloted Simulation.≫ In: *Proc. AIAA Atmospheric Flight Mechanics Conf.* 2010. DOI: 10.2514/6.2010-7941 (cit. on pp. 93, 94, 97).

[H3] D. J. Alvarez and B. Lu. ≪Piloted Simulation Study Comparing Classical, H-infinity, and Linear Parameter-Varying Control Methods.≫ In: *J. Guidance Contr. Dyn.* 34.1 (2011), pp. 164–176. DOI: 10.2514/1.50198 (cit. on pp. 91–94, 97).

[H4] H. Alwi, C. Edwards, and A. Marcos. ≪Actuator and Sensor Fault Reconstruction Using an LPV Sliding Mode Observer.≫ In: *Proc. AIAA Guidance, Navigation, Control Conf.* 2010. DOI: 10.2514/6.2010-8157 (cit. on p. 91).

[H5] N. Aouf, D. G. Bates, I. Postlethwaite, and B. Boulet. ≪Scheduling Schemes for an Integrated Flight and Propulsion Control System.≫ In: *Contr. Eng. Prac.* 10 (2002). ISSN: 09670661 (cit. on pp. 93, 94).

[H6] G. J. Balas. «Linear, Parameter-Varying Control and its Application to a Turbofan Engine.» In: *Int. J. Robust Nonlinear Contr.* 12.9 (2002), pp. 763–796. ISSN: 10498923. DOI: 10.1002/rnc.704 (cit. on pp. 92–94, 97).

[H7] G. J. Balas, I. Fialho, A. K. Packard, J. Renfrow, and C. Mullaney. «On the Design of LPV Controllers for the F-14 Aircraft Lateral-Directional Axis During Powered Approach.» In: *Proc. Amer. Control Conf.* 1997 (cit. on pp. 91–94, 97).

[H8] J. M. Barker and G. J. Balas. «Flight Control of a Tailless Aircraft via Linear Parameter-Varying Techniques.» In: *Proc. AIAA Guidance, Navigation, Control Conf.* 1999. DOI: 10.2514/6.1999-4133 (cit. on pp. 92–94, 97).

[H9] Y. Bolea, V. Puig, and J. Blesa. «Gain-Scheduled Smith Predictor PID-based LPV Controller for Open-flow Canal Control.» In: *IEEE Trans. Contr. Syst. Technol.* 22.2 (2014), pp. 468–477. ISSN: 1063-6536 (cit. on pp. 92–94, 97).

[H10] H. Buschek. «Full Envelope Missile Autopilot Design Using Gain Scheduled Robust Control.» In: *J. Guidance Contr. Dyn.* 22.1 (1999), pp. 115–122. DOI: 10.2514/2.4357 (cit. on pp. 93, 97).

[H11] S. Christiansen, H.-R. Karimi, and T. Bakka. «Linear Parameter-Varying Modelling and Control of an Offshore Wind Turbine With Constrained Information.» In: *IET Contr. Theory Appl.* 8.1 (2014), pp. 22–29. ISSN: 17518644. DOI: 10.1049/iet-cta.2013.0480 (cit. on pp. 92–94, 97).

[H12] de Corcuera, A. Díaz, A. Pujana-Arrese, J. M. Ezquerra, A. Milo, and J. Landaluze. «Linear Models-Based LPV Modelling and Control for Wind Turbines.» In: *Wind Energ.* (2014), n/a. ISSN: 1095-4244. DOI: 10.1002/we.1751 (cit. on pp. 92–95, 97).

[H13] S. Fergani, O. Sename, and L. Dugard. «A LPV/H-Infinity Fault Tolerant Control of Vehicle Roll Dynamics Under Semi-Active Damper malfunction.» In: *Proc. Amer. Control Conf.* 2014 (cit. on pp. 92–94, 97).

[H14] Gang Chen, Yueming Li, Sun Jian, Zuo Yingtao, and P. Hu. «Linear Parameter Varying Control for Active Flutter Suppression Based on Adaptive Reduced Order Model.» In: *Proc. 52nd AIAA/ASME Struct., Struct. Dyn., Materials Conf.* 2011. DOI: 10.2514/6.2011-1773 (cit. on pp. 92–94, 97).

[H15] Y. Hamada, T. Ohtani, T. Kida, and T. Nagashio. «Synthesis of a Linearly Interpolated Gain Scheduling Controller for Large Flexible Spacecraft ETS-VIII.» In: *Contr. Eng. Prac.* 19.6 (2011), pp. 611–625. ISSN: 09670661. DOI: 10.1016/j.conengprac.2011.02.005 (cit. on pp. 92, 93, 97).

[H16] S. Hecker, Andreas Varga, and D. Ossmann. «Diagnosis of Actuator Faults Using LPV-Gain Scheduling Techniques.» In: *Proc. AIAA Guidance, Navigation, Control Conf.* 2011. DOI: 10.2514/6.2011-6680 (cit. on pp. 91, 93).

[H17] A. Hjartarson, P. J. Seiler, A. K. Packard, and G. J. Balas. «LPV Aeroservoelastic Control using the LPVTools Toolbox.» In: *Proc. AIAA Atmospheric Flight Mechanics Conf.* 2013. DOI: 10.2514/6.2013-4742 (cit. on pp. 92, 93).

[H18] F. A. Inthamoussou, F. D. Bianchi, H. de Battista, and R. J. Mantz. «LPV Wind Turbine Control With Anti-Windup Features Covering the Complete Wind Speed Range.» In: *IEEE Trans. Energy Convers.* 29.1 (2014), pp. 259–266. ISSN: 0885-8969. DOI: 10.1109/TEC.2013.2294212 (cit. on pp. 92–94, 96, 97).

[H19] L. H. Lee and M. S. Spillman. «Control of Slowly Varying LPV Systems - An Application to Flight Control.» In: *Proc. AIAA Guidance, Navigation, Control Conf.* 1996. DOI: 10.2514/6.1996-3805 (cit. on pp. 92–94, 97).

[H20]   A. Marcos and S. Bennani. «A Linear Parameter Varying Controller for a Re-entry Vehicle Benchmark.» In: *Advances in Aerospace Guidance, Navigation and Control*. Ed. by F. Holzapfel and S. Theil. Berlin, Heidelberg: Springer Berlin Heidelberg, 2011 (cit. on pp. 92, 93, 97).

[H21]   A. Marcos, J. Veenman, C. W. Scherer, G. de Zaiacomo, D. Mostaza, M. Kerr, H. Köroglu, and S. Bennani. «Application of LPV Modeling, Design and Analysis Methods to a Re-entry Vehicle.» In: *Proc. AIAA Guidance, Navigation, Control Conf.* 2010. DOI: 10.2514/6.2010-8192 (cit. on pp. 92–94, 97).

[H22]   J. Mueller and G. J. Balas. «Implementation and Testing of LPV Controllers for the NASA F/A-18 Systems Research Aircraft.» In: *Proc. AIAA Guidance, Navigation, Control Conf.* 2000 (cit. on pp. 92–94, 97).

[H23]   C. Roos, J.-M. Biannic, S. Tarbouriech, C. Prieur, and M. Jeanneau. «On-Ground Aircraft Control Design Using a Parameter-Varying Anti-Windup Approach.» In: *Aerospace Sci. Technol.* 14.7 (2010), pp. 459–471. ISSN: 12709638. DOI: 10.1016/j.ast.2010.02.004 (cit. on pp. 92–94, 97, 98).

[H24]   Sanketh Bhat and Rick Lind. «Linear Parameter-Varying Control for Variations in Thermal Gradients Across Hypersonic Vehicles.» In: *Proc. AIAA Guidance, Navigation, Control Conf.* 2009. DOI: 10.2514/6.2009-5952 (cit. on p. 94).

[H25]   F. A. Shirazi, K. M. Grigoriadis, and D. Viassolo. «Wind turbine Integrated Structural and LPV Control Design for Improved Closed-Loop Performance.» In: *Int. J. Contr.* 85.8 (2012), pp. 1178–1196. ISSN: 0020-7179. DOI: 10.1080/00207179.2012.679973 (cit. on pp. 93, 94, 97, 308).

[H26]   F. A. Shirazi, K. M. Grigoriadis, and D. Viassolo. «Wind Turbine Linear Parameter Varying Control Using Fast Code.» In: *Proc. ASME Dyn. Syst. Control Conf.* 2012, p. 771. ISBN: 9780791845301. DOI: 10.1115/DSCC2012-MOVIC2012-8558 (cit. on pp. 92–94, 97).

[H27]   D. Sigthorsson, A. Serrani, M. Bolender, and D. Doman. «LPV Control Design for Over-Actuated Hypersonic Vehicles Models.» In: *Proc. AIAA Guidance, Navigation, Control Conf.* 2009. DOI: 10.2514/6.2009-6280 (cit. on pp. 93, 94).

[H28]   I. Szászi, A. Marcos, G. J. Balas, and J. Bokor. «LPV Detection Filter Design for Boeing 747-100/200.» In: *Proc. AIAA Guidance, Navigation, Control Conf.* 2002. DOI: 10.2514/6.2002-4957 (cit. on pp. 91–94, 97).

[H29]   I. Szászi, A. Marcos, G. J. Balas, and J. Bokor. «Linear Parameter-Varying Detection Filter Design for a Boeing 747-100/200 Aircraft.» In: *J. Guidance Contr. Dyn.* 28.3 (2005), pp. 461–470. DOI: 10.2514/1.6689 (cit. on pp. 91–94, 97).

[H30]   B. Vanek, G. J. Balas, and R. E. Arndt. «Linear, Parameter-Varying Control of a Super-cavitating Vehicle.» In: *Contr. Eng. Prac.* 18.9 (2010), pp. 1003–1012. ISSN: 09670661. DOI: 10.1016/j.conengprac.2010.04.006 (cit. on pp. 92, 93, 97).

[H31]   B. Vanek, Z. Szabó, A. Edelmayer, and J. Bokor. «Geometric LPV Fault Detection Filter Design for Commercial Aircrafts.» In: *Proc. AIAA Guidance, Navigation, Control Conf.* 2011. DOI: 10.2514/6.2011-6681 (cit. on pp. 91, 93).

[H32]   A. P. White, G. Zhu, and J. Choi. «Hardware-in-the-Loop Simulation of Robust Gain-Scheduling Control of Port-Fuel-Injection Processes.» In: *IEEE Trans. Contr. Syst. Technol.* 19.6 (2011), pp. 1433–1443. ISSN: 1063-6536. DOI: 10.1109/TCST.2010.2095420 (cit. on pp. 92, 93, 97).

AUTHOR'S PUBLICATIONS

Peer Reviewed Publications of the Author

Journal Publications

C. Hoffmann, A. Eichler, and H. Werner. «Control of Heterogeneous Groups of Systems Interconnected Through Directed and Switching Topologies.» In: *IEEE Trans. Automat. Contr.* 60.7 (2015), pp. 1904–1909. ISSN: 0018-9286. DOI: 10.1109/TAC.2014.2362595

C. Hoffmann, S. M. Hashemi, H. S. Abbas, and H. Werner. «Synthesis of LPV Controllers With Low Implementation Complexity Based on a Reduced Parameter Set.» In: *IEEE Trans. Contr. Syst. Technol.* 22.6 (2014), pp. 2393–2398. ISSN: 1063-6536. DOI: 10.1109/TCST.2014.2303397

C. Hoffmann and H. Werner. «A Survey of Linear Parameter-Varying Control Applications Validated by Experiments or High-Fidelity Simulations.» In: *IEEE Trans. Contr. Syst. Technol.* 23.2 (2015), pp. 416–433. ISSN: 1063-6536. DOI: 10.1109/TCST.2014.2327584

Conference Publications

C. Hoffmann and H. Werner. «Control of Heterogeneous LPV Subsystems Interconnected through Arbitrary Directed and Switching Topologies.» In: *Proc. 54th IEEE Conf. Decision Control.* 2015

C. Hoffmann and H. Werner. «LFT-LPV Modeling and Control of a Control Moment Gyroscope.» In: *Proc. 54th IEEE Conf. Decision Control.* 2015

C. Hoffmann and H. Werner. «Compact LFT-LPV Modeling With Automated Parameterization for Efficient LPV Controller Synthesis.» In: *Proc. Amer. Control Conf.* 2015

C. Hoffmann and H. Werner. «Complexity of Implementation and Synthesis in Linear Parameter-Varying Control.» In: *Proc. 19th IFAC World Congr.* 2014, pp. 11749–11760

C. Hoffmann and H. Werner. «Linear Parameter-Varying Control of Complex Mechanical Systems.» In: *Proc. 19th IFAC World Congr.* 2014, pp. 6147–6152

C. Hoffmann, S. M. Hashemi, H. S. Abbas, and H. Werner. «Synthesis of LPV Controllers With Reduced Implementation Complexity.» In: *Proc. Amer. Control Conf.* 2014, pp. 3766–3771. DOI: 10.1109/ACC.2014.6858716

C. Hoffmann, A. Eichler, and H. Werner. «Control of Heterogeneous Groups of LPV Systems Interconnected Through Directed and Switching topologies.» In: *Proc. Amer. Control Conf.* 2014, pp. 5156–5161. DOI: 10.1109/ACC.2014.6858631

C. Hoffmann, S. M. Hashemi, H. S. Abbas, and H. Werner. «Benchmark Problem — Nonlinear Control of a 3-DOF Robotic Manipulator.» In: *Proc. 52nd IEEE Conf. Decision Control.* 2013, pp. 5534–5539. DOI: 10.1109/CDC.2013.6760761

C. Hoffmann, A. Eichler, and H. Werner. «Distributed Control of Linear Parameter-Varying Decomposable Systems.» In: *Proc. Amer. Control Conf.* 2013, pp. 2386–2391

C. Hoffmann, C. Radisch, and H. Werner. «Active Damping of Container Crane Load Swing by Hoisting Modulation - An LPV Approach.» In: *Proc. 51st IEEE Conf. Decision Control.* 2012, pp. 5140–5145. DOI: 10.1109/CDC.2012.6426889

C. Hoffmann, S. M. Hashemi, H. S. Abbas, and H. Werner. «Closed-Loop Stability and Performance Optimization in LPV Control Based on a Reduced Parameter Set.» In: *Proc. 51st IEEE Conf. Decision Control.* 2012, pp. 5146–5151. DOI: 10.1109/CDC.2012.6427053

Co-Authored Journal Publications

A. Eichler, C. Hoffmann, and H. Werner. «Robust Control of Decomposable LPV Systems.» In: *Automatica* 50.12 (2014), pp. 3239–3245. ISSN: 00051098. DOI: 10.1016/j.automatica.2014.10.046

Co-Authored Conference Publications

P. S. Gonzalez Cisneros, C. Hoffmann, M. Bartels, and H. Werner. «Linear Parameter-Varying Controller Design for a Nonlinear Quad-Rotor Helicopter Model for High Speed Trajectory Tracking.» In: *Proc. Amer. Control Conf.* 2016

A. Mendez Gonzalez, C. Hoffmann, and H. Werner. «LPV Formation Control for Non-Holonomic Agents with Directed and Switching Communication Topologies.» In: *Proc. 54th IEEE Conf. Decision Control.* 2015

H. S. Abbas, S. Rahme, N. Meskin, C. Hoffmann, R. Toth, and J. Mohammadpour. «Linear Parameter-Varying Control of a Copolymerization Reactor.» In: *1st IFAC Workshop LPV Syst.* 2015

A. Eichler, C. Hoffmann, and H. Werner. «Conservatism of Analysis and Controller Synthesis of Decomposable Systems.» In: *Proc. 19th IFAC World Congr.* 2014

G. Kaiser, M. Korte, Q. Liu, C. Hoffmann, and H. Werner. «Torque Vectoring for a Real, Electric Car Implementing an LPV Controller.» In: *Proc. 19th IFAC World Congr.* 2014

S. Wollnack, C. Hoffmann, and H. Werner. «Affine LPV Controller Design with Linear Growth of the Number of LMI Constraints.» In: *Proc. Amer. Control Conf.* 2013

A. Eichler, C. Hoffmann, and H. Werner. «Robust Stability Analysis of Interconnected Systems with Uncertain Time-Varying Time Delays via IQCs.» In: *Proc. 52nd IEEE Conf. Decision Control*. 2013

A. Eichler, C. Hoffmann, and H. Werner. «Robust Control of Decomposable LPV Systems Under Time-Invariant and Time-Varying Interconnection Topologies (Part 1).» In: *Proc. 52nd IEEE Conf. Decision Control*. 2013

A. Eichler, C. Hoffmann, and H. Werner. «Robust Control of Decomposable LPV Systems Under Time-Invariant and Time-Varying Interconnection Topologies (Part 2).» In: *Proc. 52nd IEEE Conf. Decision Control*. 2013

A. Eichler, C. Hoffmann, and H. Werner. «Design of Tutorial Activities and Homework Assignments for a Large-Enrollment Introductory Course in Control Systems.» In: *Proc. IFAC Symp. on Advances in Control Education*. University of Sheffield, 2013, pp. 43–48

Q. Liu, C. Hoffmann, and H. Werner. «Distributed Control of Parameter-Varying Spatially Interconnected Systems Using Parameter-Dependent Lyapunov Functions.» In: *Proc. Amer. Control Conf.* 2013, pp. 3278–3283

A. Mendez Gonzalez, C. Hoffmann, C. Radisch, and H. Werner. «LPV Observer Design and Damping Control of Container Crane Load Swing.» In: *Proc. Europ. Control Conf.* 2013

G. Kaiser, Q. Liu, C. Hoffmann, M. Korte, and H. Werner. «Torque Vectoring for an Electric Vehicle Using an LPV Drive Controller and a Torque and Slip Limiter.» In: *Proc. 51st IEEE Conf. Decision Control*. 2012, pp. 5016–5021

Theses of the Author

C. Hoffmann. «Design and Control of a Novel Portable Mechanical Ventilator.» Master's Thesis. Hamburg, Germany: Hamburg University of Technology, 2011

C. Hoffmann. «Development of a Control System for the Shanghai Subway Flood Gate System.» Project Work. Hamburg, Germany and Shanghai, China: Hamburg University of Technology and Tongji University Shanghai, 2009

C. Hoffmann. «Modelling and Control of a Cooling System for Power Electronics on a Commercial Aircraft.» Bachelor Thesis. Hamburg, Germany: Hamburg University of Technology, 2008

Presentations of the Author

C. Hoffmann and H. Werner. *Reglerentwurf für verteilte, nicht-lineare, heterogene Systeme bei zeitlich veränderlicher Interaktionstopologie mit Hilfe multiplier-basierter konvexer Optimierungsmethoden*. Boppard, Rheinland-Pfalz, Germany, 2015

CURRICULUM VITÆ

Personal Data

Surname	Hoffmann
Given Name	Christian
Date of Birth	October 9th, 1984
Place of Birth	Bremerhaven, Bremen, Deutschland

Primary and Secondary Education

08/1991–06/1995	Grundschule Harkshörn, *Norderstedt*
08/1995–06/2004	Lessing-Gymnasium, *Norderstedt*

Civil Duties and Internships

07/2004–03/2005	Military Service
05/2005–06/2005	SAM Electronics GmbH, *Hamburg*
07/2005–09/2005	ABB Automation GmbH, *Hamburg*

Tertiary Education (*Hamburg University of Technology*)

10/2005–09/2008	General Engineering Science, Major in Mechatronics, B. Sc.
10/2008–03/2011	Mechatronics, M. Sc.
04/2011–04/2015	Research Associate, Dr.-Ing.
	Institute of Control Systems

Professional Development (*Universität zu Lübeck*)

05/2015–present	Research Fellow (Postdoctoral researcher)
	Institute for Electrical Engineering in Medicine
	Degree in progress: Habilitation